

Nickel and Palladium Complexes for C–H Functionalizations of Heteroarenes: Synthesis, Scope and Mechanistic Aspects

Thesis

Submitted to AcSIR for the Award of the Degree of

DOCTOR OF PHILOSOPHY

in

Chemical Sciences



by

Dilip Kumar Pandey

(Reg. No: 10CC13J26003)

under the guidance of

Dr. Benudhar Punji



CSIR-National Chemical Laboratory

Pune-411 008, INDIA

2019




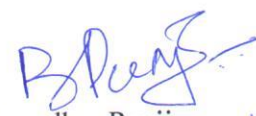
*Dedicated to
My Parents and Family*

Certificate

This is to certify that the work incorporated in this Ph.D. thesis entitled “**Nickel and Palladium Complexes for C-H Functionalizations of Heteroarenes: Synthesis, Scope and Mechanistic Aspects**” submitted by **Mr. Dilip Kumar Pandey** to Academy of Scientific and Innovative Research (AcSIR) in fulfillment of the requirements for the award of the Degree of **Doctor of Philosophy**, embodies original research work under my/our supervision/guidance. I/We further certify that this work has not been submitted to any other University or Institution in part or full for the award of any degree or diploma. Research material obtained from other sources has been duly acknowledged in the thesis. Any text, illustration, table etc., used in the thesis from other sources, have been duly cited and acknowledged.

It is also certified that this work done by the student, under my supervision, is plagiarism free.


Dilip Kumar Pandey
(Student)



Dr. Benudhar Punji
(Supervisor) 18/3/2019

Place: Pune

Declaration by the Candidate

I hereby declare that the original research work embodied in this thesis entitled, **“Nickel and Palladium Complexes for C–H Functionalizations of Heteroarenes: Synthesis, Scope and Mechanistic Aspects”** submitted to the Academy of Scientific and Innovative Research for the award of the degree of the Doctor of Philosophy (Ph.D.) is the outcome of experimental investigations carried out by me under the supervision of Dr. Benudhar Punji, Senior Scientist, CSIR-National Chemical Laboratory, Pune. I affirm that the work incorporated is original, and has not been submitted to any other academy, university or institute for the award of any degree or diploma.

18th March 2019
CSIR-National Chemical Laboratory
Pune-411008


Dilip Kumar Pandey
(Research Student)

ACKNOWLEDGEMENT

The work presented in this thesis would not have been possible without my close association with many people who were always there when I needed them the most. I take this opportunity to acknowledge them and extend my sincere gratitude for helping me make this Ph.D. thesis a possibility.

First and foremost, my special words of thanks should go to my research guide, **Dr. Benudhar Punji**, for always being so kind, helpful and motivating. His guidance helped me all the time during my research and writing of this thesis. I could not have imagined a better advisor and mentor for my Ph.D. other than him. I would like to thank him for encouraging my research and for allowing me to grow as a researcher. His advice on both research as well as on my career have been priceless. He has always been there for me with his helping hand whenever I needed it the most. His constant guidance, cooperation and support have always kept me going ahead. I owe a lot of gratitude to him for always being there for me and I feel privileged to be associated with a person like him during my life.

Besides my supervisor, I would like to thank my DAC committee members: Dr. Nandini Devi, Dr. Samir Chikkali, and Dr. Sakya Sen for their insightful comments, encouragement and also for their valuable suggestions, which helped me to widen my research from various perspectives. I am grateful to Prof. A. K. Nangia (Director, NCL), Dr. V. K. Pillai and Prof. S. Pal (Former Directors, NCL), Dr. S. S. Tambe, Head, CEPD Division, and Dr. Vivek V. Ranade (Former HOD, CEPD Division) for giving me this opportunity and providing all necessary infrastructure and facilities. I thank to the staff of Chemical Engineering Division for their innumerable help. I acknowledge the Council of Scientific and Industrial Research (CSIR), Government of India for providing me with the necessary funding and UGC for fellowship to pursue research at NCL.

My sincere thanks also go to Prof. D. S. Pandey who provided me an opportunity to join his team as M.Sc. intern, gave access to the laboratory and research facilities. I would like to acknowledge all the teachers I learnt from since my childhood, I would not have been here without their guidance, blessings and support.

My special words of gratitude to **Dr. Shrikant** and **Shahaji** for all their personal and professional support they have extended to me throughout, without them it was very difficult to come so far. I thank my fellow labmates **Dr. Hanuman, Dr. Vineeta, Ulhas, Rahul, Dipesh, Shidheswar, Vijay, Suyradev** and **Anand** for providing their help. I am also thankful to Dr.

ACKNOWLEDGEMENT

Chikkali's group members Drs. Ketan Patel, Dipa Mandal, Vijay, Swechchha, and Mr. Bhausahab, Satej, Nilesh, Anirban, Dynaneshwar, Rohit, who helped me during my Ph.D. work; also I thank my university seniors. In particular, I am grateful to **Dr. Anant Srivastava** and **Dr. Aparna Banerjee** for providing support during my journey to Ph.D.

I would like to acknowledge my college friends **Vinod, Rajeev, Shrish, Prashant and Shikher** for being my friend. Our association goes a long way since days of graduation and they have been with me ever since then as a friend, a companion. Thank you dear for being with me in ups and downs of life during all these years. I would also like to acknowledge my friend **Dharmendra** for his unconditional support to me and my family throughout my journey. I could not have asked for more than what I got from him.

I would like to thank my friends from NCL **Deepanjan, Yashpal** and **Dr. Ejaj** who have been a source of moral support to me and have extended their helping hands without fail. I would like to acknowledge my friend **Firoz** for his support without expectation. The list is endless...thanks to one and all. I find myself lucky to have friends like them in my life.

I would like to thank my friend, critic and better half **Isha** for her understanding and love during the past few years. Whenever I started losing my confidence, she came strong and boosted up my confidence. Her support and encouragement made this thesis possible.

Finally, I would like to acknowledge the people who mean world to me, my parents, uncle, aunty, my brothers and sisters. I extend my respect to my parents, my paternal and maternal grandparents, in-laws and all elders to me in the family. I can't imagine a life without their love and blessings. Thank you mom, dad, uncle and aunty for showing faith in me and giving me liberty to choose what I desired. I consider myself the luckiest in the world to have such a supportive family, standing behind me with their love and support.

I thank the Almighty for giving me the strength and patience to work through all these years so that today I could stand proud with my head held high.

Dilip Kumar Pandey

CONTENTS

List of Figures	I
List of Tables	III
List of Schemes	IV
Abbreviations	VII
Abstract	IX
Chapter 1	
Introduction	
1.1 Classification of Palladacycles	3
1.2 Methods of Preparation of Palladacycles	5
1.2.1 C–H Bond Activation	5
1.2.2 Oxidative Addition	6
1.2.3 Transmetalation	8
1.2.4 Carbopalladation and Halopalladation of Unsaturated Carbon Bonds	9
1.3 Catalytic Applications of Palladacycle Complexes	10
1.3.1 Traditional Cross-Coupling Reactions	10
1.3.1.1 Palladacycle in Heck Cross-Coupling Reactions	10
1.3.1.2 Palladacycle in Suzuki-Miyaura Coupling Reaction	11
1.3.1.3 Hiyama Coupling Reaction	13
1.3.1.4 Stille Coupling Reaction	14
1.3.1.5 Negishi Coupling Reaction	14
1.3.1.6 Sonogashira Coupling Reaction	15
1.3.2 Palladacycle Complexes in C–H Functionalization	16
1.4 Mechanistic Aspect of Palladacycle-Catalyzed Cross-Coupling Reactions	18
1.4.1 Mechanism of Heck Reaction	18
1.4.1.1 Pd(0)/Pd(II) Redox Process	18
1.4.1.2 Pd(II)/Pd(IV) Redox Process	20
1.4.2 Mechanistic Pathway for Suzuki-Miyaura Cross-Coupling Reaction	20
1.5 General Method for the Synthesis of Pincer Nickel Complexes	21
1.5.1 C–H Bond Activation Approach	21
1.5.2 Transmetalation Approach	23

CONTENTS

1.6	Catalytic Applications of Nickel Complexes	24
1.6.1	Traditional Cross-Coupling Reactions	24
1.6.1.1	Suzuki-Miyaura Coupling Reaction	24
1.6.1.2	Kumada Coupling Reaction	25
1.6.1.3	Negishi Coupling Reaction	25
1.6.1.4	Sonogashira Coupling Reaction	26
1.6.2	Nickel-Catalyzed C–H Bond Activation and Functionalization	27
1.6.2.1	Alkylation of (Hetero)Arenes	27
1.6.2.2	Arylation of (Hetero)Arenes	30
1.6.2.3	Alkenylation of (Hetero)Arenes	32
1.6.2.4	Alkynylation of (Hetero)Arenes	34
1.7	Mechanistic Aspect of Nickel-Catalyzed C–C Bond Forming Reactions Through C–H Bond Activation	36
1.7.1	Mechanistic Pathway for the Nickel-Catalyzed Alkylation Reaction	37
1.7.2	Mechanism of Nickel-Catalyzed Arylation	38
1.8	References	40

	Objective of the Present Study	50
--	---------------------------------------	----

Chapter 2

Mono- and Binuclear Palladacycles *via* Regioselective C–H Bond Activation: Syntheses, Mechanistic Insights and Catalytic Activity

2.1	Introduction	53
2.2	Results and Discussion	54
2.2.1	Synthesis of Ligands	54
2.2.2	Synthesis of Palladacycle Complexes	55
2.2.3	Derivatives of Pincer Palladacycle	58
2.2.4	Mechanistic Aspects of Regioselective Palladation	59
2.2.5	Molecular Structure of Palladium Complexes	66
2.2.6	Catalytic Activity of Palladacycle for Arylation of Azoles	70
2.3	Conclusion	75

CONTENTS

2.4	Experimental Section	75
2.5	Reference	87
	NMR Spectra of Selected Compounds	91

Chapter 3

Unactivated Alkyl Chlorides in Nickel-Catalyzed C(2)-H Alkylation of Indoles: Scope and Mechanistic Aspects

3.1	Introduction	115
3.2	Results and Discussion	116
3.2.1	Optimization of Reaction Parameters	116
3.2.2	Substrate Scope for Alkylation	119
3.2.3	Removal of Directing Group	126
3.2.4	Mechanistic Studies	127
3.2.4.1	NMR Tube Reaction	127
3.2.4.2	Probing Radical Pathway	128
3.2.4.3	Deuterium Labeling Studies	129
3.2.4.4	Electronic Effect and Reactivity Study	131
3.2.4.5	Reaction Profile using (thf) ₂ NiBr ₂ /bpy	133
3.2.4.6	Electron Paramagnetic Resonance (EPR) Studies	137
3.2.4.7	X-ray Photoelectron Spectroscopy (XPS) Studies	138
3.2.4.8	Catalytic Cycle	141
3.3	Conclusion	142
3.4	Experimental Section	143
3.5	References	179

Chapter 4

Nickel-Catalyzed C-2 Arylation of Indoles with Unactivated Aryl Chlorides

4.1	Introduction	184
4.2	Results and Discussion	185
4.2.1	Optimization of Reaction Parameters	185
4.2.2	Substrate Scope for Arylation	187

CONTENTS

4.2.3	Mechanistic Studies	190
4.2.3.1	Kinetic Analysis of Arylation of indoles	190
4.2.3.2	Probing Radical Pathway	196
4.2.3.3	Deuterium Labeling Studies	196
4.2.3.4	Effect of Indole Substitutions on Arylation	198
4.2.3.5	Catalytic Cycle	200
4.3	Conclusion	201
4.4	Experimental Section	201
4.5	References	220
	NMR Spectra of the Selected Compound	223
Chapter 5		
Synthesis and Characterization of (^QNNN^{R2})Ni Complexes, and Application in C–H Bond Functionalization		
5.1	Introduction	227
5.2	Results and Discussion	227
5.2.1	Synthesis and Characterization of (^Q NNN ^{R2}) Nickel Complexes	227
5.2.2	Molecular Structure of Nickel Complexes	229
5.2.3	Pincer Nickel Complexes in Alkylation of Indoles	232
5.2.4	Dehydrogenative Alkylation of Indoline with Primary Halides	235
5.3	Conclusion	237
5.4	Experimental Section	238
5.5	References	245
	NMR Spectra of the Selected Compounds	248
	List of Publications	256

LIST OF FIGURES

1.1	First metallacycle complex	2
1.2	Classification of palladacycle	4
1.3	Examples of palladacycles	4
1.4	Examples of ECE palladacycle	5
1.5	Palladacycles having a different ring size	5
2.1	Reaction profile for the C–H bond palladation of 6c , 7c and 8c	62
2.2	Time-dependent yields of the palladacycle 2c at different loading of K ₃ PO ₄	63
2.3	Time-dependent yields of the 5c at different concentration of Et ₃ N	64
2.4	Time-dependent yields of the 2c at different concentration of pyridine	65
2.5	Thermal ellipsoid plot of (Ph ₂ POCN ^{iPr} ₂)PdCl (2a)	67
2.6	Thermal ellipsoid plot of (Et ₂ N) ₂ POCN ^{iPr} ₂)PdCl (2b)	67
2.7	Thermal ellipsoid plot of (Ph ₂ POCN ^{iPr} ₂)PdOAc (3a)	68
2.8	Thermal ellipsoid plot of (Et ₂ N) ₂ POCN ^{iPr} ₂)PdOAc (3b)	69
2.9	Thermal ellipsoid plot of complex 5a	70
3.1	¹ H NMR spectra of controlled alkylation reaction	128
3.2	Time-dependent formation of 3aa using indoles 1a and [2-D]- 1a	130
3.3	Time-dependent formation of products 3ba and 3da	132
3.4	Time-dependent formation of products 3aa using different <i>n</i> -octyl halides	133
3.5	Time-dependent formation of 3aa using (thf) ₂ NiBr ₂ /bpy system	134
3.6	Time-dependent formation of 3aa using (A) (thf) ₂ NiBr ₂ /bpy system and (B) (bpy)NiBr ₂ catalyst	136
3.7	EPR spectrum of the incomplete alkylation reaction	138
3.8	X-ray photoelectron spectra: (A) for (Ph ₃ P) ₃ NiCl (B) for Ni(COD) ₂	139
3.9	X-ray photoelectron spectra: (A) for (thf) ₂ NiBr ₂ , (B) (thf) ₂ NiBr ₂ + bpy + LiHMDS + 1-chlorooctane (2a)	140
3.10	X-ray photoelectron spectra	140
3.11	Plausible mechanistic pathway for nickel-catalyzed alkylation of indoles	142
4.1	Time-dependent formation of 3aa	191

LIST OF FIGURES

4.2	Time-dependent formation of 3aa at different initial concentration of 1a	193
4.3	Time-dependent formation of 3aa at different initial concentration of 2a	194
4.4	Time-dependent formation of 3aa at different initial concentration of catalyst	195
4.5	Time-dependent formation of 3aa at different initial concentration of LiHMDS	196
4.6	Time-dependent formation of product 3aa using indoles 1a and [2-D]- 1a	197
4.7	Time-dependent formation of products 3ca and 3da	199
4.8	Plausible mechanistic pathway for nickel-catalyzed arylation of indoles	200
5.1	Thermal ellipsoid plot of (^Q NN ^{NMe₂})NiCl (2a)	230
5.2	Thermal ellipsoid plot of (^Q NN ^{NEt₂})NiBr (3b)	230
5.3	Thermal ellipsoid plot of (^Q NN ^{pyrrolidine})NiCl (4a)	231

LIST OF TABLES

2.1	Rate of Arylation Reaction at Different Initial Concentrations of K_3PO_4	63
2.2	Rate of Arylation Reaction at Different Initial Concentrations of Et_3N	64
2.3	Rate of Arylation Reaction at Different Initial Concentrations of Pyridine	65
2.4	Screening of Catalysts and Reaction Parameters for Arylation of Azoles	71
2.5	Scope for the Arylation of Azoles Catalyzed by 4c	73
3.1	Optimization of the Reaction Conditions	117
3.2	Scope of the Ni-Catalyzed C-2 Alkylation of Indoles with Primary Alkyl Chlorides	120
3.3	Concentration of 3aa at Different Time Intervals using $(thf)_2NiBr_2/bpy$	134
3.4	Concentration of 3aa at Different Time Intervals using $(thf)_2NiBr_2/bpy$ and $(bpy)NiBr_2$	135
4.1	Optimization of Reaction Parameters	186
4.2	Concentration of Product 3aa at Different Time Intervals	191
4.3	Rate of Arylation Reaction at Different Initial Concentrations of 1a	192
4.4	Rate of Arylation Reaction at Different Initial Concentrations of 2a	193
4.5	Rate of Arylation Reaction at Different Initial Concentrations of Catalyst	194
4.6	Rate of Arylation Reaction at Different Initial Concentrations of LiHMDS	195
5.1	Selected Bond Lengths (Å) and Angles (deg) for 2a , 3b , and 4a	232
5.2	Optimization of Reaction Conditions	233
5.3	Optimization for Dehydrogenative Alkylation of Indoline	236

LIST OF SCHEMES

1.1	Synthesis of first palladacycle complex	3
1.2	Synthesis of CE-palladacycle <i>via</i> C–H activation method	6
1.3	Synthesis of (PCP)Pd-complex <i>via</i> C–H activation process	6
1.4	Synthesis of (CN)-Pd complex by oxidative addition of C–X bond	7
1.5	Synthesis of functionality containing palladacycle <i>via</i> oxidative addition	7
1.6	Transmetalation with organo-lithium compound	8
1.7	Transmetalation by bis-cyclopalladated complex	8
1.8	Bis-cyclopalladated compounds <i>via</i> transmetalation process	9
1.9	Palladacycles <i>via</i> palladation of the unsaturated bond	9
1.10	ECE' type palladacycles <i>via</i> chloropalladation of acetylenes	10
1.11	CE type palladacycle for Heck reaction	11
1.12	Heck coupling reaction using palladium complex	11
1.13	CE-type palladacycle in Suzuki-Miyaura coupling reactions	12
1.14	Suzuki coupling reaction using complex	12
1.15	Unsymmetrical palladacycle complex for Hiyama cross-coupling	13
1.16	Hiyama cross-coupling reaction using palladacycle complex	13
1.17	Stille reaction using PCP pincer complex	14
1.18	Biphenyl analog precursors to biphenomycin antibiotics	14
1.19	Negishi coupling reaction using palladacycle complex	15
1.20	Cross-coupling reaction aryl bromide with aryl zinc using pincer complex	15
1.21	Phospha palladacycle catalyzed homogeneous Sonogashira reaction	16
1.22	Aryl halide and terminal alkynes coupling using PCP palladacycle complex	16
1.23	Arylation of azole using palladacycle catalyst	17
1.24	Arylation of azole using palladacycle catalyst	17
1.25	Heck reaction using pincer palladium complex 1.40 as dispenser of Pd(0) nanoparticles (R ¹ represents polyfluorinated chain)	19
1.26	Pd(0) nanoparticle catalyzed Heck reaction	19
1.27	Pd(II) ECE-palladacycle catalyzed Heck reaction	20
1.28	ECE-palladacycle catalyzed Suzuki reaction	21
1.29	Synthesis of PCP pincer nickel complex through C–H bond activation	22
1.30	Synthesis of bis-phosphinite POCOP-pincer nickel complexes	22

LIST OF SCHEMES

1.31	Synthesis of bis-phosphinite POCOP-pincer nickel complexes	23
1.32	Synthesis of NNN-pincer nickel complex <i>via</i> transmetalation approach	24
1.33	Suzuki-Miyaura coupling reaction by nickel	25
1.34	Nickel catalyzed Kumada coupling reaction	25
1.35	Nickel catalyzed Negishi reaction	26
1.36	Nickel catalyzed Sonogashira coupling reaction	26
1.37	Hemilabile nickel complex in Sonogashira coupling reaction	26
1.38	Synthesis of organonickel species	27
1.39	Alkylation of aromatic heterocycle with an alkyl halide	28
1.40	Alkylation of azoles using (^Q NNN ^{Me2})Ni-pincer complex	28
1.41	Aniline <i>o</i> -alkylation <i>via</i> monodentate chelation assistance	29
1.42	Chelation assisted C(2)-H alkylation of indoles	29
1.43	Alkylation of C(sp ³)-H bond of the aliphatic amide	30
1.44	Arylation of azoles with aryl halide or triflate	30
1.45	Nickel-catalyzed arylation of azoles with aryl bromide	31
1.46	Ar-H/Ar-O cross-coupling reaction	31
1.47	C(sp ²)-H bond arylation of bezo[<i>H</i>]quinolone	32
1.48	C(sp ³)-H bond arylation of aliphatic amides	32
1.49	Addition of pyridine- <i>N</i> -oxide to alkyne	33
1.50	Direct C(2)-H alkenylation of pyridine	33
1.51	C-H/C-O alkenylation of azoles	34
1.52	C(2)-H alkenylation of indole	34
1.53	Direct cross-coupling of azoles with various alkynes	35
1.54	Nickel-catalyzed C-H alkynylation of anilines	35
1.55	Alkynylation of heteroarenes	36
1.56	Alkynylation of C(sp ²)-H bond of aryl amide	36
1.57	Plausible catalytic cycle for alkylation of C(sp ³)-H bond of aliphatic amide	38
1.58	Plausible mechanism for arylation of C(sp ³)-H bond in aliphatic amide using nickel catalyst	39
2.1	Synthesis of POCN-H ligands	54

LIST OF SCHEMES

2.2	Synthesis of palladacycle complexes	56
2.3	Synthesis of acetate-bridged binuclear palladium complex 5a	57
2.4	Reactivity of 1a with Pd(OAc) ₂	58
2.5	Synthesis of POCN-pincer palladium derivatives	59
2.6	Proposed pathway for the formation of “PC”- and “POCN”-palladacycles	61
3.1	Reactivity of <i>N</i> -substituted indoles	118
3.2	Scope of C-2 alkylation of substituted indoles and pyrroles	124
3.3	Scope of C-2 alkylation of indoles with secondary alkyl bromides	125
3.4	In-situ synthesis of bis(indolyl)butane	126
3.5	Removal of 2-pyridinyl directing group	127
3.6	External additive and radical clock experiments	129
3.7	Deuterium labeling experiments	131
3.8	Controlled stoichiometric reactions	137
4.1	Screening of <i>N</i> -substituent at Indole	187
4.2	Scope of C-2 arylation of indoles with aryl chlorides	189
4.3	Scope of C-2 arylation of Substituted indoles and pyrroles	190
4.4	External additive experiment	196
4.5	Deuterium labeling experiments	198
4.6	Effect of indole substitutions on arylation	199
5.1	Synthesis of (^Q NNN ^{R2})-H pincer ligand	228
5.2	Synthesis of (^Q NNN ^{R2})NiX pincer complexes	229
5.3	Scope for alkylation of indole	234
5.4	Scope for dehydrogenative alkylation of indoline	237

ABBREVIATIONS

AgOAc	Silver acetate
AgOTf	Silver trifluoromethanesulfonate
AgCN	Silver cyanide
AgONO ₂	Silver nitrite
AgSbF ₆	Silver hexafluoroantimonate
bpy	2,2'-Bipyridine
BDMAE	Bis(2-dimethylaminoethyl) ether
BnN ₃	Benzyl azide
BINOL	1,1'-Bi-2-naphthol
Cp	Cyclopentadienyl
COD	1,5-cyclo-octadiene
Cy	Cyclohexyl
Davephos	2-Dicyclohexylphosphino-2'-(<i>N,N</i> -dimethylamino)biphenyl
DCE	1,2-dichloroethane
Dppm	bis(diphenylphosphino)methane
Dppe	1, 2-bis(diphenylphosphino)ethane
Binap	(2, 2'-bis(diphenylphosphino))-1
dcype	Dicyclophosphinoethane
Dpephos	Bis[(2diphenylphosphino)phenyl] ether
DME	Dimethoxy ethane
DMA	<i>N,N</i> -dimethylacetamide
Diglyme	Bis(2-methoxyethyl) ether
DMAP	4-Dimethylaminopyridine
DMF	<i>N,N</i> -dimethylformamide
DMSO	Dimethyl sulfoxide
D ^t BEDA	<i>N,N'</i> -Di- <i>tert</i> -butyl ethylenediamine
d ^t bpy	4,4-Di- <i>tert</i> -butyl bipyridine
dppf	1,1'-Bis(diphenylphosphino)ferrocene
dppbz	1,2-Bis(diphenylphosphanyl)benzene
(DME)NiCl ₂	Nickel(II) chloride ethylene glycol dimethyl ether
(dppf)NiCl ₂	Dichloro((diphenylphosphino)ferrocene)nickel

ABBREVIATIONS

Galvinoxyl	2,6-Di- <i>tert</i> -butyl- α -(3,5-di- <i>tert</i> -butyl-4-oxo-2,5-cyclohexadien-1-ylidene)- <i>p</i> -tolylxy
HRMS	High resolution mass spectrometry
KI	Pottasium iodide
LA	Lewis Acid
LiHMDS	Lithium bis(trimethylsilyl)amide
MesCOOH	2,4,6-trimethylbenzoic acid
Neocuproine	2,9-dimethyl-1,10-phenanthroline
NMP	1-Methyl-2-pyrrolidone
ORTEP	Oak ridge thermal-ellipsoid plot program
OTf	Trifluoromethanesulfonate
Pcyp ₃	Tricyclo pentyl phosphine
Pd ₂ (dba) ₃	Tris(dibenzylideneacetone)dipalladium(0)
Pd(COD)Cl ₂	Dichloro(1,5 cyclooctadiene)palladium(II)
Phen	1.10-Phenanthroline
Py	Pyridinyl
P(^{<i>i</i>} Pr) ₃	<i>tri</i> -Isopropyl phosphine
TEMPO	(2,2,6,6-Tetramethylpiperidin-1-yl)oxyl
TFA	Trifluoroacetic acid
TFE	Trifluoroethanol
TIPS	Triisopropylsilyl
TOF	Turnover frequency
TON	Turnover number
Xantphos	4,5 Bis(diphenylphosphino)
Xphos	2-Dicyclohexylphosphino-2',4',6'-triisopropylbiphenyl

ABSTRACT

The thesis is divided into five different chapters. Chapter-1 deals with the detailed literature survey on the synthesis of palladacycle complexes, and their applications in traditional cross-coupling as well as in direct C–H bond functionalization of arenes and heteroarenes. Mechanistic aspect of the palladium-catalyzed coupling reaction is also reviewed. Similarly, this chapter includes reports on the NNN-pincer nickel complexes, their application in traditional cross coupling and C–H functionalization, and catalytic aspects. The C–H bond functionalization of heteroarenes with simple nickel precursor is also discussed in this chapter.

Chapter-2 describes the syntheses of mono- and binuclear palladacycles *via* regioselective C–H bond activation, and application in azoles arylation. Palladacycles containing C-anionic four-electron donor (CE) or six-electron donor (ECE) ligand (E = donor group) have many attractive structural features. Generally, the selective synthesis of CE- and ECE-palladacycle requires the introduction of a site selective activating group (-SiMe₃) in the ligand backbone. Thus, in this chapter, we focussed on the syntheses of new unsymmetrical “POCN” pincer-type ligands, and their “PC”-chelated binuclear, [κ^P, κ^C -PC-PdCl]₂ (CE-type) and “POCN”-coordinated mononuclear, ($\kappa^P, \kappa^C, \kappa^N$ -POCN)PdCl (ECE'-type) palladacycle complexes *via* the regioselective C–H bond activation. More importantly, the steric and electronic influence of base on the regioselective C–H palladation is demonstrated by extensive kinetics analysis. All the palladacycles were well-characterized by various analytical techniques, including X-ray crystal structure determination. The palladacycle complexes were screened and employed as catalysts for direct C–H bond arylation of azoles with aryl iodides.

Chapter 3 describes the nickel-catalyzed chemo and regioselective C-2 alkylation of indoles with unactivated primary and secondary alkyl chlorides. We have demonstrated a new methodology, wherein a simple Ni-catalyst system (thf)₂NiBr₂/bpy was efficiently employed for the C-2 alkylation of indoles at mild condition using unactivated alkyl chlorides as coupling partners. We have successfully demonstrated various substrate scopes for alkylation of indoles using diverse unactivated alkyl chlorides. Different functional groups, like halides, alkenyl, alkynyl, ether, thioether, furanyl, pyrrolyl, indolyl and carbazolyl including acyclic and cyclic alkyls were well tolerated under optimized reaction condition. Mechanistic experiments like kinetics, external additive experiment, radical probe experiment, deuterium labeling experiments were performed to get more insight of the reaction mechanism. EPR and XPS studies were done to analyze the reactive nickel intermediate. A comprehensive mechanistic study highlights that

ABSTRACT

the alkylation proceeds through a single-electron transfer (SET) process with Ni(I)-species being the active catalyst. Overall, the alkylation follows a Ni(I)/Ni(III) pathway involving the rate-influencing two-step single-electron oxidative addition of alkyl chloride.

Chapter 4 describes regioselective nickel-catalyzed C-2 arylation of indoles with unactivated aryl chlorides. A simple nickel catalyst system Ni(OAc)₂/dppf was found to be suitable for the arylation of indole and pyrrole derivatives with diverse aryl chlorides at relatively mild conditions. Varieties of functional groups, such as -F, -OMe, -OCF₃, ether, thioether, pyrrolyl, indolyl and carbazolyl were tolerated under the reaction conditions. Detailed mechanistic study for this arylation reaction has been performed, including external additive experiments, deuterium labeling experiments and kinetic experiments to get insight of the reaction mechanism. Mechanistic study highlights that the arylation proceeds through a single-electron transfer (SET) process.

Chapter 5 discusses about the synthesis of hemilabile (O^qNNN^{R2})-H ligand and pincer nickel complexes. The synthesized complexes were characterized by different spectroscopic techniques and the structures were confirmed with the help of X-ray diffraction technique. These complexes were screened and employed for the C-H bond alkylation of indole. Selective substrates scope has been demonstrated using this nickel catalyst. This chapter also deals with the one-pot strategy for the dehydrogenative alkylation of indolines to achieve C-2 alkylated indoles *via* a monodentate-chelate assistance strategy.

Chapter 1

Introduction

This chapter describes the general classification, synthesis, and applications of palladacycle complexes. The main focus is on the palladacycle systems and their applications in the field of catalysis and C–H bond functionalization. In addition, the fundamental properties and synthetic routes of the palladacycle complexes are discussed. The utilization of palladacycle complexes in various catalytic transformations and their mechanistic study is documented in details. Similarly, nickel-catalyzed C–H functionalization such as alkylation, arylation, alkenylation, alkynylation, and the mechanistic aspect of nickel-catalyzed reaction is discussed.

Historically, there are many events responsible for the development of metallacycle chemistry. Kleiman and Dubeck in 1963 discovered the metallacycle by the reaction between Cp_2Ni and azobenzene resulting in a five-membered nickelacycle (Figure 1.1).¹ They have proposed the resultant structure by considering η^2 -coordination of the N=N π -bond to the nickel center. This cyclometallation chemistry was continued to other members of transition metals. Between the year 1965 and 1968 analogous reactions were carried out by Cope, Siekman and Friedrich with *N,N*-dimethylbenzylamines and azobenzene **1.1**, using Li_2PdCl_4 or PdCl_2 and they have isolated the first well-characterized palladacycle complex **1.2** (Scheme 1.1).^{2,3}

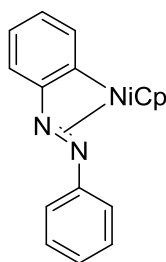
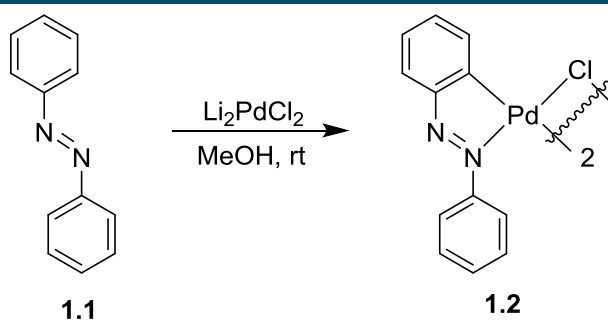


Figure 1.1 First metallacycle complex.

High thermal stability exhibited by these compounds, particularly in the solid state, is the most important factor for the development of palladacycle complexes. In 1995, Herrmann *et al.* introduced the tri-*o*-tolyl-phosphine palladacycle complex as catalyst precursor for the cross-coupling reactions.⁴ These palladacycle complexes were useful in activating more economic substrate such as aryl chlorides than those applied so far (aryl iodides or aryl triflates).⁵ Palladacycle complexes enabled the industrial application of these cross-coupling reactions. Since then, these complexes are being used as catalyst precursors or active intermediates to complex molecular transformation and have been ubiquitous in the catalytic reaction.^{6,7}



Scheme 1.1 Synthesis of first palladacycle complex.

The strong and stable chelation metal-carbon σ -bond provides high air and thermal stability to palladacycle complexes due to which it can perform various attractive catalytic transformations.⁸ Different steric and electronic properties around the palladium can be tuned by changing the substituent around the donor-atoms. These properties of palladacycles make them extraordinary catalysts for various important organic transformations, such as C–C and C–N bond forming reactions, oxidations, and many other reactions.^{9,10} The hemilabile character of such systems could provide the suitable steric, electronic and coordination demands during the different steps of a catalytic reaction.

1.1 Classification of Palladacycles

On the basis of donating ability of coordinated atoms, palladacycles can be divided into two types: C-anionic four-electron donor (CE) and six-electron donor (ECE). The ECE type of palladacycles can be further distinguished into two types: symmetrical (ECE type) and unsymmetrical (ECE' type) (Figure 1.2a-c). The CE type palladacycles (halogen or acetate bridged dimer) mostly stay in two geometric isomers *cisoid* and *transoid* conformations (Figure 1.2d-e). The CE-type palladacycles, depending upon the nature of the X-type ligands can be neutral (dimer,³ bis-cyclopalladated,¹¹ or monomeric¹²), cationic,¹³ or anionic¹⁴ (Figure 1.3).

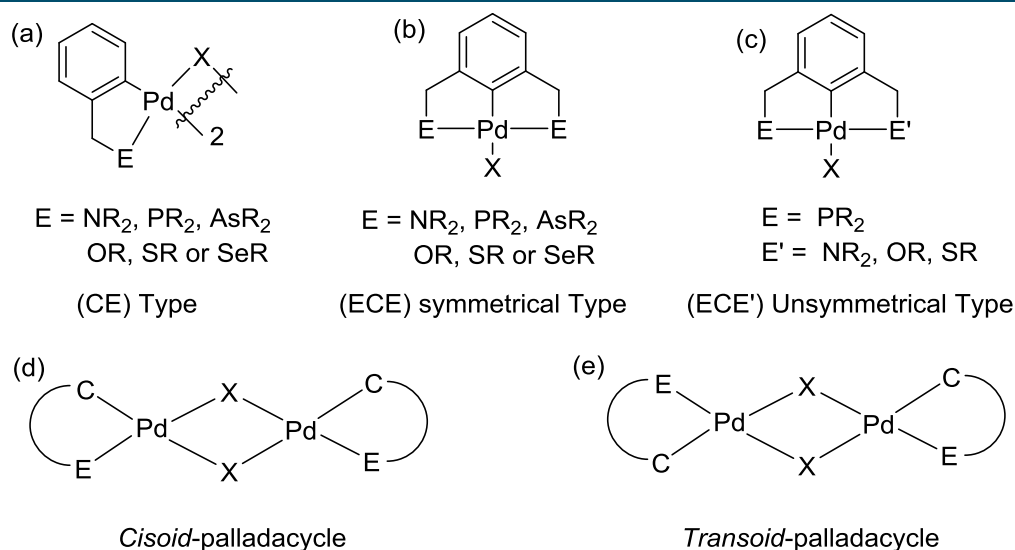


Figure 1.2 Classification of palladacycle.

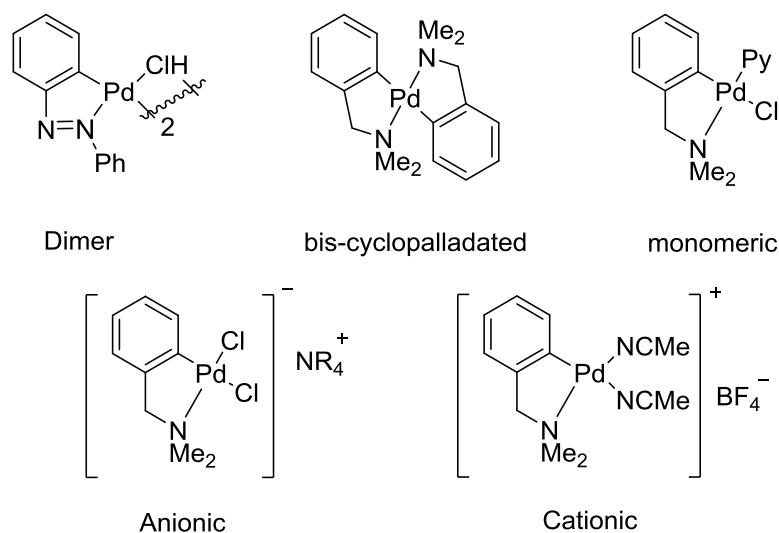


Figure 1.3 Examples of CE palladacycles.

The ECE-type palladacycles can be of two types: symmetrical¹⁵⁻¹⁸ or unsymmetrical¹⁹⁻²³ (Figure 1.4). The metalated ring size of palladacycles can vary from 3 to 11 members (Figure 1.5).²⁴⁻²⁹ Notably, the stable three and four-membered palladacycles are very limited, and examples of isolated and well-characterized compounds are very rare.

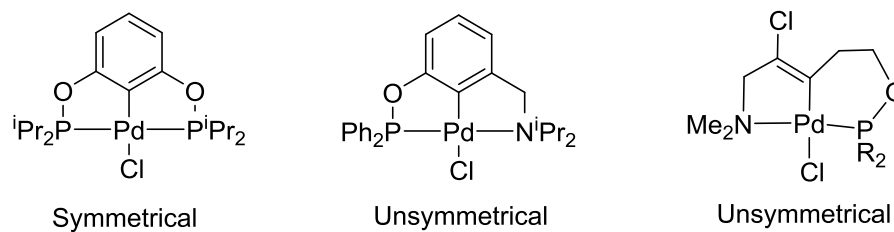


Figure 1.4 Examples of ECE palladacycle.

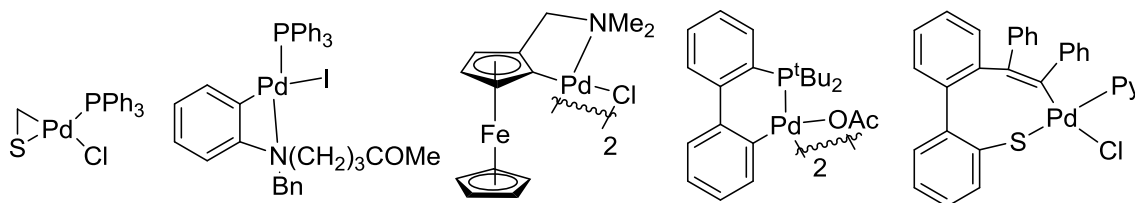


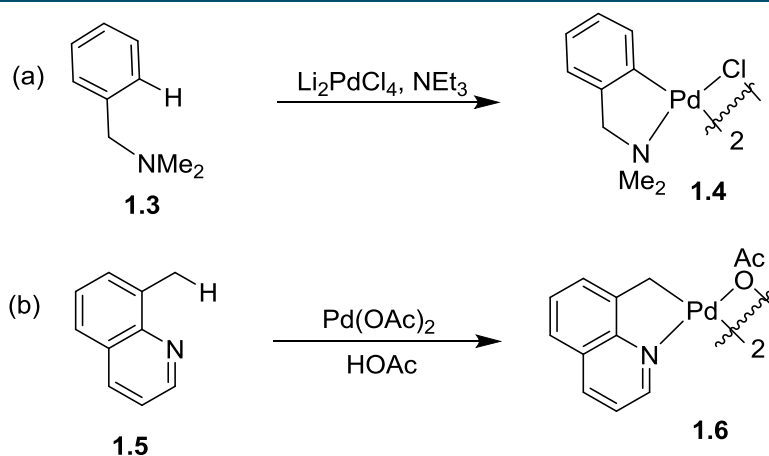
Figure 1.5 Palladacycles having a different ring size.

1.2 Methods of Preparation of Palladacycles

Palladacycles can be synthesized by means of different chemical methods such as C–H activation, oxidative addition, transmetalation, and nucleophilic addition to an unsaturated bond. The stability of these palladacycles depends on the chelate ring size. Generally, the five- and six-membered chelate rings are more stable as compared to other palladacycle due to the formation of a stable Pd–C bond, assisted by two-electron donor group coordinated to the palladium.

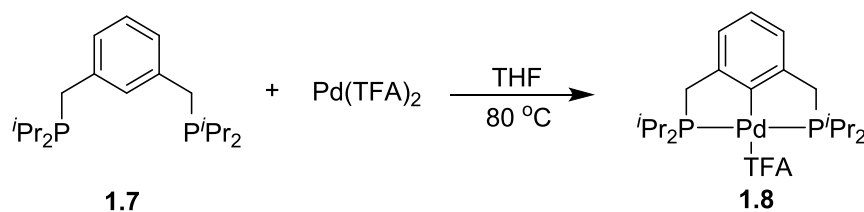
1.2.1 C–H Bond Activation

Chelation assisted palladation also called *ortho* palladation of C–H bonds are the simplest and direct method for the preparation of palladacycles.¹⁸ This method involves the C–H activation process which requires simple metal precursor compared to the procedure based on oxidative addition. For example, a common palladium precursor such as tetrachloropalladate salt (Scheme 1.2a) or palladium acetate (Scheme 1.2b) can be used for the palladation reaction.³⁰ For example, the N,N-dimethyl-1-phenylmethanamine (**1.3**) was treated with tetrachloropalladium in the presence of Et₃N to give palladacycle **1.4**. Similarly, the 8-methylquinoline (**1.5**) was treated with palladium acetate to get the complex **1.6**. These palladium precursors are cost-effective and easy to handle.



Scheme 1.2 Synthesis of CE-palladacycle *via* C–H activation method.

The C–H activation process generally depends on the ligand moieties attached to the Pd(II) metal precursor. It was demonstrated that efficient C–H functionalization can be achieved with the ligand having weakly co-ordinating side arms using Pd(II) salts, such as $\text{Pd}(\text{OCOCF}_3)_2$ ^{31,32} or $\text{Pd}(\text{BF}_4)_2(\text{CH}_3\text{CN})_4$.³³⁻³⁶ In 1997, Milstein demonstrated the synthesis of (PCP)Pd-complex (**1.8**) *via* the C–H activation of PCP pincer ligand **1.7** with $\text{Pd}(\text{TFA})_2$ salt (Scheme 1.3).³¹

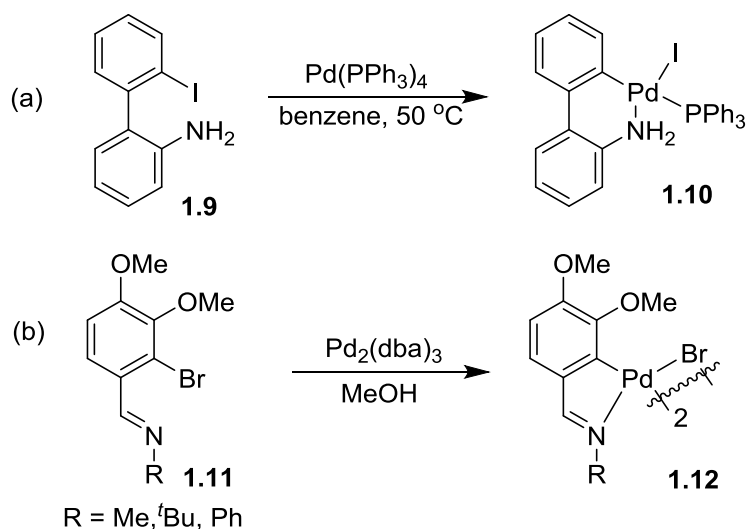


Scheme 1.3 Synthesis of (PCP)Pd-complex *via* C–H activation process.

1.2.2 Oxidative Addition

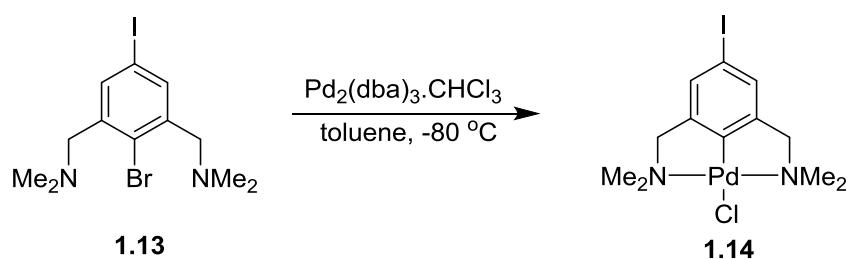
Oxidative addition method is very advantageous for the synthesis of palladacycles that cannot be obtained by C–H bond activation method. One of the most crucial differences between oxidative addition and C–H bond activation method is the need of metal precursors having different oxidation state. In the case of oxidative addition strategy, the oxidative addition of C–X bond on ligand is performed with Pd(0) species like $\text{Pd}(\text{PPh}_3)_4$ or $\text{Pd}_2(\text{dba})_3$, but in the case of C–H bond activation method the reaction is achieved with Pd(II) precursors. Many palladacycles are synthesized by adopting oxidative addition strategy. For example, complex **1.10** could be

synthesized by reacting compound **1.9** with $\text{Pd}(\text{PPh}_3)_4$ palladium precursor (Scheme 1.4a).³⁷ Similarly, the complex **1.12** was obtained by reacting compound **1.11** with $\text{Pd}_2(\text{dba})_3$ (Scheme 1.4b).^{38,39} In most of the reaction, $\text{Pd}(\text{dba})_2$, $\text{Pd}_2(\text{dba})_3$ or $\text{Pd}(\text{PPh}_3)_4$ are used as palladium precursors.



Scheme 1.4 Synthesis of (CN)-Pd complex by oxidative addition of C–X bond.

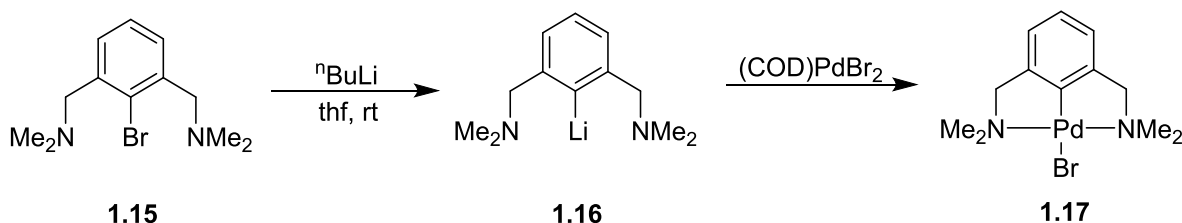
Oxidative addition is a feasible method for palladacycles containing less stable cyclic ring such as three- and four-membered rings. Moreover, this method is convenient for the synthesis of palladacycles containing reactive functionalities. For example, the complex **1.14** was derived from the ligand **1.13** *via* oxidative addition method (Scheme 1.5).⁴⁰ Palladacycle **1.14** may further undergo transformations leading to the synthesis of heterobimetallic systems. Generally, the accessibility of the halogen-containing desired starting material is the major drawback of the oxidative addition methodology, which was prepared by a multistep procedure.



Scheme 1.5 Synthesis of functionality containing palladacycle *via* oxidative addition.

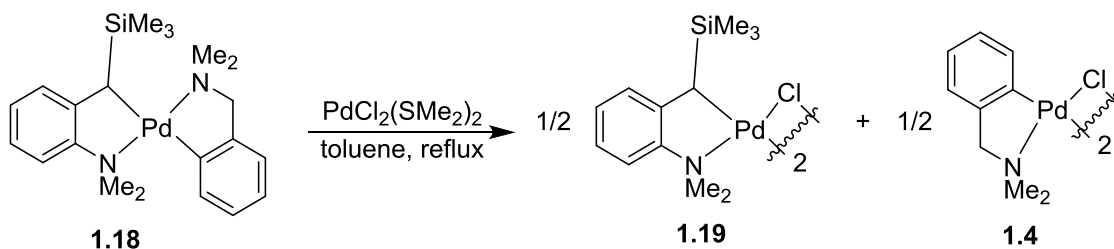
1.2.3 Transmetalation

Transmetalation is a type of organometallic reaction that involves the transfer of ligands from one metal to another. This is a more often-used methodology for the preparation of palladacycles. Generally, organolithium or organomercurial reagents are used as a transmetallating agent. For example, selective lithiation of the ligand **1.15** or by Li/halogen exchange, the organolithium reagents **1.16** can be prepared with quantitative yield and corresponding lithiated compound can be reacted with (COD)PdBr₂ to get the complex **1.17** (Scheme 1.6).⁴¹

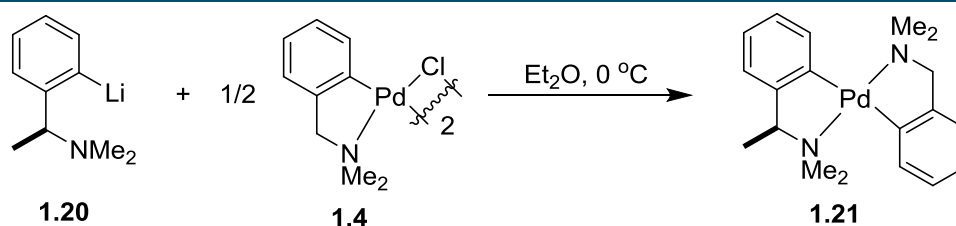


Scheme 1.6 Transmetalation with organo-lithium compound.

Some typical halogen dimer palladacycle **1.19** having labile SiMe₃ group located at the metalated carbon can be achieved by transmetalation reactions using PdCl₂(SMe)₂ with bis-cyclopalladated compounds **1.18** (Scheme 1.7).⁴² These types of transformations are not accessible through other methods. Transmetalation approach can also be used for the synthesis of bis-cyclopalladated complex. For example, the organolithium compound **1.20** with the halogen dimer palladacycles **1.4** can easily produce the bis-cyclopalladated complex **1.21** containing *N*- or *O*-donor group (Scheme 1.8).^{43,44}



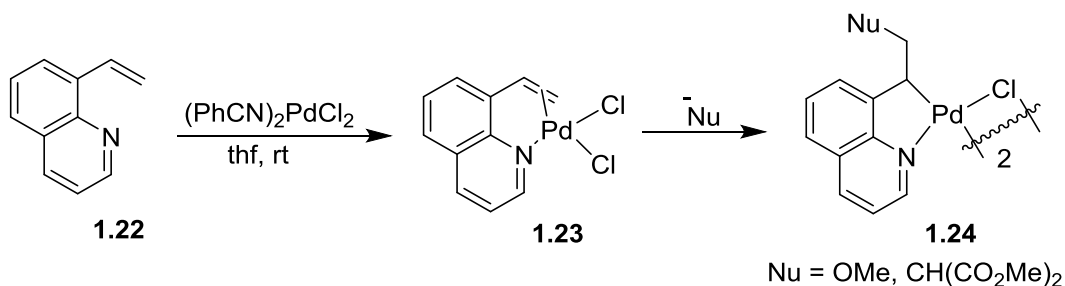
Scheme 1.7 Transmetalation by bis-cyclopalladated complex.



Scheme 1.8 Bis-cyclopalladated compounds *via* transmetalation process.

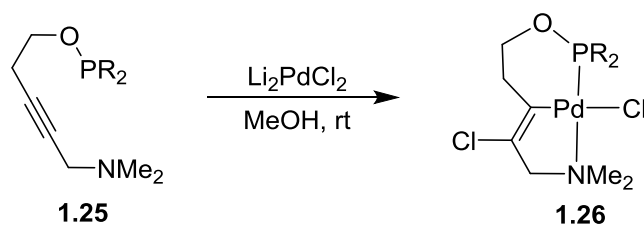
1.2.4. Carbopalladation and Halopalladation of Unsaturated Carbon Bonds

Carbopalladation and halopalladation reaction involves the first step as coordination of the olefin group to the metal centre. The C=C bond of the compound **1.22** co-ordinates to the electrophilic Pd(II) centre in a η^2 fashion to generate compound **1.23**. Attack of a nucleophile to the unsaturated carbon of compound **1.23** gives the more stable palladacycle compound **1.24**. Five-membered palladacycles are preferred over six-membered rings (Scheme 1.9).^{45,46} The formation of the intermediate generated through the chelation of both donor groups as well as C=C bond is crucial for the formation of the palladacycle.



Scheme 1.9 Palladacycles *via* palladation of the unsaturated bond.

Terminal allyl and homo-allyl alkenes can also form palladacycles very frequently than the internal alkenes.^{47,48} This type of chloropalladation reaction method is helpful for the preparation of nonsymmetrical pincer palladacycles. For example, heterosubstituted acetylenes (**1.25**) reacted with palladium precursor in the presence of methanol solvent to obtain the PCN-palladacycle **1.26** (Scheme 1.10).^{23,49}



Scheme 1.10 ECE' type palladacycles *via* chloropalladation of acetylenes.

1.3 Catalytic Applications of Palladacycle Complexes

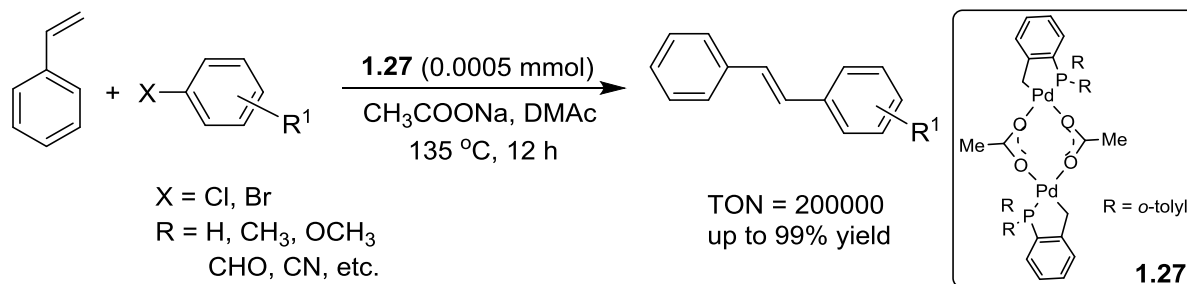
1.3.1 Traditional Cross-Coupling Reactions

High thermal stability, unique reactivity and well-defined nature of the palladacycle complexes make them useful catalysts for various practical applications. The possibility of tuning the metal reactivity *via* rational donor group variation provides access to unique reactivity through palladacycle. The literature reports show that the palladacycle complexes have been used mostly for the traditional cross-coupling reactions, which includes the C–C bond forming reaction.^{50,51} Milstein and others reported the Heck reaction catalyzed by ECE type palladacycle catalyst.^{31,52-72} Later, ECE types of palladacycle complexes were explored for other cross-coupling reactions, such as Suzuki-Miyaura reaction,⁷³⁻⁹³ Sonogashira reaction,⁹⁴⁻¹⁰² Stille coupling,^{66,103} Hiyama¹⁰⁰ and Negishi coupling.¹⁰⁴⁻¹⁰⁶

1.3.1.1 Palladacycle in Heck Cross-Coupling Reactions

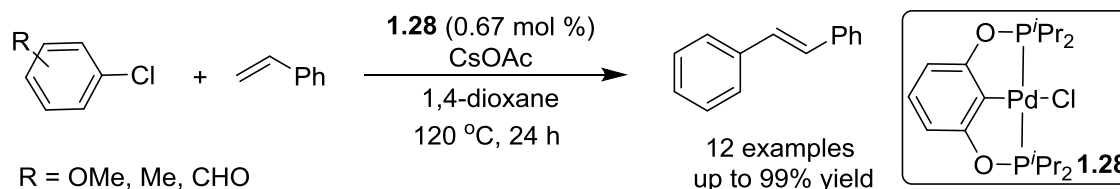
Heck reaction is synthetically most important coupling reaction. Palladium-catalyzed Heck cross-coupling reaction is basically C–C bond forming reaction between olefin and aryl halide or vinyl halide, which occurs in the presence of a base. Heck coupling reaction provides an easy access for the synthesis of various substituted alkenes and highly luminescent organic materials. This reaction also offers a convenient method for the synthesis of olefinic intermediates for pharmaceuticals, fine chemicals, and as building blocks of polymers.

The dimeric palladacycle complex $[\text{Pd}(\mu\text{-OAc})(\text{P}(\text{OPh})_2(\text{OC}_6\text{H}_4))]_2$ reported by Harmann *et al.* was employed to the various traditional cross coupling catalytic reactions like Heck coupling reaction (Scheme 1.11).⁴ The dimeric palladacycle **1.27** was found to be a good catalyst for the reaction of aryl halides with styrene in DMAc using CH_3COONa as the base at 135 °C.



Scheme 1.11 CE type palladacycle for Heck reaction.

The most challenging coupling partner for Heck reaction, such as aryl bromide and aryl chloride can be coupled with olefin by using pincer palladium complex (Scheme 1.12). Jensen and co-worker have reported coupling reaction of most challenging aryl chloride with olefin employing five-membered phosphinito palladium complex **1.28** in good yields.¹⁵ Similarly Milstein described the pincer palladium catalyzed Heck reaction of aryl iodide with methyl acrylate with high turnover numbers.³¹ In addition to these reports, there are many examples on pincer palladium catalyzed Heck reaction using various aryl halides and pseudo halides coupling partners.



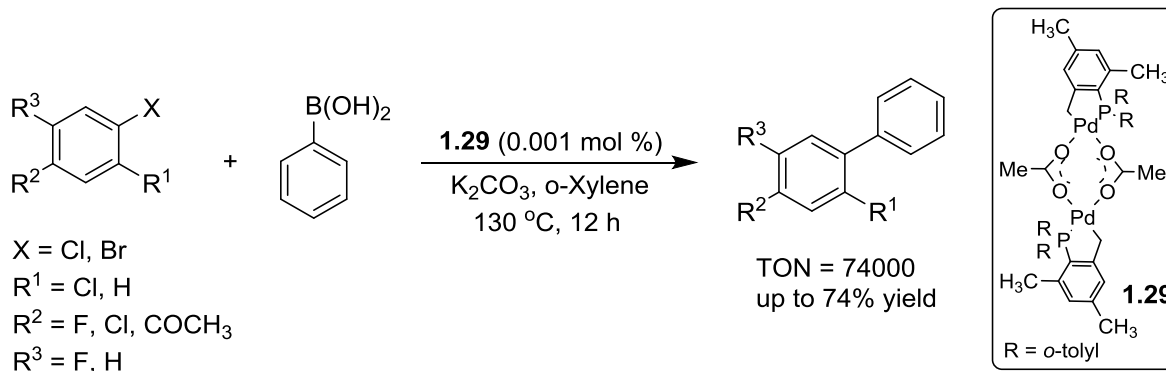
Scheme 1.12 Heck coupling reaction using palladium complex.

1.3.1.2 Palladacycle in Suzuki-Miyaura Coupling Reaction

The Suzuki-Miyaura coupling is one of the most important carbon-carbon bond forming reactions. It involves the coupling of aryl boronic acid with aryl halide under basic condition.¹⁰⁷ An important difference between the Heck-coupling and Suzuki-coupling is the transmetalation of the organoboronate species with a Pd(II) species in the Suzuki coupling, without redox reaction.¹⁰⁷

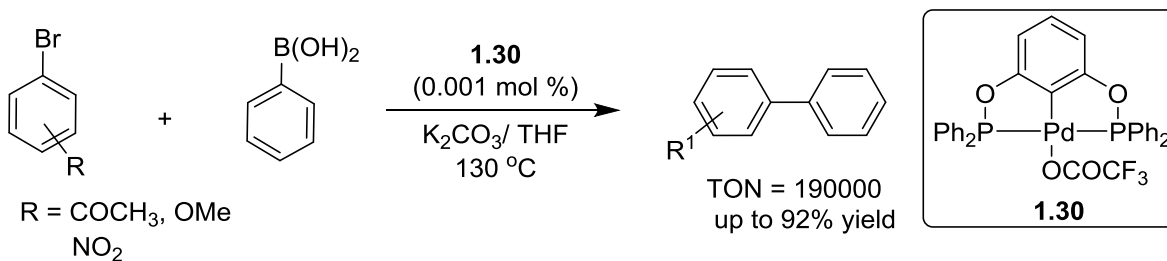
Beller *et al.* synthesized the new palladacycle complex that could be used successfully for the Suzuki reaction. The coupling of an aryl halide and phenyl boronic acid was achieved using

palladacycle catalyst **1.29** in the presence of K_2CO_3 in *o*-xylene (Scheme 1.13).¹⁰⁸ This catalytic system shows a high yield of product and TON up to 74000 was achieved using only 0.001 mol % of the catalyst. Phospha-palladacycle acetate dimer complexes were shown better activity compared to the traditional triphenyl phosphane palladium complexes $[Pd(PR_3)_n]$ for the Suzuki reaction.



Scheme 1.13 CE-type palladacycle in Suzuki-Miyaura coupling reactions.

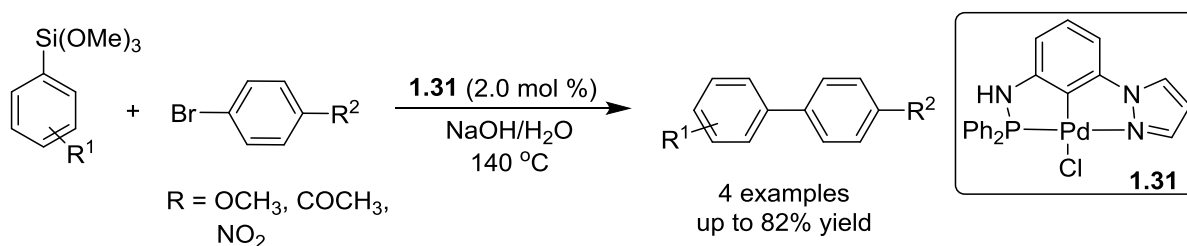
The PCP-palladium complex **1.30** was used for the cross-coupling reaction of aryl bromide with boronic acid by Welch and co-workers (Scheme 1.14).³² In this, the efficient cross-coupling of aryl boronic acid with aryl bromide was carried out by the pincer palladium complex, which resulted in turnover numbers (TON) of 190000. The reaction tolerated various functional groups like $-COCH_3$, $-NO_2$, $-OCH_3$.



Scheme 1.14 Suzuki coupling reaction using (POCOP)Pd complex.

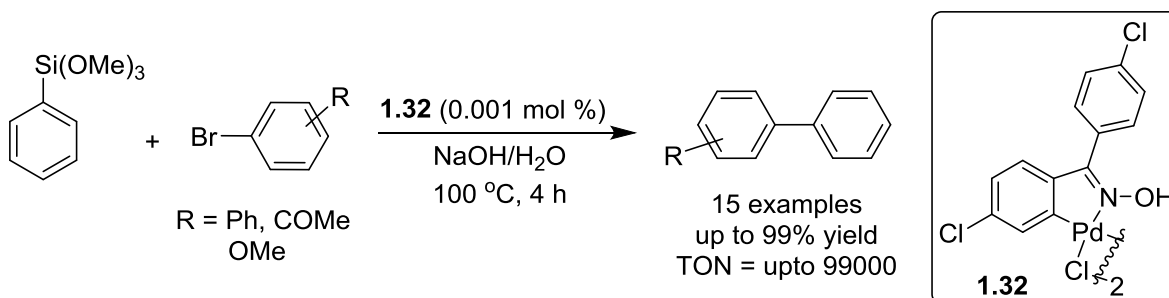
1.3.1.3 Hiyama Coupling Reaction

Hiyama coupling reaction is the cross-coupling reaction of the organosilane with an aryl halide where fluoride ions are used as a promoter. Sanmartin and Domínguez have reported the first example of Hiyama coupling reaction of the organosilane with aryl bromide using unsymmetrical palladacycle complex **1.31** to produce the corresponding coupled product (Scheme 1.15).¹⁰⁰ The coupling reaction was carried out in water, and the aq. NaOH played the role of an activator. However, the status of the catalyst was not clear in this transformation.



Scheme 1.15 Unsymmetrical palladacycle complex for Hiyama cross-coupling.

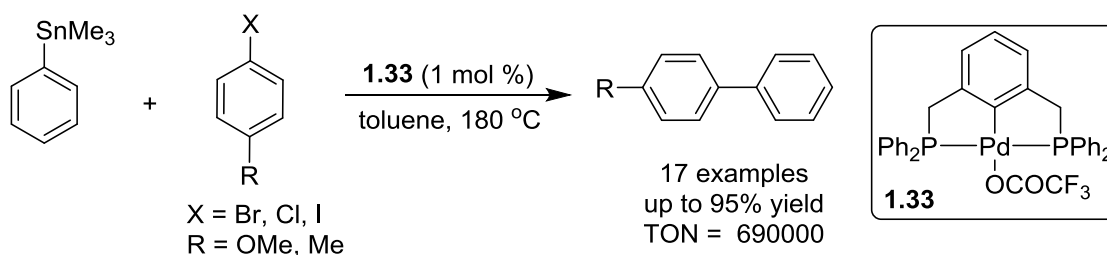
In 2006, Nájera and co-worker reported the first fluoride-free Hiyama coupling using oxime-palladacycle as a catalyst (Scheme 1.16).¹⁰⁹ The oxime-palladacycle **1.32** was shown to be very efficient catalyst that afforded the coupled product with as high as 9900 TON. In another example they have demonstrated the coupling of bromo/chloroaryl with vinylsiloxanes, where TBAB (0.5–1.0 equiv) was used as an additive and the reaction required high loading 0.1–1.5 mol % of a palladium catalyst. They have shown that the isolated palladacycle catalyst was more effective than simple palladium precursors, such as PdCl_2 and Pd(OAc)_2 .



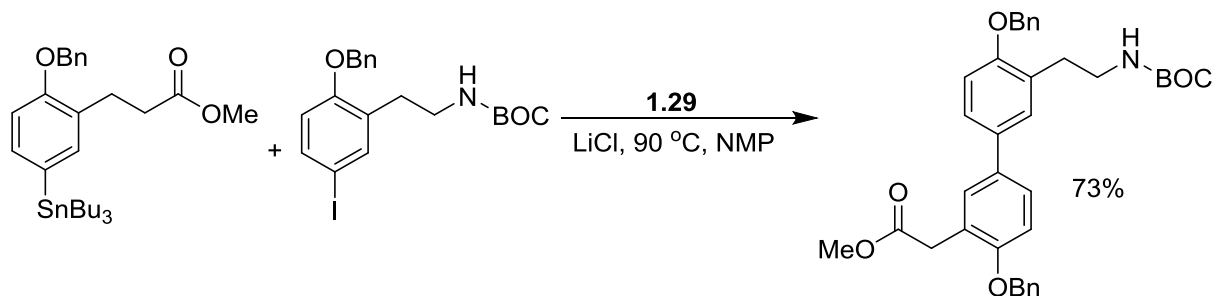
Scheme 1.16 Hiyama cross-coupling reaction using palladacycle complex.

1.3.1.4 Stille Coupling Reaction

Wendt group reported the cross-coupling reaction of the organotin reagent with a C(sp²) aromatic halide using palladacycle catalyst. They have described that the PCP palladacycle complex **1.33** catalyzes the coupling of aryl tin with aryl bromide (Scheme 1.17).¹⁰³ The process was very efficient to produce the coupled product with low catalyst loading and resulted with high TON's. In 2003, Paintner and co-worker synthesized biphenyl analogs in excellent yield using Herrmann-Beller palladacycle catalyst **1.29** *via* Stille coupling reaction (Scheme 1.18).¹¹⁰ This biphenyl precursor can be used to generate biphenomycin antibiotics.



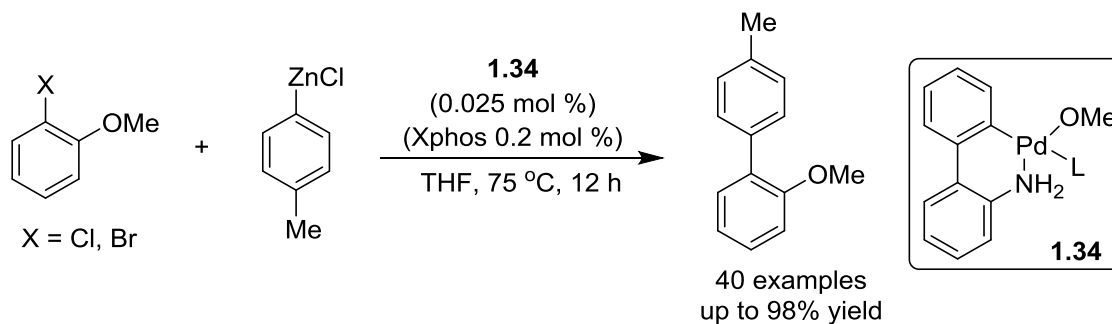
Scheme 1.17 Stille reaction using PCP pincer complex.



Scheme 1.18 Biphenyl analog precursors to biphenomycin antibiotics.

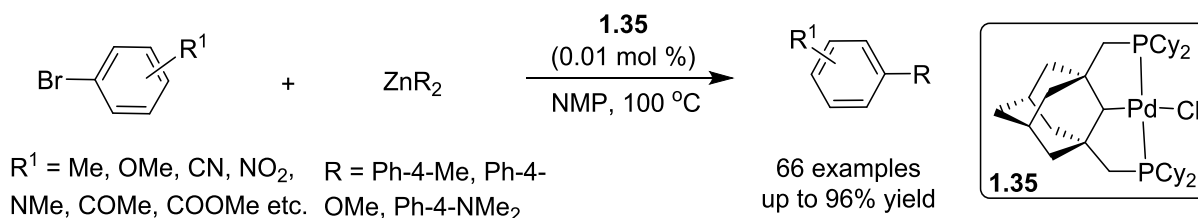
1.3.1.5 Negishi Coupling Reaction

In addition to all coupling reactions discussed, the Negishi coupling is also a synthetically important coupling reaction. In 2013, Buchwald developed the CE-type palladacycle **1.34** for the Negishi coupling reaction, which worked efficiently at ambient temperature and with low catalyst loadings. Numerous heteroaryl coupling partners, which were previously unsuccessful substrates, could be coupled successfully. In addition, they have successfully used the polyfluoroaryl zinc reagents for Negishi coupling (Scheme 1.19).¹¹¹



Scheme 1.19 Negishi coupling reaction using palladacycle complex.

Frech *et al.* developed an aliphatic phosphine based PCP-palladacycle complex **1.35** for the Negishi reaction. In this reaction, the coupled products of activated and non-activated, electronically diverse, sterically challenging and functionalized aryl bromides with diaryl zinc were successfully obtained (Scheme 1.20).¹⁰⁶ After the completion of reaction, the catalysis was continued by adding more of substrates and catalyst remained active and afforded the coupled product without a decrease in catalytic activity. The authors have demonstrated that the palladium nanoparticles were unlikely the active catalysts.

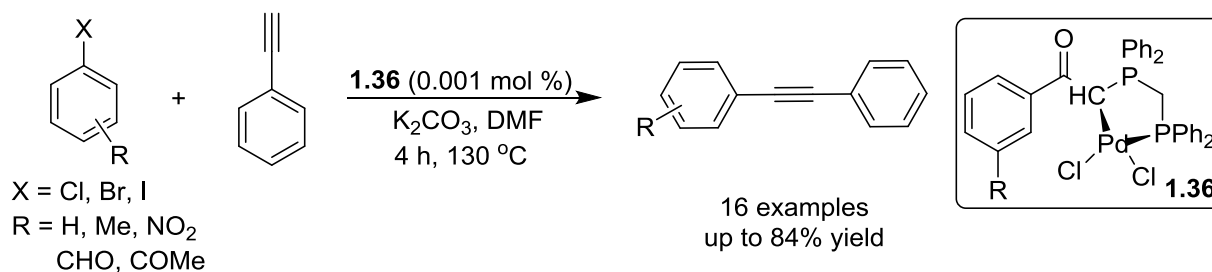


Scheme 1.20 Cross-coupling reaction aryl bromide with aryl zinc using pincer complex.

1.3.1.6 Sonogashira Coupling Reaction

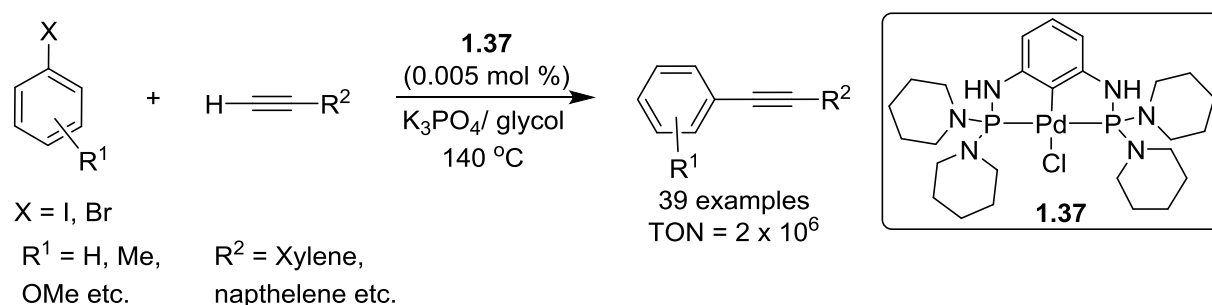
Palladium-catalyzed coupling of alkynes with aryl halides in the presence of a copper reagent is a powerful tool in organic synthesis.^{112,113} Sonogashira coupling has been applied successfully to numerous important synthetic areas such as natural product and drug synthesis, materials science and biologically important products. Sabounchei *et al.* in 2013 described the Sonogashira cross-coupling reactions by exploiting moisture and air-stable, robust phosphine-ylide palladacycle complex **1.36**.¹¹⁴ This methodology is very significant since it is additive- and amine-free reaction. With this methodology various substituted aryl halides were coupled with

phenylacetylene profitably under air, with very low catalyst loading and the corresponding cross-coupled products were obtained in good to excellent yields (Scheme 1.21).



Scheme 1.21 Phospha palladacycle catalyzed homogeneous Sonogashira reaction.

Frech and co-workers have developed aminophosphine based palladacycle catalyst **1.37** for the coupling of phenyl acetylene with aryl iodide to obtain aryl-alkyne coupled products (Scheme 1.22).⁹⁴ This reaction provided excellent TON (2×10^6) and a quantitative yield without a copper co-catalyst. The coupling reaction shows negative mercury drop test. Ambiguity was expressed regarding the status of the PCP-Palladium catalyst **1.37** in the reaction. Similarly, Gu and Chen have demonstrated that carbene based palladacycle catalysts efficiently performs Sonogashira cross-coupling reactions without the use of copper.



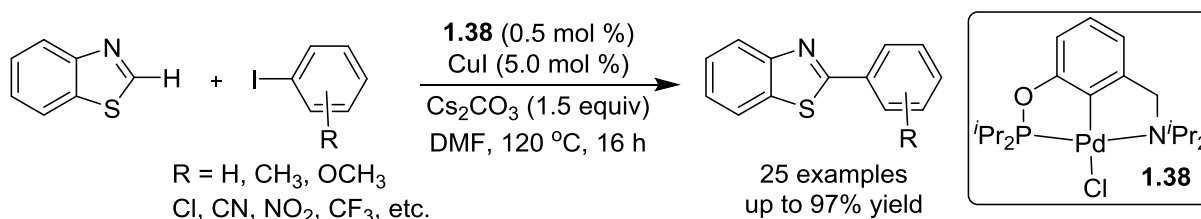
Scheme 1.22 Aryl halide and terminal alkynes coupling using PCP palladacycle complex.

1.3.2 Palladacycle Complexes in C–H Functionalization

Among the recent methodological advancement, transition metal catalyzed C–H functionalization has made shift from the classical methods of organic synthesis. The recent advancements in organometallic chemistry have made it possible to achieve site-selective C–H functionalization. Palladium has been used vigorously in C–H bond functionalization and has

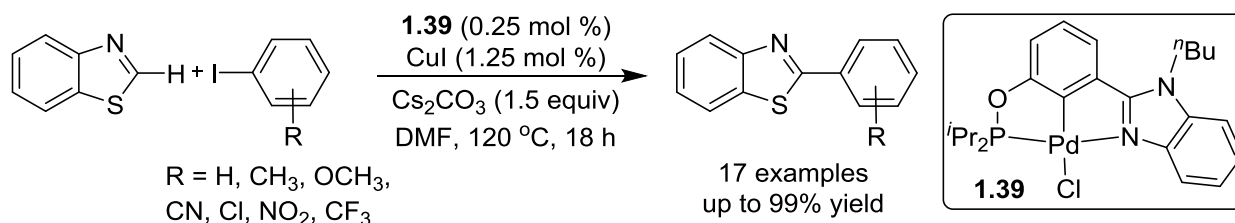
shown great reactivity in organic transformation.¹¹⁵⁻¹³¹ In that context, the arylation of azoles have attracted particular attention as they are fundamental unit of many naturally occurring compounds as well as pharmaceutical products.¹³²⁻¹³⁵

In 2014, Punji and co-workers have developed POCN-ligated palladium complex **1.38** for the direct C–H bond arylation of azoles with aryl iodides (Scheme 1.23).¹³⁶ Various heteroarenes such as benzothiazole, substituted-benzoxazoles, and 5-aryl oxazoles were arylated successfully with the diverse aryl iodides in the presence of CuI co-catalyst. The kinetic studies of isolated intermediate and Hammett plot experiments gave the preliminary insight into the mechanism of the reaction. The reaction followed a Pd(II)-Pd(IV)-Pd(II) catalytic pathway and showed that complex itself works as catalyst and palladium nanoparticles are less likely the active catalyst.



Scheme 1.23 Arylation of azole using palladacycle catalyst.

Recently, Wang and co-worker developed a new POCN-palladacycle catalyst **1.39** with (phosphinito)aryl benzimidazole ligand. The complex was synthesized by one-pot phosphorylation/palladation reaction of a (2-benzimidazolyl)-containing *m*-phenol derivative. They could able to reduce the loading of palladium catalyst and co-catalyst (CuI) for the catalytic transformation (Scheme 1.24).¹³⁷



Scheme 1.24 Arylation of azole using palladacycle catalyst.

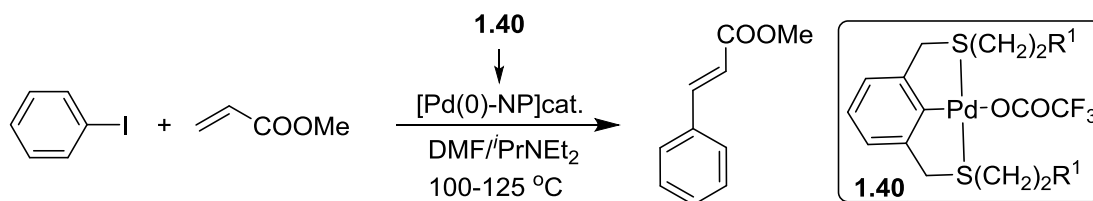
1.4 Mechanistic Aspect of Palladacycle-Catalyzed Cross-Coupling Reactions

The mechanistic pathway of the palladacycle catalyzed cross-coupling reaction is well studied. Many palladacycle catalyzed reactions are assumed to proceed through nanoparticles, though the actual role of the palladium complex is dubious. Many previous reports demonstrate that the palladacycles are the active catalyst, directly involved in the catalysis. In cross-coupling reactions, palladium undergoes redox process and proceeds *via* Pd(II)/Pd(IV) pathway.^{58, 67,74,77,89,138-140} In contrast, many studies demonstrated that the palladacycle complexes decompose to Pd(0) under the harsh conditions and the catalytic activity is exhibited from the palladium(0), such as Pd(0) nanoparticles or colloidal palladium.^{33,64,92,141-145} In such case, the palladacycle complex act as a precatalyst, and releases the palladium(0) nanoparticles or homogeneous palladium(0) that act as the catalyst. There are various methods known to detect the formation of palladium(0) nanoparticles.^{64, 92, 93,142,144,145}

1.4.1 Mechanism of Heck Reaction:

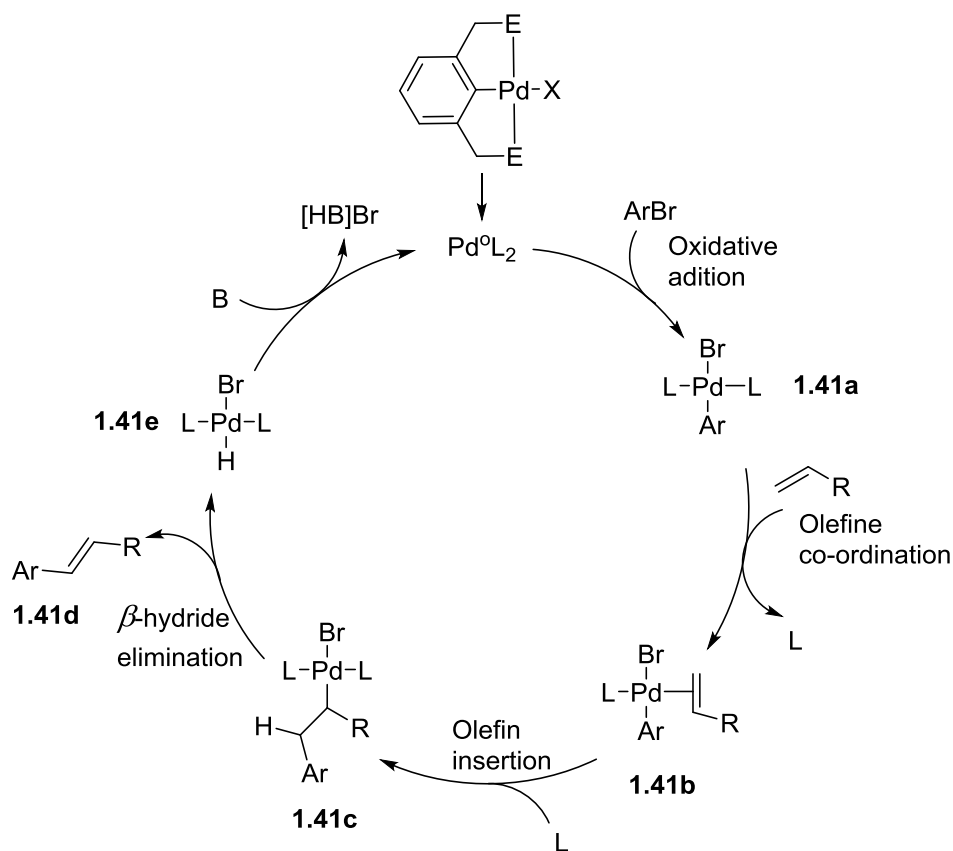
1.4.1.1 Pd(0)/Pd(II) Redox Process

Since the discovery of Heck reaction in 1971, it has become one of the standard methods of organic synthesis. There are many examples on the traditional coupling reaction which is catalyzed by the palladacycle complexes with high yield. Many reports suggest that the palladacycle complexes decompose to form Pd(0) nanoparticles or clusters upon Pd–C bond cleavage of the pincer palladium system. Hence, Pd(0) species don't have a ligand backbone. The nanoparticle catalyzed the cross-coupling reaction following the Pd(0)/Pd(II) mechanistic pathway. Jones and co-workers independently carried out several experimental studies for the mechanistic pathway of the reaction.^{33,143,144} They observed that palladium(0) nanoparticles generated from the palladacycle complex in the reaction are the actual catalyst. For example, Gladysz *et al.* have demonstrated that the cross-coupling of phenyl iodide and methyl acrylate does not catalyze directly by fluorine pincer complex **1.40**, but by the dispenses Pd(0) nanoparticles (Scheme 1.25).⁶⁴



Scheme 1.25 Heck reaction using pincer palladium complex **1.40** as dispenser of Pd(0) nanoparticles (R^1 represents polyfluorinated chain).

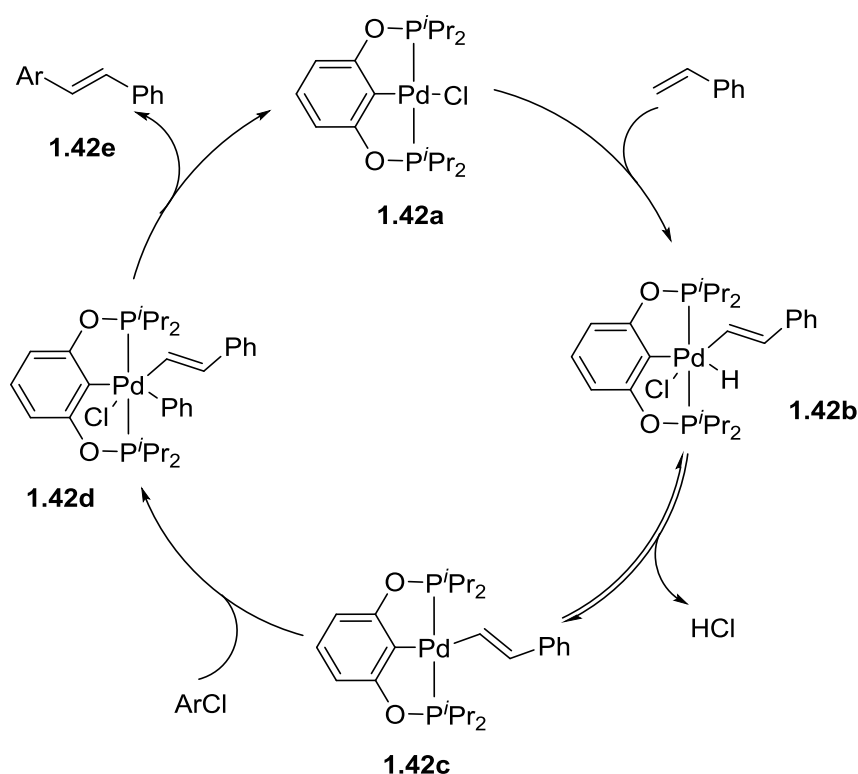
The schematic diagram of the classical catalytic cycle of Heck cross-coupling which is initiated by the oxidative addition of organohalide to the palladium(0) catalyst, released from palladacycle complex, is shown in Scheme 1.26. The first step is the oxidative addition of aryl halide to Pd(0) to form Pd(II) complex **1.41a**. In the second step, the ligand dissociation and olefin coordination gives intermediate **1.41b**, which undergoes insertion of the olefin into Pd–Ar bond to afford η^1 -alkyl-Pd complex **1.41c**. The β -hydride elimination from **1.41c** generates the coupled product **1.41d** and hydrido palladium complex **1.41e**. The complex **1.41e** upon deprotonation with base produces the Pd(0) catalyst.



Scheme 1.26 Pd(0) nanoparticle catalyzed Heck reaction.

1.4.1.2 Pd(II)/Pd(IV) Redox Process

Though some reports demonstrate the palladacycle catalyzed cross coupling proceed *via* Pd(0)/Pd(II) pathway, many others have suggested the mechanism *via* a Pd(II)/Pd(IV) process. For example, Jenson has reported Heck reaction catalyzed by ECE-type palladacycle complex, in which reaction proceeds through Pd(II)/Pd(IV) cycle (Scheme 1.27).¹⁵ This catalytic cycle starts with the oxidative addition of a vinyl C–H bond of the alkene over palladium catalyst **1.42a** to generate Pd(IV) species **1.42b**, followed by the reductive elimination of HCl to give **1.42c**. Species **1.42c** undergoes oxidative addition with aryl halide to form species **1.42d**, which undergoes reductive elimination of product **1.42e** and regenerate the pincer catalyst **1.42a**.

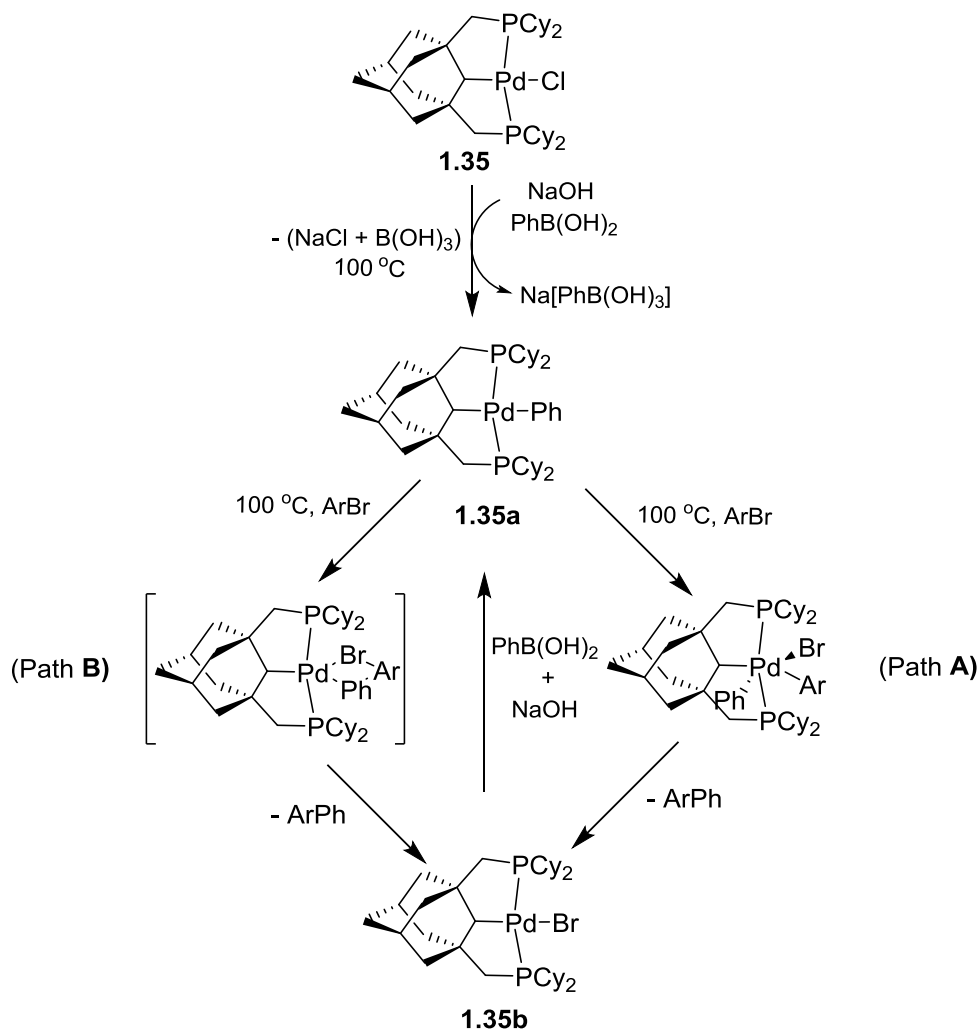


Scheme 1.27 Pd(II) ECE-palladacycle catalyzed Heck reaction.

1.4.2 Mechanistic Pathway for Suzuki-Miyaura Cross-Coupling Reaction

Frech and co-workers reported Suzuki coupling reaction of aryl boronic acid with aryl halides using PCP-palladacycle complex **1.35** (Scheme 1.28).¹⁴⁶ They have proposed a catalytic cycle, wherein the first step is the formation of the complex **1.35a** from the reaction of **1.35** with phenylboronic acid and NaOH. The hydroxide ion activates the phenylboronic acid that

promotes phenyl group transfer to the palladium center. Further, oxidative addition of aryl bromide to **1.35a** produced a neutral hexacoordinated pincer Pd(IV) species $[\text{Pd}(\text{Ar})(\text{Br})(\text{Ph})]$. The hexacoordinated Pd(IV) species gives back Pd(II) active catalyst upon reductive elimination of the coupled product (Scheme 1.28; path A). Alternately, the direct biaryl product formation at the Pd(II) center through a four-centered transition state has been proposed (Scheme 1.28; path B).



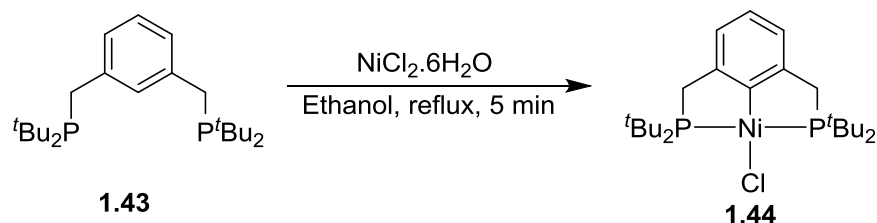
Scheme 1.28 ECE-palladacycle catalyzed Suzuki reaction.

1.5 General Method for the Synthesis of Pincer Nickel Complexes

1.5.1 C–H Bond Activation Approach

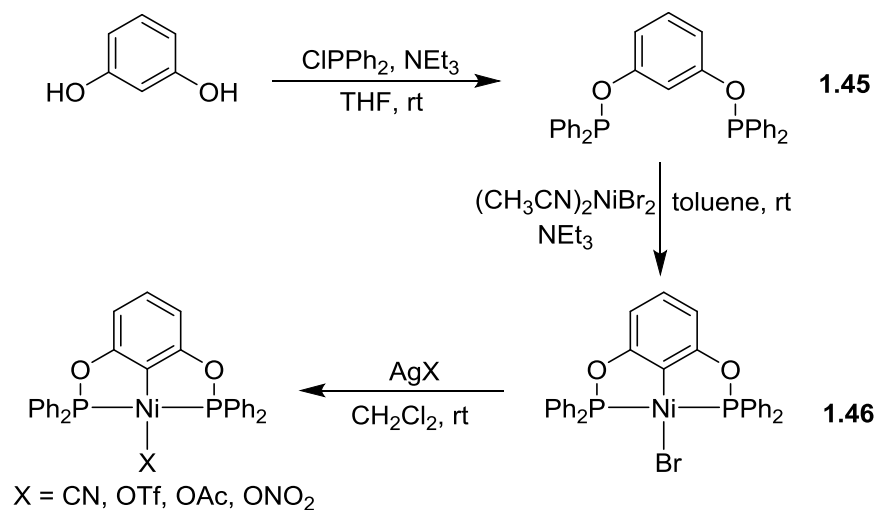
In 1976, the first pincer complex was synthesized by Shaw and co-workers, which is the best example that could be considered under the C–H activation approach (Scheme 1.29).¹⁴⁷ The

new diphosphine ligand was prepared in good yield by reacting di^tbutylphosphine with 1,3-bis(dibromomethyl)benzene in the presence of sodium acetate base. The ^tBu⁴PCP-ligand (**1.43**) upon reaction with Ni(II) chloride hexahydrate in ethanol under reflux conditions resulted in the PCP-nickel complex [(^tBu⁴PCP)NiCl] **1.44** via C–H bond activation. This complex was purified by sublimation under vacuum at very high temperature without any apparent decomposition.



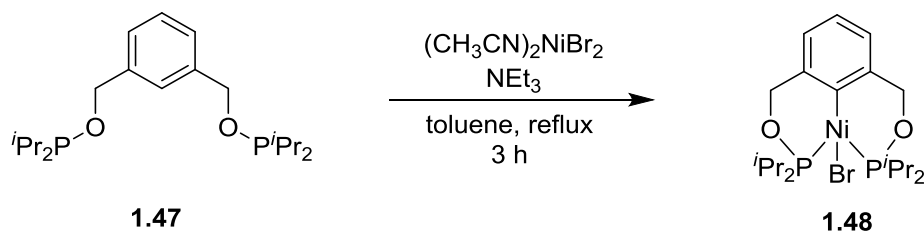
Scheme 1.29 Synthesis of PCP pincer nickel complex through C–H bond activation.

Zargarian group in 2011 synthesized the POCOP-ligand **1.45** and pincer nickel complexes (Scheme 1.30).¹⁴⁸ The POCOP ligand **1.45** was synthesized from resorcinol by treatment with ClPPh₂ in the presence of Et₃N. The POCOP ligand further on reaction with (CH₃CN)₂NiBr₂ resulted in the formation of pincer nickel complex **1.46**. The complex **1.46** was treated with AgX (X = CN, OTf, OAc, ONO₂) to develop many derivatives of pincer nickel complexes.



Scheme 1.30 Synthesis of bis-phosphinite POCOP-pincer nickel complexes.

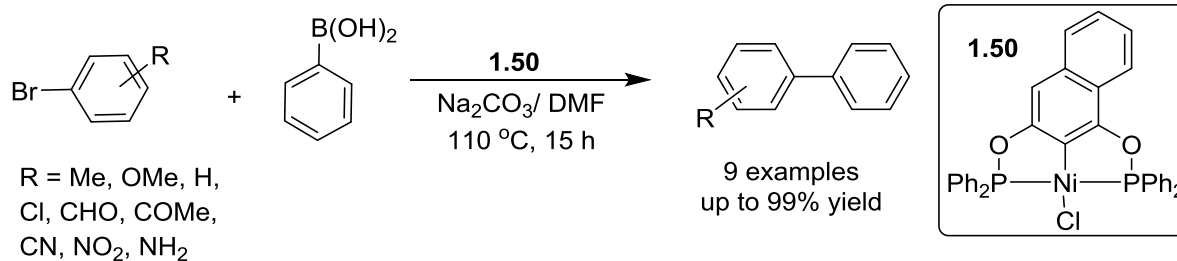
Punji group synthesized ($i\text{Pr}^4\text{POCCOP}$)NiBr complex *via* C–H bond activation (Scheme 1.31).¹⁴⁹ The $i\text{Pr}^4\text{POCCOP-H}$ ligand **1.47** was treated with $(\text{CH}_3\text{CN})_2\text{NiBr}_2$ nickel precursor in the presence of triethylamine to afford the pincer complex **1.48** *via* C(2)–H bond activation on the ligand (**1.47**). The acetate and triflate derivatives of the nickel complex were synthesized by the reaction of complex **1.48** with AgOAc and AgOTf, respectively in quantitative yields.



Scheme 1.31 Synthesis of bis-phosphinite POCOP-pincer nickel complexes.

1.5.2 Transmetalation Approach

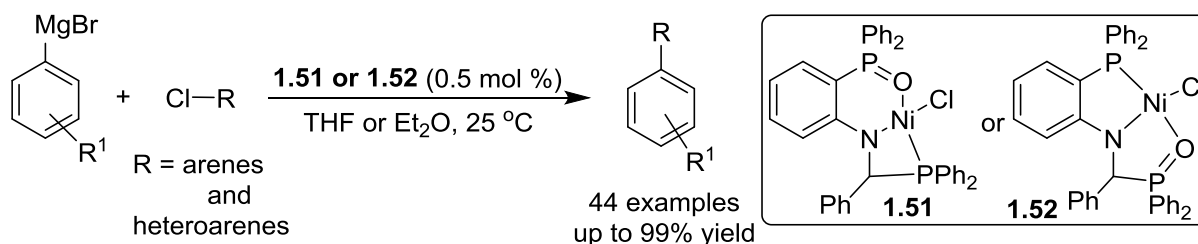
Transmetalation reaction involves the transfer of ligands from one metal to another. This methodology is useful for the synthesis of complexes whose synthesis is difficult *via* C–H activation or oxidative addition approach. Organolithium reagents are used very frequently as a transmetallating agent. Hu group synthesized NNN-pincer nickel complex by the transmetalation approach.¹⁵⁰ The complex was synthesized in three steps starting from 2-bromo-*N,N*-dimethylaniline and 2-amino-*N,N*-dimethylaniline. The first step involved the Pd(0)/dppf catalyzed C–N coupling reaction. In the second step, the C–N coupled product **1.49a** was treated with *n*-BuLi to obtain a lithiated NNN-cluster type compound **1.49b**. The final step involved the nickelation of lithiated NNN-cluster with the (dme)NiCl₂ metal precursor *via* transmetalation to give complex **1.49c** (Scheme 1.32).



Scheme 1.33 Suzuki-Miyaura coupling reaction by nickel.

1.6.1.2 Kumada Coupling Reaction

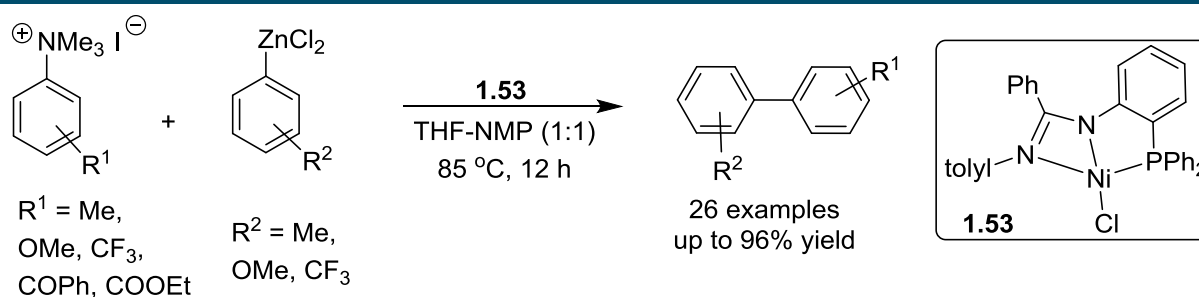
Wang and co-workers synthesized the PNO-pincer nickel complexes **1.51** and **1.52**, which showed application in the Kumada coupling reaction of (hetero)aryl/alkenyl chlorides with aryl magnesium bromides (aryl Grignard reagents) (Scheme 1.34).¹⁵³ The reactions were conducted at room temperature and tolerated various functional groups on aryl chlorides in the presence of LiCl or ZnCl₂ additives.



Scheme 1.34 Nickel catalyzed Kumada coupling reaction.

1.6.1.3 Negishi Coupling Reaction

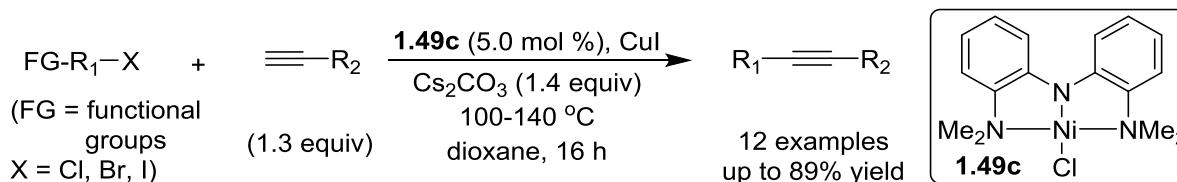
In 2012, Wang and co-workers reported the synthesis of PNN-pincer nickel complex **1.53** and employed in the Negishi coupling reaction of aryltrimethylammonium iodides with (hetero)arylzinc chlorides (Scheme 1.35).¹⁵⁴ This reaction displayed a broad substrate scope with low catalyst loading. Further, reaction proved the potential of PNN-pincer nickel catalyst system for the C–N bond activation of aryltrimethylammonium salts.



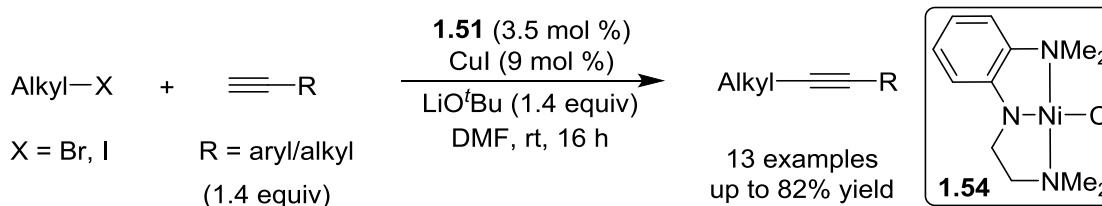
Scheme 1.35 Nickel catalyzed Negishi reaction.

1.6.1.4 Sonogashira Coupling Reaction

The nickamine catalyst **1.49c** synthesized by Hu was successfully employed in Sonogashira coupling reaction of nonactivated alkyl halides with terminal alkynes (Scheme 1.36). In 2015, Hu *et al.* synthesized a new NNN-pincer nickel complex **1.54** (Scheme 1.37).¹⁵⁵ To improve the catalytic activity of nickel catalyst, newly designed complex was synthesized in a single step from 2-bromo-*N,N*-dimethylaniline and *N,N*-dimethylethylenediamine.¹⁵⁶ One of the two aryl linkers in previous catalyst **1.49c** was replaced by an ethylene linker. The new pincer complex **1.54** was expected to be more labile, which rendered the resulting complex more reactive. Complex **1.54** was employed in the Sonogashira coupling reaction, *i.e.* direct coupling of primary alkyl halides with terminal alkynes at room temperature. In this catalysis, broad substrate scope and high functional group tolerance were observed.



Scheme 1.36 Nickel catalyzed Sonogashira coupling reaction.

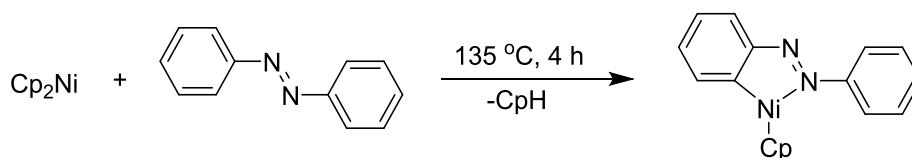


Scheme 1.37 Hemilabile nickel complex in Sonogashira coupling reaction.

1.6.2 Nickel-Catalyzed C–H Bond Activation and Functionalization

Direct C–H bond functionalization to construct C–C or C–heteroatom bond *via* transition metal catalyzed reaction is a powerful and attractive tool.¹⁵⁷⁻¹⁶⁸ Since many decades, inert C–H bond activation has been studied by using late and noble transition metal catalysts; however, their broad application is limited because of their less abundance and more cost. Compared to the 4d and 5d transition metals, 3d transition metals are in high abundance, with low cost, and unique reactivity. In addition, 3d metals are less explored in various catalytic applications. Nickel has unique activity and versatile reactivity among the first-row transition metals. Sabatier group in 1922 explained that “nickel can do all kind of work and maintain it’s activity for a long time”. The development of organo-nickel chemistry led to the discovery of several catalytic systems and many practical applications.¹⁶⁹⁻¹⁷⁴ The nickel complexes have been used in many catalytic organic transformations which contribute both in academic as well as in the industry.¹⁷⁵⁻¹⁷⁹

Kleinman and Dubeck group in 1964 reported the first nickel-mediated aromatic C–H bond activation.¹ They observed that the heating of dicyclopentadienyl nickel with an excess of diazobenzene afforded purple blue organo-nickel species (Scheme 1.38). Later, there were several publications appeared on the nickel-catalyzed C–H bond activation and functionalization.

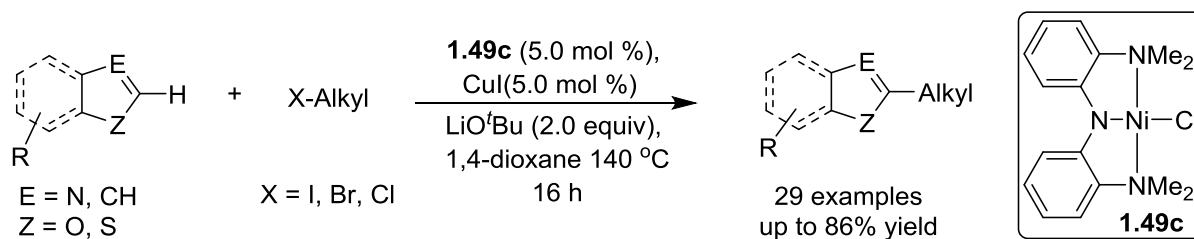


Scheme 1.38 Synthesis of organonickel species.

1.6.2.1 Alkylation of (Hetero)Arenes

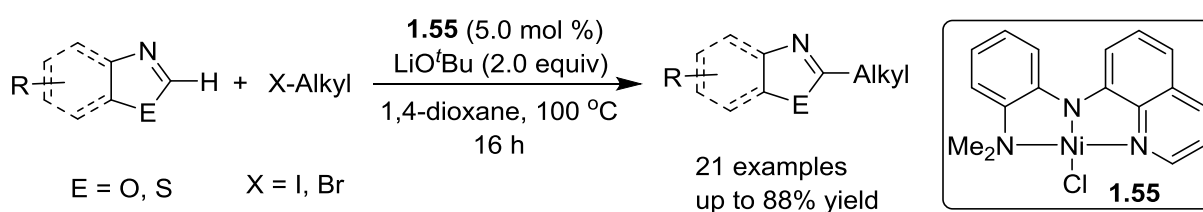
Arenes and heteroarenes alkylated compounds are important backbone of many natural products, biological compounds, and organic materials.¹⁸⁰⁻¹⁸² In 2010, Hu group reported the nickel-catalyzed C–H bond alkylation of aromatic heterocycles with unactivated alkyl halides containing the β -hydrogen (Scheme 1.39).¹⁸³ Coupling of various substituted heterocycles with diversely substituted alkyl halides was achieved using $\text{Me}_2\text{N}_2\text{N-NiCl}$ catalyst **1.49c**, CuI co-catalyst and LiO^tBu base. This methodology tolerates various functional groups, such as

methoxy and halides on oxazole and $-\text{OAr}$, $-\text{OCOAr}$, $-\text{SAr}$, $-\text{CO}$, $-\text{CN}$ groups on alkyl halide moiety, and shows excellent chemo and regioselectivity.



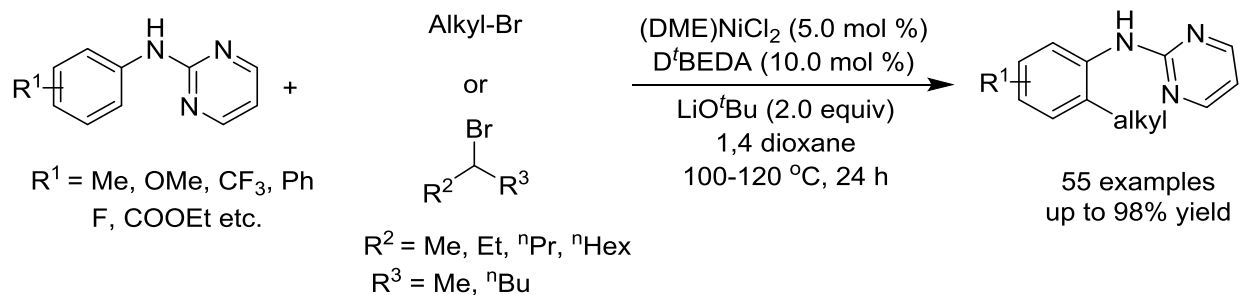
Scheme 1.39 Alkylation of aromatic heterocycle with an alkyl halide.

Punji and co-workers developed a quinolinyl-based NNN pincer nickel complex **1.55** for the direct C–H bond alkylation of challenging benzothiazole derivatives under mild reaction conditions. The coupling of azoles with alkyl halides was achieved using nickel pincer complex at 100 °C without CuI co-catalyst (Scheme 1.40).¹⁸⁴ The catalyst was recycled and reused five-times for the alkylation without affecting the catalytic activity. This catalysis showed broad substrate scope for differently substituted azoles and alkyl halides.



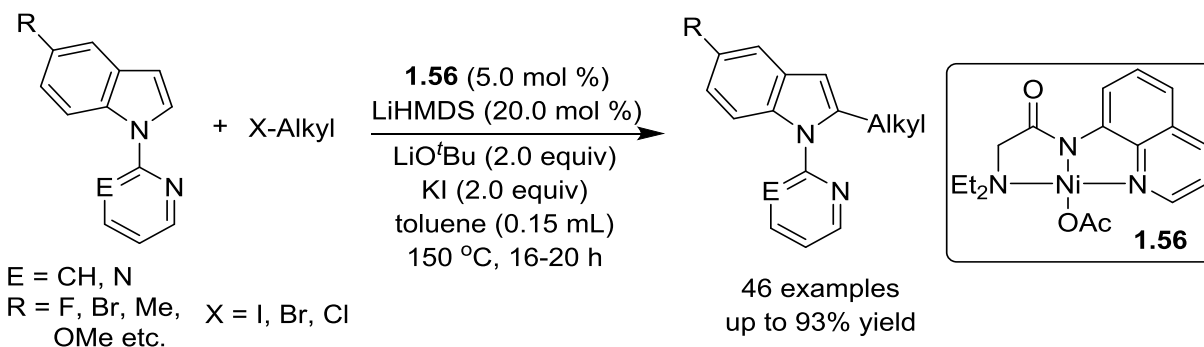
Scheme 1.40 Alkylation of azoles using $(^{\text{Q}}\text{NNN}^{\text{Me}_2})\text{Ni}$ -pincer complex.

Ackerman and co-workers developed a new methodology for *ortho* C–H alkylation of aniline with alkyl bromide using nickel catalyst *via* monodentate chelation assistance (Scheme 1.41).¹⁸⁵ Herein, the efficient cross-coupling of anilines bearing a monodentate *N*-pyrimidyl substituent with alkyl bromide can be achieved using $(\text{dme})\text{NiCl}_2/\text{D}^t\text{BEDA}$ catalyst system. Methodology provided a broad substrate scope for *o*-, *m*-, and *p*-substituted aniline. Reaction also tolerated important functional groups, such as $-\text{OMe}$, $-\text{CF}_3$, $-\text{F}$, $-\text{Cl}$, and $-\text{COOEt}$. This protocol works for both primary alkyl bromides as well as for secondary alkyl bromides.



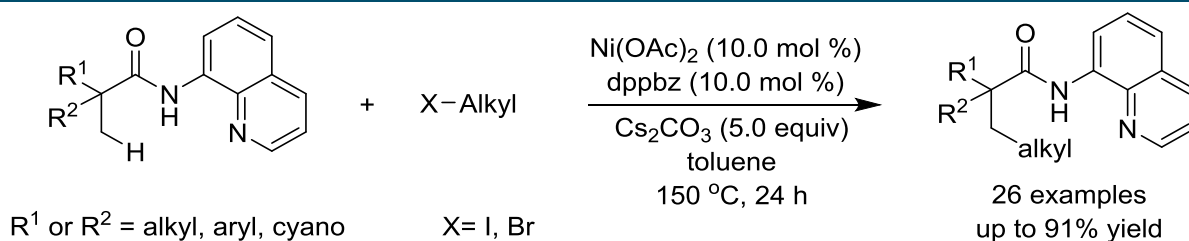
Scheme 1.41 Aniline *o*-alkylation *via* monodentate chelation assistance.

Recently, Punji and co-workers described the first example of direct C-2 alkylation of indole with alkyl halides through monodentate chelation assistance using (quinolinyl)amido-nickel catalyst **1.56**. In this methodology, the efficient coupling of indole with primary and secondary alkyl halide was achieved (Scheme 1.42).¹⁸⁶ Alkylation proceeded through C–H activation and *via* an alkyl radical intermediate. The reaction represents a good example of Ni-catalyzed monodentate-chelate-assisted C–H functionalization.



Scheme 1.42 Chelation assisted C(2)–H alkylation of indoles.

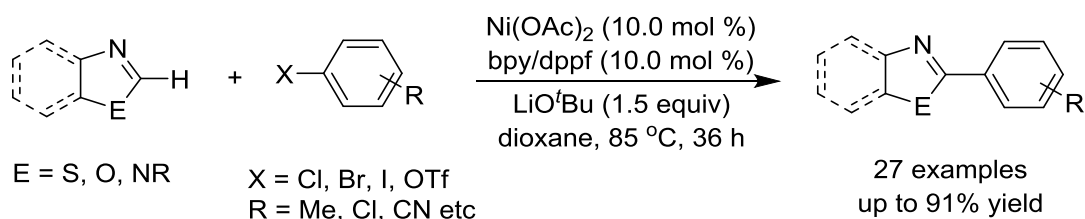
Ge *et al.* showed the direct alkylation of unactivated C(sp³)–H bond of alkyl amides with alkyl halides using nickel catalyst *via* bidentate chelation assistance (Scheme 1.43).¹⁸⁷ This method is highly selective for C–H bond alkylation of methyl group over the methylene C–H bond of the aliphatic amide. Important functional groups like alkenyl, cyano, ester, and trifluoromethyl were tolerated on aliphatic amides.



Scheme 1.43 Alkylation of $C(sp^3)$ -H bond of the aliphatic amide.

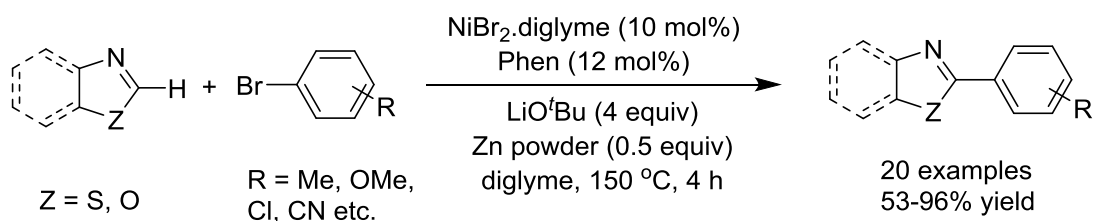
1.6.2.2 Arylation of (Hetero)Arenes

The direct C-H bond activation is more significant than the activation of C-X (X = halide or pseudohalide) bond. Especially the C-H bond arylation of heteroarenes is important because the arylated products are the fundamental unit of many naturally occurring compounds and pharmaceutical products. In 2009, the nickel-catalyzed C-H bond arylation of azoles with aryl halide was reported independently by Itami¹⁸⁸ and Miura.¹⁸⁹ Itami group described the cross-coupling of azole with aryl halides and aryl triflate using $Ni(OAc)_2/bipy$ or $Ni(OAc)_2/dppf$ catalyst in the presence of LiO^tBu (Scheme 1.44).¹⁸⁸ A number of structurally diverse heteroarenes, such as thiazoles, oxazoles, and benzimidazoles were efficiently coupled with differently substituted aryl halides.



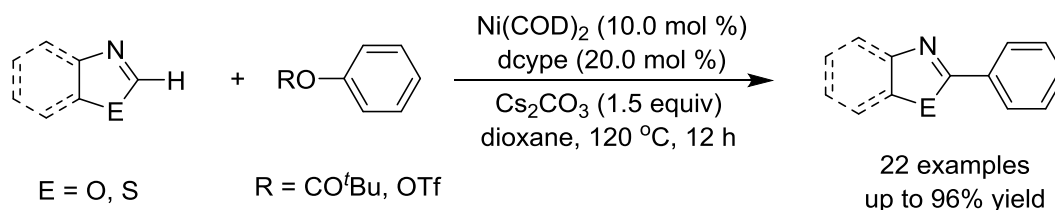
Scheme 1.44 Arylation of azoles with aryl halide or triflate.

Similarly, Miura *et al* demonstrated the arylation reaction of various azoles with aryl bromide (Scheme 1.45).¹⁸⁹ They have achieved the coupling of azoles with aryl bromide using $NiBr_2$ -diglyme/Phen catalyst system and LiO^tBu . It was observed that the use of Zn powder increases the reaction rate by reducing Ni(II) to Ni(0) active species. The reaction worked well with oxazoles and thiazoles.



Scheme 1.45 Nickel-catalyzed arylation of azoles with aryl bromide.

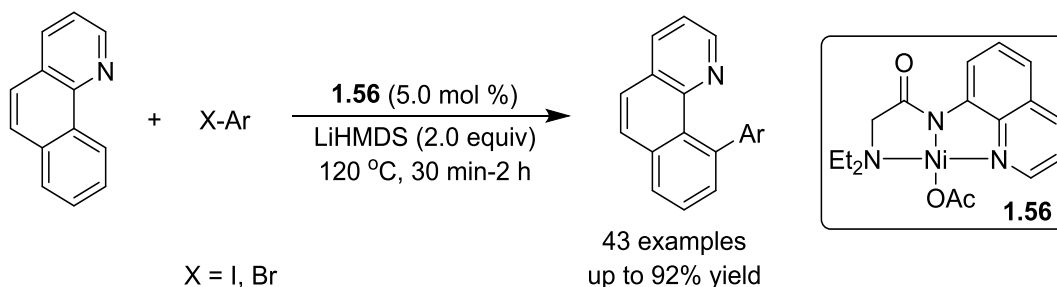
Various catalytic systems were reported for the coupling reaction of (hetero)arenes with aryl halide using nickel as a catalyst, but the use of aryl halide is still a drawback.¹⁸⁸⁻¹⁹⁰ The coupling of arenes with phenol derivatives would be more beneficial since the phenol and their derivatives are commercially available and less expensive. In 2012, Itami group demonstrated the first nickel-catalyzed Ar-H/Ar-O coupling reaction (Scheme 1.46).¹⁹¹ In this study, they have achieved the cross-coupling of variously substituted 1,3-azole and benzoxazole with phenol derivatives using $\text{Ni}(\text{COD})_2/\text{dcype}$ as a catalyst in the presence of Cs_2CO_3 . This protocol provided efficient coupling of azoles with various phenol derivatives, such as pivalates, triflates, tosylates, mesylates, carbamates, carbonates, and sulfamates, with the tolerance of functional groups $-\text{OMe}$ and $-\text{COOMe}$ on azoles.



Scheme 1.46 Ar-H/Ar-O cross-coupling reaction.

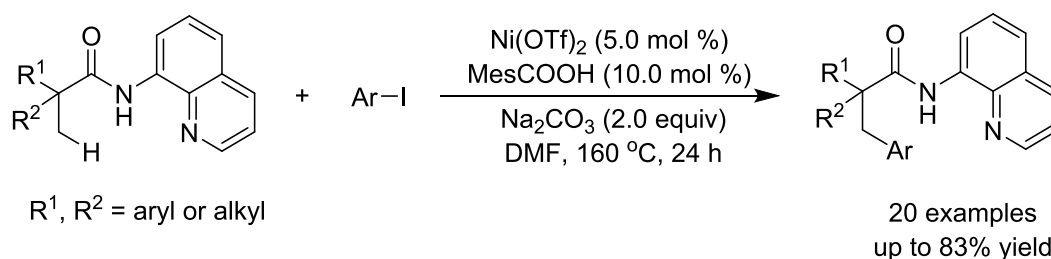
Recently, Punji and co-workers developed an efficient solvent-free method for the arylation of arenes and indoles using nickel catalyst **1.56** through the chelation assistance (Scheme 1.47).¹⁹² In this case, efficient coupling of benzo[*H*]quinoline with aryl halide was achieved using a quinolinyl based pincer nickel complex in neat condition. This methodology also worked for the arylation of indole and phenyl pyridine derivatives. This method provided a broad substrate scope for the arylation of arenes/heteroarenes with the tolerance of different

functional groups. Methodology is highly selective for monoarylation for phenyl pyridine derivatives.



Scheme 1.47 C(sp²)-H bond arylation of benzo[*H*]quinolone.

A wide variety of catalytic systems were developed for the C(sp²)-H bond arylation of arenes and heteroarenes, but the C(sp³)-H bond arylation remained challenging. In 2014, Chatani *et al.* developed the nickel-catalyzed arylation of unactivated C(sp³)-H bond in aliphatic amide using bidentate chelation assistance (Scheme 1.48).¹⁹³ The arylation of aliphatic amide containing 8-aminoquinoline as directing group with various aryl iodide was achieved using Ni(OTf)₂ as a catalyst. This reaction is highly selective for the methyl group arylation, and the methylene and benzene C-H bond remain unreacted.

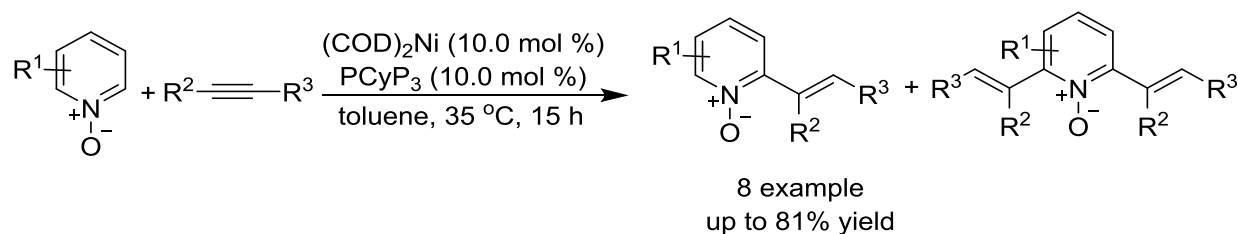


Scheme 1.48 C(sp³)-H bond arylation of aliphatic amides.

1.6.2.3 Alkenylation of (Hetero)Arenes

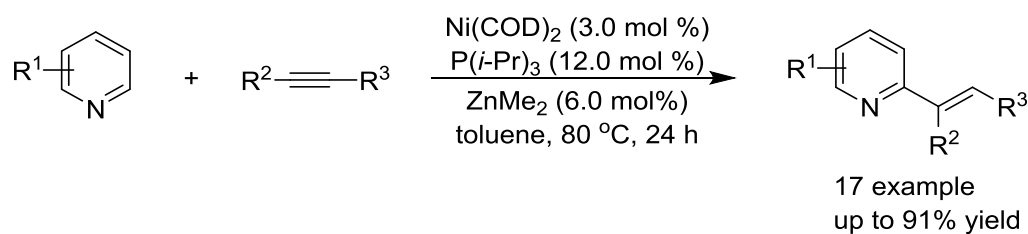
In 2007, Hiyama reported the direct C-H bond coupling of pyridine-*N*-oxide across various alkyne using nickel as a catalyst (Scheme 1.49).¹⁹⁴ Reaction was chemoselective and occurred particularly at the C-2 position of the pyridine-*N*-oxide through C-H bond activation under mild reaction condition. The coupling of substituted pyridine-*N*-oxide to symmetrical alkynes affords

good yield of the product. Also, the E-selectivity for the product can be obtained by using unsymmetrical alkynes as the coupling partner.



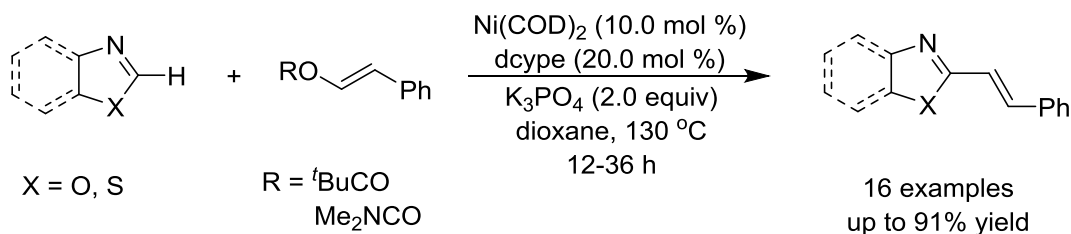
Scheme 1.49 Addition of pyridine-*N*-oxide to alkyne.

Hiyama and co-workers also reported C(2)-selective alkenylation of pyridine, which is difficult to undergo C–H functionalization.¹⁹⁵ They observed that the coupling of pyridine with alkyne produced an excellent yield of coupled product using nickel and a Lewis acid catalyst (LA) (Scheme 1.50).¹⁹⁶ It was assumed that the pyridine is activated by the coordination of pyridine nitrogen to a Lewis acid catalyst. The combination of nickel and Lewis acid catalyst gave selective C(2)–H alkenylated product in good yield. This methodology provided a wide range of alkenylated pyridines in chemo-, regio-, and stereoselective manner under the mild reaction conditions.



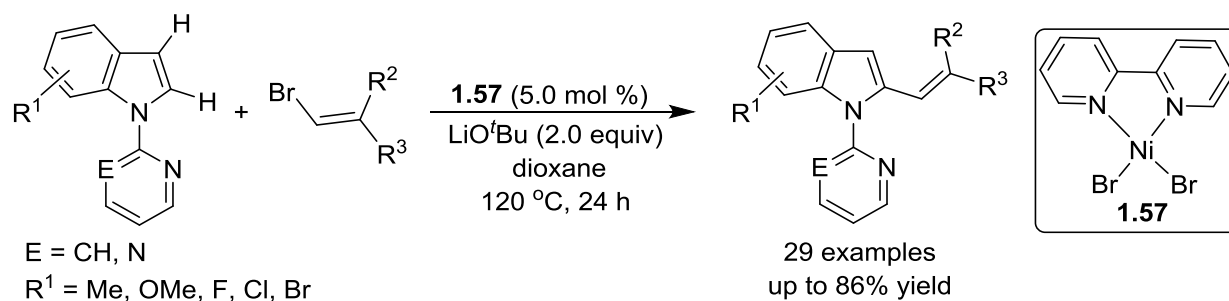
Scheme 1.50 Direct C(2)–H alkenylation of pyridine.

In 2013 Itami group demonstrated an unprecedented C–H/C–O alkenylations of heteroarenes with a Ni/dcype catalyst system using enol derivatives and α , β -unsaturated esters as alkenylating agents (Scheme 1.51).¹⁹⁷ This protocol provided a wide substrate scope for the alkenylated product. The reaction tolerated both oxazoles and azoles efficiently.



Scheme 1.51 C–H/C–O alkenylation of azoles.

Punji and co-worker recently reported the chelate assisted C-2 alkenylation of indole and related heteroarenes with alkenyl bromides using well-defined nickel catalyst **1.57** under relatively mild condition. The reaction was performed with (bpy)NiBr₂ catalyst and LiO^tBu base (Scheme 1.52).¹⁹⁸ The reaction allowed the coupling of indole derivatives with various alkenyl bromides, such as aromatic, heteroaromatics, α - and β -substituted as well as exo- and endo-cyclic alkenyl compounds.

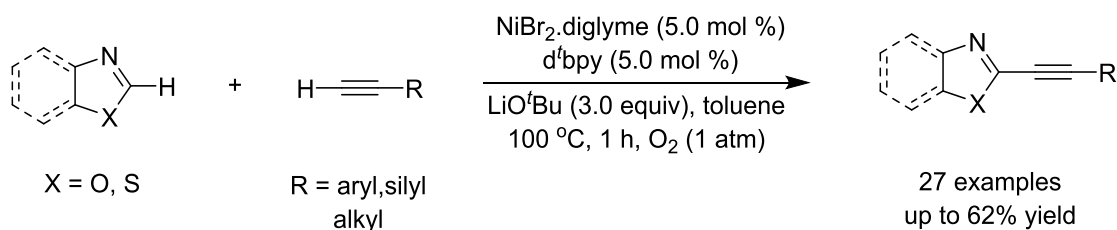


Scheme 1.52 C(2)–H alkenylation of indole .

1.6.2.4 Alkynylation of (Hetero)Arenes

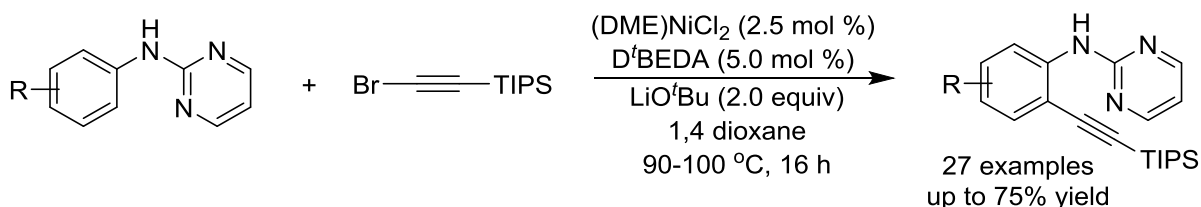
The alkynylated heteroarenes are the most fundamental and important composition of many natural products, materials, and pharmaceutical compounds.^{199,200} Various nickel catalysts were developed for the direct C(sp²)–H arylation and alkenylation reactions; however, only a few systems were reported for the C(sp²)–H alkynylation of arenes and heteroarenes using nickel catalyst.^{201–204} Miura group reported the nickel-catalyzed direct coupling of azoles and alkynes through double C–H bond activation, which is a highly challenging task due to the difficulties of catalyst control in activation of two different C–H bonds (Scheme 1.53).²⁰¹ Various azoles were coupled with alkynes in the presence of NiBr₂.diglyme/d^tbpy and LiO^tBu under O₂ atmosphere. This method furnished a new approach for the direct coupling of azoles and alkynes without

preactivation of the substrate under the O₂ atmosphere, which is beneficial from the economic prospective.



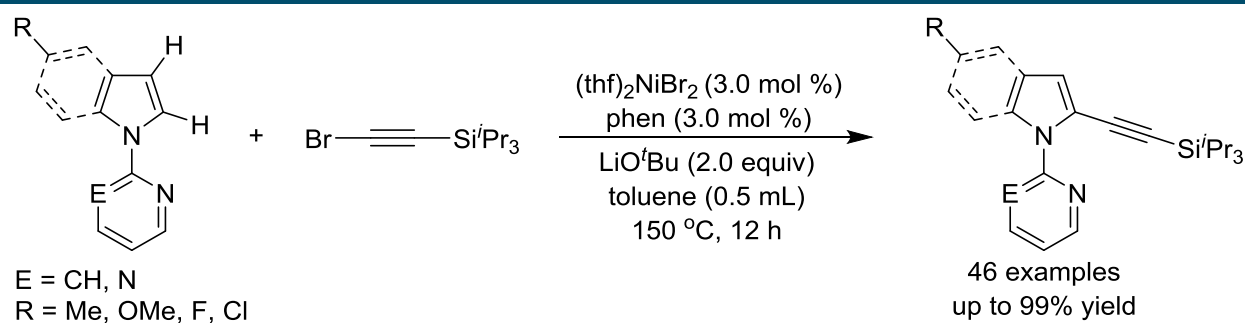
Scheme 1.53 Direct cross-coupling of azoles with various alkynes.

The monodentate chelation assisted nickel catalyzed C–H alkylation of *NH*-free aniline was successfully demonstrated by Ackermann (Scheme 1.54).²⁰⁵ They have reported excellent positional selectivity and high functional group tolerance for the alkylation reaction with excellent substrate scope. They could also be able to functionalize the C–H bond in presence of purine nucleobase. The utility of the C–H alkylation strategy was shown by a step-economical synthesis of indole.



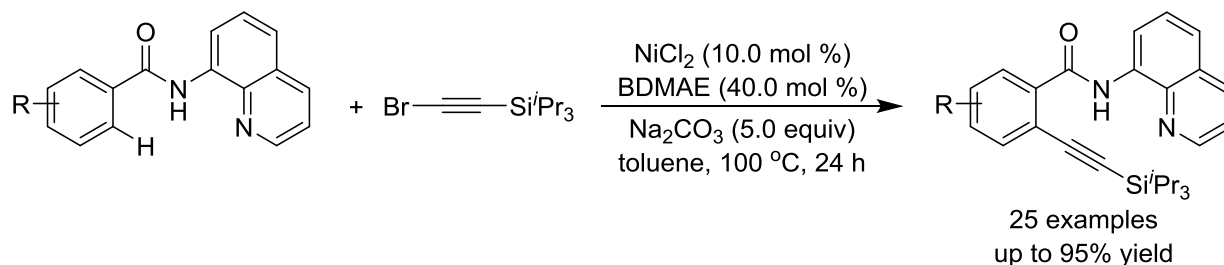
Scheme 1.54 Nickel-catalyzed C–H alkylation of anilines.

Punji group described the nickel catalyzed alkylation of heteroarenes through monodentate chelation assistance. The $(\text{thf})_2\text{NiBr}_2/\text{phen}$ catalytic system was used for the successful coupling of indoles with alkynyl bromide (Scheme 1.55).²⁰⁶ This methodology tolerated a large number of functional group including halide, nitro, ether, and nitrile. Synthetic applicability of the methodology was demonstrated by the removal of triisopropyl silyl group and further functionalization to triazolyl, benzofuranyl, alkynyl arenes derivatives. The mechanistic finding suggested that the C–H nickelation is kinetically relevant and proceeds *via* a concerted pathway



Scheme 1.55 Alkynylation of heteroarenes.

In 2015, Li described an efficient method for the *ortho*-C(sp²)-H bond alkynylation of aromatic amides using nickel catalyst *via* the chelation-assistance of 8-aminoquinoline (Scheme 1.56).²⁰² They found that NiCl₂/BDMAE catalyst system efficiently catalyzes the coupling of the aromatic amide with alkynyl bromide in the presence of Na₂CO₃ base at 100 °C to get desired couple products in good yields. Good reactivity was observed for a range of (hetero)aryl amides.



Scheme 1.56 Alkynylation of C(sp²)-H bond of aryl amide.

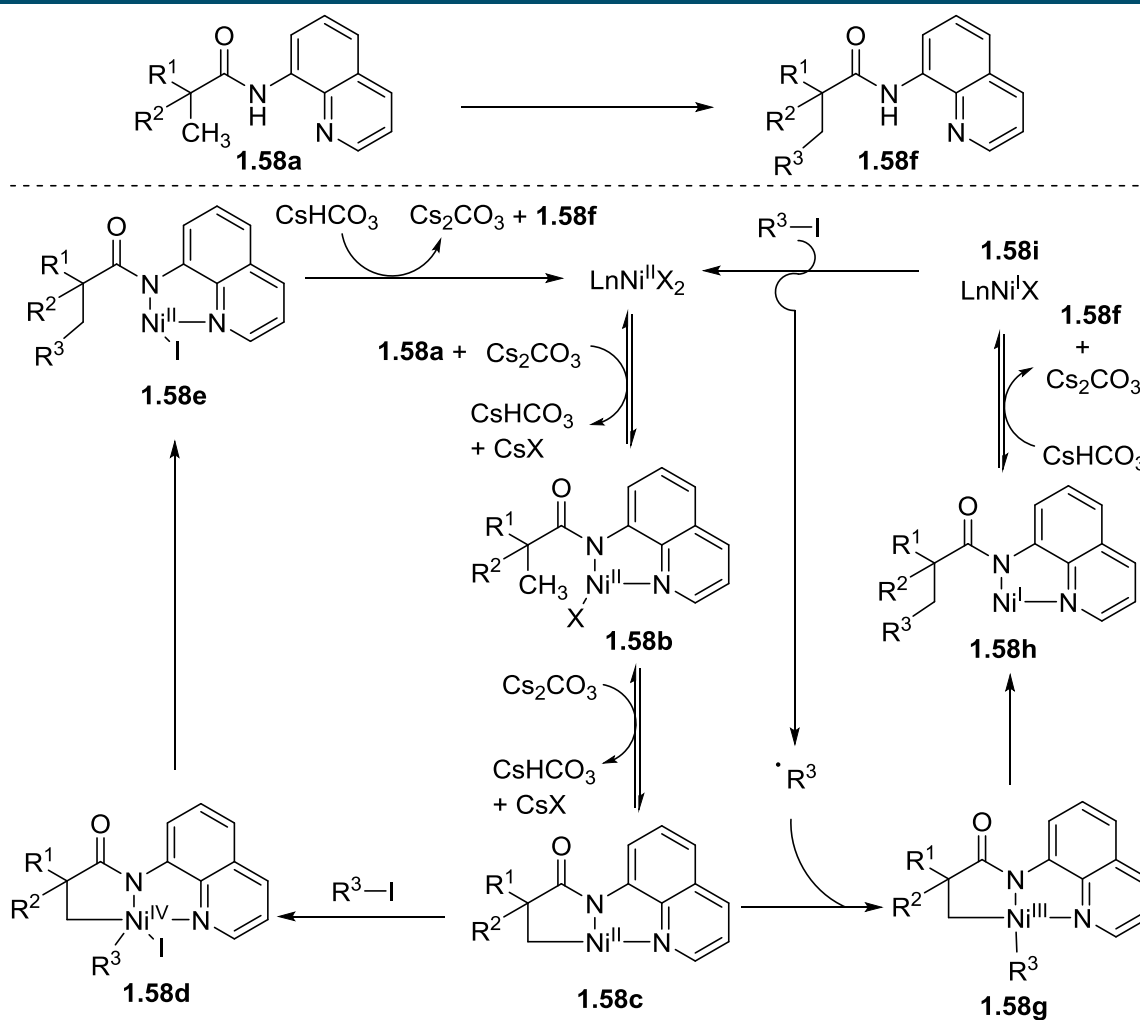
1.7 Mechanistic Aspect of Nickel-Catalyzed C–C Bond Forming Reactions through C–H Bond Activation

Generally, the organonickel species are highly reactive, and hence, they lead to the discovery of new reaction pathways. The homolytic bond cleavage in Ni–C occurs faster than the Pd–C and Pt–C,^{207,208} hence in group 10 metals the contribution of radical processes is favorable in nickel species compared to the Pd and Pt metals. Because of the involvement of one-electron process,¹⁷⁰ the nickel species showed easy access to the different oxidation states, such as Ni(0), Ni(I), Ni(II), Ni(III) and Ni(IV) during the catalytic transformation. These diverse oxidation states discover new reactive pattern beyond the traditional framework of the noble metal. There

are many reports on the C–C bond forming reaction using nickel as catalyst. In this section, the mechanistic aspect of nickel-catalyzed C–H functionalization is briefly discussed.

1.7.1 Mechanistic Pathway for the Nickel-Catalyzed Alkylation Reaction

Ge group described the nickel-catalyzed alkylation of C(sp³)–H bond of the aliphatic amide with alkyl halide *via* the bidentate chelation assistance.¹⁸⁷ On the basis of the mechanistic study, they have proposed two different pathways for the catalysis: a) Ni(II)/Ni(IV) or b) Ni(II)/Ni(III) (Scheme 1.57). The first step involves the coordination of aliphatic amide **1.58a** to the Ni(II) species, which undergoes ligand transfer process in the presence of Cs₂CO₃ to form nickel species **1.58b**. This species undergoes deprotonation in the presence of Cs₂CO₃ to form nickelacycle intermediate **1.58c**. The oxidative addition of alkyl halide to intermediate **1.58c** form the Ni(IV) species **1.58d**, which upon reductive elimination affords species **1.58e**. The protonation of **1.58e** produces the desired coupled product **1.58f** and regenerates the Ni(II) active catalyst. Alternatively, the intermediate **1.58c** could form Ni(III) species **1.58g** upon addition of alkyl radical, which on reductive elimination forms Ni(I) species **1.58h**. The species **1.58h** on protonation produces coupled product **1.58f** and generate Ni(I) species **1.58i**. From deuterium scrambling and kinetic isotope effect experiments, they have observed that the rate determining step is cyclometalation of amide **1.58a** with nickel species. The standard catalytic reaction was performed using Ni(COD)₂ as a catalyst, wherein the low yield of the desired product indicated the low probability of Ni(0) active species. Further, radical trapping experiment in the presence of TEMPO resulted in a low yield of the desired product, which indicated that the reaction proceeds through Ni(II)/Ni(III) pathway.

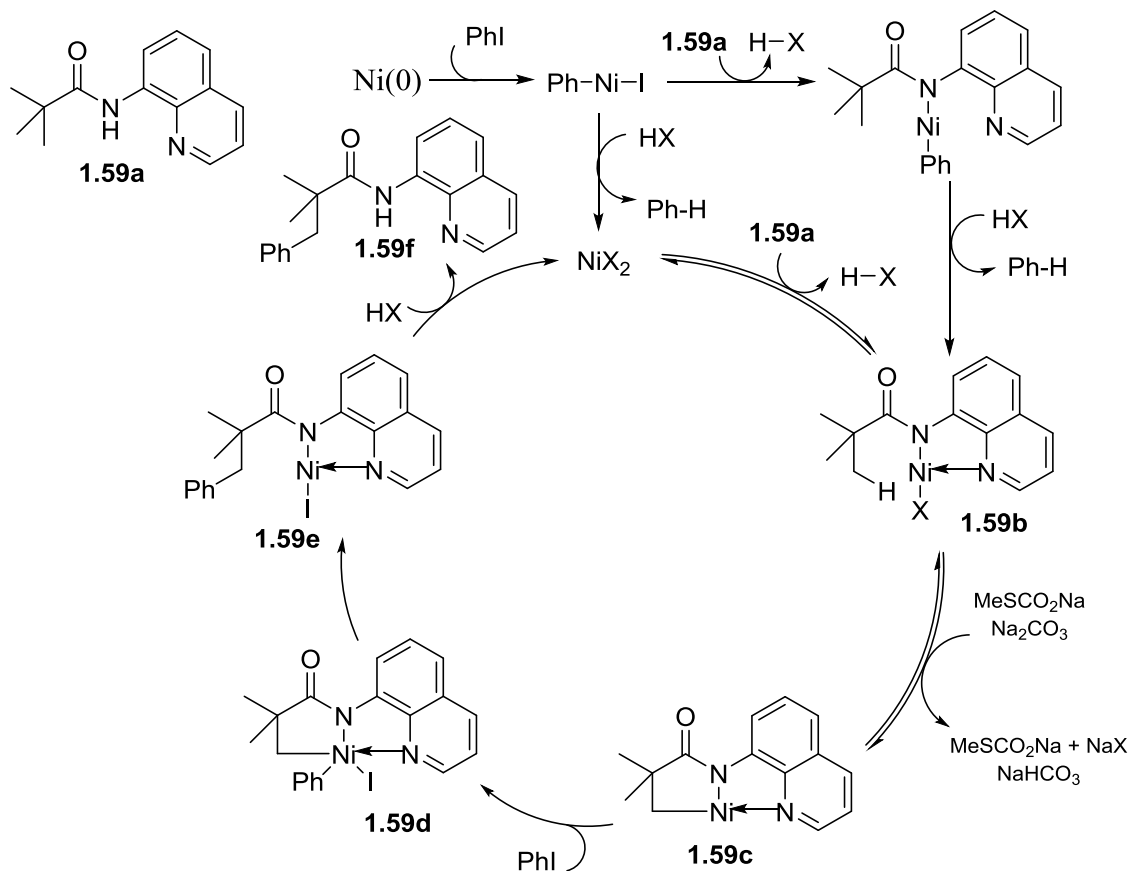


Scheme 1.57 Plausible catalytic cycle for alkylation of C(sp³)-H bond of the aliphatic amide.

1.7.2 Mechanism of Nickel-Catalyzed Arylation

The mechanistic aspects of the arylation of the aliphatic amide with aryl halide using bidentate directing group was demonstrated by Chatani.¹⁹³ The deuterium labeling experiments showed that the C-H bond breaking is a reversible process during the reaction. The product distribution study was performed to understand the difference between Ni(0) and Ni(II) catalyzed the reaction. The experiment suggested that the catalysis involves Ni(II) as an active species, and not the Ni(0). On the basis of the experimental studies, they proposed the catalytic cycle (Scheme 1.58). The catalytic cycle starts with the coordination of amide **1.59a** to Ni-centre followed by the ligand exchange in the presence of Na₂CO₃ to produce Ni-species **1.59b**, which undergoes reversible cyclometalation to give nickel species **1.59c** via the concerted-metalation-deprotonation pathway. The oxidative addition of iodobenzene to Ni(II) species **1.59c** forms a

high valent Ni(IV) species **1.59d**, which on reductive elimination afforded species **1.59e**. The species **1.59e** on protonation gives the desired arylated product **1.59f** and regenerates the Ni(II) active species. The catalytic cycle proposed to follow a Ni(II)/Ni(IV) pathway.



Scheme 1.58 Plausible mechanism for arylation of C(sp³)-H bond in aliphatic amide using nickel catalyst.

1.8 REFERENCES

- (1) Kleiman, J. P.; Dubeck, M. *J. Am. Chem. Soc.* **1963**, *85*, 1544-1545.
- (2) Cope, A. C.; Siekman, R. W. *J. Am. Chem. Soc.* **1965**, *87*, 3272-3273.
- (3) Cope, A. C.; Friedrich, E. C. *J. Am. Chem. Soc.* **1968**, *90*, 909-913.
- (4) Herrmann, W. A.; Brossmer, C.; Öfele, K.; Reisinger, C.-P.; Priermeier, T.; Beller, M.; Fischer, H. *Angew. Chem. Int. Ed. Engl.* **1995**, *34*, 1844-1848.
- (5) Corbet, J. P.; Mignani, G. *Chemical Reviews* **2006**, *106*, 2651.
- (6) Bedford, R. B.; Cazin, C. S. J.; Holder, D. *Coord. Chem. Rev.* **2004**, *248*, 2283-2321.
- (7) Herrmann, W. A.; Böhm, V. P. W.; Reisinger, C.-P. *J. Organomet. Chem.* **1999**, *576*, 23-41.
- (8) Dupont, J.; Pfeffer, M.; Spencer, J. *Eur. J. Inorg. Chem.* **2001**, 1917-1927.
- (9) Ryabov, A. D. *Synthesis* **1985**, 233-252.
- (10) Spencer, J.; Sharratt, D. P.; Dupont, J.; Monteiro, A. L.; Reis, V. I.; Stracke, M. P.; Rominger, F.; McDonald, I. M. *Organometallics* **2005**, *24*, 5665-5672.
- (11) Arlen, C.; Pfeffer, M.; Bars, O.; Grandjean, D. *J. Chem. Soc., Dalton Trans.* **1983**, 1535-1544.
- (12) Dehand, J.; Pfeffer, M.; Zinsius, M. *Inorg. Chim. Acta* **1975**, *13*, 229-232.
- (13) Dehand, J.; Jordanov, J.; Pfeffer, M.; Zinsius, M. *C. R. Hebd. Seances Acad. Sci., Ser. C* **1975**, *281*, 651.
- (14) Braunstein, P.; Dehand, J.; Pfeffer, M. *Inorg. Nucl. Chem. Lett.* **1974**, *10*, 581-585.
- (15) Morales-Morales, D.; Redon, R.; Yung, C.; Jensen, C. M. *Chem. Commun.* **2000**, 1619-1620.
- (16) Steenwinkel, P.; Gossage, R. A.; Maunula, T.; Grove, D. M.; van Koten, G. *Chem. Eur. J.* **1998**, *4*, 763-768.
- (17) Valk, J.-M.; Boersma, J.; van Koten, G. *J. Organomet. Chem.* **1994**, *483*, 213-216.
- (18) Trofimenko, S. *Inorg. Chem.* **1973**, *12*, 1215-1221.
- (19) Consorti, C. S.; Ebeling, G.; Flores, F. R.; Rominger, F.; Dupont, J. *Adv. Synth. Catal.* **2004**, *346*, 617-624.
- (20) Hou, A.-T.; Liu, Y.-J.; Hao, X.-Q.; Gong, J.-F.; Song, M.-P. *J. Organomet. Chem.* **2011**, *696*, 2857-2862.
- (21) Yang, M.-J.; Liu, Y.-J.; Gong, J.-F.; Song, M.-P. *Organometallics* **2011**, *30*, 3793-3803.

-
- (22) Zhang, B.-S.; Wang, W.; Shao, D.-D.; Hao, X.-Q.; Gong, J.-F.; Song, M.-P. *Organometallics* **2010**, *29*, 2579-2587.
- (23) Ebeling, G.; Meneghetti, M. R.; Rominger, F.; Dupont, J. *Organometallics* **2002**, *21*, 3221-3227.
- (24) McPherson, H. M.; Wardell, J. L. *Inorg. Chim. Acta* **1983**, *75*, 37-43.
- (25) Sola, D.; Vallverdu, L.; Solans, X.; Font-Bardia, M.; Bonjoch, J. *J. Am. Chem. Soc.* **2003**, *125*, 1587-1594.
- (26) Gaunt, J. C.; Shaw, B. L. *J. Organomet. Chem.* **1975**, *102*, 511-516.
- (27) Zim, D.; Buchwald, S. L. *Org. Lett.* **2003**, *5*, 2413-2415.
- (28) Maassarani, F.; Pfeffer, M.; Le Borgne, G. *Organometallics* **1987**, *6*, 2029-2043.
- (29) Dupont, J.; Pfeffer, M.; Rotteveel, M. A.; De Cian, A.; Fischer, J. *Organometallics* **1989**, *8*, 1116-1118.
- (30) Goel, A. B.; Pfeffer, M. *Inorg. Synth.* **1989**, *26*, 211.
- (31) Ohff, M.; Ohff, A.; van der Boom, M. E.; Milstein, D. *J. Am. Chem. Soc.* **1997**, *119*, 11687-11688.
- (32) Bedford, R. B.; Draper, S. M.; Noelle Scully, P.; Welch, S. L. *New J. Chem.* **2000**, *24*, 745-747.
- (33) Sommer, W. J.; Yu, K.; Sears, J. S.; Ji, Y.; Zheng, X.; Davis, R. J.; Sherrill, C. D.; Jones, C. W.; Weck, M. *Organometallics* **2005**, *24*, 4351-4361.
- (34) Gagliardo, M.; Selander, N.; Mehendale, N. C.; van Koten, G.; Klein Gebbink, R. J. M.; Szabó, K. J. *Chem. Eur. J.* **2008**, *14*, 4800-4809.
- (35) Aydin, J.; Kumar, K. S.; Eriksson, L.; Szabó, K. J. *Adv. Synth. Catal.* **2007**, *349*, 2585-2594.
- (36) Aydin, J.; Szabó, K. J. *Org. Lett.* **2008**, *10*, 2881-2884.
- (37) Driver, M. S.; Hartwig, J. F. *J. Am. Chem. Soc.* **1997**, *119*, 8232-8245.
- (38) Pfeffer, M.; Sutter-Beydoun, N.; De Cian, A.; Fischer, J. *J. Organomet. Chem.* **1993**, *453*, 139-146.
- (39) Clark, P. W.; Dyke, S. F. *J. Organomet. Chem.* **1983**, *259*, C17-C19.
- (40) Rodriguez, G.; Albrecht, M.; Schoenmaker, J.; Ford, A.; Lutz, M.; Spek, A. L.; van Koten, G. *J. Am. Chem. Soc.* **2002**, *124*, 5127-5138.
- (41) Grove, D. M.; Van Koten, G.; Louwen, J. N.; Noltes, J. G.; Spek, A. L.; Ubbels, H. J. C. *J. Am. Chem. Soc.* **1982**, *104*, 6609-6616.
-

- (42) Maassarani, F.; Pfeffer, M.; Spek, A. L.; Schreurs, A. M. M.; Van Koten, G. *J. Am. Chem. Soc.* **1986**, *108*, 4222-4224.
- (43) Dehand, J.; Mauro, A.; Osson, H.; Pfeffer, M.; de A. Santos, R. H.; Lechat, J. R. *J. Organomet. Chem.* **1983**, *250*, 537-550.
- (44) Wehman, E.; van Koten, G.; Jastrzebski, J. T. B. H.; Osson, H.; Pfeffer, M. *J. Chem. Soc. Dalton Trans.* **1988**, 2975-2981.
- (45) Dupont, J.; A.P. Halfen, R.; Schenato, R.; Berger, A.; Horner, M.; Bortoluzzi, A.; Maichle-Mossmer, C. c. *Polyhedron* **1996**, *15*, 3465-3468.
- (46) Dupont, J.; Halfen, R. A. P.; Zinn, F. K.; Pfeffer, M. *J. Organomet. Chem.* **1994**, *484*, C8-C9.
- (47) Holton, R. A.; Kjonaas, R. A. *J. Am. Chem. Soc.* **1977**, *99*, 4177-4179.
- (48) Holton, R. A.; Zoeller, J. R. *J. Am. Chem. Soc.* **1985**, *107*, 2124-2131.
- (49) Rosa, G. R.; Ebeling, G.; Dupont, J.; Monteiro, A. L. *Synthesis* **2003**, *2003*, 2894-2897.
- (50) Anastasia, L.; Negishi, E. *In Handbook of Organopalladium Chemistry for Organic Synthesis; John Wiley & Sons, Inc.: 2003*, p 311-334.
- (51) Phan, N. T. S.; Van Der Sluys, M.; Jones, C. W. *Adv. Synth. Catal.* **2006**, *348*, 609-679.
- (52) Yao, Q.; Kinney, E. P.; Zheng, C. *Org. Lett.* **2004**, *6*, 2997-2999.
- (53) Naghipour, A.; Sabounchei, S. J.; Morales-Morales, D.; Canseco-González, D.; Jensen, C. M. *Polyhedron* **2007**, *26*, 1445-1448.
- (54) Solano-Prado, M. A.; Estudiante-Negrete, F.; Morales-Morales, D. *Polyhedron* **2010**, *29*, 592-600.
- (55) Duncan, D.; Hope, E. G.; Singh, K.; Stuart, A. M. *Dalton Trans.* **2011**, *40*, 1998-2005.
- (56) Luo, Q.-L.; Tan, J.-P.; Li, Z.-F.; Qin, Y.; Ma, L.; Xiao, D.-R. *Dalton Trans.* **2011**, *40*, 3601-3609.
- (57) Yang, L.; Zhang, X.; Mao, P.; Xiao, Y.; Bian, H.; Yuan, J.; Mai, W.; Qu, L. *RSC Adv.* **2015**, *5*, 25723-25729.
- (58) Blacque, O.; Frech, C. M. *Chem. Eur. J.* **2010**, *16*, 1521-1531.
- (59) Leigh, V.; Ghattas, W.; Mueller-Bunz, H.; Albrecht, M. *J. Organomet. Chem.* **2014**, *771*, 33-39.
- (60) Yang, L. Z., X.; Mao, P.; Xiao, Y.; Bian, H.; Yuan, J.; Mai, W.; Qu, L. *RSC Adv.* **2015**, *5*, 25723-25729.
- (61) Sobhani, S.; Zeraatkar, Z.; Zarifi, F. *New J. Chem.* **2015**, *39*, 7076-7085.

- (62) Sobhani, S.; Zeraatkar, Z.; Zarifi, F. *New J. Chem.* **2016**, *40*, 8969-8969.
- (63) Yoon, M. S. R., D.; Kim, J.; Ahn, K. H. *Organometallics* **2006**, *25*, 2409-2411.
- (64) da Costa, R. C.; Jurisch, M.; Gladysz, J. A. *Inorg. Chim. Acta* **2008**, *361*, 3205-3214.
- (65) Schuster, E. M.; Botoshansky, M.; Gandelman, M. *Angew. Chem. Int. Ed.* **2008**, *47*, 4555-4558.
- (66) Bröring, M.; Kleeberg, C.; Köhler, S. *Inorg. Chem.* **2008**, *47*, 6404-6412.
- (67) Aydin, J.; Larsson, J. M.; Selander, N.; Szabó, K. J. *Org. Lett.* **2009**, *11*, 2852-2854.
- (68) Kumar, A.; Agarwal, M.; Singh, A. K.; Butcher, R. J. *Inorg. Chim. Acta* **2009**, *362*, 3208-3218.
- (69) Yoo, K. S. O. N., J.; Sakaguchi, S.; Giles, R.; Lee, J. H.; Jung, K. W. *J. Org. Chem.* **2010**, *75*, 95-101.
- (70) Wang, Z. F., X.; Fang, W.; Tu, T. *Synlett* **2011**, *2011*, 951-954.
- (71) SanMartin, R.; Inés, B.; Moure, M. J.; Herrero, M. T.; Domínguez, E. *Helvetica Chim. Acta* **2012**, *95*, 955-962.
- (72) Feng, J.; Cai, C. *J. Fluorine Chem.* **2013**, *146*, 6-10.
- (73) Lee, H. M.; Zeng, J. Y.; Hu, C.-H.; Lee, M.-T. *Inorg. Chem.* **2004**, *43*, 6822-6829.
- (74) Kjellgren, J.; Aydin, J.; Wallner, O. A.; Saltanova, I. V.; Szabó, K. J. *Chem. Eur. J.* **2005**, *11*, 5260-5268.
- (75) Hahn, F. E.; Jahnke, M. C.; Pape, T. *Organometallics* **2007**, *26*, 150-154.
- (76) Wei, W. Q., Y.; Luo, M.; Xia, P.; Wong, M. S. *Organometallics* **2008**, *27*, 2268- 2272.
- (77) Bonnet, S.; Van Lenthe, J. H.; Sieglar, M. A.; Spek, A. L.; Van Koten, G.; Gebbink, R. J. M. K. *Organometallics* **2009**, *28*, 2325-2333.
- (78) Olsson, D.; Wendt, O. F. *J. Organomet. Chem.* **2009**, *694*, 3112-3115.
- (79) Tu, T. F., X.; Wang, Z.; Liu, X. *Dalton Trans.* **2010**, *39*, 10598-10600.
- (80) Li, P.; Zhou, H.-F.; Liu, F.; Hu, Z.-X.; Wang, H.-X. *Inorg. Chem. Commun.* **2013**, *32*, 78-81.
- (81) Ramírez-Rave, S.; Estudiante-Negrete, F.; Toscano, R. A.; Hernández-Ortega, S.; Morales-Morales, D.; Grévy, J.-M. *J. Organomet. Chem.* **2014**, *749*, 287-295.
- (82) Tamizmani, M.; Kankanala, R.; Sivasankar, C. *J. Organomet. Chem.* **2014**, *763*, 6-13.
- (83) Imanaka, Y.; Hashimoto, H.; Kinoshita, I.; Nishioka, T. *Chem. Lett.* **2014**, *43*, 687- 689.
- (84) Arumugam, V. K., W.; Bhuvanesh, N. S. P.; Nallasamy, D. *RSC Adv.* **2015**, *5*, 59428-59436.

-
- (85) Liang, L.-C.; Chien, P.-S.; Song, L.-H. *J. Organomet. Chem.* **2016**, *804*, 30-34.
- (86) Baran, T.; Menteş, A. *J. Mol. Str.* **2017**, *1134*, 591-598.
- (87) Vignesh, A. K., W.; Dharmaraj, N. *ChemCatChem* **2017**, *9*, 910-914.
- (88) Churruca, F.; SanMartin, R.; Tellitu, I.; Domínguez, E. *Synlett* **2005**, 3116-3120.
- (89) Bonnet, S.; Lutz, M.; Spek, A. L.; van Koten, G.; Klein Gebbink, R. J. M. *Organometallics* **2010**, *29*, 1157-1167.
- (90) Kozlov, V. A.; Aleksanyan, D. V.; Nelyubina, Y. V.; Lyssenko, K. A.; Petrovskii, P. V.; Vasil'ev, A. A.; Odinets, I. L. *Organometallics* **2011**, *30*, 2920-2932.
- (91) Luo, Q.-L.; Tan, J.-P.; Li, Z.-F.; Nan, W.-H.; Xiao, D.-R. *J. Org. Chem.* **2012**, *77*, 8332-8337.
- (92) Kumar, S.; Rao, G. K.; Kumar, A.; Singh, M. P.; Singh, A. K. *Dalton Trans.* **2013**, *42*, 16939-16948.
- (93) Rao, G. K.; Kumar, A.; Kumar, S.; Dupare, U. B.; Singh, A. K. *Organometallics* **2013**, *32*, 2452-2458.
- (94) Bolliger, J. L.; Frech, C. M. *Adv. Synth. Catal.* **2009**, *351*, 891-902.
- (95) Gu, S.; Chen, W. *Organometallics* **2009**, *28*, 909-914.
- (96) Huynh, H. V.; Lee, C.-S. *Dalton Trans.* **2013**, *42*, 6803-6809.
- (97) Scharf, A. G., I.; Vigalok, A. *J. Am. Chem. Soc.* **2013**, *135*, 967-970.
- (98) Hung, Y.-T.; Chen, M.-T.; Huang, M.-H.; Kao, T.-Y.; Liu, Y.-S.; Liang, L.-C. *Inorg. Chem. Front.* **2014**, *1*, 405-413.
- (99) Zhang, J.-H. L., P.; Hu, W.-P.; Wang, H.-X. *Polyhedron* **2015**, *96*, 107-112.
- (100) Inés, B.; San Martin, R.; Churruca, F.; Domínguez, E.; Urriaga, M. K.; Arriortua, M. I. *Organometallics* **2008**, *27*, 2833-2839.
- (101) Bagherzadeh, M.; Mousavi, N.-A.; Zare, M.; Jamali, S.; Ellern, A.; Woo, L. K. *Inorg. Chim. Acta* **2016**, *451*, 227-232.
- (102) Kumar, S.; Saleem, F.; Mishra, M. K.; Singh, A. K. *New J. Chem.* **2017**, *41*, 2745-2755.
- (103) Olsson, D.; Nilsson, P.; El Masnaouy, M.; Wendt, O. F. *Dalton Trans.* **2005**, 1924-1929.
- (104) Liu, J.; Wang, H.; Zhang, H.; Wu, X.; Zhang, H.; Deng, Y.; Yang, Z.; Lei, A. *Chem. Eur. J.* **2009**, *15*, 4437-4445.
- (105) Wang, H.; Liu, J.; Deng, Y.; Min, T.; Yu, G.; Wu, X.; Yang, Z.; Lei, A. *Chem. Eur. J.* **2009**, *15*, 1499-1507.
- (106) Gerber, R.; Blacque, O.; Frech, C. M. *Dalton Trans.* **2011**, *40*, 8996-9003.
-

- (107) Miyaura, N.; Suzuki, A. *Chem. Rev.* **1995**, *95*, 2457-2483.
- (108) Beller, M.; Fischer, H.; Herrmann, W. A.; Öfele, K.; Brossmer, C. *Angew. Chem. Int. Ed. Engl.* **1995**, *34*, 1848-1849.
- (109) Alacid, E.; Alonso, D. A.; Botella, L.; Najera, C.; Pacheco, M. C. *The Chem. Record* **2006**, *6*, 117-132.
- (110) Paintner, F. F.; Görler, K.; Voelterb, W. *Synlett* **2003**, *4*, 522-526.
- (111) Yang, Y.; Oldenhuis, N. J.; Buchwald, S. L. *Angew. Chem. Int. Ed.* **2013**, *52*, 615 -619.
- (112) Gelman, D.; Buchwald, S. L. *Angew. Chem. Int. Ed.* **2003**, *42*, 5993-5996.
- (113) Lipshutz, B. H.; Chung, D. W.; Rich, B. *Org. Lett.* **2008**, *10*, 3793-3796.
- (114) Sabounchei, S. J.; Ahmadi, M.; Nasri, Z.; Shams, E.; Panahimehr, M. *Tetrahedron Lett.* **2013**, *54*, 4656-4660.
- (115) Mori, A.; Sekiguchi, A.; Masui, K.; Shimada, T.; Horie, M.; Osakada, K.; Kawamoto, M.; Ikeda, T. *J. Am. Chem. Soc.* **2003**, *125*, 1700-1701.
- (116) Bellina, F.; Cauteruccio, S.; Rossi, R. *Eur. J. Org. Chem.* **2006**, *2006*, 1379-1382.
- (117) Turner, G. L.; Morris, J. A.; Greaney, M. F. *Angew. Chem. Int. Ed.* **2007**, *46*, 7996-8000.
- (118) Bellina, F.; Calandri, C.; Cauteruccio, S.; Rossi, R. *Tetrahedron* **2007**, *63*, 1970-1980.
- (119) Chiong, H. A.; Daugulis, O. *Org. Lett.* **2007**, *9*, 1449-1451.
- (120) Ackermann, L.; Althammer, A.; Fenner, S. *Angew. Chem. Int. Ed.* **2009**, *48*, 201-204.
- (121) Doğan, O.; Gürbüz, N.; Özdemir, I.; Çetinkaya, B.; Şahin, O.; Büyükgüngör, O. *Dalton Trans.* **2009**, 7087-7093.
- (122) Campeau, L.-C.; Stuart, D. R.; Leclerc, J.-P.; Bertrand-Laperle, M.; Villemure, E.; Sun, H.-Y.; Lasserre, S.; Guimond, N.; Lecavallier, M.; Fagnou, K. *J. Am. Chem. Soc.* **2009**, *131*, 3291-3306.
- (123) Ackermann, L.; Barfüsser, S.; Pospesch, J. *Org. Lett.* **2010**, *12*, 724-726.
- (124) Shibahara, F.; Yamaguchi, E.; Murai, T. *Chem. Commun.* **2010**, *46*, 2471-2473.
- (125) Saha, D.; Adak, L.; Ranu, B. C. *Tetrahedron Lett.* **2010**, *51*, 5624-5627.
- (126) Demir, S.; Özdemir, İ.; Arslan, H.; VanDerveer, D. *J. Organomet. Chem.* **2011**, *696*, 2589-2593.
- (127) Özdemir, İ.; Arslan, H.; Demir, S.; VanDerveer, D.; Çetinkaya, B. *Inorg. Chem. Commun.* **2011**, *14*, 672-675.
- (128) Zhang, G.; Zhao, X.; Yan, Y.; Ding, C. *Eur. J. Org. Chem.* **2012**, *2012*, 669-672.

- (129) Shen, X.-B.; Zhang, Y.; Chen, W.-X.; Xiao, Z.-K.; Hu, T.-T.; Shao, L.-X. *Org. Lett.* **2014**, *16*, 1984-1987.
- (130) Gu, J.; Cai, C. *RSC Adv.* **2015**, *5*, 56311-56315.
- (131) Huang, J.; Chan, J.; Chen, Y.; Borths, C. J.; Baucom, K. D.; Larsen, R. D.; Faul, M. M. *J. Am. Chem. Soc.* **2010**, *132*, 3674-3675.
- (132) Razavi, H.; Palaninathan, S. K.; Powers, E. T.; Wiseman, R. L.; Purkey, H. E.; Mohamedmohaideen, N. N.; Deechongkit, S.; Chiang, K. P.; Dendle, M. T. A.; Sacchettini, J. C.; Kelly, J. W. *Angew. Chem. Int. Ed.* **2003**, *42*, 2758-2761.
- (133) Okamoto, K.; Eger, B. T.; Nishino, T.; Kondo, S.; Pai, E. F.; Nishino, T. *J. Biol. Chem.* **2003**, *278*, 1848-1855.
- (134) Coqueron, P.-Y.; Didier, C.; Ciufolini, M. A. *Angew. Chem. Int. Ed.* **2003**, *42*, 1411-1414.
- (135) Giddens, A. C.; Boshoff, H. I. M.; Franzblau, S. G.; Barry, C. E.; Copp, B. R. *Tetrahedron Lett.* **2005**, *46*, 7355-7357.
- (136) Khake, S. M.; Soni, V.; Gonnade, R. G.; Punji, B. *Dalton Trans.* **2014**, *43*, 16084-16096.
- (137) Wang, C.; Li, Y.; Lu, B.; Hao, X.-Q.; Gong, J.-F.; Song, M.-P. *Polyhedron* **2018**, *143*, 184-192.
- (138) Takemoto, T.; Iwasa, S.; Hamada, H.; Shibatomi, K.; Kameyama, M.; Motoyama, Y.; Nishiyama, H. *Tet. Lett.* **2007**, *48*, 3397-3401.
- (139) Bolliger, J. L.; Blacque, O.; Frech, C. M. *Chem. Eur. J.* **2008**, *14*, 7969-7977.
- (140) Vicente, J.; Arcas, A.; Juliá-Hernández, F.; Bautista, D. *Angew. Chem. Int. Ed.* **2011**, *50*, 6896-6899.
- (141) Dupont, J.; Consorti, C. S.; Spencer, J. *Chem. Rev.* **2005**, *105*, 2527-2572.
- (142) Eberhard, M. R. *Org. Lett.* **2004**, *6*, 2125-2128.
- (143) Yu, K.; Sommer, W.; Richardson, J. M.; Weck, M.; Jones, C. W. *Adv. Synth. Catal.* **2005**, *347*, 161-171.
- (144) Weck, M. J., C. W. *Inorg. Chem.* **2007**, *46*, 1865-1875.
- (145) Suijkerbuijk, B. M. J. M.; Martínez, S. D. H.; van Koten, G.; Klein Gebbink, R. J. M. *Organometallics* **2008**, *27*, 534-542.
- (146) Gerber, R.; Blacque, O.; Frech, C. M. *ChemCatChem* **2009**, *1*, 393-400.
- (147) Moulton, C. J.; Shaw, B. L. *J. Chem. Soc., Dalton Trans.* **1976**, 1020-1024.
- (148) Salah, A. B.; Zargarian, D. *Dalton Trans.* **2011**, *40*, 8977-8985.
- (149) Pandiri, H.; Sharma, D. M.; Gonnade, R. G.; Punji, B. *J. Chem. Sci.* **2017**, *129*, 1161-1169.

- (150) Csok, Z.; Vechorkin, O.; Harkins, S. B.; Scopelliti, R.; Hu, X. *J. Am. Chem. Soc.* **2008**, *130*, 8156-8157.
- (151) Gómez-Benítez, V.; Baldovino-Pantaleón, O.; Herrera-Álvarez, C.; Toscano, R. A.; Morales-Morales, D. *Tetrahedron Lett.* **2006**, *47*, 5059-5062.
- (152) Gu, S.; Du, J.; Huang, J.; Guo, Y.; Yang, L.; Xu, W.; Chen, W. *Dalton Trans.* **2017**, *46*, 586-594.
- (153) Liu, N.; Wang, Z.-X. *J. Org. Chem.* **2011**, *76*, 10031-10038.
- (154) Zhang, X.-Q.; Wang, Z.-X. *J. Org. Chem.* **2012**, *77*, 3658-3663.
- (155) Hu, X. *Chimia* **2012**, *66*, 154-158.
- (156) Pérez García, P. M.; Ren, P.; Scopelliti, R.; Hu, X. *ACS Catal.* **2015**, *5*, 1164-1171.
- (157) Alberico, D.; Scott, M. E.; Lautens, M. *Chem. Rev.* **2007**, *107*, 174-238.
- (158) Quasdorf, K. W.; Tian, X.; Garg, N. K. *J. Am. Chem. Soc.* **2008**, *130*, 14422-14423.
- (159) Kakiuchi, F.; Kochi, T. *Synthesis* **2008**, *2008*, 3013-3039.
- (160) Li, C.-J. *Acc. Chem. Res.* **2009**, *42*, 335-344.
- (161) Quasdorf, K. W.; Riener, M.; Petrova, K. V.; Garg, N. K. *J. Am. Chem. Soc.* **2009**, *131*, 17748-17749.
- (162) Ackermann, L.; Vicente, R.; Kapdi, A. R. *Angew. Chem. Int. Ed.* **2009**, *48*, 9792-9826.
- (163) Chen, X.; Engle, K. M.; Wang, D.-H.; Yu, J.-Q. *Angew. Chem. Int. Ed.* **2009**, *48*, 5094-5115.
- (164) Messaoudi, S.; Brion, J.-D.; Alami, M. *Eur. J. Org. Chem.* **2010**, *2010*, 6495-6516.
- (165) Sun, C.-L.; Li, B.-J.; Shi, Z.-J. *Chem. Rev.* **2011**, *111*, 1293-1314.
- (166) Yamaguchi, J.; Yamaguchi, A. D.; Itami, K. *Angew. Chem. Int. Ed.* **2012**, *51*, 8960-9009.
- (167) Mesganaw, T.; Garg, N. K. *Org. Process Res. Dev.* **2012**, *17*, 29-39.
- (168) Yu, D.-G. W., X.; Zhu, R.-Y.; Luo, S.; Zhang, X.-B.; Wang, B.-Q.; Wang, L.; Shi, Z.-J. *J. Am. Chem. Soc.* **2012**, *134*, 14638-14641.
- (169) Keim, W. E. *Angew. Chem. Int. Ed.* **1990**, *29*, 235-244.
- (170) Wilke, G. *Angew. Chem. Int. Ed.* **1988**, *27*, 185-206.
- (171) Trotaş, I.-T. Z., T.; Schüth, F. *Chem. Rev.* **2014**, *114*, 1761-1782.
- (172) Tasker, S. Z. S., E. A.; Jamison, T. F. *Nature* **2014**, *509*, 299-309.
- (173) Henrion, M.; Ritleng, V.; Chetcuti, M. J. *ACS Catal.* **2015**, *5*, 1283-1302.
- (174) Prakasham, A. P.; Ghosh, P. *Inorg. Chim. Acta* **2015**, *431*, 61-100.
- (175) Montgomery, J. *Angew. Chem. Int. Ed.* **2004**, *43*, 3890-3908.

- (176) Netherton, M. R.; Fu, G. C. *Adv. Synth. Catal.* **2004**, *346*, 1525-1532.
- (177) Terao, J.; Kambe, N. *Acc. Chem. Res.* **2008**, *41*, 1545-1554.
- (178) Denmark, S. E.; Butler, C. R., . *Chem. Commun.* **2009**, 20-33.
- (179) Jacobsen, E. N.; Breinbauer, R. *Science* **2000**, *287*, 437-438.
- (180) Carey, J. S.; Laffan, D.; Thomson, C.; Williams, M. T. *Org. Biomol. Chem.* **2006**, *4*, 2337-2347.
- (181) Godula, K.; Sames, D. *Science* **2006**, *312*, 67-72.
- (182) Kraft, A.; Grimsdale, A. C.; Holmes, A. B. *Angew. Chem. Int. Ed.* **1998**, *37*, 402-428.
- (183) Vechorkin, O.; Proust, V.; Hu, X. *Angew. Chem. Int. Ed.* **2010**, *49*, 3061-3064.
- (184) Patel, U. N.; Pandey, D. K.; Gonnade, R. G.; Punji, B. *Organometallics* **2016**, *35*, 1785-1793.
- (185) Ruan, Z.; Lackner, S.; Ackermann, L. *Angew. Chem., Int. Ed.* **2016**, *55*, 3153-3157.
- (186) Soni, V.; Jagtap, R. A.; Gonnade, R. G.; Punji, B. *ACS Catal.* **2016**, *6*, 5666-5672.
- (187) Wu, X.-L.; Zhao, Y.; Ge, H. *J. Am. Chem. Soc.* **2014**, *136*, 1789-1792.
- (188) Canivet, J.; Yamaguchi, J.; Ban, I.; Itami, K. *Org. Lett.* **2009**, *11*, 1733-1736.
- (189) Hachiya, H.; Hirano, K.; Satoh, T.; Miura, M. *Org. Lett.* **2009**, *11*, 1737-1740.
- (190) Yamamoto, T.; Muto, K.; Komiyama, M.; Canivet, J.; Yamaguchi, J.; Itami, K. *Chem. Eur. J.* **2011**, *17*, 10113-10122.
- (191) Muto, K.; Yamaguchi, J. I., K. *J. Am. Chem. Soc.* **2012**, *134*.
- (192) Jagtap, R. A.; Soni, V.; Punji, B. *ChemSusChem* **2017**, *10*, 2242-2248.
- (193) Aihara, Y.; Chatani, N. *J. Am. Chem. Soc.* **2014**, *136*, 898-901.
- (194) Kanyiva, K. S.; Nakao, Y.; Hiyama, T. *Angew. Chem. Int. Ed.* **2007**, *46*, 8872-8874.
- (195) Nakao, Y.; Kashihara, N.; Kanyiva, K. S.; Hiyama, T. *J. Am. Chem. Soc.* **2008**, *130*, 16170-16171.
- (196) Nakao, Y.; Kanyiva, K. S.; Hiyama, T. *J. Am. Chem. Soc.* **2008**, *130*, 2448-2449.
- (197) Meng, L.; Kamada, Y.; Muto, K.; Yamaguchi, J.; Itami, K. *Angew. Chem. Int. Ed.* **2013**, *52*, 10048-10051.
- (198) Jagtap, R. A.; Vinod, C. P.; Punji, B. *ACS Catalysis*, *9*, 431-441.
- (199) Kumar, D.; David, W. M.; Kerwin, S. M. *Bioorg. Med. Chem. Lett.* **2001**, *11*, 2971-2974.
- (200) Callstrom, M. R.; Neenan, T. X.; McCreery, R. L.; Alsmeyer, D. C. *J. Am. Chem. Soc.* **1990**, *112*, 4954-4956.

- (201) Matsuyama, N.; Kitahara, M.; Hirano, K.; Satoh, T.; Miura, M. *Org. Lett.* **2010**, *12*, 2358-2361.
- (202) Yi, J.; Yang, L.; Xia, C.; Li, F. *J. Org. Chem.* **2015**, *80*, 6213-6221.
- (203) Landge, V. G.; Shewale, C. H.; Jaiswal, G.; Sahoo, M. K.; Midya, S. P.; Balaraman, E. *Catal. Sci. Technol.* **2016**, *6*, 1946-1951.
- (204) Luo, F.-X.; Cao, Z.-C.; Zhao, H.-W.; Wang, D.-C.; Zhang, Y.-F.; Xu, X.; Shi, Z.-J. *Organometallics* **2017**, *36*, 18-21.
- (205) Ruan, Z.; Lackner, S.; Ackermann, L. *ACS Catal.* **2016**, *6*, 4690-4693.
- (206) Khake, S. M.; Soni, V.; Gonnade, R. G.; Punji, B. *Chem. Eur. J.* **2017**, *23*, 2907-2914.
- (207) Macgregor, S. A.; Neave, G. W.; Smith, C. *Faraday Discuss* **2003**, *124*, 111-127.
- (208) Ananikov, V. P.; Musaev, D. G.; Morokuma, K. *Organometallics* **2005**, *24*, 715-723.

Objectives of the Present Study

Literature survey demonstrates that there exist an immense interest in the chemistry of transition metal complexes and their applications in diverse catalysis and material chemistry. Particularly, considering the broad applicability of the palladacycles, the efficient and regioselective synthesis of the hemilabile ECE'-based palladacycles (both CE- and ECE'-type) by C–H bond activation is indispensable. In general, the syntheses of the arene-based ECE palladacycle, containing 1,3-donor group substituents are executed by the direct cyclopalladation at the C-2 position of the arene ligands. However, in some of the pincer-type ligands, the cyclopalladation of the C-4/C-6 position takes place to generate CE-type palladacycles. In order to obtain the selective ECE- palladacycles, in such cases, the site selectivity of the palladation is inverted by the introduction of an activating group ($-\text{SiMe}_3$) at the C-2 position. The synthesis of both the CE- and ECE/ECE'-palladacycles from a single ECE/ECE'-pincer-type ligand *via* the selective C–H bond palladation has not been precedented. In that regards, one objective of this thesis was to develop a suitable approach for the synthesis of CE and ECE type of palladacycle from a single ECE type ligand (Chapter 2). Thus, unsymmetrical pincer-type POCN–H ligands were synthesized and reactivity towards palladium was tuned to allow selective coordination of arm to metal centre. The side arm coordination followed by the regioselective C–H bond palladation to generate both types of palladacycles (CE and ECE') without installation of an activating group. In this chapter we have discussed the synthesis and mechanism of synthesis of CE and ECE type palladacycle without the introduction of an activating group *via* the selective C–H bond palladation. Application of the synthesized palladacycles was demonstrated for the direct C–H bond arylation of azoles with aryl iodides.

Further, the literature study shows that the nickel catalyst systems are highly active, and are efficient for the transformation of unreactive bonds. The nickel catalyst systems have been used for many C–C bond forming reactions, such as alkylation, arylation, alkenylation, and alkynylation using C–H activation strategy. In Chapter 3, the nickel-catalyzed coupling of unactivated alkyl chlorides with C(2)–H of indoles under mild conditions was successfully demonstrated. This method allowed the regioselective alkylation of indoles and pyrroles with primary alkyl chlorides and secondary alkyl chlorides and bromides at 60 °C. Various functionalities, such as halides, alkenyl, alkynyl, ether, thioether, furanyl, pyrrolyl, indolyl and carbazolyl including acyclic and cyclic alkyls were well tolerated under the reaction conditions. The chemoselectivity with regard to alkyl halides $\text{C}(\text{sp}^3)\text{--I}$, $\text{C}(\text{sp}^3)\text{--Br}$ or $\text{C}(\text{sp}^3)\text{--Cl}$ bond activation has been shown. The utility of this nickel-catalyzed protocol is established by the

Objectives of the Present Study

removal of trace directing group. A comprehensive mechanistic study has been demonstrated and catalytic cycle has been proposed, which follows a Ni(I)/Ni(III) pathway.

Similarly, Chapter 4 describes an effective and practical strategy for the chemoselective coupling of unactivated aryl chlorides with indoles and pyrroles using simple Ni(OAc)₂/dppf catalytic system. Optimization of reaction conditions for the arylation of indole, and the substrate scope for indole and pyrrole arylation with aryl chlorides were discussed. Reaction compatibility with a range of simple and functionalized aryl chlorides as well as electronically distinct indoles has been shown. The reaction tolerated various functionalities, such as halides, ethers, thioether and amines, as well as heterocycles indolyl, pyrrolyl, and carbazolyl. The chemo-selectivity with regard to aryl halides has been demonstrated. Mechanistic investigations by various controlled reactions, kinetic studies, and deuterium labeling experiments have been performed. On the basis of above experiments conducted and literature precedents, we have proposed the catalytic cycle which follows the Ni(II)/Ni(IV) pathway.

In the literature, we have found that hemilabile pincer ligand systems installed on the metal increase its reactivity drastically. Considering the literature reports and with our hypothesis, we have developed a series of quinolinylnyl based (^QNNN^{R2})-pincer nickel(II) complexes, which is shown in Chapter 5. The (quinolinylnyl)amine pincer ligands R₂NC₂H₄(μ-NH)C₉H₆N [^QNNN^{R2}-H; NR₂ = NMe₂, NEt₂, pyrrolidinyl], and corresponding nickel complexes [(^{R2}NNN^Q)NiX; X = Cl, Br], were synthesized in good yields. These complexes were well characterized by spectroscopy technique, elemental analysis, and HRMS. Furthermore, the molecular structures of some of these complexes were elucidated by X-ray crystallography. The synthesized pincer nickel complexes showed excellent activity for the regioselective alkylation of indoles and moderate activity for the dehydrogenative alkylation of indolines with alkyl halides. Synthesis and characterization of the nickel complexes and their applications towards C–H bond alkylation is discussed in this chapter.

Chapter 2

**Mono- and Binuclear Palladacycles *via* Regioselective C–H
Bond Activation: Syntheses, Mechanistic Insights and
Catalytic Activity**

2.1 INTRODUCTION

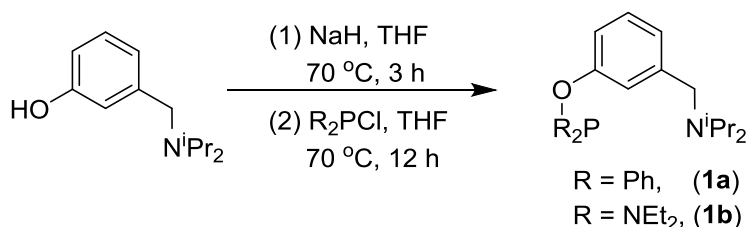
Palladacycles containing C-anionic four-electron donor (CE) or six-electron donor (ECE) ligand (E = donor group) have many attractive structural features.^{1,2} The stable chelating structure and strong metal-carbon σ -bond provides them with high air and thermal stability, whereas the appropriate tuning of the substituents on donor-atom furnishes distinct sterics and electronics around the palladium; which make the palladacycles extraordinary catalysts for various important organic transformations.³⁻¹⁴ Though, each of these palladacycles has its own unique chemistry, the ECE-pincer (NCN,¹⁵⁻²¹ PCP,²²⁻²⁸ SCS,²⁹⁻³⁴ etc.) palladium system has attracted considerable interest, as it benefits from the advantage of terdentate coordination and hence, the well-protected palladium center. Recently, the unsymmetrical ECE'-pincer palladium system having two different donor arms, typically one soft P-donor and one hard N- or O-donor, such as PCN,³⁵⁻³⁷ POCN,³⁸⁻⁴² and PCO⁴³ has given particular attention, as such system renders complementary properties of both the hard/soft donor as well as that of the distinct electron-donor/acceptor ability. In addition, the hemilabile palladacycles could provide suitable sterics, electronics, and coordination demands needed on the different steps of a catalytic reaction, and might produce the interesting structural motifs on stoichiometric reactions.

Considering the broad applicability of the palladacycles, the efficient and regioselective synthesis of the hemilabile ECE'-based palladacycles (both CE- and ECE'-type) by C-H bond activation is indispensable. In general, the syntheses of the arene-based ECE pincer-palladium complexes, containing 1,3-donor group substituents, are executed by the direct cyclopalladation at C-2 position of the arene ligands; which usually promoted by the coordination of the donor groups on ligand prior to the intramolecular C(2)-H bond activation.⁴⁴⁻⁴⁸ However, in some of the pincer-type ligands, the cyclopalladation of C-2 does not occur and instead the C-4/C-6 palladation takes place to generate CE-type palladacycles.^{49,50} In order to obtain the selective ECE-pincer palladacycles, in such cases, the site selectivity of the palladation is inverted by the introduction of an activating group ($-\text{SiMe}_3$) at C-2 position.⁵⁰⁻⁵² Surprisingly, the synthesis of both the CE- and ECE/ECE'-palladacycles from a single ECE/ECE' pincer-type ligand *via* the selective C-H bond palladation has not been precedented in the literature. We assumed that in an unsymmetrical pincer-type ligand POCN-H, as it contain two different donor groups with the distinct donating ability, the reactivity of the ligand towards palladium could be tuned to allow

only P- or both N- and P-coordination, which would be followed by the regioselective C–H bond palladation to generate both type of palladacycles (CE- and ECE'-type), without being the introduction of an activating group (-SiMe₃). With this in mind, in this chapter, we describe the syntheses of two unsymmetrical POCN pincer-type ligands, and their regioselective C–H bond palladation to accomplish both the “PC”-chelate binuclear [κ^P, κ^C -PC-PdCl]₂ (CE-type) and “POCN”-coordinated mononuclear ($\kappa^P, \kappa^C, \kappa^N$ -POCN)PdCl (ECE'-type) palladacycles. Furthermore, the influence of base on the regioselective C–H bond activation is demonstrated, and the mechanistic aspect of the same has been elucidated. All the palladacycles were screened as a catalyst precursor for the direct C–H bond arylation of azoles with aryl iodides and some of them were efficiently employed in the synthesis of a variety of 2-arylated azoles.

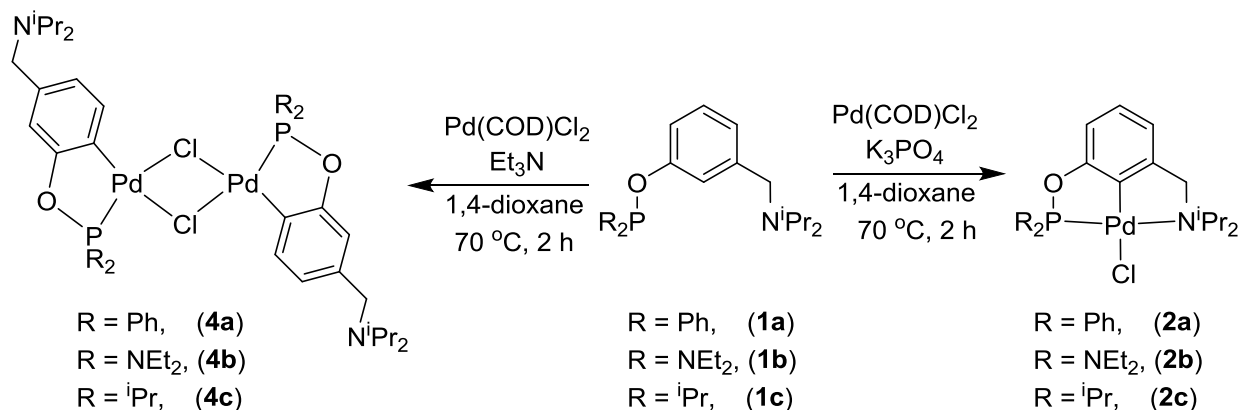
2.2 RESULTS AND DISCUSSION

2.2.1 Synthesis of Ligands. The $R^2\text{POCN}^{i\text{Pr}}_2\text{-H}$ [3-R₂PO-C₆H₄-1-CH₂NⁱPr₂ (R = Ph, **1a**; R = Et₂N, **1b**)] pincer ligands were synthesized following the procedure similar to the synthesis of analogous compounds.⁵³ Hence, the treatment of 3-((diisopropylamino)methyl)phenol with NaH, followed by the reaction with relevant chlorophosphine produced the hybrid ligands **1a** and **1b** in good yields (Scheme 2.1). The ³¹P{¹H} NMR spectra of **1a** and **1b** showed single resonances at 109.7 and 131.8 ppm, respectively; which were comparable with the ³¹P NMR data of the similar compounds *i.e.* ^{Ph}4POCOP-H¹² (δ_P 114.0 ppm) and 4-Me-C₆H₄-OP(NEt₂)₂⁵⁴ (δ_P 133.0 ppm). In the ¹H NMR spectra of both the compounds, the -CH₂ protons on -CH₂NⁱPr₂ group appeared around 3.60 ppm as singlets. Further, the assigned molecular structures of the compounds **1a** and **1b** are consistent with the observed ¹H and ¹³C NMR data. These compounds were used for the metallation reactions without further purification.



Scheme 2.1 Synthesis of POCN–H ligands.

2.2.2 Synthesis of Palladacycle Complexes. Following previous protocol for the synthesis of POCN pincer-palladium complexes,⁵³ the reactions of **1a** and **1b** with Pd(COD)Cl₂ in the presence of inorganic base K₃PO₄ in 1,4-dioxane produced the pincer-ligated complexes { $\kappa^P, \kappa^C, \kappa^N$ -2-(R₂PO)-C₆H₃-6-(CH₂NⁱPr₂)}PdCl [(^{R2}POCN^{iPr2})PdCl; R = Ph (**2a**) and R = Et₂N (**2b**)] (Scheme 2.2). The ³¹P{¹H} NMR spectra of **2a** and **2b** displayed singlets at 150.0 and 142.3 ppm, respectively. In the ¹H NMR spectrum of **2a**, the -CH₃ protons (12H) of isopropyl groups appeared as two set of doublets in contrast to a single set of doublet observed for the same (12H) in **1a**, which could be due to the magnetic non-equivalency of -CH₃ protons, generated upon the coordination of N-arm of the ligand to the palladium center. The two -CH protons on the isopropyl groups appeared as an octet, which might be due to the partial overlapping of the two septets for each -CH of the -N{CH(CH₃)₂}₂ group. Similarly, the -CH₃ protons on isopropyl groups of the **2b** resonate differently and appeared as two distinct doublets. The appearance of two set of doublets for the -CH₃ protons on -N{CH(CH₃)₂}₂ groups in the complexes **2a** and **2b**, in contrast to single set of doublet in the ligands **1a** and **1b**, could be considered as an indication of the nitrogen-arm coordination to the palladium center. Further, the peak of -CH₂ protons on the -CH₂NⁱPr₂ group of **2a** and **2b** deshielded (~ 0.4 ppm) compared to the respective ligands, and appeared around 4.0 ppm as singlets. The POCN-pincer palladium complexes **2a** and **2b** were further characterized by ¹³C NMR, MALDI-TOF measurements and elemental analyses. The proton and carbon peaks chemical shift in both the complexes were fully assigned by the 2D NMR studies, after establishing the atom connectivity and spatial relationship. The molecular structures of **2a** and **2b** were also established by the single crystal X-ray diffraction studies.

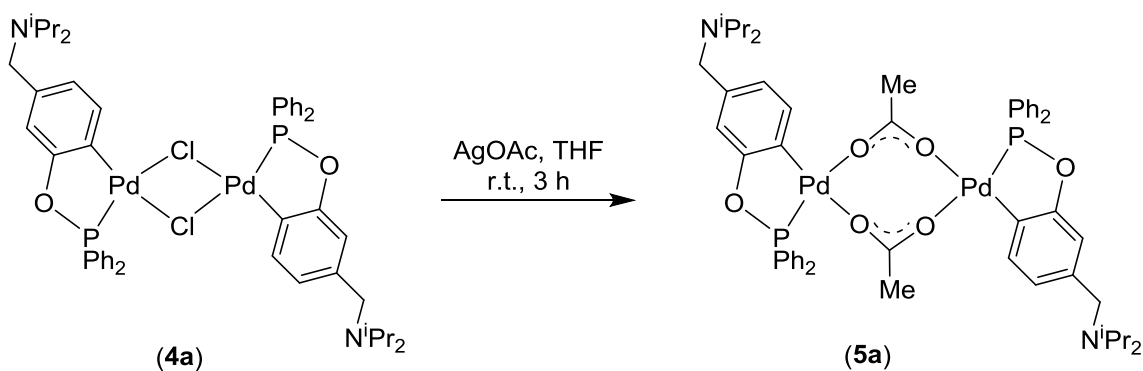


Scheme 2.2 Synthesis of palladacycle complexes.

To our surprise, the reaction of **1a**, **1b** and **1c**⁵³ with Pd(COD)Cl₂ in the presence of Et₃N as base in 1,4-dioxane produced the binuclear *ortho*-palladated complexes [$\{\kappa^P, \kappa^C$ -2-(R₂PO)-C₆H₃-4-(CH₂NⁱPr₂) $\}(\mu\text{-Cl})\text{Pd}]_2$ (R = Ph (**4a**), Et₂N (**4b**), ⁱPr (**4c**)), with the chloride as a bridging ligand between the two palladium centers (Scheme 2.2). In the binuclear complexes (**4a**, **4b** and **4c**), each palladium center is coordinated by the P-atom, and the C-atom that is *ortho* to –OPR₂ and *para* to –CH₂NⁱPr₂ group. Unlike the pincer-ligated complexes **2a**, **2b**, and **2c**,⁵³ the N-arm of the ligand in binuclear complexes (**4a**, **4b** and **4c**) does not involved in the coordination to palladium center. It should be noted that the triethylamine (Et₃N) is commonly used as a base for the synthesis of pincer-ligated palladium complexes; however, in the current ligand systems the formation of non-pincer *ortho*-palladated binuclear complexes were observed in the presence of Et₃N, even though the ligands are of pincer-type. To our knowledge, this represents the first example of a base-assisted site selective palladation to accomplish both the bidentate-coordinated palladacycles (**4a-4c**) and tridentate-coordinated pincer palladium complexes (**2a-2c**) from the pincer-type ligands, though the site selective palladation has been known by the introduction of an activating group (i.e. –SiMe₃).^{49-52,55,56} The ³¹P NMR spectrum of **4a** displayed two singlets at 152.9 and 152.2 ppm in 1.5 : 1 ratio. The two different peaks could be due to the existence of *cis* and *trans* isomers for the complex **4a** in solution.⁵⁷ Though, the ³¹P NMR data of **4a** is suggestive of two isomers, the ¹H NMR spectrum displayed a single set of peaks. The –CH₃ protons on the –NⁱPr₂ group showed only one broad singlet at 1.00 ppm, suggesting the N-arm of the ligand is not involved in the coordination to Pd-center. Further, the peak at 3.55 ppm for the

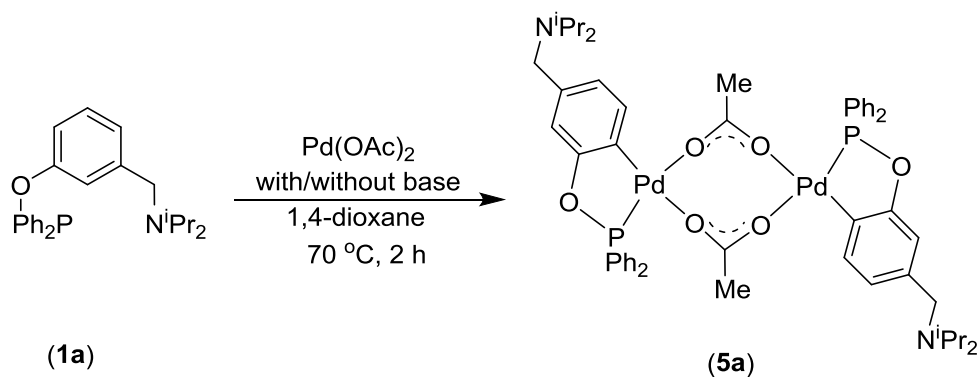
$-\text{CH}_2$ protons on $-\text{CH}_2\text{N}^i\text{Pr}_2$ group is indicative of a non-coordinating N-arm. The MALDI-TOF spectrum of **4a** displayed the molecular ion peak at 1063.3624, which is consistent with the existence of a binuclear complex. Similar to the complex **4a**, the ^{31}P NMR spectrum of binuclear complex **4b** displayed two singlets at 137.7 (76%) and 137.9 (24%) ppm for the two different isomers. The ^1H NMR spectrum showed a single set of peaks and the splitting pattern of the proton peaks resemble to that observed for a non-coordinating $-\text{CH}_2\text{N}^i\text{Pr}_2$ group. The ^{31}P NMR spectrum of the complex **4c** showed two singlets at 200.0 and 199.0 ppm for the presumed two isomers in 1.9:1 ratio. The ^1H NMR spectrum exhibited a single set of peaks with the distinctive of non-coordinated $-\text{CH}_2\text{N}^i\text{Pr}_2$ and coordinated $-\text{OP}^i\text{Pr}_2$ groups. The MALDI-TOF measurement displayed the peaks at 1043.4058 $(\text{M}+\text{H})^+$ and 927.3241 $(\text{M}+\text{H})^+$ for the binuclear complexes **4b** and **4c**, respectively.

To synthesize the derivative of a binuclear complex, the complex **4a** was treated with AgOAc which generated the acetate-bridged binuclear complex $[\{\kappa^P, \kappa^C\text{-}2\text{-(Ph}_2\text{PO)-C}_6\text{H}_3\text{-}4\text{-(CH}_2\text{N}^i\text{Pr}_2)\}(\mu\text{-OAc})\text{Pd}]_2$ (**5a**) (Scheme 2.3). The ^{31}P NMR spectrum of **5a** displayed a singlet at 151.0 ppm, which is slightly shielded than that observed for the chloro-bridged complex **4a**. Unlike the complex **4a**, the acetate-bridged binuclear complex **5a** exists as a single isomer in solution as indicated from the ^{31}P NMR data. The ^1H NMR data of **5a** resembled with that of the **4a**, except that the $-\text{CH}_3$ protons of bridged-acetate show a singlet at 2.17 ppm. Further, the ^{13}C NMR data and elemental analysis of **5a** is in good agreement with the assigned structure. The molecular structure of complex **5a** was further confirmed by X-ray diffraction study.



Scheme 2.3 Synthesis of acetate-bridged binuclear palladium complex **5a**.

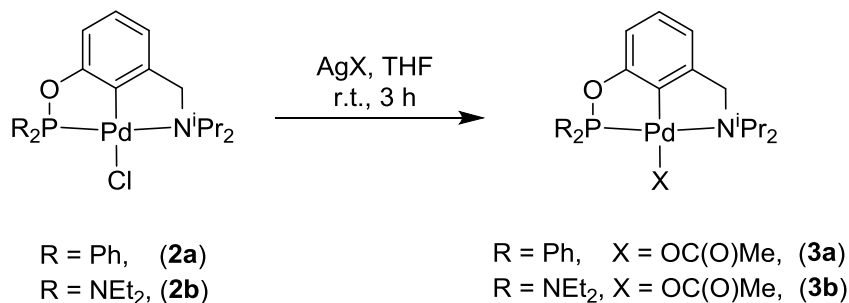
In a different note, the C–H bond palladation of the ligand $R^2\text{POCN}^{i\text{Pr}^2}\text{-H}$ was explored with other palladium precursor like $\text{Pd}(\text{OAc})_2$. Surprisingly, the reaction of $\text{Ph}^2\text{POCN}^{i\text{Pr}^2}\text{-H}$ (**1a**) with $\text{Pd}(\text{OAc})_2$ in the presence of K_3PO_4 produced the *ortho*-palladated binuclear complex **5a**, rather than the expected mono-nuclear pincer complex (Scheme 2.4). Further, the same reaction in the presence of Et_3N or even in the absence of a base afforded the binuclear complex **5a**. These results indicated that the base has no influence on the regioselective palladation of the ligand **1a** while $\text{Pd}(\text{OAc})_2$ is used as a palladium source. This distinct reactivity of **1a** with $\text{Pd}(\text{OAc})_2$ than with the $\text{Pd}(\text{COD})\text{Cl}_2$ towards the regioselective palladation can be attributable to the electrophilic character of $\text{Pd}(\text{OAc})_2$. The high electrophilicity of $\text{Pd}(\text{OAc})_2$ could accelerate the electrophilic attack of the Pd-center on arene ring of the POCN–H ligand after the P-arm coordination, leading to complex **5a**, rather than allowing both the P- and N-arm coordination and $\text{C}_{\text{ipso}}\text{-H}$ bond palladation.



Scheme 2.4 Reactivity of **1a** with $\text{Pd}(\text{OAc})_2$.

2.2.3 Derivatives of Pincer Palladacycle. The treatment of $(\text{POCN})\text{PdCl}$ complexes **2a** and **2b** with AgOAc in THF at room temperature resulted in the formation of complexes $\{\kappa^P, \kappa^C, \kappa^N\text{-}2\text{-}(\text{R}_2\text{PO})\text{-C}_6\text{H}_3\text{-}6\text{-(CH}_2\text{N}^i\text{Pr}_2)\}\text{Pd}(\text{OAc})$ [$\text{R} = \text{Ph}$ (**3a**) and $\text{R} = \text{Et}_2\text{N}$ (**3b**)] in good yields (Scheme 2.5). The ^{31}P NMR spectra of the complexes **3a** and **3b** displayed single resonances at 143.8 and 142.3 ppm, respectively. In the ^1H NMR spectra, the $-\text{OCOCH}_3$ protons appeared as singlets at 1.86 and 1.92 ppm for **3a** and **3b**, respectively. Other ^1H and ^{13}C NMR peaks for the complexes **3a** and **3b** as well as their splitting patterns are largely resembled with that observed in the

respective spectra of the complexes **2a** and **2b**. Moreover, the MALDI-TOF and elemental analyses of both the complexes are in accord with the assigned molecular structures. The complexes **3a** and **3b** were further characterized by ^{13}C NMR, elemental analyses and single crystal X-ray diffraction studies.

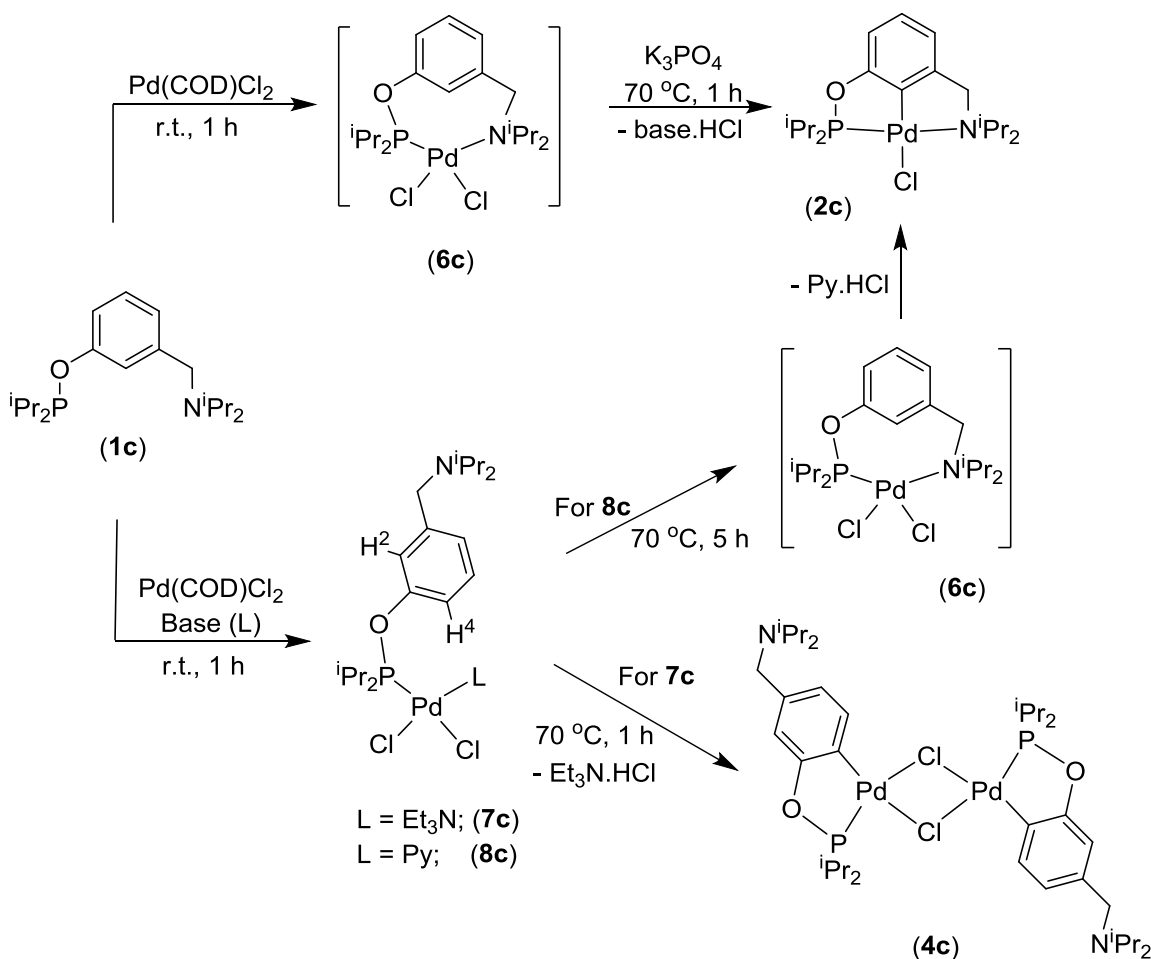


Scheme 2.5 Synthesis of POCN-pincer palladium derivatives.

2.2.4 Mechanistic Aspects of Regioselective Palladation. The reactions of the ligands **1a-1c** with $\text{Pd}(\text{COD})\text{Cl}_2$ in the presence of K_3PO_4 produce the pincer complexes **2a-2c** by the arene C(2)-H bond activation of the 1,3-donor group substituted ligands **1a-1c**, whereas the similar reactions in the presence of triethylamine exclusively furnished the non-pincer *ortho*-palladated binuclear complexes **4a-4c** through the C(4)-H bond activation, leaving the N-arm non-coordinated. In view of the synthetic aspect of the palladacycle complexes, this regioselective C-H bond palladation is unique as a base could decide the outcome of the products formation, *i.e.* mononuclear pincer complex or binuclear non-pincer complex. This distinct reactivity of the hybrid ligands **1a-1c** motivated us to investigate the mechanistic aspects of the regioselective palladation reaction. We have chosen **1c** as a model ligand to study its reactivity with $\text{Pd}(\text{COD})\text{Cl}_2$ under controlled reaction conditions, and the progress of the reaction was monitored by the ^{31}P NMR analysis. Initially, the ligand **1c** was treated with $\text{Pd}(\text{COD})\text{Cl}_2$ in 1,4-dioxane in the absence of base at room temperature (Scheme 2.6). After 1 h, the ^{31}P NMR spectrum of the crude reaction mixture displayed two singlets at 198.2 and 141.6 ppm. The peak at 198.2 ppm corresponds to the pincer-ligated complex **2c**. The phosphorous peak at δ_{P} 141.6 ppm was tentatively assigned for the intermediate complex **6c**, as the HRMS (ESI) measurement of the crude reaction mixture showed a mass peak at m/z 522.0696 (m/z Calcd for $[\mathbf{6c}+\text{Na}]^+ =$

522.0682). Several attempts to isolate the pure product of **6c** were unsuccessful, as the reactions were always resulted with the mixture of both **2c** and **6c**. However, upon addition of K_3PO_4 to the reaction mixture, a clean conversion of the mixture to the compound **2c** was occurred at elevated temperature. This suggests that the chelate complex **6c** is most likely an active intermediate for the formation of pincer-complex **2c** in the presence of K_3PO_4 . Similar type of chelate complex intermediate $[\kappa^S, \kappa^S-(MeS-CH_2)_2-C_6H_4-PdCl_2]$ for the synthesis of symmetrical pincer complex $[\kappa^S, \kappa^C, \kappa^S-(MeS-CH_2)_2-C_6H_3-PdCl]$ has previously been described.³⁰ Further, to understand the effect of Et_3N on the palladation reaction, the ligand **1c** was treated with $Pd(COD)Cl_2$ in the presence of Et_3N (1.2 equiv) in 1,4-dioxane at room temperature and the progress of the reaction was monitored by ^{31}P NMR analysis. After stirring the reaction mixture for 1 h, the ligand peak at δ_P 148.8 ppm completely disappeared and the formation of a new peak at δ_P 143.6 ppm was observed, with a minor formation of the complex **4c** (δ_P 200.6 ppm). The peak at δ_P 143.6 ppm was tentatively assigned to the intermediate palladium complex **7c** (Scheme 2.6), as the phosphorous ligands environment in **6c** and **7c** are almost similar and the ^{31}P NMR chemical shifts for both of them were around in the same region (δ_P 141.6 and 143.6 ppm). Attempt to the isolation and characterization of the presumed intermediate **7c** was unsuccessful, as the probable hemilabile species **7c** was completely transformed into the thermodynamically stable product **4c** during the work-up process. Assuming that the hemilabile nature of Et_3N ligand might play a role in the instability of **7c**, the ligand **1c** was treated with $Pd(COD)Cl_2$ in the presence of pyridine (1.2 equiv) in 1,4-dioxane. After the reaction mixture was stirred at room temperature for 1 h, the ^{31}P NMR measurement of the reaction mixture displayed a peak at 144.9 ppm with the complete disappearance of the peak correspond to **1c**. The ^{31}P NMR peak at 144.9 ppm was assigned to the complex **8c**. The compound **8c** was isolated and fully characterized by the major spectroscopic techniques. In the 1H NMR spectrum of **8c**, the downfield shift (ca. 0.6 ppm) of the C(2)-H and C(6)-H protons on pyridine moiety suggests the pyridine ligand coordination to the palladium center. Further, the HRMS (ESI) analysis of the complex **8c** confirmed the assigned molecular structure. Since the ^{31}P NMR chemical shifts of the three intermediate complexes (**6c**, **7c** and **8c**) were around the same region, we assumed that the assigned structures for these intermediates are appropriate. To our surprise, when the complex **8c** was heated in 1,4-dioxane at 70 °C for 5 h, the formation of pincer complex **2c** was

observed, instead of the expected *ortho*-palladacycle complex **4c**. The formation of the pincer complex **2c** from the intermediate **8c** can be attributable to the easy displacement of the less bulky pyridine ligand by the $-\text{CH}_2\text{N}^i\text{Pr}_2$ ligand arm leading to the formation of an intermediate species **6c**, which is followed by the C(2)–H bond palladation. However, in the case of intermediate **7c**, the steric hindrance between $-\text{CH}_2\text{N}^i\text{Pr}_2$ group and coordinated Et_3N ligand might keep the $-\text{CH}_2\text{N}^i\text{Pr}_2$ unit away from the palladium center and allow the C(4)–H bond activation to produce the complex **4c**.



Scheme 2.6 Proposed pathway for the formation of "PC"- and "POCN"-palladacycles.

Further to gain more insight into the influence of bases during the course of C–H bond palladation reaction, the kinetics of the electrophilic palladation step in the formation of **2c** and **4c** from the **6c** (or **8c**) and **7c**, respectively, were determined. All the kinetic experiments were performed after being the in-situ generation of the intermediate species **6c**, **7c** and **8c**. Initially the rates for the formation of products **2c** and **4c** were determined by employing one equiv of bases K_3PO_4 , Et_3N and pyridine. The reaction profile for the C–H bond palladation on **6c**, **7c** and **8c** over a period of 45 min is shown in Figure 2.1. As displayed, the rate for the formation of **4c** from the **7c** ($1.14 \times 10^{-3} \text{ Mmin}^{-1}$) is approximately four times faster than the formation of **2c** from the **8c** ($0.296 \times 10^{-3} \text{ Mmin}^{-1}$). This indicates that the Et_3N base was dissociated faster than the pyridine from the respective species **7c** and **8c**.

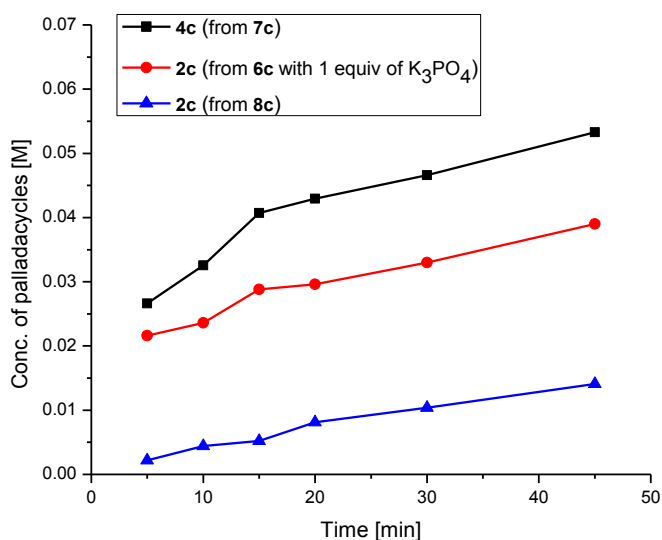


Figure 2.1 Reaction profile for the C–H bond palladation of **6c**, **7c** and **8c** at 70 °C.

Again, the kinetic of the C–H bond palladation was studied by determining the rates of palladacycle formation with varying concentration of bases using the initial rate approximation. Figure 2.2 shows the rate of the palladation reaction is almost same for the various concentration of the K_3PO_4 , suggesting the reaction is zeroth-order in the concentration of K_3PO_4 . Notably, the rates of the C–H bond palladation reactions in **7c** and **8c** decreases with the increased concentration of Et_3N and pyridine (Figure 2.3 and Figure 2.4). These results suggest that the

dissociation of the coordinated bases from the species **7c** and **8c** might be suppressed with the high concentration of bases (Et_3N and pyridine).

Rate Order Determination for K_3PO_4 (Table 2.1, Figure 2.2): To determine the order of the palladation reaction on K_3PO_4 , the initial rates at different initial concentrations (1 equiv, 3 equiv, 10 equiv) of K_3PO_4 were recorded. The final data was obtained by averaging the results of two independent trials for each experiment.

Table 2.1 Rate of Arylation Reaction at Different Initial Concentrations of K_3PO_4

Experiment	Conc. of K_3PO_4 [equiv]	Initial rate [Mmin^{-1}] $\times 10^{-3}$
1	1.0	0.466
2	3.0	0.302
3	10.0	0.360

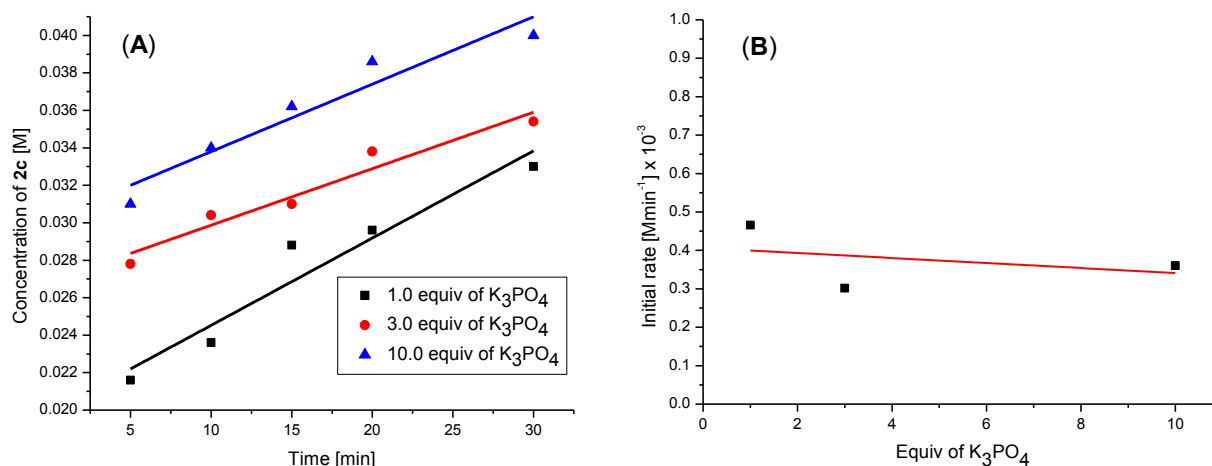


Figure 2.2 (A) Time-dependent yields of the palladacycle **2c** at different loading of K_3PO_4 . (B) The dependence of initial palladation reaction rates on the loading of K_3PO_4 .

Rate Order Determination for Et_3N (Table 2.2, Figure 2.3): To determine the order of the palladation reaction on Et_3N , the initial rates at different initial concentrations (0.074, 0.222, 0.444 and 0.742 [M]) of Et_3N were recorded. The final data was obtained by averaging the results of two independent trials for each experiment.

Table 2.2 Rate of Arylation Reaction at Different Initial Concentrations of Et₃N

Experiment	Conc. of Et ₃ N [M]	Initial Rate [Mmin ⁻¹] x 10 ⁻³
1	0.074	1.14
2	0.222	1.69
3	0.444	0.80
4	0.742	0.702

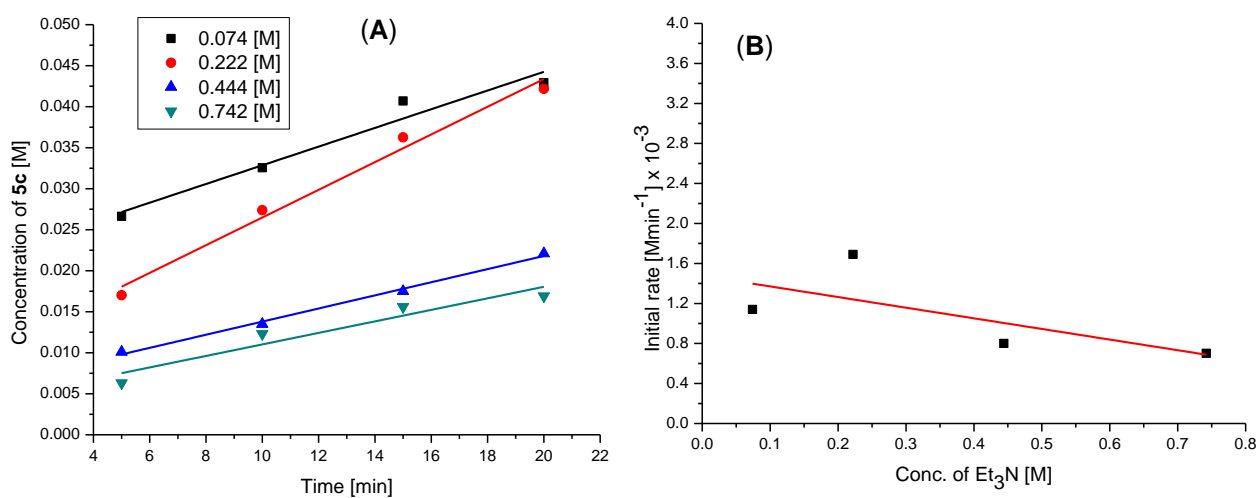


Figure 2.3 (A) Time-dependent yields of the palladacycle **5c** at different concentration of Et₃N. (B) The dependence of initial palladation reaction rates on the concentration of Et₃N.

Rate Order Determination for pyridine (Table 2.3, Figure 2.4): To determine the order of the palladation reaction on pyridine, the initial rates at different initial concentrations (0.074, 0.222, 0.444 and 0.742 [M]) of pyridine were recorded. The final data was obtained by averaging the results of two independent trials for each experiment.

Table 2.3 Rate of Arylation Reaction at Different Initial Concentrations of pyridine

Experiment	Conc. of pyridine [M]	Initial rate [Mmin^{-1}] $\times 10^{-3}$
1	0.074	0.296
2	0.222	0.280
3	0.444	0.135
4	0.742	0.134

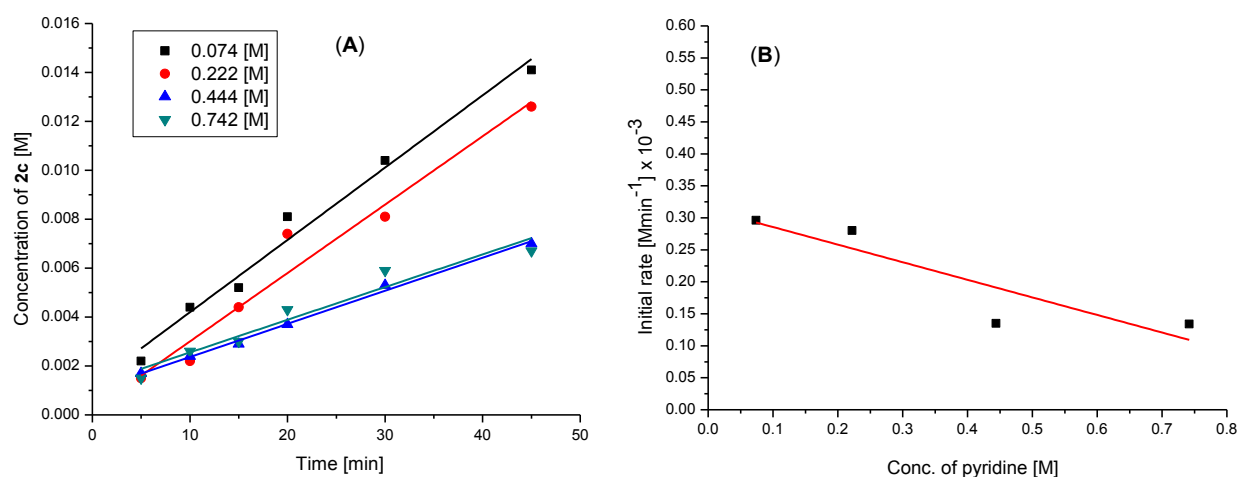


Figure 2.4 (A) Time-dependent yields of the palladacycle **2c** at different concentration of pyridine. (B) The dependence of initial palladation reaction rates on the concentration of pyridine.

On the basis of all the experimental findings, the pathway for the formation “POCN”-pincer palladium and “PC”-chelate palladium complex can drawn as shown in scheme 2.6. Thus, the formation of pincer complex **2c** occurred *via* the chelate intermediate species **6c** in the presence of an inorganic base K_3PO_4 , whereas the binuclear complex **4c** was formed *via* the Lewis base-coordinated intermediate **7c**. Notably, the Lewis base-coordinated intermediate might leads to the formation of pincer complex (as seen in the case of **8c**), provided the dangling non-coordinated arm ($-\text{CH}_2\text{N}^i\text{Pr}_2$) displaced the coordinated-base (L) and generates the chelate species **6c**. Hence, we proposed that the primary requirement for the synthesis of a chloro-bridged binuclear complex could be the use of a coordinating Lewis base (L); and secondly, the substantial steric hindrance between the coordinated-base and the dangling arm ($-\text{CH}_2\text{N}^i\text{Pr}_2$) to

avoid the formation of intermediate **6c**. We assume that the steric between the N-arm ($-\text{CH}_2\text{N}^i\text{Pr}_2$) and coordinated ligand (L) was very crucial to the specific palladacycle formation, than the electronic factor (Et_3N vs Py). This can be further outlined on the fact that the ligand **1c** reacted with $\text{Pd}(\text{COD})\text{Cl}_2$ and Et_3N to produces the non-pincer complex **4c**; whereas a slightly less bulky ligand $\text{Ph}_2\text{PO}-\text{C}_6\text{H}_4-\text{CH}_2\text{NET}_2$ upon the reaction with PdCl_2 and Et_3N , generated the pincer-ligated palladium complex.

2.2.5 Molecular Structure of Palladium Complexes. The crystals of the complexes **2a**, **2b**, **3a**, **3b** and **5a**, suitable for the X-ray diffraction study were obtained from the slow evaporation of petroleum ether solution of the complexes at room temperature. The ORTEP diagrams are shown in Figure 2.5-2.9 and the selected bond lengths and bond angles are given in the respective figure captions. In the structures of **2a** and **2b**, the geometry around the palladium is distorted square planar. The Pd–C bond lengths, 1.9514(16) and 1.960(2) Å in **2a** and **2b**, respectively; are comparable with the Pd–C bond length (1.957(2) Å) in the similar complex (3-MeO- $\text{Ph}_2\text{POCN}^{\text{Me}_2}$) PdCl .⁴¹ The Pd–Cl bond length (2.3848(4) Å) in **2a** is slightly shorter than the Pd–Cl bond length (2.4082(6) Å) observed in **2b**, which might be due to the σ -donor strength exerted by the ($^{\text{Et}_2\text{N}}_2\text{POCN}^{i\text{Pr}_2}$) moiety upon the palladium in **2b** being stronger than that of the ($^{\text{Ph}_2}\text{POCN}^{i\text{Pr}_2}$) moiety in complex **2a**. The Pd–P bond length (2.1885(4) Å) in **2a** is comparable with that of the complex (3-MeO- $\text{Ph}_2\text{POCN}^{\text{Me}_2}$) PdCl (Pd–P = 2.1858(6) Å).⁴¹ However, the Pd–P bond length (2.1951(6) Å) in **2b** is significantly shorter than the Pd–P bond lengths (2.284(2), 2.277(2) Å) in the symmetrical pincer complex ($^{\text{Et}_2\text{N}}_4\text{POCOP}$) PdI .²⁷ The Pd(1)–N(1) bond length (2.2032(13) Å) in **2a** is slightly shorter than the Pd(1)–N(1) bond length (2.2204(17) Å) in ($^{i\text{Pr}_2}\text{POCN}^{i\text{Pr}_2}$) PdCl , whereas the Pd(1)–N(1) bond length (2.2361(16) Å) in **2b** is slightly longer than that observed in complex ($^{i\text{Pr}_2}\text{POCN}^{i\text{Pr}_2}$) PdCl .⁵³ For the complexes **2a** and **2b**, the P–Pd–N bond angles are 161.10(4) and 161.30(5)°, respectively; which are smaller than the corresponding bond angle (P–Pd–N, 162.10(5)°) in the ($^{i\text{Pr}_2}\text{POCN}^{i\text{Pr}_2}$) PdCl complex.

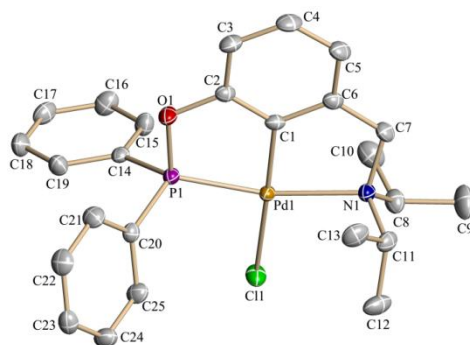


Figure 2.5 Thermal ellipsoid plot of $(\text{Ph}_2\text{POCN}^{\text{iPr}_2})\text{PdCl}$ (**2a**). All the hydrogen atoms are omitted for clarity. Selected bond lengths (Å): Pd(1)–C(1), 1.9514(16); Pd(1)–P(1), 2.1885(4); Pd(1)–N(1), 2.2032(13); Pd(1)–Cl(1), 2.3848(4). Selected bond angles (°): C(1)–Pd(1)–P(1), 80.52(5); C(1)–Pd(1)–N(1), 81.72(6); P(1)–Pd(1)–N(1), 161.10(4); C(1)–Pd(1)–Cl(1), 176.08(5); P(1)–Pd(1)–Cl(1), 98.672(16); N(1)–Pd(1)–Cl(1), 99.48(4).

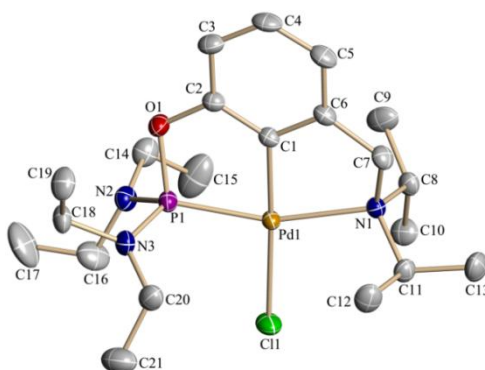


Figure 2.6 Thermal ellipsoid plot of $(\text{Et}_2\text{N})_2\text{POCN}^{\text{iPr}_2}\text{PdCl}$ (**2b**). All the hydrogen atoms are omitted for clarity. Selected bond lengths (Å): Pd(1)–C(1), 1.960(2); Pd(1)–P(1), 2.1951(6); Pd(1)–N(1), 2.2361(16); Pd(1)–Cl(1), 2.4082(6). Selected bond angles (°): C(1)–Pd(1)–P(1), 80.26(6); C(1)–Pd(1)–N(1), 81.09(8); P(1)–Pd(1)–N(1), 161.30(5); C(1)–Pd(1)–Cl(1), 176.84(6); P(1)–Pd(1)–Cl(1), 97.42(2); N(1)–Pd(1)–Cl(1), 101.27(5).

For the complexes **3a** and **3b**, the coordination geometry around the palladium is slightly distorted from the expected square planar geometry. The acetate ligand in both the complexes binds as η^1 -coordinated fashion, and the Pd–O bond lengths (2.084(2) Å in **3a**, 2.1247(12) Å in **3b**) are similar to those found in other examples of palladium-acetate complexes, wherein the acetate ligand is *trans* to aryl groups.^{58,59} The Pd–C bond lengths (1.952(3) and 1.9510(17) Å) in **3a** and **3b** are comparable with the Pd–C bond lengths in their halide counterparts **2a** and **2b**, which is in line with the similar *trans* influence of both chloride and acetate ligands. However, the Pd–P bond lengths (2.2136(8) and 2.2140(5) Å) in the **3a** and **3b** are slightly longer than the corresponding Pd–P bond lengths in halide derivatives **2a** and **2b**. The P(1)–Pd(1)–O(2) bond angles in **3a** and **3b** are 102.90(6)° and 102.48(4)°, whereas the N(1)–Pd(1)–O(2) bond angles are 93.34(9)° and 95.14(5)°. This indicates that the O(2) atom of OC(O)CH₃ ligand is aligned more towards N-arm than the P-arm, whereas the carbonyl oxygen O(3) is closer to the P-center than the N-center in both the complexes **3a** and **3b**.

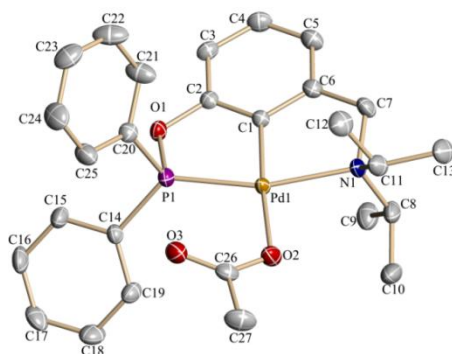


Figure 2.7 Thermal ellipsoid plot of (^{Ph}₂POCN^{iPr}₂)PdOAc (**3a**). All the hydrogen atoms are omitted for clarity. Selected bond lengths (Å): Pd(1)–C(1), 1.952(3); Pd(1)–P(1), 2.2136(8); Pd(1)–N(1), 2.207(2); Pd(1)–O(2), 2.084(2); C(26)–O(2), 1.276(4); C(26)–O(3), 1.243(4). Selected bond angles (°): C(1)–Pd(1)–P(1), 81.21(8); C(1)–Pd(1)–N(1), 82.44(10); P(1)–Pd(1)–N(1), 162.89(6); C(1)–Pd(1)–O(2), 175.64(10); P(1)–Pd(1)–O(2), 102.90(6); N(1)–Pd(1)–O(2), 93.34(9).

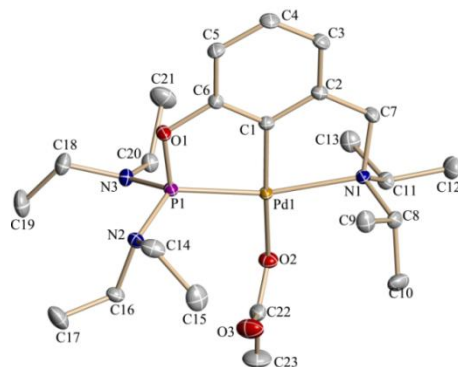


Figure 2.8 Thermal ellipsoid plot of $(\text{Et}^2\text{N})_2\text{POCN}^{\text{iPr}2}\text{PdOAc}$ (**3b**). All the hydrogen atoms are omitted for clarity. Selected bond lengths (Å): Pd(1)–C(1), 1.9510(17); Pd(1)–P(1), 2.2140(5); Pd(1)–N(1), 2.2295(14); Pd(1)–O(2), 2.1247(12). Selected bond angles (°): C(1)–Pd(1)–P(1), 80.77(6); C(1)–Pd(1)–N(1), 81.97(7); P(1)–Pd(1)–N(1), 162.35(4); C(1)–Pd(1)–O(2), 170.84(6); P(1)–Pd(1)–O(2), 102.48(4); N(1)–Pd(1)–O(2), 95.14(5).

In the binuclear palladium complex **5a**, each palladium center is ligated with one P-center, one C-center and the third and fourth coordination sites are occupied by the oxygen-atoms of two bridged acetate ligands to form a C_2 -symmetry molecule. Both the palladium centers are slightly distorted from the expected square planar geometry. The five-membered palladacycle rings containing Pd-, P- and O-atoms are in *transoid* conformation.⁵⁷ The eight-membered ring containing two palladium and two acetate ligands form a boat conformation, with both the palladium occupying apical positions. The distance between the two palladium centers is 3.408 Å, which is longer than the sum of their van der Waals' radii (3.26 Å), and hence not considered as a bonding interaction. The Pd–C(1) bond length is 2.002(4) Å, which is slightly longer than the Pd–C bond length (1.952(3) Å) in pincer complex **3a**. The Pd–P(1) bond length (2.1730(12) Å) is significantly shorter than the Pd–P(1) bond length (2.216(1) Å) found in a similar palladacycle binuclear complex.¹⁰ The Pd–O(3) bond length (2.139(3) Å) *trans* to the Pd–C is slightly longer than the Pd–O(2) bond length (2.093(3) Å) located in the *cis* position, which could be due to the strong *trans* effect of the carbon compared to the phosphorus-atom ligand. The P–Pd–C bond angle is 79.51(12)°, whereas the O(2)–Pd–O(3) bond angle is a perfect right angle (90.06(11)°).

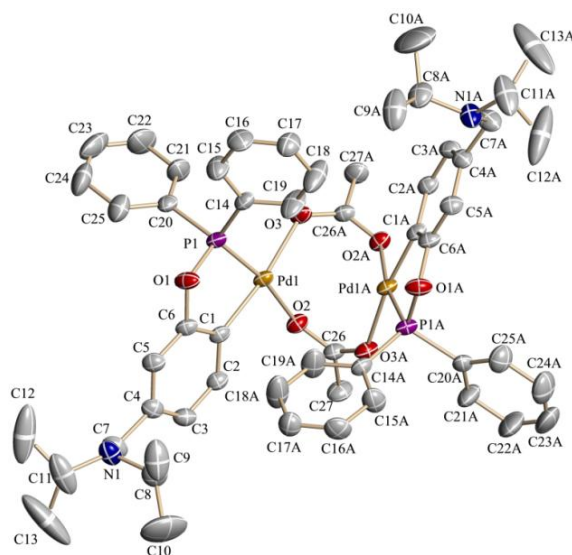
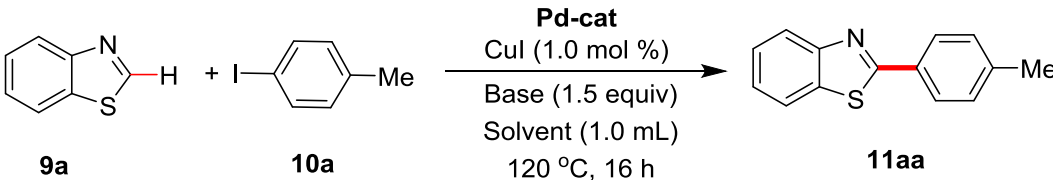


Figure 2.9 Thermal ellipsoid plot of complex **5a**. All the hydrogen atoms are omitted for clarity. Selected bond lengths (Å): Pd(1)–C(1), 2.002(4); Pd(1)–P(1), 2.1730(12); Pd(1)–O(2), 2.093(3); Pd(1)–O(3), 2.139(3); C(26)–O(3), 1.249(5); C(26)–O(3A), 1.253(5). Selected bond angles (°): C(1)–Pd(1)–P(1), 79.51(12); C(1)–Pd(1)–O(2), 92.23(15); P(1)–Pd(1)–O(2), 169.83(9); C(1)–Pd(1)–O(3), 171.83(14); P(1)–Pd(1)–O(3), 97.33(9); O(2)–Pd(1)–O(3), 90.06(11).

2.2.6 Catalytic Activity of Palladacycle for the Arylation of Azoles. All the complexes (**2a–5a**; 0.5 mol % for mononuclear complex, 0.25 mol % for binuclear complexes) were screened for the C–H bond arylation of benzothiazole (**9a**, 0.3 mmol) with 4-iodotoluene (**10a**, 0.45 mmol), employing CuI co-catalyst in the presence of K_3PO_4 in DMF as solvent (Table 2.4, Entries 1-11). Interestingly, the coupled product 2-(*p*-tolyl)benzothiazole (**11aa**) could be obtained in 93% isolated yield, when the binuclear palladacycle **4c** (0.25 mol %) was used as a catalyst in the presence of CuI and K_3PO_4 in DMF (Entry 6). Notably, the palladacycles containing $iPr_2POCN^{iPr_2}$ -ligand backbone (**2c** and **4c**) were shown superior activities than those having $Ph_2POCN^{iPr_2}$ -backbone (**2a**, **3a** and **4a**), whereas the palladacycles with $(Et_2N)_2POCN^{iPr_2}$ -backbone (**2b**, **3b** and **4b**) exhibited very poor catalytic performances (Entries 1-11). The use of Cs_2CO_3 base, which shown to be ideal base for the **2c**-catalyzed arylation, was less efficient with the

catalyst **4c**. The arylation reaction in the polar solvents like DMSO and DMA also gave moderate to good yields of coupled product (Entries 15-16).

Table 2.4 Screening of Catalysts and Reaction Parameters for Arylation of Azoles^a

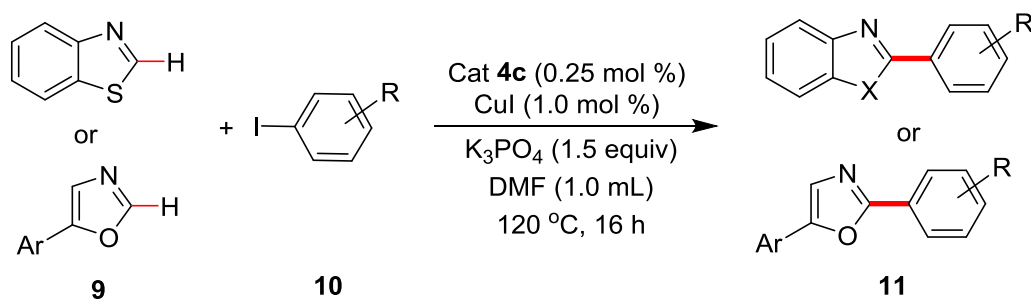


Entry	[Pd]	Base	Solvent	11aa (%) ^b
1	2a	K ₃ PO ₄	DMF	59
2	2b	K ₃ PO ₄	DMF	11
3	2c	K ₃ PO ₄	DMF	90 (88)
4	4a	K ₃ PO ₄	DMF	92
5	4b	K ₃ PO ₄	DMF	15
6	4c	K₃PO₄	DMF	95 (93)^c
7	3a	K ₃ PO ₄	DMF	58
8	3b	K ₃ PO ₄	DMF	4
9	5a	K ₃ PO ₄	DMF	79
10	4c	KOAc	DMF	46
11	4c	K ₂ CO ₃	DMF	50
12	4c	CS ₂ CO ₃	DMF	46
13	4c	K ₃ PO ₄	DMSO	85 (84) ^c
14	4c	K ₃ PO ₄	DMA	63
15	4c	K ₃ PO ₄	NMP	5
16	4c	K ₃ PO ₄	Toluene	29

^aReaction conditions: Benzothiazole (0.041 g, 0.3 mmol), 4-iodotoluene (0.098 g, 0.45 mmol), [Pd] (0.5 mol % per Pd), base (0.45 mmol), solvent (1.0 mL). ^bGC yields using *para*-xylene as internal standard, ^cisolated yields.

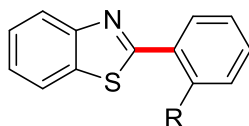
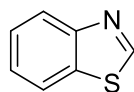
Having the optimized reaction conditions in hand, a number of substituted 5-aryl oxazoles were subjected to the direct arylation with 4-iodotoluene (Table 2.5, Entries 2-6). Hence, by employing 0.25 mol % of the catalyst **4c** and 1.0 mol % of CuI, the azoles containing electronically different aryl-substituents reacted efficiently with 4-iodotoluene to give the coupled products in good yields. Functional groups like -Cl, -CF₃ and -OMe as well as heteroarene substituent pyridine were tolerated on the azole substrates. Furthermore, the versatility of the catalyst **4c** in the arylation of azoles with the functionalized aryl iodide electrophiles was tested. Thus, the benzothiazole was very efficiently coupled with the aryl iodides bearing a variety of important functional groups, such as -OMe, -F, -Cl, -CF₃ and -CN (Table 2.5, Entries 7-11). The coupling of highly electron-deficient aryl iodides with benzothiazole gave very low yields of coupled products (**11ag**, **11ah**). The tolerability of -F, -Cl and -CN functional groups in the coupled products (**11ac**, **11ad**, **11af**) is very important, as they could be employed for further functionalization. The aryl iodides having *ortho*-substituents were also employed for the arylation, giving the desired products in moderate to good yields (Entries 14-16). Further, the heteroarene electrophiles also reacted with benzothiazole to produce the coupled products (**11ap**, **11aq**) in moderate yields.

Though, the palladacycle catalyst **4c** showed similar activity as the previously described pincer palladium catalyst **2c** for the arylation of azoles, the excellent performance of the catalyst **4c** in the presence of less expensive base (K₃PO₄) makes this catalyst superior. The C-H bond arylation of azoles were well preceded by *in situ* generated palladium catalysts employing high loading of the precious metal.⁶⁰⁻⁶³ However, the well-defined palladacycle **4c** catalyzes the arylation of azoles only with 0.25 mol % of the catalyst loading.

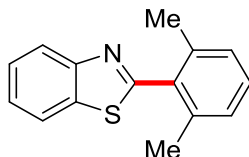
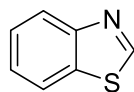
Table 2.5 Scope for the Arylation of Azoles Catalyzed by **4c**^a

entry	azoles (9)	product (11)	yield (%) ^b
1			93
2			64
3			67
4			75
5			87
6			81
7			R = OMe 96

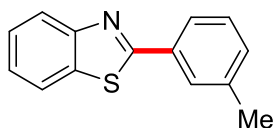
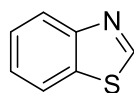
8		R = F	(11ac)	76
9		R = Cl	(11ad)	79
10		R = CF ₃	(11ae)	90
11		R = CN	(11af)	86
12		R = NO ₂	(11ag)	26
13		R = COOMe	(11ah)	37



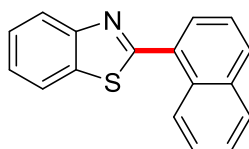
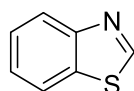
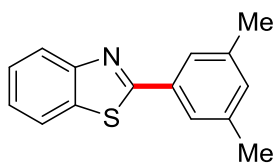
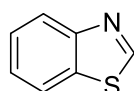
14		R = Me	(11ai)	91
15		R = OMe	(11aj)	72
16		R = Cl	(11ak)	79



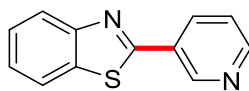
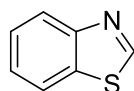
17			(11al)	40
18			(11am)	75



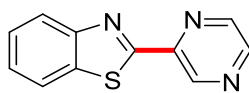
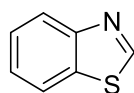
19			(11an)	65
20			(11ao)	97



21			(11ap)	54
----	--	--	--------	----



22			(11aq)	68
----	--	--	--------	----



^aReaction conditions: Azole (0.3 mmol), aryl iodide (0.45 mmol), K₃PO₄ (0.096 g, 0.45 mmol), catalyst **4c** (0.0007 g, 0.25 mol %), CuI (0.0006 g, 1.0 mol %), DMF (1.0 mL), 120 °C, 16 h.

^bYields of isolated compound

2.3 CONCLUSION

In summary, two unsymmetrical POCN ligands, and a series of mononuclear pincer palladium complexes and chloro-bridged binuclear palladacycles were synthesized *via* the regioselective C–H bond activation of the POCN–H ligands. Hence, the palladation reactions of the POCN–H ligands bearing isopropyl substituents on N-atom produced “PC”-palladacycles **4a–4c** in the presence of Et₃N, whereas the same ligands in the presence of K₃PO₄ or pyridine afforded “POCN”-pincer palladium complexes; *via* the selective activation of the arene C(4)–H and C(2)–H bond, respectively. All the palladacycles were fully characterized by multinuclear NMR studies and the molecular structures of many complexes were established by X-ray crystal structure determination. The influence of base on the regioselective C–H palladation to form chloro-bridged binuclear palladacycle or pincer palladium complex has been investigated, which suggests that the regioselectivity was dictated by the coordinating ability of the external base as well as the sterics between the base and nitrogen-ligand arm, rather than the electronics. The palladacycle **4c** shows excellent catalytic activity for the arylation of azoles with aryl iodides employing a relatively moderate and inexpensive base K₃PO₄, under the mild reaction conditions. A number of 5-aryl azoles and benzothiazole were arylated with substituted aryl iodides containing numerous functional groups (–F, –Cl, –CN, –CF₃ etc.).

2.4 EXPERIMENTAL SECTION

General Information. All manipulations were conducted under an argon atmosphere either in a glove box or using standard Schlenk techniques in pre-dried glass wares. The catalytic reactions were performed in flame-dried reaction vessels with rubber septa. Solvents were dried over Na/benzophenone or CaH₂ and distilled prior to use. DMF was dried over CaH₂, distilled under vacuum and stored over 4 Å molecular sieves. Liquid reagents were flushed with argon prior to use. The POCN-H ligand **1c**,⁵³ 3-((diisopropylamino)methyl)phenol,⁵³ and 5-aryl azoles⁶⁴ were synthesized according to previously described procedures. All other chemicals were obtained from commercial sources and were used without further purification. Yields refer to isolated compounds, estimated to be > 95% pure as determined by ¹H-NMR. TLC: TLC Silica gel 60 F₂₅₄. Detection under UV light at 254 nm. Chromatography: Separations were carried out on Spectrochem silica gel (0.120-0.250 mm, 60-120 mesh, for organic compounds) and neutral

alumina (for inorganic complexes). High resolution mass spectroscopy (HRMS) mass spectra were recorded on a Thermo Scientific Q-Exactive, Accela 1250 pump and MALDI-TOF mass spectra on AB SCIEX TOF/TOFTM 5800/4800 plus. M. p.: Büchi 540 capillary melting point apparatus, values are uncorrected. NMR (¹H and ¹³C) spectra were recorded at 400 or 500 (¹H), 100 or 125 (¹³C, DEPT (distortionless enhancement by polarization transfer)}, 377 (¹⁹F) and 162 or 202 MHz (³¹P{¹H}), respectively on Bruker AV 400 and AV 500 spectrometers in CDCl₃ solutions, if not otherwise specified; chemical shifts (δ) are given in ppm. The ¹H and ¹³C NMR spectra are referenced to residual solvent signals (CDCl₃: δ H = 7.26 ppm, δ C = 77.2 ppm) and ³¹P{¹H} NMR chemical shifts are referenced to an external standard, H₃PO₄ in D₂O solvent (δ 0.0 ppm), in a sealed capillary tube.

GC Method. Gas Chromatography analyses were performed using a Shimadzu GC-2010 gas chromatograph equipped with a Shimadzu AOC-20s autosampler and a Restek RTX-5 capillary column (30 m x 250 μm). The instrument was set to an injection volume of 1 μL, an inlet split ratio of 10:1, and inlet and detector temperatures of 250 and 320 °C, respectively. UHP-grade argon was used as carrier gas with a flow rate of 30 mL/min. The temperature program used for all the analyses is as follows: 80 °C, 1 min; 30 °C/min to 200 °C, 2 min; 30 °C/min to 260 °C, 3 min; 30 °C/min to 300 °C, 3 min.

Response factors for all the necessary compounds with respect to standard mesitylene were calculated from the average of three independent GC runs.

2.4.1 Synthesis of ^{R2}POCN^{iPr2}-H (R = Ph, **1a; R = Et₂N, **1b**).** To the suspension of NaH (0.30 g, 12.50 mmol) in THF (10 mL) was added a solution of 3-(diisopropylamino)methyl phenol (2.0 g, 9.65 mmol) in THF (20 mL) and the resulting mixture was refluxed at 70 °C for 3 h. After the reaction mixture was cooled to room temperature, a solution of chlorophosphine, R₂PCl (2.13 g, 9.65 mmol for R = Ph; 2.03 g, 9.65 mmol for R = Et₂N) in THF (20 mL) was added and resulting reaction mixture was further refluxed at 70 °C for 12 h. The reaction mixture was cooled to ambient temperature and volatiles were evaporated under reduced pressure. The compounds were extracted with *n*-hexane (60 mL x 3) and the combined *n*-hexane solutions were evaporated under vacuum to obtain oily products of ^{R2}POCN^{iPr2}-H.

Ph²POCN^{iPr2}-H (1a): Yield = 3.20 g, 85%; ¹H-NMR (500 MHz, CDCl₃): δ = 7.61-7.56 (m, 4H, Ar-H), 7.37-7.32 (m, 6H, Ar-H), 7.21 (s, 1H, Ar-H), 7.14 (dd, *J* = 7.9, 7.6 Hz, 1H, Ar-H), 7.01 (d, *J* = 7.3 Hz, 1H, Ar-H), 6.95 (d, *J* = 6.7 Hz, 1H, Ar-H), 3.58 (s, 2H, CH₂), 2.95 (sept, *J* = 6.7 Hz, 2H, CH(CH₃)₂), 0.96 (d, *J* = 6.4 Hz, 12H, CH₃); ¹³C-NMR (100 MHz, CDCl₃): δ = 157.4 (d, *J*_{P-C} = 9.0 Hz, C_q), 145.4 (C_q), 141.1 (d, *J*_{P-C} = 18.2 Hz, 2C, C_q), 130.7 (2C, CH), 130.5 (2C, CH), 129.6 (2C, CH), 129.0 (CH), 128.5 (d, *J*_{P-C} = 6.4 Hz, 4C, CH), 121.9 (CH), 118.1 (d, *J* = 10.9, CH), 116.6 (d, *J* = 10.0 Hz, CH), 48.8 (CH₂), 47.9 (2C, CH(CH₃)₂), 20.8 (4C, CH(CH₃)₂); ³¹P{¹H}NMR (202 MHz, CDCl₃): δ = 109.7 (s).

(Et₂N)²POCN^{iPr2}-H (1b): Yield = 3.10 g, 84%; ¹H-NMR (500 MHz, CDCl₃): δ = 7.14 (vt, *J* = 7.7 Hz, 1H, Ar-H), 7.07 (s, 1H, Ar-H), 6.97 (d, *J* = 7.3 Hz, 1H, Ar-H), 6.83 (d, *J* = 7.8 Hz, 1H, Ar-H), 3.60 (s, 2H, CH₂), 3.22-3.10 (m, 4H, CH₂CH₃), 3.09-2.95 (m, 4H, CH₂CH₃; 2H, CH(CH₃)₂), 1.05 (t, *J* = 6.8 Hz, 12H, N(CH₂CH₃)₂), 1.01 (d, *J* = 6.6 Hz, 12H, CH(CH₃)₂); ¹³C-NMR (100 MHz, CDCl₃): δ = 155.8 (d, *J*_{P-C} = 7.7 Hz, C_q), 144.9 (C_q), 128.7 (CH), 121.3 (CH), 118.9 (d, *J*_{P-C} = 10.8 Hz, CH), 117.4 (d, *J*_{P-C} = 9.3 Hz, CH), 48.9 (CH₂), 47.8 (2C, CH(CH₃)₂), 39.1 (d, *J*_{P-C} = 19.3 Hz, 4C, CH₂CH₃), 20.9 (4C, CH(CH₃)₂), 14.8 (d, *J*_{P-C} = 3.1 Hz, 4C, CH₂CH₃); ³¹P{¹H}NMR (202 MHz, CDCl₃): δ = 131.8 (s).

2.4.2 Synthesis of (^{R2}POCN^{iPr2})PdCl (R = Ph, **2a; R = Et₂N, **2b**).** A mixture of Pd(COD)Cl₂ (0.058 g, 0.203 mmol for compound **2a**; 0.15 g, 0.525 mmol for compound **2b**), appropriate amount of (^{R2}POCN^{iPr2})-H (0.079 g, 0.203 mmol of **1a**; 0.20 g, 0.525 mmol of **1b**) and K₃PO₄ (0.047 g, 0.223 mmol for compound **2a**; 0.122 g, 0.577 mmol for compound **2b**) was taken in a schlenk flask and 1,4-dioxane (20 mL) was added into it. The reaction mixture was heated at 70 °C for 2 h under argon atmosphere. The yellow suspension formed was cooled to ambient temperature, filtered through cannula and the volatile were evaporated under reduced pressure. The crude product was purified by column chromatography using neutral alumina (petroleum ether/EtOAc : 10/1). The X-ray quality single crystals were obtained by the slow evaporation of *petroleum ether* solution of the compounds at room temperature.

(Ph²POCN^{iPr2})PdCl (2a): Yield = 0.019 g, 18%; M. p. = 209 °C; ¹H-NMR (500 MHz, CDCl₃): δ = 8.03-7.99 (m, 4H, Ar-H), 7.52-7.44 (m, 6H, Ar-H), 6.98 (dd, *J* = 7.6, 7.3 Hz, 1H,

Ar-H), 6.72 (d, $J = 7.6$ Hz, 1H, Ar-H), 6.68 (d, $J = 7.3$ Hz, 1H, Ar-H), 4.14 (s, 2H, CH_2), 3.61 (apparent octet, $J = 6.1$ Hz, 2H, $\text{CH}(\text{CH}_3)_2$), 1.69 (d, $J = 6.1$ Hz, 6H, $\text{CH}(\text{CH}_3)_2$), 1.23 (d, $J = 6.1$ Hz, 6H, $\text{CH}(\text{CH}_3)_2$); ^{13}C -NMR (100 MHz, CDCl_3): $\delta = 162.1$ (d, $J_{\text{P-C}} = 10.0$ Hz, C_q), 153.6 (C_q), 144.5 (C_q), 133.8 (d, $J_{\text{P-C}} = 54.0$ Hz, 2C, C_q), 132.0 (4C, CH), 131.9 (2C, CH), 129.0 (d, $J_{\text{P-C}} = 13.2$ Hz, 4C, CH), 126.8 (CH), 115.4 (CH), 109.2 (d, $J_{\text{P-C}} = 17.7$ Hz, CH), 61.6 (CH_2), 57.6 (2C, $\text{CH}(\text{CH}_3)_2$), 22.8 (2C, $\text{CH}(\text{CH}_3)_2$), 19.7 (2C, $\text{CH}(\text{CH}_3)_2$); $^{31}\text{P}\{^1\text{H}\}$ NMR (202 MHz, CDCl_3): $\delta = 150.0$ (s); MALDI-TOF: m/z calcd for $\text{C}_{25}\text{H}_{29}\text{ClNOPPd-Cl}^+ [\text{M-Cl}]^+$ 496.1022, found 496.1617; elemental analysis calcd (%) for $\text{C}_{25}\text{H}_{29}\text{ClNOPPd}$: C 56.40, H 5.49, N 2.63; found: C 55.84, H 5.41, N 2.23.

(Et^2N) $^2\text{POCN}^{\text{iPr}2}\text{PdCl}$ (2b**):** Yield = 0.079 g, 29%; M. p. = 105 °C; ^1H -NMR (500 MHz, CDCl_3): $\delta = 6.94$ (dd, $J = 7.9, 7.6$ Hz, 1H, Ar-H), 6.63 (d, $J = 7.3$ Hz, 1H, Ar-H), 6.55 (d, $J = 7.9$ Hz, 1H, Ar-H), 4.01 (s, 2H, CH_2), 3.52 (apparent octet, $J = 6.4$ Hz, 2H, $\text{CH}(\text{CH}_3)_2$), 3.36-3.22 (m, 8H, CH_2CH_3), 1.62 (d, $J = 6.4$ Hz, 6H, $\text{CH}(\text{CH}_3)_2$), 1.17-1.13 (m, 6H, $\text{CH}(\text{CH}_3)_2$); 12H, (CH_2CH_3) $_4$; ^{13}C -NMR (100 MHz, CDCl_3): $\delta = 157.5$ (d, $J_{\text{P-C}} = 15.4$ Hz, C_q), 153.6 (d, $J_{\text{P-C}} = 2.3$ Hz, C_q), 143.1 (d, $J_{\text{P-C}} = 2.3$ Hz, C_q), 126.6 (CH), 115.0 (CH), 108.2 (d, $J_{\text{P-C}} = 19.3$, CH), 60.7 (d, $J_{\text{P-C}} = 2.3$ Hz, CH_2), 57.0 (d, $J_{\text{P-C}} = 3.1$ Hz, 2C, $\text{CH}(\text{CH}_3)_2$), 40.3 (d, $J_{\text{P-C}} = 9.3$ Hz, 4C, CH_2CH_3), 22.6 (2C, $\text{CH}(\text{CH}_3)_2$), 19.5 (2C, $\text{CH}(\text{CH}_3)_2$), 14.4 (d, $J_{\text{P-C}} = 2.3$ Hz, 4C, CH_2CH_3); $^{31}\text{P}\{^1\text{H}\}$ NMR (202 MHz, CDCl_3): $\delta = 142.3$ (s); MALDI-TOF: m/z calcd for $\text{C}_{21}\text{H}_{39}\text{ClN}_3\text{OPPd-Cl}^+ [\text{M-Cl}]^+$ 486.1866, found 486.2410; elemental analysis calcd (%) for $\text{C}_{21}\text{H}_{39}\text{ClN}_3\text{OPPd}$: C 48.28, H 7.53, N 8.04; found: C 48.22, H 7.60, N 7.62.

2.4.3 Representative Procedure for Synthesis of ($\text{R}^2\text{POCN}^{\text{iPr}2}$)Pd(OAc)

Synthesis of ($\text{Ph}^2\text{POCN}^{\text{iPr}2}$)Pd(OAc) (3a**):** To the mixture of 2,6-(Ph_2PO)(C_6H_3)($\text{CH}_2\text{-N}^{\text{iPr}2}$)PdCl, **2a** (0.020 g, 0.038 mmol) and AgOAc (0.008 g, 0.046 mmol) was added THF (10 mL) and the reaction mixture was stirred at room temperature for 3 h. The solvent was evaporated under reduced pressure and the compound was extracted with Et_2O (10 mL x 3). Upon evaporation of diethyl ether, the compound **3a** was obtained as a light yellow solid. The compound **3a** was recrystallized from petroleum ether solution by slow evaporation to obtain X-ray quality single crystals. Yield = 0.013 g, 62%; M. p. = 182 °C; ^1H -NMR (400 MHz, CDCl_3): $\delta = 7.90$ -7.84 (m, 4H, Ar-H), 7.49-7.40 (m, 6H, Ar-H), 6.92 (vt, $J = 7.8$ Hz, 1H, Ar-H), 6.61 (d, J

= 7.3 Hz, 1H, Ar-H), 6.57 (d, $J = 8.1$ Hz, 1H, Ar-H), 4.16 (s, 2H, CH₂), 3.53 (apparent octet, $J = 6.1$ Hz, 2H, CH(CH₃)₂), 1.86 (s, 3H, COCH₃), 1.60 (d, $J = 6.4$ Hz, 6H, CH(CH₃)₂), 1.28 (d, $J = 6.6$ Hz, 6H, CH(CH₃)₂); ¹³C-NMR (100 MHz, CDCl₃): $\delta = 175.0$ (CO), 162.3 (d, $J_{P-C} = 11.0$ Hz, C_q), 153.2 (C_q), 143.0 (C_q), 135.4 (d, $J_{P-C} = 58.6$ Hz, 2C, C_q), 132.7 (d, $J_{P-C} = 13.4$ Hz, 4C, CH), 131.2 (d, $J_{P-C} = 2.3$ Hz, 2C, CH), 128.3 (d, $J_{P-C} = 12.1$ Hz, 4C, CH), 126.4 (CH), 114.5 (CH), 108.6 (d, $J_{P-C} = 16.6$ Hz), 61.4 (CH₂), 57.3 (2C, CH(CH₃)₂), 31.1 (COCH₃), 22.2 (2C, CH(CH₃)₂), 19.5 (2C, CH(CH₃)₂); ³¹P{¹H}NMR (202 MHz, CDCl₃): $\delta = 143.8$ (s); MALDI-TOF: m/z calcd for C₂₇H₃₂NO₃PPd-OAc⁺ [M-OAc]⁺ 496.1022, found 496.1594; elemental analysis calcd (%) for C₂₇H₃₂NO₃PPd: C 58.33, H 5.80, N 2.52; found: C 58.42, H 6.20, N 1.84.

Synthesis of (^{Et₂N})₂POCN^{iPr₂})Pd(OAc) (3b): The representative procedure was followed, using **2b** (0.058 g, 0.111 mmol) and AgOAc (0.022 g, 0.133 mmol). Yield = 0.040 g, 66%; M. p. = 86 °C; ¹H-NMR (500 MHz, CDCl₃): $\delta = 6.93$ (vt, $J = 7.7$, 1H, Ar-H), 6.59 (d, $J = 7.5$, 1H, Ar-H), 6.53 (d, $J = 7.7$ Hz, 1H, Ar-H), 4.02 (s, 2H, CH₂), 3.38 (apparent octet, $J = 6.2$ Hz, 2H, CH(CH₃)₂), 3.32-3.21 (m, 8H, CH₂CH₃), 1.92 (s, 3H, COCH₃), 1.53 (d, $J = 6.4$ Hz, 6H, CH(CH₃)₂), 1.23 (d, $J = 6.4$ Hz, 6H, CH(CH₃)₂), 1.13 (t, $J = 7.0$ Hz, 12H, CH₂CH₃); ¹³C-NMR (125 MHz, CDCl₃): $\delta = 175.9$ (CO), 157.7 (d, $J_{P-C} = 14.3$ Hz, C_q), 153.6 (d, $J_{P-C} = 1.9$ Hz, C_q), 140.6 (C_q), 126.3 (CH), 114.6 (CH), 108.0 (d, $J_{P-C} = 19.1$ Hz, CH), 60.4 (d, $J_{P-C} = 2.9$ Hz, CH₂), 56.8 (d, $J_{P-C} = 2.9$ Hz, 2C, CH(CH₃)₂), 40.4 (d, $J_{P-C} = 10.5$ Hz, 4C, CH₂CH₃), 24.7 (COCH₃), 21.9 (2C, CH(CH₃)₂), 19.3 (2C, CH(CH₃)₂), 14.4 (d, $J_{P-C} = 2.9$ Hz, 4C, CH₂CH₃); ³¹P{¹H}NMR (202 MHz, CDCl₃): $\delta = 142.3$ (s); MALDI-TOF: m/z calcd for C₂₃H₄₂N₃O₃PPd-OAc⁺ [M-OAc]⁺ 486.1866, found 486.2420; elemental analysis calcd (%) for C₂₃H₄₂N₃O₃PPd: C 50.60, H 7.75, N 7.70; found: C 52.37, H 8.35, N 6.80.

2.4.4 Procedure for Synthesis of [κ^P, κ^C -4-^{iPr₂}NCH₂-C₆H₃-Pd(μ -Cl)-(2-OPR₂)]₂ (R = Ph, **4a; R = Et₂N, **4b**; R = ^{iPr}, **4c**).** A mixture of Pd(COD)Cl₂ (0.306 g, 1.07 mmol for **4a**; 0.550 g, 1.93 mmol for **4b**; 0.088 g, 0.308 mmol for **4c**), (^{R₂}POCN^{iPr₂})-H (0.420 g, 1.07 mmol of **1a**; 0.735 g, 1.93 mmol of **1b**; 0.100 g, 0.309 mmol of **1c**) and Et₃N (0.18 mL, 1.28 mmol for **4a**; 0.32 mL, 2.30 mmol for **4b**; 0.05 mL, 0.370 mmol for **4c**) was taken in a schlenk flask and 1,4-dioxane (30 mL) was added into it. The reaction mixture was heated at 70 °C for 2 h under argon atmosphere. The yellow suspension formed was cooled to ambient temperature and the volatile were

evaporated under reduced pressure. The compounds was purified by column chromatography on neutral alumina (petroleum ether:EtOAc / 10:1) to yielded the desired complexes (**4a**, **4b**, **4c**) as light yellow solid.

[κ^P, κ^C -4- i Pr₂NCH₂-C₆H₃-Pd(μ -Cl)-(2-OPPh₂)₂]₂ (4a**):** Yield = 0.138 g, 24%; M. p. = 114-116 °C; ¹H-NMR (500 MHz, CDCl₃): δ = 8.02-7.76 (m, 8H, Ar-H), 7.57-7.35 (m, 14H, Ar-H), 6.99 (br s, 2H, Ar-H), 6.83 (br s, 2H, Ar-H), 3.55 (s, 4H, CH₂), 3.00 (br s, 4H, CH(CH₃)₂), 1.00 (br s, 24H, CH(CH₃)₂); ¹³C-NMR (100 MHz, CDCl₃): δ = 164.3 (2C, C_q), 143.3 (2C, C_q), 135.8 (2C, CH), 132.8 (4C, C_q), 132.5 (4C, CH), 132.3 (d, J_{P-C} = 13.6 Hz, 8C, CH), 132.1 (2C, C_q), 129.0 (d, J_{P-C} = 10.9 Hz, 8C, CH), 122.0 (2C, CH), 111.4 (2C, CH), 48.7 (2 CH₂), 47.9 (4C, CH(CH₃)₂), 20.9 (8C, CH(CH₃)₂); ³¹P{¹H}NMR (202 MHz, CDCl₃): δ = 152.9 (s, major, 57%), 152.2 (s, minor, 43%); MALDI-TOF: m/z calcd for C₅₀H₅₈Cl₂N₂O₂P₂Pd₂+H⁺ [M+H]⁺ 1063.1498, found 1063.3624; elemental analysis calcd (%) for C₅₀H₅₈Cl₂N₂O₂P₂Pd₂: C 56.40, H 5.49, N 2.63; found: C 55.22, H 5.15, N 2.25.

[κ^P, κ^C -4- i Pr₂NCH₂-C₆H₃-Pd(μ -Cl)-(2-OP(NEt₂)₂)₂]₂ (4b**):** Yield = 0.320 g, 32%; M. P. = 188-190 °C; ¹H-NMR (500 MHz, CDCl₃): δ = 7.47 (dd, J = 6.8, 6.5 Hz, 2H, Ar-H), 6.89-6.77 (m, 4H, Ar-H), 3.55 (s, 4H, CH₂), 3.48-3.34 (m, 8H, CH₂CH₃), 3.29-3.17 (m, 8H, CH₂CH₃), 3.04-2.96 (m, 4H, CH(CH₃)₂), 1.17 (t, J = 7.0 Hz, 24H, CH₂CH₃), 1.00 (d, J = 6.0, 24H, CH(CH₃)₂); ¹³C-NMR (100 MHz, CDCl₃): δ = 158.3 (d, J_{P-C} = 18.1 Hz, 2C, C_q), 142.4 (2C, C_q), 136.1 (2C, CH), 132.5 (2C, C_q), 121.5 (2C, CH), 110.7 (d, J_{P-C} = 20.9, 2C, CH), 48.7 (2 CH₂), 47.8 (4C, CH(CH₃)₂), 40.5 (d, J_{P-C} = 9.1 Hz, 8C, CH₂CH₃), 20.9 (8C, CH(CH₃)₂), 14.3 (8C, CH₂CH₃); ³¹P{¹H}NMR (202 MHz, CDCl₃): δ = 137.7 (s, major, 76%), 137.9 (s, minor, 24%); MALDI-TOF: m/z calcd for C₄₂H₇₈Cl₂N₆O₂P₂Pd₂+H⁺ [M+H]⁺ 1043.3186, found 1043.4058; elemental analysis calcd (%) for C₄₂H₇₈Cl₂N₆O₂P₂Pd₂: C 48.28, H 7.53, N 8.04; found: C 47.62, H 7.59, N 6.86.

[κ^P, κ^C -4- i Pr₂NCH₂-C₆H₃-Pd(μ -Cl)-(2-OP^{*i*}Pr₂)₂]₂ (4c**):** Yield: 0.102 g, 71%; M. p. = 153-154 °C; ¹H-NMR (400 MHz, CDCl₃): δ = 7.60-7.36 (m, 2H, Ar-H), 6.90-9.74 (m, 4H, Ar-H), 3.54 (br s, 4H, CH₂), 3.01 (br s, 4H, N{CH(CH₃)₂})₂, 2.41 (br s, 4H, P{CH(CH₃)₂})₂, 1.44 (d, J = 12.7 Hz, 12H, PCH(CH₃)₂), 1.31 (dd, J = 15.9, 6.9 Hz, 12H, PCH(CH₃)₂), 1.01 (br s, 24H, NCH(CH₃)₂); ¹³C-NMR (100 MHz, CDCl₃): δ = 165.5 (d, J_{P-C} = 6.2 Hz, 2C, C_q), 142.8 (2C, C_q), 135.8 (2C, CH), 131.9 (2C, C_q), 121.6 (2C, CH), 110.5 (d, J_{P-C} = 16.2 Hz, 2C, CH), 48.7 (2C,

CH₂), 47.8 (4C, N{CH(CH₃)₂})₂), 29.5 (d, $J_{P-C} = 29.3$ Hz, 4C, P{CH(CH₃)₂})₂), 20.9 (4C, PCH(CH₃)₂), 17.8 (4C, PCH(CH₃)₂), 17.0 (8C, NCH(CH₃)₂); ³¹P {¹H}-NMR (202 MHz, CDCl₃): $\delta = 200.0$ (s, major, 65%), 199.0 (s, minor, 35%); MALDI-TOF: m/z calcd for C₃₈H₆₆Cl₂N₂O₂P₂Pd₂+H [M+H]⁺ 927.2124, found 927.3241; elemental analysis calcd (%) for C₃₈H₆₆Cl₂N₂O₂P₂Pd₂: C 49.15, H 7.16, N 3.02; found: C 49.12, H 7.34, N 2.69.

Synthesis of [κ^P, κ^C -4-ⁱPr₂NCH₂-C₆H₃-Pd(μ -OAc)-(2-OPPh₂)₂]₂ (5a). To the mixture of **4a** (0.040 g, 0.038 mmol) and AgOAc (0.014 g, 0.084 mmol) was added THF (10 mL) and the reaction mixture was stirred at room temperature for 3 h. The solvent was evaporated under reduced pressure and the compound was extracted with Et₂O (10 mL x 3). Upon evaporation of diethyl ether, the compound **5a** was obtained as a light yellow solid. The compound **5a** was further recrystallized from *petroleum ether* solution to obtain X-ray quality crystals at room temperature. Yield = 0.024 g, 57%; M. p. = 192 °C; ¹H-NMR (400 MHz, CDCl₃): $\delta = 7.89$ -7.70 (m, 6H, Ar-H), 7.51-7.04 (m, 16H, Ar-H), 6.84 (br s, 2H, Ar-H), 6.66 (d, $J = 7.6$ Hz, 2H, Ar-H), 3.55 (s, 4H, CH₂), 3.05 (sept, $J = 6.4$ Hz, 4H, CH(CH₃)₂), 2.17 (s, 6H, COCH₃), 1.04 (d, $J = 6.4$ Hz, 24H, CH(CH₃)₂); ¹³C-NMR (100 MHz, CDCl₃): $\delta = 181.4$ (2C, C_q), 164.5 (d, $J_{P-C} = 14.6$ Hz, 2C, C_q), 141.9 (2C, C_q), 134.7 (2C, CH), 132.6-131.2 (m, 20C), 128.6-128.3 (m, 6C), 121.8 (2C, CH), 111.0 (2C, CH), 48.7 (2C, CH₂), 47.6 (4C, CH(CH₃)₂), 25.4 (2C, COCH₃), 21.0 (8C, CH(CH₃)₂); ³¹P{¹H}NMR (202 MHz, CDCl₃): $\delta = 151.0$ (s); HRMS (ESI): m/z calcd for C₅₄H₆₆N₂O₆P₂Pd₂+H [M+H]⁺ 1113.2539, found 1113.2501; elemental analysis calcd (%) for C₅₄H₆₆N₂O₆P₂Pd₂: C 58.23, H 5.97, N 2.51; found: C 57.69, H 6.02, N 2.13.

Synthesis of { κ^P -(3-ⁱPr₂NCH₂)-C₆H₄-(2-OPⁱPr₂)}(Py)PdCl₂ (8c). A mixture of Pd(COD)Cl₂ (0.044 g, 0.154 mmol), **1c** (0.050 g, 0.155 mmol) and pyridine (0.015 mL, 0.185 mmol) was taken in a Schlenk flask and 1,4-dioxane (10 mL) was added into it. The reaction mixture was stirred at room temperature for 1 h under argon atmosphere and the volatiles were evaporated under reduced pressure to obtain light-yellow compound of **8c**. Yield: 0.065 g, 73%; ¹H-NMR (500 MHz, C₆D₆): $\delta = 9.08$ (br s, 2H, Py-H), 7.99 (s, 1H, Ar-H), 7.62 (d, $J = 7.3$ Hz, 1H, Ar-H), 7.15 (t, $J = 7.9$ Hz, 1H, Ar-H), 7.07 (d, $J = 7.3$ Hz, 1H, Ar-H), 6.67 (br s, 1H, Py-H), 6.40 (br s, 2H, Py-H), 3.55 (s, 2H, CH₂), 2.96 (sept, $J = 6.7$ Hz, 2H, NCH(CH₃)₂), 2.86 (app octet, $J = 7.6$ Hz, 2H, PCH(CH₃)₂), 1.48 (dd, $J = 18.0, 7.3$ Hz, 6H, PCH(CH₃)₂), 1.40 (dd, $J = 16.2, 7.0$ Hz, 6H, PCH(CH₃)₂), 0.95 (d, $J = 6.7$, 12H, NCH(CH₃)₂); ¹³C-NMR (125 MHz,

C₆D₆): δ = 155.5 (d, J_{P-C} = 8.6 Hz, C_q), 151.6 (CH), 145.7 (C_q), 137.9 (CH), 129.4 (CH), 128.7 (2C, CH), 124.3 (CH), 123.7 (CH), 120.6 (d, J_{P-C} = 5.7 Hz, CH), 118.9 (d, J_{P-C} = 5.7 Hz, CH), 49.5 (CH₂), 48.5 (2C, NCH(CH₃)₂), 31.5 (d, J_{P-C} = 31.5 Hz, 2C, PCH(CH₃)₂), 21.3 (4C, NCH(CH₃)₂), 19.2 (2C, PCH(CH₃)₂), 18.0 (2C, PCH(CH₃)₂); ³¹P {¹H}-NMR (202 MHz, C₆D₆): δ = 144.4 (s); HRMS (ESI): m/z . calcd for C₂₄H₃₉Cl₂N₂OPPd+H [M+H]⁺ 579.1285, found 579.1282.

2.4.5 Representative Procedure for the Arylation of Azoles: Synthesis of 2-(*p*-tolyl)benzo[*d*]thiazole (11aa). To a flame-dried screw-capped Schlenk tube equipped with magnetic stir bar was introduced CuI in CH₃CN [0.0006 g, 0.003 mmol, 1.0 mol %, 0.1 mL from the stock solution (0.036 g in CH₃CN (6.0 mL))] and the solvent was evaporated to dryness under vacuum. Then, 4-iodotoluene **10a** (0.098 g, 0.45 mmol), K₃PO₄ (0.096 g, 0.45 mmol) and benzothiazole **9a** (0.041 g, 0.30 mmol) were added under argon. The screw-capped Schlenk tube with the mixture was then evacuated and refilled with argon. To the above mixture was added Pd-catalyst **4c** (0.00075 mmol, 0.25 mol % (0.5 mol % per Pd), 1.0 mL of 0.00075 M stock solution in DMF) in DMF under argon. The resultant reaction mixture was then stirred at 120 °C in a pre-heated oil bath for 16 h. At ambient temperature, H₂O (10 mL) was added and the reaction mixture was extracted with EtOAc (15 mL x 3). The combined organic layers were dried over MgSO₄ and the solvent was evaporated *in vacuo*. The remaining residue was purified by column chromatography on silica gel (*petroleum ether*/EtOAc 30/1 → 20/1) to yield **11aa** (0.063 g, 93%) as an off-white solid.

All the isolated coupled products (**11aa-11aq**) were characterized by ¹H and ¹³C-NMR techniques and well compared with the literature reports.

2.4.6 Kinetic Measurements for Palladation Reactions

Rate Order Determination: The rate order of palladation reaction for each base was determined by the initial rate method. The data of the concentration of the product *vs* time (min) plot was fitted linear with OriginPro 8. The slope of the linear fitting represents the reaction rate. The order of the reaction was then determined by plotting the reaction rate *vs* the initial concentration of base.

Procedure for Rate Order Determination for K_3PO_4 : To a 25 mL round-bottom flask equipped with magnetic stir bar was introduced Pd(COD)Cl₂ (0.106 g, 0.371 mmol) and **1c** (0.120 g, 0.371 mmol), and 1,4-dioxane (5.0 mL) was added inside the glove-box, which makes 0.0742 M concentration of the reaction mixture. The reaction mixture was then stirred at room temperature for 1 h and 0.5 mL of the reaction mixture was drawn to a NMR tube. The ³¹P NMR measurement of the reaction mixture indicated the formation of the species **7c**. To the above reaction mixture appropriate amount K₃PO₄ was added and the reaction mixture was heated in an oil bath at 70 °C. At regular intervals (5, 10, 15, 20 and 30 min), 0.5 mL of the reaction mixture was drawn to the NMR tube and ³¹P NMR analyses were carried out for each sample. The concentration of the product formed in each sample was determined from the integral percentage of the product with respect to the starting compound **7c**.

Procedure Rate Order Determination for Et₃N: To a 25 mL round-bottom flask equipped with magnetic stir bar was introduced Pd(COD)Cl₂ (0.106 g, 0.371 mmol) and **1c** (0.120 g, 0.371 mmol), and 1,4-dioxane (5.0 mL) was added inside the glove-box, which makes 0.0742 M concentration of the reaction mixture. To the above reaction mixture appropriate amount Et₃N was added and stirred at room temperature for 1 h. About 0.5 mL of the reaction mixture was drawn to a NMR tube, whose ³¹P NMR measurement indicated the formation of the species **8c**. The reaction mixture on the flask was then heated in an oil bath at 70 °C. At regular intervals (5, 10, 15, 20, 30 and 45 min), 0.5 mL of the reaction mixture was drawn to the NMR tube and ³¹P NMR analyses were carried out for each sample. The concentration of the product (**5c**) formed in each sample was determined from the integral percentage of the product with respect to the starting compound **8c**.

Procedure Rate Order Determination for Pyridine: To a 25 mL round-bottom flask equipped with magnetic stir bar was introduced Pd(COD)Cl₂ (0.106 g, 0.371 mmol) and **1c** (0.120 g, 0.371 mmol), and 1,4-dioxane (5.0 mL) was added inside the glove-box, which makes 0.0742 M concentration of the reaction mixture. To the above reaction mixture appropriate amount pyridine was added and stirred at room temperature for 1 h. About 0.5 mL of the reaction mixture was drawn to a NMR tube, whose ³¹P NMR measurement indicated the formation of the species **9c**. The reaction mixture on the flask was then heated in an oil bath at 70 °C. At regular intervals (5, 10, 15, 20, 30 and 45 min), 0.5 mL of the reaction mixture was drawn to the NMR

tube and ^{31}P NMR analyses were carried out for each sample. The concentration of the product (**2c**) formed in each sample was determined from the integral percentage of the product with respect to the starting compound **9c**.

2.4.7 X-ray Structure Determination. X-ray intensity data measurements of compounds **2a**, **2b**, **3a**, **3b** and **5a** were carried out on a Bruker SMART APEX II CCD diffractometer with graphite-monochromatized ($\text{MoK}\alpha = 0.71073 \text{ \AA}$) radiation between $150(2) - 296(2) \text{ K}$. The X-ray generator was operated at 50 kV and 30 mA. A preliminary set of cell constants and an orientation matrix were calculated from three sets of 12 frames (total 36 frames). Data were collected with ω scan width of 0.5° at eight different settings of φ and 2θ with a frame time of 10 sec keeping the sample-to-detector distance fixed at 5.00 cm for all the compounds. The X-ray data collection was monitored by APEX2 program (Bruker, 2006).⁶⁵ All the data were corrected for Lorentzian, polarization and absorption effects using SAINT and SADABS programs (Bruker, 2006). SHELX-97 was used for structure solution and full matrix least-squares refinement on F^2 .⁶⁶ Hydrogen atoms were placed in geometrically idealized position and constrained to ride on their parent atoms.

Table 2.6 Crystal Data and Structure Refinement for Complexes 2a, 2b and 3a

	2a	2b	3a
Empirical formula	C ₂₅ H ₂₉ ClNOPd	C ₂₁ H ₃₉ ClN ₃ OPd	C ₂₇ H ₃₂ NO ₃ PPd
Formula weight	532.31	522.37	555.91
Temperature (K)	150(2)	296(2)	200(2)
Crystal system	monoclinic	monoclinic	monoclinic
Space group	<i>P2₁/c</i>	<i>P2₁/c</i>	<i>P2₁/c</i>
<i>a</i> /Å	16.5228(14)	7.9316(3)	10.7002(3)
<i>b</i> /Å	10.2622(9)	13.8355(5)	15.0417(4)
<i>c</i> /Å	14.7716(13)	22.8534(8)	15.7925(4)
α /°	90	90	90
β /°	110.312(3)	98.291(2)	99.1280(10)
γ /°	90	90	90
<i>V</i> (Å ³)	2348.9(4)	2481.67(16)	2509.60(12)
<i>Z</i>	4	4	4
ρ_{calc} , (Mg/m ³)	1.505	1.398	1.471
ε (mm ⁻¹)	0.989	0.936	0.832
<i>F</i> (000)	1088	1088	1144
Crystal size (mm)	0.65 x 0.58 x 0.52	0.67 x 0.22 x 0.16	0.41 x 0.37 x 0.22
θ (min, max) (°)	2.38 to 25.00	1.73 to 25.00	1.88 to 25.00
R(int)	0.0227	0.0376	0.0265
Independent reflections	4137	4372	4410
Completeness to θ	99.9 %	100.0 %	100.0 %
Max. and min. transmission	0.6274, 0.5658	0.8647, 0.5729	0.8382, 0.7267
Data / restraints / parameters	4137 / 0 / 275	4372 / 0 / 261	4410 / 0 / 303
GOF (<i>F</i> ²)	1.093	1.155	1.027
R1, wR2 (<i>I</i> > 2 σ (<i>I</i>))	0.0167, 0.0428	0.0241, 0.0600	0.0294, 0.0648
R1, wR2 (all data)	0.0170, 0.0430	0.0256, 0.0613	0.0317, 0.0660

Table 2.7 Crystal Data and Structure Refinement for Complexes 3b and 5a

	3b	5a
Empirical formula	C ₂₃ H ₄₂ N ₃ O ₃ PPd	C ₅₄ H ₆₄ N ₂ O ₆ P ₂ Pd ₂
Formula weight	545.97	1111.81
Temperature (K)	200(2)	200(2)
Crystal system	monoclinic	monoclinic
Space group	<i>P</i> 2 ₁ / <i>c</i>	<i>P</i> 2 ₁ / <i>c</i>
<i>a</i> /Å	11.5217(7)	11.1190(2)
<i>b</i> /Å	12.4022(8)	11.0743(3)
<i>c</i> /Å	18.4419(12)	21.2441(5)
α /°	90	90
β /°	101.270(2)	99.9410(10)
γ /°	90	90
<i>V</i> (Å ³)	2584.4(3)	2576.62(10)
<i>Z</i>	4	2
ρ_{calc} , (Mg/m ³)	1.403	1.433
ε (mm ⁻¹)	0.807	0.810
<i>F</i> (000)	1144	1144
Crystal size (mm)	0.39 x 0.32 x 0.21	0.42 x 0.31 x 0.21
θ (min, max) (°)	1.80 to 25.00	1.84 to 25.00
R(int)	0.0202	0.0289
Independent reflections	4553	4483
Completeness to θ	100.0 %	98.3 %
Max. and min. transmission	0.8487, 0.7436	0.8483, 0.7272
Data / restraints / parameters	4553 / 0 / 289	4483 / 0 / 303
GOF (<i>F</i> ²)	1.160	1.000
R1, wR2 (<i>I</i> > 2 σ (<i>I</i>))	0.0204, 0.0541	0.0452, 0.0744
R1, wR2 (all data)	0.0220, 0.0558	0.0620, 0.0805

2.5 REFERENCES

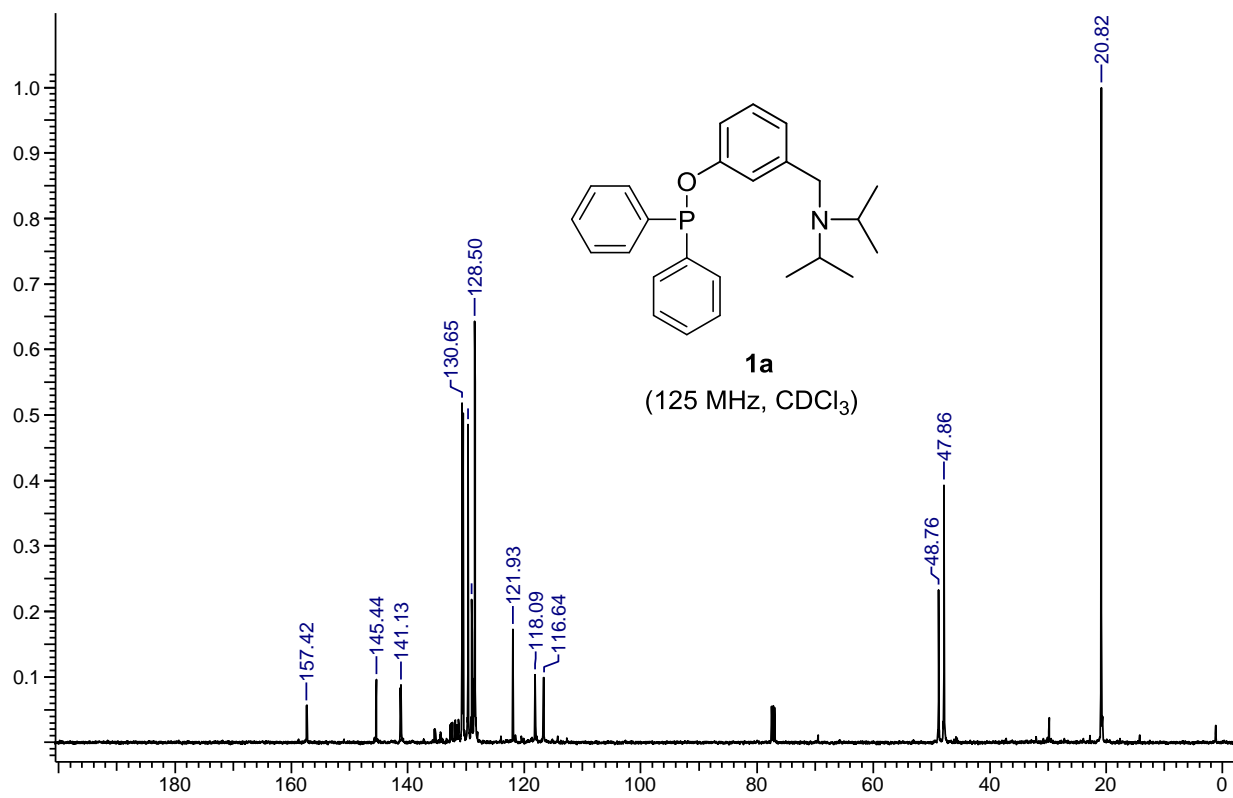
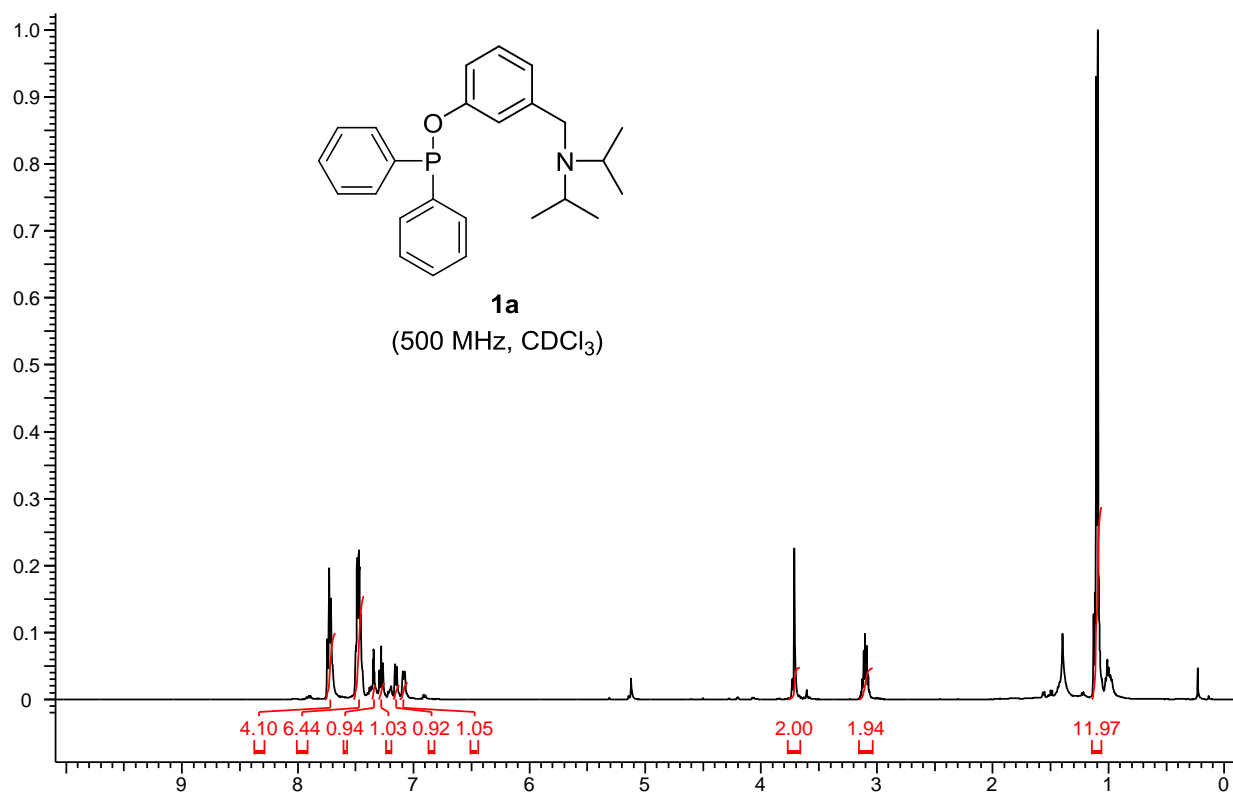
- (1) Albrecht, M.; van Koten, G. *Angew. Chem. Int. Ed.* **2001**, *40*, 3750-3781.
- (2) Dupont, J.; Consorti, C. S.; Spencer, J. *Chem. Rev.* **2005**, *105*, 2527-2572.
- (3) Herrmann, W. A.; Böhm, V. P. W.; Reisinger, C.-P. *J. Organomet. Chem.* **1999**, *576*, 23-41.
- (4) Dupont, J.; Pfeffer, M.; Spencer, J. *Eur. J. Inorg. Chem.* **2001**, 1917-1927.
- (5) Bedford, R. B. *Chem. Commun.* **2003**, 1787-1796.
- (6) van der Boom, M. E.; Milstein, D. *Chem. Rev.* **2003**, *103*, 1759-1792.
- (7) Singleton, J. T. *Tetrahedron* **2003**, *59*, 1837-1857.
- (8) Omae, I. *Coord. Chem. Rev.* **2004**, *248*, 995-1023.
- (9) Selander, N.; Szabó, K. J. *Chem. Rev.* **2011**, *111*, 2048-2076.
- (10) Herrmann, W. A.; Brossmer, C.; Öfele, K.; Reisinger, C.-P.; Priermeier, T.; Beller, M.; Fischer, H. *Angew. Chem. Int. Ed. Engl.* **1995**, *34*, 1844-1848.
- (11) Beller, M.; Fischer, H.; Herrmann, W. A.; Öfele, K.; Brossmer, C. *Angew. Chem. Int. Ed. Engl.* **1995**, *34*, 1848-1849.
- (12) Bedford, R. B.; Draper, S. M.; Noelle Scully, P.; Welch, S. L. *New J. Chem.* **2000**, *24*, 745-747.
- (13) Rossin, A.; Bottari, G.; Lozano-Vila, A. M.; Paneque, M.; Peruzzini, M.; Rossi, A.; Zanobini, F. *Dalton Trans.* **2013**, *42*, 3533-3541.
- (14) Bruneau, A.; Roche, M.; Alami, M.; Messaoudi, S. *ACS Catal.* **2015**, *5*, 1386-1396.
- (15) Lagunas, M.-C.; Gossage, R. A.; Spek, A. L.; van Koten, G. *Organometallics* **1998**, *17*, 731-741.
- (16) Jung, I. G.; Son, S. U.; Park, K. H.; Chung, K.-C.; Lee, J. W.; Chung, Y. K. *Organometallics* **2003**, *22*, 4715-4720.
- (17) Canty, A. J.; Denney, M. C.; van Koten, G.; Skelton, B. W.; White, A. H. *Organometallics* **2004**, *23*, 5432-5439.
- (18) Takenaka, K.; Uozumi, Y. *Org. Lett.* **2004**, *6*, 1833-1835.
- (19) Takenaka, K.; Uozumi, Y. *Adv. Synth. Catal.* **2004**, *346*, 1693-1696.
- (20) Takenaka, K.; Minakawa, M.; Uozumi, Y. *J. Am. Chem. Soc.* **2005**, *127*, 12273-12281.

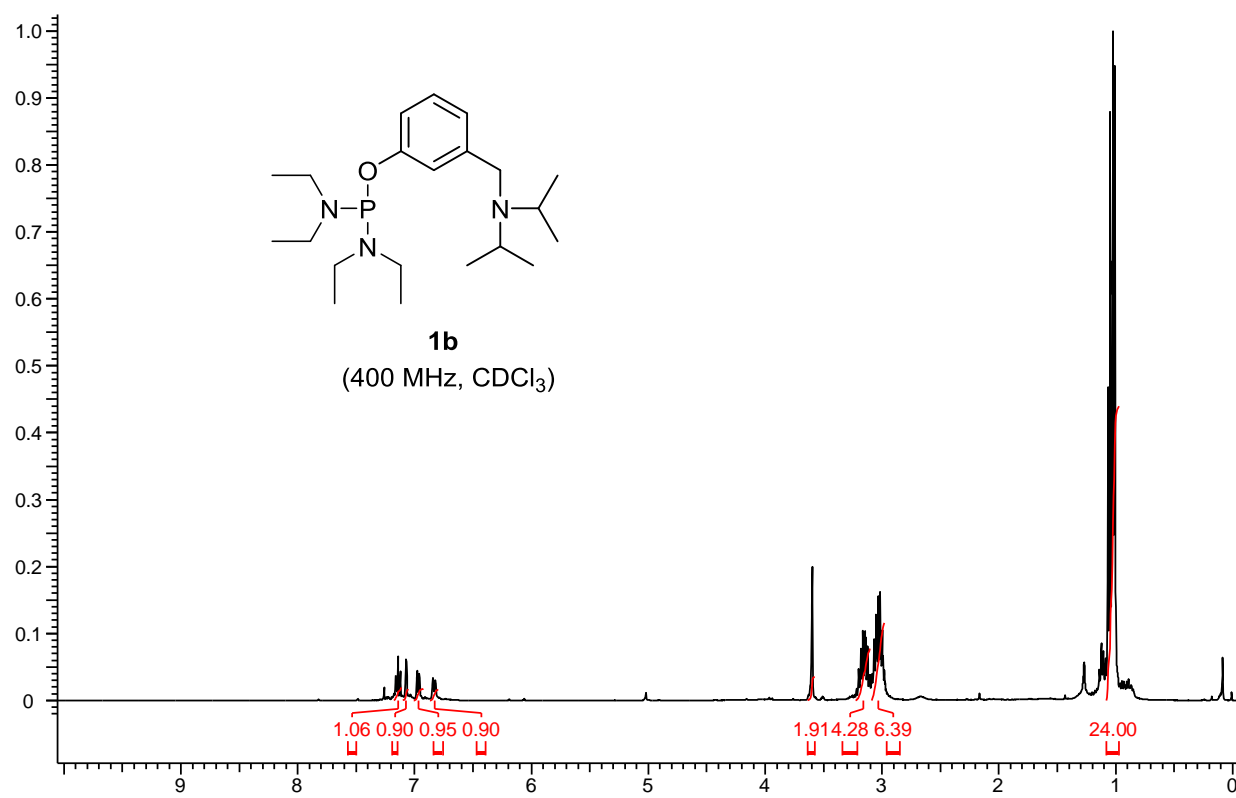
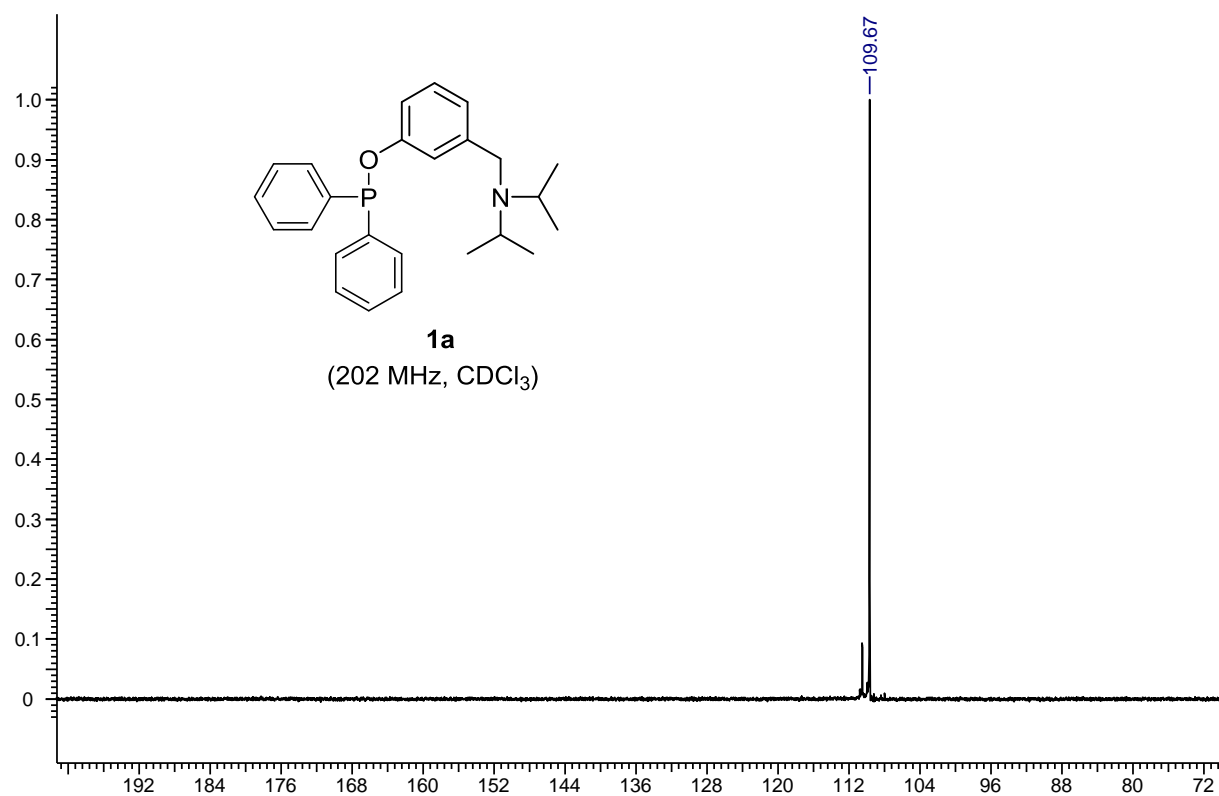
-
- (21) Soro, B.; Stoccoro, S.; Minghetti, G.; Zucca, A.; Cinellu, M. A.; Manassero, M.; Gladiali, S. *Inorg. Chim. Acta* **2006**, *359*, 1879-1888.
- (22) Moulton, C. J.; Shaw, B. L. *J. Chem. Soc., Dalton Trans.* **1976**, 1020-1024.
- (23) Ohff, M.; Ohff, A.; van der Boom, M. E.; Milstein, D. *J. Am. Chem. Soc.* **1997**, *119*, 11687-11688.
- (24) Morales-Morales, D.; Grause, C.; Kasaoka, K.; Redón, R.; Cramer, R. E.; Jensen, C. M. *Inorg. Chim. Acta* **2000**, *300-302*, 958-963.
- (25) Eberhard, M. R.; Wang, Z.; Jensen, C. M. *Chem. Commun.* **2002**, 818-819.
- (26) Baber, R. A.; Bedford, R. B.; Betham, M.; Blake, M. E.; Coles, S. J.; Haddow, M. F.; Hursthouse, M. B.; Orpen, A. G.; Pilarski, L. T.; Pringle, P. G.; Wingad, R. L. *Chem. Commun.* **2006**, 3880-3882.
- (27) Kimura, T.; Uozumi, Y. *Organometallics* **2006**, *25*, 4883-4887.
- (28) Naghipour, A.; Sabounchei, S. J.; Morales-Morales, D.; Canseco-González, D.; Jensen, C. M. *Polyhedron* **2007**, *26*, 1445-1448.
- (29) Kanbara, T.; Yamamoto, T. *J. Organomet. Chem.* **2003**, *688*, 15-19.
- (30) Lucena, N.; Casabó, J.; Escriche, L.; Sánchez-Castelló, G.; Teixidor, F.; Kivekäs, R.; Sillanpää, R. *Polyhedron* **1996**, *15*, 3009-3018.
- (31) Yu, K.; Sommer, W.; Weck, M.; Jones, C. W. *J. Catal.* **2004**, *226*, 101-110.
- (32) Akaiwa, M.; Kanbara, T.; Fukumoto, H.; Yamamoto, T. *J. Organomet. Chem.* **2005**, *690*, 4192-4196.
- (33) Cervantes, R.; Castillejos, S.; Loeb, S. J.; Ortiz-Frade, L.; Tiburcio, J.; Torrens, H. *Eur. J. Inorg. Chem.* **2006**, 1076-1083.
- (34) Bergbreiter, D. E.; Osburn, P. L.; Frels, J. D. *Adv. Synth. Catal.* **2005**, *347*, 172-184.
- (35) Ebeling, G.; Meneghetti, M. R.; Rominger, F.; Dupont, J. *Organometallics* **2002**, *21*, 3221-3227.
- (36) Consorti, C. S.; Ebeling, G.; Flores, F. R.; Rominger, F.; Dupont, J. *Adv. Synth. Catal.* **2004**, *346*, 617-624.
- (37) Fleckhaus, A.; Mousa, A. H.; Lawal, N. S.; Kazemifar, N. K.; Wendt, O. F. *Organometallics* **2015**, *34*, 1627-1634.
- (38) Gong, J.-F.; Zhang, Y.-H.; Song, M.-P.; Xu, C. *Organometallics* **2007**, *26*, 6487-6492.
-

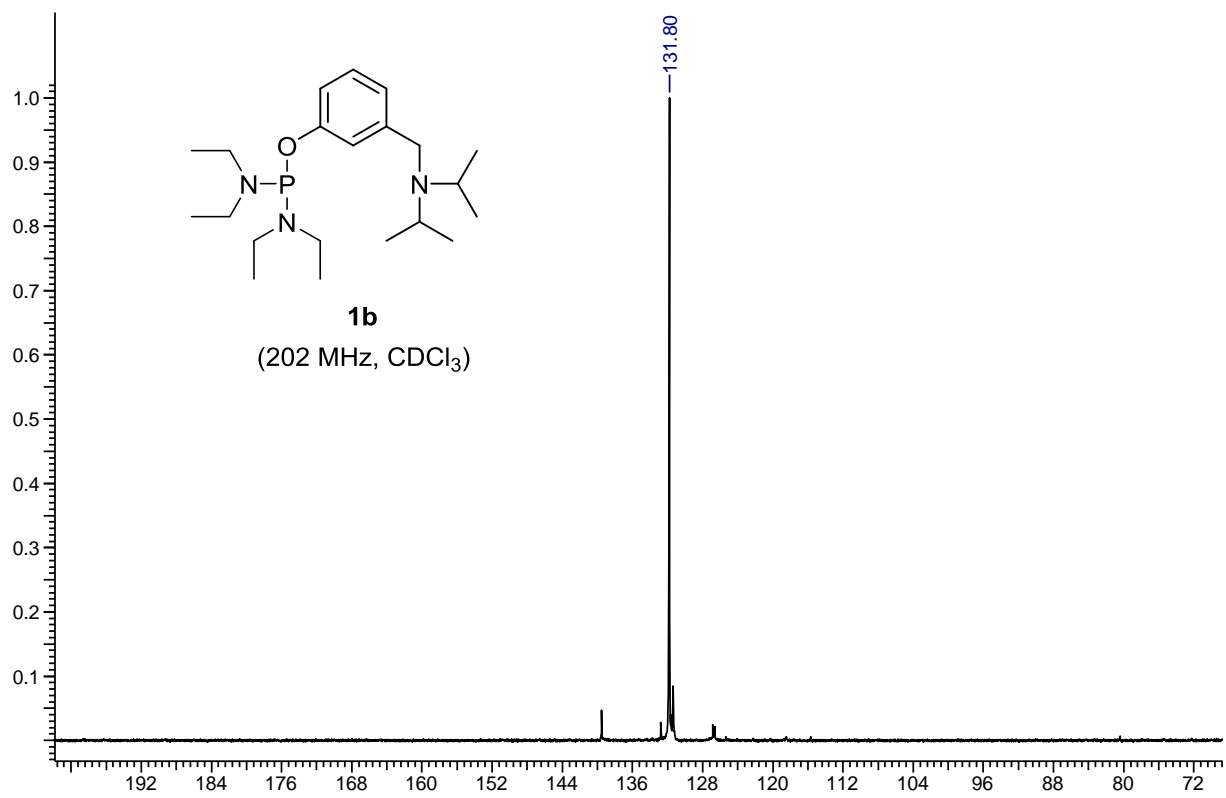
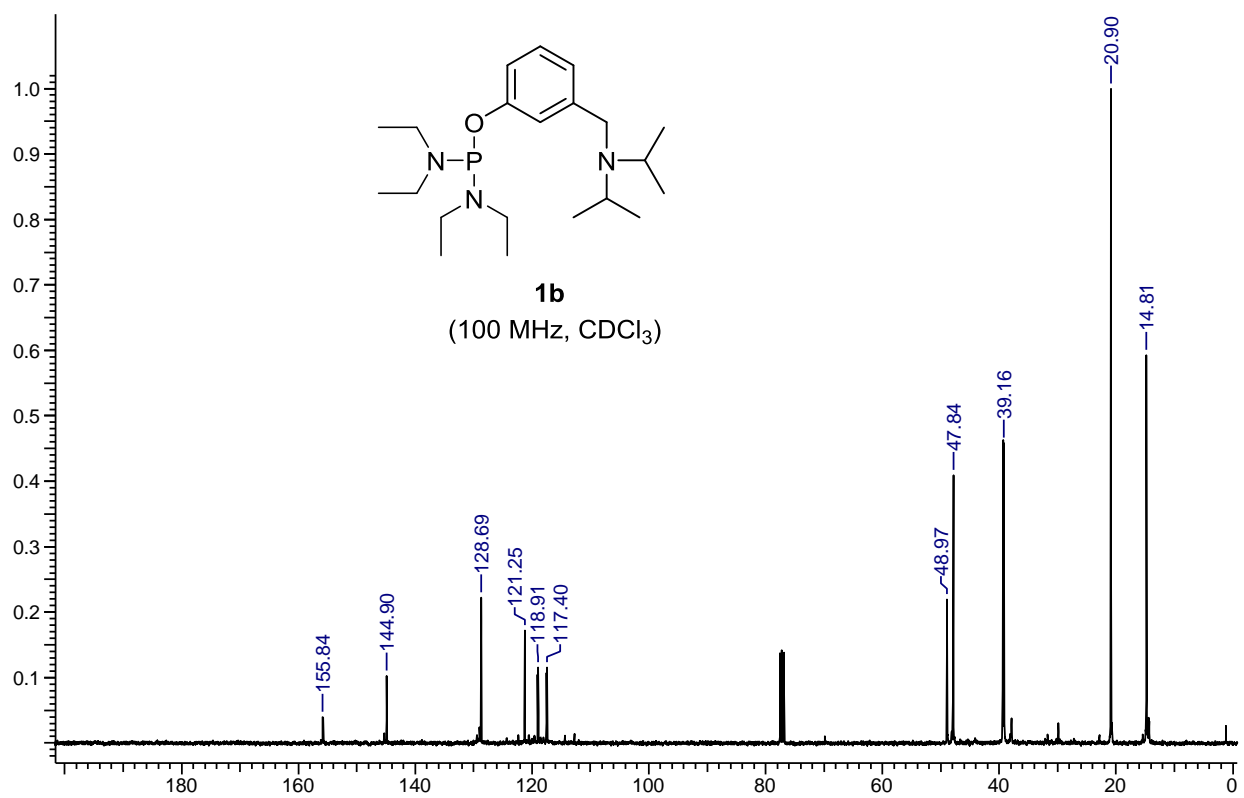
- (39) Niu, J.-L.; Chen, Q.-T.; Hao, X.-Q.; Zhao, Q.-X.; Gong, J.-F.; Song, M.-P. *Organometallics* **2010**, *29*, 2148-2156.
- (40) Yang, M.-J.; Liu, Y.-J.; Gong, J.-F.; Song, M.-P. *Organometallics* **2011**, *30*, 3793-3803.
- (41) Li, J.; Sieglar, M.; Lutz, M.; Spek, A. L.; Klein Gebbink, R. J. M.; van Koten, G. *Adv. Synth. Catal.* **2010**, *352*, 2474-2488.
- (42) Motoyama, Y.; Shimozone, K.; Nishiyama, H. *Inorg. Chim. Acta* **2006**, *359*, 1725-1730.
- (43) Fulmer, G. R.; Kaminsky, W.; Kemp, R. A.; Goldberg, K. I. *Organometallics* **2011**, *30*, 1627-1636.
- (44) Dani, P.; Karlen, T.; Gossage, R. A.; Smeets, W. J. J.; Spek, A. L.; van Koten, G. *J. Am. Chem. Soc.* **1997**, *119*, 11317-11318.
- (45) Newkome, G. R.; Puckett, W. E.; Gupta, V. K.; Kiefer, G. E. *Chem. Rev.* **1986**, *86*, 451-489.
- (46) Vigalok, A.; Uzan, O.; Shimon, L. J. W.; Ben-David, Y.; Martin, J. M. L.; Milstein, D. *J. Am. Chem. Soc.* **1998**, *120*, 12539-12544.
- (47) Gusev, D. G.; Madott, M.; Dolgushin, F. M.; Lyssenko, K. A.; Antipin, M. Y. *Organometallics* **2000**, *19*, 1734-1739.
- (48) Adams, J. J.; Lau, A.; Arulsamy, N.; Roddick, D. M. *Inorg. Chem.* **2007**, *46*, 11328-11334.
- (49) Trofimenko, S. *Inorg. Chem.* **1973**, *12*, 1215-1221.
- (50) Steenwinkel, P.; Gossage, R. A.; Maunula, T.; Grove, D. M.; van Koten, G. *Chem. Eur. J.* **1998**, *4*, 763-768.
- (51) Steenwinkel, P.; James, S. L.; Grove, D. M.; Kooijman, H.; Spek, A. L.; van Koten, G. *Organometallics* **1997**, *16*, 513-515.
- (52) Steenwinkel, P.; Gossage, R. A.; van Koten, G. *Chem. Eur. J.* **1998**, *4*, 759-762.
- (53) Khake, S. M.; Soni, V.; Gonnade, R. G.; Punji, B. *Dalton Trans.* **2014**, *43*, 16084-16096.
- (54) Nifant'ev, E. E.; Rasadkina, E. N.; Slit'kov, P. V.; Vasyanina, L. K. *Phosphorus, Sulfur, and Silicon and Rel. Elem.* **2003**, *178*, 2465-2477.
- (55) Valk, J.-M.; van Belzen, R.; Boersma, J.; Spek, A. L.; van Koten, G. *J. Chem. Soc., Dalton Trans.* **1994**, 2293-2302.
- (56) Valk, J.-M.; Boersma, J.; van Koten, G. *J. Organomet. Chem.* **1994**, *483*, 213-216.

-
- (57) Zanini, M. L.; Meneghetti, M. R.; Ebeling, G.; Livotto, P. R.; Rominger, F.; Dupont, J. *Inorg. Chim. Acta* **2003**, *350*, 527-536.
- (58) Johansson, R.; Jarenmark, M.; Wendt, O. F. *Organometallics* **2005**, *24*, 4500-4502.
- (59) Canty, A. J.; Minchin, N. J.; Skelton, B. W.; White, A. H. *J. Chem. Soc., Dalton Trans.* **1987**, 1477-1483.
- (60) Pivsa-Art, S.; Satoh, T.; Kawamura, Y.; Miura, M.; Nomura, M. *Bull. Chem. Soc. Jpn.* **1998**, *71*, 467-473.
- (61) Bellina, F.; Cauteruccio, S.; Rossi, R. *Eur. J. Org. Chem.* **2006**, *2006*, 1379-1382.
- (62) Ackermann, L.; Althammer, A.; Fenner, S. *Angew. Chem. Int. Ed.* **2009**, *48*, 201-204.
- (63) Shibahara, F.; Yamaguchi, E.; Murai, T. *Chem. Commun.* **2010**, *46*, 2471-2473.
- (64) van Leusen, A. M.; Hoogenboom, B. E.; Siderius, H. *Tetrahedron Lett.* **1972**, *13*, 2369-2372.
- (65) APEX2, SAINT and SADABS. *Bruker AXS Inc.*, Madison, Wisconsin, USA **2006**.
- (66) Sheldrick, G. M. *Acta Crystallogr.* **2008**, *A64*, 112-122.

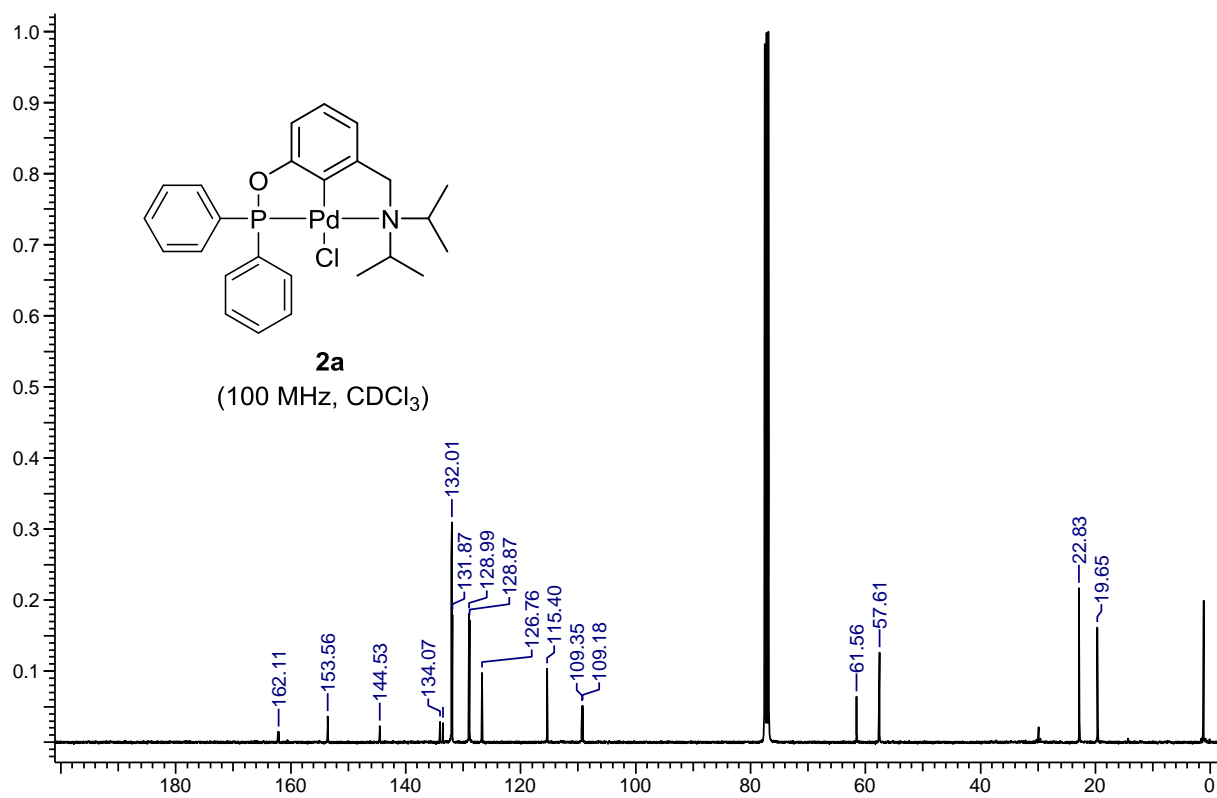
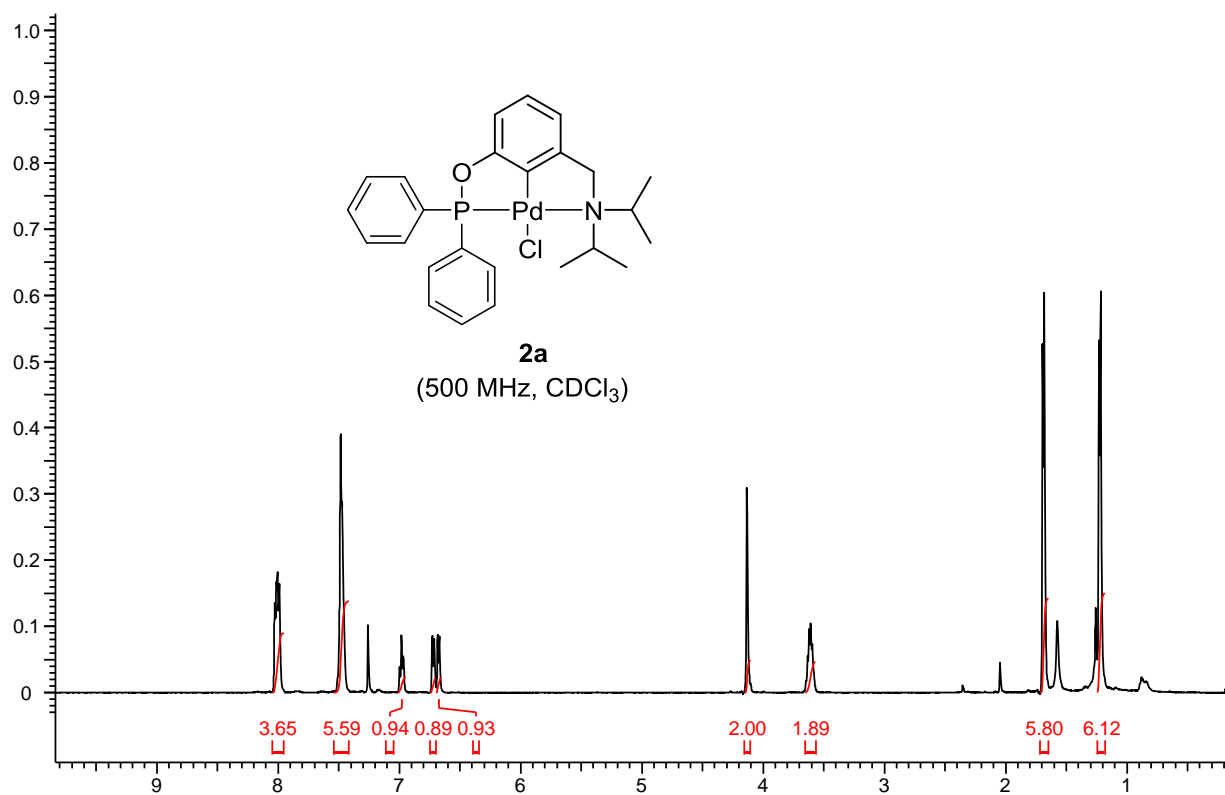
NMR Spectra of Ligands and Complexes

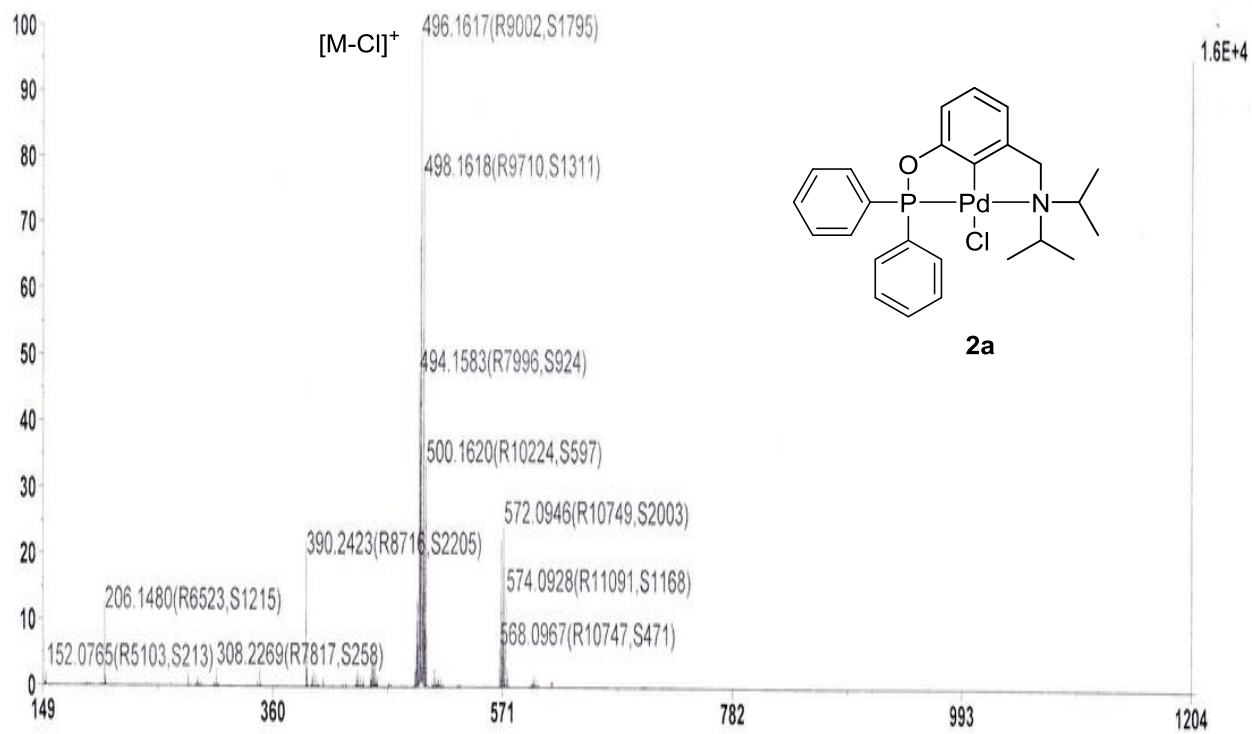
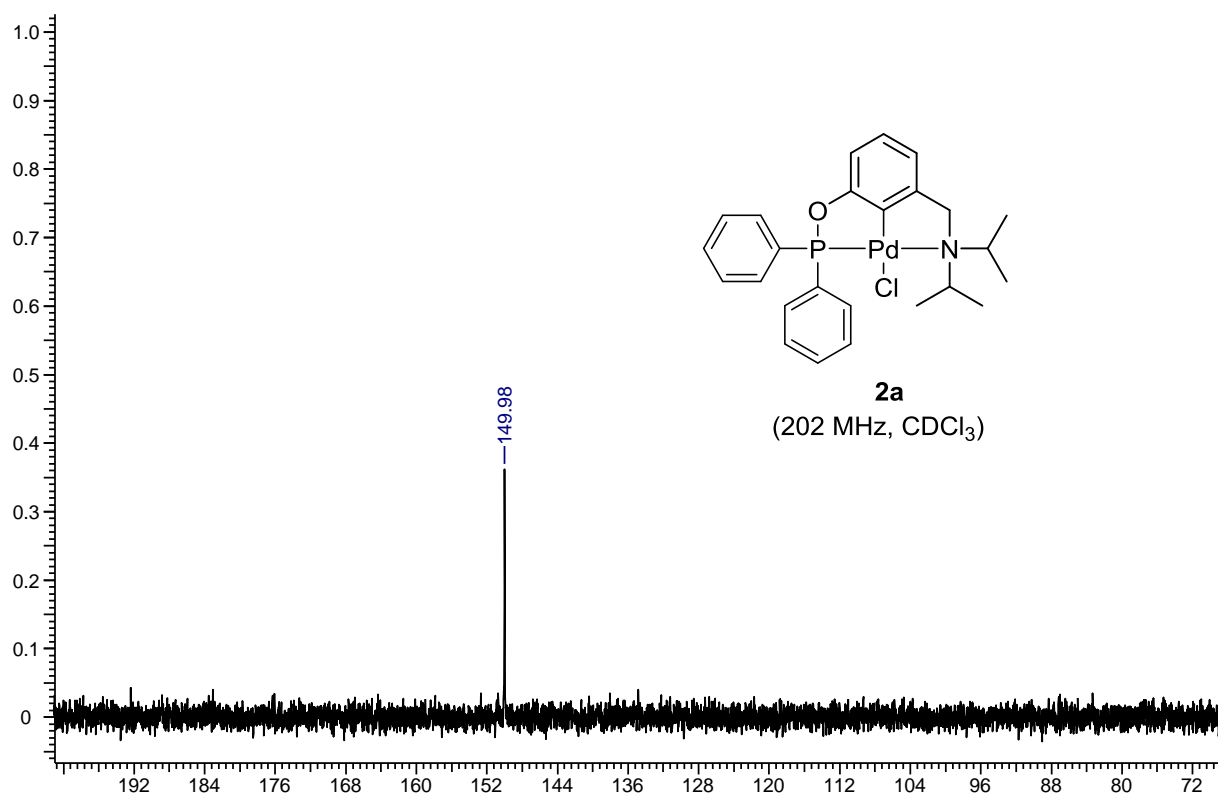


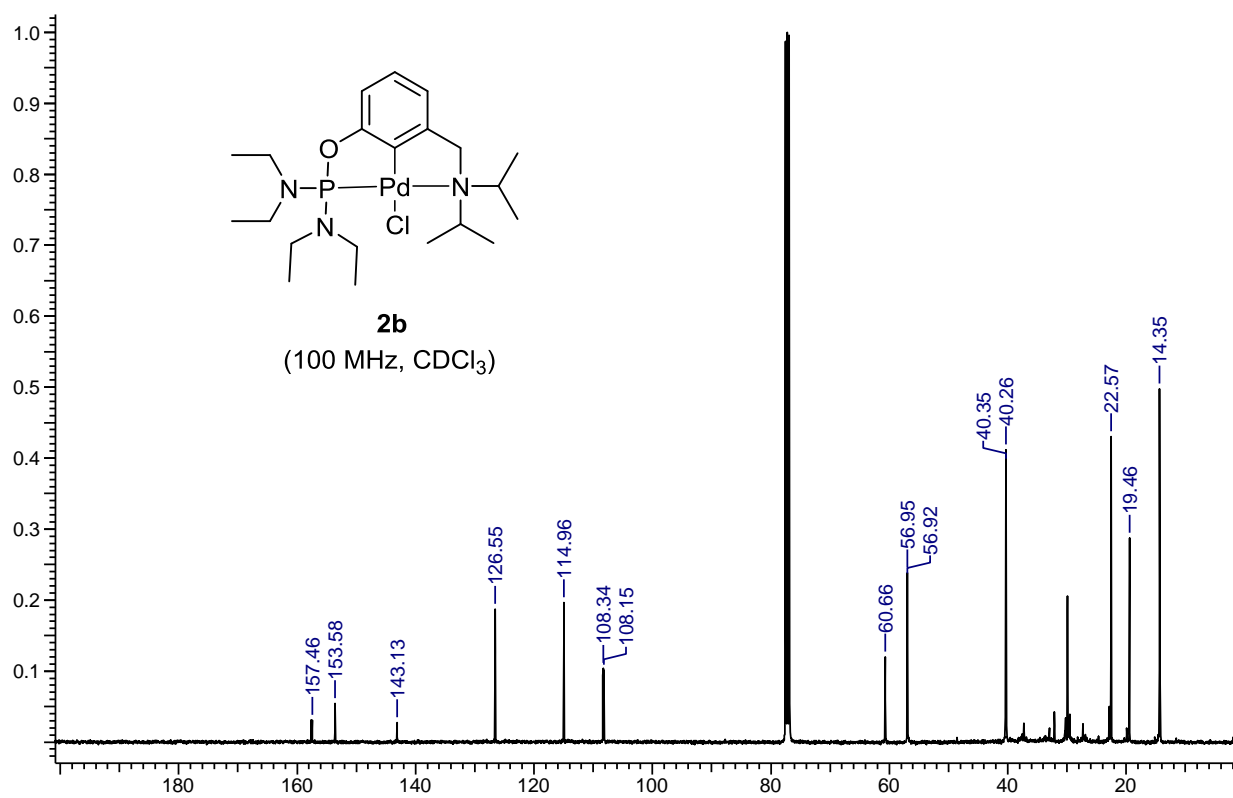
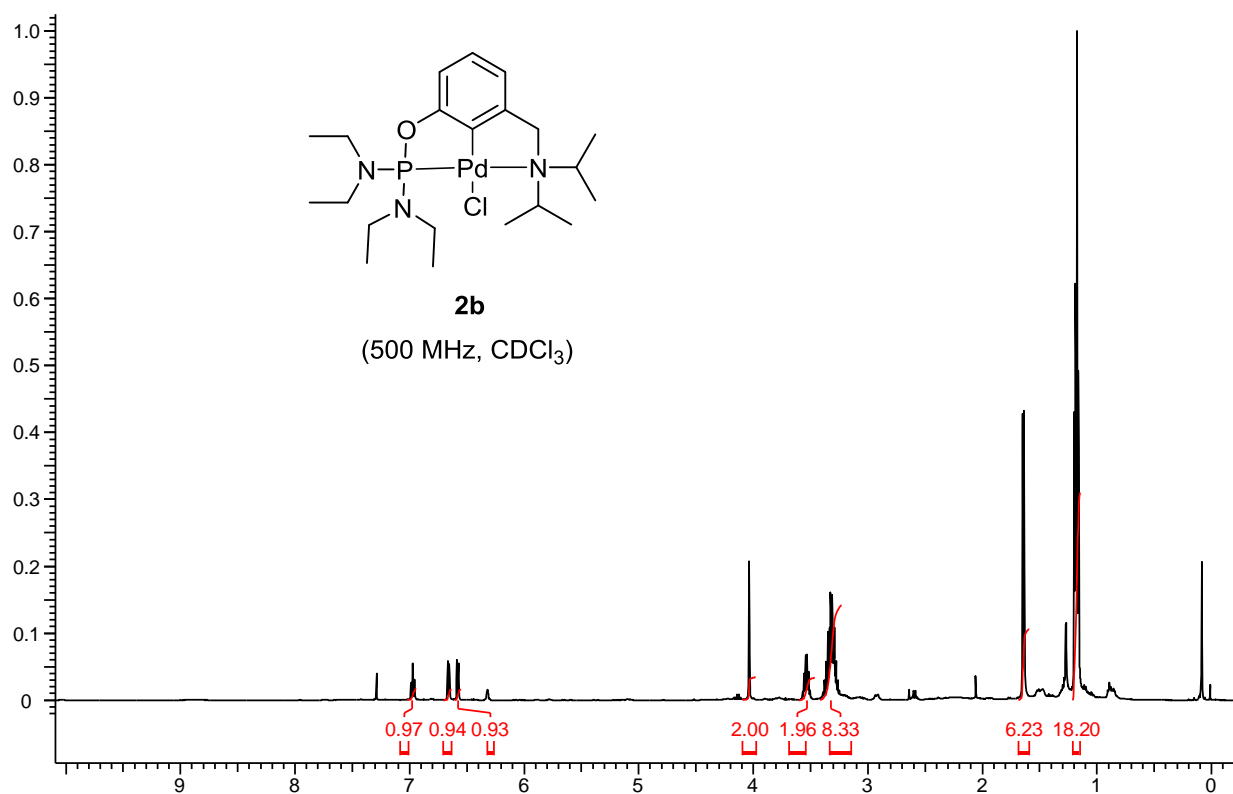


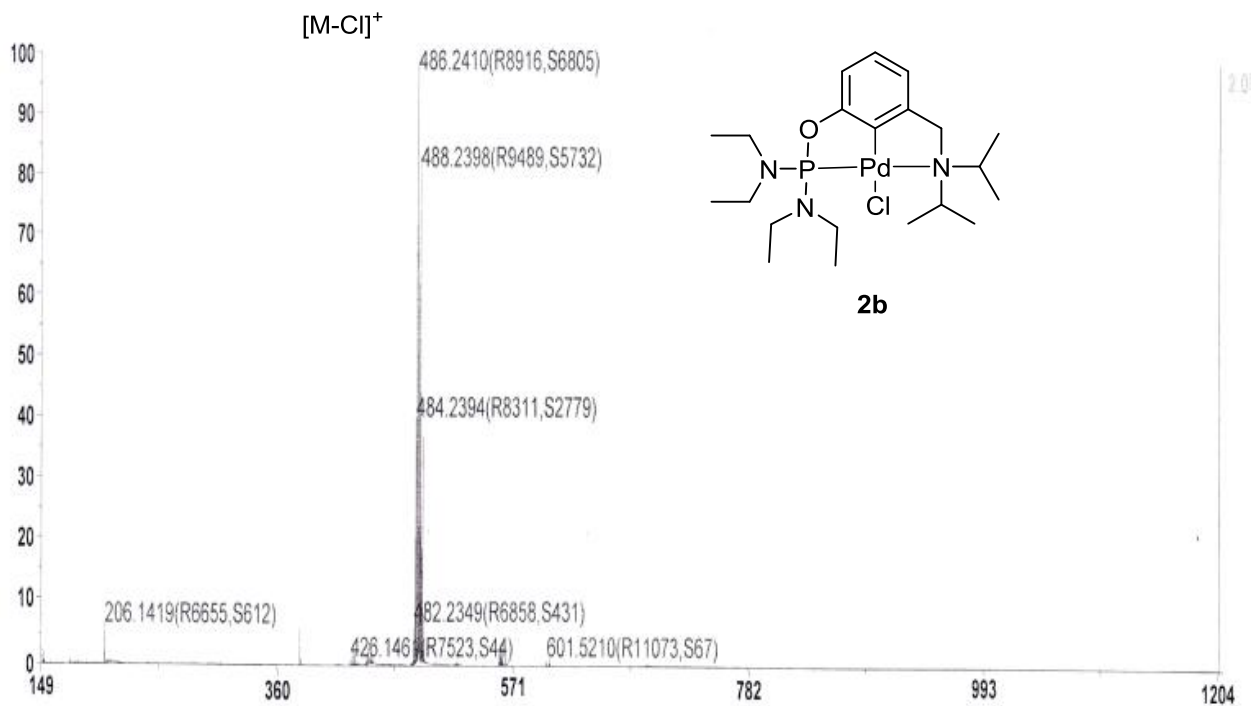
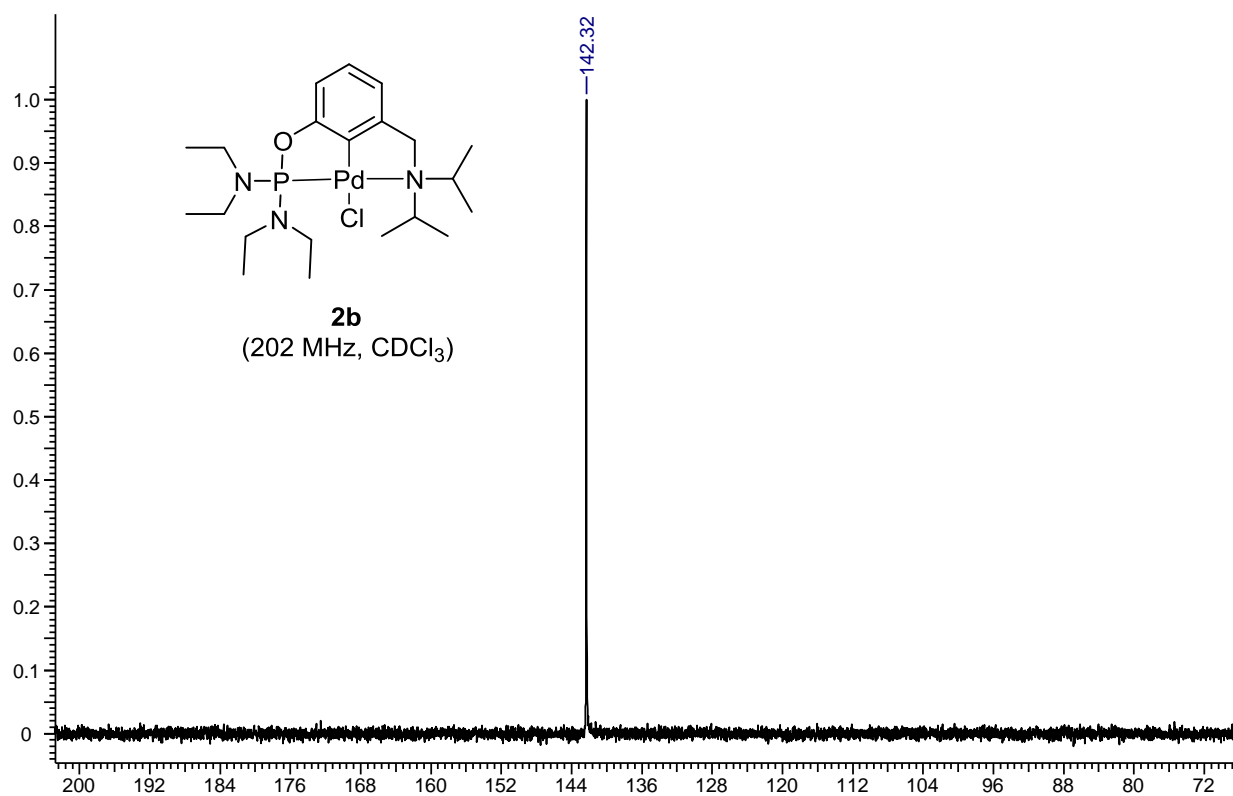


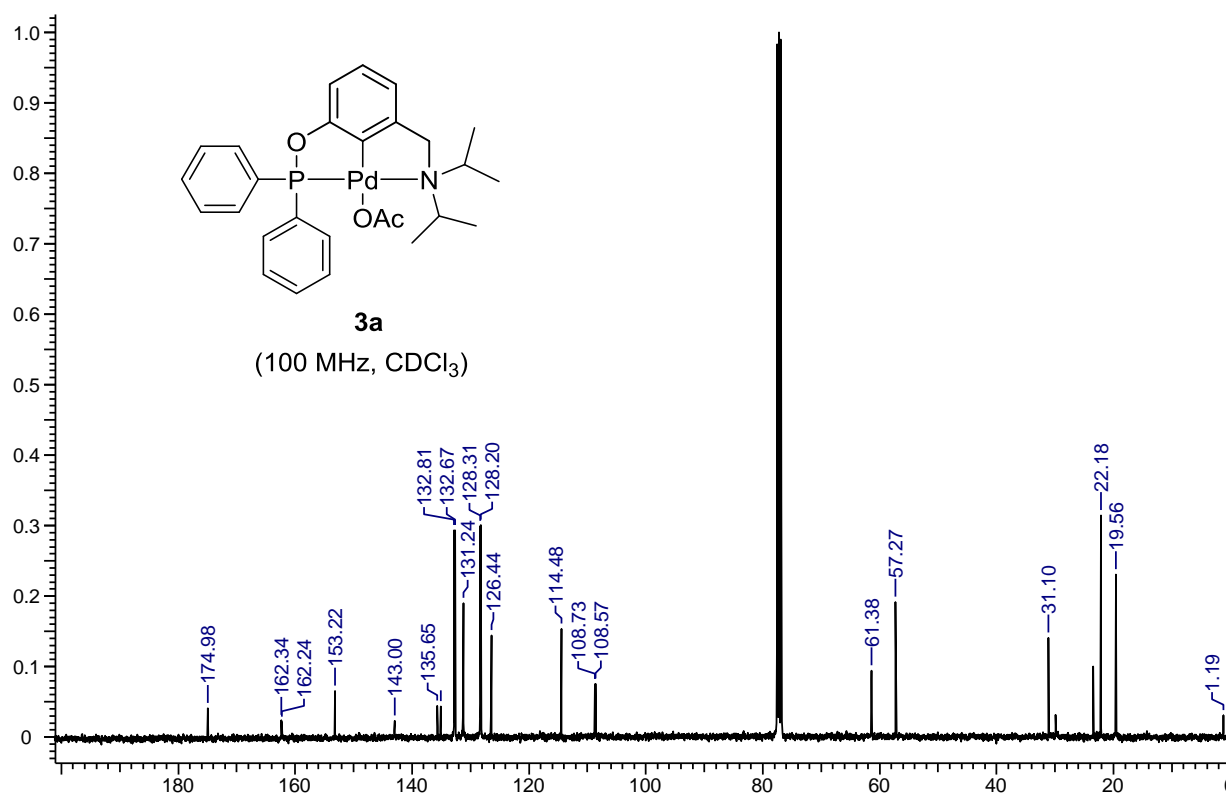
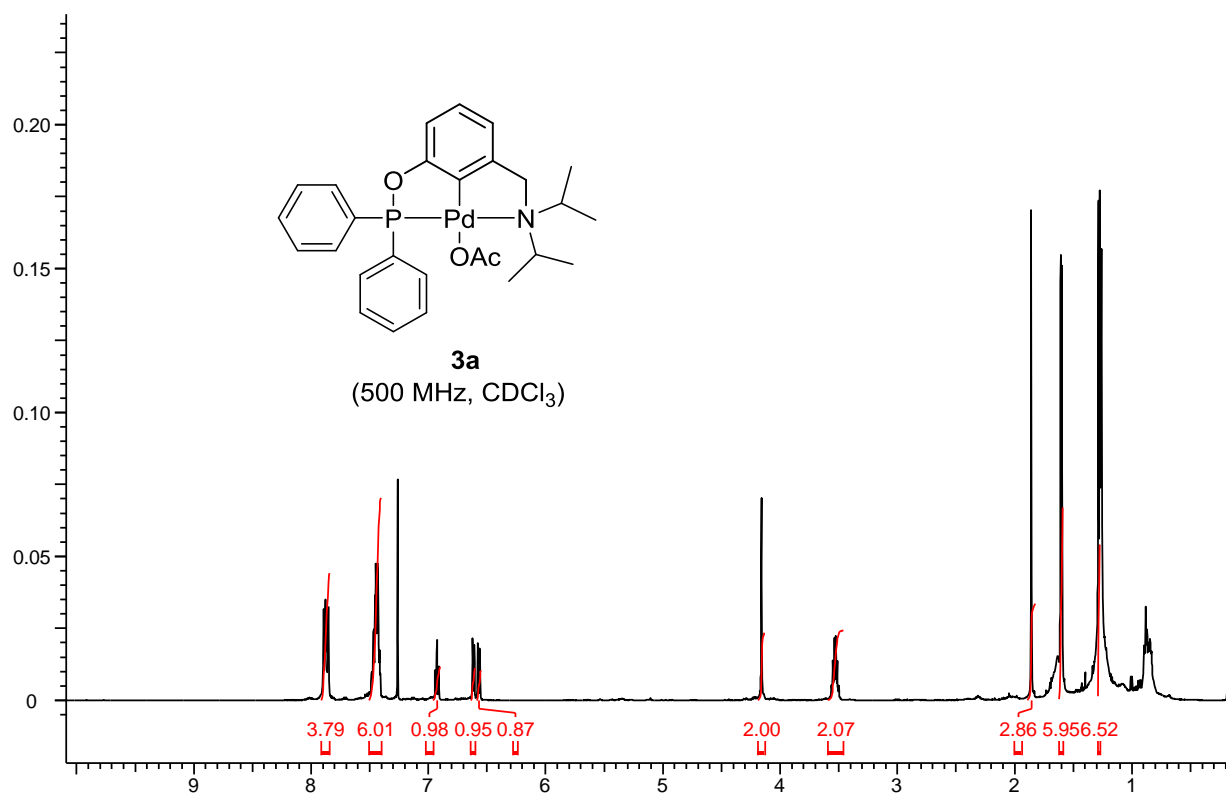
NMR and Mass Spectra of Complexes

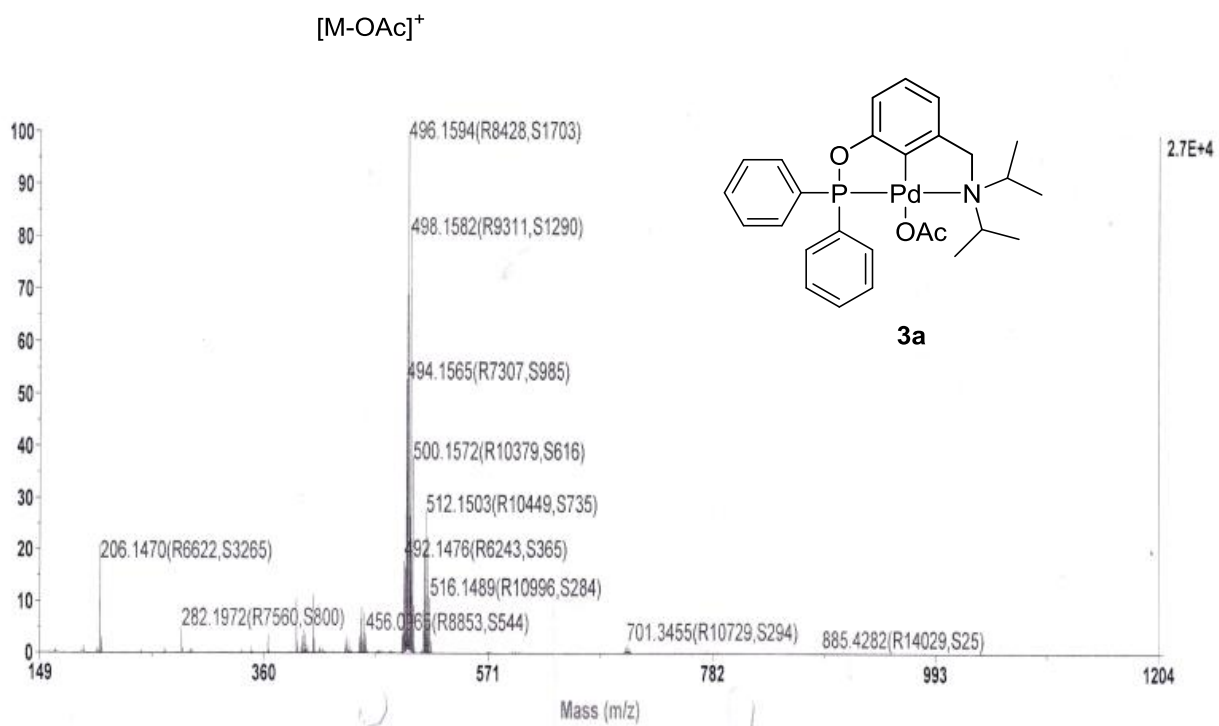
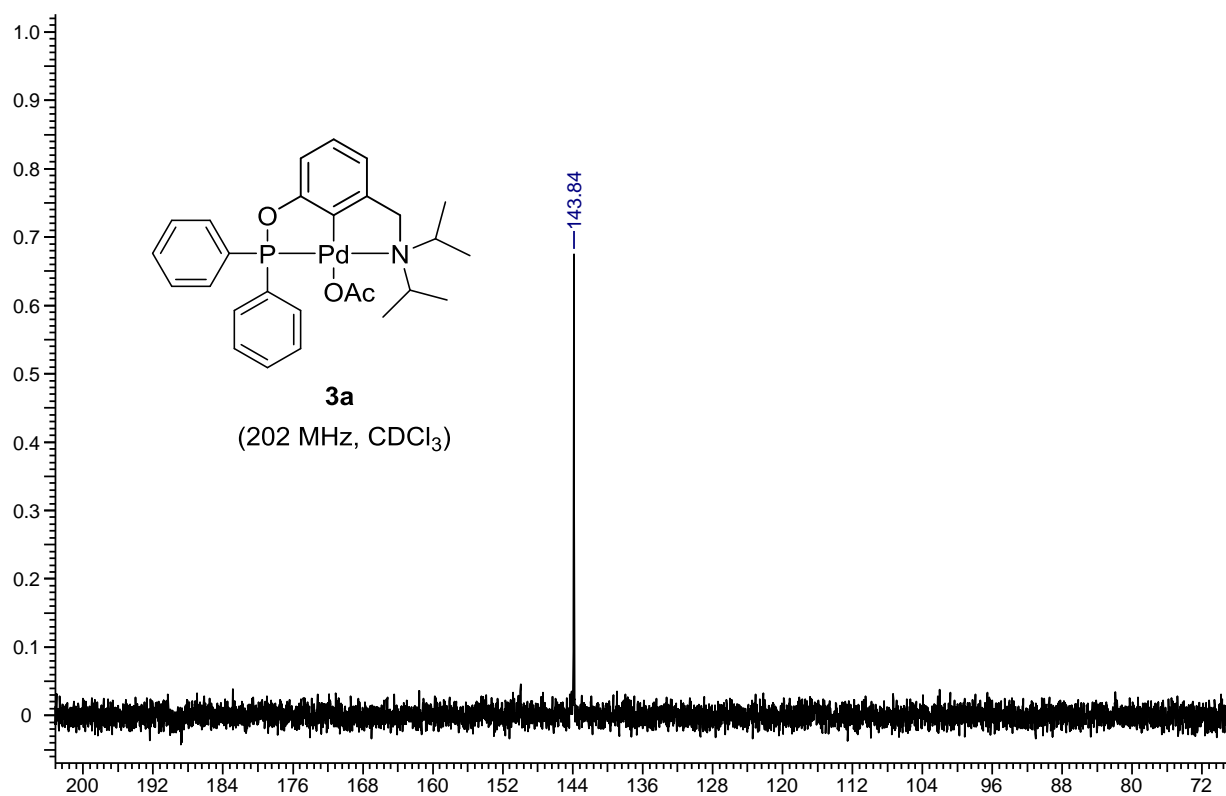


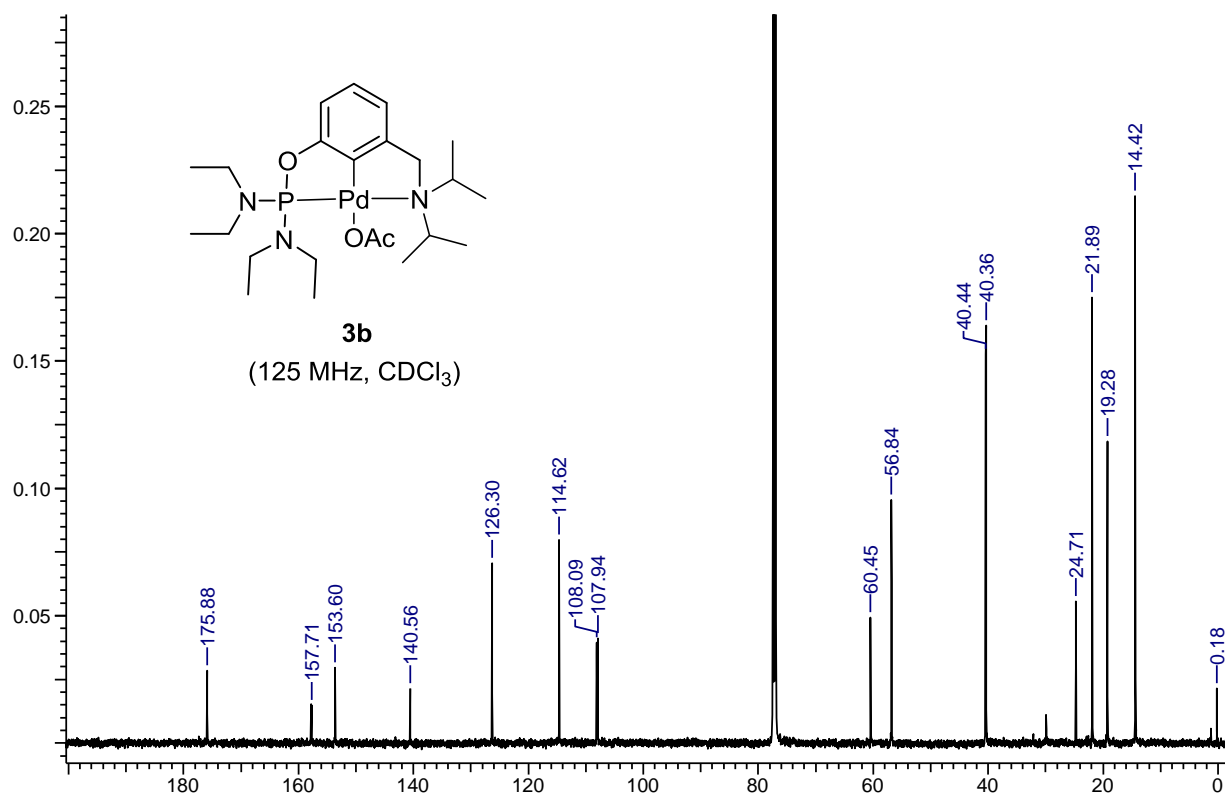
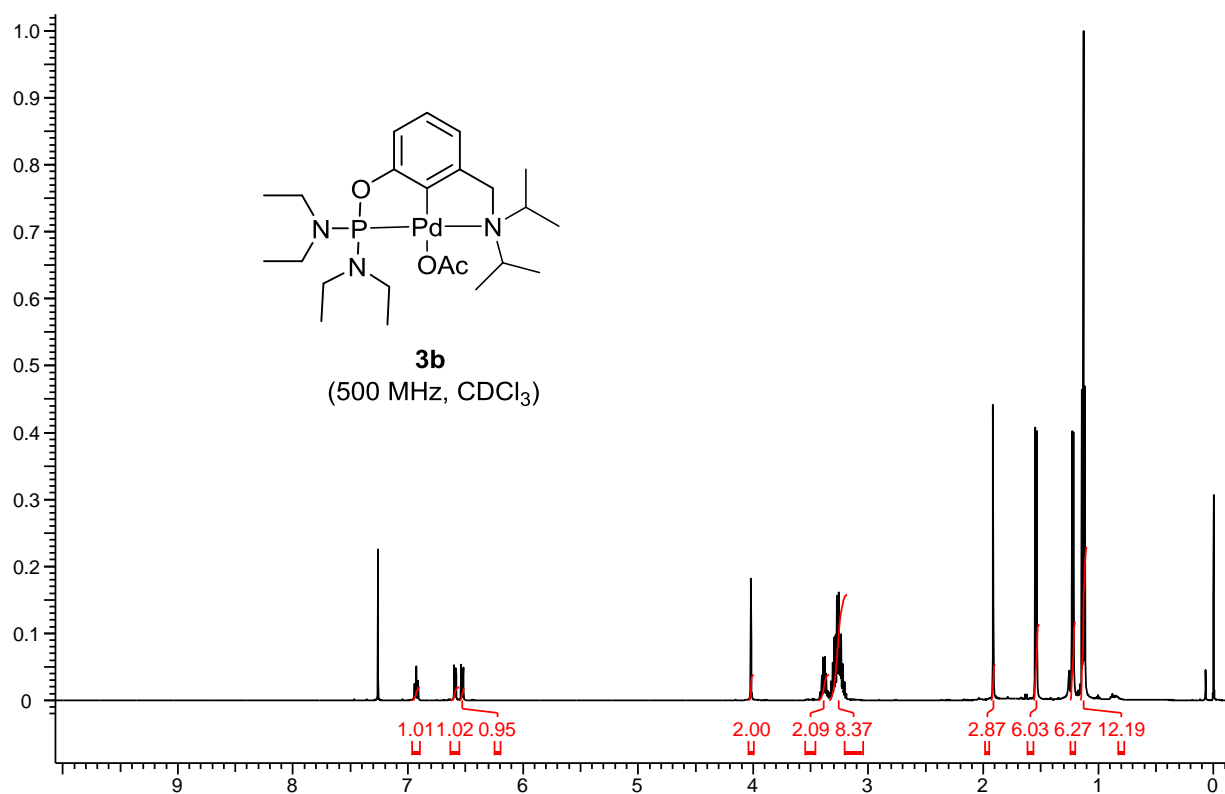


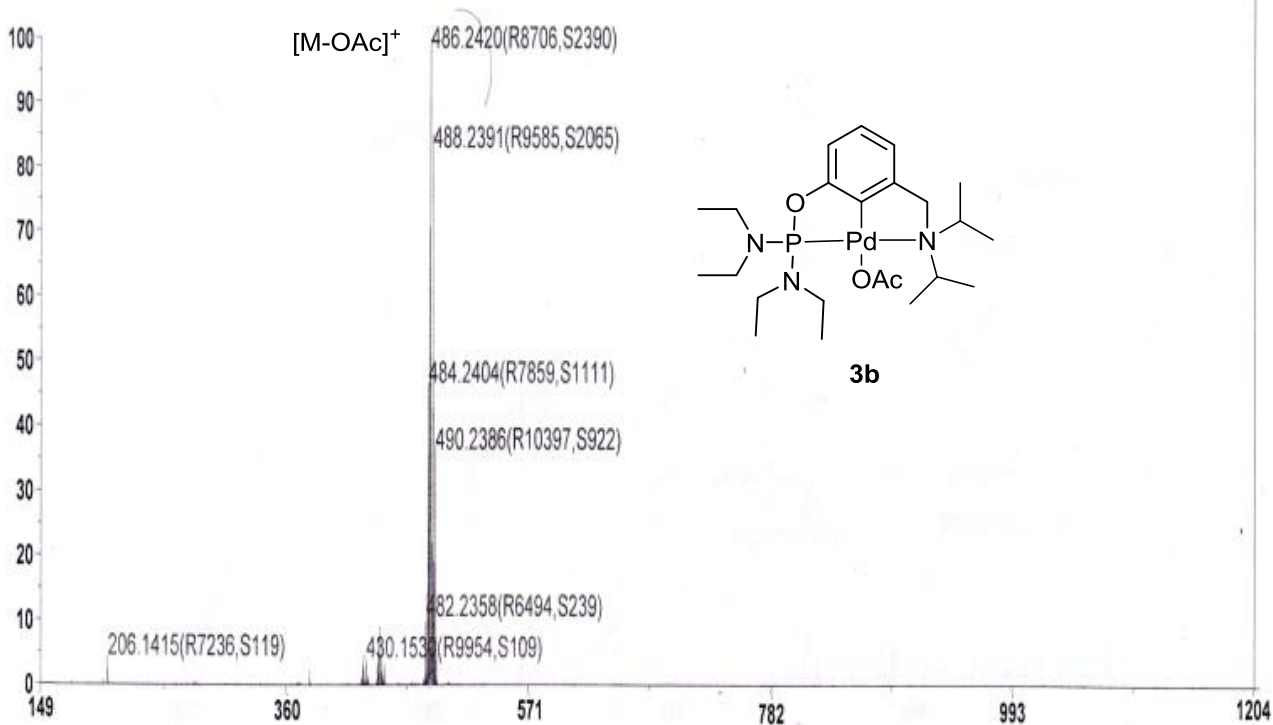
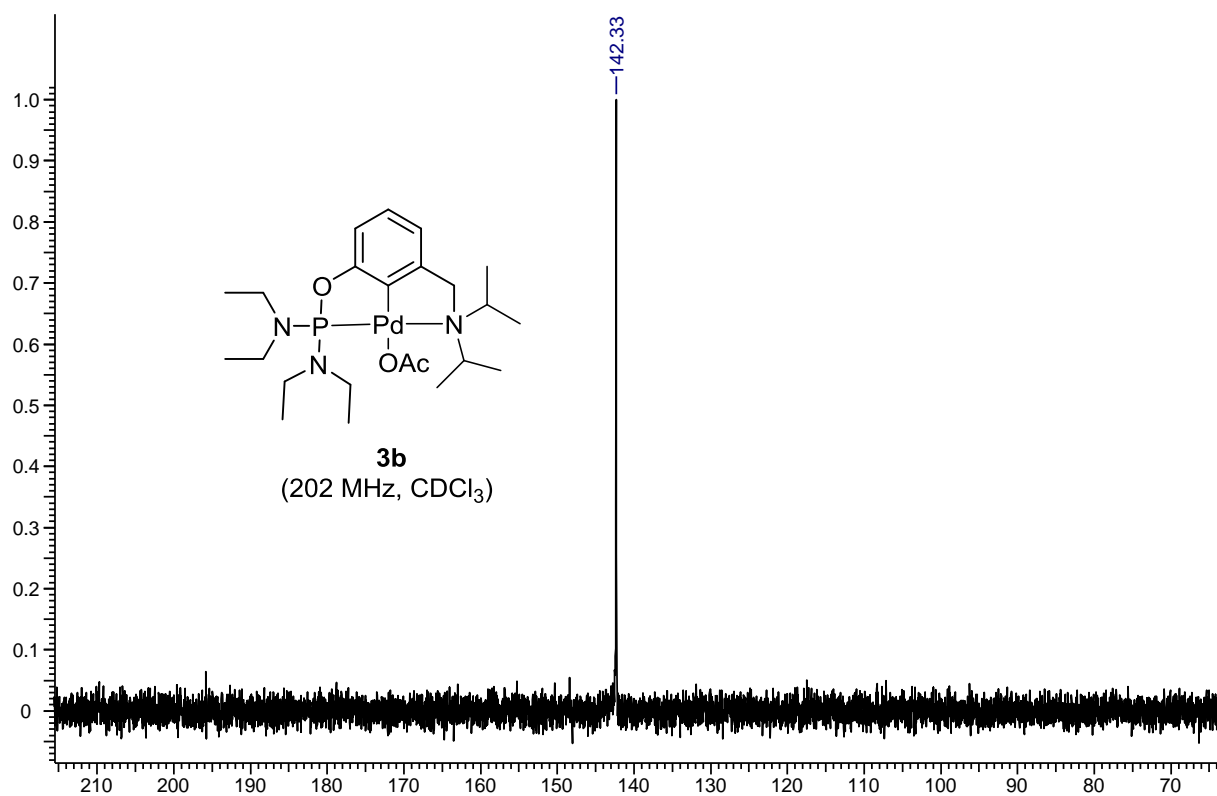


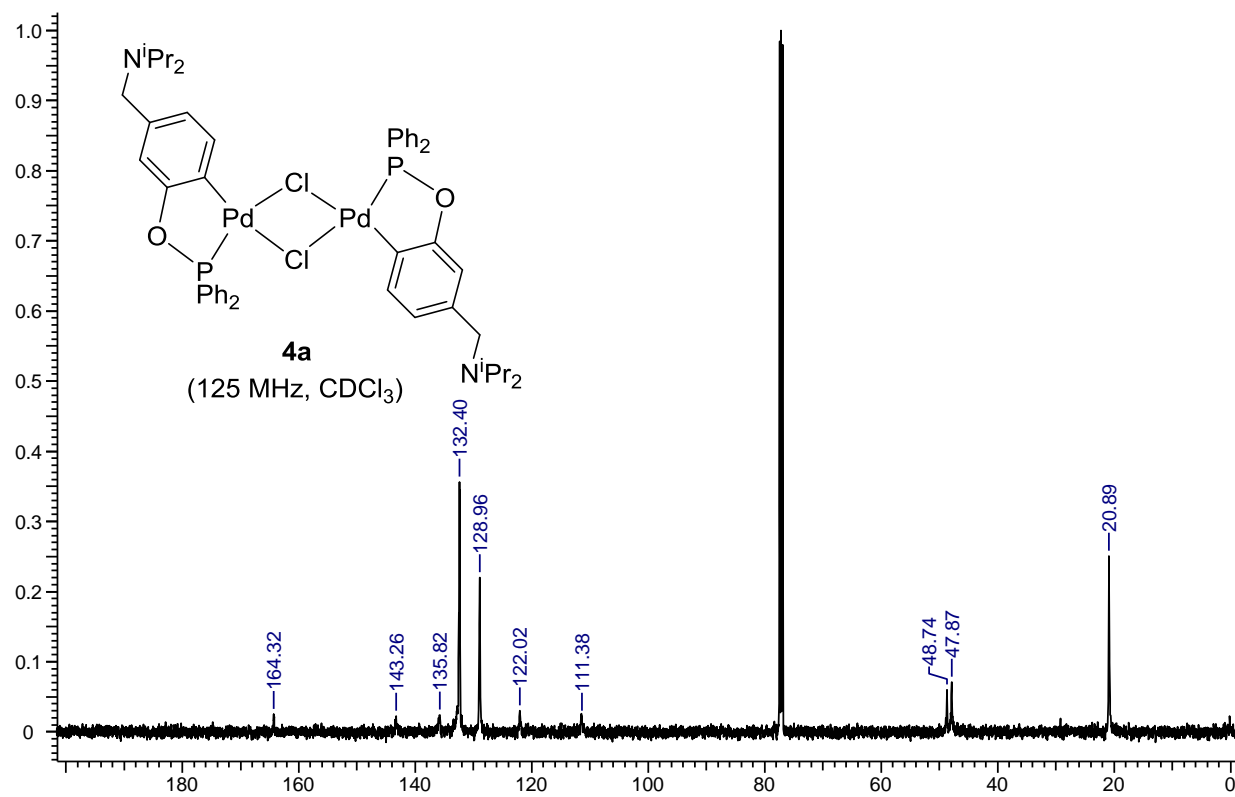
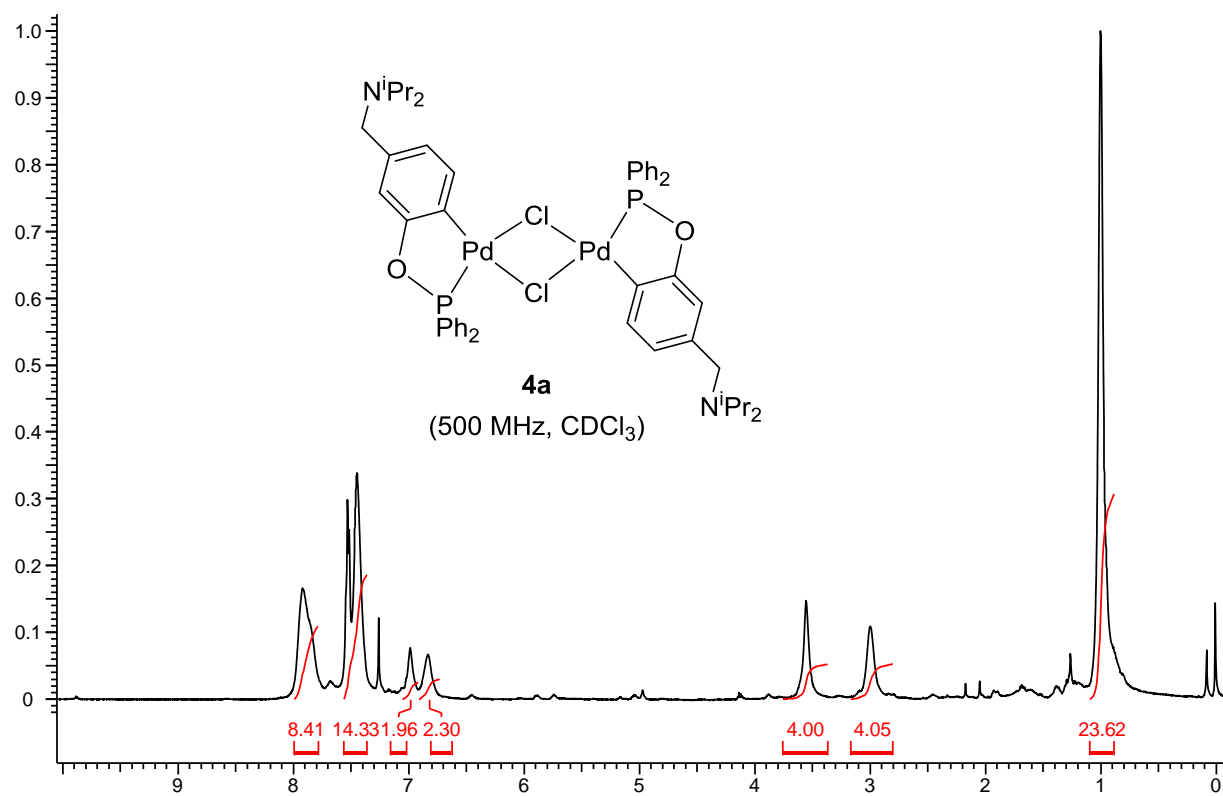


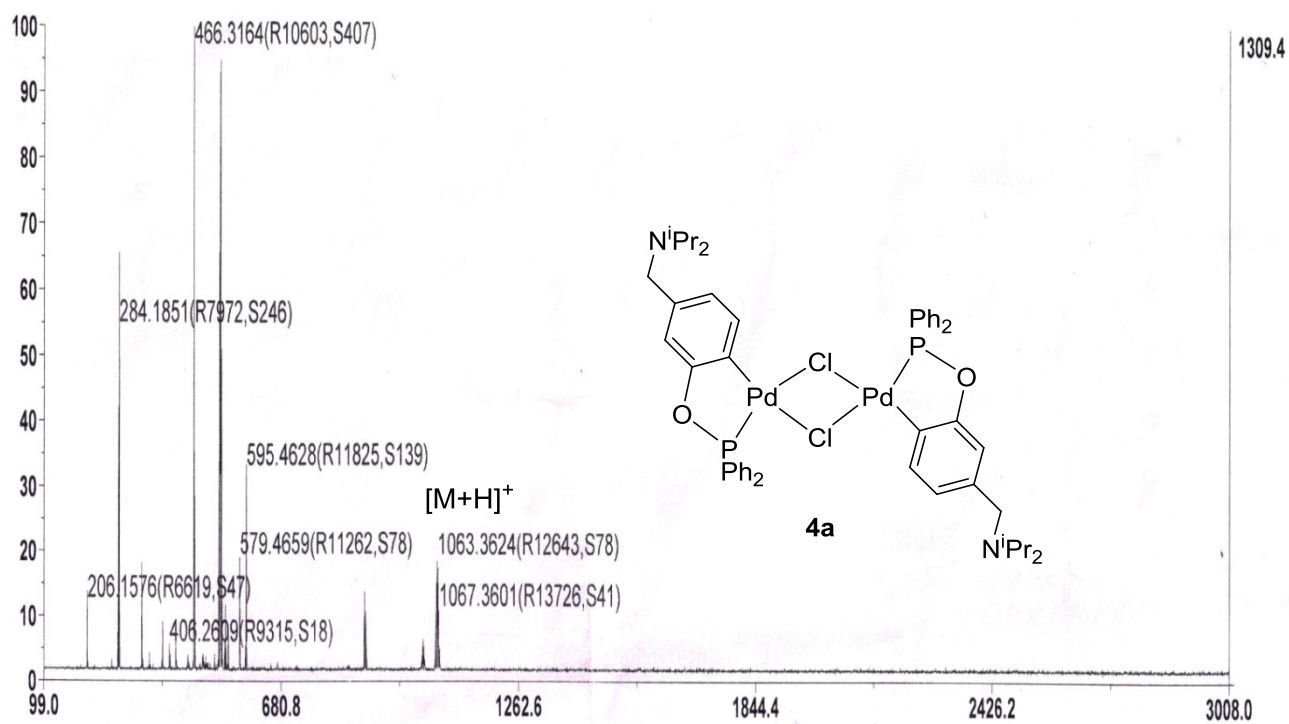
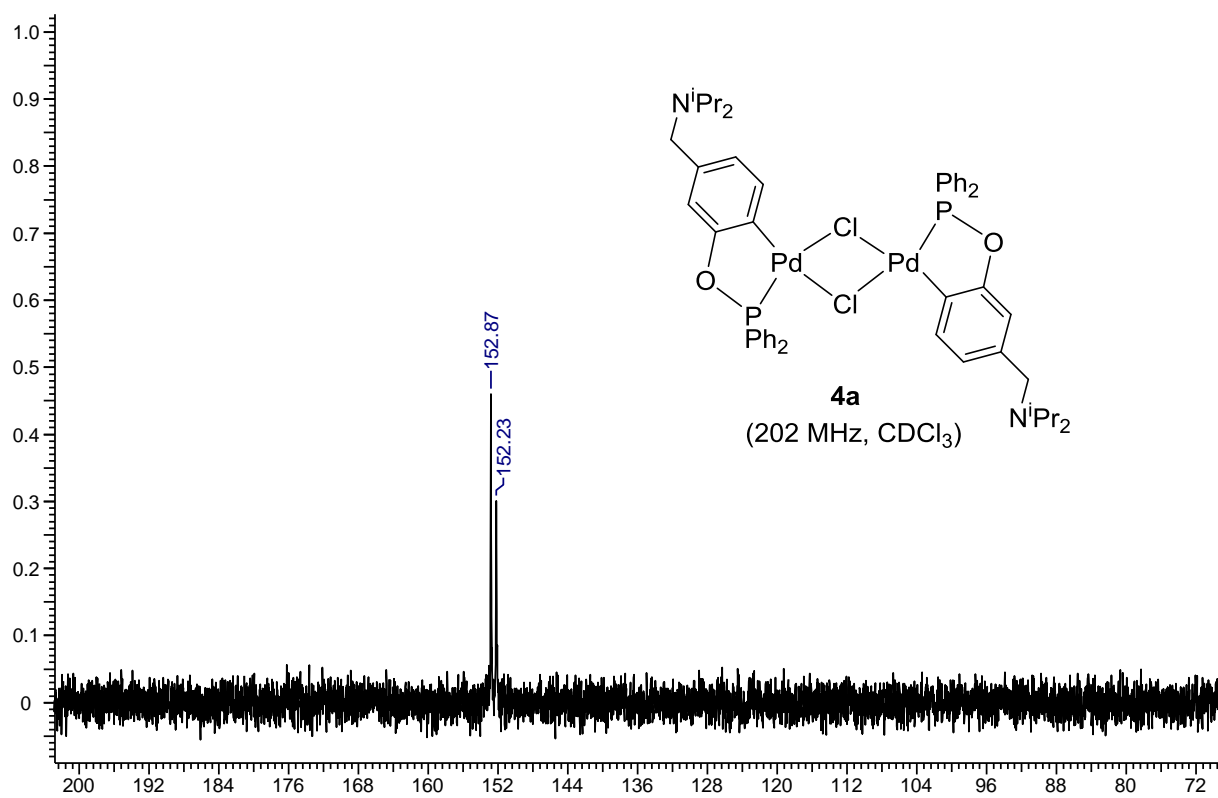


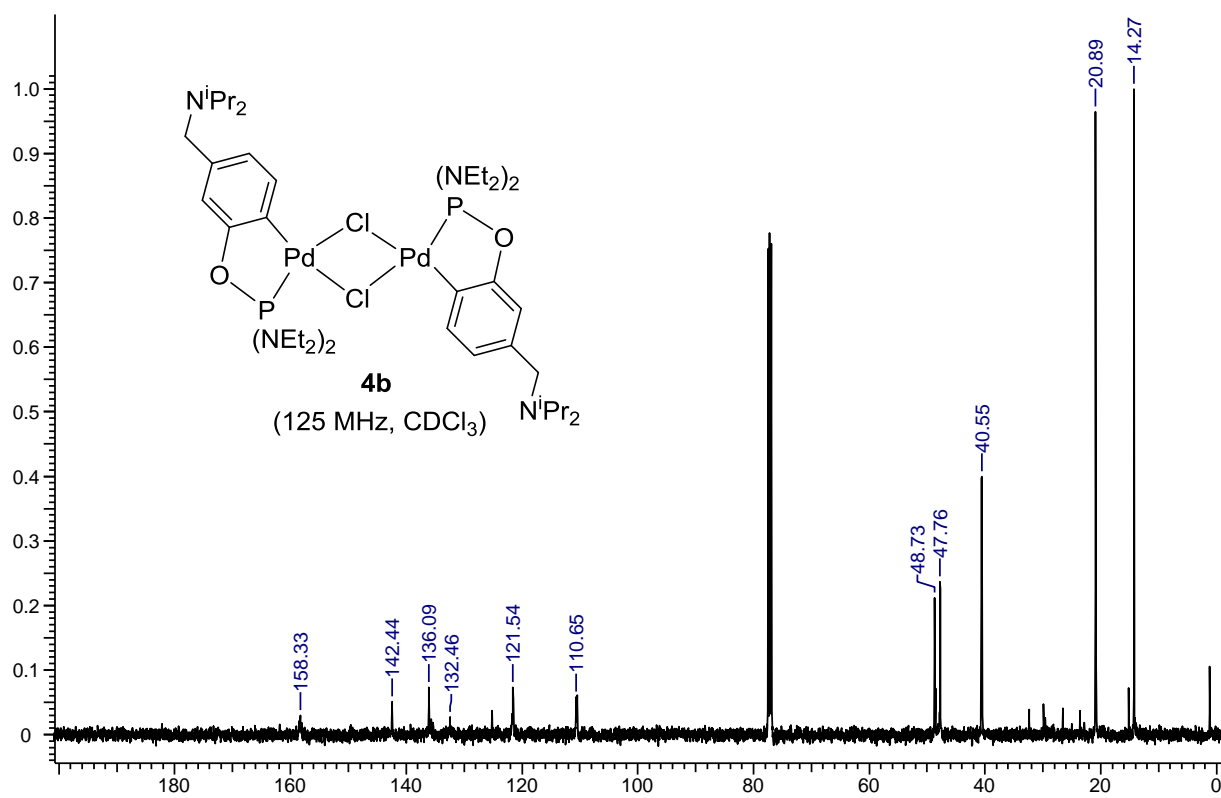
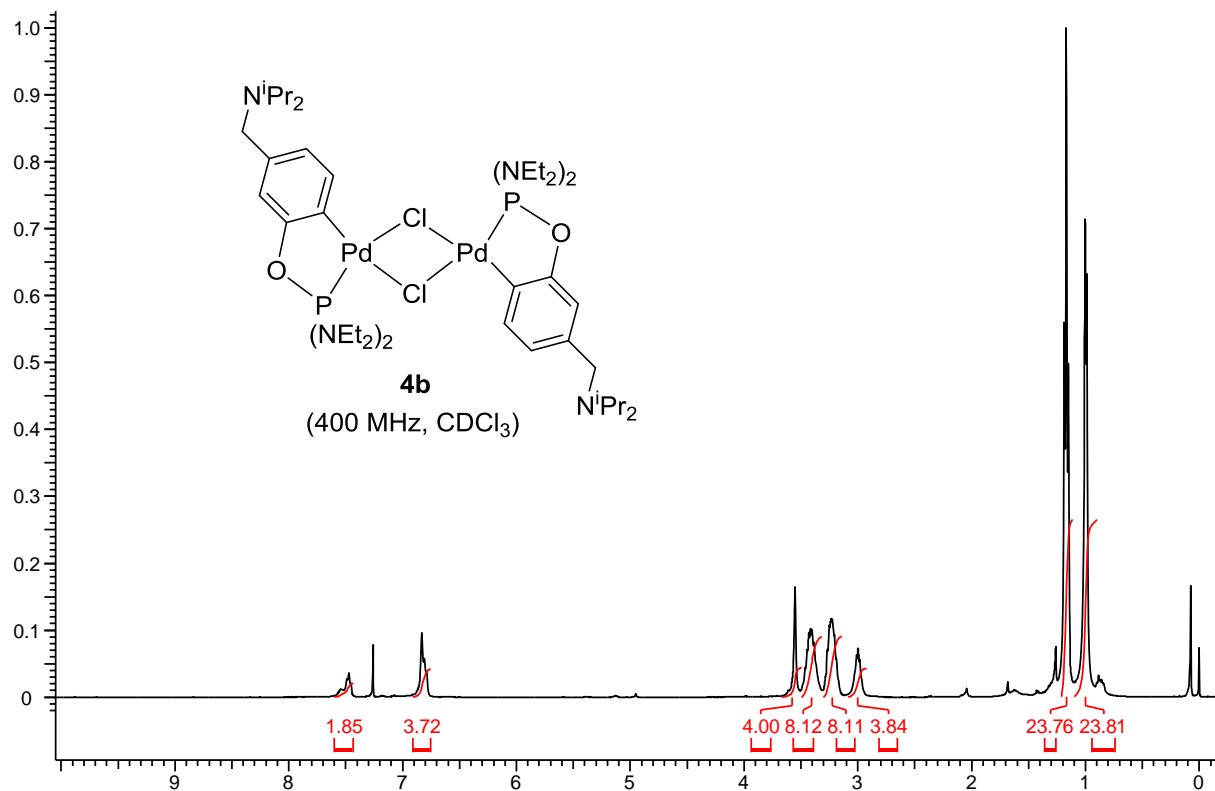


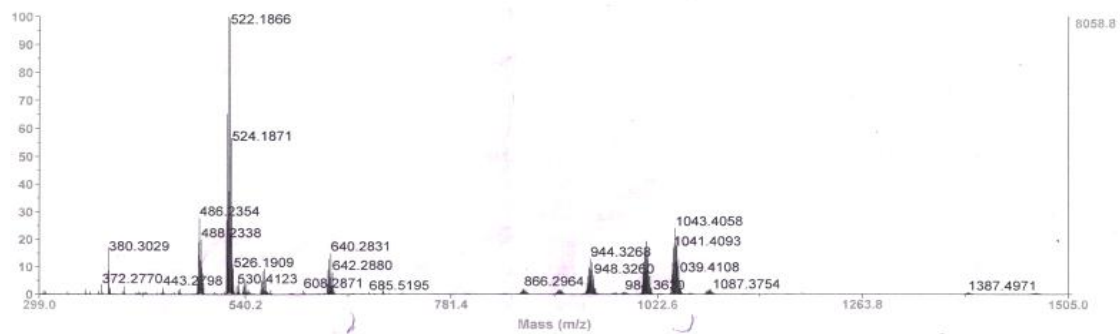
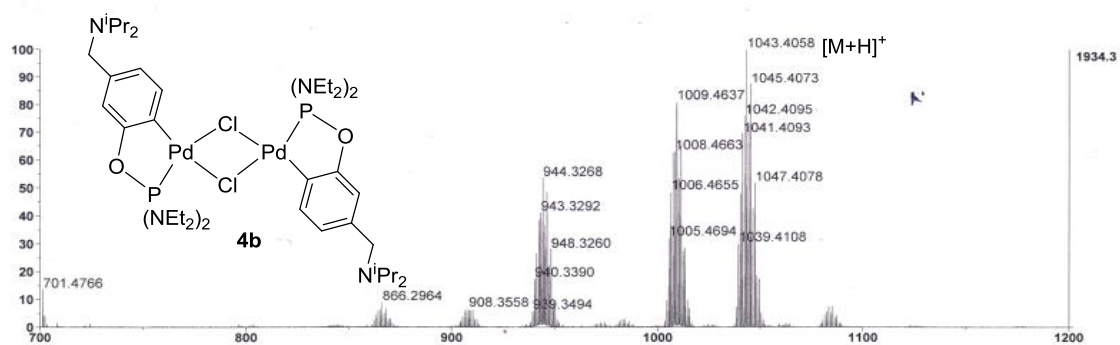
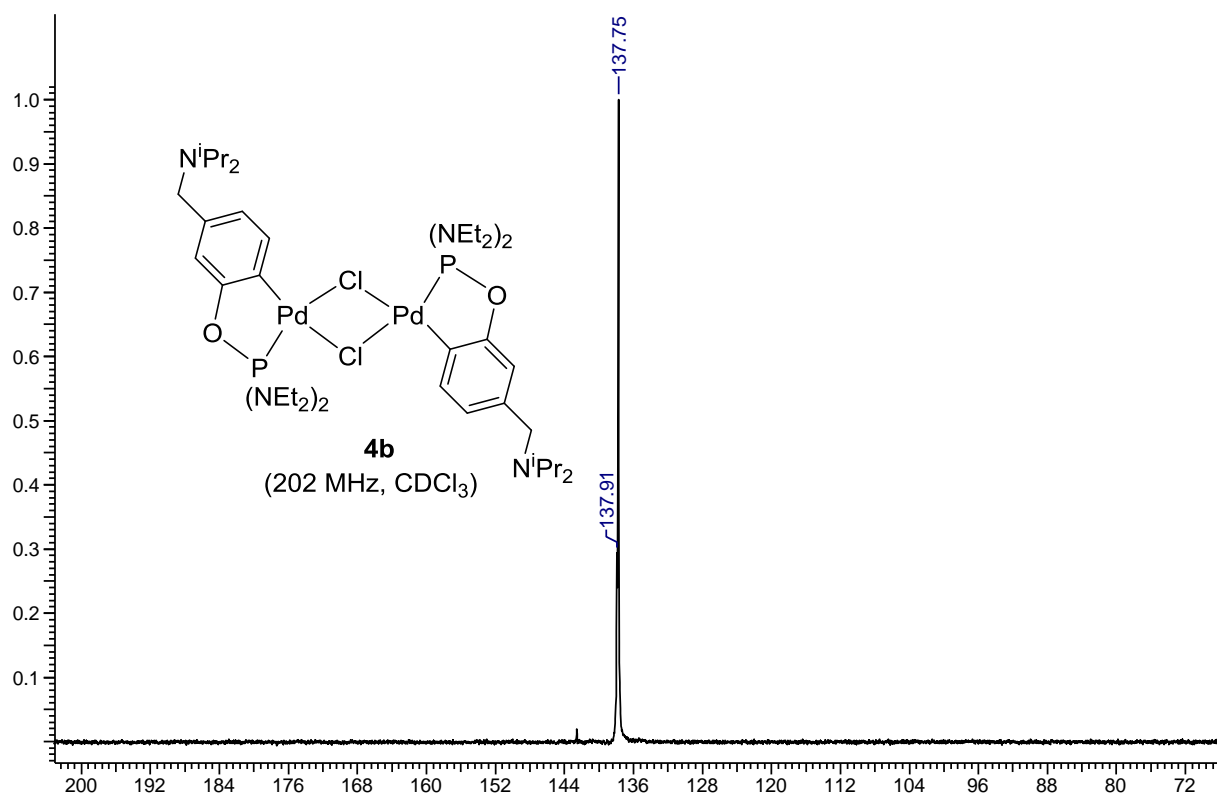


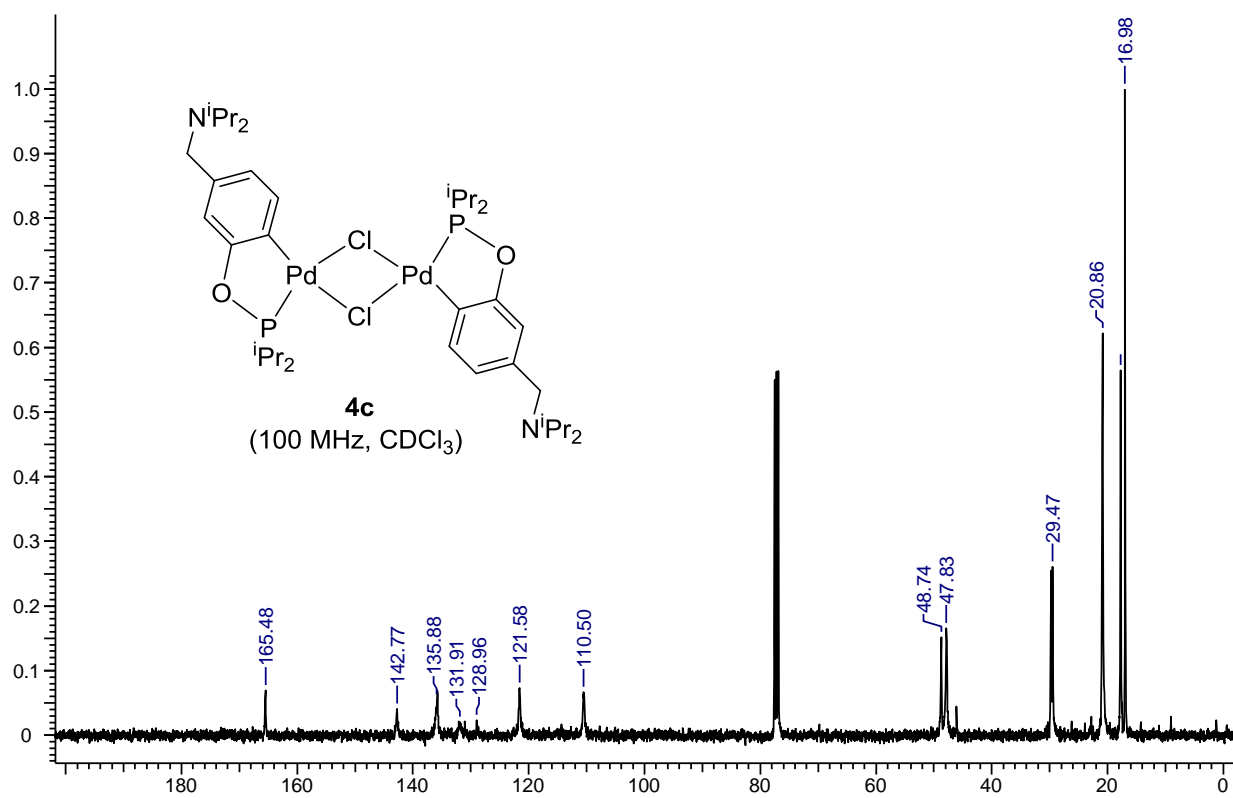
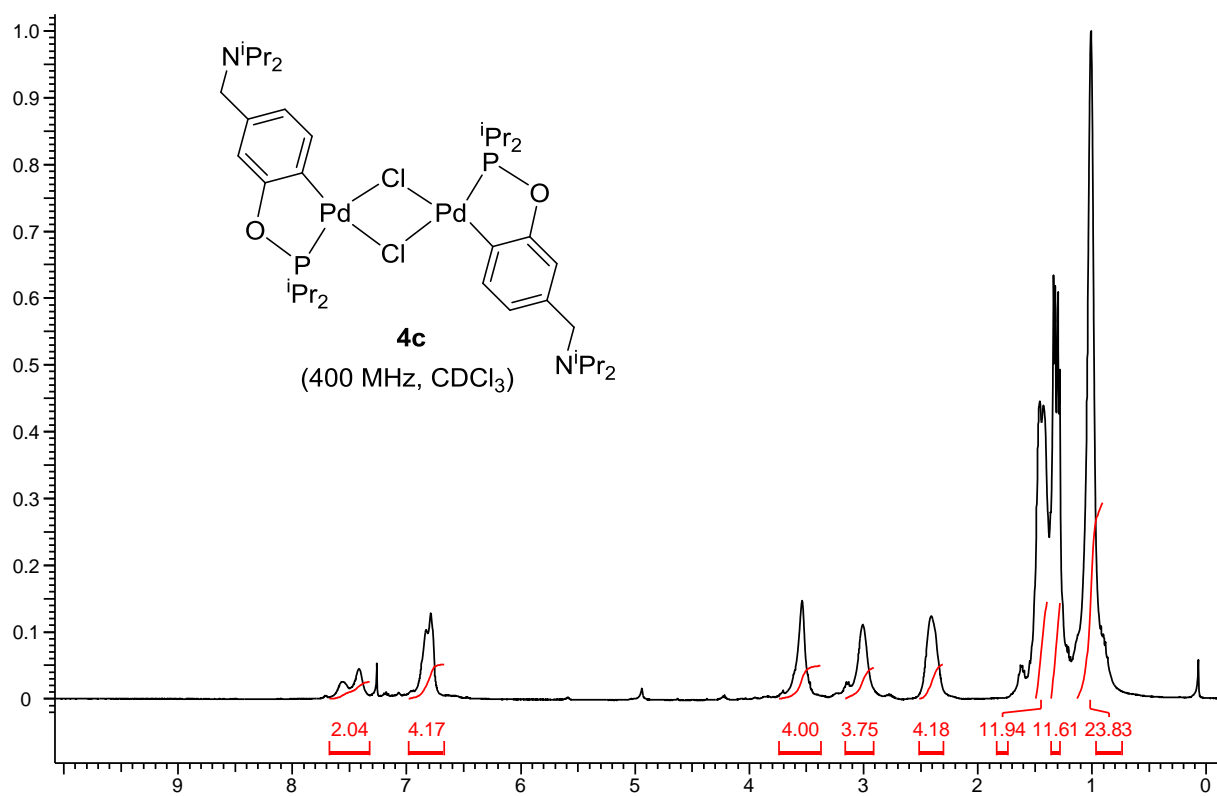


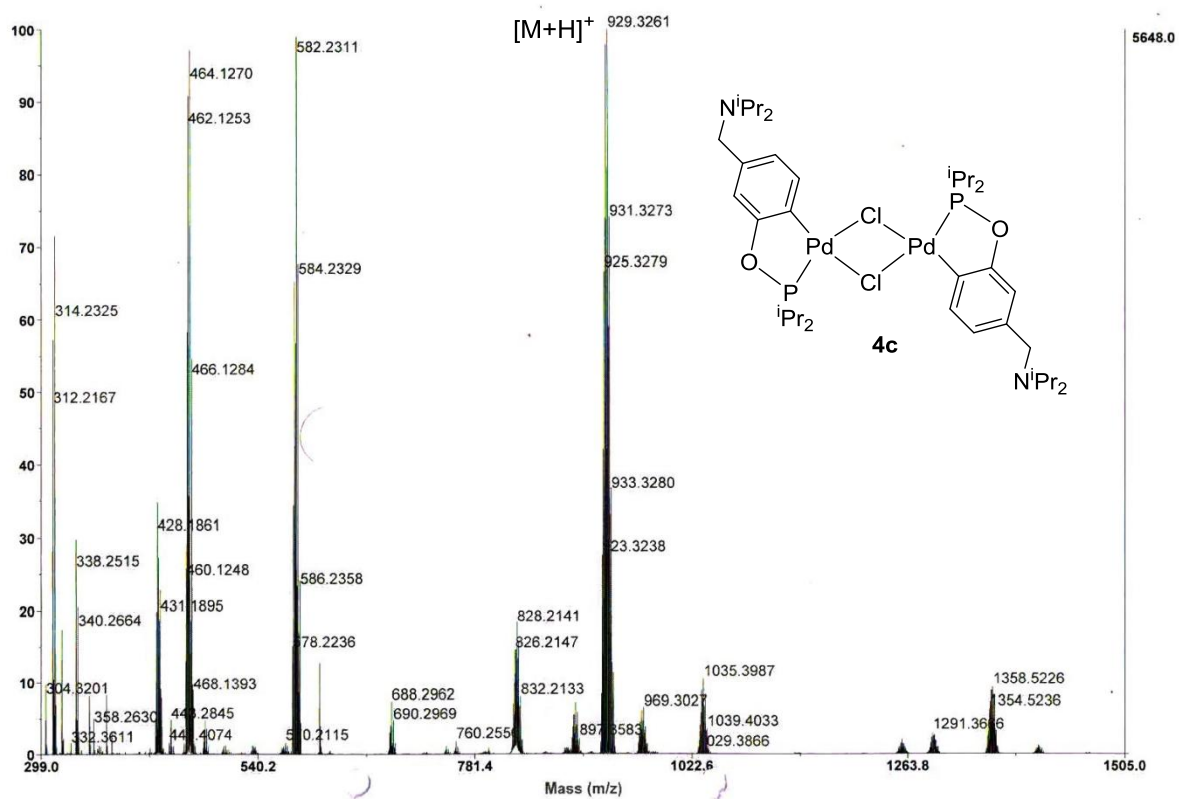
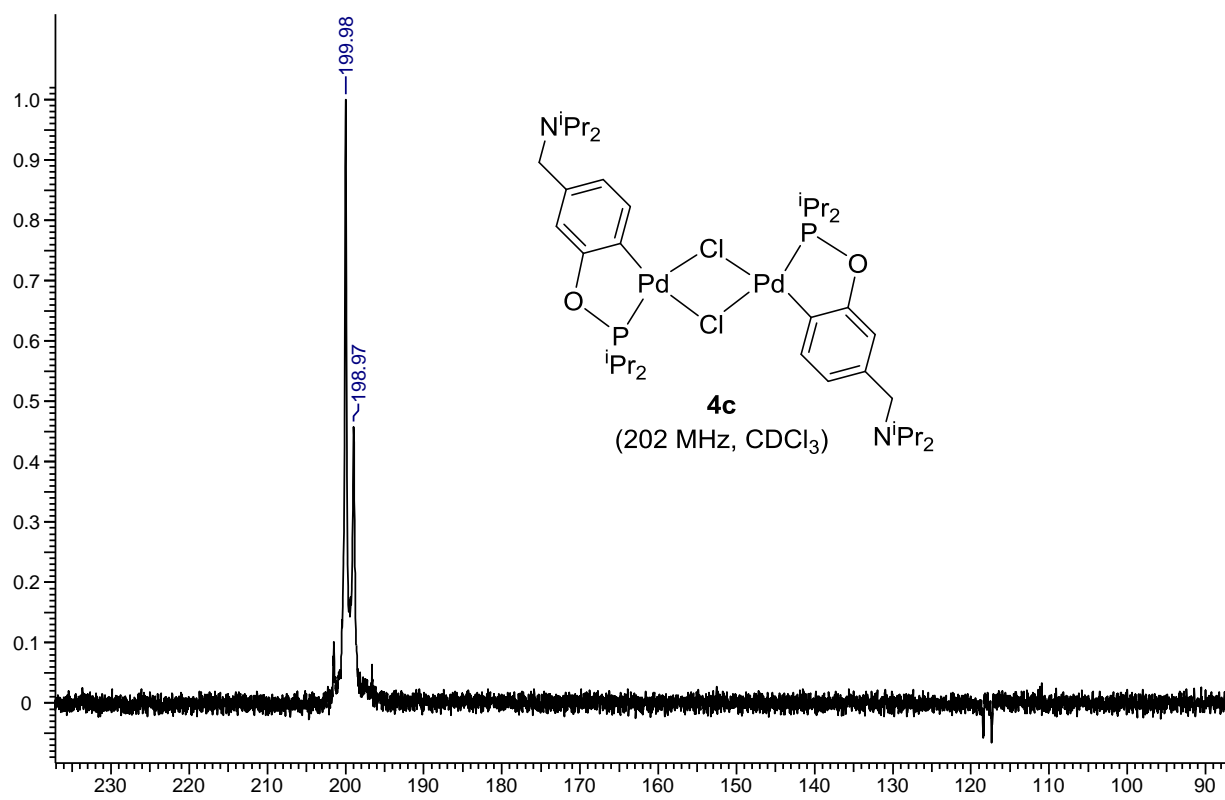


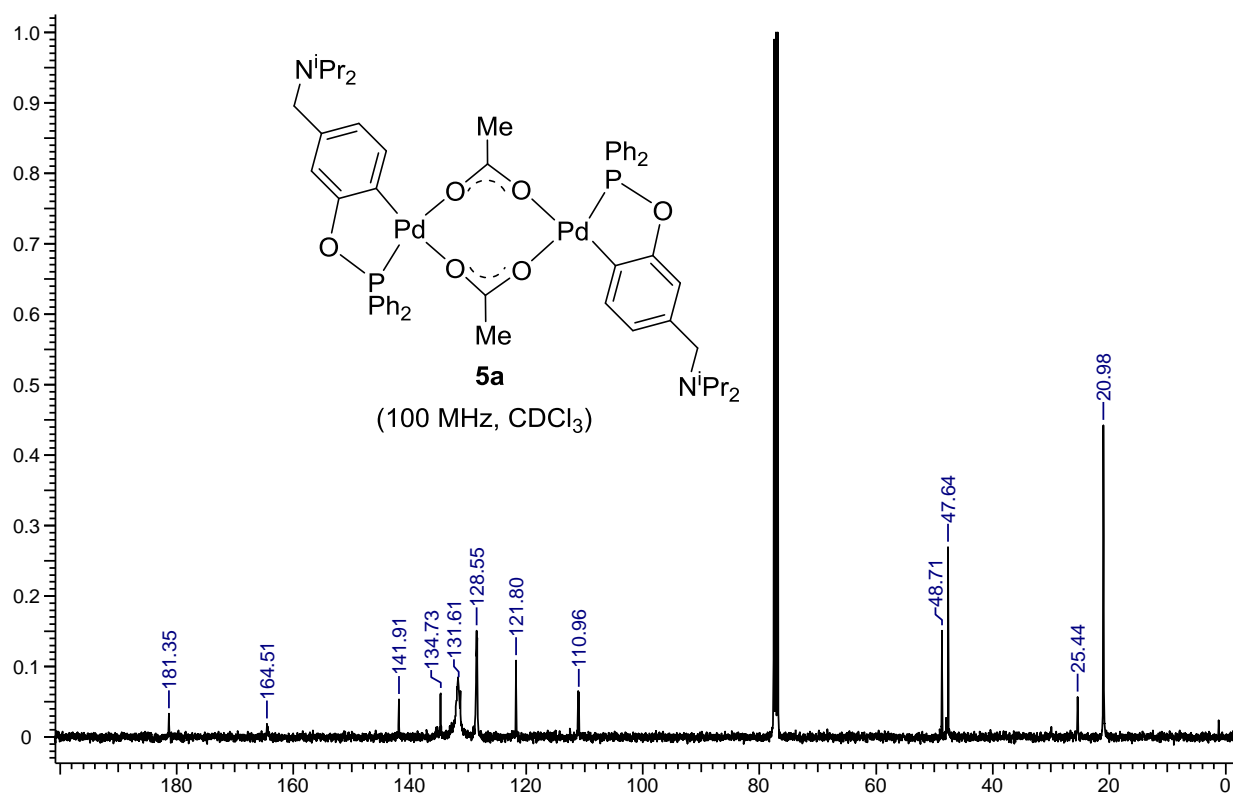
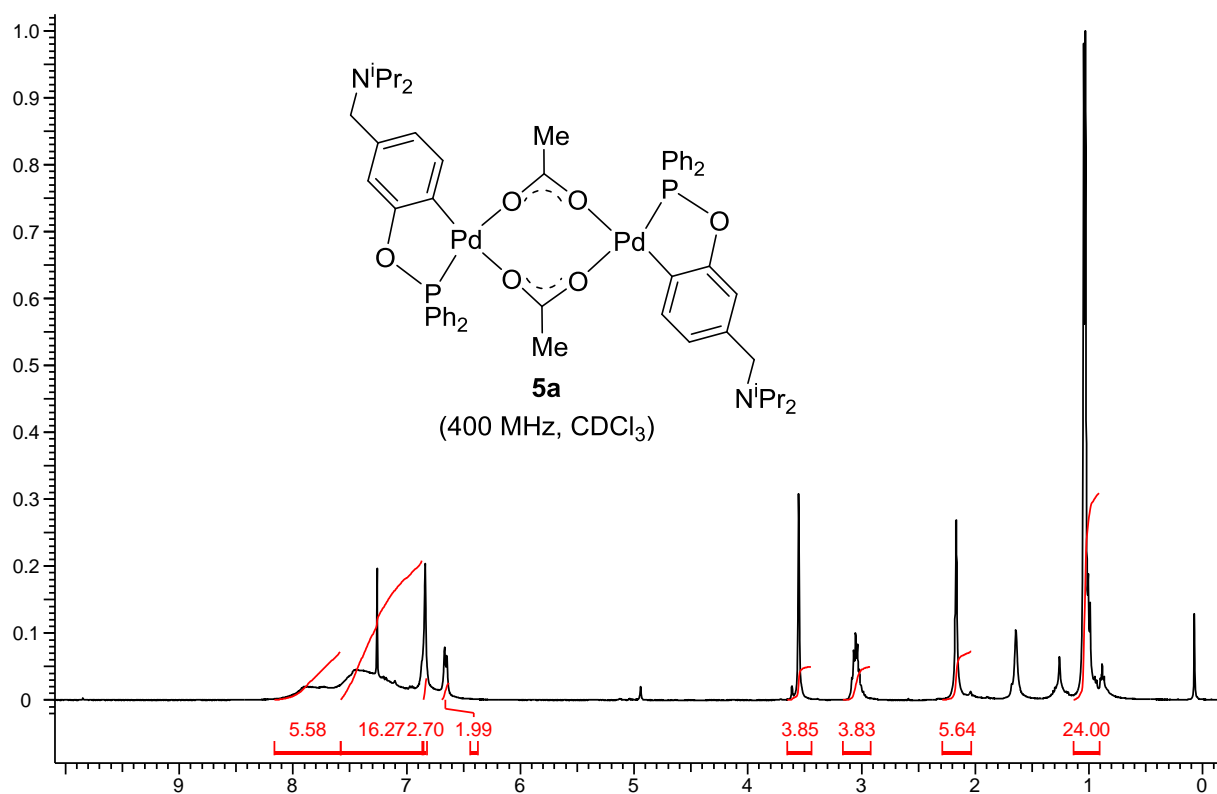


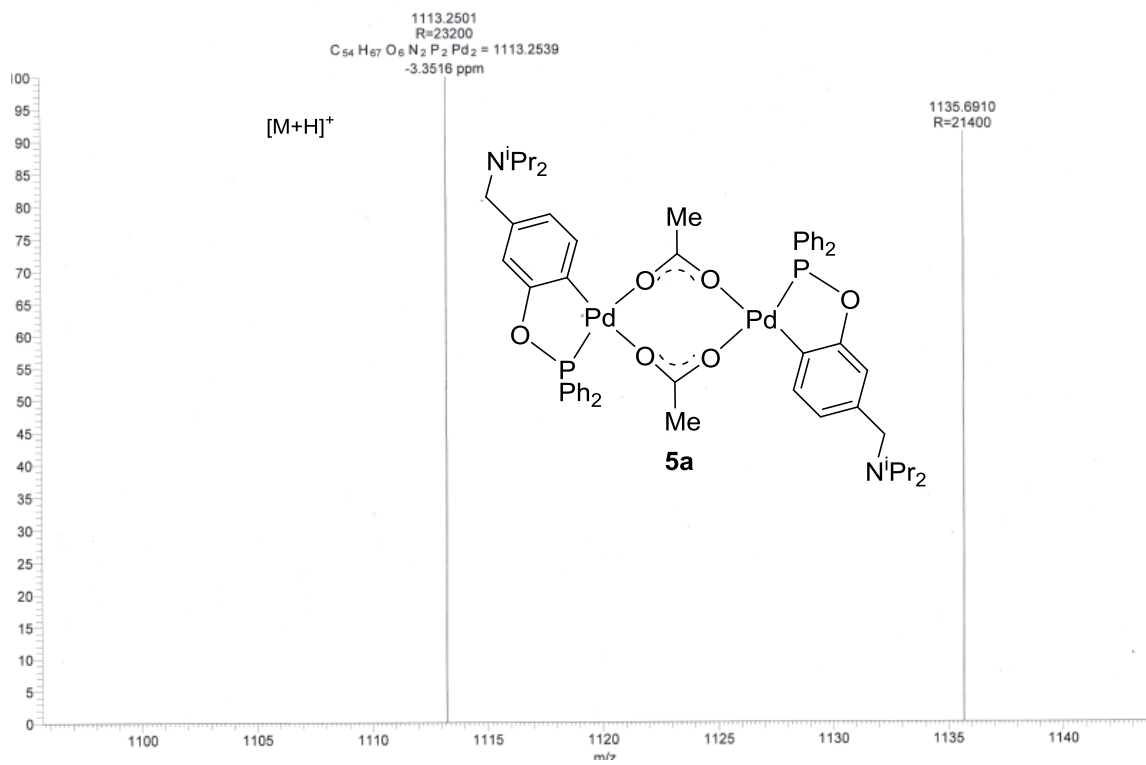
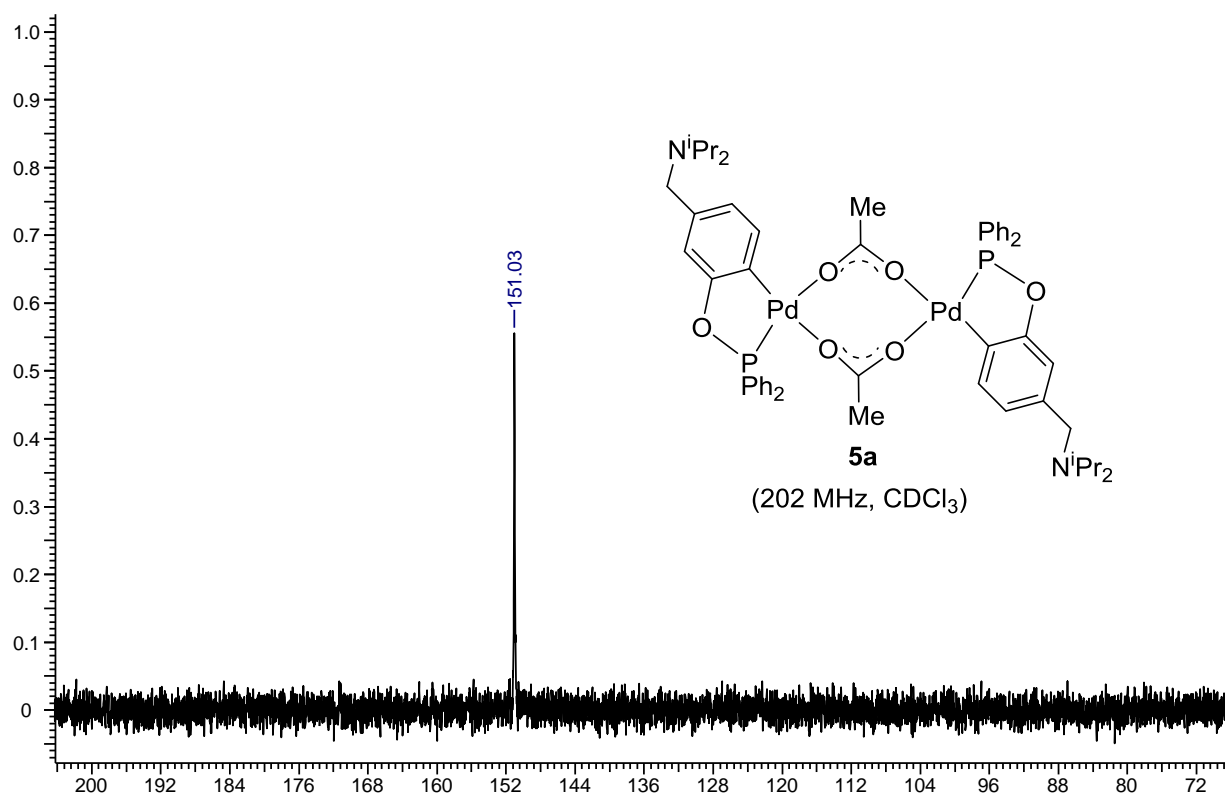


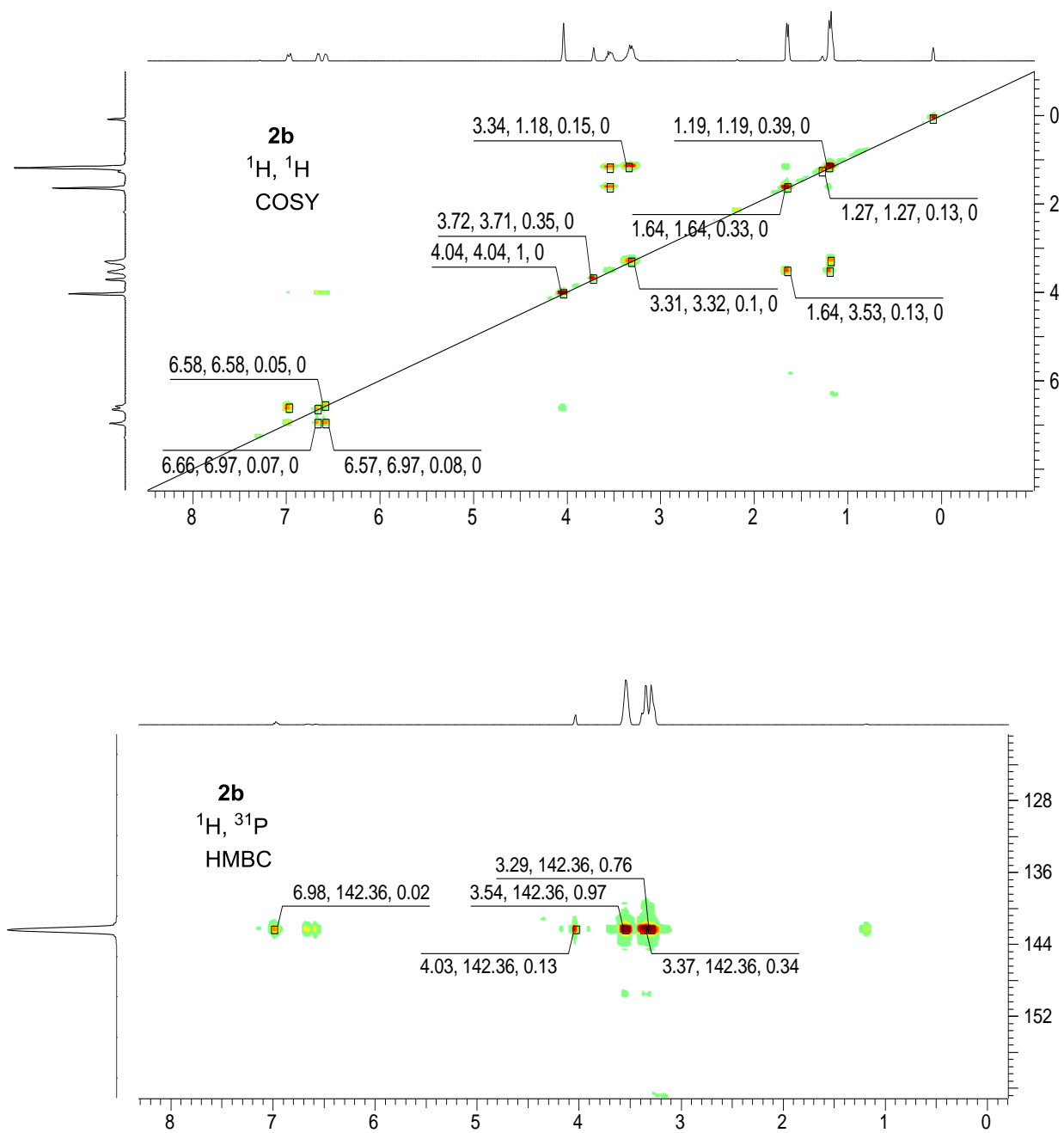


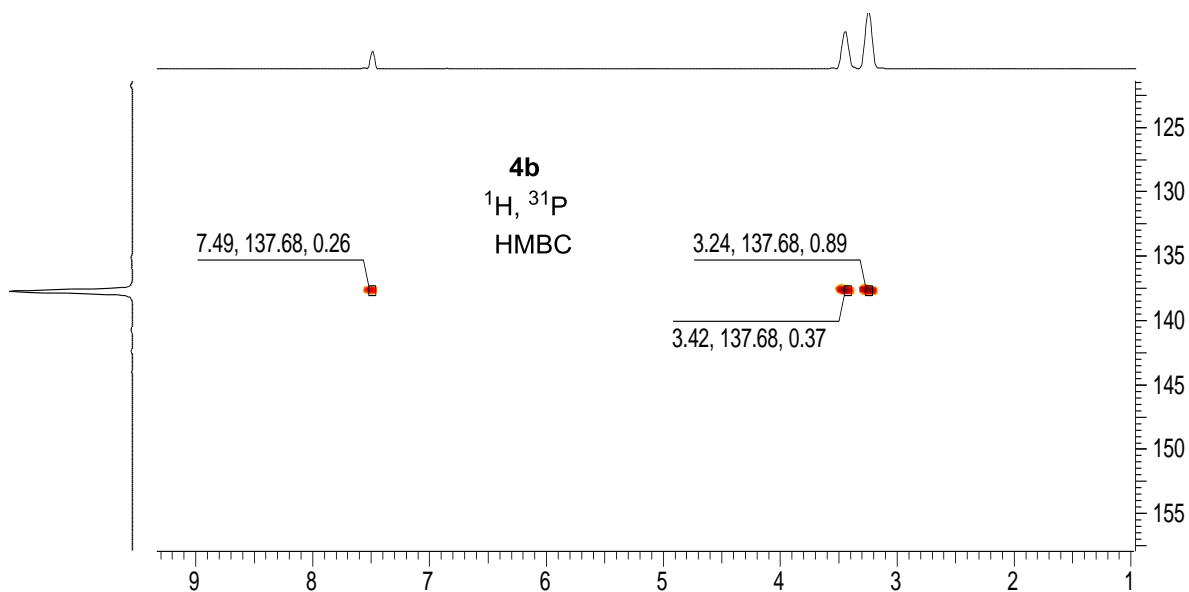
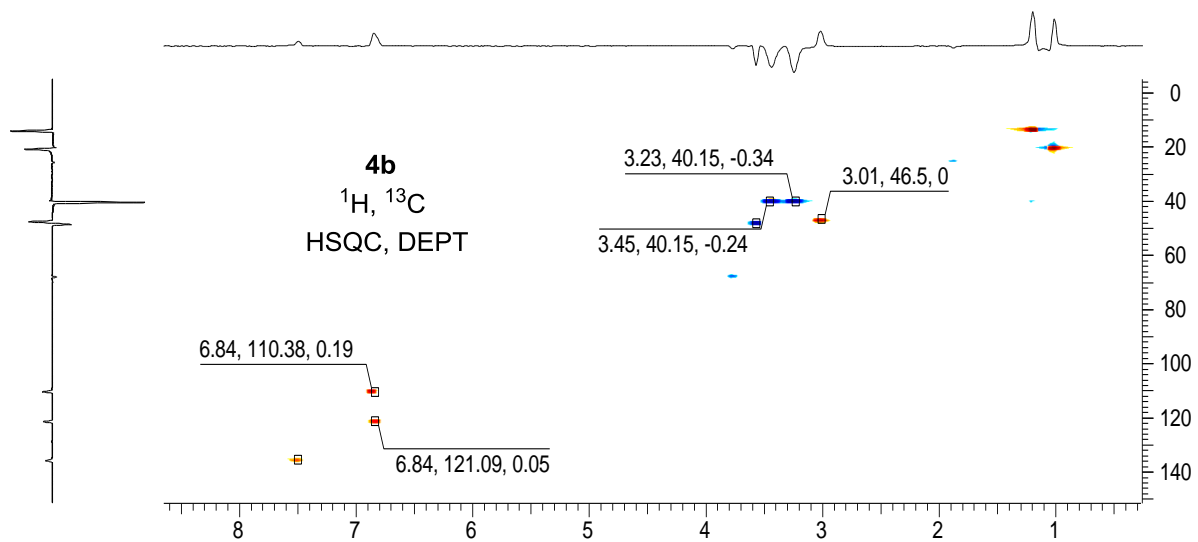


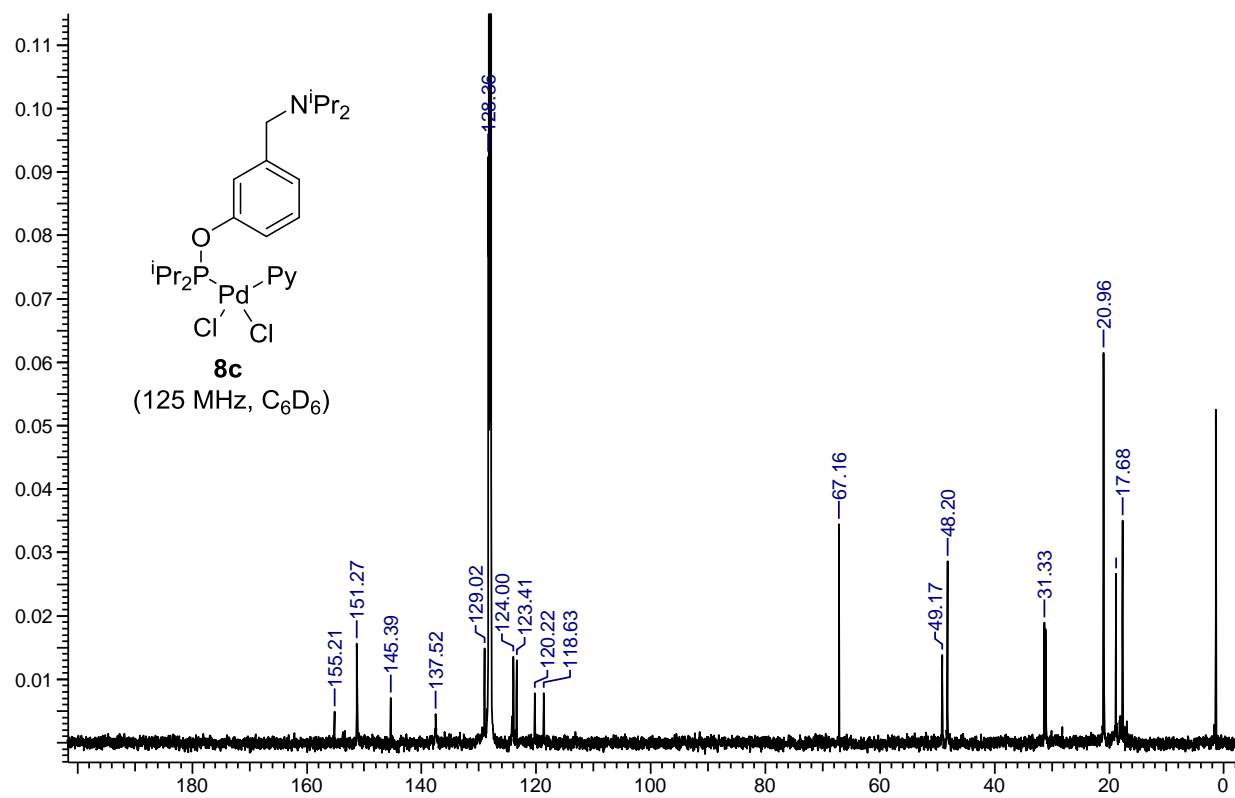
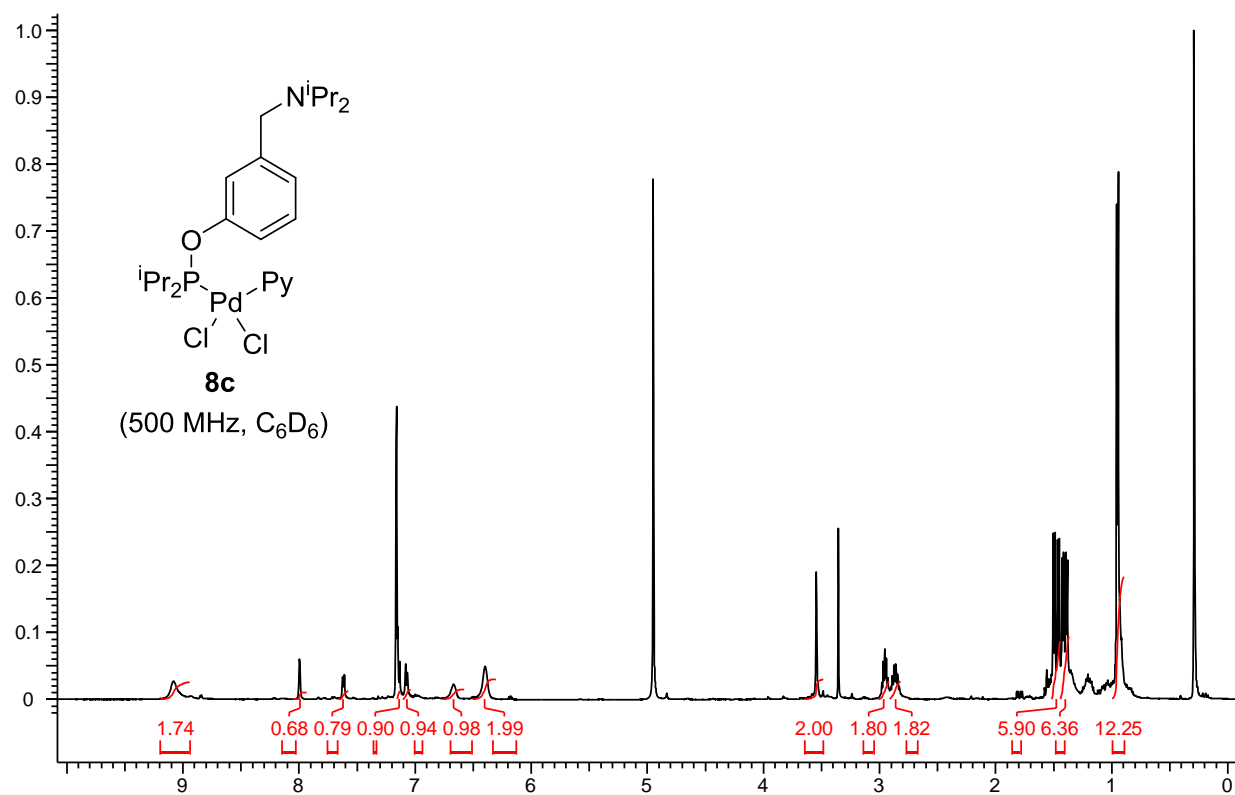


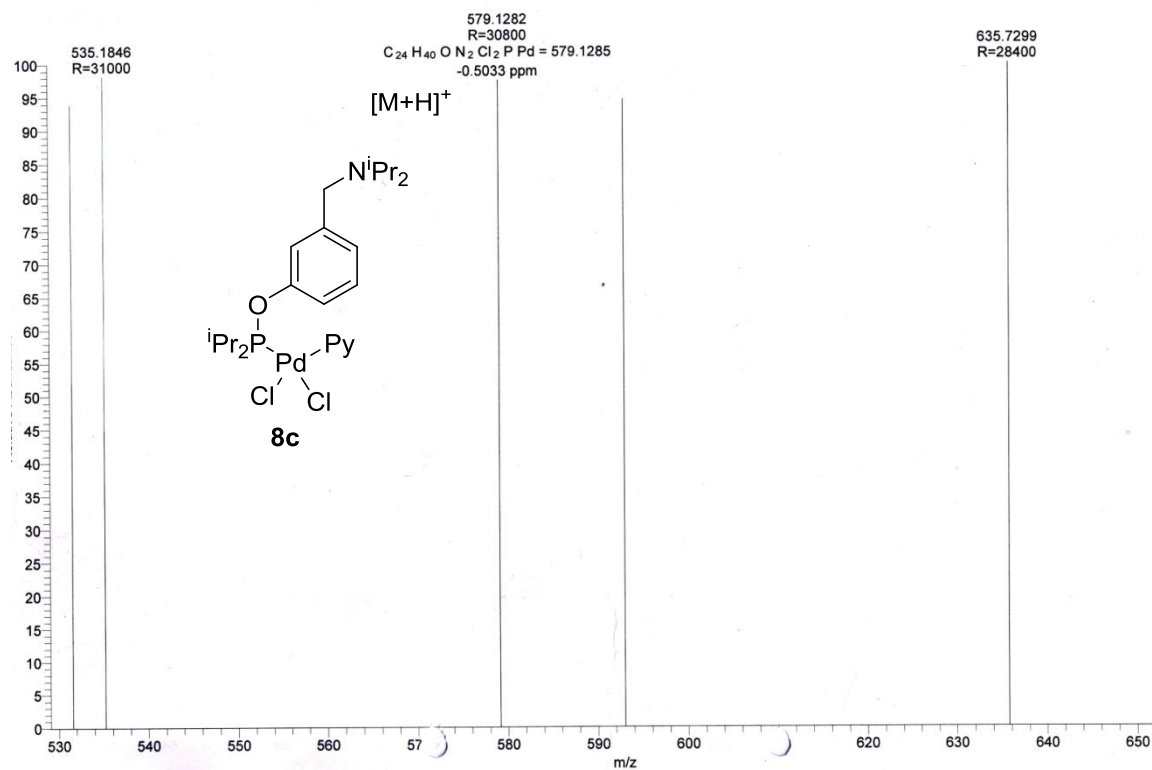
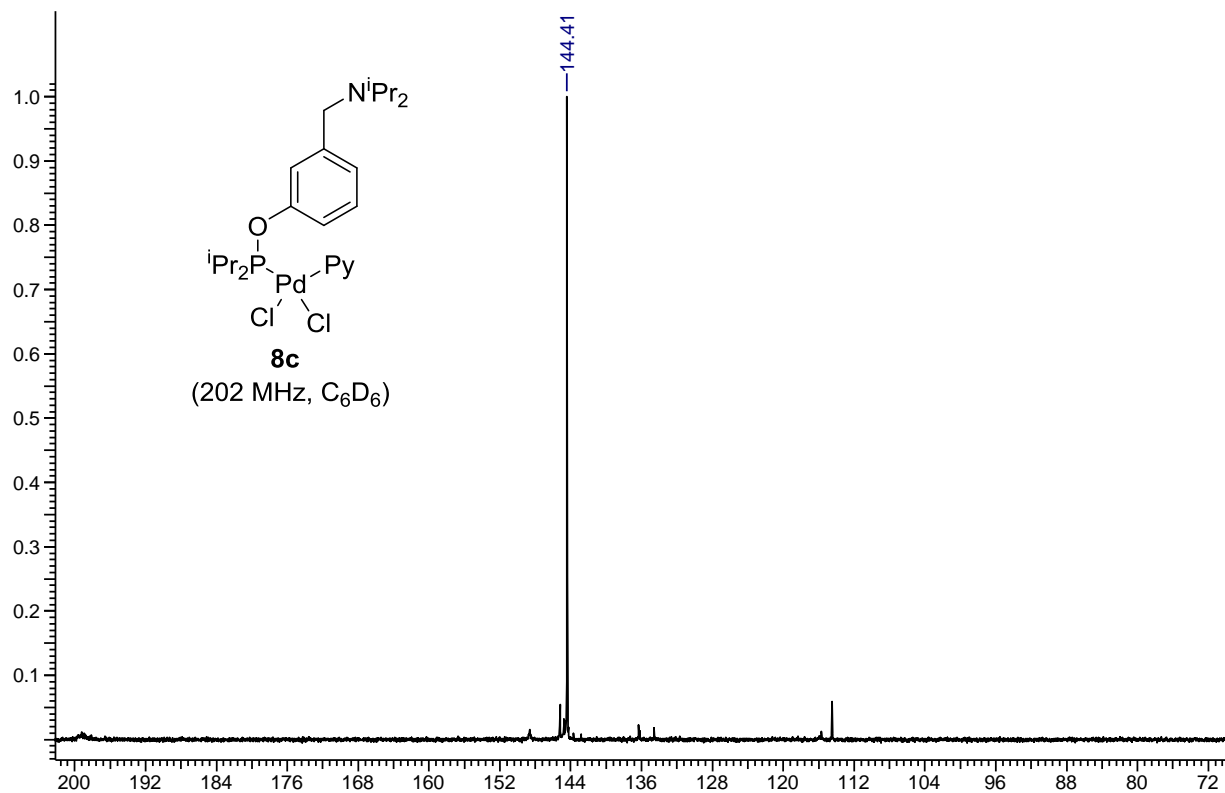




2D NMR Spectra of **2b** and **4b**



NMR and Mass Spectra of **8c**



Chapter 3

Unactivated Alkyl Chlorides in Nickel-Catalyzed C(2)–H Alkylation of Indoles: Scope and Mechanistic Aspects

3.1 INTRODUCTION

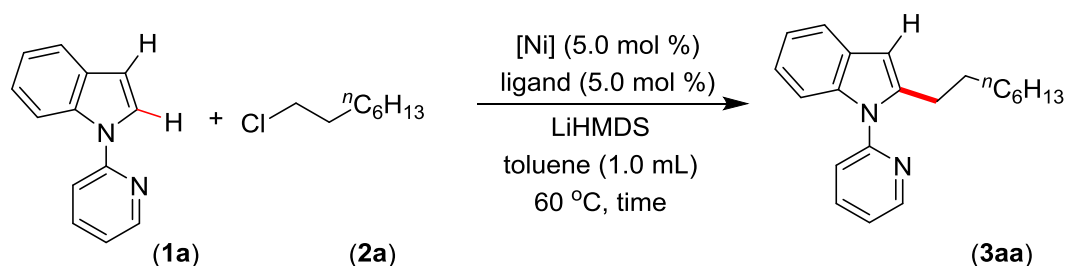
Functionalized heterocycles are highly valuable compounds that occur in many natural products, vital drug candidates, and exhibits significant biological activity.¹⁻⁶ Therefore, direct and regioselective C–H functionalization⁷⁻¹⁵ of heteroarenes,¹⁶⁻²⁰ including that of privileged indoles,²¹⁻²⁴ by the transition-metal-catalyzed protocol has attracted considerable attention. Particularly, selective alkylation of indoles is highly significant as the alkyl indoles are the precursor for many medicinally important alkaloids,²⁵⁻²⁸ and alkyl-functionality can significantly alter the biological and physicochemical properties, such as metabolic stability and lipophilicity. The biggest hurdles in the development of alkylation protocol using unactivated alkyl halides, especially those with β -hydrogen atoms, are the reluctance of these electrophiles to undergo oxidative addition and their tendency to competitive side reactions (β -hydrogen elimination and hydrodehalogenation). Although the C-3 alkylation of indoles can be achieved by catalytic Friedel-Crafts alkylation, allylic alkylation, and conjugate addition,²⁹⁻³³ the regioselective direct C(2)–H alkylation of indoles with alkyl halides are extremely limited.³⁴⁻⁴² For example, Bach has demonstrated the C2-alkylation of indoles with alkyl bromides *via* a norbornene-mediated Catellani-type reaction,⁴³⁻⁴⁷ employing a precious Pd-catalyst in high loadings (>10 mol %). On the contrary, we have reported an inexpensive nickel-catalyst for the C2-alkylation of indoles with alkyl iodides,⁴⁸ wherein a high reaction temperature (150 °C) is essential for the successful alkylation.

Surprisingly, to date, the selective alkylation of indoles (even arenes) has been achieved primarily by employing reactive alkyl iodides or bromides. However, attempts to use more challenging and inexpensive alkyl chloride coupling partners have been less successful, and only a cobalt-catalyzed method has been reported employing an excess of a sensitive Grignard base, CyMgCl, with limited scope.⁴⁹ Therefore, a generalized direct C2-alkylation of indoles and related heteroarenes using readily available and less expensive alkyl chlorides, and a user-friendly base under mild conditions is highly desirable. In this chapter, we demonstrate the C–H alkylation of indoles with alkyl chlorides using a nature-abundant and inexpensive Ni(II)-catalyst at mild reaction conditions, which delivered highly chemo- and regioselective alkyl indoles. The detailed mechanistic investigation has been conducted, including stoichiometric and controlled reactivity studies, kinetics analysis, deuterium labeling and electronic effect studies, EPR and

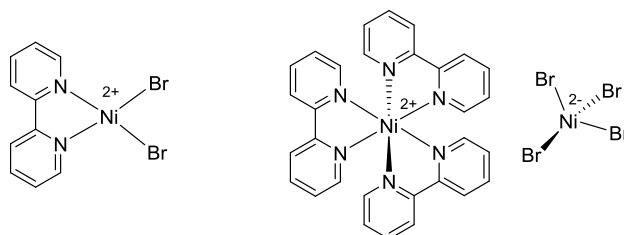
XPS analysis. These studies suggested a single-electron transfer (SET) pathway for the nickel-catalyzed alkylation that proceeds *via* a Ni(I)/Ni(III) route involving the rate-influencing oxidative addition of alkyl chloride.

3.2 RESULTS AND DISCUSSION

3.2.1 Optimization of Reaction Parameters. We have initiated optimization study for the coupling of 1-(pyridin-2-yl)-1*H*-indole (**1a**) with 1-chlorooctane (**2a**) employing Ni(OAc)₂/1,10-phenanthroline (phen) catalyst system, and a non-nucleophilic LiHMDS base in toluene (Table 3.1). Initial experiments were conducted to screen suitable reaction temperature and were found that the coupled product 2-octyl-1-(pyridin-2-yl)-1*H*-indole (**3aa**) could be obtained in 17% yield at as low as 60 °C. The alkylation reaction employing other nickel precursors like (CH₃CN)₂NiBr₂, Ni(OTf)₂, (dme)₂NiCl₂ or (thf)₂NiBr₂ along with phen gave improved yield, and the product **3aa** was obtained in 86% with the (thf)₂NiBr₂/phen catalyst system (entries 1-5). Among various nitrogen-donor ligands screened (entries 5-8), the 2,2'-bipyridine (bpy) ligand was slightly superior to others. Remarkably, the reaction could be completed in 5 h affording the alkylation product **3aa** in 88% isolated yield (entry 9). Notably, under the optimized conditions, the oxidative coupling of indole with toluene derivative was not detected, as was seen in our previous protocol.⁴⁸ The alkylation reaction was less effective when performed at 40 °C or 50 °C. As the (thf)₂NiBr₂/bpy catalyst system afforded a quantitative yield of **3aa**, we have employed the synthesized complexes (bpy)NiBr₂ and (bpy)_{1.5}NiBr₂ as catalysts for the alkylation reaction. Notably, the reaction was relatively slow while using the isolated complex and required 16-20 h for complete conversion (entries 11-14). We assumed that the formation of an active catalyst either from (bpy)NiBr₂ or (bpy)_{1.5}NiBr₂ is slow compared to the same from (thf)₂NiBr₂/bpy *in-situ* system.

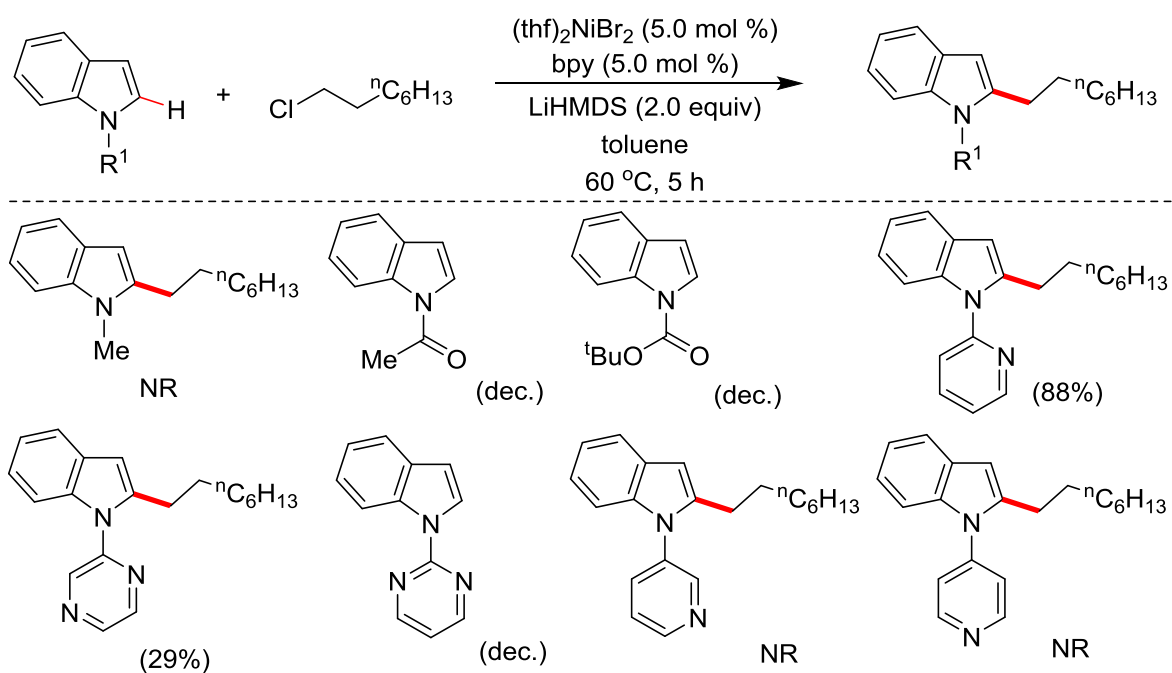
Table 3.1 Optimization of the Reaction Conditions^a

entry	[Ni]	ligand	t (h)	3aa (%) ^b
1	Ni(OAc) ₂	phen	24	17
2	(CH ₃ CN) ₂ NiBr ₂	phen	24	38
3	Ni(OTf) ₂	phen	24	82
4	(dme)NiCl ₂	phen	24	72
5	(thf) ₂ NiBr ₂	phen	24	86
6	(thf) ₂ NiBr ₂	bpy	24	92
7	(thf) ₂ NiBr ₂	d ^t Bu-bpy	24	87
8	(thf) ₂ NiBr ₂	neocuprine	24	90
9	(thf)₂NiBr₂	bpy	5	92 (88)^c
10 ^d	(thf) ₂ NiBr ₂	bpy	12	57
11	(bpy)NiBr ₂	-	5	15
12	(bpy)NiBr ₂	-	16	86
13	(bpy) ₃ Ni.NiBr ₄	-	5	52
14	(bpy) ₃ Ni.NiBr ₄	-	16	86



^aReaction Conditions: **1a** (0.039 g, 0.2 mmol), **2a** (0.059 g, 0.4 mmol), [Ni] cat (0.01 mmol, 5 mol %), ligand (0.01 mmol, 5 mol %), LiHMDS (0.067 g, 0.4 mmol). ^b¹H NMR yield using CH₂Br₂ as internal standard. ^cIsolated yield. ^dReaction performed at 50 °C.

The indole **1a** bearing 2-pyridinyl as directing group efficiently coupled with 1-chlorooctane (**2a**) to afford 2-octyl indole (**3aa**) in 88% yield employing $(\text{thf})_2\text{NiBr}_2/\text{bpy}$ in the presence of LiHMDS at 60 °C. Thus, the possibility of other substituents/directing groups at the *N*-center of indole moiety was explored (Scheme 3.1). Notably, the free-NH indole was decomposed under the standard catalytic conditions, whereas *N*-Me indole was unreactive. Similarly, the indole bearing *N*-acetyl and *N*-Boc directing groups decomposes to intractable materials. To our surprise, the indole bearing easily removable group such as 2-pyrimidinyl was not effective under the catalytic conditions, whereas 2-pyrazinyl indole afforded 29% of desired alkylation product. Further, to understand the electronic impact *versus* the coordinating ability of *N*-pyridinyl group, 3-pyridinyl and 4-pyridinyl-substituted indoles were subjected to the alkylation reaction, wherein alkylation was not observed. All these findings indicate that the *N*-donor atom at the 2-position of the nitrogen-substituent is necessary for the alkylation of indoles under the standard optimized conditions.



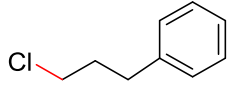
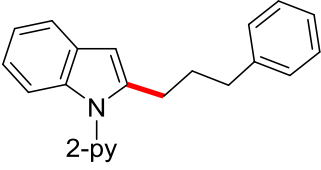
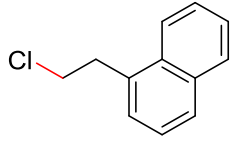
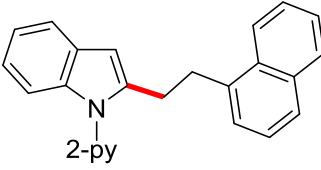
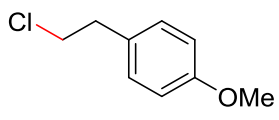
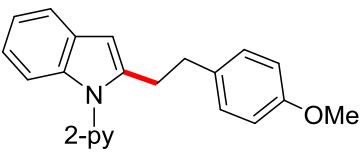
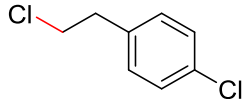
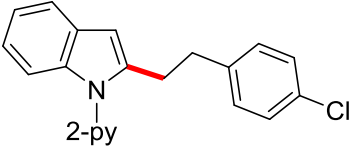
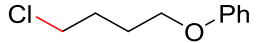
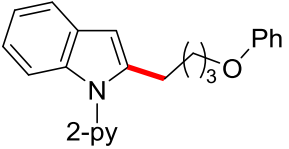
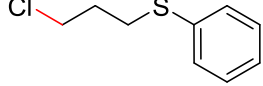
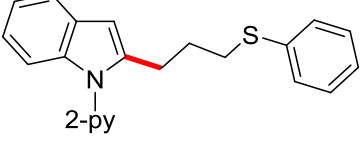
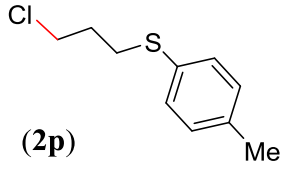
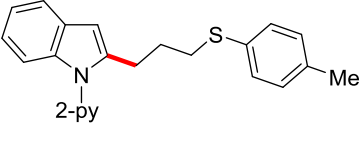
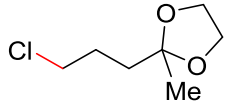
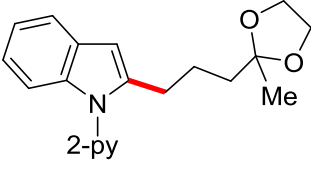
Scheme 3.1 Reactivity of *N*-substituted indoles.

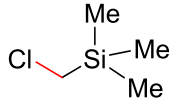
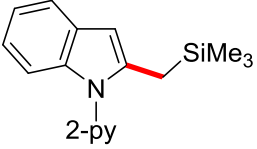
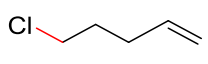
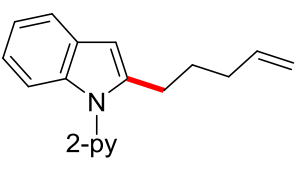
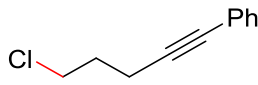
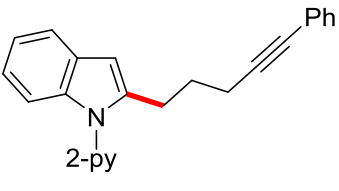
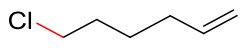
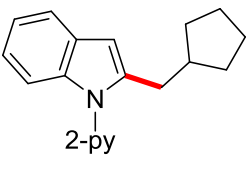
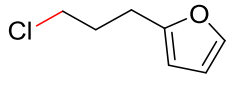
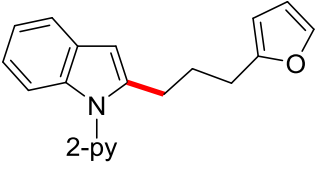
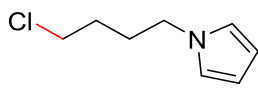
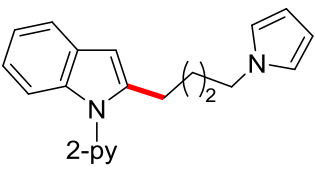
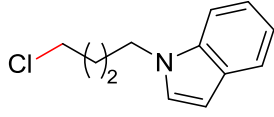
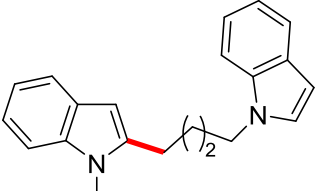
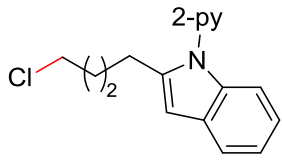
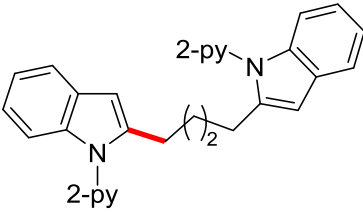
3.2.2 Substrate Scope for Alkylation. Upon achieving the 2-alkylation of indoles with alkyl chloride using an inexpensive $(\text{thf})_2\text{NiBr}_2/\text{bpy}$ catalyst in the presence of LiHMDS, we started to explore the scope of the alkylation (Table 3.2). It was found that the reaction is compatible with a variety of simple and functionalized alkyl chlorides as the coupling partners. Alkyl chlorides with different chain lengths or branching were efficiently coupled, and the reaction proceeded smoothly at 60 °C affording good to excellent yields of the desired products (entries 1-7). The 1-bromo-4-chlorobutane and 1-iodo-4-chlorobutane electrophiles chemoselectively reacted with indole **1a** at 40 °C (or at 60 °C) and produced 2-(4-chlorobutyl)-1-(pyridin-2-yl)-1*H*-indole (**3ah**) leaving -Cl functionality untouched. Similarly, 1,6-dichlorohexane efficiently reacted on one $\text{C}(\text{sp}^3)\text{-Cl}$ to give product **3ai** in 80% yield (entry 9). Notably, in all these cases exclusive mono-indolation products were obtained, and the bis-indolation of electrophile was not observed. The coupling of $\text{C}(\text{sp}^3)\text{-Br}$ and $\text{C}(\text{sp}^3)\text{-I}$ sites in the presence of a $\text{C}(\text{sp}^3)\text{-Cl}$ bond as well as selective one $\text{C}(\text{sp}^3)\text{-Cl}$ coupling (in case of 1,6-dichlorohexane) is highly significant, as the resulted products can be used for further functionalization. The aryl-substituted alkyl chlorides also smoothly coupled with indole (entries 10-13). Interestingly, the activation of $\text{C}(\text{sp}^3)\text{-Cl}$ was highly selective in the presence of a $\text{C}(\text{sp}^2)\text{-Cl}$ bond (entry 13), and the coupling of $\text{C}(\text{sp}^2)\text{-Cl}$ with indole $\text{C}(2)\text{-H}$ was not observed. The reaction delivered an array of 2-alkylated indoles with diverse functional groups, such as phenyl ether (entry 14), thioether (entries 15 and 16), ketal (entry 17), silyl (entry 18), alkenyl (entry 19) and alkynyl (entry 20). Tolerability of such functionalities has not been preceded, not even with the precious metal catalyzed alkylation. The reaction was sensitive to the ester, -CN, -NO₂ functionalities and the electrophiles containing such groups were decomposed under the reaction conditions (for details see Supporting Information). Notably, the use of 6-chlorohex-1-ene as electrophile produced 2-(cyclopentyl methyl)-1-(pyridin-2-yl)-1*H*-indole (**3au**) in 78% yield as the major product *via* a radical cyclization, and only a trace (9%) of direct alkylation product, 2-(hex-5-en-1-yl)-1-(pyridin-2-yl)-1*H*-indole was observed (entry 21). The alkyl chlorides containing heterocycles, such as furan, pyrrole, indole, and carbazole efficiently reacted with indole and delivered the desired alkylation products in moderate to good yields (entries 22-27). The observed low yield during the alkylation of indole with 9-(2-chloroethyl)-9*H*-carbazole (**2a'**) arises due to the severe proto-de-alkylation of coupling partner resulting in the formation of 9*H*-carbazole (entry 27). Notably, in all cases, regioselective $\text{C}(2)\text{-H}$ alkylation was realized, and neither C-3 alkylation

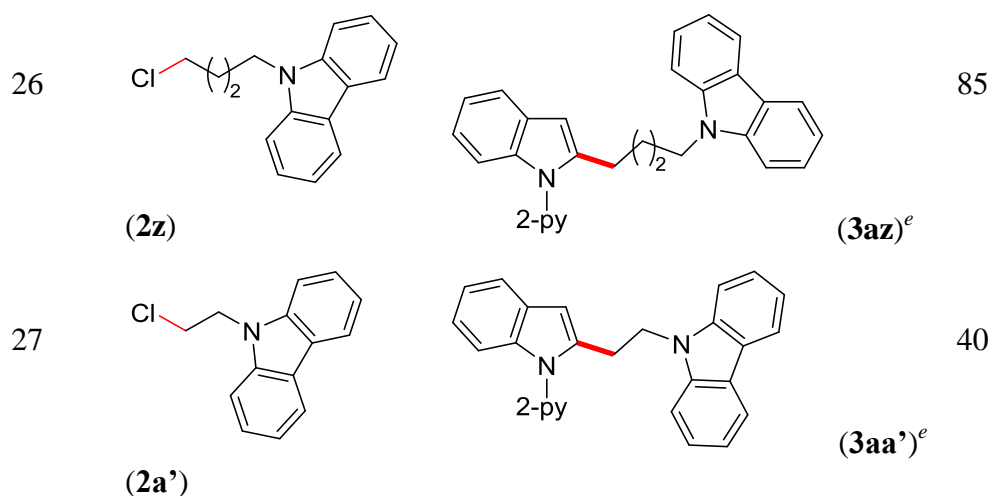
nor C-2/C-3 double alkylation was observed, which is very crucial, as the C(3)-H can further be functionalized by the electrophilic activation.

Table 3.2 Scope of the Ni-Catalyzed C-2 Alkylation of Indoles with Primary Alkyl Chlorides^a

entry	alkyl halide (2)	product (3)	yield (%) ^b
1	R = ⁿ C ₆ H ₁₃ (2a)	R = ⁿ C ₆ H ₁₃ (3aa)	88
2	R = ⁿ C ₂ H ₅ (2b)	R = ⁿ C ₂ H ₅ (3ab)	94
3	R = ⁿ C ₄ H ₉ (2c)	R = ⁿ C ₄ H ₉ (3ac)	90
4	R = ⁿ C ₈ H ₁₇ (2d)	R = ⁿ C ₈ H ₁₇ (3ad)	87
5	R = ⁿ C ₁₀ H ₂₁ (2e)	R = ⁿ C ₁₀ H ₂₁ (3ae)	88
6	R = ⁿ C ₁₂ H ₂₅ (2f)	R = ⁿ C ₁₂ H ₂₅ (3af)	88
7	 (2g)	 (3ag)	93
8 ^{c,d}	 (2h) X = Br (2h') X = I	 (3ah)	84 81
9	 (2i)	 (3ai) ^e	80

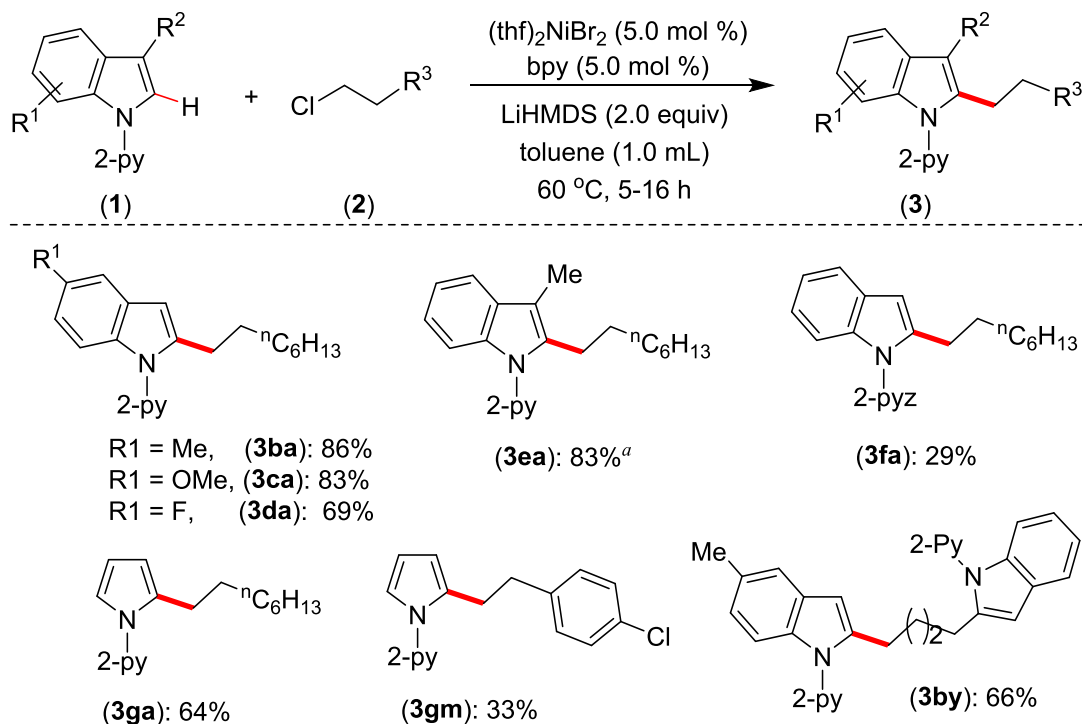
10	 (2j)	 2-py (3aj)^d	96
11	 (2k)	 2-py (3ak)^e	75
12	 (2l)	 2-py (3al)^d	81
13	 (2m)	 2-py (3am)^d	62
14	 (2n)	 2-py (3an)^e	73
15	 (2o)	 2-py (3ao)^f	55
16	 (2p)	 2-py (3ap)^f	61
17	 (2q)	 2-py (3aq)^d	42

18	 (2r)	 2-py (3ar)^d	55
19	 (2s)	 2-py (3as)^d	93
20	 (2t)	 2-py (3at)^d	53
21	 (2u)	 2-py (3au)^d	78
22	 (2v)	 2-py (3av)^f	60
23	 (2w)	 2-py (3aw)^d	84
24	 (2x)	 2-py (3ax)^d	75
25	 (2y)	 2-py (3ay)^d	65



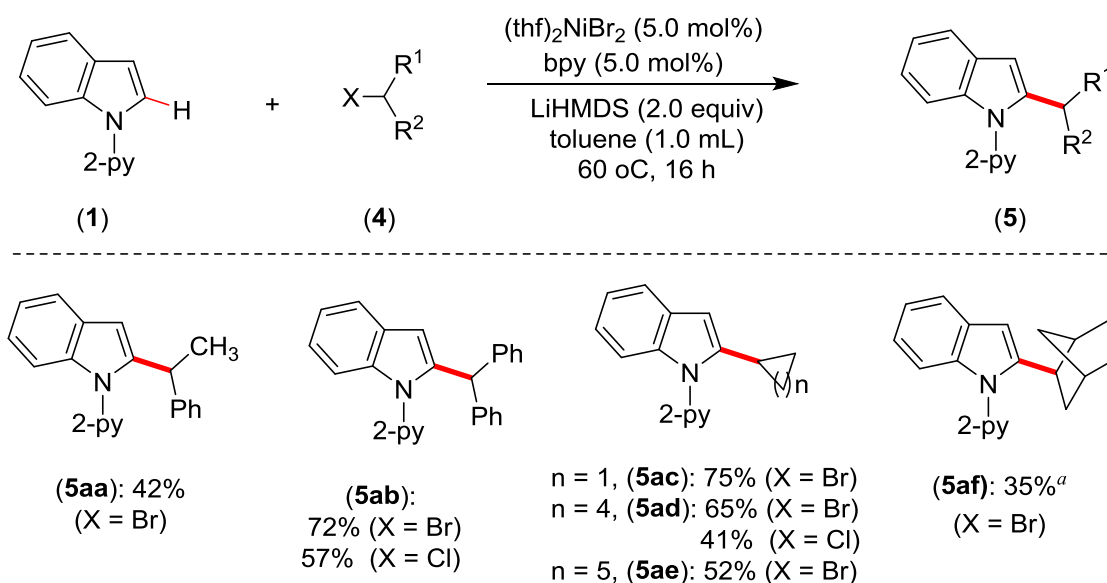
^aConditions: indole **1** (0.20 mmol), alkyl halide **2** (0.40 mmol), LiHMDS (0.067 g, 0.40 mmol), (thf)₂NiBr₂ (0.0037 g, 0.01 mmol), bpy (0.0016 g, 0.01 mmol), toluene (1.0 mL). ^bYield of isolated compound. ^cSimilar results at 40 °C or 60 °C. Entries 1-7: reaction time is 5 h. ^dReaction time 16 h. ^eReaction time 24 h. ^fReaction performed at 80 °C for 24 h

Further, the scope of various indole and pyrrole substrates was explored with alkyl chlorides (Scheme 3.2). Indoles with electron-donating and electron-withdrawing substituents at the C5 position smoothly participated in the alkylation to deliver the coupled products **3ba-3da** and **3by** in moderate to good yields. Sensitive and important functional groups like nitro, cyano, and bromo were not tolerated in the indole backbone. The sterically hindered C-3 substituted indole (**1e**) could be alkylated with good activity. In addition to indoles, the pyrrole moiety was alkylated at the C2 position to deliver selective mono-alkylation products **3ga** and **3gm**.



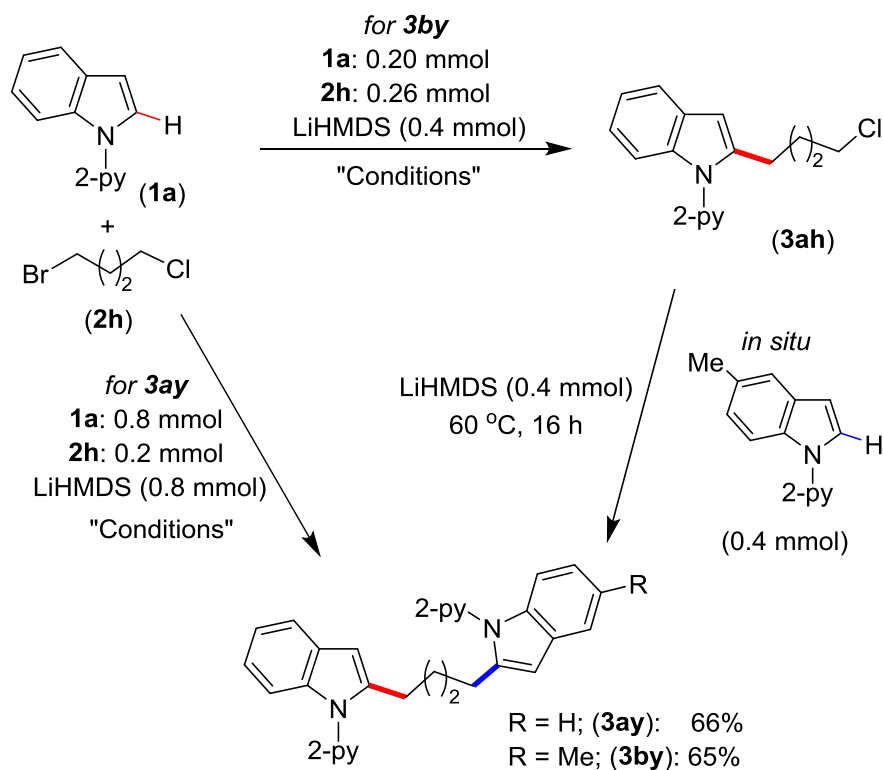
Scheme 3.2 Scope of C-2 alkylation of substituted indoles and pyrroles. ^aYield by ¹H NMR. For **3ba-3fa** reaction time is 5 h. For **3da**, **3by**, **3ga** and **3gm** reaction time is 16 h.

The optimized reaction condition was further explored to the coupling of secondary alkyl bromides with 1-(pyridin-2-yl)-1*H*-indole (Scheme 3.3). Thus, the acyclic phenyl-substituted secondary alkyl bromides were efficiently coupled at the C-2 position of indole to afford the desired products (**5aa**, **5ab**) in moderate to good yields. Similarly, the cyclic secondary alkyl halides (**4c-e**) with different ring-size were reacted in moderate to good activity. The electrophile 2-bromobicyclo[2.2.1]heptane (**4f**) gave the alkylated product **5af** in 35% yield. Especially, the kinetically favored undesired β -elimination over the reductive elimination is responsible for the lower yields of the coupling of many secondary alkyl halides. The coupling reaction has not occurred with tertiary alkyl chlorides, such as *tert*-butyl chloride and 1-chloroadamantane.



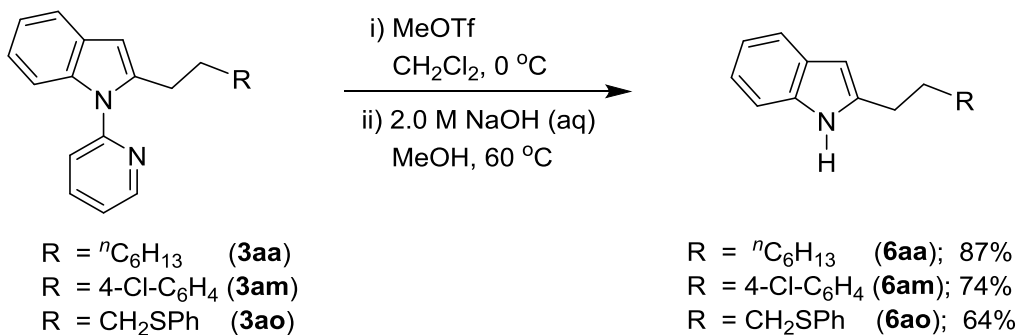
Scheme 3.3 Scope of C-2 alkylation of indoles with secondary alkyl halides. ^aYield by ¹H NMR.

It is noteworthy that when 1-bromo-4-chlorobutane (**2h**; 2.0 equiv) was used as a coupling partner for the alkylation of indole, the alkylated product **3ah** was exclusively obtained by C(sp³)–Br bond activation leaving the C(sp³)–Cl bond untouched. Thus, we have performed alkylation reaction employing 1-bromo-4-chlorobutane (**2h**) electrophile to synthesize symmetrical and unsymmetrical bis(indolyl)butane derivatives in a single pot (Scheme 3.4). The indole **1a** (4.0 equiv) upon treatment with 1-bromo-4-chlorobutane (**2h**, 1.0 equiv) under the standard alkylation conditions at 60 °C for 16 h afforded the symmetrical bis(indolyl)butane **3ay** in 66% yield. However, the unsymmetrical bis(indolyl)butane **3by** was isolated in 65% yield by the reaction of 1-bromo-4-chlorobutane (**2h**) with indoles **1a** and **1b** in a sequential manner in one pot. The demonstrated protocol provides a unique approach for the synthesis of bis(indolyl)alkyl derivatives, which can be extended for the development many other such symmetrical and unsymmetrical scaffolds.



Scheme 3.4 In-situ synthesis of bis(indolyl)butane. $(\text{thf})_2\text{NiBr}_2$ (0.02 mmol), bpy (0.02 mmol), toluene (2.0 mL), 60 °C, 16 h.

3.2.3 Removal of Directing Group. Considering the importance of functionalized free *N*-H indoles, we have demonstrated the utility of our developed protocol with the removal of a 2-pyridinyl group. Thus, the C-2 alkylated indoles **3aa**, **3am**, and **3ao** were treated with MeOTf followed by the reaction in NaOH (2.0 M) led to the formation of C-2 alkylated free *N*-H indoles **6aa**, **6am**, and **6ao**, respectively (Scheme 3.5).^{50,51} The resulted indoles can be easily functionalized at C(3)-H and/or *N*-H to synthesize diverse biologically active compounds.^{5,52}



Scheme 3.5 Removal of 2-pyridinyl directing group.

3.2.4 MECHANISTIC STUDIES

3.2.4.1 NMR Tube Reaction. We sought to study the detailed reaction mechanism of the nickel-catalyzed C-2 alkylation of indole considering the unique activity of $(\text{thf})_2\text{NiBr}_2/\text{bpy}$ under mild conditions. The ^1H NMR analysis of the mixture $(\text{thf})_2\text{NiBr}_2$, bpy and LiHMDS showed a single broad peak at 10.69 ppm for the (bpy)Ni protons, which accounts for > 98 % w.r.t. internal standard (Figure 3.1). The broad single peak indicates that the generated nickel species could be the paramagnetic Ni(I) and/or tetrahedral Ni(II) species (conclusive identification was demonstrated by EPR and XPS). Upon addition of substrates **1a** and **2a** to the reaction mixture, the peak corresponds to (bpy)Ni is completely disappeared, and signals for the product **3aa** and unreacted substrate **1a** were appeared. These observations clearly indicate that the involved nickel catalyst is paramagnetic in nature.^{53,54}

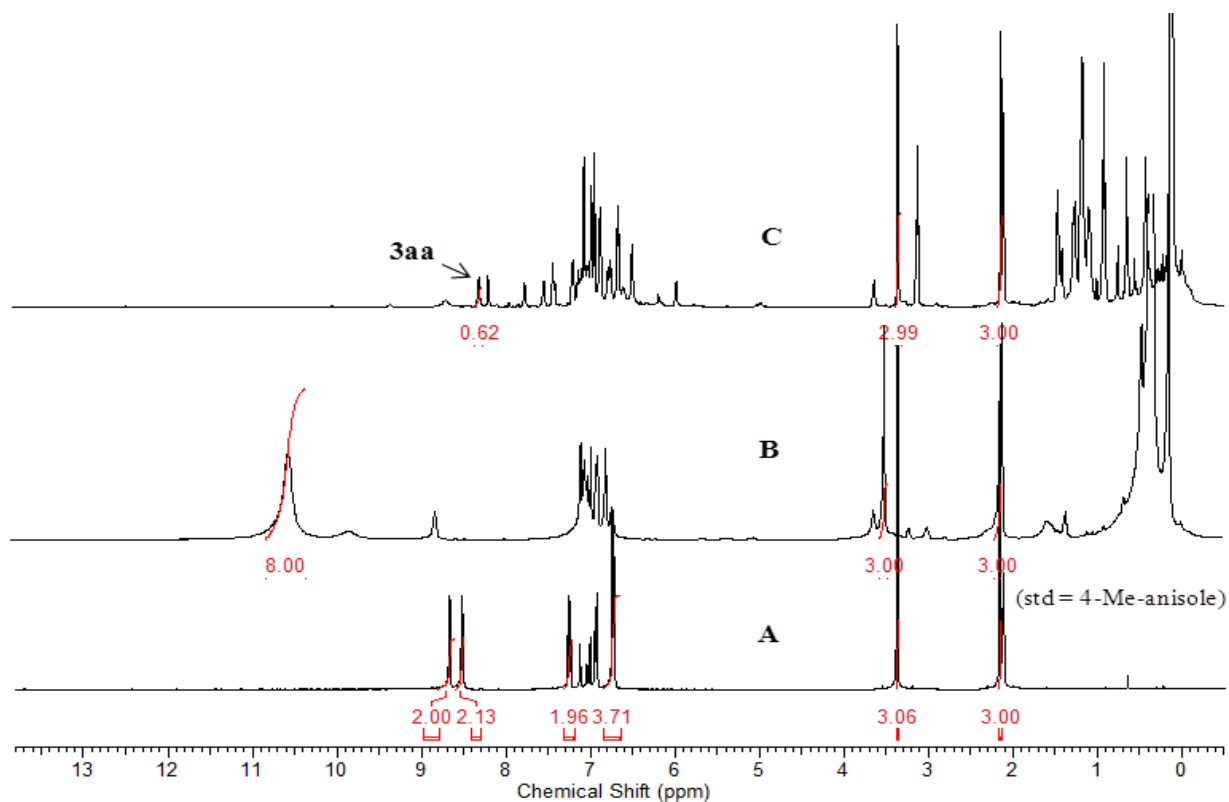
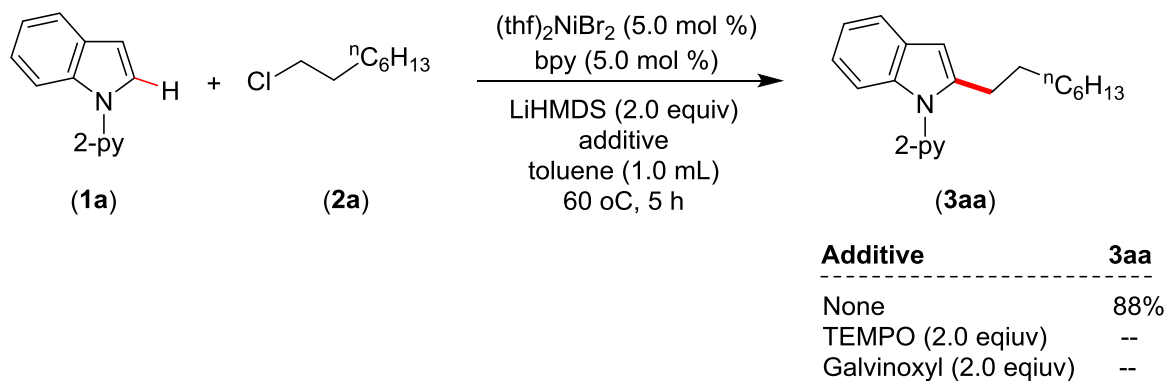


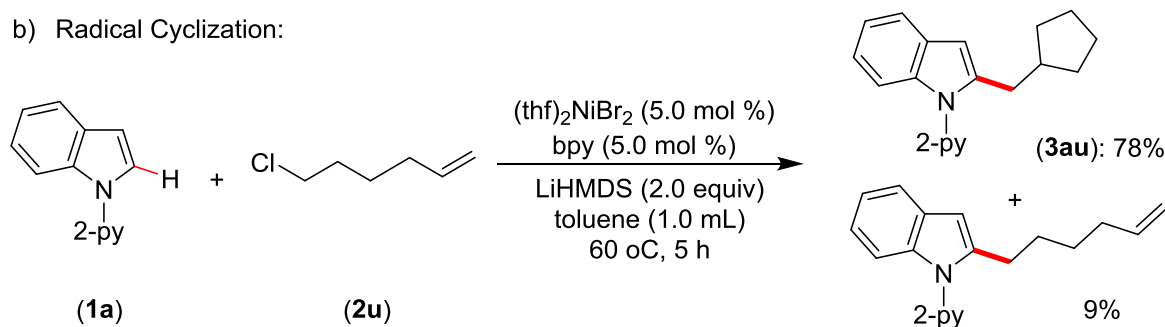
Figure 3.1 ^1H NMR spectra of controlled alkylation reaction: (A) bpy in toluene- d_8 , (B) bpy + $(\text{thf})_2\text{NiBr}_2$ + LiHMDS in toluene- d_8 after heating 15 min at 60 $^\circ\text{C}$, (C) bpy + $(\text{thf})_2\text{NiBr}_2$ + LiHMDS + indole **1a** + 1-chlorooctane (**2a**) in toluene- d_8 after heating 15 min at 60 $^\circ\text{C}$.

3.2.4.2 Probing Radical Pathway. The standard alkylation reaction was performed in the presence of radical scavengers, TEMPO (2.0 equiv) or galvinoxyl (2.0 equiv), wherein the reaction was completely inhibited (Scheme 3.6a). This suggests the involvement of a radical intermediate during the alkylation process. Unfortunately, the coupling of presumed radical species with TEMPO or galvinoxyl was not detected. The reaction of indole **1a** with 6-chlorohex-1-ene afforded 9% of direct coupled product 2-(hex-5-en-1-yl)-1-(pyridin-2-yl)-1*H*-indole, whereas 78% of 2-(cyclopentylmethyl)-1-(pyridin-2-yl)-1*H*-indole (**3au**) was obtained *via* the radical cyclization (Scheme 3.6b). This finding highlights that the major pathway of the alkylation reaction involves an alkyl radical intermediate.

a) External Additive Experiments:



b) Radical Cyclization:



Scheme 3.6 External additive and radical clock experiments.

3.2.4.3 Deuterium Labeling Studies. The rate of nickel-catalyzed alkylation reaction was determined to gain information about the catalytic process. In a standard rate measurement, the indole **1a** (0.039 g, 0.20 mmol, 0.2 M) was treated with 1-chlorooctane (0.059 g, 0.40 mmol, 0.4 M) in the presence of $(\text{thf})_2\text{NiBr}_2$ (0.0037 g, 0.01 mmol, 0.01 M), bpy (0.0016 g, 0.01 mmol) and LiHMDS (0.067 g, 0.40 mmol, 0.4 M) in toluene (Figure 3.2). The kinetic profile shows that the alkylation was consistent with the formation **3aa** in 6 % and 17 % after 30 and 60 min, respectively (Figure 3.5). The initial rate of the alkylation was determined to be $7.3 \times 10^{-4} \text{ M min}^{-1}$. Notably, the rate of alkylation was unexpectedly slow ($1.8 \times 10^{-4} \text{ M min}^{-1}$) when defined nickel complex $(\text{bpy})\text{NiBr}_2$ was employed instead of $(\text{thf})_2\text{NiBr}_2/\text{bpy}$ catalyst system, which could be due to the slower formation of active Ni-catalyst from $(\text{bpy})\text{NiBr}_2$ than the $(\text{thf})_2\text{NiBr}_2/\text{bpy}$ system. This is also consistent with the finding that a longer reaction time is required while using $(\text{bpy})\text{NiBr}_2$ as a catalyst. To know the essence of indole C–H bond activation in the alkylation reaction, and probable involvement of the same in the rate

influencing step, the initial rates of the alkylation reaction using indoles **1a** and [2-D]-**1a** were determined. The kinetic isotope effect (KIE) value was found to be 1.12, which indicates that the C–H bond activation is unlikely involved in the rate-limiting step (Figure 3.2).⁵⁵

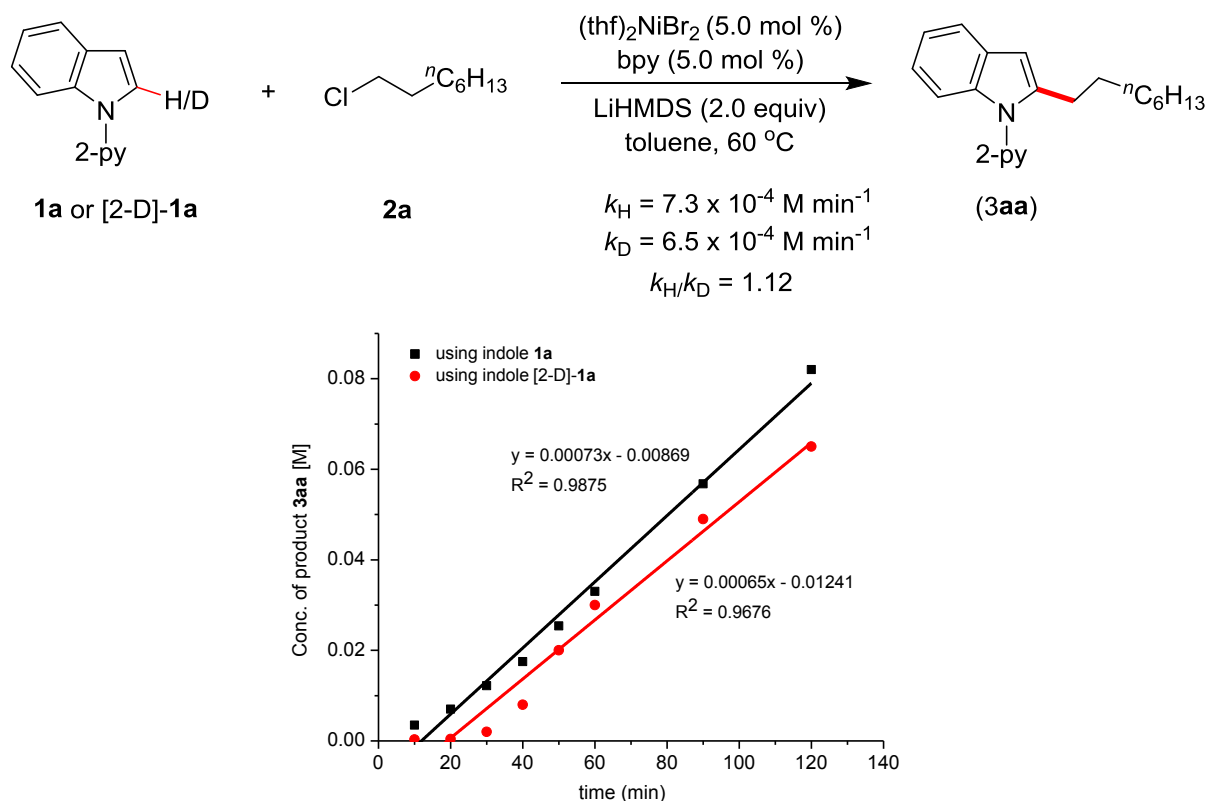
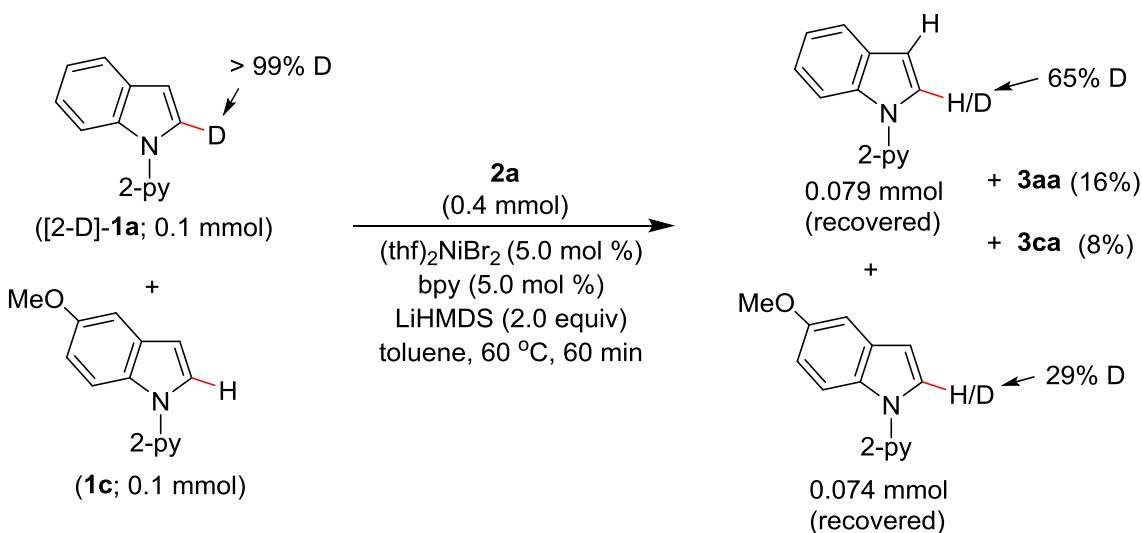


Figure 3.2 Time-dependent formation of product **3aa** using indoles **1a** and [2-D]-**1a**.

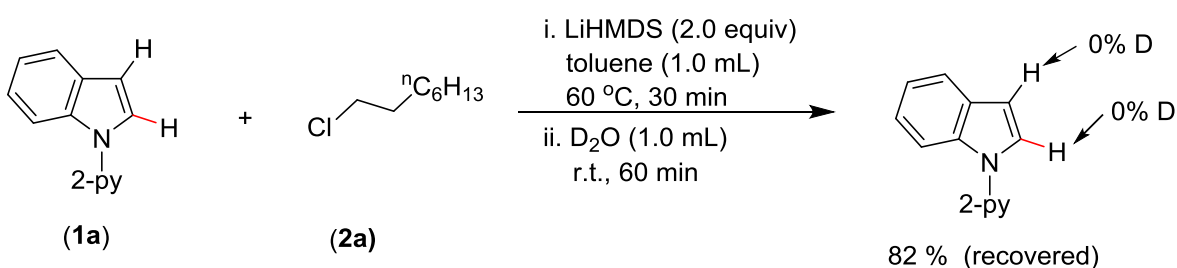
An alkylation reaction was performed using indole [2-D]-**1a** and 5-methoxy-1-(pyridine-2-yl)-1*H*-indole (**1c**) in the same reaction vessel under standard catalytic conditions, and the reaction was stopped at an early reaction time (60 min). The recovery and ${}^1\text{H}$ NMR analysis of the starting precursors [2-D]-**1a** and **1c** shows a substantial H/D exchange between the two substrates at C(2)–H position (Scheme 3.7a), highlighting the reversibility of C–H nickelation during the reaction. Further, the standard alkylation reaction (both in the presence or absence of $(\text{thf})_2\text{NiBr}_2/\text{bpy}$) was heated at $60\text{ }^\circ\text{C}$ for 1 h, and the reaction mixture was quenched with D_2O (Scheme 3.7b). The ${}^1\text{H}$ NMR analysis of the recovered starting compound does not show the

incorporation of deuterium at C(2)–H or C(3)–H of indole **1a**, which suggests that the indole C–H nickelation *via* a simple base-mediated deprotonation pathway is remote.

a) *H/D* Scrambling Experiment:



b) *H/D* Scrambling:



Scheme 3.7 Deuterium labeling experiments.

3.2.4.4 Electronic Effect and Reactivity Study. Initial rates of the alkylation reaction for electronically distinct indoles were determined to understand the electronic effects on the reaction. As shown in Figure 3.3, the electron-donating substituent significantly favors the alkylation reaction suggesting the C(2)–H acidity of the indole moiety is irrelevant, and supports an electrophilic type of C–H nickelation.^{56,57} The rates of the alkylation employing different alkyl halides, 1-chlorooctane, 1-bromooctane, and 1-iodooctane, were measured to establish the nature of the C–halide bond activation. Figure 3.4 shows the initial rate of alkylation employing

1-iodooctane and 1-bromooctane was found to be 7.6 and 4.4 times faster than that with the 1-chlorooctane. The greater efficiency of the cross-coupling reaction using 1-iodooctane over 1-bromooctane and 1-chlorooctane suggests the crucial role of C–halide bond activation. Considering the unlikeliness of C–H nickelation or reductive elimination as the rate influencing step,^{55,58} we assume that the C(alkyl)–Cl bond activation could possibly be the rate-limiting step during the alkylation. This is also supported by the finding that the rate of reaction is faster with an indole bearing electron-donating substituent, wherein an electron-rich indolyl ligated nickel would favor the oxidative addition of C–Cl.

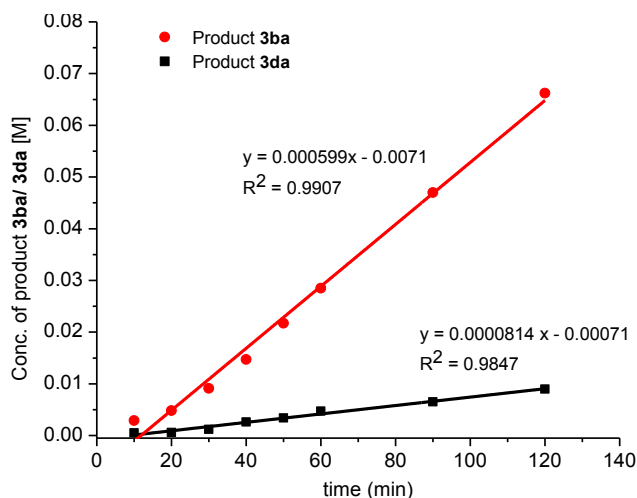
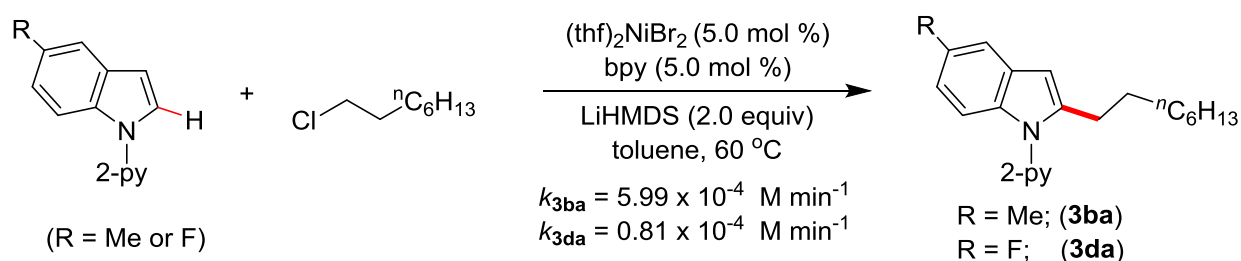


Figure 3.3 Time-dependent formation of products **3ba** and **3da**.

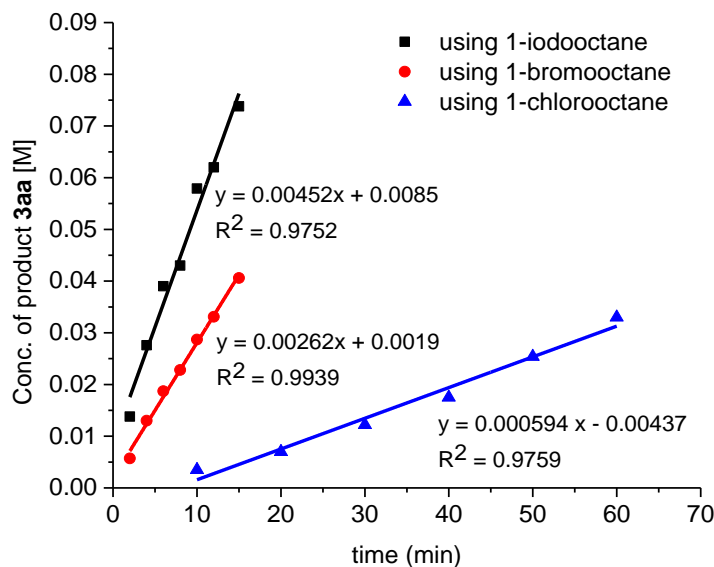
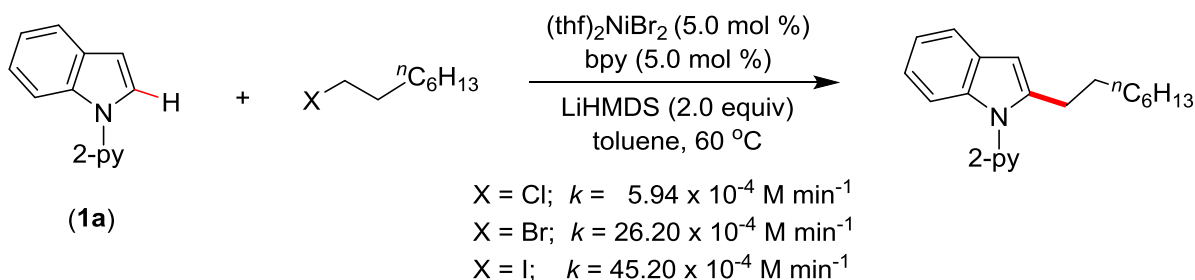


Figure 3.4 Time-dependent formations of products **3aa** using different *n*-octyl halides.

3.2.4.5 Reaction Profile using $(\text{thf})_2\text{NiBr}_2/\text{bpy}$: The kinetic analysis of the alkylation reaction was performed to understand the rate of reaction as well as the reactivity of nickel catalyst. In a standard kinetic experiment, a teflon-screw capped tube equipped with magnetic stir bar was introduced $(\text{thf})_2\text{NiBr}_2$, bpy, LiHMDS, 1-chlorooctane and 1-(pyridin-2-yl)-1*H*-indole, then toluene (required amount) was added to make the total volume 1.0 mL. To the reaction mixture *n*-hexadecane was added as an internal standard. The reaction mixture was then stirred at 60 °C in a pre-heated oil bath and at regular intervals (10, 20, 30, 40, 50, 60, 90, 120, 180, 240 and 300 min) the progress of the reaction was monitored by the GC analysis (Table 3.3). The data of the concentration of the product vs time (min) plot was drawn with Origin Pro 8. For the reaction rate, the data were fitted linear (excluding induction period) with Origin Pro 8 and the rate was determined by initial rate method. The reaction profile of the nickel-catalyzed alkylation of

indole with alkyl chloride over a period of 300 min has shown in Figure 3.5. The reaction profile shows that the reaction doesn't need an induction period and alkylation product formed from the beginning. This suggests that $(\text{thf})_2\text{NiBr}_2$ is an active catalyst species.

Table 3.3 Concentration of Product 3aa at Different Time Intervals using $(\text{thf})_2\text{NiBr}_2/\text{bpy}$

Time (min)	Conc. of 3aa [M]
10	0.003
20	0.007
30	0.012
40	0.017
50	0.025
60	0.033
90	0.057
120	0.082
180	0.118
240	0.134
300	0.141

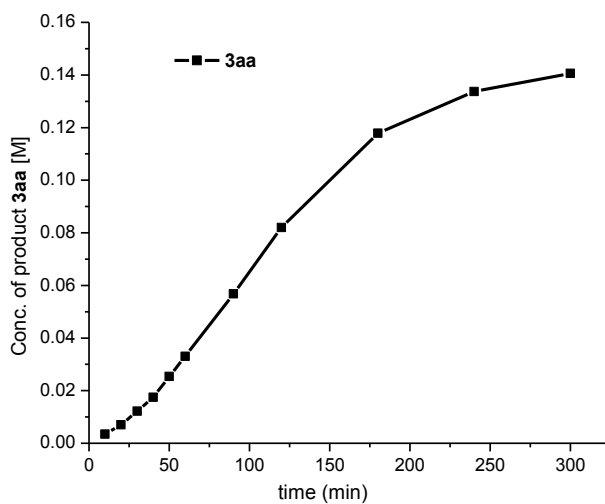


Figure 3.5 Time-dependent formation of **3aa** using $(\text{thf})_2\text{NiBr}_2/\text{bpy}$ system.

To understand the kinetics as well as the reactivity of the alkylation reaction using isolated catalyst, kinetic reaction was performed. In a standard kinetic experiment, a Teflon-screw capped tube equipped with magnetic stir bar was introduced (bpy)NiBr₂, LiHMDS, 1-chlorooctane and 1-(pyridin-2-yl)-1*H*-indole, then toluene (required amount) was added to make the total volume 1.0 mL. To the reaction mixture *n*-hexadecane (0.025 mL) was added as an internal standard. The reaction mixture was then stirred at 60 °C in a pre-heated oil bath and at regular intervals (30, 60, 90, 120, 150, 180, 210, 240, 300 and 360 min) the progress of the reaction was monitored by the GC analysis (Table 3.4). The data of the concentration of the product vs time (min) plot was drawn with Origin Pro 8. For the reaction rate, the data were fitted linear (excluding induction period) with Origin Pro 8 and the rate was determined by initial rate method. By comparing the rate of the reaction using isolated catalyst and *in-situ* catalyst, we could observe that the rate of reaction is 4.1 times faster with the *in-situ* catalyst as compared to isolated catalyst (Figure 3.6).

Table 3.4 Concentration of Product 3aa at Different Time Intervals using (thf)₂NiBr₂/bpy and (bpy)NiBr₂

(thf) ₂ NiBr ₂ /bpy		(bpy)NiBr ₂	
Time (min)	Conc. of 3aa [M]	Time (min)	Conc. of 3aa [M]
10	0.003	30	0.004
20	0.007	60	0.010
30	0.012	90	0.015
40	0.017	120	0.020
50	0.025	150	0.026
60	0.033	180	0.031
90	0.057	210	0.036
120	0.082	240	0.042
		300	0.052
		360	0.063

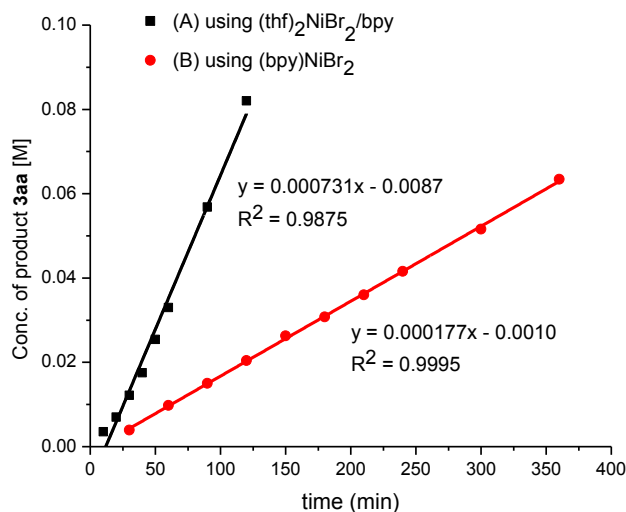
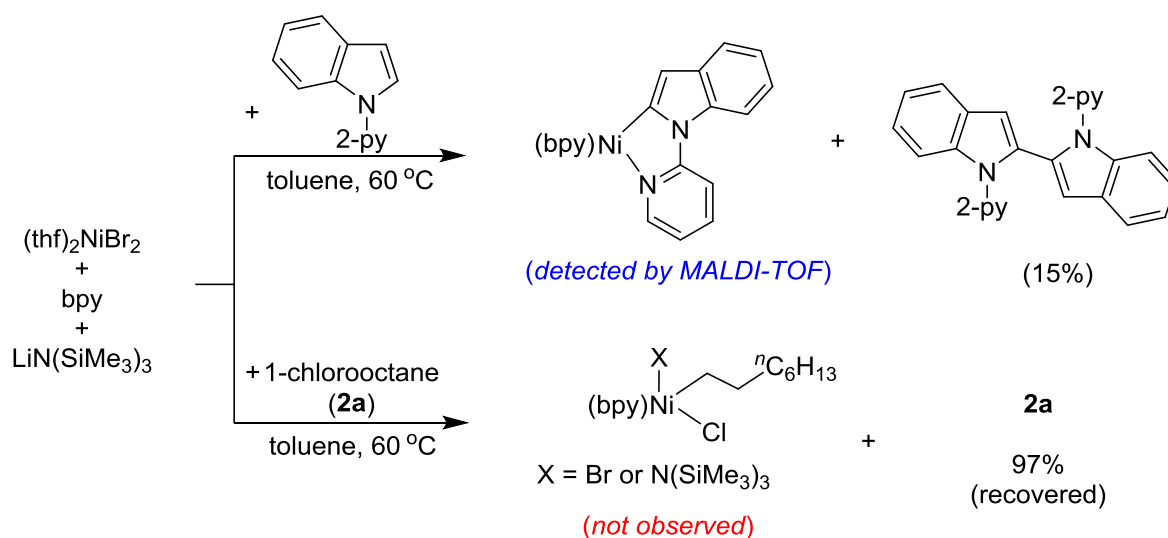


Figure 3.6 Time-dependent formation of **3aa** using (A) $(\text{thf})_2\text{NiBr}_2/\text{bpy}$ system and (B) $(\text{bpy})\text{NiBr}_2$ catalyst.

In an attempt to isolate possible catalytic intermediate, stoichiometric and controlled experiments were conducted (Scheme 3.8). The stoichiometric reaction of $(\text{thf})_2\text{NiBr}_2/\text{bpy}$ with indole **1a** in the presence of LiHMDS at 60 °C resulted in the formation of 1,1'-di(pyridin-2-yl)-1*H*,1'*H*-2,2'-biindole (self-coupling of **1a**) in 15%, and unreacted indole (57%) was recovered. We were unable to isolate the possible intermediate $(\text{bpy})\text{Ni}(2\text{-indolyl-2-pyridine})$; however, this species was detected by the MALDI-TOF analysis of the reaction mixture. The oxidative self-coupling of indole might occur *via* the Ni(II)-mediated process in the presence of LiHMDS. Notably, self-coupling of indole was not observed in the presence of electrophile 1-chloroalkane during the standard alkylation conditions. Additionally, oxidative coupling of indole was significant while increasing the catalyst loadings, which led to the reduced yield of desired alkylation product. These findings strongly suggest that Ni(II)-species is unlikely the active catalyst, as increase in loading of $(\text{thf})_2\text{NiBr}_2$ diminishes the yield of alkylation. Considering the detection of intermediate $(\text{bpy})\text{Ni}(\text{I})(2\text{-indolyl-2-pyridine})$ and EPR findings, we tentatively assumed a Ni(I)-species as the active catalyst. Notably, the treatment of $(\text{thf})_2\text{NiBr}_2/\text{bpy}$ with 1-chlorooctane in the presence of LiHMDS at 60 °C did not lead to any product, and the electrophile 1-chlorooctane was recovered in 97%. These controlled stoichiometric reactions also highlight that the Ni-species reacts with indole **1a** prior to the alkyl chloride.



Scheme 3.8 Controlled stoichiometric reactions.

3.2.4.6 Electron Paramagnetic Resonance (EPR) Studies. To know the identity of radical species, the EPR measurements were performed on a frozen (100 K) aliquot of the incomplete alkylation reaction as well as for other controlled reaction mixture. Thus, the data collected from the EPR experiment of the incomplete reaction between $(\text{thf})_2\text{NiBr}_2$, bpy and LiHMDS (60 °C, 30 min) exhibits a rhombic spectrum ($g_1 > g_2 > g_3$). After simulating the data with the Easyspin software,⁵⁹ the g -values ($g_1 = 2.385$, $g_2 = 2.137$ and $g_3 = 2.082$) were obtained (Figure 3.7). The g -factor ($g_{\text{av}} = 2.201$) is suggestive of the unpaired spin resides in an orbital with significant metal character (Ni^{I}), as the g -values for free-radical nature of an unpaired electron and Ni-centered radical are typically observed in the range of 2.002-2.004^{60,61} and 2.15-2.20,⁶²⁻⁶⁴ respectively. The observation of Ni(I)-species from the reaction mixture of $(\text{thf})_2\text{NiBr}_2$ + bpy + LiHMDS suggests that the one-electron reduction of Ni(II) to Ni(I) in the presence of LiHMDS is feasible. Notably, the EPR measurements of other controlled experiments, such as i) $(\text{thf})_2\text{NiBr}_2$ + bpy + LiHMDS + indole **1a**, ii) $(\text{thf})_2\text{NiBr}_2$ + bpy + LiHMDS + 1-chlorooctane (**2a**) and iii) $(\text{thf})_2\text{NiBr}_2$ + bpy + LiHMDS + **1a** + **2a** (standard reaction) in toluene resulted with the spectra that were too complicated to make any concrete judgments on the nature of the radical species. Additionally, we were unable to trace the organic radical by EPR analysis though the radical clock experiment strongly suggests the intermediacy of an alkyl radical.

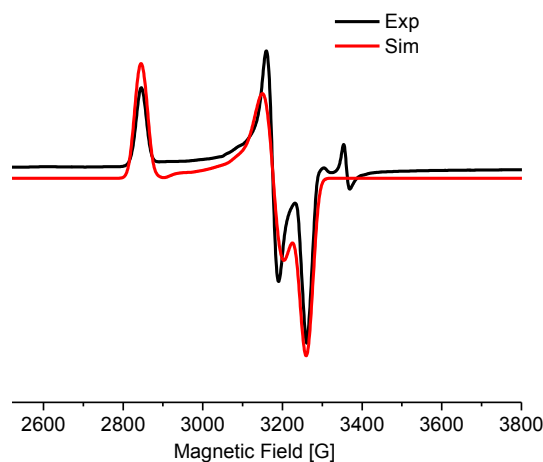


Figure 3.7 EPR spectrum of the incomplete alkylation reaction. Rhombic symmetry with g anisotropy values, g_{xx} (2.385), g_{yy} (2.137), g_{zz} (2.082). The g -values are derived from simulation of the EPR spectrum.

3.2.4.7 X-ray Photoelectron Spectroscopy (XPS) Studies. We have extended our study to the XPS analysis of controlled reactions to establish the oxidation state of involved Ni-species. The XPS analyses of controlled reactions were performed to establish the oxidation state of involved Ni-species, and compared them with the XPS spectrum of standard Ni(0), Ni(I) and Ni(II) compounds. The Ni $2p_{3/2}$ XPS spectrum of complex $(COD)_2Ni$ displays a peak at 852.6 eV correspond to Ni(0)-species (Figure 3.8(B)).⁶⁵ Similarly, the complex $(Ph_3P)_3NiCl$ ⁶⁶ shows a peak at 853.4 eV, which is assigned to Ni(I)-species (Figure 3.8(A)). The additional peak at 856.0 eV is due to the Ni(II) species that might have formed upon oxidation of Ni(I) during the experimental procedure. The complex $(thf)_2NiBr_2$ displays a sharp peak centered around 856.0 eV, which is assigned to Ni(II)-species (Figure 3.9(A)). Notably, the XPS spectrum of the reaction mixture between $(thf)_2NiBr_2$, bpy and LiHMDS (10 equiv), upon heating at 60 °C for 30 min, is much broader with a larger FWHM indicating the multiple oxidation states (Figure 3.10(A)). We could fit two peaks in the main $2p_{3/2}$ photoelectron peak at 853.4 eV and 856.0 eV. The peak corresponding to 856.0 eV is assigned to (bpy)Ni(II)-species, whereas the peak at 853.4 eV has binding energy value greater than Ni(0) (852.6 eV).⁶⁵ As the binding energy observed (853.4 eV) is higher than Ni(0) and lower than the same found for Ni(II), we can assign the peak at 853.4 eV as a Ni(I) intermediate. This peak is also matching with the peak observed

for $(\text{Ph}_3\text{P})_3\text{NiCl}(\text{Ni}^{\text{I}})$. The observation from this controlled experiment is consistent with the EPR finding that an odd electron nickel species, *i.e.* Ni(I), is generated from the Ni(II) complex in the presence of LiHMDS. The XPS analysis of controlled reaction, $(\text{thf})_2\text{NiBr}_2 + \text{bpy} + \text{LiHMDS} + \text{indole } \mathbf{1a}$, shows three peaks at 853.4 eV, 854.8 eV and 856.0 eV (Figure 3.10(B)). The peaks at 853.4 eV and 856.0 eV are for Ni(I) and Ni(II), respectively. However, the peak at 854.8 eV has slightly lower binding energy than the peaks observed for $(\text{bpy})\text{Ni}(\text{II})$ or $(\text{thf})_2\text{Ni}(\text{II})$, thus could be due to an electron-rich Ni(II)-species, $(\text{bpy})\text{Ni}(\text{II})\text{X}(2\text{-indolyl-2-pyridine})$. The XPS analysis of standard alkylation reaction, *i.e.* $(\text{thf})_2\text{NiBr}_2 + \text{bpy} + \text{LiHMDS} + \text{indole } \mathbf{1a} + \mathbf{2a}$ (Figure 3.10(C)) also exhibited three peaks at 853.4 eV [Ni(I)], 854.8 eV [Ni(II)] and 856.0 eV [Ni(II)]. Notably, the XPS analysis of the reaction without indole $\mathbf{1a}$, but in the presence of $\mathbf{2a}$ [*i.e.* $(\text{thf})_2\text{NiBr}_2 + \text{bpy} + \text{LiHMDS} + 1\text{-chlorooctane } (\mathbf{2a})$], showed the presence of only Ni(II) species (856.0 eV), which is consistent with the findings of stoichiometric reaction (Figure 3.9(B)). All the XPS findings, along with the EPR and stoichiometry experiments, unanimously support the Ni(I)-species as an active catalyst. This is also consistent with the radical manifold of the alkylation, wherein a Ni(I) species is expected to trigger the two-step one-electron oxidative addition of alkyl chloride in a facile manner.

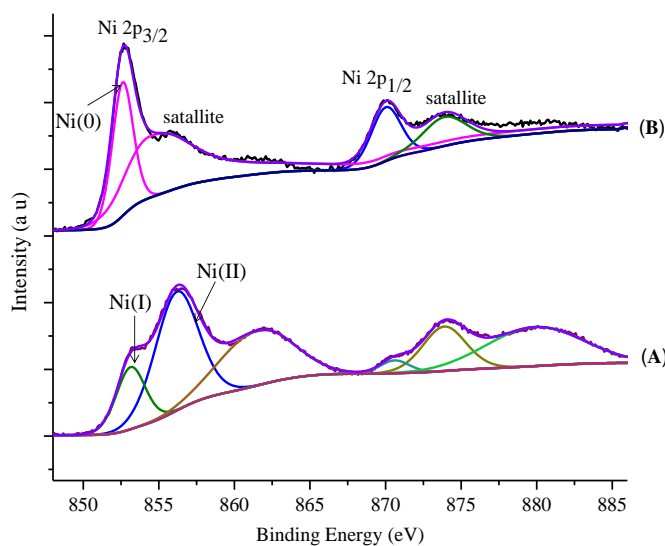


Figure 3.8 X-ray photoelectron spectra: (A) for $(\text{Ph}_3\text{P})_3\text{NiCl}$ [shows some Ni(II) also], (B) for $\text{Ni}(\text{COD})_2$.

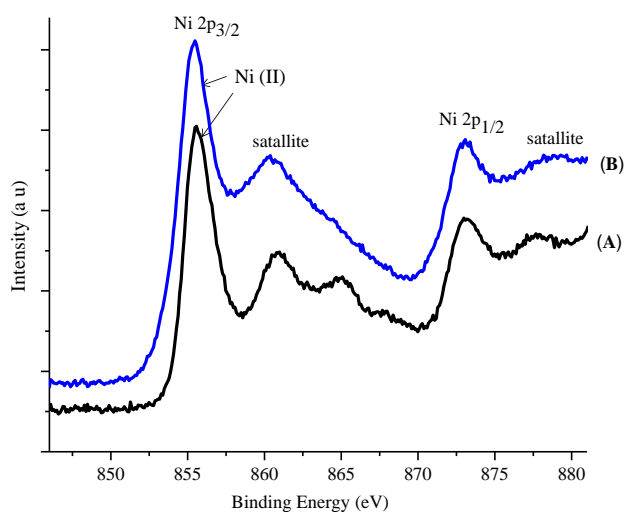


Figure 3.9 X-ray photoelectron spectra: (A) for $(\text{thf})_2\text{NiBr}_2$, (B) $(\text{thf})_2\text{NiBr}_2 + \text{bpy} + \text{LiHMDS} + 1\text{-chlorooctane (2a)}$.

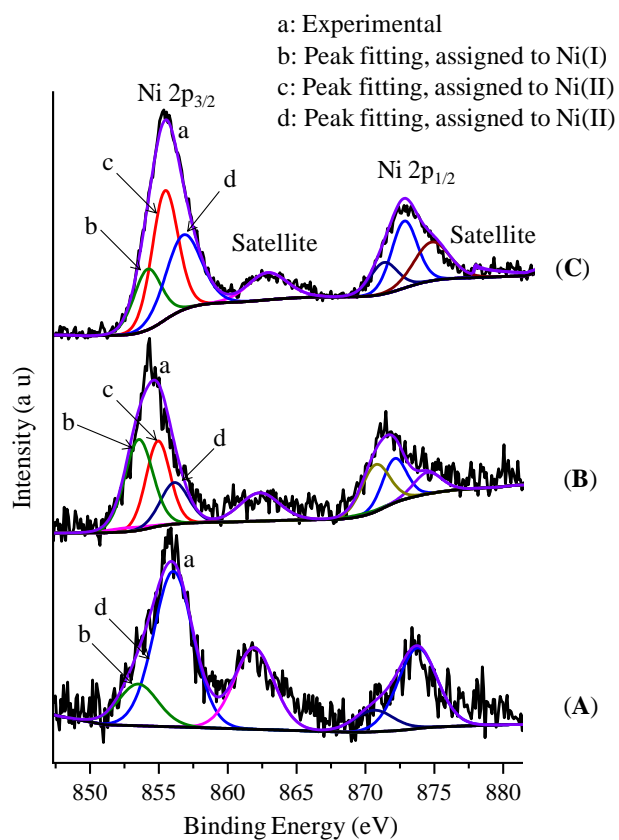


Figure 3.10 X-ray photoelectron spectra: (A) $(\text{thf})\text{NiBr}_2 + \text{bpy} + \text{LiHMDS}$, (B) $(\text{thf})\text{NiBr}_2 + \text{bpy} + \text{LiHMDS} + \mathbf{1a}$, (C) $(\text{thf})\text{NiBr}_2 + \text{bpy} + \text{LiHMDS} + \mathbf{1a} + \mathbf{2a}$ (standard reaction).

3.2.4.8 Catalytic Cycle. On the basis of our mechanistic investigation and literature precedents,⁶⁷⁻⁷² we proposed a reaction mechanism for the Ni-catalyzed alkylation of indoles with alkyl chlorides (Figure 3.11). The Ni(II)-species is first reduced to an active Ni(I)-species in the presence of $\text{LiN}(\text{SiMe}_3)_2$ (proved by both EPR and XPS analysis). One-electron reduction of Ni(II) by $\text{LiN}(\text{SiMe}_3)_2$ could occur *via* the displacement of a $\bullet\text{N}(\text{SiMe}_3)_3$ radical.^{62,73} The indole **1a** then reacts with the active low-valent Ni(I) (**A**) to deliver the intermediate species **B**. This step is a reversible process as exemplified by the deuterium labeling study. The nickel complex **B** would prompt the radical generation from alkyl chloride in the rate-limiting step, and undergo a one-electron oxidation to produce the intermediate **C**. Radical clock experiment strongly supports the single-electron transfer (SET) path and the intermediacy of an alkyl radical. We believe that the reaction of nickel species **A** with alkyl chloride is unlikely to occur at the first place because the resulted penta-coordinated $(\text{bpy})\text{Ni}(\text{X})(\text{Cl})\text{alkyl}$ would be non-reactive with (2-*py*)-indole (**1a**) *via* a nitrogen-coordinative C–H activation protocol. Further, the reaction of alkyl chloride would be preferred to a more electron-rich Ni-center in **B** than with the nickel species **A**, which is also illustrated by the controlled stoichiometric reactions. The nitrogen (*N*₂-*py*)-decoordination and subsequent recombination of the alkyl radical could deliver the complex **D**. As a minor path, alkyl chloride **2** can undergo $2e^-$ oxidative addition to produce **D**. Upon reductive elimination of the alkylated product **3** from complex **D**, the active catalyst **A** will be generated. All the elementary steps are strongly supported by our experimental findings. The presentation of an inclusive mechanism on the nickel-catalyzed C–H alkylation has rarely been found in the literature, though many proposals are documented.⁷⁴⁻⁷⁷ Although our studies support a mono-nuclear SET pathway for the reaction, the possibility of a bimetallic pathway for the activation of alkyl chloride cannot be ruled out.

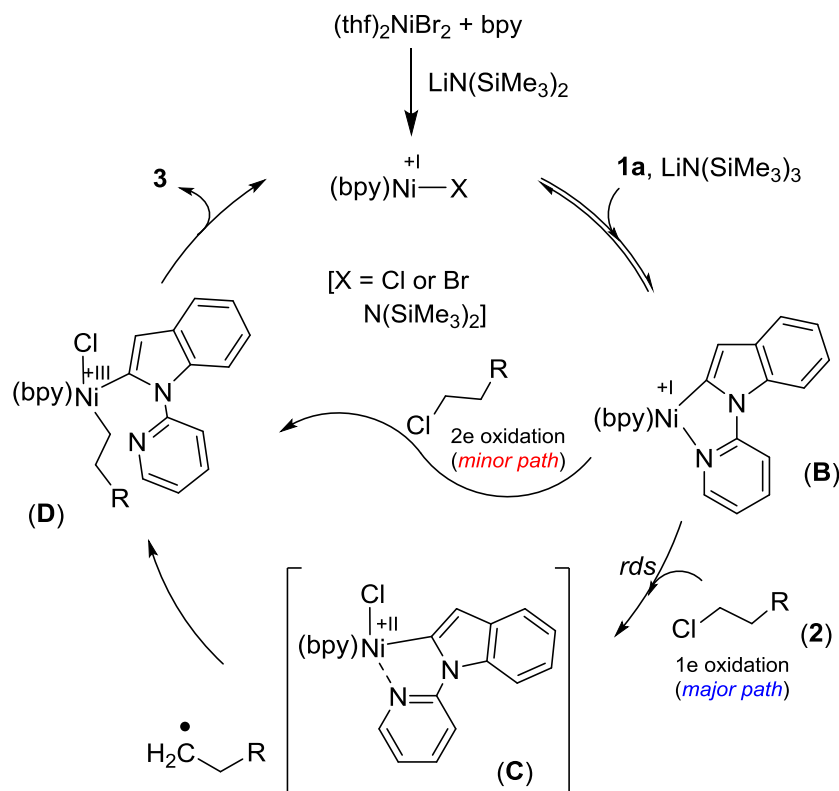


Figure 3.11 Plausible mechanistic pathway for nickel-catalyzed alkylation of indoles.

3.3 CONCLUSION

In summary, we have developed a mild and efficient protocol for the chemo- and regioselective coupling of unactivated alkyl chlorides with indoles and pyrroles. The use of an inexpensive and air-stable bpy ligand along with a naturally-abundant nickel for the coupling of challenging alkyl chlorides makes it a unified approach. This reaction is compatible with a wide range of simple and functionalized primary alkyl chlorides and secondary alkyl bromides as well as electronically distinct indoles. The chemoselectivity with regard to alkyl halides is especially excellent with the selective $\text{C}(\text{sp}^3)\text{-I}$, $\text{C}(\text{sp}^3)\text{-Br}$ or $\text{C}(\text{sp}^3)\text{-Cl}$ bond activation. Further, a $\text{C}(\text{sp}^3)\text{-Cl}$ bond preferentially activated and coupled over the $\text{C}(\text{sp}^2)\text{-Cl}$ bond. The utility of this nickel-catalyzed protocol is demonstrated by the removal of trace directing group. A comprehensive mechanistic study of the alkylation reaction by kinetics analysis, controlled and labeling experiments allowed us to propose a reliable mechanistic cycle that follows a SET process involving the rate influencing alkyl-Cl bond activation. EPR and XPS analyses indicated

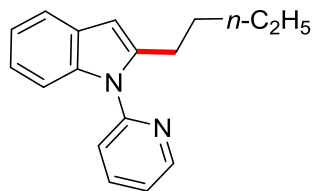
the involvement of a Ni(I) active species, thus strongly supporting a Ni(I)/Ni(III) pathway for the alkylation.

3.4 EXPERIMENTAL

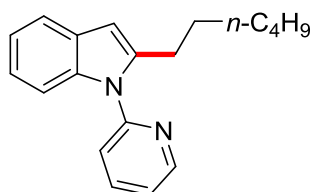
3.4.1 Representative Procedure for Alkylation

Synthesis of 2-Octyl-1-(pyridin-2-yl)-1*H*-indole (3aa): To a flame-dried screw-cap tube (5 mL) equipped with a magnetic stir bar were introduced 1-pyridin-2-yl-1*H*-indole (**1a**, 0.039 g, 0.20 mmol), 1-chlorooctane (**2a**, 0.059 g, 0.40 mmol), (thf)₂NiBr₂ (0.0037 g, 0.01 mmol, 5.0 mol %), bpy (0.0016 g, 0.01 mmol) and LiHMDS (0.067 g, 0.40 mmol) inside the glove box. To the above mixture in the tube was added toluene (1.0 mL), and the resultant reaction mixture was stirred at 60 °C in a preheated oil bath for 5 h. At ambient temperature, the reaction mixture was quenched with distilled H₂O (10 mL) and neutralized with 2N HCl (0.5 mL). The crude product was then extracted with EtOAc (20 mL x 3). The combined organic extract was dried over Na₂SO₄, and the volatiles were evaporated *in vacuo*. The remaining residue was purified by column chromatography on neutral alumina (petroleum ether/EtOAc: 50/1) to yield **3aa** (0.054 g, 88%) as a light yellow liquid. ¹H-NMR (500 MHz, CDCl₃): δ = 8.69 (d, *J* = 3.4 Hz, 1H, Ar-H), 7.94-7.83 (td, *J* = 7.8, 1.6 Hz, 1H, Ar-H), 7.65-7.56 (m, 1H, Ar-H), 7.44 (d, *J* = 8.0 Hz, 1H, Ar-H), 7.39-7.29 (m, 2H, Ar-H), 7.20-7.08 (m, 2H, Ar-H), 6.48 (s, 1H, Ar-H), 2.87 (t, *J* = 7.6 Hz, 2H, CH₂), 1.59 (quin, *J* = 7.4 Hz, 2H, CH₂), 1.40-1.28 (m, 4H, CH₂), 1.27-1.23 (m, 6H, CH₂), 0.90 (t, *J* = 7.1 Hz, 3H, CH₃). ¹³C{¹H}-NMR (125 MHz, CDCl₃): δ = 151.8 (C_q), 149.8 (CH), 141.9 (C_q), 138.4 (CH), 137.4 (C_q), 128.8 (C_q), 122.1 (CH), 121.6 (CH), 121.3 (CH), 120.7 (CH), 120.0 (CH), 110.2 (CH), 102.2 (CH), 32.0 (CH₂), 29.5 (2C, CH₂), 29.3 (CH₂), 28.7 (CH₂), 27.6 (CH₂), 22.8 (CH₂), 14.3 (CH₃). HRMS (ESI): *m/z* Calcd for C₂₁H₂₆N₂+H⁺ [M+H]⁺ 307.2169; Found 307.2160. The ¹H and ¹³C spectra are consistent with those reported in the literature.⁴⁸

3.4.2 Characterization Data of Alkylated Compounds

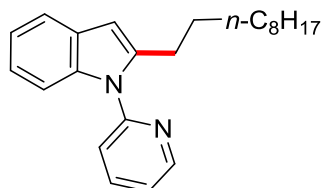


2-Butyl-1-(pyridin-2-yl)-1H-indole (3ab): The representative procedure was followed, using substrate **1a** (0.039 g, 0.20 mmol) and 1-chlorobutane (**2b**; 0.037 g, 0.40 mmol), and the reaction mixture was stirred for 5 h. Purification by column chromatography on neutral alumina (petroleum ether/EtOAc: 50/1) yielded **3ab** (0.047 g, 94%) as a light yellow liquid. $^1\text{H-NMR}$ (500 MHz, CDCl_3): δ = 8.68 (dd, J = 4.6, 1.1 Hz, 1H, Ar-H), 7.89 (td, J = 7.7, 2.1 Hz, 1H, Ar-H), 7.66-7.56 (m, 1H, Ar-H), 7.44 (d, J = 8.0 Hz, 1H, Ar-H), 7.38-7.28 (m, 2H, Ar-H), 7.21-7.07 (m, 2H, Ar-H), 6.47 (s, 1H, Ar-H), 2.86 (t, J = 7.6 Hz, 2H, CH_2), 1.57 (quin, J = 7.6 Hz, 2H, CH_2), 1.41-1.32 (m, 2H, CH_2), 0.88 (t, J = 7.2 Hz, 3H, CH_3). $^{13}\text{C}\{^1\text{H}\}$ -NMR (125 MHz, CDCl_3): δ = 151.8 (C_q), 149.8 (CH), 141.9 (C_q), 138.4 (CH), 137.4 (C_q), 128.8 (C_q), 122.2 (CH), 121.7 (CH), 121.3 (CH), 120.7 (CH), 120.0 (CH), 110.2 (CH), 102.2 (CH), 30.9 (CH_2), 27.3 (CH_2), 22.5 (CH_2), 14.0 (CH_3). HRMS (ESI): m/z Calcd for $\text{C}_{17}\text{H}_{18}\text{N}_2+\text{H}^+$ $[\text{M}+\text{H}]^+$ 251.1543; Found 251.1543. The ^1H and ^{13}C spectra are consistent with those reported in the literature.⁴⁸

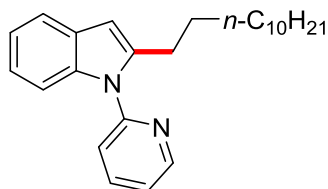


2-Hexyl-1-(pyridin-2-yl)-1H-indole (3ac): The representative procedure was followed, using substrate **1a** (0.039 g, 0.20 mmol) and 1-chlorohexane (**2c**; 0.048 g, 0.40 mmol), and the reaction mixture was stirred for 5 h. Purification by column chromatography on neutral alumina (petroleum ether/EtOAc: 50/1) yielded **3ac** (0.050 g, 90%) as a light yellow liquid. $^1\text{H-NMR}$ (500 MHz, CDCl_3): δ = 8.68 (dd, J = 4.8, 1.0 Hz, 1H, Ar-H), 7.88 (td, J = 7.7, 1.7 Hz, 1H, Ar-H), 7.65-7.56 (m, 1H, Ar-H), 7.44 (d, J = 8.0 Hz, 1H, Ar-H), 7.39-7.28 (m, 2H, Ar-H), 7.21-7.09 (m, 2H, Ar-H), 6.48 (s, 1H, Ar-H), 2.86 (t, J = 7.6 Hz, 2H, CH_2), 1.59 (quin, J = 7.6 Hz, 2H, CH_2), 1.35-1.17 (m, 6H, CH_2), 0.88 (t, J = 6.9 Hz, 3H, CH_3). $^{13}\text{C}\{^1\text{H}\}$ -NMR (125 MHz,

CDCl₃): δ = 151.8 (C_q), 149.8 (CH), 141.9 (C_q), 138.4 (CH), 137.4 (C_q), 128.8 (C_q), 122.1 (CH), 121.7 (CH), 121.3 (CH), 120.7 (CH), 120.0 (CH), 110.2 (CH), 102.2 (CH), 31.7 (CH₂), 29.1 (CH₂), 28.7 (CH₂), 27.6 (CH₂), 22.7 (CH₂), 14.2 (CH₃). HRMS (ESI): m/z Calcd for C₁₉H₂₂N₂+H⁺ [M+H]⁺ 279.1856; Found 279.1853. The ¹H and ¹³C spectra are consistent with those reported in the literature.⁴⁸

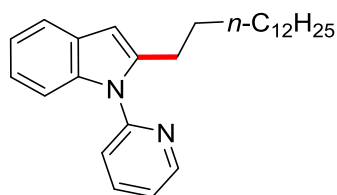


2-Decyl-1-(pyridin-2-yl)-1H-indole (3ad): The representative procedure was followed, using substrate **1a** (0.039 g, 0.20 mmol) and 1-chlorodecane (**2d**; 0.071 g, 0.40 mmol), and the reaction mixture was stirred for 5 h. Purification by column chromatography on neutral alumina (petroleum ether/EtOAc: 50/1) yielded **3ad** (0.058 g, 87%) as a light yellow liquid. ¹H-NMR (400 MHz, CDCl₃): δ = 8.68 (br s, 1H, Ar-H), 7.89 (t, J = 7.3 Hz, 1H, Ar-H), 7.64-7.54 (m, 1H, Ar-H), 7.43 (d, J = 7.9 Hz, 1H, Ar-H), 7.33 (d, J = 4.9 Hz, 2H, Ar-H), 7.21-7.07 (m, 2H, Ar-H), 6.46 (s, 1H, Ar-H), 2.85 (t, J = 7.6 Hz, 2H, CH₂), 1.66-1.54 (m, 2H, CH₂), 1.32-1.22 (m, 14H, CH₂), 0.95-0.85 (m, 3H, CH₃). ¹³C{¹H}-NMR (100 MHz, CDCl₃): δ = 151.7 (C_q), 149.8 (CH), 141.9 (C_q), 138.4 (CH), 137.4 (C_q), 128.8 (C_q), 122.2 (CH), 121.6 (CH), 121.3 (CH), 120.7 (CH), 120.0 (CH), 110.2 (CH), 102.2 (CH), 32.0 (CH₂), 29.7 (CH₂), 29.6 (CH₂), 29.5 (3C, CH₂), 28.7 (CH₂), 27.6 (CH₂), 22.8 (CH₂), 14.3 (CH₃). HRMS (ESI): m/z Calcd for C₂₃H₃₀N₂+H⁺ [M+H]⁺ 335.2482; Found 335.2479. The ¹H and ¹³C spectra are consistent with those reported in the literature.⁴⁸

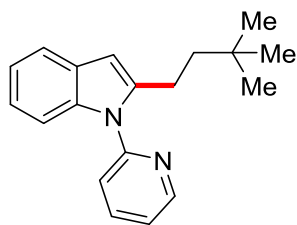


2-Dodecyl-1-(pyridin-2-yl)-1H-indole (3ae): The representative procedure was followed, using substrate **1a** (0.039 g, 0.20 mmol) and 1-chlorododecane (**2e**; 0.082 g, 0.40 mmol), and the reaction mixture was stirred for 5 h. Purification by column chromatography on neutral alumina

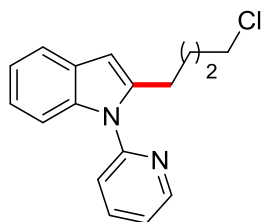
(petroleum ether/EtOAc: 50/1) yielded **3ae** (0.064 g, 88%) as a light yellow liquid. $^1\text{H-NMR}$ (500 MHz, CDCl_3): δ = 8.72-8.64 (m, 1H, Ar-H), 7.88 (td, J = 7.8, 1.9 Hz, 1H, Ar-H), 7.63-7.56 (m, 1H, Ar-H), 7.44 (d, J = 8.0 Hz, 1H, Ar-H), 7.38-7.29 (m, 2H, Ar-H), 7.18-7.10 (m, 2H, Ar-H), 6.48 (s, 1H, Ar-H), 2.86 (t, J = 7.4 Hz, 2H, CH_2), 1.64-1.54 (m, 2H, CH_2), 1.35-1.23 (m, 18H, CH_2), 0.92 (td, J = 6.9, 1.5 Hz, 3H, CH_3). $^{13}\text{C}\{^1\text{H}\}$ -NMR (125 MHz, CDCl_3): δ = 151.8 (C_q), 149.8 (CH), 141.9 (C_q), 138.4 (CH), 137.4 (C_q), 128.8 (C_q), 122.1 (CH), 121.6 (CH), 121.3 (CH), 120.6 (CH), 120.0 (CH), 110.2 (CH), 102.2 (CH), 32.1 (CH_2), 29.8 (2C, CH_2), 29.6 (CH_2), 29.5 (3C, CH_2), 29.5 (CH_2), 28.7 (CH_2), 27.6 (CH_2), 22.8 (CH_2), 14.3 (CH_3). HRMS (ESI): m/z Calcd for $\text{C}_{25}\text{H}_{34}\text{N}_2+\text{H}^+$ $[\text{M}+\text{H}]^+$ 363.2795; Found 363.2791. The ^1H and ^{13}C spectra are consistent with those reported in the literature.⁴⁸



2-Tetradecyl-1-(pyridin-2-yl)-1H-indole (3af): The representative procedure was followed, using substrate **1a** (0.039 g, 0.20 mmol) and 1-chlorotetradecane (**2f**; 0.093 g, 0.40 mmol), and the reaction mixture was stirred for 5 h. Purification by column chromatography on neutral alumina (petroleum ether/EtOAc: 50/1) yielded **3af** (0.069 g, 88%) as a light yellow liquid. $^1\text{H-NMR}$ (500 MHz, CDCl_3): δ = 8.67 (d, J = 4.6 Hz, 1H, Ar-H), 7.92-7.86 (m, 1H, Ar-H), 7.61-7.56 (m, 1H, Ar-H), 7.43 (d, J = 8.0 Hz, 1H, Ar-H), 7.32 (dd, J = 7.4, 4.4 Hz, 2H, Ar-H), 7.19-7.06 (m, 2H, Ar-H), 6.45 (s, 1H, Ar-H), 2.84 (t, J = 7.6 Hz, 2H, CH_2), 1.62-1.50 (m, 2H, CH_2), 1.36-1.24 (m, 22H, CH_2), 0.90 (t, J = 6.9 Hz, 3H, CH_3). $^{13}\text{C}\{^1\text{H}\}$ -NMR (125 MHz, CDCl_3): δ = 151.8 (C_q), 149.8 (CH), 142.0 (C_q), 138.4 (CH), 137.5 (C_q), 128.9 (C_q), 122.2 (CH), 121.7 (CH), 121.4 (CH), 120.7 (CH), 120.0 (CH), 110.2 (CH), 102.2 (CH), 32.1 (CH_2), 29.8 (5C, CH_2), 29.7 (CH_2), 29.5 (3C, CH_2), 28.8 (CH_2), 27.6 (CH_2), 22.9 (CH_2), 14.3 (CH_3). HRMS (ESI): m/z Calcd for $\text{C}_{27}\text{H}_{38}\text{N}_2+\text{H}^+$ $[\text{M}+\text{H}]^+$ 391.3005; Found 391.2980. The ^1H and ^{13}C spectra are consistent with those reported in the literature.⁴⁸

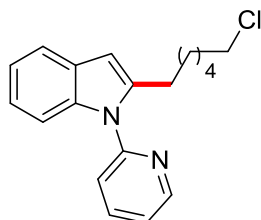


2-(3,3-Dimethylbutyl)-1-(pyridin-2-yl)-1H-indole (3ag): The representative procedure was followed, using substrate **1a** (0.039 g, 0.20 mmol), 1-chloro-3,3-dimethylbutane (**2g**; 0.048 g, 0.40 mmol) and the reaction mixture was stirred at 60 °C for 5 h. Purification by column chromatography on neutral alumina (petroleum ether/EtOAc: 50/1) yielded **3ag** (0.052 g, 93%) as a light yellow liquid. $^1\text{H-NMR}$ (400 MHz, CDCl_3): δ = 8.67 (dd, J = 4.6, 1.5 Hz, 1H, Ar-H), 7.89 (td, J = 7.6, 2.3 Hz, 1H, Ar-H), 7.57 (t, J = 4.6 Hz, 1H, Ar-H), 7.45 (d, J = 7.6 Hz, 1H, Ar-H), 7.34-7.31 (m, 2H, Ar-H), 7.14-7.11 (m, 2H, Ar-H), 6.45 (s, 1H, Ar-H), 2.85-2.81 (m, 2H, CH_2), 1.47-1.43 (m, 2H, CH_2), 0.84 (s, 9H, CH_3). $^{13}\text{C}\{^1\text{H}\}$ -NMR (100 MHz, CDCl_3): δ = 151.6 (C_q), 149.7 (CH), 142.4 (C_q), 138.3 (CH), 137.3 (C_q), 128.7 (C_q), 122.1 (CH), 121.5 (CH), 121.2 (CH), 120.6 (CH), 119.9 (CH), 110.0 (CH), 102.0 (CH), 43.2 (CH_2), 30.4 (C_q), 29.2 (3C, CH_3), 22.9 (CH_2). HRMS (ESI): m/z Calcd for $\text{C}_{19}\text{H}_{22}\text{N}_2+\text{H}^+$ $[\text{M}+\text{H}]^+$ 279.1856; Found 279.1854.

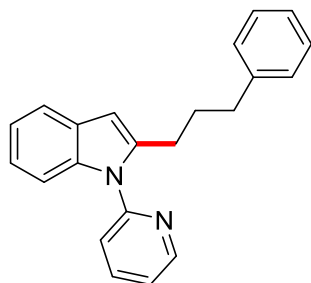


2-(4-Chlorobutyl)-1-(pyridin-2-yl)-1H-indole (3ah): The representative procedure was followed, using substrate **1a** (0.039 g, 0.20 mmol) and 1-bromo-4-chlorobutane (**2h**; 0.068 g, 0.40 mmol) or 1-iodo-4-chlorobutane (**2h'**; 0.087 g, 0.40 mmol), and the reaction mixture was stirred for 16 h. Purification by column chromatography on neutral alumina (petroleum ether/EtOAc: 50/1) yielded **3ah** {0.048 g, 84% (using **2h**) and 0.046 g, 81% (using **2h'**)} as a light yellow liquid. $^1\text{H-NMR}$ (500 MHz, CDCl_3): δ = 8.67 (dd, J = 4.8, 1.3 Hz, 1H, Ar-H), 7.90 (td, J = 7.6, 1.9 Hz, 1H, Ar-H), 7.63-7.55 (m, 1H, Ar-H), 7.45 (d, J = 8.0 Hz, 1H, Ar-H), 7.37-7.29 (m, 2H, Ar-H), 7.19-7.10 (m, 2H, Ar-H), 6.47 (s, 1H, Ar-H), 3.49 (t, J = 6.5 Hz, 2H, CH_2), 2.90 (t, J = 7.4 Hz, 2H, CH_2), 1.84-1.76 (m, 2H, CH_2), 1.76-1.68 (m, 2H, CH_2). $^{13}\text{C}\{^1\text{H}\}$ -NMR

(125 MHz, CDCl₃): δ = 151.6 (C_q), 149.8 (CH), 140.9 (C_q), 138.5 (CH), 137.4 (C_q), 128.7 (C_q), 122.3 (CH), 121.9 (CH), 121.3 (CH), 120.8 (CH), 120.1 (CH), 110.2 (CH), 102.6 (CH), 44.9 (CH₂), 32.2 (CH₂), 26.8 (CH₂), 25.9 (CH₂). HRMS (ESI): m/z Calcd for C₁₇H₁₇N₂Cl+H⁺ [M+H]⁺ 285.1153; Found 285.1156.

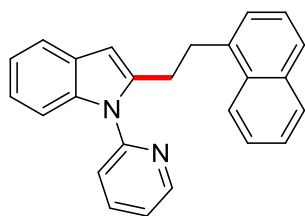


2-(6-Chlorohexyl)-1-(pyridin-2-yl)-1H-indole (3ai): The representative procedure was followed, using substrate **1a** (0.039 g, 0.20 mmol), 1,6-dichlorohexane (**2i**; 0.062 g, 0.40 mmol) and the reaction mixture was stirred at 60 °C for 24 h. Purification by column chromatography on neutral alumina (petroleum ether/EtOAc: 50/1) yielded **3ai** (0.050 g, 80%) as a light yellow liquid. ¹H-NMR (400 MHz, CDCl₃): δ = 8.67-8.66 (m, 1H, Ar-H), 7.89 (td, J = 7.6, 2.3 Hz, 1H, Ar-H), 7.58-7.56 (m, 1H, Ar-H), 7.44-7.42 (m, 1H, Ar-H), 7.34-7.30 (m, 2H, Ar-H), 7.13-7.11 (m, 2H, Ar-H), 6.44 (s, 1H, Ar-H), 3.48 (t, J = 6.9 Hz, 2H, CH₂), 2.85 (t, J = 7.6 Hz, 2H, CH₂), 1.74-1.67 (m, 2H, CH₂), 1.61-1.53 (m, 2H, CH₂), 1.40-1.30 (m, 4H, CH₂). ¹³C{¹H}-NMR (100 MHz, CDCl₃): δ = 151.6 (C_q), 149.7 (CH), 141.5 (C_q), 138.4 (CH), 137.3 (C_q), 128.7 (C_q), 122.1 (CH), 121.7 (CH), 121.2 (CH), 120.6 (CH), 119.9 (CH), 110.14 (CH), 102.2 (CH), 45.1 (CH₂), 32.5 (CH₂), 28.5 (CH₂), 28.4 (CH₂), 27.3 (CH₂), 26.6 (CH₂). HRMS (ESI): m/z Calcd for C₁₉H₂₁ClN₂+H⁺ [M+H]⁺ 313.1466; Found 313.1464.

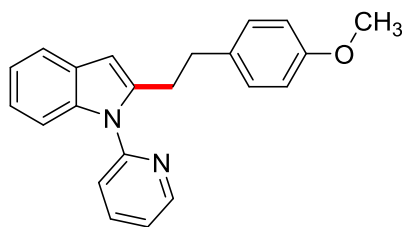


2-(3-Phenylpropyl)-1-(pyridin-2-yl)-1H-indole (3aj): The representative procedure was followed, using substrate **1a** (0.039 g, 0.20 mmol) and (3-chloropropyl)benzene (**2j**; 0.062 g, 0.40 mmol), and the reaction mixture was stirred for 16 h. Purification by column

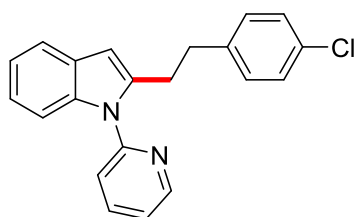
chromatography on neutral alumina (petroleum ether/EtOAc: 50/1) yielded **3aj** (0.060 g, 96%) as a light yellow liquid. $^1\text{H-NMR}$ (500 MHz, CDCl_3): $\delta = 8.71\text{-}8.61$ (m, 1H, Ar-H), 7.86 (td, $J = 7.8, 1.9$ Hz, 1H, Ar-H), 7.65-7.57 (m, 1H, Ar-H), 7.42 (d, $J = 8.0$ Hz, 1H, Ar-H), 7.39-7.34 (m, 1H, Ar-H), 7.34-7.30 (m, 1H, Ar-H), 7.30-7.25 (m, 2H, Ar-H), 7.24-7.07 (m, 5H, Ar-H), 6.51 (s, 1H, Ar-H), 2.93 (t, $J = 7.6$ Hz, 2H, CH_2), 2.66 (t, $J = 7.6$ Hz, 2H, CH_2), 1.92 (quin, $J = 7.6$ Hz, 2H, CH_2). $^{13}\text{C}\{^1\text{H}\}\text{-NMR}$ (125 MHz, CDCl_3): $\delta = 151.6$ (C_q), 149.8 (CH), 142.1 (C_q), 141.3 (C_q), 138.4 (CH), 137.4 (C_q), 128.8 (C_q), 128.6 (2C, CH), 128.4 (2C, CH), 125.9 (CH), 122.1 (CH), 121.8 (CH), 121.2 (CH), 120.8 (CH), 120.1 (CH), 110.2 (CH), 102.5 (CH), 35.5 (CH_2), 30.5 (CH_2), 27.2 (CH_2). HRMS (ESI): m/z Calcd for $\text{C}_{22}\text{H}_{20}\text{N}_2+\text{H}^+$ $[\text{M}+\text{H}]^+$ 313.1699; Found 313.1696. The ^1H and ^{13}C spectra are consistent with those reported in the literature.⁴⁸



2-(2-(Naphthalen-1-yl)ethyl)-1-(pyridin-2-yl)-1H-indole (3ak): The representative procedure was followed using, substrate **1a** (0.039 g, 0.20 mmol), 1-(2-chloroethyl)naphthalene (**2k**; 0.076 g, 0.40 mmol) and the reaction mixture was stirred for 24 h. Purification by column chromatography on neutral alumina (petroleum ether/EtOAc: 50/1) yielded **3ak** (0.052 g, 75%) as a pale yellow solid. $^1\text{H-NMR}$ (500 MHz, CDCl_3): $\delta = 8.65$ (d, $J = 3.8$ Hz, 1H, Ar-H), 7.90 (d, $J = 8.4$ Hz, 1H, Ar-H), 7.87-7.83 (m, 1H, Ar-H), 7.83-7.77 (m, 1H, Ar-H), 7.71 (d, $J = 8.0$ Hz, 1H, Ar-H), 7.69-7.61 (m, 1H, Ar-H), 7.47 (m, 2H, Ar-H), 7.40-7.32 (m, 3H, Ar-H), 7.31-7.22 (m, 2H, Ar-H), 7.22-7.13 (m, 2H, Ar-H), 6.64 (s, 1H, Ar-H), 3.46-3.37 (m, 2H, CH_2), 3.36-3.27 (m, 2H, CH_2). $^{13}\text{C}\{^1\text{H}\}\text{-NMR}$ (125 MHz, CDCl_3): $\delta = 151.5$ (C_q), 149.8 (CH), 141.2 (C_q), 138.4 (CH), 137.7 (C_q), 137.4 (C_q), 134.0 (C_q), 131.9 (C_q), 128.9 (CH), 128.8 (C_q), 127.0 (CH), 126.3 (CH), 126.0 (CH), 125.7 (CH), 125.6 (CH), 123.8 (CH), 122.2 (CH), 122.0 (CH), 121.3 (CH), 120.9 (CH), 120.2 (CH), 110.2 (CH), 102.7 (CH), 33.2 (CH_2), 29.0 (CH_2). HRMS (ESI): m/z Calcd for $\text{C}_{25}\text{H}_{20}\text{N}_2+\text{H}^+$ $[\text{M}+\text{H}]^+$ 348.1699; Found 348.1696.

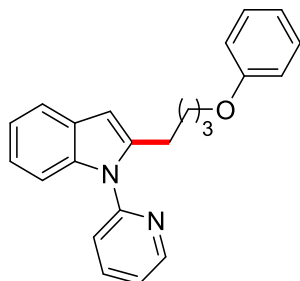


2-(4-Methoxyphenethyl)-1-(pyridin-2-yl)-1H-indole (3al): The representative procedure was followed using, substrate **1a** (0.039 g, 0.20 mmol), 1-(2-chloroethyl)-4-methoxybenzene (**2l**; 0.068 g, 0.40 mmol) and the reaction mixture was stirred for 16 h. Purification by column chromatography on neutral alumina (petroleum ether/EtOAc: 20/1) yielded **3al** (0.053 g, 81%) as a white solid. $^1\text{H-NMR}$ (400 MHz, CDCl_3): δ = 8.69 (d, J = 3.7 Hz, 1H, Ar-H), 7.88 (t, J = 7.3 Hz, 1H, Ar-H), 7.72-7.55 (m, 1H, Ar-H), 7.42 (d, J = 7.9 Hz, 1H, Ar-H), 7.40-7.28 (m, 2H, Ar-H), 7.23-7.13 (m, 2H, Ar-H), 7.06 (d, J = 8.5 Hz, 2H, Ar-H), 6.82 (d, J = 7.9 Hz, 2H, Ar-H), 6.53 (s, 1H, Ar-H), 3.79 (s, 3H, OCH_3), 3.17 (t, J = 7.9 Hz, 2H, CH_2), 2.97-2.83 (m, 2H, CH_2). $^{13}\text{C}\{^1\text{H}\}$ -NMR (100 MHz, CDCl_3): δ = 158.0 (C_q), 151.6 (C_q), 149.8 (CH), 141.0 (C_q), 138.4 (CH), 137.3 (C_q), 133.7 (C_q), 129.4 (2C, CH), 128.7 (C_q), 122.2 (CH), 121.9 (CH), 121.2 (CH), 120.8 (CH), 120.2 (CH), 113.9 (2C, CH), 110.2 (CH), 102.6 (CH), 55.3 (OCH_3), 34.5 (CH_2), 30.0 (CH_2). HRMS (ESI): m/z Calcd for $\text{C}_{22}\text{H}_{20}\text{N}_2\text{O}+\text{H}^+$ $[\text{M}+\text{H}]^+$ 329.1648; Found 329.1645.

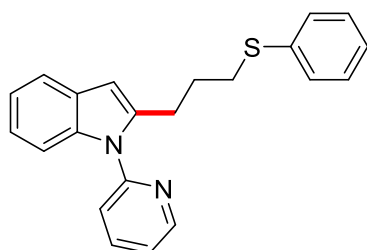


2-(4-Chlorophenethyl)-1-(pyridin-2-yl)-1H-indole (3am): The representative procedure was followed using, substrate **1a** (0.039 g, 0.20 mmol), 1-chloro-4-(2-chloroethyl)benzene (**2m**; 0.070 g, 0.40 mmol) and the reaction mixture was stirred for 16 h. Purification by column chromatography on neutral alumina (petroleum ether/EtOAc: 30/1) yielded **3am** (0.041 g, 62%) as a pale yellow solid. $^1\text{H-NMR}$ (400 MHz, CDCl_3): δ = 8.69 (br s, 1H, Ar-H), 7.89 (br s, 1H, Ar-H), 7.62 (br s, 1H, Ar-H), 7.51-7.30 (m, 3H, Ar-H), 7.30-7.12 (m, 4H, Ar-H), 7.03 (br s, 2H, Ar-H), 6.50 (br s, 1H, Ar-H), 3.19 (br s, 2H, CH_2), 3.07-2.79 (m, 2H, CH_2). $^{13}\text{C}\{^1\text{H}\}$ -NMR (100 MHz, CDCl_3): δ = 151.3 (C_q), 149.6 (CH), 140.5 (C_q), 139.9 (C_q), 138.7 (CH), 137.3 (C_q),

131.8 (C_q), 129.9 (2C, CH), 128.7 (C_q), 128.5 (2C, CH), 122.2 (CH), 122.0 (CH), 121.2 (CH), 120.9 (CH), 120.2 (CH), 110.2 (CH), 102.9 (CH), 34.8 (CH₂), 29.6 (CH₂). HRMS (ESI): *m/z* Calcd for C₂₁H₁₇ClN₂+H⁺ [M+H]⁺ 333.1153; Found 333.1151.

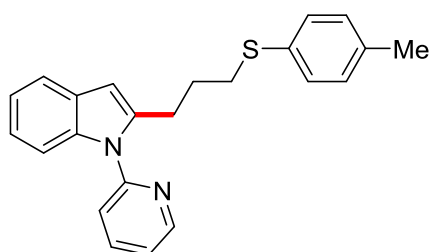


2-(4-Phenoxybutyl)-1-(pyridin-2-yl)-1H-indole (3an): The representative procedure was followed, using substrate **1a** (0.039 g, 0.20 mmol) and (4-chlorobutoxy)benzene (**2n**; 0.074 g, 0.40 mmol), and the reaction mixture was stirred for 24 h. Purification by column chromatography on neutral alumina (petroleum ether/EtOAc: 20/1) yielded **3an** (0.050 g, 73%) as a light yellow liquid. ¹H-NMR (400 MHz, CDCl₃): δ = 8.63 (d, *J* = 3.7 Hz, 1H, Ar-H), 7.99-7.77 (m, 1H, Ar-H), 7.69-7.52 (m, 1H, Ar-H), 7.43 (d, *J* = 7.9 Hz, 1H, Ar-H), 7.38-7.20 (m, 4H, Ar-H), 7.20-7.05 (m, 2H, Ar-H), 6.92 (t, *J* = 7.0 Hz, 1H, Ar-H), 6.84 (d, *J* = 7.9 Hz, 2H, Ar-H), 6.48 (s, 1H, Ar-H), 3.90 (t, *J* = 5.5 Hz, 2H, CH₂), 2.94 (t, *J* = 7.0 Hz, 2H, CH₂), 1.83-1.67 (m, 4H, CH₂). ¹³C{¹H}-NMR (125 MHz, CDCl₃): δ = 159.1 (C_q), 151.7 (C_q), 149.8 (CH), 141.2 (C_q), 138.4 (CH) 137.4 (C_q), 129.5 (2C, CH), 128.7 (C_q), 122.2 (CH), 121.8 (CH), 121.2 (CH), 120.8 (CH), 120.7 (CH), 120.1 (CH), 114.6 (2C, CH), 110.2 (CH), 102.5 (CH), 67.5 (CH₂), 29.0 (CH₂), 27.3 (CH₂), 25.3 (CH₂). HRMS (ESI): *m/z* Calcd for C₂₃H₂₂N₂O+H⁺ [M+H]⁺ 343.1805; Found 343.1803.

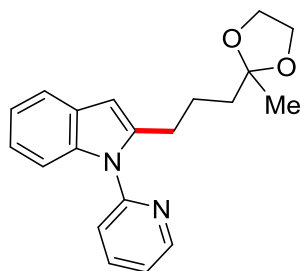


2-(3-(Phenylthio)propyl)-1-(pyridin-2-yl)-1H-indole (3ao): The representative procedure was followed, using substrate **1a** (0.039 g, 0.20 mmol), (3-chloropropyl)(phenyl)sulfane (**2o**; 0.075 g,

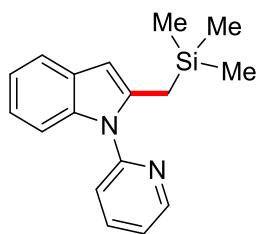
0.40 mmol) and the reaction mixture was stirred at 80 °C for 24 h. Purification by column chromatography on neutral alumina (petroleum ether/EtOAc: 10/1) yielded **3ao** (0.038 g, 55%) as a light yellow liquid. $^1\text{H-NMR}$ (500 MHz, CDCl_3): δ = 8.67 (d, J = 3.4 Hz, 1H, Ar-H), 7.88 (td, J = 7.6, 1.9 Hz, 1H, Ar-H), 7.62 (m, 1H, Ar-H), 7.45 (d, J = 8.0 Hz, 1H, Ar-H), 7.38-7.31 (m, 2H, Ar-H), 7.30-7.29 (m, 4H, Ar-H), 7.22-7.18 (m, 3H, Ar-H), 6.50 (s, 1H, Ar-H), 3.05 (t, J = 7.6 Hz, 2H, CH_2), 2.96 (t, J = 7.2 Hz, 2H, CH_2), 1.99-1.93 (m, 2H, CH_2). $^{13}\text{C}\{^1\text{H}\}$ -NMR (125 MHz, CDCl_3): δ = 151.4 (C_q), 149.7 (CH), 140.2 (C_q), 138.3 (CH), 137.3 (C_q), 136.5 (C_q), 129.1 (2C, CH), 128.9 (2C, CH), 128.6 (C_q), 125.8 (CH), 122.1 (CH), 121.8 (CH), 121.0 (CH), 120.0 (CH), 121.0 (CH), 110.12 (CH), 102.7 (CH), 33.0 (CH_2), 28.1 (CH_2), 26.4 (CH_2). HRMS (ESI): m/z . Calcd for $\text{C}_{22}\text{H}_{20}\text{N}_2\text{S}+\text{H}^+$ $[\text{M}+\text{H}]^+$ 345.1420; Found 345.1420.



1-(Pyridin-2-yl)-2-(3-(p-tolylthio)propyl)-1H-indole (3ap): The representative procedure was followed, using substrate **1a** (0.039 g, 0.20 mmol), (3-chloropropyl)(p-tolyl)sulfane (**2p**; 0.080 g, 0.40 mmol) and the reaction mixture was stirred at 80 °C for 24 h. Purification by column chromatography on neutral alumina (petroleum ether/EtOAc: 10/1) yielded **3ap** (0.044 g, 61%) as a light yellow liquid. $^1\text{H-NMR}$ (500 MHz, CDCl_3): δ = 8.66 (br s, 1H, Ar-H), 7.89 (t, J = 7.6 Hz, 1H, Ar-H), 7.60 (m, 1H, Ar-H), 7.44 (d, J = 7.6 Hz, 1H, Ar-H), 7.35-7.32 (m, 2H, Ar-H), 7.22 (m, 2H, Ar-H), 7.16 (m, 2H, Ar-H), 7.09 (d, J = 7.6 Hz, 2H, Ar-H), 6.46 (s, 1H, Ar-H), 3.03 (t, J = 7.2 Hz, 2H, CH_2), 2.90 (t, J = 7.2 Hz, 2H, CH_2), 2.35 (s, 3H, CH_3), 1.93-1.90 (m, 2H, CH_2). $^{13}\text{C}\{^1\text{H}\}$ -NMR (125 MHz, CDCl_3): δ = 151.4 (C_q), 149.6 (CH), 140.2 (C_q), 138.2 (CH), 137.3 (C_q), 136.0 (C_q), 132.5 (C_q), 130.0 (2C, CH), 129.6 (2C, CH), 128.5 (C_q), 122.0 (CH), 121.7 (CH), 121.0 (CH), 120.6 (CH), 119.9 (CH), 110.0 (CH), 102.6 (CH), 33.8 (CH_2), 28.2 (CH_2), 26.4 (CH_2), 21.0 (CH_3). HRMS (ESI): m/z . Calcd for $\text{C}_{23}\text{H}_{22}\text{N}_2\text{S}+\text{H}^+$ $[\text{M}+\text{H}]^+$ 359.1576; Found 359.1575.

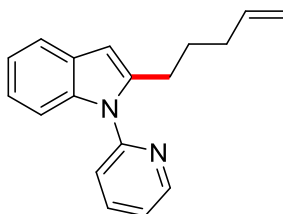


2-(3-(2-Methyl-1,3-dioxolan-2-yl)propyl)-1-(pyridin-2-yl)-1H-indole (3aq): The representative procedure was followed, using substrate **1a** (0.039 g, 0.20 mmol) and 2-(4-chlorobutyl)-2-methyl-1,3-dioxolane (**2q**; 0.066 g, 0.40 mmol), and the reaction mixture was stirred for 16 h. Purification by column chromatography on neutral alumina (petroleum ether/EtOAc: 50/1) yielded **3aq** (0.027 g, 42%) as a light yellow liquid. $^1\text{H-NMR}$ (500 MHz, CDCl_3): δ = 8.72-8.54 (m, 1H, Ar-H), 7.89 (br s, 1H, Ar-H), 7.64-7.52 (m, 1H, Ar-H), 7.44 (d, J = 7.6 Hz, 1H, Ar-H), 7.38-7.28 (m, 2H, Ar-H), 7.17-7.03 (m, 2H, Ar-H), 6.48 (s, 1H, Ar-H), 4.01-3.77 (m, 4H, CH_2), 2.86 (d, J = 6.9 Hz, 2H, CH_2), 1.68 (br s, 4H, CH_2), 1.27 (s, 3H, CH_3). $^{13}\text{C}\{^1\text{H}\}$ -NMR (125 MHz, CDCl_3): δ = 151.7 (C_q), 149.8 (CH), 141.4 (C_q), 138.4 (CH), 137.4 (C_q), 128.8 (C_q), 122.2 (CH), 121.7 (CH), 121.3 (CH), 120.7 (CH), 120.1 (CH), 110.2 (CH), 110.1 (C_q), 102.4 (CH), 64.8 (2C, CH_2), 38.8 (CH_2), 27.7 (CH_2), 24.0 (CH_3), 23.1 (CH_2). HRMS (ESI): m/z Calcd for $\text{C}_{20}\text{H}_{22}\text{O}_2\text{N}_2+\text{Na}^+$ $[\text{M}+\text{Na}]^+$ 345.1573; Found 345.1567.

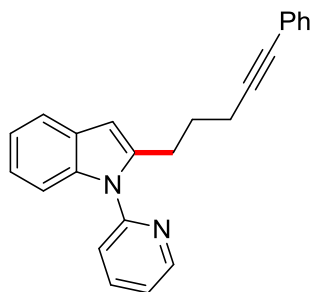


1-(Pyridin-2-yl)-2-((trimethylsilyl)methyl)-1H-indole (3ar): The representative procedure was followed, using substrate **1a** (0.039 g, 0.20 mmol) and (chloromethyl)trimethylsilane (**2r**; 0.049 g, 0.40 mmol), and the reaction mixture was stirred for 16 h. Purification by column chromatography on neutral alumina (petroleum ether/EtOAc: 50/1) yielded **3ar** (0.031 g, 55%) as a light yellow liquid. $^1\text{H-NMR}$ (400 MHz, CDCl_3): δ = 8.68 (dt, J = 5.0, 0.9 Hz, 1H, Ar-H), 7.88 (td, J = 7.8, 1.8 Hz, 1H, Ar-H), 7.54 (d, J = 7.8 Hz, 1H, Ar-H), 7.47-7.41 (m, 1H, Ar-H), 7.35-7.28 (m, 2H, Ar-H), 7.17-7.06 (m, 2H, Ar-H), 6.31 (s, 1H, Ar-H), 2.46 (s, 2H, CH_2), -0.09

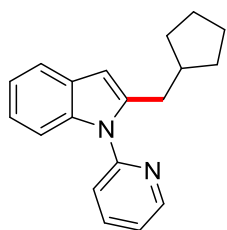
(s, 9H, CH₃). ¹³C{¹H}-NMR (100 MHz, CDCl₃): δ = 151.85 (C_q), 149.6 (CH), 139.8 (C_q), 138.2 (CH), 137.2 (C_q), 129.3 (C_q), 122.0 (CH), 121.7 (CH), 120.9 (CH), 120.8 (CH), 119.3 (CH), 110.1 (CH), 101.7 (CH), 17.5 (CH₂), -1.3 (3C, CH₃). HRMS (ESI): *m/z* Calcd for C₁₇H₂₀N₂Si+H⁺ [M+H]⁺ 281.1469; Found 281.1471.



2-(Pent-4-en-1-yl)-1-(pyridin-2-yl)-1H-indole (3as): The representative procedure was followed using, substrate **1a** (0.039 g, 0.20 mmol), 5-chloropent-1-ene (**2s**; 0.042 g, 0.40 mmol) and the reaction mixture was stirred for 16 h. Purification by column chromatography on neutral alumina (petroleum ether/EtOAc: 50/1) yielded **3as** (0.049 g, 93%) as a pale yellow solid. ¹H-NMR (500 MHz, CDCl₃): δ = 8.68 (d, *J* = 4.6 Hz, 1H, Ar-H), 7.89 (t, *J* = 7.6 Hz, 1H, Ar-H), 7.66-7.55 (m, 1H, Ar-H), 7.45 (d, *J* = 7.6 Hz, 1H, Ar-H), 7.40-7.27 (m, 2H, Ar-H), 7.07-7.20 (m, 2H, Ar-H), 6.49 (s, 1H, Ar-H), 5.85-5.70 (m, 1H, CH), 4.89-5.06 (m, 2H, CH₂), 2.89 (t, *J* = 7.6 Hz, 2H, CH₂), 2.10 (quin, *J* = 6.9 Hz, 2H, CH₂), 1.69 (quin, *J* = 7.5 Hz, 2H, CH₂). ¹³C{¹H}-NMR (125 MHz, CDCl₃): δ = 151.6 (C_q), 149.8 (CH), 141.4 (C_q), 138.5 (CH), 138.4 (CH), 137.4 (C_q), 128.7 (C_q), 122.2 (CH), 121.7 (CH), 121.2 (CH), 120.7 (CH), 120.0 (CH), 115.0 (CH₂), 110.2 (CH), 102.4 (CH), 33.4 (CH₂), 27.9 (CH₂), 27.0 (CH₂). HRMS (ESI): *m/z* Calcd for C₁₈H₁₈N₂+H⁺ [M+H]⁺ 263.1543; Found 263.1541. The ¹H and ¹³C spectra are consistent with those reported in the literature.⁴⁸

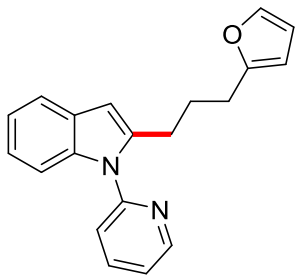


2-(5-Phenylpent-4-yn-1-yl)-1-(pyridin-2-yl)-1H-indole (3at): The representative procedure was followed, using substrate **1a** (0.039 g, 0.20 mmol) and (5-chloropent-1-yn-1-yl)benzene (**2t**; 0.071 g, 0.40 mmol), and the reaction mixture was stirred for 16 h. Purification by column chromatography on neutral alumina (petroleum ether/EtOAc: 20/1) yielded **3at** (0.036 g, 53%) as a light yellow liquid. $^1\text{H-NMR}$ (400 MHz, CDCl_3): δ = 8.76-8.53 (m, 1H, Ar-H), 7.85 (td, J = 7.6, 1.8 Hz, 1H, Ar-H), 7.66-7.54 (m, 1H, Ar-H), 7.49-7.39 (m, 1H, Ar-H), 7.39-7.30 (m, 3H, Ar-H), 7.30-7.21 (m, 4H, Ar-H), 7.20-7.06 (m, 2H, Ar-H), 6.51 (s, 1H, Ar-H), 3.04 (t, J = 7.6 Hz, 2H, CH_2), 2.43 (t, J = 6.9 Hz, 2H, CH_2), 1.97-1.75 (m, 2H, CH_2). $^{13}\text{C}\{^1\text{H}\}$ -NMR (100 MHz, CDCl_3): δ = 151.6 (C_q), 149.9 (CH), 140.6 (C_q), 138.5 (CH), 137.4 (C_q), 131.7 (2C, CH), 128.7 (C_q), 128.3 (2C, CH), 127.7 (CH), 124.0 (C_q), 122.3 (CH), 121.9 (CH), 121.3 (CH), 120.8 (CH), 120.1 (CH), 110.3 (CH), 102.8 (CH), 89.8 (C_q), 81.3 (C_q), 29.9 (CH_2), 28.0 (CH_2), 26.7 (CH_2). HRMS (ESI): m/z Calcd for $\text{C}_{24}\text{H}_{20}\text{N}_2+\text{H}^+$ $[\text{M}+\text{H}]^+$ 337.1699; Found 337.1699.

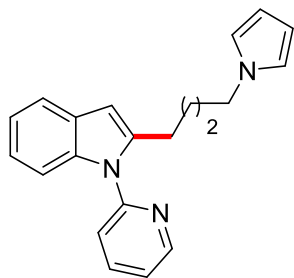


2-(Cyclopentylmethyl)-1-(pyridin-2-yl)-1H-indole (3au): The representative procedure was followed, using substrate **1a** (0.039 g, 0.20 mmol), 6-chloro-1-hexene (**2u**; 0.047 g, 0.40 mmol) and the reaction mixture was stirred for 16 h. Purification by column chromatography on neutral alumina (petroleum ether/EtOAc: 50/1) yielded **3au** (0.043 g, 78%) as a light yellow liquid. $^1\text{H-NMR}$ (400 MHz, CDCl_3): δ = 8.87-8.57 (m, 1H, Ar-H), 7.89 (t, J = 7.3 Hz, 1H, Ar-H), 7.59 (d, J = 4.9 Hz, 1H, Ar-H), 7.43 (d, J = 7.9 Hz, 1H, Ar-H), 7.39-7.28 (m, 2H, Ar-H), 7.23-7.07 (m, 2H, Ar-H), 6.48 (s, 1H, Ar-H), 2.86 (d, J = 6.7 Hz, 2H, CH_2), 2.22-1.93 (m, 1H, CH), 1.73 (d, J

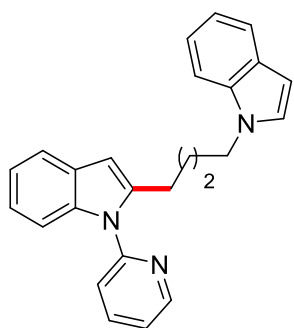
= 6.7 Hz, 2H, CH₂), 1.66-1.47 (m, 4H, CH₂), 1.25-1.00 (m, 2H, CH₂). ¹³C{¹H}-NMR (125 MHz, CDCl₃): δ = 151.8 (C_q), 149.8 (CH), 141.4 (C_q), 138.4 (CH), 137.4 (C_q), 128.8 (C_q), 122.2 (CH), 121.6 (CH), 121.4 (CH), 120.7 (CH), 120.0 (CH), 110.2 (CH), 102.9 (CH), 39.3 (CH), 33.8 (CH₂), 32.8 (2C, CH₂), 25.2 (2C, CH₂). HRMS (ESI): *m/z* Calcd for C₁₉H₂₀N₂+H⁺ [M+H]⁺ 277.1699; Found 277.1700. The ¹H and ¹³C spectra are consistent with those reported in the literature.⁴⁸



2-(3-(Furan-2-yl)propyl)-1-(pyridin-2-yl)-1H-indole (3av): The representative procedure was followed, using substrate **1a** (0.039 g, 0.20 mmol), 2-(3-chloropropyl)furan (**2v**; 0.058 g, 0.40 mmol) and the reaction mixture was stirred at 80 °C for 16 h. Purification by column chromatography on neutral alumina (petroleum ether/EtOAc: 5/1) yielded **3av** (0.036 g, 60%) as a light yellow liquid. ¹H-NMR (400 MHz, CDCl₃): δ = 8.64 (dd, *J* = 5.3, 2.3 Hz, 1H, Ar-H), 7.90-7.86 (td, *J* = 7.6, 1.5 Hz, 1H, Ar-H), 7.58 (t, *J* = 4.6 Hz, 1H, Ar-H), 7.42 (d, *J* = 7.6 Hz, 1H, Ar-H), 7.34-7.30 (m, 2H, Ar-H), 7.27-2.25 (m, 1H, Ar-H), 7.16-7.11 (m, 2H, Ar-H), 6.49 (s, 1H, Ar-H), 6.26-6.25 (m, 1H, Ar-H), 5.93 (d, *J* = 3.0 Hz, 1H, Ar-H), 2.90 (t, *J* = 7.6 Hz, 2H, CH₂), 2.64 (t, *J* = 7.6 Hz, 2H, CH₂), 1.91 (pent, *J* = 7.6 Hz, 2H, CH₂). ¹³C{¹H}-NMR (100 MHz, CDCl₃): δ = 155.7 (C_q), 151.5 (C_q), 149.7 (CH), 140.9 (C_q), 140.9 (CH), 138.4 (CH), 137.3 (C_q), 128.7 (C_q), 122.1 (CH), 121.7 (CH), 121.1 (CH), 120.7 (CH), 120.0 (CH), 110.2 (CH), 110.1 (CH), 105.0 (CH), 102.5 (CH), 27.5 (CH₂), 27.1 (CH₂), 26.9 (CH₂). HRMS (ESI): *m/z* Calcd for C₂₀H₁₈N₂O+H⁺ [M+H]⁺ 303.1492; Found 303.1490.

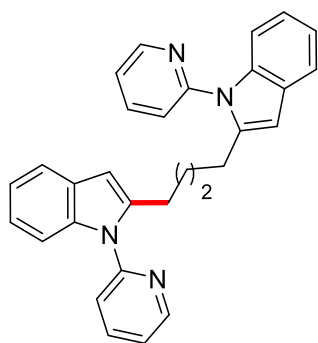


2-(4-(1H-Pyrrol-1-yl)butyl)-1-(pyridin-2-yl)-1H-indole (3aw): The representative procedure was followed, using substrate **1a** (0.039 g, 0.20 mmol) and 1-(4-chlorobutyl)-1H-pyrrole (**2w**; 0.063 g, 0.40 mmol), and the reaction mixture was stirred for 16 h. Purification by column chromatography on neutral alumina (petroleum ether/EtOAc: 20/1) yielded **3aw** (0.053 g, 84%) as a light yellow liquid. $^1\text{H-NMR}$ (400 MHz, CDCl_3): δ = 8.66 (br s, 1H, Ar-H), 8.01-7.79 (m, 1H, Ar-H), 7.79-7.61 (m, 2H, Ar-H), 7.46-7.28 (m, 3H, Ar-H), 7.28-7.15 (m, 3H, Ar-H), 7.08 (br s, 1H, Ar-H), 6.53 (br s, 1H, Ar-H), 6.47 (br s, 1H, Ar-H), 4.23-3.99 (m, 2H, CH_2), 3.14-2.84 (m, 2H, CH_2), 2.03-1.81 (m, 2H, CH_2), 1.63 (d, J = 7.3 Hz, 2H, CH_2). $^{13}\text{C}\{^1\text{H}\}$ -NMR (100 MHz, CDCl_3): δ = 151.5 (C_q), 149.7 (CH), 140.9 (C_q), 138.5 (CH), 137.3 (C_q), 128.6 (C_q), 122.2 (CH), 121.8 (CH), 121.2 (CH), 120.8 (CH), 120.5 (2C, CH), 120.0 (CH), 110.2 (CH), 108.0 (2C, CH), 102.5 (CH), 49.3 (CH_2), 31.1 (CH_2), 27.0 (CH_2), 25.8 (CH_2). HRMS (ESI): m/z Calcd for $\text{C}_{21}\text{H}_{21}\text{N}_3+\text{H}^+$ $[\text{M}+\text{H}]^+$ 316.1808; Found 316.1806.

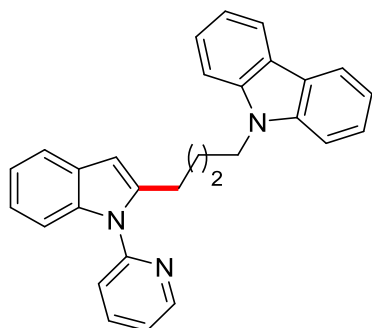


2-(4-(1H-Indol-1-yl)butyl)-1-(pyridin-2-yl)-1H-indole (3ax): The representative procedure was followed, using substrate **1a** (0.039 g, 0.20 mmol) and 1-(4-chlorobutyl)-1H-indole (**2x**; 0.083 g, 0.40 mmol), and the reaction mixture was stirred for 16 h. Purification by column chromatography on neutral alumina (petroleum ether/EtOAc: 20/1) yielded **3ax** (0.055 g, 75%) as a light yellow liquid. $^1\text{H-NMR}$ (400 MHz, CDCl_3): δ = 8.65 (d, J = 3.7 Hz, 1H, Ar-H), 7.95-7.78 (m, 1H, Ar-H), 7.70 (d, J = 7.3 Hz, 1H, Ar-H), 7.67-7.58 (m, 1H, Ar-H), 7.42-7.28 (m, 4H,

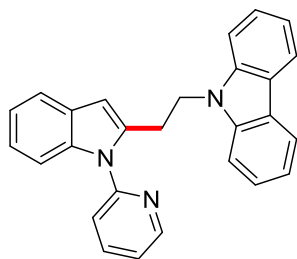
Ar-H), 7.28-7.12 (m, 4H, Ar-H), 7.07 (d, $J = 3.1$ Hz, 1H, Ar-H), 6.52 (d, $J = 2.4$ Hz, 1H, Ar-H), 6.46 (s, 1H, Ar-H), 4.11 (t, $J = 7.0$ Hz, 2H, Ar-H), 2.93 (t, $J = 7.6$ Hz, 2H, CH₂), 2.02-1.80 (m, 2H, CH₂), 1.70-1.54 (m, 2H, CH₂). ¹³C{¹H}-NMR (125 MHz, CDCl₃): $\delta = 151.4$ (C_q), 149.7 (CH), 140.8 (C_q), 138.4 (CH), 137.4 (C_q), 136.0 (C_q), 128.7 (C_q), 128.6 (C_q), 127.9 (CH), 122.2 (CH), 121.9 (CH), 121.4 (CH), 121.1 (CH), 121.1 (CH), 120.8 (CH), 120.1 (CH), 119.3 (CH), 110.2 (CH), 109.5 (CH), 102.5 (CH), 101.0 (CH), 46.2 (CH₂), 29.8 (CH₂), 27.1 (CH₂), 26.0 (CH₂). HRMS (ESI): m/z Calcd for C₂₅H₂₃N₃+H⁺ [M+H]⁺ 366.1965; Found 366.1967.



1,4-Bis(1-(pyridin-2-yl)-1H-indol-2-yl)butane (3ay): The representative procedure was followed, using substrate **1a** (0.039 g, 0.20 mmol) and 2-(4-chlorobutyl)-1-(pyridin-2-yl)-1H-indole (**2y**, 0.114 g, 0.40 mmol), and the reaction mixture was stirred for 16 h. Purification by column chromatography on neutral alumina (petroleum ether/EtOAc: 10/1) yielded **3ay** (0.058 g, 65%) as a light yellow solid. ¹H-NMR (500 MHz, CDCl₃): $\delta = 8.56$ (dd, $J = 5.0, 0.8$ Hz, 2H, Ar-H), 7.75 (td, $J = 7.7, 2.1$ Hz, 2H, Ar-H), 7.59-7.50 (m, 2H, Ar-H), 7.34 (d, $J = 8.0$ Hz, 2H, Ar-H), 7.31-7.27 (m, 2H, Ar-H), 7.27-7.21 (m, 2H, Ar-H), 7.16-7.08 (m, 4H, Ar-H), 6.34 (s, 2H, Ar-H), 2.81 (br s, 4H, CH₂), 1.55-1.48 (m, 4H, CH₂). ¹³C{¹H}-NMR (125 MHz, CDCl₃): $\delta = 151.6$ (2C, C_q), 149.7 (2C, CH), 141.3 (2C, C_q), 138.4 (2C, CH), 137.4 (2C, C_q), 128.7 (2C, C_q), 122.1 (2C, CH), 121.7 (2C, CH), 121.2 (2C, CH), 120.7 (2C, CH), 120.0 (2C, CH), 110.2 (2C, CH), 102.4 (2C, CH), 28.1 (2C, CH₂), 27.3 (2C, CH₂). HRMS (ESI): m/z Calcd for C₃₀H₂₆N₄+H⁺ [M+H]⁺ 443.2230; Found 443.2235.

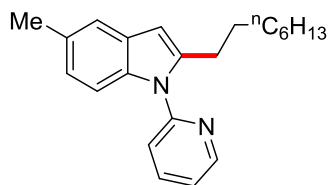


9-(4-(1-(Pyridin-2-yl)-1H-indol-2-yl)butyl)-9H-carbazole (3az): The representative procedure was followed, using substrate **1a** (0.039 g, 0.20 mmol) and 9-(4-chlorobutyl)-8a,9a-dihydro-9H-carbazole (**2z**; 0.103 g, 0.40 mmol), and the reaction mixture was stirred for 24 h. Purification by column chromatography on neutral alumina (petroleum ether/EtOAc: 10/1) yielded **3az** (0.071 g, 85%) as a pale yellow liquid. $^1\text{H-NMR}$ (500 MHz, CDCl_3): δ = 8.71-8.49 (m, 1H, Ar-H), 8.19 (d, J = 7.6 Hz, 2H, Ar-H), 7.76 (t, J = 7.4 Hz, 1H, Ar-H), 7.66 (d, J = 6.9 Hz, 1H, Ar-H), 7.52 (t, J = 7.4 Hz, 2H, Ar-H), 7.43-7.36 (m, 3H, Ar-H), 7.35-7.27 (m, 3H, Ar-H), 7.28- 7.16 (m, 3H, Ar-H), 6.46 (s, 1H, Ar-H), 4.30 (t, J = 6.7 Hz, 2H, CH_2), 2.95 (t, J = 7.2 Hz, 2H, CH_2), 2.03-1.87 (m, 2H, CH_2), 1.73-1.57 (m, 2H, CH_2). $^{13}\text{C}\{^1\text{H}\}$ -NMR (125 MHz, CDCl_3): δ = 151.4 (C_q), 149.6 (CH), 140.8 (C_q), 140.5 (2C, C_q), 138.3 (CH), 137.3 (C_q), 128.6 (C_q), 125.7 (2C, CH), 122.9 (2C, C_q), 122.1 (CH), 121.8 (CH), 120.9 (CH), 120.8 (CH), 120.4 (2C, CH), 120.1 (CH), 118.9 (2C, CH), 110.1 (CH), 108.8 (2C, CH), 102.5 (CH), 42.8 (CH_2), 28.7 (CH_2), 27.3 (CH_2), 26.3 (CH_2). HRMS (ESI): m/z Calcd for $\text{C}_{29}\text{H}_{25}\text{N}_3+\text{H}^+$ $[\text{M}+\text{H}]^+$ 416.2121; Found 416.2121. The ^1H and ^{13}C spectra are consistent with those reported in the literature.⁴⁸

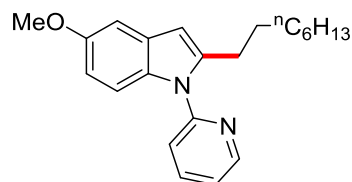


9-(4-(1-(Pyridin-2-yl)-1H-indol-2-yl)ethyl)-9H-carbazole (3aa'): The representative procedure was followed, using substrate **1a** (0.039 g, 0.20 mmol) and 9-(2-chloroethyl)-9H-carbazole (**2a'**; 0.092 g, 0.40 mmol), and the reaction mixture was stirred for 24 h. Purification by column chromatography on neutral alumina (petroleum ether/EtOAc: 20/1) yielded **3aa'** (0.031 g, 40%)

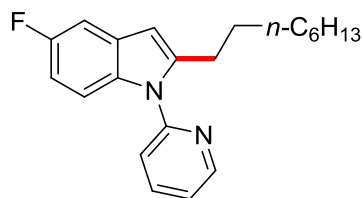
as a light yellow liquid. $^1\text{H-NMR}$ (500 MHz, CDCl_3): δ = 8.59 (d, J = 3.8 Hz, 1H, Ar-H), 8.06 (d, J = 7.6 Hz, 2H, Ar-H), 7.71 (s, 1H, Ar-H), 7.67-7.58 (m, 1H, Ar-H), 7.45-7.34 (m, 2H, Ar-H), 7.31 (d, J = 7.2 Hz, 1H, Ar-H), 7.25-7.14 (m, 7H, Ar-H), 7.09 (d, J = 8.0 Hz, 1H, Ar-H), 6.66 (s, 1H, Ar-H), 4.61 (t, J = 7.6 Hz, 2H, CH_2), 3.46 (t, J = 7.4 Hz, 2H, CH_2). $^{13}\text{C}\{^1\text{H}\}$ -NMR (125 MHz, CDCl_3): δ = 151.1 (C_q), 149.6 (CH), 140.2 (2C, C_q), 138.5 (CH), 138.2 (C_q), 137.3 (C_q), 128.7 (C_q), 125.7 (2C, CH), 123.1 (2C, C_q), 122.3 (CH), 122.0 (CH), 121.1 (CH), 120.7 (CH), 120.4 (CH), 120.4 (2C, CH), 119.1 (2C, CH), 110.3 (CH), 108.6 (2C, CH), 103.9 (CH), 43.9 (CH_2), 27.0 (CH_2). HRMS (ESI): m/z Calcd for $\text{C}_{27}\text{H}_{22}\text{N}_2+\text{H}^+$ $[\text{M}+\text{H}]^+$ 388.1808; Found 388.1810.



2-Octyl-1-(5-methylpyridin-2-yl)-1H-indole (3ba): The representative procedure was followed, using substrate **1b** (0.042 g, 0.20 mmol) and 1-chlorooctane (**2a**; 0.059 g, 0.40 mmol), and the reaction mixture was stirred for 5 h. Purification by column chromatography on neutral alumina (petroleum ether/EtOAc: 50/1) yielded **3ba** (0.055 g, 86%) as a light yellow liquid. $^1\text{H-NMR}$ (400 MHz, CDCl_3): δ = 8.69 (d, J = 4.2 Hz, 1H, Ar-H), 7.98-7.85 (m, 1H, Ar-H), 7.50-7.38 (m, 2H, Ar-H), 7.33 (dd, J = 7.0, 5.2 Hz, 1H, Ar-H), 7.27 (d, J = 8.5 Hz, 1H, Ar-H), 6.99 (d, J = 7.9 Hz, 1H, Ar-H), 6.41 (s, 1H, Ar-H), 2.88 (t, J = 7.6 Hz, 2H, CH_2), 2.49 (s, 3H, CH_3), 1.67-1.53 (m, 2H, CH_2), 1.44-1.20 (m, 10H, CH_2), 0.92 (t, J = 6.7 Hz, 3H, CH_3). $^{13}\text{C}\{^1\text{H}\}$ -NMR (100 MHz, CDCl_3): δ = 151.9 (C_q), 149.7 (CH), 142.0 (C_q), 138.3 (CH), 135.7 (C_q), 129.9 (C_q), 129.1 (C_q), 123.1 (CH), 121.9 (CH), 121.1 (CH), 119.8 (CH), 109.9 (CH), 101.9 (CH), 32.0 (CH_2), 29.5 (2C, CH_2), 29.3 (CH_2), 28.8 (CH_2), 27.7 (CH_2), 22.8 (CH_2), 21.5 (CH_3), 14.3 (CH_3). HRMS (ESI): m/z Calcd for $\text{C}_{22}\text{H}_{28}\text{N}_2+\text{H}^+$ $[\text{M}+\text{H}]^+$ 321.2325; Found 321.2323. The ^1H and ^{13}C spectra are consistent with those reported in the literature.⁴⁸

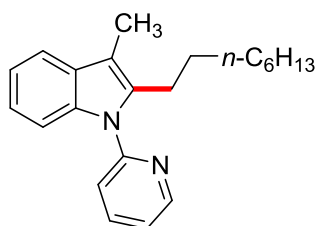


2-Octyl-1-(5-methoxypyridin-2-yl)-1H-indole (3ca): The representative procedure was followed, using substrate **1c** (0.045 g, 0.20 mmol) and 1-chlorooctane (**2a**; 0.059 g, 0.40 mmol), and the reaction mixture was stirred for 5 h. Purification by column chromatography on neutral alumina (petroleum ether/EtOAc: 50/1) yielded **3ca** (0.056 g, 83%) as a light yellow liquid. ^1H NMR (400 MHz, CDCl_3): δ = 8.68 (d, J = 3.7 Hz, 1H, Ar-H), 8.03-7.79 (m, 1H, Ar-H), 7.43 (d, J = 7.9 Hz, 1H, Ar-H), 7.38-7.21 (m, 2H, Ar-H), 7.09 (s, 1H, Ar-H), 6.90-6.73 (m, 1H, Ar-H), 6.41 (s, 1H, Ar-H), 3.88 (s, 3H, OCH_3), 2.86 (t, J = 7.6 Hz, 2H, CH_2), 1.70-1.50 (m, 2H, CH_2), 1.41-1.19 (m, 10H, CH_2), 0.90 (t, J = 6.7 Hz, 3H, CH_3). $^{13}\text{C}\{^1\text{H}\}$ -NMR (100 MHz, CDCl_3): δ = 154.9 (C_q), 151.9 (C_q), 149.7 (CH), 142.5 (C_q), 138.4 (CH), 132.5 (C_q), 129.3 (C_q), 121.9 (CH), 121.0 (CH), 111.1 (CH), 111.0 (CH), 102.3 (CH), 102.1 (CH), 56.0 (OCH_3), 32.0 (CH_2), 29.5 (2C, CH_2), 29.3 (CH_2), 28.8 (CH_2), 27.7 (CH_2), 22.8 (CH_2), 14.2 (CH_3). HRMS (ESI): m/z Calcd for $\text{C}_{22}\text{H}_{28}\text{N}_2\text{O}+\text{H}^+$ $[\text{M}+\text{H}]^+$ 337.2274; Found 337.2270. The ^1H and ^{13}C spectra are consistent with those reported in the literature.⁴⁸

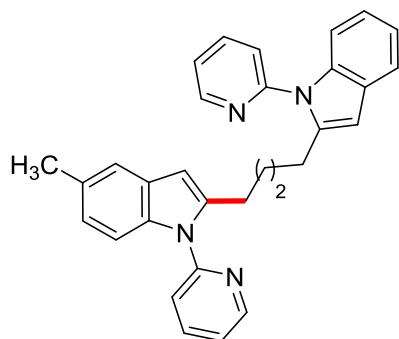


2-Octyl-1-(5-fluoropyridin-2-yl)-1H-indole (3da): The representative procedure was followed, using substrate **1d** (0.042 g, 0.20 mmol) and 1-chlorooctane (**2a**; 0.059 g, 0.40 mmol), and the reaction mixture was stirred for 16 h. Purification by column chromatography on neutral alumina (petroleum ether/EtOAc: 50/1) yielded **3da** (0.045 g, 69%) as a light yellow liquid. ^1H -NMR (400 MHz, CDCl_3): δ = 8.84-8.60 (m, 1H, Ar-H), 8.07-7.81 (m, 1H, Ar-H), 7.54-7.34 (m, 2H, Ar-H), 7.33-7.14 (m, 2H, Ar-H), 7.00-6.78 (m, 1H, Ar-H), 6.43 (s, 1H, Ar-H), 3.05- 2.75 (m, 2H, CH_2), 1.78-1.49 (m, 2H, CH_2), 1.26 (br s, 10H, CH_2), 1.06-0.81 (m, 3H, CH_3). $^{13}\text{C}\{^1\text{H}\}$ -NMR (100 MHz, CDCl_3): δ = 158.6 (d, $^1J_{\text{C-F}}$ = 235.0 Hz, C_q), 151.6 (C_q), 149.9 (CH), 143.6 (C_q), 138.5 (CH), 134.0 (C_q), 129.2 (d, $^3J_{\text{C-F}}$ = 10.0 Hz, C_q), 122.4 (CH), 121.2 (CH), 110.9 (d,

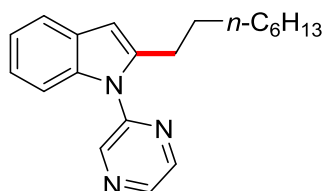
$^3J_{\text{C-F}} = 10.0$ Hz, CH), 109.5 (d, $^2J_{\text{C-F}} = 25.4$ Hz, CH), 105.1 (d, $^2J_{\text{C-F}} = 24.0$ Hz, CH), 102.1 (d, $^4J_{\text{C-F}} = 4.0$ Hz, CH), 32.0 (CH₂), 29.5 (2C, CH₂), 29.3 (CH₂), 28.7 (CH₂), 27.7 (CH₂), 22.8 (CH₂), 14.3 (CH₃). $^{19}\text{F-NMR}$ (377 MHz, CDCl₃): $\delta = -124.2$ (s). HRMS (ESI): m/z Calcd for C₂₁H₂₅FN₂+H⁺ [M+H]⁺ 325.2075; Found 325.2073. The ^1H and ^{13}C spectra are consistent with those reported in the literature.⁴⁸



3-Methyl-2-octyl-1-(pyridin-2-yl)-1H-indole (3ea): The representative procedure was followed, using substrate **1e** (0.042 g, 0.20 mmol) and 1-chlorooctane (**2a**; 0.059 g, 0.40 mmol), and the reaction mixture was stirred for 5 h. Purification by column chromatography on neutral alumina (petroleum ether/EtOAc: 50/1) yielded **3ea** (0.053 g, 83%) as a light yellow liquid. ^1H NMR (400 MHz, CDCl₃): $\delta = 8.67$ (d, $J = 3.7$ Hz, 1H, Ar-H), 7.88 (t, $J = 7.6$ Hz, 1H, Ar-H), 7.58 (d, $J = 7.9$ Hz, 1H, Ar-H), 7.44 (d, $J = 7.9$ Hz, 1H, Ar-H), 7.35 (d, $J = 7.3$ Hz, 1H, Ar-H), 7.33-7.27 (m, 1H, Ar-H), 7.23-7.12 (m, 2H, Ar-H), 2.94 (t, $J = 7.6$ Hz, 2H, CH₂), 2.36 (s, 3H, CH₃), 1.44-1.34 (m, 2H, CH₂), 1.33-1.15 (m, 10H, CH₂), 0.90 (t, $J = 7.0$ Hz, 3H, CH₃). $^{13}\text{C}\{^1\text{H}\}$ -NMR (125 MHz, CDCl₃): $\delta = 152.1$ (C_q), 149.7 (CH), 138.3 (CH), 137.4 (C_q), 136.7 (C_q), 129.6 (C_q), 121.8 (CH), 121.8 (CH), 121.2 (CH), 120.2 (CH), 118.3 (CH), 110.0 (CH), 109.8 (C_q), 32.0 (CH₂), 29.5 (CH₂), 29.3 (2C, CH₂), 29.2 (CH₂), 24.8 (CH₂), 22.8 (CH₂), 14.2 (CH₃), 9.0 (CH₃). HRMS (ESI): m/z Calcd for C₂₂H₂₈N₂+H⁺ [M+H]⁺ 321.2325; Found 321.2323. The ^1H and ^{13}C spectra are consistent with those reported in the literature.⁴⁸

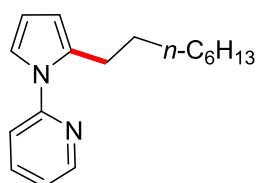


5-Methyl-1-(pyridin-2-yl)-2-(4-(1-(pyridin-2-yl)-1H-indol-2-yl)butyl)-1H-indole (3by): The representative procedure was followed, using 5-methyl-1-(pyridin-2-yl)-1H-indole (**1b**; 0.042 g, 0.20 mmol), 2-(4-chlorobutyl)-1-(pyridin-2-yl)-1H-indole (**2y**, 0.114 g, 0.40 mmol), and the reaction mixture was stirred for 16 h. Purification by column chromatography on neutral alumina (petroleum ether/EtOAc: 10/1) yielded **3by** (0.060 g, 66%) as a light yellow solid. $^1\text{H-NMR}$ (500 MHz, CDCl_3): $\delta = 8.64\text{--}8.49$ (m, 2H, Ar-H), 7.80-7.71 (m, 2H, Ar-H), 7.59-7.50 (m, 1H, Ar-H), 7.37-7.27 (m, 4H, Ar-H), 7.25-7.16 (m, 3H, Ar-H), 7.16-7.08 (m, 2H, Ar-H), 6.94 (d, $J = 8.4$ Hz, 1H, Ar-H), 6.34 (s, 1H, Ar-H), 6.27 (s, 1H, Ar-H), 2.80 (br s, 4H, CH_2), 2.44 (s, 3H, CH_3), 1.48-1.56 (m, 4H, CH_2). $^{13}\text{C}\{^1\text{H}\}\text{-NMR}$ (125 MHz, CDCl_3): $\delta = 151.8$ (C_q), 151.6 (C_q), 149.7 (CH), 149.6 (CH), 141.3 (2C, C_q), 138.3 (2C, CH), 137.4 (C_q), 135.7 (C_q), 129.9 (C_q), 129.0 (C_q), 128.7 (C_q), 123.1 (CH), 122.1 (CH), 121.9 (CH), 121.7 (CH), 121.3 (CH), 121.0 (CH), 120.7 (CH), 120.0 (CH), 119.8 (CH), 110.2 (CH), 109.9 (CH), 102.4 (CH), 102.1 (CH), 28.1 (2C, CH_2), 27.4 (CH_2), 27.3 (CH_2), 21.6 (CH_3). HRMS (ESI): m/z Calcd for $\text{C}_{31}\text{H}_{28}\text{N}_4+\text{H}^+$ $[\text{M}+\text{H}]^+$ 457.2387; Found 457.2388.

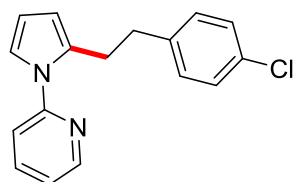


2-Octyl-1-(pyrazin-2-yl)-1H-indole (3fa): The representative procedure was followed, using substrate 1-(pyrazin-2-yl)-1H-indole (**1f**; 0.039 g, 0.20 mmol), 1-chlorooctane (**2a**; 0.059 g, 0.40 mmol) and the reaction mixture was stirred for 5 h. Purification by column chromatography on neutral alumina (petroleum ether/EtOAc: 50/1) yielded **3fa** (0.018 g, 29%) as a brown liquid. $^1\text{H-NMR}$ (400 MHz, CDCl_3): $\delta = 8.79$ (s, 1H, Ar-H), 8.65-8.60 (m, 1H, Ar-H), 8.56 (d, $J = 3.0$ Hz,

¹H, Ar-H), 7.61-7.54 (m, 1H, Ar-H), 7.41-7.34 (m, 1H, Ar-H), 7.19-7.12 (m, 2H, Ar-H), 6.49 (s, 1H, Ar-H), 2.82 (t, $J = 7.6$ Hz, 2H, CH₂), 1.57 (pent, $J = 7.6$ Hz, 2H, CH₂), 1.29-1.22 (m, 10H, CH₂), 0.86 (t, $J = 6.9$ Hz, 3H, CH₃). ¹³C{¹H}-NMR (100 MHz, CDCl₃): $\delta = 148.4$ (C_q), 143.7 (CH), 142.6 (CH), 142.2 (CH), 141.7 (C_q), 137.1 (C_q), 129.0 (C_q), 122.2 (CH), 121.4 (CH), 120.2 (CH), 109.9 (CH), 103.5 (CH), 31.8 (CH₂), 29.7 (CH₂), 29.3 (CH₂), 29.2 (CH₂), 28.7 (CH₂), 27.5 (CH₂), 22.7 (CH₂), 14.1 (CH₃). HRMS (ESI): m/z Calcd for C₂₀H₂₅N₃+H⁺ [M+H]⁺ 308.2121; Found 308.2119.

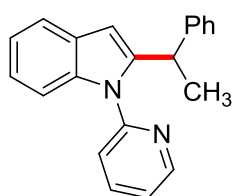


2-(2-Octyl-1H-pyrrol-1-yl)pyridine (3ga): The representative procedure was followed, using substrate **1g** (0.029 g, 0.20 mmol) and 1-chlorooctane (**2a**; 0.059 g, 0.40 mmol), and the reaction mixture was stirred for 16 h. Purification by column chromatography on neutral alumina (petroleum ether/EtOAc: 50/1) yielded **3ga** (0.033 g, 64%) as a light yellow liquid. ¹H-NMR (500 MHz, CDCl₃) $\delta = 8.52$ (d, $J = 3.4$ Hz, 1H, Ar-H), 7.78 (t, $J = 6.9$ Hz, 1H, Ar-H), 7.29 (d, $J = 8.0$ Hz, 1H, Ar-H), 7.20 (dd, $J = 6.9, 5.3$ Hz, 1H, Ar-H), 7.01 (br s, 1H, Ar-H), 6.24 (t, $J = 2.9$ Hz, 1H, Ar-H), 6.09 (br s, 1H, Ar-H), 2.81 (t, $J = 7.6$ Hz, 2H, CH₂), 1.62-1.49 (m, 2H, CH₂), 1.30-1.22 (m, 10H, CH₂), 0.87 (t, $J = 6.9$ Hz, 3H, CH₃). ¹³C{¹H}-NMR (125 MHz, CDCl₃): $\delta = 153.2$ (C_q), 149.0 (CH), 138.3 (CH), 134.6 (C_q), 121.2 (CH), 120.6 (CH), 117.8 (CH), 109.1 (CH), 108.8 (CH), 32.0 (CH₂), 29.6 (CH₂), 29.5 (CH₂), 29.4 (2C, CH₂), 27.7 (CH₂), 22.8 (CH₂), 14.3 (CH₃). HRMS (ESI): m/z Calcd for C₁₇H₂₄N₂+H⁺ [M+H]⁺ 257.2012; Found 257.2012.

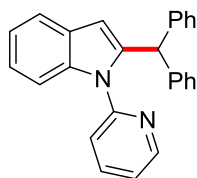


2-(2-(4-Chlorophenethyl)-1H-pyrrol-1-yl)pyridine (3gm): The representative procedure was followed, using substrate **1g** (0.029 g, 0.20 mmol), 1-chloro-4-(2-chloroethyl)benzene (**2m**; 0.070 g, 0.40 mmol) and the reaction mixture was stirred for 24 h. Purification by column

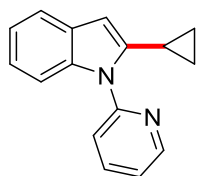
chromatography on neutral alumina (petroleum ether/EtOAc: 50/1) yielded **3gm** (0.019 g, 33%) as a brown liquid. $^1\text{H-NMR}$ (500 MHz, CDCl_3): δ = 8.54 (d, J = 4.2 Hz, 1H, Ar-H), 7.79 (t, J = 7.4 Hz, 1H, Ar-H), 7.30-7.25 (m, 1H, Ar-H), 7.23-7.19 (m, 3H, Ar-H), 7.08-7.03 (m, 2H, Ar-H), 7.01 (s, 1H, Ar-H), 6.26 (s, 1H, Ar-H), 6.13 (s, 1H, Ar-H), 3.17 (t, J = 7.9 Hz, 2H, CH_2), 2.86 (t, J = 7.4 Hz, 2H, CH_2). $^{13}\text{C}\{^1\text{H}\}$ -NMR (125 MHz, CDCl_3): δ = 152.9 (C_q), 148.7 (CH), 140.3 (C_q), 138.3 (CH), 133.2 (C_q), 131.5 (C_q), 129.7 (2C, CH), 128.3 (2C, CH), 121.1 (CH), 120.5 (CH), 117.3 (CH), 109.4 (CH), 109.2 (CH), 35.4 (CH_2), 29.6 (CH_2). HRMS (ESI): m/z Calcd for $\text{C}_{17}\text{H}_{15}\text{ClN}_2+\text{H}^+$ $[\text{M}+\text{H}]^+$ 283.0997; Found 283.0996.



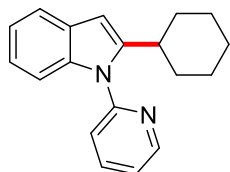
2-(1-Phenylethyl)-1-(pyridin-2-yl)-1H-indole (5aa): The representative procedure was followed, using substrate **1a** (0.039 g, 0.20 mmol), (1-bromoethyl)benzene (**4a**; 0.074 g, 0.40 mmol) and the reaction mixture was stirred for 16 h. Purification by column chromatography on neutral alumina (petroleum ether/EtOAc: 50/1) yielded **5aa** (0.025 g, 42%) as a light yellow liquid. $^1\text{H-NMR}$ (400 MHz, CDCl_3): δ = 8.58 (br s, 1H, Ar-H), 8.17 (d, J = 7.9 Hz, 1H, Ar-H), 7.89-7.77 (m, 1H, Ar-H), 7.63 (s, 1H, Ar-H), 7.52 (d, J = 8.5 Hz, 1H), 7.44-7.23 (m, 6H, Ar-H), 7.22-7.03 (m, 3H, Ar-H), 4.41 (q, J = 7.3 Hz, 1H, CH), 1.77 (d, J = 7.3 Hz, 3H, CH_3). $^{13}\text{C}\{^1\text{H}\}$ -NMR (100 MHz, CDCl_3): δ = 152.7 (C_q), 149.2 (CH) 146.4 (C_q), 138.5 (CH) 135.9 (C_q), 129.9 (C_q), 128.6 (2C, CH), 127.7 (2C, CH), 126.3 (CH), 124.2 (C_q), 123.3 (CH), 123.1 (CH), 121.0 (CH), 120.2 (CH), 119.9 (CH), 114.6 (CH), 113.0 (CH), 37.1 (CH), 22.5 (CH_3). HRMS (ESI): m/z Calcd for $\text{C}_{21}\text{H}_{18}\text{N}_2+\text{H}^+$ $[\text{M}+\text{H}]^+$ 299.1543; Found 299.1541. The ^1H and ^{13}C spectra are consistent with those reported in the literature.⁴⁸



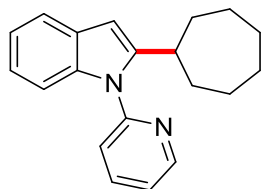
2-Benzhydryl-1-(pyridin-2-yl)-1H-indole (5ab): The representative procedure was followed using, substrate **1a** (0.039 g, 0.20 mmol), (bromomethylene)dibenzene (**4b**; 0.099 g, 0.40 mmol) and the reaction mixture was stirred for 16 h. Purification by column chromatography on neutral alumina (petroleum ether/EtOAc: 50/1) yielded **5ab** (0.052 g, 72%) as a pale yellow solid. $^1\text{H-NMR}$ (500 MHz, CDCl_3): δ = 8.65 (d, J = 3.8 Hz, 1H, Ar-H), 8.37 (d, J = 8.4 Hz, 1H, Ar-H), 7.91-7.79 (m, 1H, Ar-H), 7.53-7.34 (m, 14H, Ar-H), 7.23 (t, J = 6.9 Hz, 2H, Ar-H), 5.86 (s, 1H, CH). $^{13}\text{C}\{^1\text{H}\}$ -NMR (125 MHz, CDCl_3): δ = 152.6 (C_q), 149.0 (CH), 143.5 (2C, C_q), 138.4 (CH), 136.0 (C_q), 129.80 (C_q), 129.2 (4C, CH), 128.6 (4C, CH), 126.6 (2C, CH), 125.7 (CH), 123.5 (CH), 122.8 (C_q), 121.2 (CH), 120.4 (CH), 119.9 (CH), 114.6 (CH), 113.3 (CH), 48.9 (CH). HRMS (ESI): m/z Calcd for $\text{C}_{26}\text{H}_{20}\text{N}_2+\text{H}^+$ $[\text{M}+\text{H}]^+$ 361.1699; Found 361.1698. The ^1H and ^{13}C spectra are consistent with those reported in the literature.⁴⁸



2-Cyclopropyl-1-(pyridin-2-yl)-1H-indole (5ac): The representative procedure was followed, using substrate **1a** (0.039 g, 0.20 mmol) and bromocyclopropane (**4c**, 0.048 g, 0.40 mmol) and the reaction mixture was stirred for 16 h. Column chromatography on neutral alumina (petroleum ether/EtOAc: 50/1) afforded the **5ac** (0.035 g, 75%). $^1\text{H-NMR}$ (500 MHz, CDCl_3): δ = 8.69 (d, J = 5.0 Hz, 1H, Ar-H), 7.93-7.82 (m, 1H, Ar-H), 7.60-7.51 (m, 2H, Ar-H), 7.46 (dd, J = 6.3, 2.5 Hz, 1H, Ar-H), 7.32 (dd, J = 7.1, 5.1 Hz, 1H, Ar-H), 7.19-7.08 (m, 2H, Ar-H), 6.29 (s, 1H, Ar-H), 2.03 (br s, 1H, CH), 0.95-0.86 (m, 2H, CH_2), 0.71-0.83 (m, 2H, CH_2). $^{13}\text{C}\{^1\text{H}\}$ -NMR (125 MHz, CDCl_3): δ = 151.9 (C_q), 149.6 (CH), 143.4 (C_q), 138.2 (CH), 137.5 (C_q), 128.6 (C_q), 121.9 (2C, CH), 121.2 (CH), 120.9 (CH), 120.0 (CH), 110.7 (CH), 100.0 (CH), 8.8 (CH), 8.4 (2C, CH_2). HRMS (ESI): m/z Calcd for $\text{C}_{16}\text{H}_{14}\text{N}_2+\text{H}^+$ $[\text{M}+\text{H}]^+$ 235.1230; Found 235.1232. The ^1H and ^{13}C spectra are consistent with those reported in the literature.⁴⁸

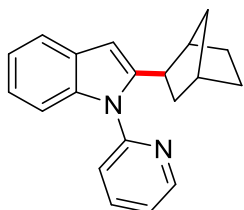


2-Cyclohexyl-1-(pyridin-2-yl)-1H-indole (5ad): The representative procedure was followed, using substrate **1a** (0.039 g, 0.20 mmol) and bromocyclohexane (**4d**; 0.065 g, 0.40 mmol), and the reaction mixture was stirred for 16 h. Purification by column chromatography on neutral alumina (petroleum ether/EtOAc: 50/1) yielded **5ad** (0.036 g, 65%) as a light yellow liquid. $^1\text{H-NMR}$ (500 MHz, CDCl_3): δ = 8.76-8.62 (m, 1H, Ar-H), 7.90 (td, J = 7.7, 1.7 Hz, 1H, Ar-H), 7.60 (dd, J = 5.9, 2.9 Hz, 1H, Ar-H), 7.45 (d, J = 7.6 Hz, 1H, Ar-H), 7.34 (dd, J = 7.1, 5.1 Hz, 1H, Ar-H), 7.32-7.23 (m, 1H, Ar-H), 7.18-7.07 (m, 2H, Ar-H), 6.46 (s, 1H, Ar-H), 3.07-2.96 (m, 1H, CH), 1.92 (d, J = 12.6 Hz, 2H, CH_2), 1.75 (dd, J = 8.6, 3.6 Hz, 2H, CH_2), 1.48-1.36 (m, 2H, CH_2), 1.31-1.17 (m, 4H, CH_2). $^{13}\text{C}\{^1\text{H}\}$ -NMR (125 MHz, CDCl_3): δ = 151.9 (C_q), 149.8 (CH), 147.4 (C_q), 138.5 (CH), 137.5 (C_q), 128.7 (C_q), 122.3 (CH), 121.7 (CH), 121.6 (CH), 120.6 (CH), 120.1 (CH), 110.1 (CH), 100.0 (CH), 35.8 (CH), 33.4 (2C, CH_2), 26.6 (2C, CH_2), 26.3 (CH_2). HRMS (ESI): m/z Calcd for $\text{C}_{19}\text{H}_{20}\text{N}_2+\text{H}^+$ $[\text{M}+\text{H}]^+$ 277.1699; Found 277.1700. The ^1H and ^{13}C spectra are consistent with those reported in the literature.⁴⁸



2-Cycloheptyl-1-(pyridin-2-yl)-1H-indole (5ae): The representative procedure was followed, using substrate **1a** (0.039 g, 0.20 mmol), bromocycloheptane (**4e**; 0.071 g, 0.40 mmol) and the reaction mixture was stirred for 16 h. Purification by column chromatography on neutral alumina (petroleum ether/EtOAc: 50/1) yielded **5ae** (0.030 g, 52%) as a light yellow liquid. $^1\text{H-NMR}$ (400 MHz, CDCl_3): δ = 8.69 (d, J = 3.7 Hz, 1H, Ar-H), 7.91 (t, J = 7.0 Hz, 1H, Ar-H), 7.63-7.50 (m, 1H, Ar-H), 7.44 (d, J = 7.9 Hz, 1H, Ar-H), 7.40-7.32 (m, 1H, Ar-H), 7.31-7.20 (m, 1H, Ar-H), 7.19-7.04 (m, 2H, Ar-H), 6.47 (s, 1H, Ar-H), 3.33-3.09 (m, 1H, CH), 1.97 (dt, J = 6.9, 3.6 Hz, 2H, CH_2), 1.80-1.65 (m, 4H, CH_2), 1.57 (br s, 4H, CH_2), 1.42-1.31 (m, 2H, CH_2). $^{13}\text{C}\{^1\text{H}\}$ -NMR (100 MHz, CDCl_3): δ = 151.9 (C_q), 149.9 (CH), 148.5 (C_q), 138.5 (CH) 137.5

(C_q), 128.7 (C_q), 122.3 (CH), 121.9 (CH), 121.6 (CH), 120.6 (CH), 120.1 (CH), 110.1 (CH), 100.0 (CH), 37.0 (CH), 35.0 (2C, CH₂), 28.4 (2C, CH₂), 26.8 (2C, CH₂). HRMS (ESI): *m/z* Calcd for C₂₀H₂₂N₂+H⁺ [M+H]⁺ 291.1856; Found 291.1855. The ¹H and ¹³C spectra are consistent with those reported in the literature.⁴⁸

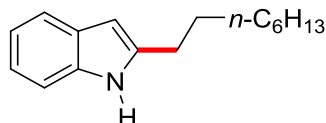


2-((1R,2R,4S)-Bicyclo[2.2.1]heptan-2-yl)-1-(pyridin-2-yl)-1H-indole (5af): The representative procedure was followed, using substrate **1a** (0.039 g, 0.20 mmol), 2-bromobicyclo[2.2.1]heptane (**4f**; 0.070 g, 0.40 mmol) and the reaction mixture was stirred for 16 h. Purification by column chromatography on neutral alumina (petroleum ether/EtOAc: 50/1) yielded **5af** (0.02 g, 35%) as a pale yellow solid. ¹H-NMR (500 MHz, CDCl₃): δ = 8.73-8.64 (m, 1H, Ar-H), 7.90 (td, *J* = 7.7, 1.7 Hz, 1H, Ar-H), 7.61-7.55 (m, 1H, Ar-H), 7.44 (d, *J* = 8.0 Hz, 1H, Ar-H), 7.34 (dd, *J* = 7.2, 5.3 Hz, 1H, Ar-H), 7.27-7.22 (m, 1H, Ar-H), 7.15-7.07 (m, 2H, Ar-H), 6.43 (s, 1H, Ar-H), 3.12 (dd, *J* = 8.4, 5.7 Hz, 1H, CH), 2.33 (br s, 1H, CH), 2.28 (br s, 1H, CH), 1.67-1.56 (m, 2H, CH₂), 1.55-1.38 (m, 3H, CH₂), 1.21-1.10 (m, 3H, CH₂). ¹³C{¹H}-NMR (125 MHz, CDCl₃): δ = 152.0 (C_q), 149.8 (CH), 146.9 (C_q), 138.4 (CH), 137.8 (C_q), 128.6 (C_q), 122.3 (CH), 121.9 (CH), 121.7 (CH), 120.6 (CH), 120.1 (CH), 110.1 (CH), 100.4 (CH), 42.3 (CH) 39.8 (CH) 38.3 (CH₂) 36.8 (CH) 36.4 (CH₂), 29.9 (CH₂), 28.9 (CH₂). HRMS (ESI): *m/z* Calcd for C₂₀H₂₀N₂+H⁺ [M+H]⁺ 289.1699; Found 289.1700.

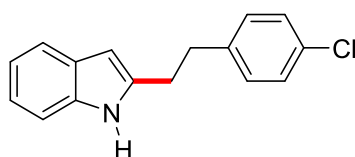
3.4.3 Procedure for Removal of Directing Group

Representative Procedure: Synthesis of 2-Octyl-1H-indole (6aa): To an oven dried Schlenk tube, **3aa** (0.035 g, 0.11 mmol) was introduced and CH₂Cl₂ (5.0 mL) was added into it. Methyl trifluoromethanesulfonate, MeOTf (0.036 g, 0.22 mmol) was added drop wise *via* a syringe to the reaction mixture at 0 °C and the resultant reaction mixture was stirred at room temperature for 16 h. The volatiles were removed under vacuum and the residue was redissolved in MeOH (2.0 mL). To the resultant mixture, NaOH (2M aq, 2.0 mL) solution was added and the

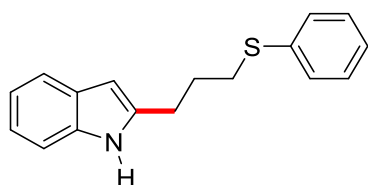
reaction mixture was stirred at 60 °C for 12 h. At ambient temperature, the volatiles were evaporated under reduced pressure, and the resulting residue was extracted with EtOAc (15 mL x 3). The combined organic extract was washed with brine, dried over Na₂SO₄ and the volatiles were evaporated in *vacuo*. The remaining residue was purified by column chromatography on neutral alumina (petroleum ether/EtOAc: 50/1) to yield **6aa** (0.022 g, 87%) as a light yellow liquid.



2-Octyl-1H-indole (6aa): ¹H-NMR (400 MHz, CDCl₃): δ = 7.85 (br s, 1H, NH), 7.53 (d, *J* = 7.3 Hz, 1H, Ar-H), 7.30 (d, *J* = 7.9 Hz, 1H, Ar-H), 7.08 (d, *J* = 7.9 Hz, 1H, Ar-H), 7.11 (d, *J* = 8.5 Hz, 1H, Ar-H), 6.24 (s, 1H, Ar-H), 2.75 (t, *J* = 7.6 Hz, 2H, CH₂), 1.91-1.63 (m, 2H, CH₂), 1.28 (br s, 10H, CH₂), 0.89 (t, *J* = 6.4 Hz, 3H, CH₃). ¹³C{¹H}-NMR (100 MHz, CDCl₃): δ = 140.2 (C_q), 136.0 (C_q), 129.1 (C_q), 121.1 (CH), 119.9 (CH), 119.7 (CH), 110.4 (CH), 99.6 (CH), 32.0 (CH₂), 29.9 (CH₂), 29.6 (CH₂), 29.5 (CH₂), 29.4 (CH₂), 28.5 (CH₂), 22.8 (CH₂), 14.3 (CH₃). HRMS (ESI): *m/z* Calcd for C₁₆H₂₃N+H⁺ [M+H]⁺ 230.1903 Found 230.1905. The ¹H and ¹³C spectra are consistent with those reported in the literature.⁴⁸



2-(4-Chlorophenethyl)-1H-indole (6am): The representative procedure was followed, using substrate **3am** (0.035 g, 0.105 mmol) and methyl trifluoromethanesulfonate, MeOTf (0.069 g, 0.42 mmol). Purification by column chromatography on neutral alumina (petroleum ether/EtOAc: 50/1) yielded **6am** (0.020 g, 74%) as a light yellow solid. ¹H-NMR (400 MHz, CDCl₃): δ = 7.95 (br s, 1H, NH), 7.72 (d, *J* = 7.9 Hz, 1H, Ar-H), 7.54-7.38 (m, 3H, Ar-H), 7.38-7.22 (m, 4H, Ar-H), 6.44 (s, 1H, Ar-H), 3.20-2.93 (m, 4H, CH₂). ¹³C{¹H}-NMR (100 MHz, CDCl₃): δ = 139.7 (C_q), 138.6 (C_q), 136.0 (C_q), 132.2 (C_q), 130.0 (2C, CH), 128.8 (2C, CH), 128.7 (C_q), 121.4 (CH), 120.1 (CH), 119.9 (CH), 110.5 (CH), 100.2 (CH), 35.2 (CH₂), 30.2 (CH₂). HRMS (ESI): *m/z* Calcd for C₁₆H₁₄NCl+H⁺ [M+H]⁺ 256.0888; Found 256.0891.



2-(3-(Phenylthio)propyl)-1H-indole (6ao): The representative procedure was followed, using substrate **3ao** (0.04 g, 0.116 mmol) and methyl trifluoromethanesulfonate, MeOTf (0.076 g, 0.464 mmol). Purification by column chromatography on neutral alumina (petroleum ether/EtOAc: 50/1) yielded **6ao** (0.020 g, 64%) as a brown solid. $^1\text{H-NMR}$ (400 MHz, CDCl_3): δ = 7.88 (br s, 1H, NH), 7.55 (d, J = 7.9 Hz, 1H, Ar-H), 7.40-7.35 (m, 2H, Ar-H), 7.34-7.29 (m, 3H, Ar-H), 7.26-7.20 (m, 1H, Ar-H), 7.19-7.08 (m, 2H, Ar-H), 6.28 (s, 1H, Ar-H), 3.02 (t, J = 7.3 Hz, 2H, CH_2), 2.95 (t, J = 7.3 Hz, 2H, CH_2), 2.09 (app. pent, J = 7.3 Hz, 2H, CH_2). $^{13}\text{C}\{^1\text{H}\}$ -NMR (100 MHz, CDCl_3): δ = 138.3 (C_q), 136.1 (C_q), 135.9 (C_q), 129.4 (2C, CH), 128.9 (2C, CH), 128.8 (C_q), 126.1 (CH), 121.2 (CH), 119.8 (CH), 119.7 (CH), 110.3 (CH), 110.0 (CH), 32.9 (CH_2), 28.5 (CH_2), 26.8 (CH_2). HRMS (ESI): m/z Calcd for $\text{C}_{17}\text{H}_{17}\text{NS}+\text{H}^+$ $[\text{M}+\text{H}]^+$ 268.1154; Found 268.1155.

3.4.4 Procedure for NMR Tube Experiment

To a J-Young NMR tube, the ligand bpy (0.006 g, 0.04 mmol) was introduced, 4-MeO-C₆H₅-Me (0.005 mL, 0.04 mmol, internal standard) and toluene- d^8 (0.5 mL) was added into it. The ^1H NMR analysis shows the expected signals for the bpy compound. To the NMR tube, $(\text{thf})_2\text{NiBr}_2$ (0.015 g, 0.04 mmol) and LiHMDS (0.027 g, 0.16 mmol) were added and the reaction mixture was heated at 60 °C for 15 min. The ^1H NMR analysis shows a broad signal at 10.69 ppm for all the bpy protons (coordinated to Ni) and a signal at 0.08 ppm for the unreacted LiHMDS. In addition, de-coordinated THF protons are visible. This suggests the probable formation of a paramagnetic bpy-coordinated nickel species during the reaction. To the same NMR tube, indole **1a** (0.008 g, 0.04 mmol) and 1-chlorooctane (**2a**; 0.006 g, 0.04 mmol) were added and the reaction was further heated at 60 °C for 15 min in a preheated oil bath. The ^1H NMR analysis of the reaction mixture shows the same broad signal at 10.69 ppm in addition to the peaks correspond to the product **3aa**. This strongly suggests the existence of a paramagnetic (bpy)Ni species during the reaction.

3.4.5 External Additive Experiments

Procedure: The representative procedure of the alkylation reaction was followed using indole **1a** (0.039 g, 0.20 mmol), 1-chlorooctane (0.059 g, 0.40 mmol), (thf)₂NiBr₂ (0.0037 g, 0.01 mmol, 5.0 mol %), bpy (0.0016 g, 0.01 mmol, 5.0 mol %), LiHMDS (0.067 g, 0.40 mmol), TEMPO (0.062 g, 0.40 mmol) or galvinoxyl (0.169 g, 0.40 mmol) and the reaction mixture was stirred for 5 h. The GC analysis of the crude reaction mixture does not show the formation of product **3aa**. In addition, the coupled product of TEMPO and galvinoxyl with *n*-octyl was not detected in the GCMS.

3.4.6 Radical Clock Experiment

Procedure: The representative procedure of the alkylation reaction was followed, using indole **1a** (0.039 g, 0.20 mmol), 6-chloro-1-hexene (**2u**; 0.047 g, 0.40 mmol) and the reaction mixture was stirred for 16 h. Purification by column chromatography on neutral alumina (petroleum ether/EtOAc 50/1) yielded **3au** (0.043 g, 78%) and direct coupled product 2-(hex-5-en-1-yl)-1-(pyridin-2-yl)-1*H*-indole (0.005 g, 9% (GC yield)).

3.4.7 Procedure for One Pot Double Alkylation

Synthesis of 1,4-Bis(1-(pyridin-2-yl)-1*H*-indol-2-yl)butane (3ay): To a screw-cap tube (5 mL) equipped with a magnetic stir bar were introduced 1-bromo-4-chlorobutane (**2h**, 0.035 g, 0.20 mmol), 1-pyridin-2-yl-1*H*-indole (**1a**, 0.156 g, 0.80 mmol), (thf)₂NiBr₂ (0.0073 g, 0.02 mmol), bpy (0.003 g, 0.02 mmol), LiHMDS (0.134 g, 0.80 mmol) inside the glove box. To the above mixture in the tube was added toluene (2.0 mL), and the resultant reaction mixture was stirred at 60 °C in a preheated oil bath for 16 h. At ambient temperature, the reaction mixture was quenched with distilled H₂O (10 mL) and then neutralized with 2N HCl (2.0 mL). The crude product was then extracted with EtOAc (20 mL x 3). The combined organic extract was dried over Na₂SO₄, and the volatiles were evaporated *in vacuo*. The remaining residue was purified by column chromatography on basic alumina (petroleum ether/EtOAc 10/1) to yield **3ay** (0.058 g, 66%) as a light yellow solid.

Synthesis of 5-Methyl-1-(pyridin-2-yl)-2-(4-(1-(pyridin-2-yl)-1*H*-indol-2-yl)butyl)-1*H*-indole (3by): To a screw-cap tube (5 mL) equipped with a magnetic stir bar were introduced 1-pyridin-2-yl-1*H*-indole (**1a**, 0.039 g, 0.20 mmol), 1-bromo-4-chlorobutane (**2h**, 0.045 g, 0.26

mmol), (thf)NiBr₂ (0.0073 g, 0.02 mmol), bpy (0.003 g, 0.02 mmol), LiHMDS (0.067 g, 0.40 mmol) inside the glove box. To the above mixture in the tube was added toluene (2.0 mL), and the resultant reaction mixture was stirred at 60 °C in a preheated oil bath for 16 h. At ambient temperature, the reaction tube was transferred to the glove box and 5-methyl-1-(pyridin-2-yl)-1*H*-indole (**1b**, 0.083 g, 0.40 mmol) and LiHMDS (0.067 g, 0.40 mmol) were added into it. The resultant reaction mixture was again stirred at 60 °C for 16 h. At ambient temperature, the reaction mixture was quenched with distilled H₂O (10 mL) and then neutralized with 2N HCl (2.0 mL). The crude product was then extracted with EtOAc (20 mL x 3). The combined organic extract was dried over Na₂SO₄, and the volatiles were evaporated *in vacuo*. The remaining residue was purified by column chromatography on basic alumina (petroleum ether/EtOAc 10/1) to yield **3by** (0.059 g, 65%) as a light yellow solid.

3.4.8 Procedure for Stoichiometric Reaction

Procedure (without addition of 1-chlorooctane). To a Teflon-screw capped tube equipped with magnetic stir bar were introduced (thf)₂NiBr₂ (0.037 g, 0.10 mmol), bpy (0.016 g, 0.10 mmol), LiHMDS (0.033 g, 0.20 mmol), indole **1a** (0.039 g, 0.20 mmol) and *n*-hexadecane (0.025 mL, 0.085 mmol, internal standard), and toluene (1.0 mL) was added. The reaction mixture was then stirred at 60 °C for 4 h in a pre-heated oil bath. At ambient temperature, the reaction was quenched with H₂O (5 mL) and an aliquot was subjected to GC analysis. The GC spectrum shows the presence of dimer of indole (15%) and indole **1a** (57%).

Procedure (without addition of indole). To a Teflon-screw capped tube equipped with magnetic stir bar were introduced (thf)₂NiBr₂ (0.037 g, 0.10 mmol), bpy (0.016 g, 0.10 mmol), LiHMDS (0.033 g, 0.20 mmol), 1-chlorooctane (0.030 g, 0.20 mmol) and *n*-hexadecane (0.025 mL, 0.085 mmol, internal standard), and toluene (1.0 mL). The reaction mixture was then stirred at 60 °C for 4 in a pre-heated oil bath. At ambient temperature, the reaction was quenched with H₂O (5 mL) and an aliquot was subjected to GC analysis. The GC spectrum shows the presence of 1-chlorooctane (97%), and no other products (1-octene or *n*-octane) from this reaction were observed.

3.4.9 Kinetics Experiments

3.4.9.1 Reaction Profile for Indole Alkylation

Representative Procedure (*Using in-situ generated catalyst*): To a Teflon-screw capped tube equipped with magnetic stir bar were introduced $(\text{thf})_2\text{NiBr}_2$ (0.0037 g, 0.01 mmol, 0.01 M), bpy (0.0016 g, 0.01 mmol), LiHMDS (0.067 g, 0.40 mmol), indole **1a** (0.039 g, 0.20 mmol, 0.2 M), 1-chlorooctane (0.059 g, 0.40 mmol, 0.4 M) and *n*-hexadecane (0.025 mL, 0.085 mmol, 0.085 M, internal standard), and toluene (0.87 mL) was added to make the total volume to 1.0 mL. The reaction mixture was then stirred at 60 °C in a pre-heated oil bath. At regular intervals (10, 20, 30, 40, 50, 60, 90, 120, 180, 240, 300 min) the reaction vessel was cooled to ambient temperature and an aliquot of sample was withdrawn to the GC vial. The sample was diluted with acetone and subjected to GC analysis. The concentration of the product **3aa** obtained in each sample was determined with respect to the internal standard *n*-hexadecane. The data of the concentration of the product *vs* time (min) plot was drawn with Origin Pro 8. The data's were taken from the average of two independent experiments.

Procedure for Kinetic Experiment (*Using isolated complex*): Representative procedure of kinetic experiment (Sec 12.1.1) was followed using $(\text{bpy})\text{NiBr}_2$ (0.0037 g, 0.01 mmol, 0.01 M), LiHMDS (0.067 g, 0.40 mmol), indole **1a** (0.039 g, 0.20 mmol, 0.2 M) and 1-chlorooctane (0.059 g, 0.40 mmol, 0.4 M) and *n*-hexadecane (0.025 mL, 0.085 mmol, 0.085 M, internal standard). An aliquot of sample was withdrawn to the GC vial at regular intervals (10, 20, 30, 40, 50, 60, 90, 120 min, etc.). The data of the concentration of the product *vs* time (min) plot was drawn and fitted linear with Origin Pro 8, and the rate was determined by the initial rate method (up to 360 minutes). The slope of the linear fitting represents the reaction rate. These data were taken from the average of two independent experiments.

3.4.9.2 Kinetics for Electronic Effect Study

Procedure for Reaction Rates with Different Indole Derivatives: Representative procedure of the kinetic experiment was followed using $(\text{thf})_2\text{NiBr}_2$ (0.0037 g, 0.01 mmol, 0.01 M), bpy (0.0016 g, 0.01 mmol), LiHMDS (0.067 g, 0.40 mmol), substrate 5-methyl-1-(pyridin-2-yl)-1*H*-indole (**1b**; 0.042 g, 0.20 mmol, 0.2 M) or 5-fluoro-1-(pyridin-2-yl)-1*H*-indole (**1d**; 0.042 g, 0.20 mmol, 0.2 M), 1-chlorooctane (0.059 g, 0.40 mmol, 0.4 M) and *n*-hexadecane (0.025

mL, 0.085 mmol, 0.085 M, internal standard), and toluene (0.87 mL). The concentration of the product **3ba** (or **3da**) obtained in each sample was determined with respect to the internal standard *n*-hexadecane. The data were collected till 120 min. The data of the concentration of the product *vs* time (min) plot was drawn and fitted linear with Origin Pro 8, and the rate was determined by the initial rate method (up to 120 minutes). The slope of the linear fitting represents the reaction rate. These data were taken from the average of three independent experiments.

3.4.9.3 Procedure for the Reaction Rates with Different Octyl Halides: Representative procedure of kinetic experiment (Sec 12.1.1) was followed using (thf)₂NiBr₂ (0.0037 g, 0.01 mmol, 0.01 M), bpy (0.0016 g, 0.01 mmol), LiHMDS (0.067 g, 0.40 mmol), substrate **1a** (0.039 g, 0.20 mmol, 0.2 M) 1-bromooctane (0.077 g, 0.40 mmol, 0.4 M) or 1-iodooctane (0.096 g, 0.40 mmol, 0.4 M) and *n*-hexadecane (0.025 mL, 0.085 mmol, 0.085 M, internal standard), and toluene (0.87 mL). The concentration of the product **3aa** obtained in each sample was determined with respect to the internal standard *n*-hexadecane. The data were collected till 120 min. The data of the concentration of the product *vs* time (min) plot was drawn and fitted linear with Origin Pro 8, and the rate was determined by the initial rate method (up to 120 minutes). The slope of the linear fitting represents the reaction rate. These data were taken from the average of three independent experiments.

3.4.10 Deuterium Labeling Experiments

3.4.10.1 Procedure for Kinetic Isotope Effect (KIE) Study: Representative procedure of kinetic experiment (Sec 12.1.1) was followed using (thf)₂NiBr₂ (0.0037 g, 0.01 mmol, 0.01 M), bpy (0.0016 g, 0.01 mmol), LiHMDS (0.067 g, 0.40 mmol), indole **1a** (0.039 g, 0.20 mmol, 0.2 M) or [2-D]-**1a** (0.039 g, 0.20 mmol, 0.2 M), and 1-chlorooctane (0.059 g, 0.40 mmol, 0.4 M), and *n*-hexadecane (0.025 mL, 0.085 mmol, 0.085 M, internal standard), and toluene (0.87 mL). The concentration of the product **3aa** obtained in each sample was determined with respect to the internal standard *n*-hexadecane. The data of the concentration of the product *vs* time (min) plot was drawn and fitted linear with Origin Pro 8, and the rate was determined by initial rate method (up to 120 minutes). The slope of the linear fitting represents the reaction rate.

3.4.10.2 Procedure for H/D Scrambling Experiment (Intermolecular): To a screw-capped tube equipped with magnetic stir bar were introduced 1-(pyridine-2-yl)-1*H*-indole-2-*d* ([2-D]-**1a**; 0.019 g, 0.10 mmol), 5-methoxy-1-(pyridine-2-yl)-1*H*-indole (**1c**; 0.022 g, 0.10 mmol), 1-chlorooctane (**2a**; 0.059 g, 0.40 mmol), (thf)₂NiBr₂ (0.0037 g, 0.01 mmol, 0.01 M), bpy (0.0016 g, 0.01 mmol), LiHMDS (0.067 g, 0.40 mmol) inside the glove-box. To the above mixture toluene (1.0 mL) was added and the resultant reaction mixture was stirred at 60 °C in a preheated oil bath for 60 min. At ambient temperature, the reaction mixture was quenched with distilled H₂O (10 mL). The crude product was then extracted with EtOAc (20 mL x 3). The combined organic extract was dried over Na₂SO₄ and the volatiles were evaporated in *vacuo*. The remaining residue was subjected to column chromatography on neutral alumina (petroleum ether/EtOAc: 20/1) to recover the starting compounds. The ¹H NMR analysis of the recovered compound **1c** shows 29% incorporation of deuterium at the C(2)-H, whereas compound [2-D]-**1a** shows 35% loss of deuterium.

3.4.10.3 Procedure for Deuterium Incorporation Experiment (using D₂O): To a screw-capped tube equipped with magnetic stir bar were introduced 1-(pyridine-2-yl)-1*H*-indole (**1a**; 0.039 g, 0.20 mmol), 1-chlorooctane (0.059 g, 0.40 mmol), (thf)₂NiBr₂ (0.0037 g, 0.01 mmol, 0.01 M), bpy (0.0016 g, 0.01 mmol), LiHMDS (0.067 g, 0.40 mmol) inside the glove-box. To the above mixture toluene (1.0 mL) was added and the resultant reaction mixture was stirred at 60 °C in a preheated oil bath for 30 min. At ambient temperature, D₂O (1.0 mL) was added to the reaction mixture under argon and was stirred for 1 h. Reaction mixture was quenched with distilled H₂O (10 mL). The crude product was then extracted with EtOAc (20 mL x 3). The combined organic extract was dried over Na₂SO₄ and the volatiles were evaporated in *vacuo*. The ¹H NMR analysis of the recovered compound does not show incorporation of deuterium at the C(2)-H of indole **1a**. This experiment in the absence of nickel catalyst (thf)₂NiBr₂/bpy also shows the same result.

3.4.11 Procedure for EPR Study

Representative Procedure: To a flame-dried screw-cap tube equipped with magnetic stir bar were introduced 1-(175pyridine-2-yl)-1*H*-indole (**1a**; 0.019 g, 0.10 mmol), 1-chlorooctane (**2a**; 0.030 g, 0.20 mmol), (thf)₂NiBr₂ (0.011 g, 0.03 mmol, 30.0 mol %), bpy (0.005 g, 0.03

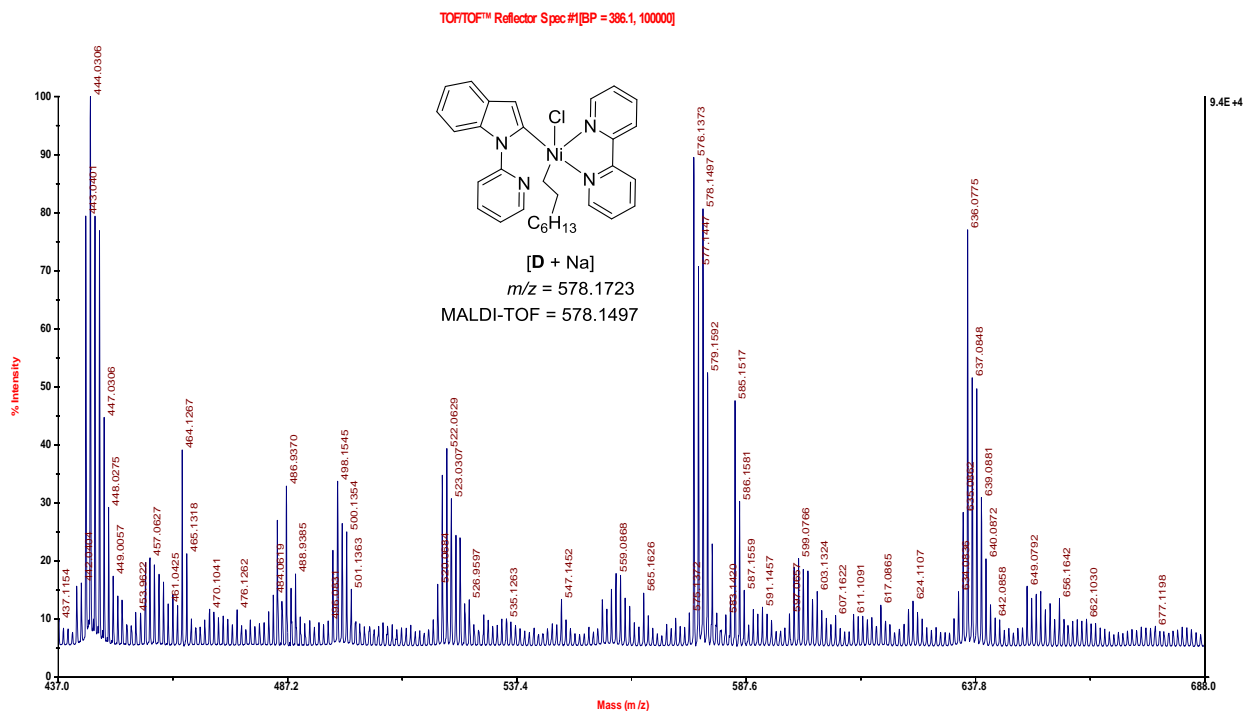
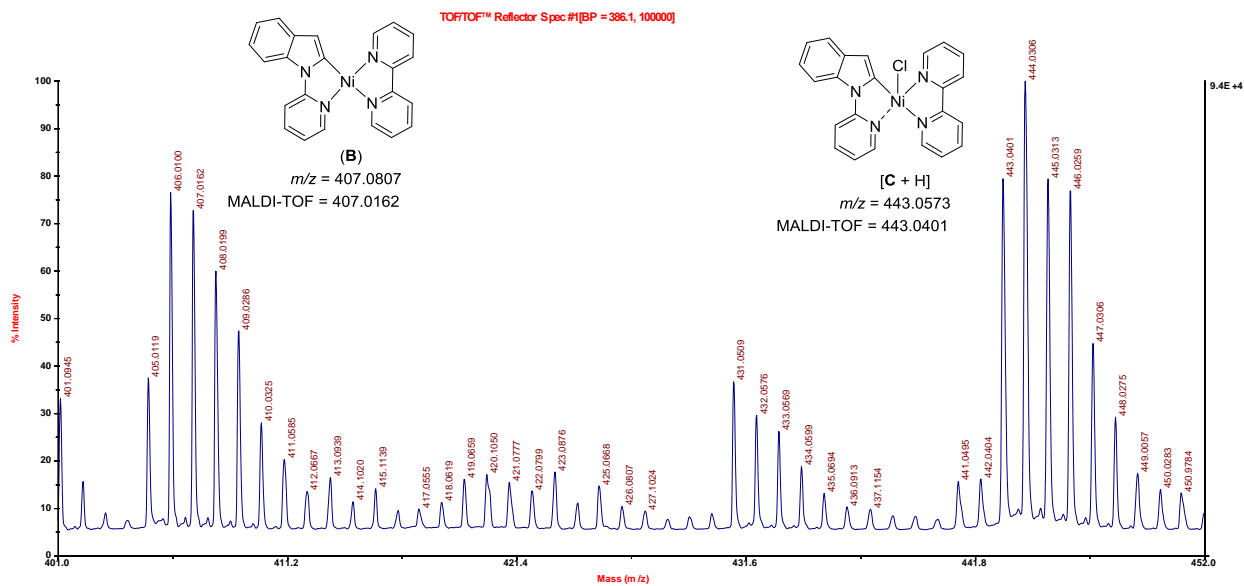
mmol, 30.0 mol %) and LiHMDS (0.033 g, 0.20 mmol) inside the glove box. To the above mixture in the tube was added toluene (1.0 mL) and the resultant reaction mixture was immersed in a preheated oil bath at 60 °C and stirred for 30 min. At ambient temperature, the reaction tube was transferred to the glove box, and an aliquot of the reaction mixture was transferred to an EPR tube and frozen at 100 K, which was then subjected to EPR measurement.

The representative procedure was followed to perform EPR experiments for other controlled reactions:

- (i) (thf)₂NiBr₂ + bpy + LiHMDS
- (ii) (thf)₂NiBr₂ + bpy + LiHMDS + indole **1a**
- (iii) (thf)₂NiBr₂ + bpy + LiHMDS + 1-chlorooctane (**2a**)

3.4.12 Procedure for XPS Analysis

Representative Procedure: To a flame-dried screw-cap tube equipped with magnetic stir bar were introduced 1-(pyridin-2-yl)-*1H*-indole (**1a**; 0.019 g, 0.10 mmol), 1-chlorooctane (**2a**; 0.030 g, 0.20 mmol), (thf)₂NiBr₂ (0.009 g, 0.025 mmol), bpy (0.004 g, 0.025 mol) and LiHMDS (0.033 g, 0.2 mmol) inside the glove box. To the above mixture in tube was added toluene (0.5 mL). The resultant reaction mixture in the tube was immersed in a preheated oil bath at 60 °C and stirred for 30 min. At ambient temperature, the reaction tube was transferred to the glove box. The sample for XPS analysis was prepared inside the glove box. After sample preparation, the sample was transferred to a vacuum transfer module which was subsequently evacuated in the antechamber of the glove box. The samples were loaded onto the spectrometer using this vacuum transfer module and subsequently pumped down by turbo molecular pumps connected to the load lock chamber. This allowed efficient transfer of the samples without being exposed to the atmosphere. The charge correction was done with C1s at 284.6 eV as standard. The peak fitting of the individual core-levels were done using Avantage software with a Shirley type background. The representative procedure was followed to perform XPS experiments for other controlled reaction:



3.5 REFERENCES

- (1) Horton, D. A.; Bourne, G. T.; Smythe, M. L. *Chem. Rev.* **2003**, *103*, 893-930.
- (2) Tois, J.; Franzén, R.; Koskinen, A. *Tetrahedron* **2003**, *59*, 5395-5405.
- (3) Chen, F.-E.; Huang, J. *Chem. Rev.* **2005**, *105*, 4671-4706.
- (4) Walker, S. R.; Carter, E. J.; Huff, B. C.; Morris, J. C. *Chem. Rev.* **2009**, *109*, 3080-3098.
- (5) Kochanowska-Karamyan, A. J.; Hamann, M. T. *Chem. Rev.* **2010**, *110*, 4489-4497.
- (6) Melander, R. J.; Minvielle, M. J.; Melander, C. *Tetrahedron* **2014**, *70*, 6363-6372.
- (7) Lyons, T. W.; Sanford, M. S. *Chem. Rev.* **2010**, *110*, 1147-1169.
- (8) Ackermann, L. *Chem. Rev.* **2011**, *111*, 1315-1345.
- (9) Wencel-Delord, J.; Droge, T.; Liu, F.; Glorius, F. *Chem. Soc. Rev.* **2011**, *40*, 4740-4761.
- (10) Yamaguchi, J.; Yamaguchi, A. D.; Itami, K. *Angew. Chem. Int. Ed.* **2012**, *51*, 8960-9009.
- (11) Zhang, F.; Spring, D. R. *Chem. Soc. Rev.* **2014**, *43*, 6906-6919.
- (12) Zhang, M.; Zhang, Y.; Jie, X.; Zhao, H.; Li, G.; Su, W. *Org. Chem. Front.* **2014**, *1*, 843-895.
- (13) Cernak, T.; Dykstra, K. D.; Tyagarajan, S.; Vachal, P.; Krska, S. W. *Chem. Soc. Rev.* **2016**, *45*, 546-576.
- (14) Gensch, T.; Hopkinson, M. N.; Glorius, F.; Wencel-Delord, J. *Chem. Soc. Rev.* **2016**, *45*, 2900-2936.
- (15) Wedi, P.; van Gemmeren, M. *Angew. Chem. Int. Ed.* **2018**, *57*, 13016-13027.
- (16) Ackermann, L. *Chem. Commun.* **2010**, *46*, 4866-4877.
- (17) Hirano, K.; Miura, M. *Synlett* **2011**, *2011*, 294-307.
- (18) Han, W.; Ofial, A. R. *Synlett* **2011**, 1951-1955.
- (19) Cho, S. H.; Kim, J. Y.; Kwak, J.; Chang, S. *Chem. Soc. Rev.* **2011**, *40*, 5068-5083.
- (20) Yamaguchi, J.; Muto, K.; Itami, K. *Top. Curr. Chem.* **2016**, *374*, 55.
- (21) Joucla, L.; Djakovitch, L. *Adv. Synth. Catal.* **2009**, *351*, 673-714.
- (22) Sandtorv, A. H. *Adv. Synth. Catal.* **2015**, *357*, 2403-2435.
- (23) Leitch, J.; Bhonoah, Y.; Frost, C. G. *ACS Catal.* **2017**, *7*, 5618-5627.
- (24) Chen, J.; Jia, Y. *Org. Biomol. Chem.* **2017**, *15*, 3550-3567.
- (25) Sundberg, R. J.; Luis, J. G.; Parton, R. L.; Schreiber, S.; Srinivasan, P. C.; Lamb, P.; Forcier, P.; Bryan, R. F. *J. Org. Chem.* **1978**, *43*, 4859-4865.
- (26) Mohan, B. N., D.; Vedachalam, M.; Srinivasan, P. C. *Synthesis* **1985**, 188-190.

- (27) Hashimoto, C.; Husson, H.-P. *Tetrahedron Lett.* **1988**, *29*, 4563-4566.
- (28) Dolušić, E.; Larrieu, P.; Blanc, S.; Sapunarić, F.; Norberg, B.; Moineaux, L.; Colette, D.; Stroobant, V.; Pilotte, L.; Colau, D.; Ferain, T.; Fraser, G.; Galeni, M.; Frère, J. M.; Masereel, B.; Van den Eynde, B.; Wouters, J.; Frédérick, R. *Bioorg. Med. Chem.* **2011**, *19*, 1550-1561.
- (29) Cacchi, S.; Fabrizi, G. *Chem. Rev.* **2005**, *105*, 2873-2920.
- (30) Seregin, I. V.; Gevorgyan, V. *Chem. Soc. Rev.* **2007**, *36*, 1173-1193.
- (31) Bandini, M.; Eichholzer, A. *Angew. Chem. Int. Ed.* **2009**, *48*, 9608-9644.
- (32) Putra, A. E.; Takigawa, K.; Tanaka, H.; Ito, Y.; Oe, Y.; Ohta, T. *Eur. J. Org. Chem.* **2013**, *2013*, 6344-6354.
- (33) Gao, J.; Wu, H.; Xiang, B.; Yu, W.; Han, L.; Jia, Y. *J. Am. Chem. Soc.* **2013**, *135*, 2983-2986.
- (34) Nakao, Y.; Kashihara, N.; Kanyiva, K. S.; Hiyama, T. *Angew. Chem. Int. Ed.* **2010**, *49*, 4451-4454.
- (35) Pan, S.; Ryu, N.; Shibata, T. *J. Am. Chem. Soc.* **2012**, *134*, 17474-17477.
- (36) Pan, S.; Shibata, T. *ACS Catal.* **2013**, *3*, 704-712.
- (37) Zhang, Y.; Liu, X.; Zhao, X.; Zhang, J.; Zhou, L.; Lin, L.; Feng, X. *Chem. Commun.* **2013**, *49*, 11311-11313.
- (38) Schramm, Y.; Takeuchi, M.; Semba, K.; Nakao, Y.; Hartwig, J. F. *J. Am. Chem. Soc.* **2015**, *137*, 12215-12218.
- (39) Shibata, T.; Ryu, N.; Takano, H. *Adv. Synth. Catal.* **2015**, *357*, 1131-1135.
- (40) Lee, P.-S.; Yoshikai, N. *Org. Lett.* **2015**, *17*, 22-25.
- (41) Lu, P.; Feng, C.; Loh, T.-P. *Org. Lett.* **2015**, *17*, 3210-3213.
- (42) Loup, J.; Zell, D.; Oliveira, J. C. A.; Keil, H.; Stalke, D.; Ackermann, L. *Angew. Chem. Int. Ed.* **2017**, *56*, 14197-14201.
- (43) Jiao, L.; Bach, T. *J. Am. Chem. Soc.* **2011**, *133*, 12990-12993.
- (44) Jiao, L.; Herdtweck, E.; Bach, T. *J. Am. Chem. Soc.* **2012**, *134*, 14563-14572.
- (45) Jiao, L.; Bach, T. *Synthesis* **2014**, *46*, 35-41.
- (46) Wegmann, M.; Henkel, M.; Bach, T. *Org. Biomol. Chem.* **2018**, *16*, 5376-5385.
- (47) Wang, H.; Yu, S.; Qi, Z.; Li, X. *Org. Lett.* **2015**, *17*, 2812-2815.
- (48) Soni, V.; Jagtap, R. A.; Gonnade, R. G.; Punji, B. *ACS Catal.* **2016**, *6*, 5666-5672.

-
- (49) Punji, B.; Song, W.; Shevchenko, G. A.; Ackermann, L. *Chem. – Eur. J.* **2013**, *19*, 10605-10610.
- (50) Tiwari, V. K.; Kamal, N.; Kapur, M. *Org. Lett.* **2015**, *17*, 1766-1769.
- (51) Ackermann, L.; Lygin, A. V. *Org. Lett.* **2011**, *13*, 3332-3335.
- (52) Chu, U. B.; Vorperian, S. K.; Satyshur, K.; Eickstaedt, K.; Cozzi, N. V.; Mavlyutov, T.; Hajipour, A. R.; Ruoho, A. E. *Biochemistry* **2014**, *53*, 2956–2965.
- (53) Broomhead, J. A.; Dwyer, F. P. *Aust. J. Chem.* **1961**, *14*, 250-252.
- (54) Khrizanforov, M.; Khrizanforova, V.; Mamedov, V.; Zhukova, N.; Strekalova, S.; Grinenko, V.; Gryaznova, T.; Sinyashin, O.; Budnikova, Y. *J. Org. Chem.* **2016**, *820*, 82-88.
- (55) Simmons, E. M.; Hartwig, J. F. *Angew. Chem. Int. Ed.* **2012**, *51*, 3066-3072.
- (56) Davies, D. L.; Al-Duaij, O.; Fawcett, J.; Giardiello, M.; Hilton, S. T.; Russell, D. R. *Dalton Trans.* **2003**, 4132-4138.
- (57) Li, L.; Brennessel, W. W.; Jones, W. D. *J. Am. Chem. Soc.* **2008**, *130*, 12414-12419.
- (58) Hartwig, J. F. *Organotransition Metal Chemistry - From Bonding to Catalysis; University Science Books: Mill Valley, California, USA* **2010**.
- (59) Stoll, S.; Schweiger, A. *J. Mag. Reson.* **2006**, *178*, 42-55.
- (60) Chen, W.-C.; Hsu, Y.-C.; Shih, W.-C.; Lee, C.-Y.; Chuang, W.-H.; Tsai, Y.-F.; Chen, P. P.-Y.; Ong, T.-G. *Chem. Commun.* **2012**, *48*, 6702-6704.
- (61) Chen, J.; Wu, J. *Angew. Chem. Int. Ed.* **2017**, *56*, 3951-3955.
- (62) Lipschutz, M. I.; Yang, X.; Chatterjee, R.; Tilley, T. D. *J. Am. Chem. Soc.* **2013**, *135*, 15298-15301.
- (63) Zheng, B.; Tang, F.; Luo, J.; Schultz, J. W.; Rath, N. P.; Mirica, L. M. *J. Am. Chem. Soc.* **2014**, *136*, 6499-6504.
- (64) Xu, H.; Diccianni, J. B.; Katigbak, J.; Hu, C.; Zhang, Y.; Diao, T. *J. Am. Chem. Soc.* **2016**, *138*, 4779-4786.
- (65) Grosvenor, A. P.; Biesinger, M. C.; Smart, R. S. C.; McIntyre, N. S. *Surf. Sci.* **2006**, *600*, 1771-1779.
- (66) Hwang, S. J.; Powers, D. C.; Maher, A. G.; Nocera, D. G. *Chem. Sci.* **2015**, *6*, 917-922.
- (67) Anderson, T. J.; Jones, G. D.; Vacic, D. A. *J. Am. Chem. Soc.* **2004**, *126*, 8100-8101.
- (68) Lin, X.; Phillips, D. L. *J. Org. Chem.* **2008**, *73*, 3680-3688.
-

- (69) Lu, Z.; Wilsily, A.; Fu, G. C. *J. Am. Chem. Soc.* **2011**, *133*, 8154-8157.
- (70) Dudnik, A. S.; Fu, G. C. *J. Am. Chem. Soc.* **2012**, *134*, 10693-10697.
- (71) Zultanski, S. L.; Fu, G. C. *J. Am. Chem. Soc.* **2013**, *135*, 624-627.
- (72) Hu, X. *Chem. Sci.* **2011**, *2*, 1867-1886.
- (73) Laskowski, C. A.; Morello, G. R.; Saouma, C. T.; Cundari, T. R.; Hillhouse, G. L. *Chem. Sci.* **2013**, *4*, 170-174.
- (74) Aihara, Y.; Chatani, N. *J. Am. Chem. Soc.* **2013**, *135*, 5308-5311.
- (75) Wu, X.-L.; Zhao, Y.; Ge, H. *J. Am. Chem. Soc.* **2014**, *136*, 1789-1792.
- (76) Ackermann, L.; Punji, B.; Song, W. *Adv. Synth. Catal.* **2011**, *353*, 3325-3329.
- (77) Obata, A.; Ano, Y.; Chatani, N. *Chem. Sci.* **2017**, *8*, 6650-6655.

Chapter 4

Nickel-Catalyzed C-2 Arylation of Indoles with Unactivated Aryl Chlorides

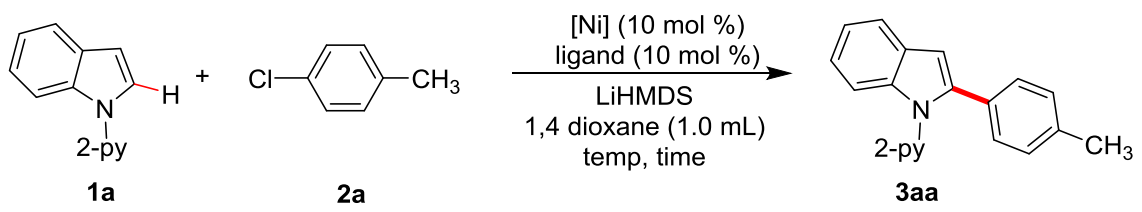
4.1 INTRODUCTION

The ubiquitous feature of indole motif in bioactive natural and pharmaceutical products¹⁻⁸ makes it the fourth most prevalent hetero-aromatic compound, which is present in 24 current marketed pharmaceuticals.⁹ This instigates the continuing interest in the C–H functionalization and late-stage modifications of biologically significant indoles.¹⁰⁻¹⁸ To accomplish the purpose, transition-metal catalyzed C–H functionalization appears to be a powerful tool. Although traditional cross-coupling methods, namely Suzuki, Negishi, and Stille coupling reactions have been widely utilized to build aryl–indolyl bonds at each position of indoles, the transition metal catalyzed C–H arylation¹⁹⁻³⁶ are considered to be an environmentally friendly and benign method for the synthesis of diverse biaryl motifs. The indole scaffold has been widely used in both direct and directed C–H functionalization.^{21,37-39} There are many reports for indole arylation using different transition metals such as Rh,⁴⁰ Pd,^{41,42} Ru,⁴³ However, current studies are being focused on the C–H bond functionalization using naturally abundant and inexpensive 3d metals⁴⁴⁻⁴⁸ like Co⁴⁹ and Cu.⁵⁰⁻⁵² Furthermore, most of the indole arylation reactions were performed either using pseudo-halides⁵³⁻⁵⁶ or by oxidative coupling;⁵⁷ and only few reports are known using aryl halides.^{22,42} Several distinct arylation reactions involving activated C–H bond containing heterocycles have been reported using nickel as a catalyst.⁵⁸⁻⁶⁴ Recently, our group and others have demonstrated the arylation of indoles,⁶⁵ but was limited with low yield and scope. However, the use of unactivated aryl chlorides⁴² in the arylation of indoles was not explored using an inexpensive nickel catalyst.

To address the limitations on existing indole C-2 arylation methods and to promote sustainable and environmentally benign protocols, in this chapter, we demonstrate the nickel-catalyzed C–H arylation of indoles with unactivated aryl chlorides. Reaction was performed at low temperature (80 °C) without the use of solvent. A detailed mechanistic investigation has been performed, including controlled reactivity study, kinetic study, deuterium labeling and electronic effect study. These studies established a single-electron transfer (SET) pathway for the nickel-catalyzed indole arylation that involves the rate-influencing oxidative addition of aryl chloride.

4.2 RESULTS AND DISCUSSION

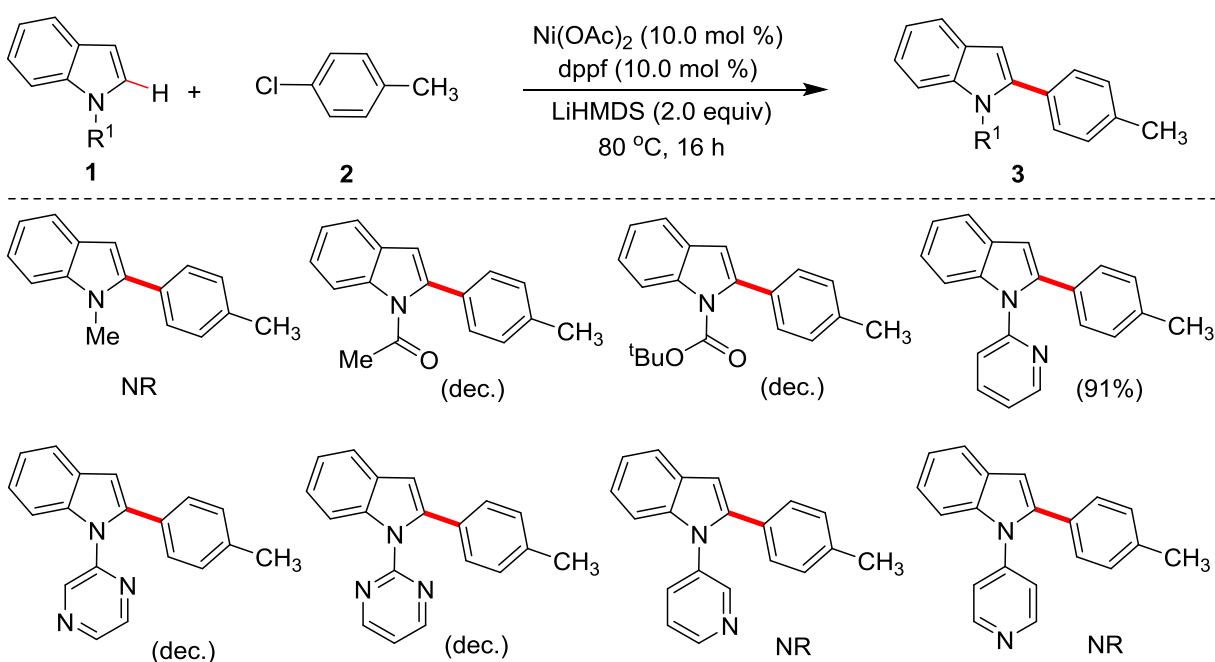
4.2.1 Optimization of Reaction Parameters. We have initiated the optimization for the coupling of 1-(pyridin-2-yl)-1*H*-indole (**1a**) with 1-chloro-4-methylbenzene (**2a**) employing Ni(OAc)₂/xantphos catalyst system, and a non-nucleophilic base LiHMDS in 1,4-dioxane (Table 4.1). Initial experiments were conducted to find the suitable temperature and it was found that the couple product 1-(pyridin-2-yl)-2-(*p*-tolyl)-1*H*-indole (**3aa**) could be obtained in 43% yield at 110 °C (entry 1). Arylation reaction employing other bidentate phosphine ligands like binap, dpephos, dppe, and monodentate PPh₃ gave improved yield, and the product **3aa** was obtained in 89% isolated yield with Ni(OAc)₂/dppf catalyst system (Table 1, entries 2-7). Various nickel precursors were screened like (thf)₂NiBr₂, Ni(OTf)₂, (dme)NiCl₂, but found to be less effective than Ni(OAc)₂ (entries 8-10). The reaction in other solvents such as toluene, *p*-xylene, mesitylene was found to be less effective (entries 11-13). Surprisingly, arylation reaction worked efficiently without the use of solvent at 80 °C, and afforded **3aa** in 91% isolated yield (entry 14). The reaction without dppf ligand gave 55% yield of the arylated product (entry 15), whereas the reaction without Ni(OAc)₂ did not give **3aa** (entry 16). The isolated complex (dppf)NiCl₂ was found to be less effective for the arylation reaction (entry 17-18). The reaction provided 75% of product **3aa** when performed with 5 mol % of catalyst loading (entry 19).

Table 4.1. Optimization of Reaction Parameters^a


entry	[Ni]	ligand	temp. (°C)	time (h)	yield (%) ^b
1	Ni(OAc) ₂	xantphos	110	24	43
2	Ni(OAc) ₂	binap	110	24	74
3	Ni(OAc) ₂	dpephos	110	24	77
4	Ni(OAc) ₂	dppe	110	24	74
5	Ni(OAc) ₂	dcype	110	24	67
6	Ni(OAc) ₂	PPh ₃	110	24	60
7	Ni(OAc) ₂	dppf	110	24	94(89) ^c
8	(thf) ₂ NiBr ₂	dppf	110	24	75
9	Ni(OTf) ₂	dppf	110	24	60
10	(dme)NiCl ₂	dppf	110	24	55
11 ^d	Ni(OAc) ₂	dppf	110	24	65
12 ^e	Ni(OAc) ₂	dppf	110	24	68
13 ^f	Ni(OAc) ₂	dppf	110	24	66
14^g	Ni(OAc)₂	dppf	80	16	96 (91)^c
15 ^g	Ni(OAc) ₂	-	80	16	55
16 ^g	-	dppf	80	16	-
17 ^g	(dppf)NiCl ₂	-	80	16	65
18 ^{g,h}	(dppf)NiCl ₂	-	80	16	73
19 ^{g,i}	Ni(OAc) ₂	dppf	80	16	75

^aReaction Conditions: Indole **1a** (0.039 g, 0.20 mmol), **2a** (0.051 g, 0.40 mmol), [Ni] cat (0.02 mmol, 10 mol %), ligand (0.02 mmol, 10 mol %), LiHMDS (0.067 g, 0.40 mmol), solvent (1.0 mL). ^bNMR yield using CH₂Br₂ as internal standard. ^cIsolated yield. ^dtoluene as a solvent. ^e*p*-Xylene as a solvent. ^fMesitylene as a solvent. ^gWithout solvent. ^hAgOAc (10 mol %), ⁱCat (5.0 mol %).

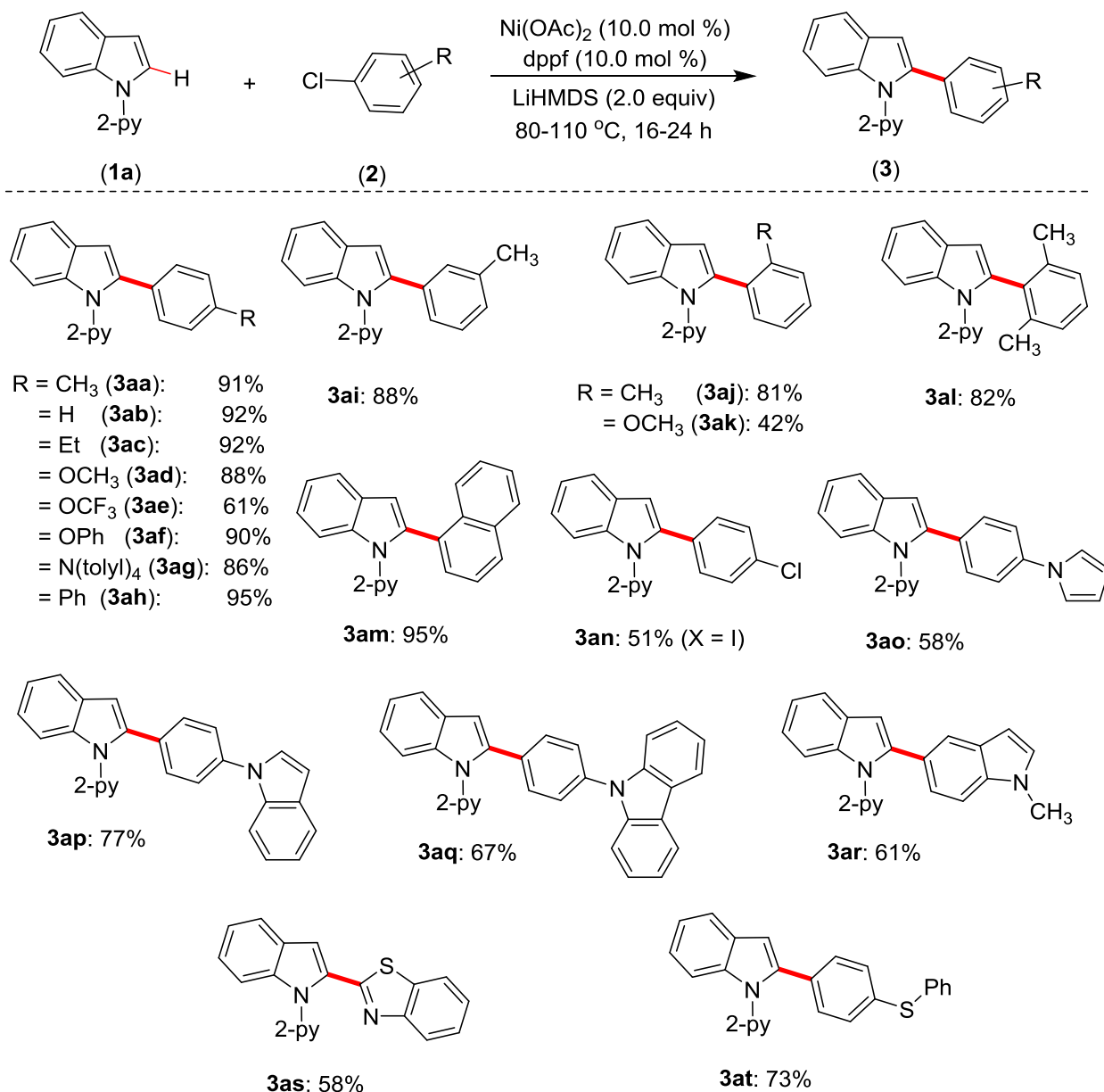
Screening of *N*-substituent at indole: We successfully optimized the reaction condition for the arylation of indole **1a** containing 2-pyridinyl as directing group with 1-chloro-4-methylbenzene (**2a**) to afford the product 1-(pyridin-2-yl)-2-(p-tolyl)-1*H*-indole (**3aa**) in 91% yield. Thus, the effectiveness of other substituents/directing group at *N*-center of the indole was investigated (Scheme 4.1). The free-NH indole decomposed under the reaction conditions whereas *N*-Me indole was non-reactive. Indole bearing *N*-acetyl and *N*-Boc directing groups were decomposed. The directing groups, 2-pyrimidinyl and 2-pyrazinyl were not effective under the catalytic reaction condition. Notably, the 3-pyridinyl and 4-pyridinyl-substituted indoles were ineffective and arylation was observed. All these findings suggest that directing group 2-pyridinyl, at the *N*-substituent of indole is essential for the effective arylation of indoles under the reaction conditions.



Scheme 4.1 Screening of *N*-substituent at indole.

4.2.2 Substrate Scope for Arylation. After successfully optimizing the 2-arylation of indole with unactivated aryl chloride using inexpensive Ni(OAc)₂/dppf catalyst system, we explored the scope of the arylation (Scheme 4.2). It was observed that reaction was compatible with a variety of simple and functionalized aryl chlorides as the coupling partners. The optimized reaction tolerated various functional group on the electrophile, such as -Ph, -Me, -OMe, -CF₃, -OPh. Aryl

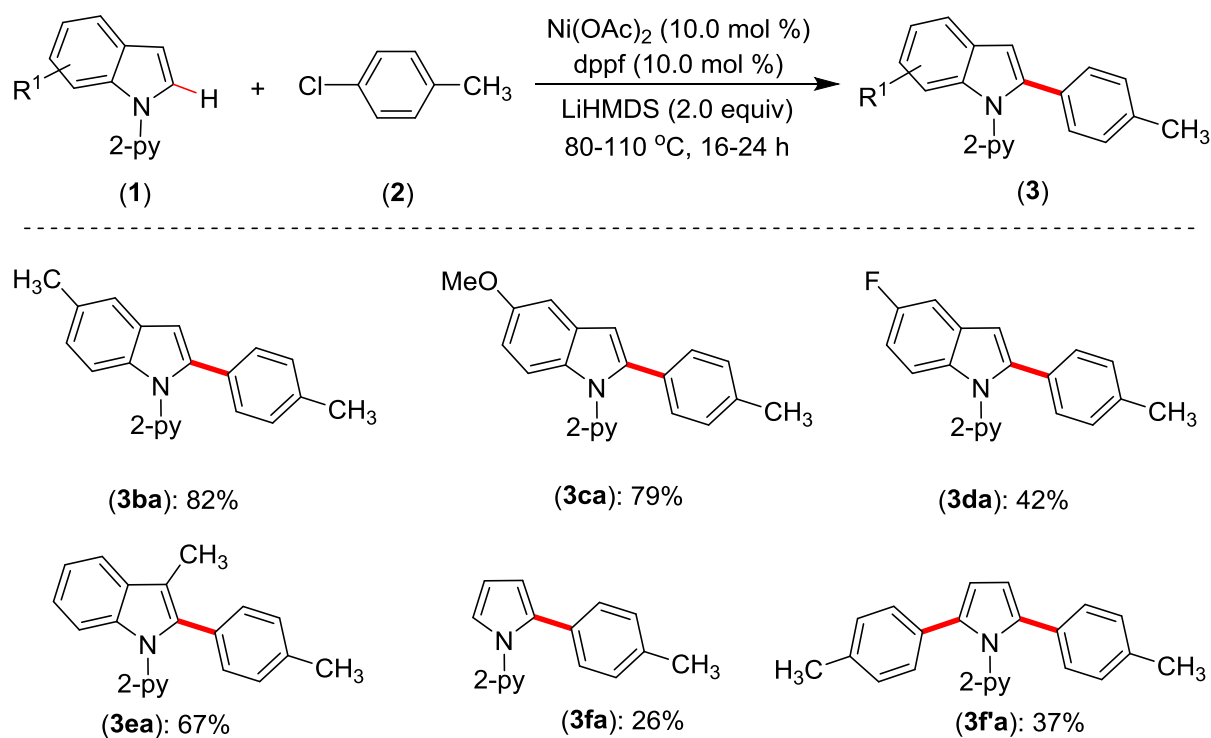
chlorides with different functionality at the *para* position of the phenyl ring were efficiently coupled (**3aa-3ah**). Functionality at the *ortho*- and *meta*- position of the aryl chloride electrophile ring was well tolerated (**3ai-3ak**). More bulkier 2-chloro-1,3-dimethylbenzene reacted to give a couple product **3al** in 82% yield. The reaction was chemoselective in terms of aryl halide, with only C(sp²)-I bond activated under the reaction condition when arylation was carried out with 1-iodo-4-chlorobenzene. The aryl chloride having nitrogen-containing heterocycle like *N*-pyrrolyl, *N*-indolyl, *N*-carbazolyl at *para* position reacted smoothly and delivered the desired arylated product in moderate to good yields (**3ao-3aq**). The 5-chloro-1-methyl-1*H*-indole was coupled with indole at C-2 position successfully to give the product **3ar** in 61% yield. Similarly 2-chlorobenzo[*d*]thiazole was coupled successfully with indole affording 58% of product **3as**. The sulphur containing electrophile was coupled with indole to give a good yield of **3at**. The reaction was sensitive to the -CN, and -NO₂ functionalities and the substrates were decomposed under reaction conditions.



Scheme 4.2 Scope of C-2 arylation of indoles with aryl chlorides. Yield of isolated products are given.

The reaction of aryl chlorides with substituted indole was explored to get more applicability of the methodology. The substituted indoles were tolerated well with the optimized condition (Scheme 4.3). The 5-methyl and 5-methoxy indole were arylated with aryl chloride to give good yield of products **3ba-3ca**. When 5-fluoroindole was subjected to the arylation under the optimized condition, the reaction needed an elevated temperature (110 °C) to give **3da** in

moderate yield. The 3-methyl-indole upon arylation with chlorotoluene gave the product **3ea** in 67% yield. Arylation of pyrrolpyridine under the reaction condition afforded a mixture of mono (**3fa**) and di-arylated (**3f'a**) products in 26% and 37% yields, respectively.



Scheme 4.3 Scope of C-2 arylation of substituted indoles and pyrrole.

4.2.3 MECHANISTIC STUDIES

4.2.3.1 Kinetic Analysis of Arylation of indoles

Reaction profile. After successful optimization and wide substrate scope for indole arylation, we were desirous to explore the detail mechanism of the nickel-catalyzed arylation reaction. In that context we initiated the kinetic study with the reaction profile analysis and rate order determination. The kinetic experiments were performed in flame-dried screw cap tubes under an argon atmosphere. In the standard reaction, the tube was charged with $\text{Ni}(\text{OAc})_2$ (0.02 mmol, 0.02 M), dppf (0.02 mmol, 0.02 M), LiHMDS (0.067 g, 0.40 mmol, 0.40 M), 4-chlorotoluene (0.051 mL, 0.40 mmol, 0.40 M), indole pyridine (0.039 g, 0.20 mmol, 0.20 M), *n*-hexadecane (0.025 mL, 0.085 M, internal standard), and 1,4-dioxane (0.89 mL) was added to make the total volume to 1.0 mL. The tube containing the reaction mixture was heated at 110 °C

in a preheated oil bath and progress of the arylation reaction was monitored by gas chromatography (GC) at regular intervals (Table 4.2). The reaction profile for the nickel-catalyzed arylation of **1a** up to 1440 min is shown in Figure 4.1. The formation of the arylation product followed a linear line, and the induction period for the production of **3aa** was not observed.

Table 4.2 Concentration of Product 3aa at Different Time Intervals

Time (min)	Conc. of 3aa [M]	Time (min)	Conc. of 3aa [M]
15	0.0046	120	0.0454
30	0.0126	240	0.069
45	0.0186	480	0.0989
60	0.0249	720	0.117
75	0.0318	960	0.1321
90	0.0355	1200	0.1464
105	0.0389	1440	0.1594

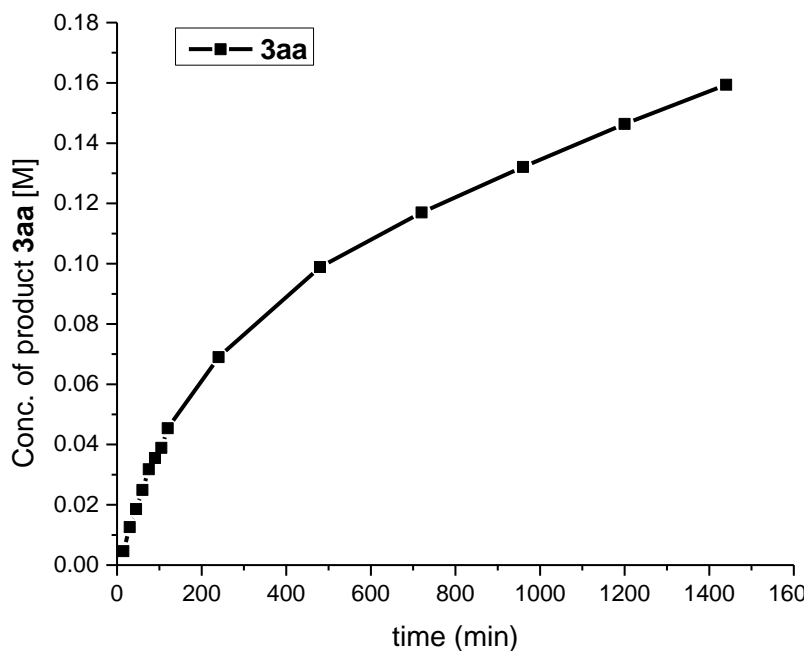


Figure 4.1 Time-dependent formation of **3aa**.

Rate Order Determination

The rate order of the arylation reaction with various reaction components was determined by the initial rate method. The data of the concentration of the product vs time (min) plot was fitted linear with Origin Pro 8. The slope of the linear fitting represents the reaction rate. The order of the reaction was then determined by plotting $\log(\text{rate})$ vs $\log(\text{conc})$ for a particular component.

Rate Order Determination on 1-(pyridin-2-yl)-1H-indole (Table 4.3 and Figure 4.2): To determine the order of the arylation reaction on 1-(pyridin-2-yl)-1H-indole, initial rates at different initial concentrations of 1-(pyridin-2-yl)-1H-indole were recorded. The final data was obtained by averaging the results of three independent experiments for same initial concentration. Concentration of the product obtained in each sample was determined with respect to the internal standard *n*-hexadecane.

The rate order of the arylation reaction in each component was independently determined using the initial rate approximation. The rate order of the arylation reaction with varying initial concentrations of indole (**1a**) suggests that the reaction is fractional-order (slope 0.60, Figure 4.2B) in the concentration of indole, which indicates a complex reaction mechanism w.r.t. indole.

Table 4.3. Rate of Arylation Reaction at Different Initial Concentrations of 1-(pyridin-2-yl)-1H-indole

Experiment	Amount of Indole (g)	Initial Conc. of Indole [M]	Initial Rate [Mmin ⁻¹] x 10 ⁻⁴
1	0.019	0.1	2.687
2	0.039	0.2	3.767
3	0.078	0.4	6.268
4	0.116	0.6	7.960

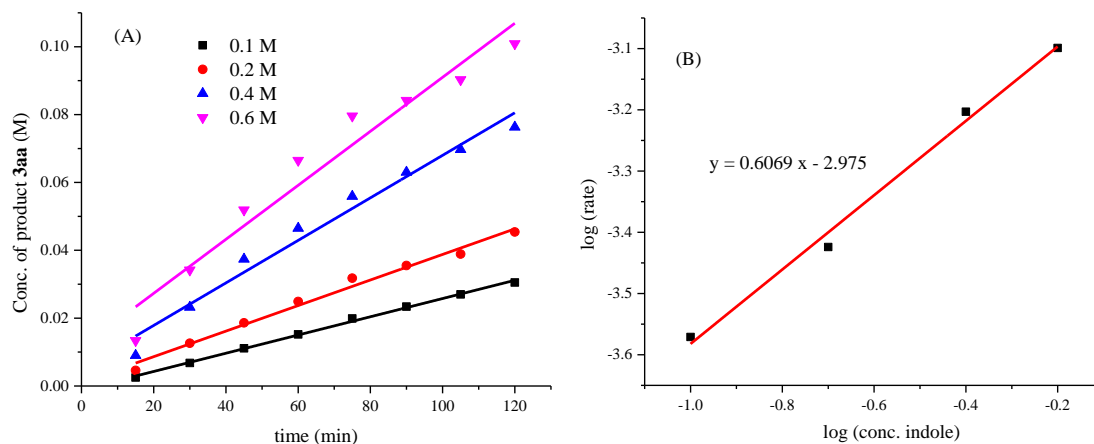


Figure 4.2 (A) Time-dependent formation of **3aa** at different initial concentration of indole pyridine. (B) Plot of $\log(\text{rate})$ vs $\log(\text{conc. indole pyridine})$.

Rate Order Determination on 4-Chlorotoluene (Table 4.4, Figure 4.3). To determine the order of the arylation reaction on 4-chlorotoluene, the initial rates at different initial concentrations of 4-chlorotoluene were recorded. The final data was obtained by averaging the results of three independent experiments for same initial concentration. The rate of the arylation reaction is almost similar when different initial concentrations of 4-chlorotoluene were used, suggesting that the reaction is zeroth-order in the concentration of 4-chlorotoluene.

Table 4.4 Rate of Arylation Reaction at Different Initial Concentrations of 4-Chlorotoluene

Experiment	Amount of 4-chlorotoluene (g)	Initial Conc. of 4-chlorotoluene [M]	Initial Rate [Mmin^{-1}] $\times 10^{-4}$
1	0.025	0.2	3.402
2	0.051	0.4	3.767
3	0.076	0.6	3.246
4	0.101	0.8	3.512

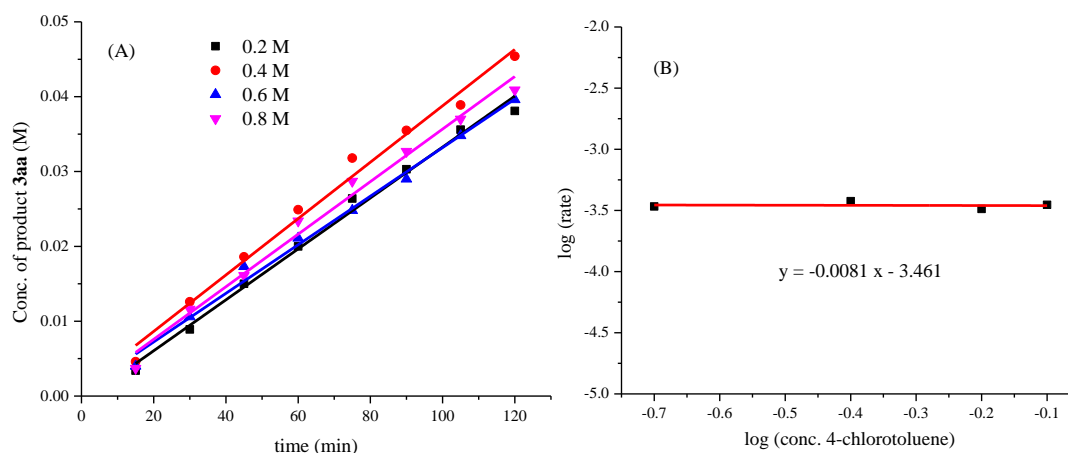


Figure 4.3 (A) Time-dependent formation of **3aa** at different initial concentration of 4-chlorotoluene. (B) Plot of $\log(\text{rate})$ vs $\log(\text{conc. 4-chlorotoluene})$.

Rate Order Determination on Catalyst (Table 4.5, Figure 4.4). To determine the order of the arylation reaction on catalyst, the initial rates at different initial concentrations of catalyst were recorded. The final data was obtained by averaging the results of three independent experiments for the same initial concentration. The reaction rate on various loadings of catalyst was measured by the initial rate of the product formation (Figure 4.4A). The plot of $\log(\text{rate})$ vs $\log(\text{conc. cat})$ provides a slope of 0.44 (Figure 4.4B), suggesting that the reaction is fractional rate order in the loading of catalyst. Considering the involvement of the catalyst in multiple steps in the catalysis, the observed rate order seems to be reasonable.

Table 4.5 Rate of Arylation Reaction at Different Initial Concentrations of Catalyst

Experiment	Amount of Catalyst (g)	Initial Conc. of Catalyst [M]	Initial Rate [Mmin^{-1}] $\times 10^{-4}$
1	0.0017	0.01	3.005
2	0.0035	0.02	3.767
3	0.0053	0.03	4.625
4	0.0071	0.04	5.779

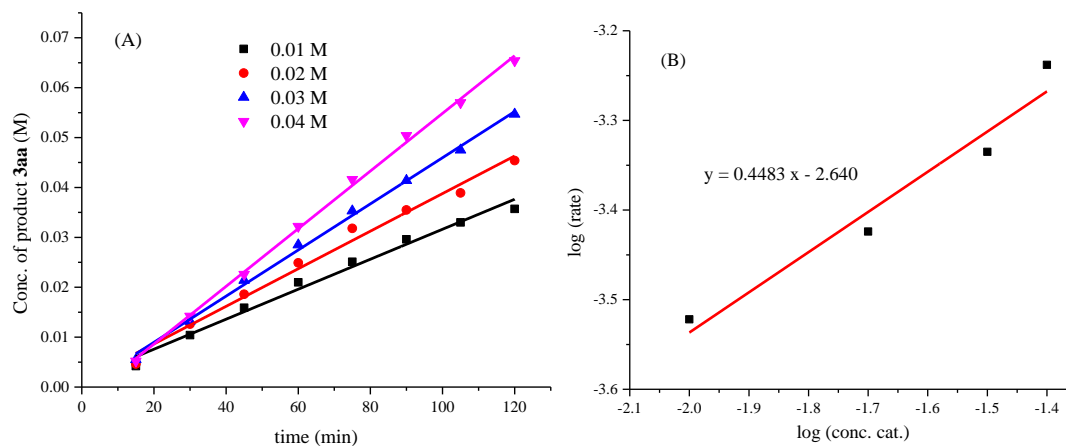


Figure 4.4 (A) Time-dependent formation of **3aa** at different initial concentration of catalyst. (B) Plot of $\log(\text{rate})$ vs $\log(\text{conc. catalyst})$.

Rate Order Determination on LiHMDS (Table 4.6, Figure 4.5). To determine the order of the arylation reaction on LiHMDS, the initial rates at different initial concentrations of LiHMDS were recorded. The final data was obtained by averaging the results of three independent experiments for same initial concentration. The rate order determination of the arylation reaction to different initial concentrations of LiHMDS showed slope of 0.45 indicating the reaction is fractional order w.r.t. concentration of LiHMDS (Figure 4.5B).

Table 4.6. Rate of Arylation Reaction at Different Initial Concentrations of LiHMDS

Experiment	Amount of LiHMDS (g)	Initial Conc. of LiHMDS [M]	Initial Rate [Mmin^{-1}] $\times 10^{-4}$
1	0.033	0.2	2.443
2	0.067	0.4	3.767
3	0.100	0.6	4.328
4	0.134	0.8	4.545

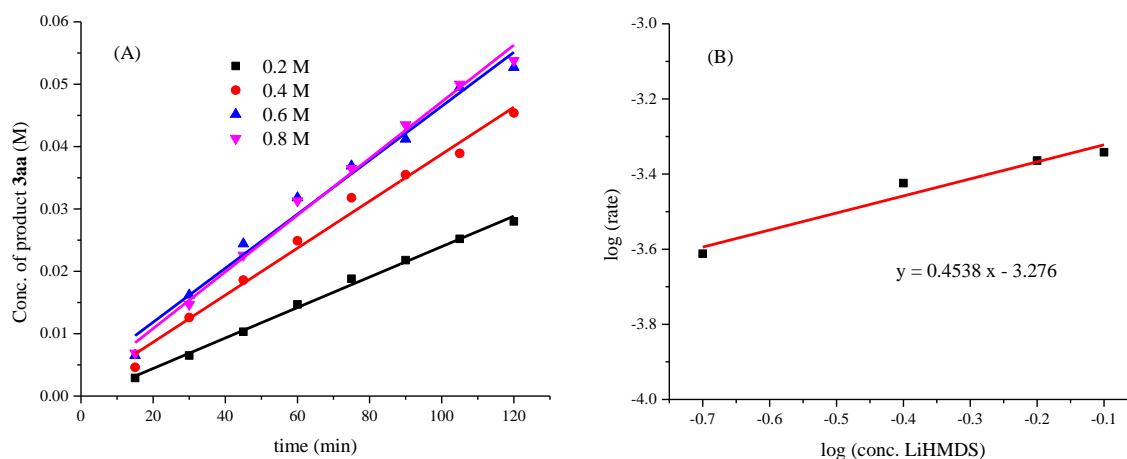
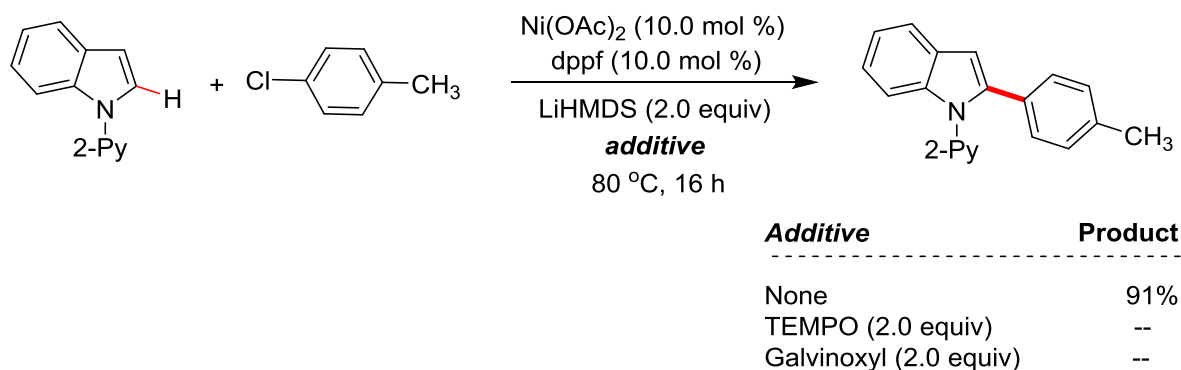


Figure 4.5 (A) Time-dependent formation of **3aa** at different initial concentration of LiHMDS. (B) Plot of $\log(\text{rate})$ vs $\log(\text{conc. LiHMDS})$.

4.2.3.2 Probing Radical Pathway. The standard arylation reaction was performed in the presence of radical scavengers, TEMPO (2.0 equiv) or galvinoxyl (2.0 equiv) wherein the complete inhibition of the reaction was observed (Scheme 4.4). This suggests the probable involvement of a radical intermediate during the arylation process. Unfortunately, the radical species coupled with TEMPO or galvinoxyl was not detected.



Scheme 4.4 External additive experiment.

4.2.3.3 Deuterium Labeling Studies.

To get the more insight of indole C–H bond activation in arylation reaction, and probable involvement of the same in the rate limiting step, initial rates of the reaction using indole **1a** and [2-D]-**1a** were determined. The rate of the arylation reaction using **1a** ($3.767 \times 10^{-4} \text{ Min}^{-1}$) was

found slightly slower than the rate with [2-D]-**1a** ($4.726 \times 10^{-4} \text{ Min}^{-1}$) (Figure 4.1). The kinetic isotopic effect (KIE) value $k_{\text{H}}/k_{\text{D}} = 0.80$ was observed, which indicates that the C–H bond activation is not involved in rate determining step.

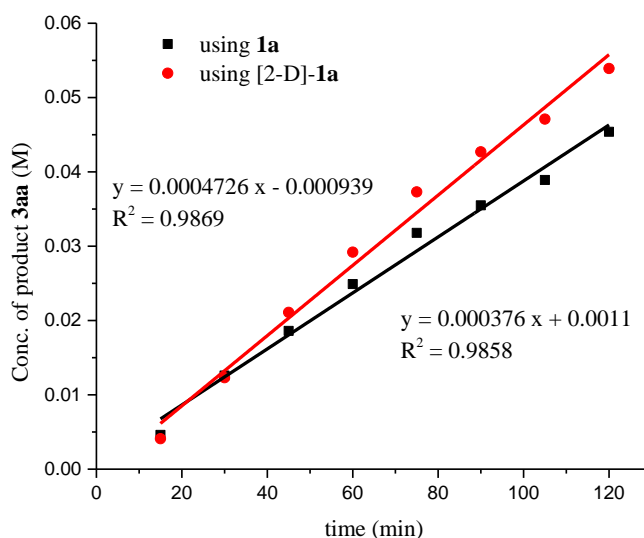
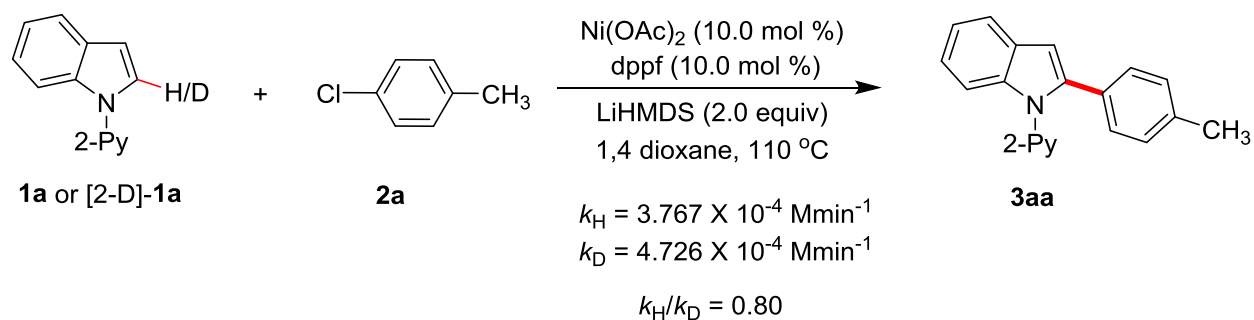
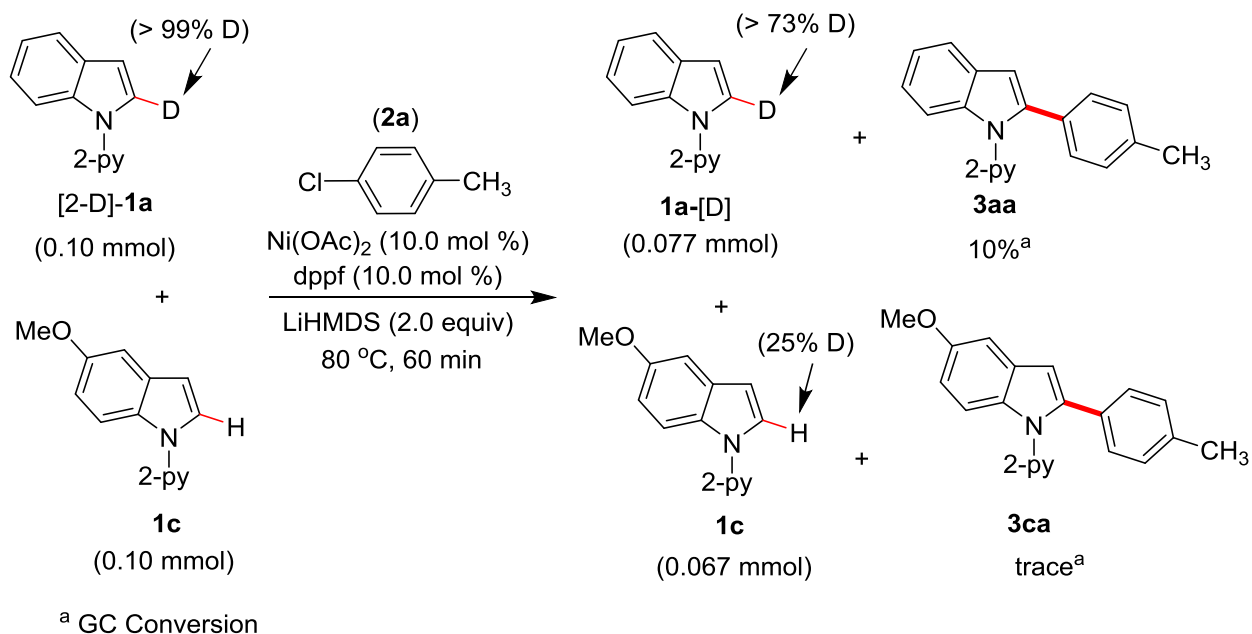


Figure 4.6 Time-dependent formation of product **3aa** using indoles **1a** and [2-D]-**1a**.

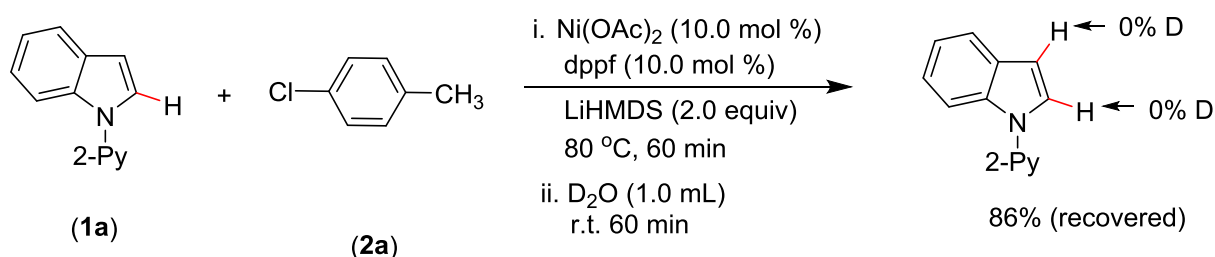
The arylation reaction using indole [2-D]-**1a** and 5-methoxy-1-(pyridine-2-yl)-1*H*-indole (**1c**) was performed in one pot using standard reaction conditions. After 60 min, the reaction was quenched and both the substrates were recovered. The ^1H NMR analysis of the recovered compound [2-D]-**1a** and **1c** demonstrated a considerable H/D exchange at C(2)–H position (Scheme 4.5a). This clearly evident the reversibility of C–H nickelation step during the reaction. Further, the standard arylation reaction both in the presence and absence of $\text{Ni(OAc)}_2/\text{dppf}$ catalyst system was performed for 60 min, and the reaction mixture was quenched with D_2O (Scheme 4.5b). The starting compound was recovered *via* column chromatography and the ^1H NMR analysis was performed. The ^1H NMR spectrum indicates no deuterium incorporation at

C(2)–H or C(3)–H of indole **1a**. This observation clearly suggests that the indole C–H nickelation *via* a simple base-mediated deprotonation pathway is remote.

(a) H/D Scrambling Experiment:



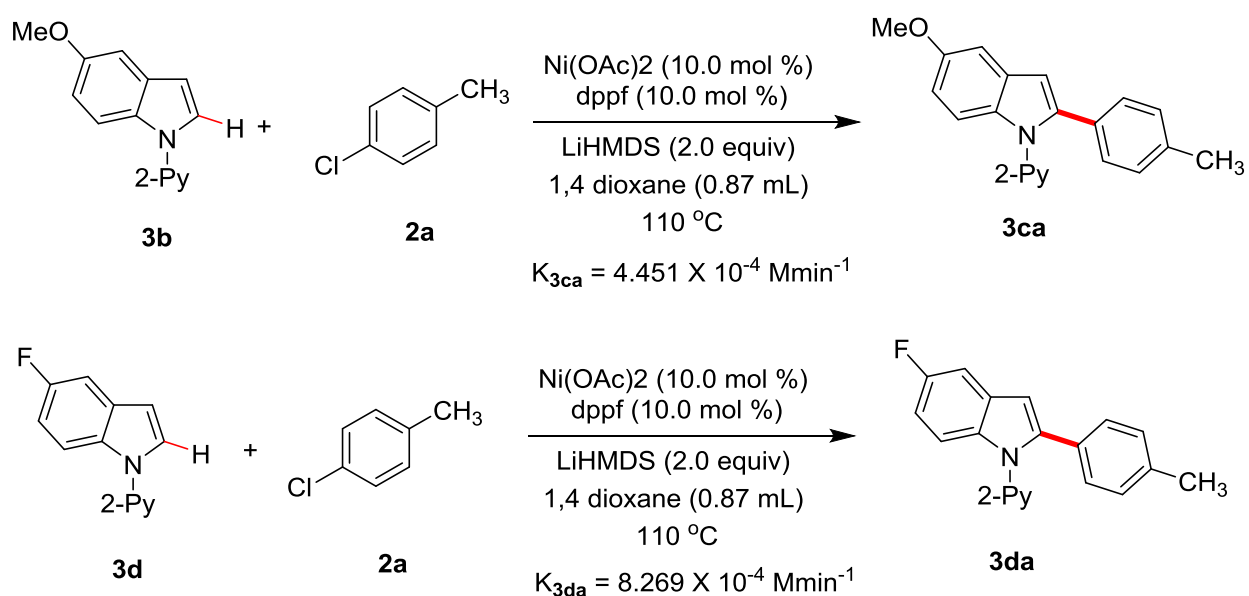
b) Deuterium Incorporation



Scheme 4.5 Deuterium labeling experiments.

4.2.3.4 Effect of Indole Substitutions on Arylation (Electronic Effect): The rates of the coupling of 5-methoxy-1-(pyridin-2-yl)-1*H*-indole (**3b**), 5-fluoro-1-(pyridin-2-yl)-1*H*-indole (**3d**) with 4-chlorotoluene were determined in order to understand the electronic influence of the substrates on arylation reaction (Scheme 4.6 Figure 4.7). The arylation reaction is faster with an electronically deficient indole compared to the electronically rich counterpart. This suggests the

possibility of generation of electronegative nickel species during the transition state of the catalysis, and hence, transition state is stabilized by the electron-withdrawing substituent on the indole.



Scheme 4.6 Effect of indole substitutions on arylation.

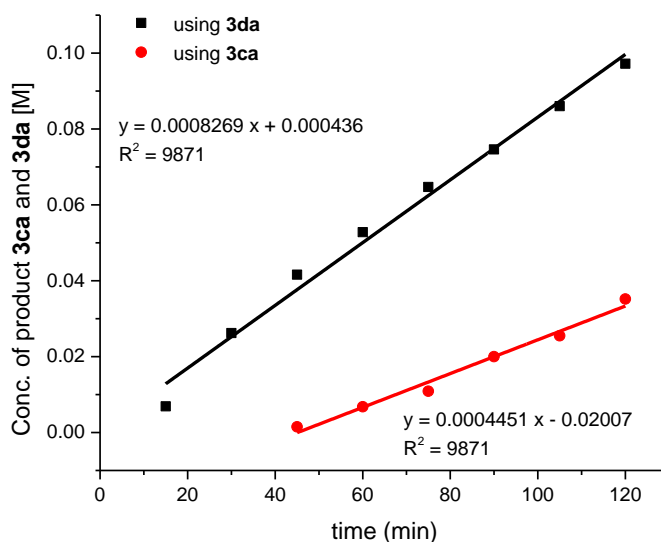


Figure 4.7 Time-dependent formation of products **3ca** and **3da**.

4.2.3.5 Catalytic Cycle. With the support of our mechanistic observation and the previous literature, we proposed a reaction mechanism for the Ni-catalyzed arylation of indoles with aryl chlorides (Figure 4.7). Two reaction pathways are possible. Path I includes the reaction of Ni(II)-species (**A**) with the indole **1a** to provide the intermediate species **B**. Deuterium labeling study suggest the reversibility of the this step. The nickel complex **B** would generate the radical species by reacting with aryl chloride by one-electron oxidation process in the rate-limiting step to produce the intermediate **C**. The pyridine nitrogen decoordination and recombination of the aryl radical generate the complex **D**. Reductive elimination from the complex **D** would result with arylated product **3** and the active catalyst **A**. Alternately, in path II, the aryl chloride would be activated in a bimetallic oxidative fashion to give (2-py-indolyl)Ni^{III}Cl(X) (**C**) and [Ni^{III}(4-MeC₆H₄)] (**E**). Reductive elimination from **E** would produce (dppf)Ni(I)(X) species (**F**) along with arylated product **3**. Disproportionation reaction between species **F** and **C** would regenerates **A** and **B** which completes the catalytic cycle.

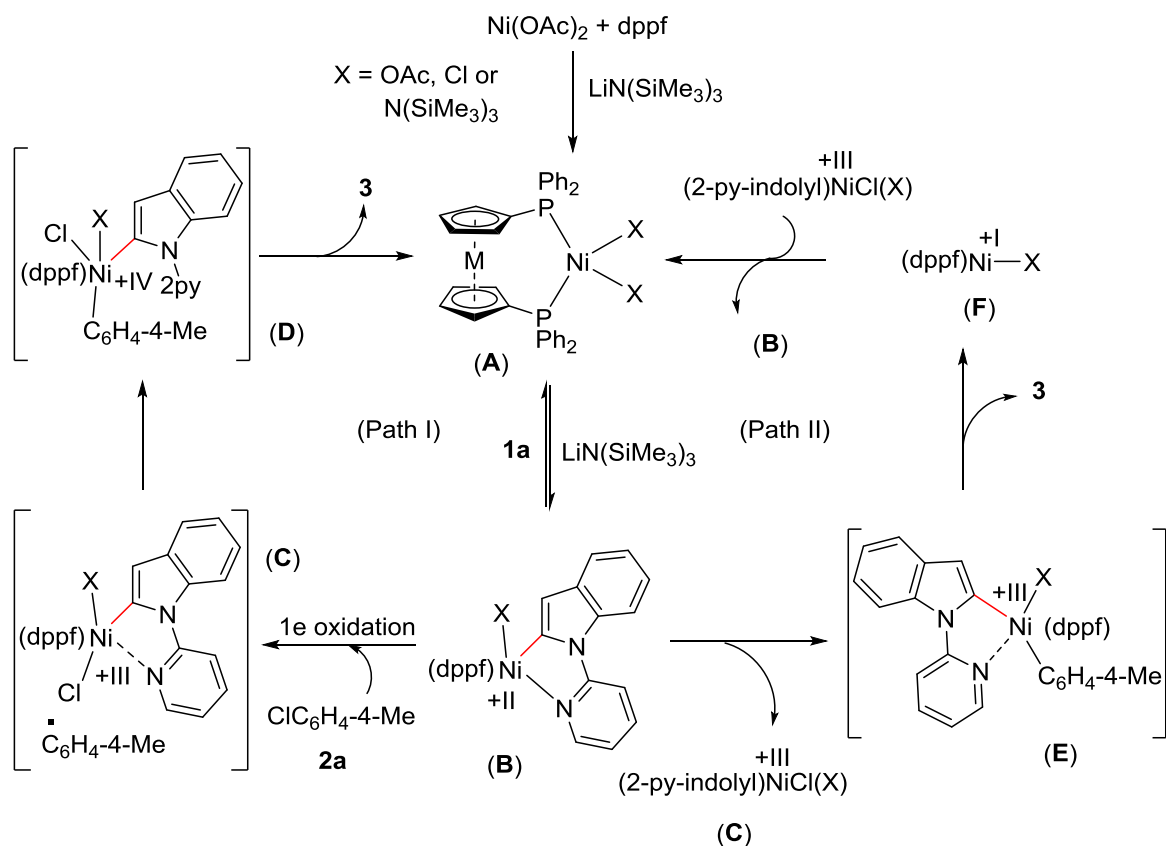


Figure 4.8 Plausible mechanistic pathway for nickel-catalyzed arylation of indoles.

4.3 CONCLUSION

In summary, we have developed a protocol for the coupling of unactivated aryl chlorides with indoles and pyrroles. The use of an inexpensive and air-stable dppf ligand along with a naturally abundant nickel for the coupling of challenging aryl chlorides makes it a desirable approach. This reaction was compatible with a range of simple and functionalized aryl chlorides as well as electronically distinct indoles. The reaction tolerated various functional groups, such as halides, ethers, and amines, as well as heterocyclic pyrrolyl, indolyl and carbazolyl. Based on the mechanistic experiments conducted by kinetics analysis, controlled and labeling experiments, we proposed two probable mechanistic cycles that follows a single electron transfer (SET) pathway involving the rate influencing aryl–Cl bond activation.

4.4 EXPERIMENTAL

4.4.1 General Experimental

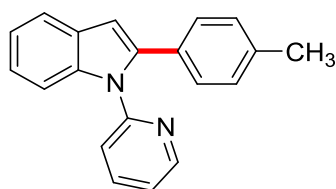
All manipulations were conducted under an argon atmosphere either in a glove box or using standard Schlenk techniques in pre-dried glass wares. The catalytic reactions were performed in flame-dried reaction vessels with Teflon screw cap. Solvents were dried over Na/benzophenone and distilled prior to use. Liquid reagents were flushed with argon prior to use. All other chemicals were obtained from commercial sources and were used without further purification. The aryl chloride electrophiles **2f**,⁶⁶ **2g**,⁶⁷ **2o**,⁶⁸ **2p**,⁶⁹ **2q**,⁷⁰ **2r**,⁷¹ **2t**,⁷² were prepared following the literature procedure. High resolution mass spectroscopy (HRMS) mass spectra were recorded on a Thermo Scientific Q-Exactive, Accela 1250 pump. NMR: (¹H and ¹³C) spectra were recorded at 400 or 500 MHz (¹H), 100 or 125 MHz (¹³C, DEPT (distortionless enhancement by polarization transfer)), 377 MHz (¹⁹F), respectively in CDCl₃ solutions, if not otherwise specified; chemical shifts (δ) are given in ppm. The ¹H and ¹³C NMR spectra are referenced to residual solvent signals (CDCl₃: δ H = 7.26 ppm, δ C = 77.2 ppm).

4.4.2 Representative Procedure for the Arylation

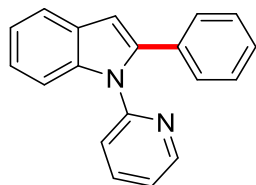
Synthesis of 1-(Pyridin-2-yl)-2-(*p*-tolyl)-*H*-indole (3aa): To a flame-dried screw-cap tube (5 mL) equipped with a magnetic stir bar were introduced 1-pyridin-2-yl-1*H*-indole (**1a**, 0.039 g, 0.20 mmol), 1-chloro-4-methylbenzene (**2a**, 0.051 g, 0.40 mmol), Ni(OAc)₂ (0.02 mmol, 10.0 mol %), dppf (0.02 mmol, 10.0 mol %) and LiHMDS (0.067 g, 0.40 mmol) inside the glove box.

The resultant reaction mixture was stirred at 80 °C in a preheated oil bath for 16 h. At ambient temperature, the reaction mixture was quenched with distilled H₂O (10 mL) and then neutralized with 2N HCl (0.5 mL). The crude product was then extracted with EtOAc (20 mL × 3). The combined organic extract was dried over Na₂SO₄, and the volatiles were evaporated *in vacuo*. The remaining residue was purified by column chromatography on silica gel (petroleum ether/EtOAc: 20/1).

4.4.3 Characterization Data of Arylated Indole Derivatives

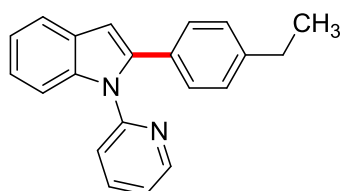


1-(Pyridin-2-yl)-2-(*p*-tolyl)-*H*-indole (3aa): (0.052 g, 91%) as a light yellow solid. ¹H-NMR (500 MHz, CDCl₃): δ = 8.68 (dd, *J* = 5.0, 1.1 Hz, 1H, Ar-H), 7.76-7.67 (m, 2H, Ar-H), 7.65 (td, *J* = 7.8, 1.9 Hz, 1H, Ar-H), 7.29-7.16 (m, 5H, Ar-H), 7.12 (d, *J* = 8.0 Hz, 2H, Ar-H), 6.93 (d, *J* = 8.0 Hz, 1H, Ar-H), 6.81 (s, 1H, Ar-H), 2.37 (s, 3H, CH₃). ¹³C{¹H}-NMR (125 MHz, CDCl₃): δ = 152.4 (C_q), 149.3 (CH), 140.3 (C_q), 138.6 (C_q), 137.9 (CH), 137.5 (C_q), 130.0 (C_q), 129.2 (2C, CH), 129.0 (C_q), 128.8 (2C, CH), 123.0 (CH), 122.2 (CH), 121.7 (CH), 121.5 (CH), 120.6 (CH), 111.7 (CH), 105.3 (CH), 21.4 (CH₃). HRMS (ESI): *m/z* Calcd for C₂₀H₁₆N₂+H⁺ [M+H]⁺ 285.1386; Found 285.1384. The ¹H and ¹³C spectra are consistent with those reported in the literature.⁶⁵

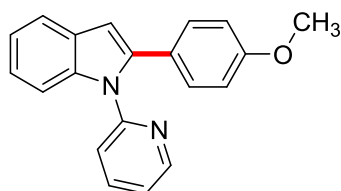


2-Phenyl-1-(pyridin-2-yl)-*H*-indole (3ab): The representative procedure was followed, using substrate **1a** (0.039 g, 0.20 mmol) and chlorobenzene (**2b**; 0.045 g, 0.40 mmol), and the reaction mixture was stirred for 16 h. Purification by column chromatography on silica gel (petroleum ether/EtOAc: 20/1) yielded **3ab** (0.050 g, 92%) as a light yellow solid. ¹H-NMR (400 MHz, CDCl₃): δ = 8.64 (d, *J* = 3.7 Hz, 1H, Ar-H), 7.77-7.64 (m, 2H, Ar-H), 7.60 (td, *J* = 7.6, 1.8 Hz,

1H, Ar-H), 7.32-7.25 (m, 5H, Ar-H), 7.25-7.17 (m, 3H, Ar-H), 6.89 (d, $J = 7.9$ Hz, 1H, Ar-H), 6.82 (s, 1H, Ar-H). $^{13}\text{C}\{^1\text{H}\}$ -NMR (100 MHz, CDCl_3): $\delta = 152.2$ (C_q), 149.3 (CH), 140.1 (C_q), 138.7 (C_q), 137.9 (CH), 132.8 (C_q), 128.9 (C_q), 128.9 (2C, CH), 128.5 (2C, CH), 127.6 (CH), 123.2 (CH), 122.2 (CH), 121.8 (CH), 121.5 (CH), 120.7 (CH), 111.7 (CH), 105.8 (CH). HRMS (ESI): m/z Calcd for $\text{C}_{19}\text{H}_{14}\text{N}_2+\text{H}^+$ $[\text{M}+\text{H}]^+$ 271.1230; Found 271.1229. The ^1H and ^{13}C spectra are consistent with those reported in the literature.⁷³

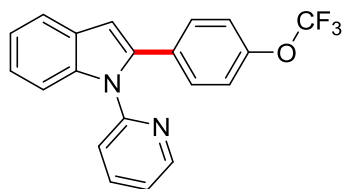


2-(4-Ethylphenyl)-1-(pyridin-2-yl)-1H-indole (3ac): The representative procedure was followed, using substrate **1a** (0.039 g, 0.20 mmol) and 1-chloro-4-ethylbenzene (**2c**; 0.056 g, 0.40 mmol), and the reaction mixture was stirred for 16 h. Purification by column chromatography on silica gel (petroleum ether/EtOAc: 20/1) yielded **3ac** (0.055 g, 92%) as a light yellow solid. ^1H -NMR (400 MHz, CDCl_3): $\delta = 8.74$ -8.64 (m, 1H, Ar-H), 7.77-7.69 (m, 2H, Ar-H), 7.65 (td, $J = 7.8, 1.9$ Hz, 1H, Ar-H), 7.30-7.21 (m, 5H, Ar-H), 7.19-7.11 (m, 2H, Ar-H), 6.95 (d, $J = 8.4$ Hz, 1H, Ar-H), 6.84 (s, 1H, Ar-H), 2.68 (q, $J = 7.6$ Hz, 2H, CH_2), 1.28 (t, $J = 7.6$ Hz, 3H, CH_3). $^{13}\text{C}\{^1\text{H}\}$ -NMR (100 MHz, CDCl_3): $\delta = 152.4$ (C_q), 149.3 (CH), 143.8 (C_q), 140.3 (C_q), 138.6 (C_q), 137.9 (CH), 130.1 (C_q), 129.0 (C_q), 128.8 (2C, CH), 128.0 (2C, CH), 123.0 (CH), 122.3 (CH), 121.7 (CH), 121.4 (CH), 120.6 (CH), 111.6 (CH), 105.4 (CH), 28.7 (CH_2), 15.5 (CH_3). HRMS (ESI): m/z Calcd for $\text{C}_{21}\text{H}_{18}\text{N}_2+\text{H}^+$ $[\text{M}+\text{H}]^+$ 299.1543; Found 299.1541. The ^1H and ^{13}C spectra are consistent with those reported in the literature.⁵⁷

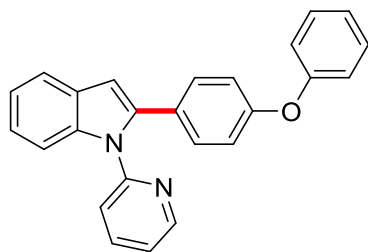


2-(4-Methoxyphenyl)-1-(pyridin-2-yl)-1H-indole (3ad): The representative procedure was followed, using substrate **1a** (0.039 g, 0.20 mmol) and 1-chloro-4-methoxybenzene (**2d**; 0.057 g, 0.40 mmol), and the reaction mixture was stirred for 16 h. Purification by column chromatography on silica gel (petroleum ether/EtOAc: 20/1) yielded **3ad** (0.053 g, 88%) as a

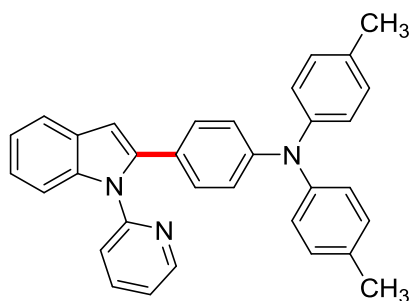
light yellow solid. $^1\text{H-NMR}$ (400 MHz, CDCl_3): δ = 8.65 (d, J = 3.8 Hz, 1H, Ar-H), 7.76-7.55 (m, 3H, Ar-H), 7.30-7.12 (m, 5H, Ar-H), 6.89 (d, J = 7.6 Hz, 1H, Ar-H), 6.82 (d, J = 8.4 Hz, 2H, Ar-H), 6.74 (s, 1H, Ar-H), 3.79 (s, 3H, CH_3). $^{13}\text{C}\{^1\text{H}\}$ -NMR (100 MHz, CDCl_3): δ = 159.2 (C_q), 152.3 (C_q), 149.3 (CH), 140.0 (C_q), 138.5 (C_q), 137.9 (CH), 130.1 (2C, CH), 128.9 (C_q), 125.3 (C_q), 122.8 (CH), 122.2 (CH), 121.7 (CH), 121.4 (CH), 120.5 (CH), 114.0 (2C, CH), 111.6 (CH), 104.8 (CH), 55.4 (CH_3). HRMS (ESI): m/z Calcd for $\text{C}_{20}\text{H}_{16}\text{N}_2\text{O}+\text{H}^+$ $[\text{M}+\text{H}]^+$ 301.1335; Found 301.1334. The ^1H and ^{13}C spectra are consistent with those reported in the literature.⁶⁵



1-(Pyridin-2-yl)-2-(4-(trifluoromethoxy)phenyl)-1H-indole (3ae): The representative procedure was followed, using substrate **1a** (0.039 g, 0.20 mmol) and 1-chloro-4-(trifluoromethoxy)benzene (**2e**; 0.079 g, 0.40 mmol), and the reaction mixture was stirred for 16 h. Purification by column chromatography on silica gel (petroleum ether/EtOAc: 20/1) yielded **3ae** (0.043 g, 61%) as a light yellow liquid. $^1\text{H-NMR}$ (500 MHz, CDCl_3): δ = 8.67 (d, J = 3.8 Hz, 1H, Ar-H), 7.79-7.68 (m, 2H, Ar-H), 7.66 (d, J = 8.4 Hz, 1H, Ar-H), 7.33-7.23 (m, 5H, Ar-H), 7.15 (d, J = 8.0 Hz, 2H, Ar-H), 6.99 (d, J = 8.0 Hz, 1H, Ar-H) 6.84 (s, 1H, Ar-H). $^{13}\text{C}\{^1\text{H}\}$ -NMR (125 MHz, CDCl_3): δ = 151.9 (C_q), 149.6 (CH), 148.7 (C_q), 138.7 (d, $^3J_{\text{C-F}}$ = 11.6 Hz, C_q), 138.3 (CH), 131.6 (C_q), 130.1 (2C, CH), 128.9 (CH), 128.7 (C_q), 128.5 (CH), 123.6 (CH), 123.2 (CH), 122.2 (d, $^4J_{\text{C-F}}$ = 2.3 Hz, CH), 121.7 (CH), 120.8 (C_q), 121.0 (2C, CH), 111.6 (CH), 106.3 (CH). $^{19}\text{F-NMR}$ (377 MHz, CDCl_3): δ = -57.8 (s). HRMS (ESI): m/z Calcd for $\text{C}_{20}\text{H}_{13}\text{ON}_2\text{F}_3+\text{H}^+$ $[\text{M}+\text{H}]^+$ 355.1053; Found 355.1050.

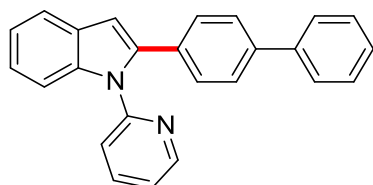


2-(4-Phenoxyphenyl)-1-(pyridin-2-yl)-1H-indole (3af): The representative procedure was followed, using substrate **1a** (0.039 g, 0.20 mmol) and 1-chloro-4-phenoxybenzene (**2f**; 0.082 g, 0.40 mmol), and the reaction mixture was stirred for 16 h. Purification by column chromatography on silica gel (petroleum ether/EtOAc: 20/1) yielded **3af** (0.065 g, 90%) as a light yellow solid. $^1\text{H-NMR}$ (400 MHz, CDCl_3): δ = 8.68 (dd, J = 5.3, 1.5 Hz, 1H, Ar-H), 7.76-7.64 (m, 3H, Ar-H), 7.43-7.34 (m, 2H, Ar-H), 7.30-7.21 (m, 5H, Ar-H), 7.19-7.12 (m, 1H, Ar-H), 7.07 (d, J = 7.6 Hz, 2H, Ar-H), 7.01-6.91 (m, 3H, Ar-H), 6.82 (s, 1H, Ar-H). $^{13}\text{C}\{^1\text{H}\}$ -NMR (100 MHz, CDCl_3): δ = 157.1 (C_q), 156.8 (C_q), 152.2 (C_q), 149.4 (CH), 139.6 (C_q), 138.6 (C_q), 138.0 (CH), 130.3 (2C, CH), 130.0 (2C, CH), 128.9 (C_q), 127.7 (C_q), 123.8 (CH), 123.1 (CH), 122.2 (CH), 121.9 (CH), 121.5 (CH), 120.6 (CH), 119.5 (2C, CH), 118.5 (2C, CH), 111.6 (CH), 105.3 (CH). HRMS (ESI): m/z Calcd for $\text{C}_{25}\text{H}_{18}\text{N}_2\text{O}+\text{H}^+$ $[\text{M}+\text{H}]^+$ 363.1492; Found 363.1492.

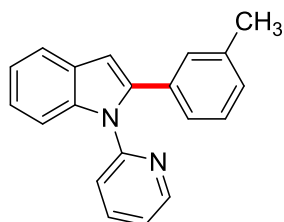


4-Methyl-N-(4-(1-(pyridin-2-yl)-1H-indol-2-yl)phenyl)-N-(p-tolyl)aniline (3ag): The representative procedure was followed, using substrate **1a** (0.039 g, 0.20 mmol) and 4-chloro-*N,N*-di-*p*-tolylaniline (**2g**; 0.123 g, 0.40 mmol), and the reaction mixture was stirred for 16 h. Purification by column chromatography on silica gel (petroleum ether/EtOAc: 10/1) yielded **3ag** (0.080 g, 0.86%) as a light yellow solid. $^1\text{H-NMR}$ (400 MHz, CDCl_3): δ = 8.67-8.57 (m, 1H, Ar-H), 7.72-7.57 (m, 3H, Ar-H), 7.25-7.12 (m, 3H, Ar-H), 7.09-7.02 (m, 6H, Ar-H), 7.01-6.94 (m, 5H, Ar-H), 6.87 (d, J = 8.4 Hz, 2H, Ar-H), 6.73 (s, 1H, Ar-H), 2.29 (s, 6H, CH_3). $^{13}\text{C}\{^1\text{H}\}$ -NMR (125 MHz, CDCl_3): δ = 152.4 (C_q), 149.3 (CH), 147.7 (C_q), 145.0 (2C, C_q), 140.3 (C_q), 138.6 (C_q), 137.9 (CH), 133.1 (2C, C_q), 130.1 (4C, CH), 129.5 (2C, CH), 129.0 (C_q), 125.0 (C_q),

125.2 (4C, CH), 122.8 (CH), 122.3 (CH), 121.8 (CH), 121.4 (2C, CH), 121.3 (CH), 120.4 (CH), 111.5 (CH), 104.7 (CH), 21.0 (2C, CH₃). HRMS (ESI): m/z Calcd for C₃₃H₂₇N₃+H⁺ [M+H]⁺ 466.2278; Found 466.2276.

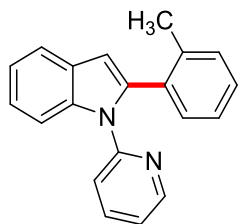


2-([1,1'-Biphenyl]-4-yl)-1-(pyridin-2-yl)-1H-indole (3ah): The representative procedure was followed, using substrate **1a** (0.039 g, 0.20 mmol) and 4-chloro-1,1'-biphenyl (**2h**; 0.075 g, 0.40 mmol), and the reaction mixture was stirred for 16 h. Purification by column chromatography on silica gel (petroleum ether/EtOAc: 20/1) yielded **3ah** (0.066 g, 95%) as a light yellow solid. ¹H-NMR (500 MHz, CDCl₃): δ = 8.76-8.61 (m, 1H, Ar-H), 7.78-7.69 (m, 2H, Ar-H), 7.67 (t, J = 7.2 Hz, 1H, Ar-H), 7.61 (d, J = 7.6 Hz, 2H, Ar-H), 7.55 (d, J = 8.0 Hz, 2H, Ar-H), 7.46 (t, J = 7.2 Hz, 2H, Ar-H), 7.38 (m, 3H, Ar-H), 7.30-7.20 (m, 3H, Ar-H), 7.00 (d, J = 8.0 Hz, 1H, Ar-H), 6.90 (s, 1H, Ar-H). ¹³C{¹H}-NMR (125 MHz, CDCl₃): δ = 152.3 (C_q), 149.4 (CH), 140.5 (C_q), 140.2 (C_q), 139.8 (C_q), 138.8 (C_q), 138.0 (CH), 131.8 (C_q), 129.2 (2C, CH), 129.0 (2C, CH), 128.9 (C_q), 127.6 (CH), 127.1 (2C, CH), 127.0 (2C, CH), 123.3 (CH), 122.3 (CH), 121.9 (CH), 121.6 (CH), 120.8 (CH), 111.7 (CH), 105.9 (CH). HRMS (ESI): m/z Calcd for C₂₅H₁₈N₂+H⁺ [M+H]⁺ 347.1543; Found 347.1541.

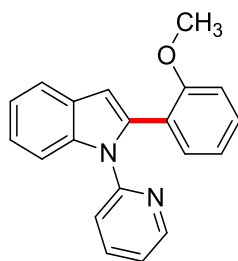


1-(Pyridin-2-yl)-2-(*m*-tolyl)-1H-indole (3ai): The representative procedure was followed, using substrate **1a** (0.039 g, 0.20 mmol) and 1-chloro-3-methylbenzene (**2i**; 0.051 g, 0.40 mmol), and the reaction mixture was stirred for 16 h. Purification by column chromatography on silica gel (petroleum ether/EtOAc: 20/1) yielded **3ai** (0.050 g, 88%) as a light yellow solid. ¹H-NMR (400 MHz, CDCl₃): δ = 8.65 (d, J = 4.6 Hz, 1H, Ar-H), 7.69 (t, J = 7.6 Hz, 2H, Ar-H), 7.62 (t, J = 7.6 Hz, 1H, Ar-H), 7.28-7.16 (m, 4H, Ar-H), 7.14 (d, J = 7.6 Hz, 1H, Ar-H), 7.11-7.05 (m, 1H, Ar-

H), 7.01 (d, $J = 7.6$ Hz, 1H, Ar-H), 6.91 (d, $J = 7.6$ Hz, 1H, Ar-H), 6.81 (s, 1H, Ar-H) 2.30 (s, CH₃). ¹³C{¹H}-NMR (100 MHz, CDCl₃): $\delta = 152.3$ (C_q), 149.3 (CH), 140.3 (C_q), 138.6 (C_q), 138.2 (C_q), 137.9 (CH), 132.7 (C_q), 129.6 (CH), 128.9 (C_q), 128.4 (CH), 128.3 (CH), 126.0 (CH), 123.1 (CH), 122.2 (CH), 121.7 (CH), 121.5 (CH), 120.7 (CH), 111.6 (CH), 105.6 (CH), 21.6 (CH₃). HRMS (ESI): m/z Calcd for C₂₀H₁₆N₂+H⁺ [M+H]⁺ 285.1386; Found 285.1385. The ¹H and ¹³C spectra are consistent with those reported in the literature.⁵⁷

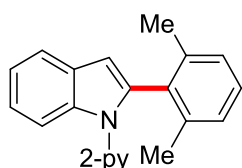


1-(Pyridin-2-yl)-2-(*o*-tolyl)-1*H*-indole (3aj): The representative procedure was followed, using substrate **1a** (0.039 g, 0.20 mmol) and 1-chloro-2-methylbenzene (**2j**; 0.051 g, 0.40 mmol), and the reaction mixture was stirred for 16 h. Purification by column chromatography on silica gel (petroleum ether/EtOAc: 20/1) yielded **3aj** (0.046 g, 81%) as a light yellow solid. ¹H-NMR (400 MHz, CDCl₃): $\delta = 8.66$ -8.53 (m, 1H, Ar-H), 7.88 (d, $J = 7.6$ Hz, 1H, Ar-H), 7.74-7.65 (m, 1H, Ar-H), 7.50 (td, $J = 7.8, 1.9$ Hz, 1H, Ar-H), 7.36-7.31 (m, 1H, Ar-H), 7.31-7.21 (m, 3H, Ar-H), 7.21-7.10 (m, 3H, Ar-H), 6.72 (d, $J = 7.6$ Hz, 1H, Ar-H), 6.69 (s, 1H, Ar-H), 2.08 (s, 3H, CH₃). ¹³C{¹H}-NMR (125 MHz, CDCl₃): $\delta = 152.0$ (C_q), 149.0 (CH), 139.1 (C_q), 137.7 (CH), 137.6 (C_q), 137.3 (C_q), 132.9 (C_q), 131.2 (CH), 130.3 (CH), 128.8 (C_q), 128.4 (CH), 125.8 (CH), 123.0 (CH), 121.4 (CH), 121.2 (CH) 120.7 (CH), 120.5 (CH), 112.1 (CH), 106.3 (CH), 20.3 (CH₃). HRMS (ESI): m/z Calcd for C₂₀H₁₆N₂+H⁺ [M+H]⁺ 285.1386; Found 285.1385. The ¹H and ¹³C spectra are consistent with those reported in the literature.⁶⁵

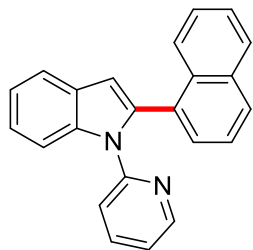


2-(2-Methoxyphenyl)-1-(pyridin-2-yl)-1*H*-indole (3ak): The representative procedure was followed, using substrate **1a** (0.039 g, 0.20 mmol) and 1-chloro-2-methoxybenzene (**2k**; 0.057 g,

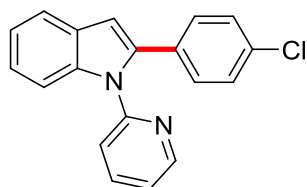
0.40 mmol), and the reaction mixture was stirred for 16 h. Purification by column chromatography on silica gel (petroleum ether/EtOAc: 20/1) yielded **3ak** (0.025 g, 42%) as a light yellow solid. $^1\text{H-NMR}$ (400 MHz, CDCl_3): δ = 8.58 (dd, J = 4.6, 1.5 Hz, 1H, Ar-H), 7.81 (d, J = 8.4 Hz, 1H, Ar-H), 7.67 (d, J = 6.9 Hz, 1H, Ar-H), 7.56 (td, J = 7.8, 1.9 Hz, 1H, Ar-H), 7.48 (dd, J = 7.6, 1.5 Hz, 1H, Ar-H), 7.32 (td, J = 7.6, 1.5 Hz, 1H, Ar-H), 7.27-7.11 (m, 3H, Ar-H), 7.02 (t, J = 7.6 Hz, 1H, Ar-H), 6.90 (d, J = 7.6 Hz, 1H, Ar-H), 6.78-6.70 (m, 2H, Ar-H), 3.32 (s, 3H, CH_3). $^{13}\text{C}\{^1\text{H}\}\text{-NMR}$ (100 MHz, CDCl_3): δ = 156.5 (C_q), 152.9 (C_q), 148.8 (CH), 137.5 (C_q), 137.4 (CH), 137.3 (C_q), 131.8 (CH), 129.9 (CH), 128.8 (C_q), 123.0 (CH), 122.5 (C_q), 121.1 (CH), 121.0 (CH), 121.0 (CH), 120.6 (CH), 119.8 (CH), 111.8 (CH), 110.9 (CH), 106.3 (CH), 54.9 (CH_3). HRMS (ESI): m/z Calcd for $\text{C}_{20}\text{H}_{16}\text{N}_2\text{O}+\text{H}^+$ $[\text{M}+\text{H}]^+$ 301.1335; Found 301.1334. The ^1H and ^{13}C spectra are consistent with those reported in the literature.⁵⁴



2-(3,5-Dimethylphenyl)-1-(pyridin-2-yl)-1H-indole (3al): The representative procedure was followed, using substrate **1a** (0.039 g, 0.20 mmol) and 2-chloro-1,3-dimethylbenzene (**2l**; 0.056 g, 0.40 mmol), and the reaction mixture was stirred for 16 h. Purification by column chromatography on silica gel (petroleum ether/EtOAc: 20/1) yielded **3al** (0.049 g, 82%) as a light yellow solid. $^1\text{H-NMR}$ (400 MHz, CDCl_3): δ = 8.56-8.50 (m, 1H, Ar-H), 7.87 (d, J = 8.4 Hz, 1H, Ar-H), 7.72-7.67 (m, 1H, Ar-H), 7.49 (td, J = 7.8, 1.9 Hz, 1H, Ar-H), 7.34-7.20 (m, 2H, Ar-H), 7.20-7.13 (m, 1H, Ar-H), 7.10 (dd, J = 6.9, 5.3 Hz, 1H, Ar-H), 7.03 (d, J = 7.6 Hz, 2H, Ar-H), 6.71 (d, J = 7.6 Hz, 1H, Ar-H), 6.57 (s, 1H, Ar-H), 2.09 (s, 6H, CH_3). $^{13}\text{C}\{^1\text{H}\}\text{-NMR}$ (100 MHz, CDCl_3): δ = 151.8 (C_q), 149.0 (CH), 138.6 (2c, C_q), 137.7 (CH), 137.6 (C_q), 136.8 (C_q), 132.7 (C_q), 129.0 (C_q), 128.6 (CH), 127.4 (2C, CH), 122.7 (CH), 121.3 (CH), 121.2 (CH), 120.5 (CH), 119.6 (CH), 112.4 (CH), 105.6 (CH), 20.8 (2C, CH_3). HRMS (ESI): m/z Calcd for $\text{C}_{21}\text{H}_{18}\text{N}_2+\text{H}^+$ $[\text{M}+\text{H}]^+$ 299.1543; Found 299.1541.

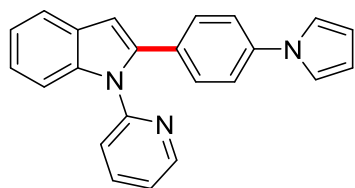


2-(Naphthalen-1-yl)-1-(pyridin-2-yl)-1H-indole (3am): The representative procedure was followed, using substrate **1a** (0.039 g, 0.20 mmol) and 1-chloronaphthalene (**2m**; 0.065 g, 0.40 mmol), and the reaction mixture was stirred for 16 h. Purification by column chromatography on silica gel (petroleum ether/EtOAc: 20/1) yielded **3am** (0.061 g, 95%) as a light yellow solid. $^1\text{H-NMR}$ (400 MHz, CDCl_3): δ = 8.50 (d, J = 3.8 Hz, 1H, Ar-H), 8.01 (d, J = 8.4 Hz, 1H, Ar-H), 7.87 (d, J = 8.4 Hz, 1H, Ar-H), 7.80 (d, J = 8.4 Hz, 2H, Ar-H), 7.72 (d, J = 6.9 Hz, 1H, Ar-H), 7.44-7.22 (m, 7H, Ar-H), 6.97 (dd, J = 6.9, 5.3 Hz, 1H, Ar-H), 6.85 (s, 1H, Ar-H), 6.62 (d, J = 8.4 Hz, 1H, Ar-H). $^{13}\text{C}\{^1\text{H}\}$ -NMR (100 MHz, CDCl_3): δ = 152.0 (C_q), 148.9 (CH), 137.8 (C_q), 137.7 (C_q), 137.6 (CH), 133.6 (C_q), 132.3 (C_q), 130.7 (C_q), 129.1 (CH), 128.8 (C_q), 128.7 (CH), 128.3 (CH), 126.6 (CH), 126.1 (2C, CH), 125.2 (CH), 123.3 (CH), 121.6 (CH), 121.3 (CH), 120.8 (CH), 120.7 (CH), 112.1 (CH), 107.8 (CH). HRMS (ESI): m/z Calcd for $\text{C}_{23}\text{H}_{16}\text{N}_2+\text{H}^+$ $[\text{M}+\text{H}]^+$ 321.1386; Found 321.1385.

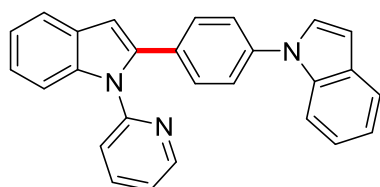


2-(4-Chlorophenyl)-1-(pyridin-2-yl)-1H-indole (3an): The representative procedure was followed, using substrate **1a** (0.039 g, 0.20 mmol) and 1-chloro-4-iodobenzene (**2n**; 0.095 g, 0.40 mmol), and the reaction mixture was stirred for 16 h. Purification by column chromatography on silica gel (petroleum ether/EtOAc: 20/1) yielded **3an** (0.031 g, 51%) as a light yellow liquid. $^1\text{H-NMR}$ (400 MHz, CDCl_3): δ = 8.68-8.52 (m, 1H, Ar-H), 7.70-7.57 (m, 3H, Ar-H), 7.31-7.13 (m, 7H, Ar-H), 6.92 (d, J = 7.6 Hz, 1H, Ar-H), 6.79 (s, 1H, Ar-H). $^{13}\text{C}\{^1\text{H}\}$ -NMR (100 MHz, CDCl_3): δ = 151.9 (C_q), 149.5 (CH), 138.9 (C_q), 138.7 (C_q), 138.2 (CH), 133.6 (C_q), 131.3 (C_q), 130.0 (2C, CH), 128.7 (2C, CH), 128.4 (C_q), 123.5 (CH), 122.1 (CH), 122.0 (CH), 121.7 (CH), 120.8 (CH), 111.6 (CH), 106.1 (CH). HRMS (ESI): m/z Calcd for $\text{C}_{19}\text{H}_{13}\text{ClN}_2+\text{H}^+$ $[\text{M}+\text{H}]^+$

305.0840; Found 305.0841. The ^1H and ^{13}C spectra are consistent with those reported in the literature.⁶⁵

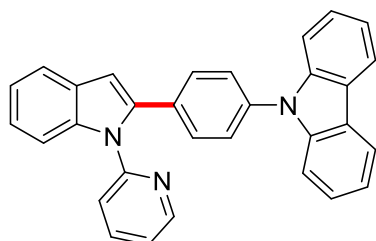


2-(4-(1H-pyrrol-1-yl)phenyl)-1-(pyridin-2-yl)-1H-indole (3ao): The representative procedure was followed, using substrate **1a** (0.039 g, 0.20 mmol) and 1-(4-chlorophenyl)-1H-pyrrole (**2o**; 0.071 g, 0.40 mmol), and the reaction mixture was stirred for 16 h. Purification by column chromatography on silica gel (petroleum ether/EtOAc: 10/1) yielded **3ao** (0.039 g, 58%) as a brown solid. ^1H -NMR (400 MHz, CDCl_3): δ = 8.78-8.60 (m, 1H, Ar-H), 7.81-7.62 (m, 3H, Ar-H), 7.42-7.31 (m, 4H, Ar-H), 7.31-7.22 (m, 3H, Ar-H), 7.12 (br s, 2H, Ar-H), 7.01 (d, J = 7.9 Hz, 1H, Ar-H), 6.87 (s, 1H, Ar-H), 6.38 (br s, 2H, Ar-H). $^{13}\text{C}\{^1\text{H}\}$ -NMR (100 MHz, CDCl_3): δ = 152.2 (C_q), 149.5 (CH), 139.9 (C_q), 139.3 (C_q), 138.8 (C_q), 138.1 (CH), 130.1 (C_q), 130.0 (2C, CH), 128.9 (C_q), 123.3 (CH), 122.2 (CH), 122.0 (CH), 121.6 (CH), 120.8 (CH), 120.2 (2C, CH), 119.2 (2C, CH), 111.6 (CH), 110.9 (2C, CH), 105.8 (CH). HRMS (ESI): m/z Calcd for $\text{C}_{23}\text{H}_{17}\text{N}_3+\text{H}^+$ $[\text{M}+\text{H}]^+$ 336.1495; Found 336.1492. The ^1H and ^{13}C spectra are consistent with those reported in the literature.⁶⁵

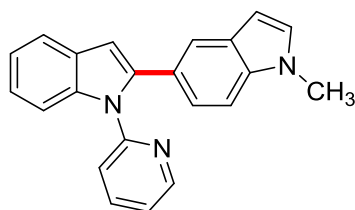


2-(4-(1H-Indol-1-yl)phenyl)-1-(pyridin-2-yl)-1H-indole (3ap): The representative procedure was followed, using substrate **1a** (0.039 g, 0.20 mmol) and 1-(4-chlorophenyl)-1H-indole (**2p**; 0.091 g, 0.40 mmol), and the reaction mixture was stirred for 16 h. Purification by column chromatography on silica gel (petroleum ether/EtOAc: 10/1) yielded **3ap** (0.059 g, 77%) as a light yellow solid. ^1H -NMR (400 MHz, CDCl_3): δ = 8.69 (d, J = 3.8 Hz, 1H, Ar-H), 7.81-7.66 (m, 4H, Ar-H), 7.60 (d, J = 7.6 Hz, 1H, Ar-H), 7.50-7.37 (m, 4H, Ar-H), 7.34 (d, J = 3.1 Hz, 1H, Ar-H), 7.32-7.13 (m, 5H, Ar-H), 7.06 (d, J = 8.4 Hz, 1H, Ar-H), 6.91 (s, 1H, Ar-H), 6.71 (d, J = 3.1 Hz, 1H, Ar-H). $^{13}\text{C}\{^1\text{H}\}$ -NMR (100 MHz, CDCl_3): δ = 152.1 (C_q), 149.5 (CH), 139.2

(C_q), 139.0 (C_q), 138.8 (C_q), 138.2 (CH), 135.7 (C_q), 130.8 (C_q), 129.9 (2C, CH), 129.6 (C_q), 128.8 (C_q), 127.8 (CH), 124.0 (2C, CH), 123.4 (CH), 122.6 (CH), 122.2 (CH), 122.1 (CH), 121.7 (CH), 121.3 (CH), 120.8 (CH), 120.7 (CH), 111.6 (CH), 110.7 (CH), 106.0 (CH), 104.1 (CH). HRMS (ESI): m/z Calcd for C₂₇H₁₉N₃+H⁺ [M+H]⁺ 386.1652; Found 386.1648.

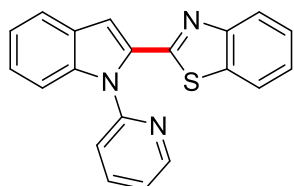


9-(4-(1-(Pyridin-2-yl)-1H-indol-2-yl)phenyl)-9H-carbazole (3aq): The representative procedure was followed, using substrate **1a** (0.039 g, 0.20 mmol) and 9-(4-chlorophenyl)-9H-carbazole (**2q**; 0.111 g, 0.40 mmol), and the reaction mixture was stirred for 16 h. Purification by column chromatography on silica gel (petroleum ether/EtOAc: 10/1) yielded **3aq** (0.058 g, 67%) as a light yellow solid. ¹H-NMR (500 MHz, CDCl₃): δ = 8.76-8.65 (m, 1H, Ar-H), 8.16 (d, J = 7.6 Hz, 2H, Ar-H), 7.84-7.65 (m, 3H, Ar-H), 7.56-7.47 (m, 4H, Ar-H), 7.46-7.38 (m, 4H, Ar-H), 7.37-7.20 (m, 5H, Ar-H), 7.11 (d, J = 8.0 Hz, 1H, Ar-H), 6.95 (s, 1H, Ar-H). ¹³C{¹H}-NMR (125 MHz, CDCl₃): δ = 152.1 (C_q), 149.6 (CH), 140.8 (2C, C_q), 139.3 (C_q), 138.9 (C_q), 138.3 (CH), 137.0 (C_q), 131.8 (C_q), 130.1 (2C, CH), 128.9 (C_q), 126.9 (2C, CH), 126.1 (2C, CH), 123.7 (2C, C_q), 123.5 (CH), 122.3 (CH), 122.2 (CH), 121.7 (CH), 120.9 (CH), 120.5 (2C, CH), 120.3 (2C, CH), 111.6 (CH), 109.9 (2C, CH), 106.3 (CH). HRMS (ESI): m/z Calcd for C₃₁H₂₁N₃+H⁺ [M+H]⁺ 436.1808; Found 436.1804. The ¹H and ¹³C spectra are consistent with those reported in the literature.⁶⁵

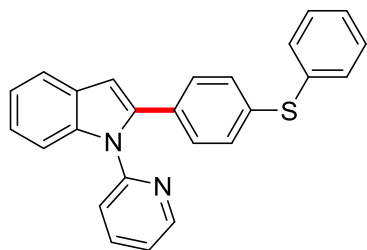


1'-Methyl-1-(pyridin-2-yl)-1H,1'H-2,5'-biindole (3ar): The representative procedure was followed, using substrate **1a** (0.039 g, 0.20 mmol) and 5-chloro-1-methyl-1H-indole (**2r**; 0.066 g, 0.40 mmol), and the reaction mixture was stirred for 16 h. Purification by column chromatography on silica gel (petroleum ether/EtOAc: 20/1) yielded **3ar** (0.040 g, 61%) as a

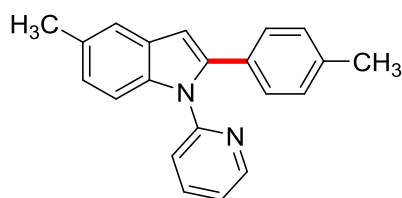
light yellow solid. $^1\text{H-NMR}$ (400 MHz, CDCl_3): δ = 8.68 (dd, J = 5.3, 1.5 Hz, 1H, Ar-H), 7.80-7.73 (m, 1H, Ar-H), 7.71-7.67 (m, 1H, Ar-H), 7.64 (d, J = 1.5 Hz, 1H, Ar-H), 7.52 (td, J = 7.8, 1.9 Hz, 1H, Ar-H), 7.25-7.16 (m, 4H, Ar-H), 7.11 (dd, J = 8.4, 1.5 Hz, 1H, Ar-H), 7.06 (d, J = 3.1 Hz, 1H, Ar-H), 6.84 (d, J = 8.4 Hz, 1H, Ar-H), 6.80 (s, 1H, Ar-H), 6.46 (d, J = 3.1 Hz, 1H, Ar-H), 3.77 (s, 3H, CH_3). $^{13}\text{C}\{^1\text{H}\}\text{-NMR}$ (125 MHz, CDCl_3): δ = 152.6 (C_q), 149.1 (CH), 141.7 (C_q), 138.4 (C_q), 137.8 (CH), 136.3 (C_q), 129.7 (CH), 129.1 (C_q), 128.5 (C_q), 124.1 (C_q), 123.1 (CH), 122.6 (CH), 122.3 (CH), 121.6 (CH), 121.5 (CH), 121.3 (CH), 120.3 (CH), 111.7 (CH), 109.2 (CH), 105.0 (CH), 101.5 (CH), 33.0 (CH_3). HRMS (ESI): m/z Calcd for $\text{C}_{22}\text{H}_{17}\text{N}_3+\text{H}^+$ $[\text{M}+\text{H}]^+$ 324.1495; Found 324.1494.



2-(1-(Pyridin-2-yl)-1H-indol-2-yl)benzo[d]thiazole (3as): The representative procedure was followed, using substrate **1a** (0.039 g, 0.20 mmol) and 2-chlorobenzo[d]thiazole (**2s**; 0.068 g, 0.40 mmol), and the reaction mixture was stirred for 16 h. Purification by column chromatography on silica gel (petroleum ether/EtOAc: 20/1) yielded **3as** (0.038 g, 58%) as a light yellow solid. $^1\text{H-NMR}$ (400 MHz, CDCl_3): δ = 8.64 (d, J = 3.8 Hz, 1H, Ar-H), 7.87-7.77 (m, 3H, Ar-H), 7.74 (d, J = 7.6 Hz, 1H, Ar-H), 7.46 (d, J = 8.4 Hz, 1H, Ar-H), 7.43-7.34 (m, 4H, Ar-H), 7.34-7.27 (m, 2H, Ar-H), 7.27-7.20 (m, 1H, Ar-H). $^{13}\text{C}\{^1\text{H}\}\text{-NMR}$ (100 MHz, CDCl_3): δ = 159.2 (C_q), 153.7 (C_q), 151.4 (C_q), 149.5 (CH), 139.8 (C_q), 138.3 (CH), 135.2 (C_q), 132.7 (C_q), 127.9 (C_q), 126.3 (CH), 125.2 (CH), 125.1 (CH), 123.4 (CH), 123.0 (CH), 122.9 (CH), 121.9 (CH), 121.8 (CH), 121.4 (CH), 111.5 (CH), 109.9 (CH). HRMS (ESI): m/z Calcd for $\text{C}_{20}\text{H}_{13}\text{N}_3\text{S}+\text{H}^+$ $[\text{M}+\text{H}]^+$ 328.0903; Found 328.0900.

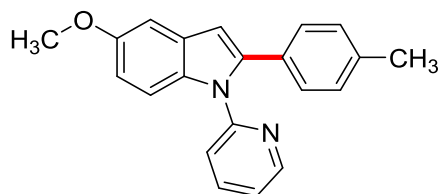


2-(4-(Phenylthio)phenyl)-1-(pyridin-2-yl)-1H-indole (3at): The representative procedure was followed, using substrate **1a** (0.039 g, 0.20 mmol) and (4-chlorophenyl)(phenyl)sulfane (**2t**; 0.088 g, 0.40 mmol), and the reaction mixture was stirred for 16 h. Purification by column chromatography on silica gel (petroleum ether/EtOAc: 20/1) yielded **3at** (0.055 g, 73%) as a light yellow solid. $^1\text{H-NMR}$ (400 MHz, CDCl_3): δ = 8.65 (dd, J = 4.6, 1.5 Hz, 1H, Ar-H), 7.74-7.66 (m, 3H, Ar-H), 7.44-7.38 (m, 2H, Ar-H), 7.37-7.29 (m, 3H, Ar-H), 7.25-7.22 (m, 3H, Ar-H), 7.21 (s, 4H, Ar-H), 6.96 (d, J = 8.4 Hz, 1H, Ar-H), 6.83 (s, 1H, Ar-H). $^{13}\text{C}\{^1\text{H}\}$ -NMR (100 MHz, CDCl_3): δ = 152.0 (C_q), 149.4 (CH), 139.3 (C_q), 138.7 (C_q), 138.1 (CH), 135.8 (C_q), 134.8 (C_q), 131.9 (2C, CH), 131.2 (C_q), 130.1 (2C, CH), 129.4 (2C, CH), 129.4 (2C, CH), 128.8 (C_q), 127.7 (CH), 123.3 (CH), 122.1 (CH), 121.9 (CH), 121.6 (CH), 120.8 (CH), 111.6 (CH), 105.9 (CH). HRMS (ESI): m/z Calcd for $\text{C}_{25}\text{H}_{18}\text{N}_2\text{S}+\text{H}^+$ $[\text{M}+\text{H}]^+$ 379.1263; Found 379.1261.

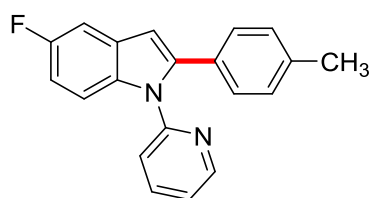


5-Methyl-1-(pyridin-2-yl)-2-(p-tolyl)-1H-indole (3ba): The representative procedure was followed, using substrate 5-methyl-1-(pyridin-2-yl)-1H-indole (**3b**) (0.042 g, 0.20 mmol) and 1-chloro-4-methylbenzene (**2a**; 0.051 g, 0.40 mmol), and the reaction mixture was stirred for 16 h. Purification by column chromatography on silica gel (petroleum ether/EtOAc: 20/1) yielded **3ba** (0.049 g, 82%) as a light yellow solid. $^1\text{H-NMR}$ (400 MHz, CDCl_3): δ = 8.62 (dd, J = 4.6, 1.5 Hz, 1H, Ar-H), 7.65-7.52 (m, 2H, Ar-H), 7.43 (s, 1H, Ar-H), 7.22-7.11 (m, 3H, Ar-H), 7.10-6.98 (m, 3H, Ar-H), 6.86 (d, J = 8.4 Hz, 1H, Ar-H), 6.69 (s, 1H, Ar-H), 2.45 (s, 3H, CH_3), 2.32 (3H, CH_3). $^{13}\text{C}\{^1\text{H}\}$ -NMR (100 MHz, CDCl_3): δ = 152.5 (C_q), 149.2 (CH), 140.2 (C_q), 137.8 (CH), 137.3 (C_q), 137.0 (C_q), 130.7 (C_q), 130.1 (C_q), 129.5 (C_q), 129.1 (2C, CH), 128.7 (2C, CH), 124.5 (CH), 122.1 (CH), 121.5 (CH), 120.3 (CH), 111.4 (CH), 105.1 (CH), 21.6 (CH_3),

21.4 (CH₃). HRMS (ESI): m/z Calcd for C₂₁H₁₈N₂+H⁺ [M+H]⁺ 299.1543; Found 299.1541. The ¹H and ¹³C spectra are consistent with those reported in the literature.⁶⁵

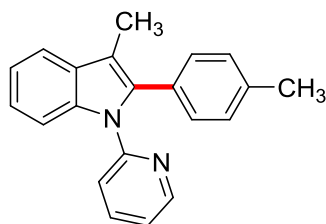


5-Methoxy-1-(pyridin-2-yl)-2-(p-tolyl)-1H-indole (3ca): The representative procedure was followed, using substrate 5-methoxy-1-(pyridin-2-yl)-1H-indole (**3c**) (0.045 g, 0.20 mmol) and 1-chloro-4-methylbenzene (**2a**; 0.051 g, 0.40 mmol), and the reaction mixture was stirred for 16 h. Purification by column chromatography on silica gel (petroleum ether/EtOAc: 20/1) yielded **3ca** (0.050 g, 79%) as a light yellow solid. ¹H-NMR (500 MHz, CDCl₃): δ = 8.66-8.59 (m, 1H, Ar-H), 7.65-7.55 (m, 2H, Ar-H), 7.20 (dd, J = 7.1, 5.1 Hz, 1H, Ar-H), 7.18-7.14 (m, 2H, Ar-H), 7.12 (d, J = 2.7 Hz, 1H, Ar-H), 7.08 (m, 2H, Ar-H), 6.90-6.81 (m, 2H, Ar-H), 6.70 (s, 1H, Ar-H), 3.88 (s, 3H, OCH₃), 2.33 (s, 3H, CH₃). ¹³C{¹H}-NMR (125 MHz, CDCl₃): δ = 155.4 (C_q), 152.5 (C_q), 149.2 (CH), 140.8 (C_q), 137.9 (CH), 137.5 (C_q), 133.9 (C_q), 130.0 (C_q), 129.5 (C_q), 129.2 (2C, CH), 128.8 (2C, CH), 122.0 (CH), 121.5 (CH), 112.8 (CH), 112.6 (CH), 105.3 (CH), 102.5 (CH). 56.0 (OCH₃), 21.4 (CH₃). HRMS (ESI): m/z Calcd for C₂₁H₁₈N₂O+H⁺ [M+H]⁺ 315.1492; Found 315.1490.

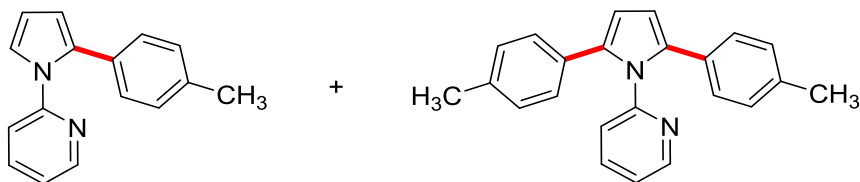


5-Fluoro-1-(pyridin-2-yl)-2-(p-tolyl)-1H-indole (3da): The representative procedure was followed, using substrate 5-fluoro-1-(pyridin-2-yl)-1H-indole (**3d**) (0.042 g, 0.20 mmol) and 1-chloro-4-methylbenzene (**2a**; 0.051 g, 0.40 mmol), and the reaction mixture was stirred for 16 h. Purification by column chromatography on silica gel (petroleum ether/EtOAc: 20/1) yielded **3da** (0.025 g, 41%) as a light yellow solid. ¹H-NMR (400 MHz, CDCl₃): δ = 8.69-8.61 (m, 1H, Ar-H), 7.66-7.58 (m, 2H, Ar-H), 7.32-7.27 (m, 1H, Ar-H), 7.26-7.21 (m, 1H, Ar-H), 7.18-7.13 (m, 2H, Ar-H), 7.13-7.05 (m, 2H, Ar-H), 6.95 (td, J = 9.2, 3.1 Hz, 1H, Ar-H), 6.85 (d, J = 7.6 Hz,

1H, Ar-H), 6.72 (s, 1H, Ar-H), 2.34 (s, 3H, CH₃). ¹³C{¹H}-NMR (100 MHz, CDCl₃): δ = 158.9 (C_q), 157.7 (C_q), 152.1 (C_q), 149.3 (CH), 141.7 (C_q), 138.0 (CH), 136.5 (d, ¹J_{C-F} = 279.9 Hz, C_q), 129.5 (d, ³J_{C-F} = 19.2 Hz, C_q), 129.3 (C_q), 129.2 (CH), 128.8 (CH), 128.7 (d, ²J_{C-F} = 35.5 Hz, CH), 122.2 (CH), 121.9 (CH), 112.6 (d, ⁴J_{C-F} = 9.6 Hz, CH), 111.5 (d, ³J_{C-F} = 25.9 Hz, CH), 105.6 (CH), 105.3 (CH), 105.1 (d, ⁴J_{C-F} = 3.8 Hz, CH), 21.4 (CH₃). ¹⁹F-NMR (377 MHz, CDCl₃): δ = -123.08 (s). HRMS (ESI): *m/z* Calcd for C₂₀H₁₅N₂F+H⁺ [M+H]⁺ 303.1292.



3-Methyl-1-(pyridin-2-yl)-2-(p-tolyl)-1H-indole (3ea): The representative procedure was followed, using substrate 3-methyl-1-(pyridin-2-yl)-1H-indole (**3e**) (0.042 g, 0.20 mmol) and 1-chloro-4-methylbenzene (**2a**; 0.051 g, 0.40 mmol), and the reaction mixture was stirred for 16 h. Purification by column chromatography on silica gel (petroleum ether/EtOAc: 20/1) yielded **3ea** (0.040 g, 67%) as a light yellow liquid. ¹H-NMR (400 MHz, CDCl₃): δ = 8.62 (d, *J* = 3.7 Hz, 1H, Ar-H), 7.77 (d, *J* = .3 Hz, 1H, Ar-H), 7.66 (d, *J* = 6.7 Hz, 1H, Ar-H), 7.56 (t, *J* = 7.0 Hz, 1H, Ar-H), 7.39-7.23 (m, 3H, Ar-H), 7.20-7.11 (m, 4H, Ar-H), 6.78 (d, *J* = 7.9 Hz, 1H, Ar-H), 2.42 (s, 3H, CH₃), 2.38 (s, 3H, CH₃). ¹³C{¹H}-NMR (100 MHz, CDCl₃): δ = 152.5 (C_q), 149.0 (CH), 137.6 (CH), 137.4 (C_q), 137.2 (C_q), 135.9 (C_q), 130.3 (2C, CH), 129.9 (C_q), 129.6 (C_q), 129.1 (2C, CH), 123.2 (CH), 121.7 (CH), 121.0 (CH), 121.0 (CH), 118.9 (CH), 112.5 (C_q), 111.6 (CH), 21.4 (CH₃), 9.7 (CH₃). HRMS (ESI): *m/z* Calcd for C₂₁H₁₈N₂+H⁺ [M+H]⁺ 299.1543; Found 299.1541. The ¹H and ¹³C spectra are consistent with those reported in the literature.⁶⁵



2-(2-(p-Tolyl)-1H-pyrrol-1-yl)pyridine (3fa): The representative procedure was followed, using substrate 2-(1H-pyrrol-1-yl)pyridine (**3f**) (0.029 g, 0.20 mmol) and 1-chloro-4-

methylbenzene (**2a**; 0.051 g, 0.40 mmol), and the reaction mixture was stirred for 16 h. Purification by column chromatography on silica gel (petroleum ether/EtOAc: 20/1) yielded **3fa** (0.012 g, 26%) as a light yellow liquid. $^1\text{H-NMR}$ (400 MHz, CDCl_3): δ = 8.57-8.42 (m, 1H, Ar-H), 7.52 (td, J = 7.8, 1.9 Hz, 1H, Ar-H), 7.39-7.31 (m, 1H, Ar-H), 7.19-7.12 (m, 1H, Ar-H), 7.07 (m, 4H, Ar-H), 6.79 (d, J = 8.4 Hz, 1H, Ar-H), 6.44-6.33 (m, 2H, Ar-H), 2.33 (CH_3). $^{13}\text{C}\{^1\text{H}\}$ -NMR (100 MHz, CDCl_3): δ = 152.3 (C_q), 149.0 (CH), 137.5 (CH), 136.5 (C_q), 133.3 (C_q), 130.4 (C_q), 129.1 (2C, CH), 128.4 (2C, CH), 123.3 (CH), 121.3 (CH), 119.4 (CH), 112.2 (CH), 110.0 (CH), 21.3 (CH_3). HRMS (ESI): m/z Calcd for $\text{C}_{16}\text{H}_{14}\text{N}_2+\text{H}^+$ $[\text{M}+\text{H}]^+$ 235.1230; Found 235.1228.

2-(2,5-Di-*p*-tolyl-1*H*-pyrrol-1-yl)pyridine (3f'a**):** (0.024 g, 37%) as a light yellow solid. $^1\text{H-NMR}$ (400 MHz, CDCl_3): δ = 8.67-8.57 (m, 1H, Ar-H), 7.76 (td, J = 7.8, 1.9 Hz, 1H, Ar-H), 7.38 (dd, J = 6.9, 5.3 Hz, 2H, Ar-H), 7.17 (m, 8H, Ar-H), 6.62 (s, 2H, Ar-H), 2.46 (s, 6H, CH_3). $^{13}\text{C}\{^1\text{H}\}$ -NMR (100 MHz, CDCl_3): δ = 152.6 (C_q), 149.1 (CH), 137.8 (CH), 136.1 (2C, C_q), 136.0 (2C, C_q), 130.5 (C_q), 129.2 (C_q), 128.9 (4C, CH), 128.5 (4C, CH), 124.0 (CH), 122.7 (CH), 110.1 (2C, CH), 21.3 (2C, CH_3). HRMS (ESI): m/z Calcd for $\text{C}_{23}\text{H}_{20}\text{N}_2+\text{H}^+$ $[\text{M}+\text{H}]^+$ 325.1699; Found 325.1695.

4.4.4 Procedure for External Additive Experiment: The representative procedure of arylation was followed, using substrate **1a** (0.039 g, 0.20 mmol), 4-chlorotoluene (0.051 g, 0.40 mmol), $\text{Ni}(\text{OAc})_2$ (0.0035 g, 0.02 mmol, 10.0 mol %), dppf (0.011 g, 0.02 mmol, 10.0 mol %), LiHMDS (0.067 g, 0.40 mmol), TEMPO (0.062 g, 0.40 mmol) or galvinoxyl (0.169 g, 0.40 mmol) and the reaction mixture was stirred for 16 h. The GC analysis of the crude reaction mixture does not show the formation of product **3aa**. In addition, the coupled product of TEMPO and galvinoxyl with aryl was not detected in the GCMS.

4.4.5 Procedure for Deuterium Labeling Experiments

Procedure for KIE Study: To the Teflon-screw capped tube equipped with magnetic stir bar was introduced catalyst $\text{Ni}(\text{OAc})_2$ (0.0035 g, 0.02 mmol, 0.02 M), dppf (0.0011 g, 0.02 mmol, 10.0 mol %), LiHMDS (0.067 g, 0.40 mmol), substrate **1a** (0.039 g, 0.20 mmol, 0.2 M) or [2-D]-**1a** (0.039 g, 0.20 mmol, 0.2 M), and 4-chlorotoluene (0.051 g, 0.40 mmol, 0.4 M), to the reaction mixture *n*-hexadecane (0.025 mL, 0.085 mmol, 0.085 M) was added as an internal

standard and 1,4 dioxane (0.87 mL) was added to make the total volume to 1.0 mL. The reaction mixture was then stirred at 110 °C in a pre-heated oil bath. At regular intervals (15, 30, 45, 60, 75, 90, 105, 120 min) the reaction vessel was cooled to ambient temperature and an aliquot of sample was withdrawn to the GC vial. The sample was diluted with acetone and subjected to GC analysis. The concentration of the product **3aa** obtained in each sample was determined with respect to the internal standard *n*-hexadecane. The data of the concentration of the product vs time (min) plot was drawn and fitted linear with Origin Pro 8, and the rate was determined by initial rate method (up to 120 minutes). The slope of the linear fitting represents the reaction rate.

Procedure for H/D Scrambling: To a Teflon-screw capped tube equipped with magnetic stir bar were introduced 1-(pyridine-2-yl)-1*H*-indole-2-*d* ([2-D]-**1a**; 0.019 g, 0.10 mmol), 5-methoxy-1-(pyridine-2-yl)-1*H*-indole (**1c**; 0.022 g, 0.10 mmol), 4-chlorotoluene (**2a**; 0.051 g, 0.40 mmol), cat Ni(OAc)₂ (0.0035 g, 0.02 mmol, 10.0 mol %), dppf (0.0011 g, 0.02 mmol, 10.0 mol %), LiHMDS (0.067 g, 0.40 mmol) inside the glove-box. The resultant reaction mixture was stirred at 80 °C in a preheated oil bath for 60 min. At ambient temperature, the reaction mixture was quenched with distilled H₂O (10 mL). The crude product was then extracted with EtOAc (20 mL x 3). The combined organic extract was dried over Na₂SO₄ and the volatiles were evaporated in *vacuo*. The remaining residue was subjected to column chromatography on silica gel (petroleum ether/EtOAc: 20/1) to recover the starting compounds **1a** and **1c**. The ¹H NMR analysis of the compound show 25% incorporation of deuterium at C(2)-H of 5-methoxy-1-(pyridine-2-yl)-1*H*-indole **1c**.

Procedure for Deuterium Incorporation Experiment: To a screw-capped tube equipped with magnetic stir bar was introduced 1-(pyridine-2-yl)-1*H*-indole (**1a**; 0.039 g, 0.20 mmol), 4-chlorotoluene (0.051 g, 0.40 mmol), Ni(OAc)₂ (0.0035 g, 0.02 mmol, 10.0 mol %), dppf (0.011 g, 0.02 mmol, 10.0 mol %), LiHMDS (0.067 g, 0.40 mmol) inside the glove-box. The resultant reaction mixture was stirred at 80 °C in a preheated oil bath for 60 min. At ambient temperature, D₂O (1.0 mL) was added to the reaction mixture under argon and stirred for 1 h. Reaction mixture was quenched with distilled H₂O (10 mL). The crude product was then extracted with EtOAc (20 mL x 3). The combined organic extract was dried over Na₂SO₄ and the volatiles were evaporated in *vacuo*. The ¹H NMR analysis of the compound **1a** does not show incorporation of deuterium at C(2)-H position.

4.4.6 Kinetics Experiments

Representative Procedure for Kinetic Experiment: To the Teflon-screw capped tube equipped with magnetic stir bar was introduced catalyst Ni(OAc)₂ (0.0035 g, 0.02 mmol, 0.02 M), dppf (0.011 g, 0.02 mmol, 10.0 mol %), LiHMDS (0.067 g, 0.40 mmol), substrate **1a** (0.039 g, 0.20 mmol, 0.2 M) and 4-chlorotoluene (0.0051 g, 0.40 mmol, 0.4 M), to the reaction mixture *n*-hexadecane (0.025 mL, 0.085 mmol, 0.085 M, internal standard) and toluene (0.87 mL) was added to make the total volume to 1.0 mL. The reaction mixture was then stirred at 110 °C in a pre-heated oil bath. At regular intervals (15, 30, 45, 60, 75, 90, 105, 120, 240, 480, 720, 960, 1200, 1440 min) the reaction vessel was cooled to ambient temperature and an aliquot of sample was withdrawn to the GC vial. The sample was diluted with acetone and subjected to GC analysis. The concentration of the product **3aa** obtained in each sample was determined with respect to the internal standard *n*-hexadecane. The data of the concentration of the product vs time (min) plot was drawn with Origin Pro 8. The data's were taken from the average of two independent experiments.

Representative Procedure for Rate Order Determination

Rate Order Determination on 1-(pyridin-2-yl)-1H-indole: In standard experiment, a Teflon-screw cap tube equipped with magnetic stir bar was introduced catalyst Ni(OAc)₂ (0.02 mmol), dppf (0.02 mmol, 0.02 M), LiHMDS (0.067 g, 0.4 mmol), 4-chlorotoluene (0.051 mL, 0.40 mmol, 0.40 M), specific amount of **1a**, *n*-hexadecane (0.025 mL, internal standard), and 1,4-dioxane (appropriate amount) was added to make the total volume to 1.0 mL. The reaction mixture was then heated at 110 °C in a pre-heated oil bath. At regular intervals (15, 30, 45, 60, 75, 90, 105, 120 min, etc.), the reaction vessel was cooled to ambient temperature and an aliquot of sample was withdrawn to the GC vial. The sample was diluted with acetone and subjected to GC analysis. The concentration of the product **3aa** obtained in each sample was determined with respect to the internal standard *n*-hexadecane.

Rate Order Determination on 4-chloro toluene: Representative procedure of rate order determination was followed, employing 1-(pyridin-2-yl)-1H-indole (0.2 M), Ni(OAc)₂ (0.02 mmol), dppf (0.02 M), LiHMDS (0.4 M), and *n*-hexadecane (0.085 M) and specific amount of 4-chlorotoluene in 1,4-dioxane. The data of the concentration of the **3aa** vs time (min) plot was fitted linear with Origin Pro 8. The order of the reaction was then determined by plotting the log(rate) vs log(conc. **2a**) for component **2a**.

Rate Order Determination on catalyst: Representative procedure of rate order determination was followed, employing 1-(pyridin-2-yl)-1*H*-indole (0.20 M), 4-chlorotoluene (0.40 M), LiHMDS (0.40 M) and *n*-hexadecane (0.085 M) and specific amount of catalyst in 1,4-dioxane. The data of the concentration of the **3aa** vs time (min) plot was fitted linear with Origin Pro 8. The order of the reaction was then determined by plotting the log(rate) vs log(conc. cat.) for component catalyst.

Rate Order Determination on LiHMDS: Representative procedure of rate order determination was followed, employing 1-(pyridin-2-yl)-1*H*-indole (0.2 M), 4-chlorotoluene (0.40 M), Ni(OAc)₂ (0.02 mmol), dppf (0.02 M), and *n*-hexadecane (0.085 M) and specific amount of LiHMDS in 1,4-dioxane. The data of the concentration of the **3aa** vs time (min) plot was fitted linear with Origin Pro 8. The order of the reaction was then determined by plotting the log(rate) vs log(conc. LiHMDS) for component LiHMDS.

Kinetic Experiments (Electronic Effect)

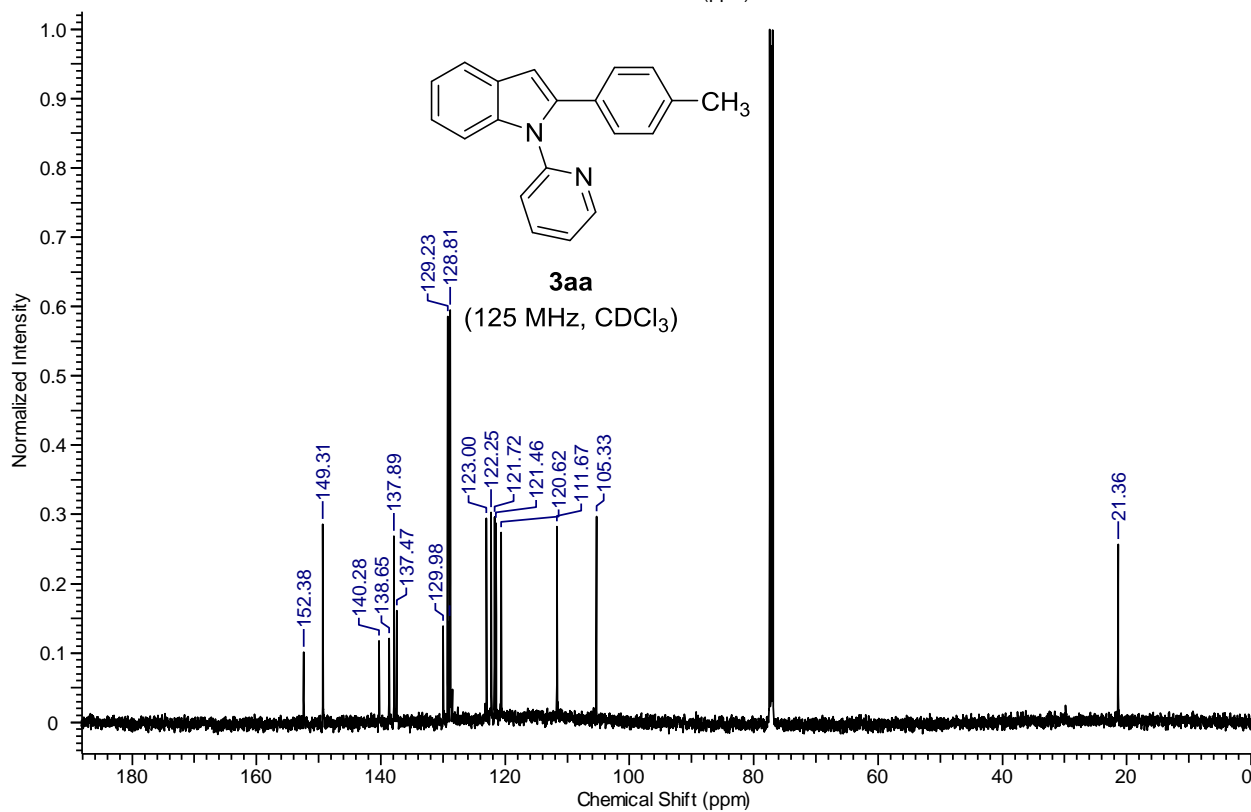
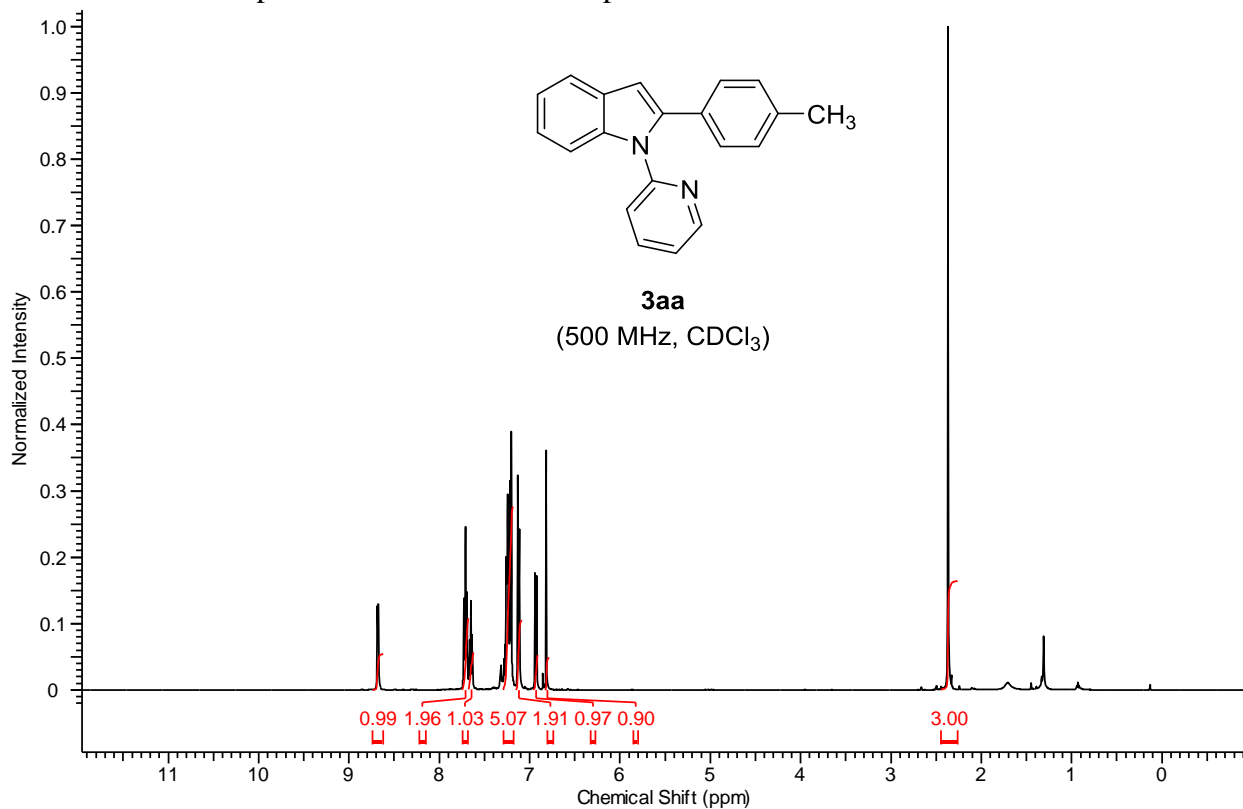
Representative Procedure: To the Teflon-screw capped tube equipped with magnetic stir bar was introduced catalyst Ni(OAc)₂ (0.0035 g, 0.02 mmol, 0.02 M), dppf (0.0011 g, 0.02 mmol, 10.0 mol %), LiHMDS (0.067 g, 0.40 mmol), substrate 5-methoxy-1-(pyridin-2-yl)-1*H*-indole (**1c**) (0.045 g, 0.20 mmol, 0.2 M) or 5-fluoro-1-(pyridin-2-yl)-1*H*-indole (**1d**) (0.042 g, 0.20 mmol, 0.2 M), and 4-chlorotoluene (0.051 g, 0.40 mmol, 0.4 M), to the reaction mixture *n*-hexadecane (0.025 mL, 0.085 mmol, 0.085 M, internal standard) and 1,4 dioxane (0.87 mL) was added to make the total volume 1.0 mL. The reaction mixture was then stirred at 110 °C in a pre-heated oil bath. At regular intervals (15, 30, 45, 60, 75, 90, 105, 120 min) the reaction vessel was cooled to ambient temperature and an aliquot of sample was withdrawn to the GC vial. The sample was diluted with acetone and subjected to GC analysis. The concentration of the product **3ca** (or **3da**) obtained in each sample was determined with respect to the internal standard *n*-hexadecane. The data of the concentration of the product vs time (min) plot was drawn and fitted linear with Origin Pro 8, and the rate was determined by the initial rate method (up to 120 minutes). The slope of the linear fitting represents the reaction rate. The data's were taken from the average of three independent experiments.

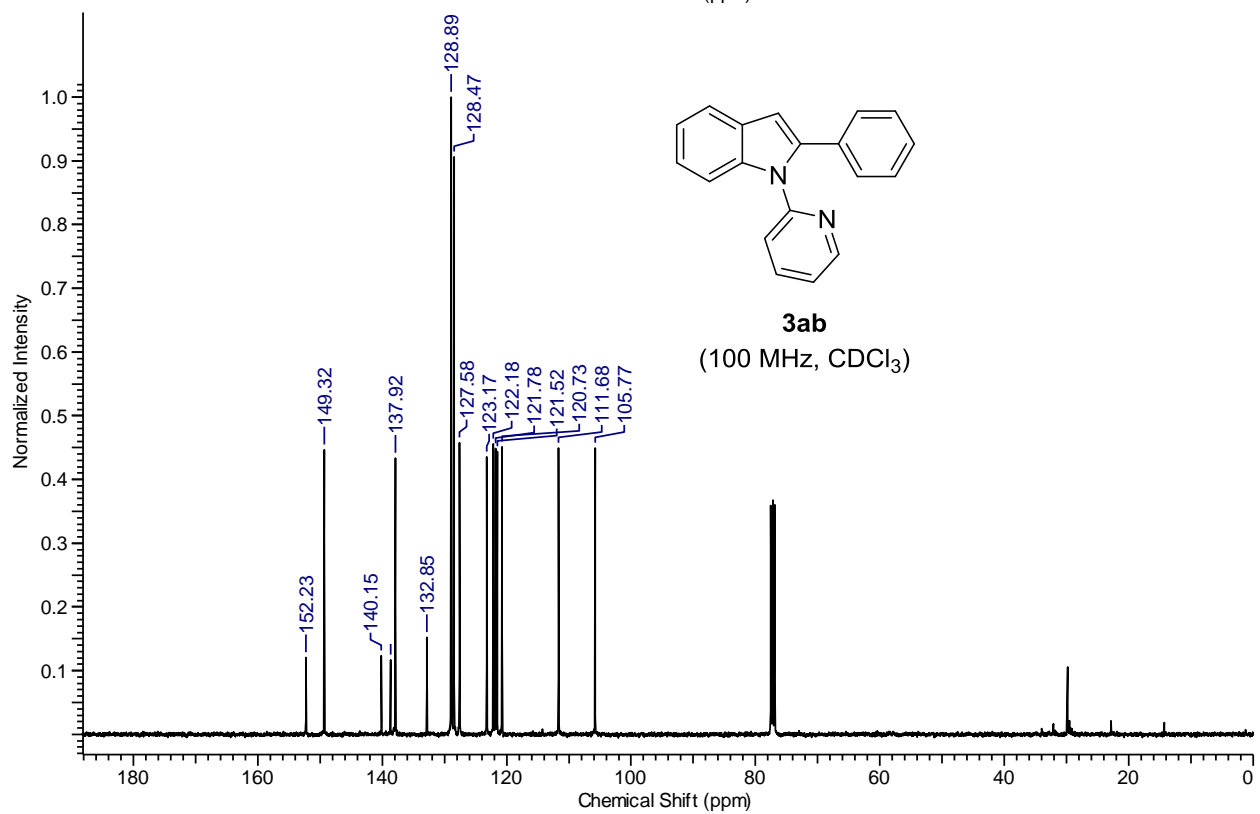
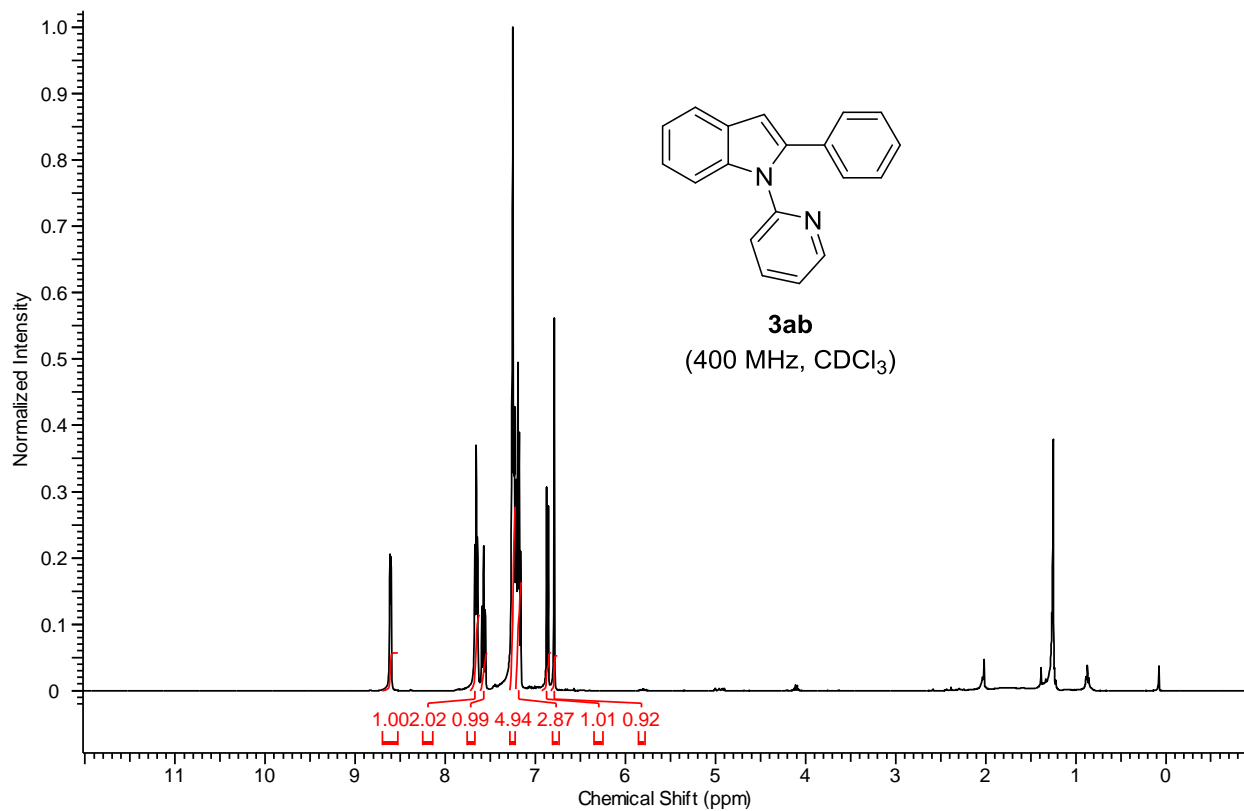
4.5 REFERENCES

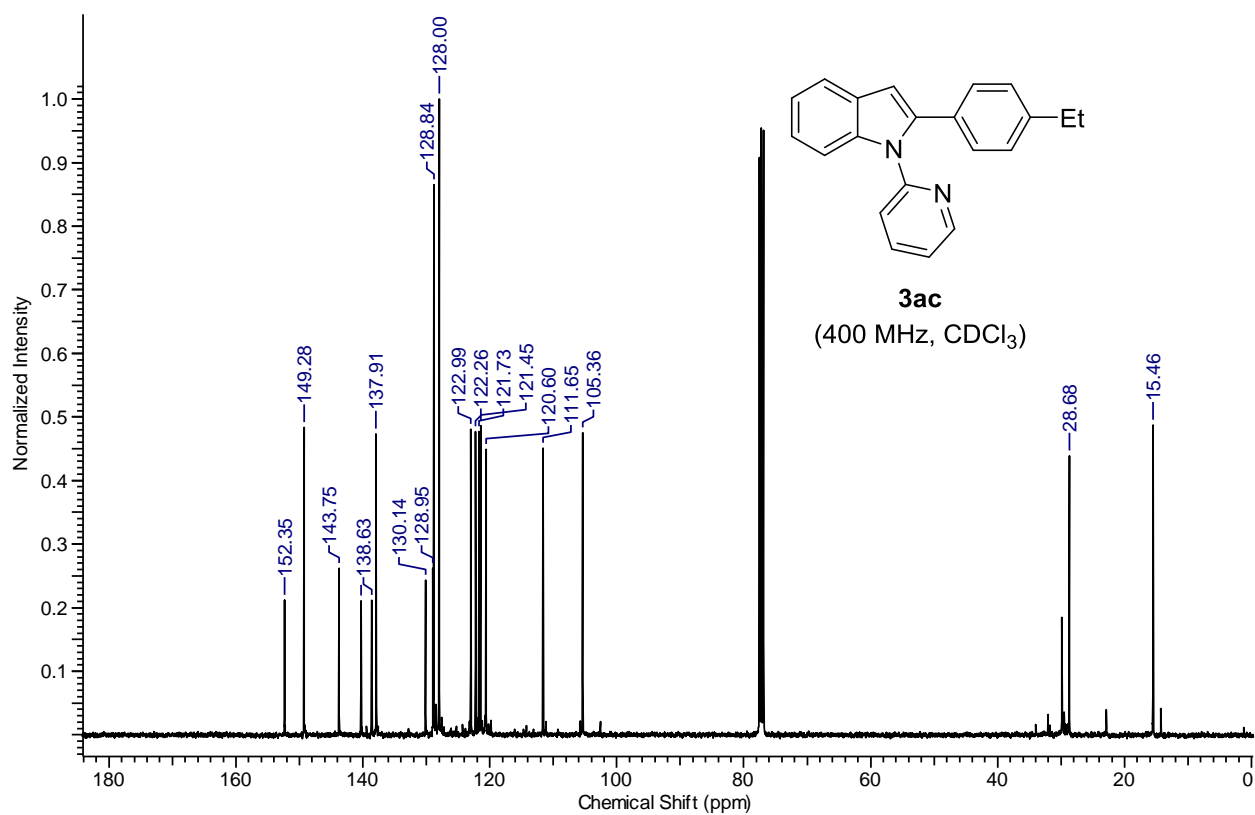
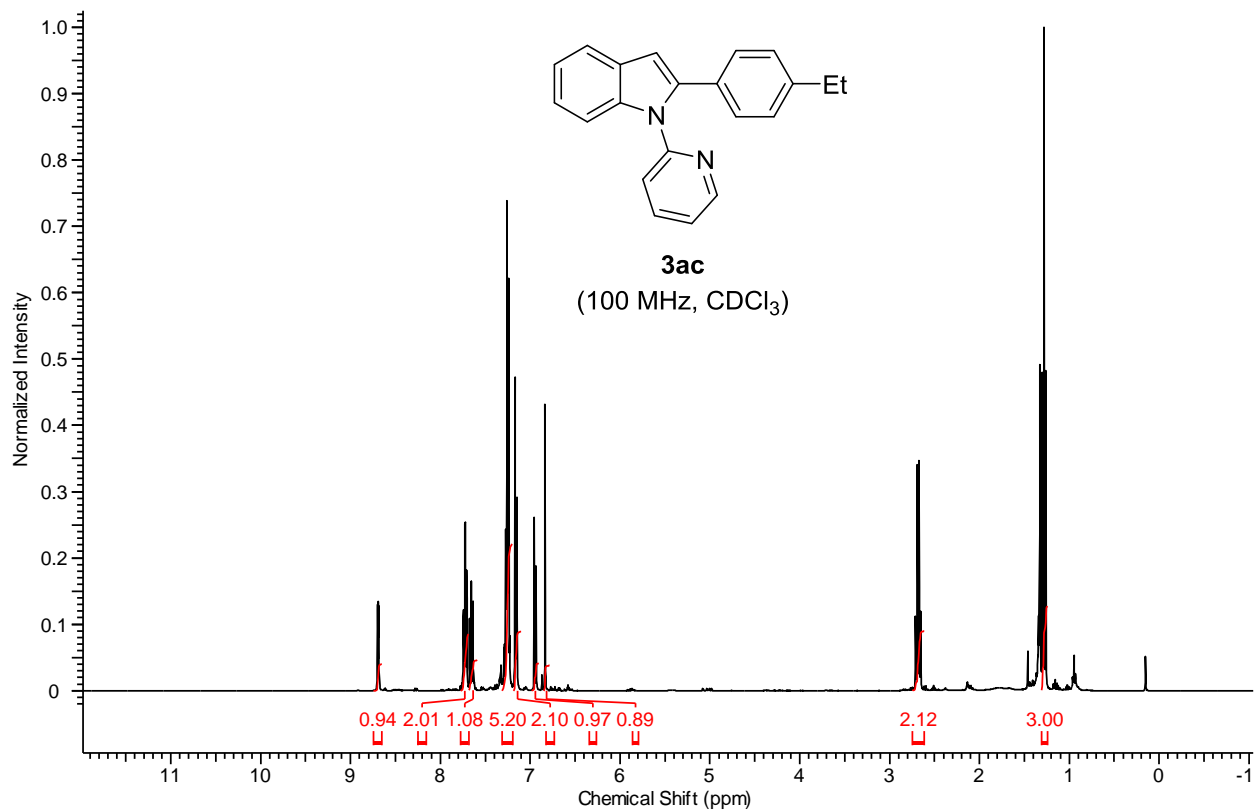
- (1) Sundberg, R. J. *In Comprehensive Heterocyclic Chemistry, 2nd ed.*; Katritzky, A. R., Rees, C. W., Eds.; Pergamon Press: Oxford, **1996**, 2, 119-206.
- (2) Gribble, G. W. *J. Chem. Soc., Perkin Trans. 1* **2000**, 1045-1075.
- (3) Garg, N. K.; Sarpong, R.; Stoltz, B. M. *J. Am. Chem. Soc.* **2002**, *124*, 13179-13184.
- (4) Horton, D. A.; Bourne, G. T.; Smythe, M. L. *Chem. Rev.* **2003**, *103*, 893-930.
- (5) Chen, F.-E.; Huang, J. *Chem. Rev.* **2005**, *105*, 4671-4706.
- (6) Walker, S. R.; Carter, E. J.; Huff, B. C.; Morris, J. C. *Chem. Rev.* **2009**, *109*, 3080-3098.
- (7) Zhou, G.; Wu, D.; Snyder, B.; Ptak, R. G.; Kaur, H.; Gochin, M. *J. Med. Chem.* **2011**, *54*, 7220-7231.
- (8) Melander, R. J.; Minvielle, M. J.; Melander, C. *Tetrahedron* **2014**, *70*, 6363-6372.
- (9) Taylor, R. D.; MacCoss, M.; Lawson, A. D. G. *J. Med. Chem.* **2014**, *57*, 5845-5859.
- (10) Leitch, J. A.; Cook, H. P.; Bhonoah, Y.; Frost, C. G. *J. Org. Chem.* **2016**, *81*, 10081-10087.
- (11) Leitch, J. A.; Wilson, P. B.; McMullin, C. L.; Mahon, M. F.; Bhonoah, Y.; Williams, I. H.; Frost, C. G. *ACS Catal.* **2016**, *6*, 5520-5529.
- (12) Ma, W.; Dong, H.; Wang, D.; Ackermann, L. *Adv. Synth. Catal.* **2017**, *359*, 966-973.
- (13) Yamaguchi, J.; Muto, K.; Itami, K. *Top. Curr. Chem.* **2016**, *374*, 55.
- (14) Brown, J. A.; Cochrane, A. R.; Irvine, S.; Kerr, W. J.; Mondal, B.; Parkinson, J. A.; Paterson, L. C.; Reid, M.; Tuttle, T.; Andersson, S.; Nilsson, G. N. *Adv. Synth. Catal.* **2014**, *356*, 3551-3562.
- (15) Lyons, T. W.; Sanford, M. S. *Chem. Rev.* **2010**, *110*, 1147-1169.
- (16) Colby, D. A.; Bergman, R. G.; Ellman, J. A. *Chem. Rev.* **2010**, *110*, 624-655.
- (17) Ackermann, L. *Chem. Rev.* **2011**, *111*, 1315-1345.
- (18) Cernak, T.; Dykstra, K. D.; Tyagarajan, S.; Vachal, P.; Krska, S. W. *Chem. Soc. Rev.* **2016**, *45*, 546-576.
- (19) Ackermann, L.; Barfüßer, S. *Synlett.* **2009**, 808-812.
- (20) Ackermann, L.; Barfüßer, S.; Pospesch, J. *Org. Lett.* **2010**, *12*, 724-726.
- (21) Ackermann, L.; Vicente, R.; Kapdi, A. R. *Angew. Chem. Int. Ed.* **2009**, *48*, 9792-9826.
- (22) Bellina, F.; Calandri, C.; Cauteruccio, S.; Rossi, R. *Tetrahedron* **2007**, *63*, 1970-1980.
- (23) Bellina, F.; Cauteruccio, S.; Rossi, R. *Eur. J. Org. Chem.* **2006**, *2006*, 1379-1382.
- (24) Bensaid, S.; Doucet, H. *ChemSusChem* **2012**, *5*, 1559-1567.

- (25) Ben-Yahia, A.; Naas, M.; El Kazzouli, S.; Essassi, E. M.; Guillaumet, G. *Eur. J. Org. Chem.* **2012**, 7075-7081.
- (26) Campeau, L.-C.; Bertrand-Laperle, M.; Leclerc, J.-P.; Villemure, E.; Gorelsky, S. I.; Fagnou, K. *J. Am. Chem. Soc.* **2008**, *130*, 3276-3277.
- (27) Chen, J.; Jia, Y. *Org. Biomol. Chem.* **2017**, *15*, 3550-3567.
- (28) Daugulis, O.; Zaitsev, V. G. *Angew. Chem. Int. Ed.* **2005**, *44*, 4046-4048.
- (29) Deprez, N. R.; Kalyani, D.; Krause, A.; Sanford, M. S. *J. Am. Chem. Soc.* **2006**, *128*, 4972-4973.
- (30) Derridj, F.; Gottumukkala, A. L.; Djebbar, S.; Doucet, H. *Eur. J. Inorg. Chem.* **2008**, 2550-2559.
- (31) Feng, J.; Lu, G.; Lv, M.; Cai, C. *J. Organomet. Chem.* **2014**, *761*, 28-31.
- (32) Ferguson, D. M.; Rudolph, S. R.; Kalyani, D. *ACS Catal.* **2014**, *4*, 2395-2401.
- (33) Funaki, K.; Sato, T.; Oi, S. *Org. Lett.* **2012**, *14*, 6186-6189.
- (34) Giri, R.; Maugel, N.; Li, J.-J.; Wang, D.-H.; Breazzano, S. P.; Saunders, L. B.; Yu, J.-Q. *J. Am. Chem. Soc.* **2007**, *129*, 3510-3511.
- (35) Gu, J.; Cai, C. *RSC Adv.* **2015**, *5*, 56311-56315.
- (36) Phipps, R. J.; Gaunt, M. J. *Science* **2009**, *323*, 1593-1597.
- (37) Sandtorv, A. H. *Adv. Synth. Catal.* **2015**, *357*, 2403-2435.
- (38) Joucla, L.; Djakovitch, L. *Adv. Synth. Catal.* **2009**, *351*, 673-714.
- (39) Yang, Y.; Gao, P.; Zhao, Y.; Shi, Z. *Angew. Chem. Int. Ed.* **2017**, *56*, 3966-3971.
- (40) Wang, X.; Lane, B. S.; Sames, D. *J. Am. Chem. Soc.* **2005**, *127*, 4996-4997.
- (41) Gemoets, H. P. L.; Kalvet, I.; Nyuchev, A. V.; Erdmann, N.; Hessel, V.; Schoenebeck, F.; Noël, T. *Chem. Sci.* **2017**, *8*, 1046-1055.
- (42) Lane, B. S.; Brown, M. A.; Sames, D. *J. Am. Chem. Soc.* **2005**, *127*, 8050-8057.
- (43) Nareddy, P.; Jordan, F.; Szostak, M. *Org. Lett.* **2018**, *20*, 341-344.
- (44) Miao, J.; Ge, H. *Eur. J. Org. Chem.* **2015**, *2015*, 7859-7868.
- (45) Moselage, M.; Sauermann, N.; Richter, S. C.; Ackermann, L. *Angew. Chem. Int. Ed.* **2015**, *54*, 6352-6355.
- (46) Moselage, M.; Li, J.; Ackermann, L. *ACS Catal.* **2016**, *6*, 498-525.
- (47) Su, B.; Cao, Z.-C.; Shi, Z.-J. *Acc. Chem. Res.* **2015**, *48*, 886-896.
- (48) Kulkarni, A. A.; Daugulis, O. *Synthesis* **2009**, 4087-4109.

- (49) Zhu, X.; Su, J.; Du, C.; Wang, Z.-L.; Ren, C.; Niu, J.; Song, M. *Org. Lett.* **2017**, *19*, 596-599.
- (50) Yang, Y.; Li, R.; Zhao, Y.; Zhao, D.; Shi, Z. *J. Am. Chem. Soc.* **2016**, *138*, 8734-8737.
- (51) Barbero, N.; SanMartin, R.; DomÁnguez, E. *Tetrahedron Lett.* **2009**, *50*, 2129-2131.
- (52) Phipps, R. J.; Grimster, N. P.; Gaunt, M. J. *J. Am. Chem. Soc.* **2008**, *130*, 8172-8174.
- (53) Song, W.; Ackermann, L. *Angew. Chem. Int. Ed.* **2012**, *51*, 8251-8254.
- (54) Wu, H.; Liu, T.; Cui, M.; Li, Y.; Jian, J.; Wang, H.; Zeng, Z. *Org. Biomol. Chem.* **2017**, *15*, 536-540.
- (55) Zhou, J.; Hu, P.; Zhang, M.; Huang, S.; Wang, M.; Su, W. *Chem. – Eur. J.* **2010**, *16*, 5876-5881.
- (56) Zhao, S.; Liu, B.; Zhan, B.-B.; Zhang, W.-D.; Shi, B.-F. *Org. Lett.* **2016**, *18*, 4586-4589.
- (57) Tiwari, V. K.; Kamal, N.; Kapur, M. *Org. Lett.* **2015**, *17*, 1766-1769.
- (58) Yamaguchi, J.; Muto, K.; Itami, K. *Eur. J. Org. Chem.* **2013**, 19-30.
- (59) Muto, K.; Hatakeyama, T.; Yamaguchi, J.; Itami, K. *Chem. Sci.* **2015**, *6*, 6792-6798.
- (60) Hyodo, I.; Tobisu, M.; Chatani, N. *Chem. Asian J.* **2012**, *7*, 1357-1365.
- (61) Fernández-Salas, J. A.; Marelli, E.; Nolan, S. P. *Chem. Sci.* **2015**, *6*, 4973-4977.
- (62) Hachiya, H.; Hirano, K.; Satoh, T.; Miura, M. *Org. Lett.* **2009**, *11*, 1737-1740.
- (63) Hachiya, H.; Hirano, K.; Satoh, T.; Miura, M. *Angew. Chem. Int. Ed.* **2010**, *49*, 2202-2205.
- (64) Kobayashi, O.; Uruguchi, D.; Yamakawa, T. *Org. Lett.* **2009**, *11*, 2679-2682.
- (65) Jagtap, R. A.; Soni, V.; Punji, B. *ChemSusChem* **2017**, *10*, 2242-2248.
- (66) Begum, T.; Mondal, M.; Borpuzari, M. P.; Kar, R.; Gogoi, P. K.; Bora, U. *Eur. J. Org. Chem.* **2017**, *2017*, 3244-3248.
- (67) Cai, L.; Qian, X.; Song, W.; Liu, T.; Tao, X.; Li, W.; Xie, X. *Tetrahedron* **2014**, *70*, 4754-4759.
- (68) Chen, H.; Han, J.; Wang, L. *Beilstein J. Org. Chem.* **2018**, *14*, 354-363.
- (69) Hong, X.; Tan, Q.; Liu, B.; Xu, B. *Angew. Chem. Int. Ed.* **2017**, *56*, 3961-3965.
- (70) Wang, L.; Ji, E.; Liu, N.; Dai, B. *Synthesis* **2016**, *48*, 737-750.
- (71) Song, J.; Cui, J.; Liang, H.; Liu, Q.; Dong, Y.; Liu, H. *Asian J. Org. Chem.* **2017**, *7*, 341-345.
- (72) Liu, C.; Szostak, M. *Chem. Commun.* **2018**, *54*, 2130-2133.
- (73) Wang, L.; Qu, X.; Li, Z.; Peng, W.-M. *Tetrahedron Lett.* **2015**, *56*, 3754-3757.

^1H and ^{13}C NMR Spectra of the Selected Compound





Chapter 5

**Synthesis and Characterization of (^QNNN^{R2})Ni Complexes,
and Application in C–H Bond Functionalization**

5.1 INTRODUCTION

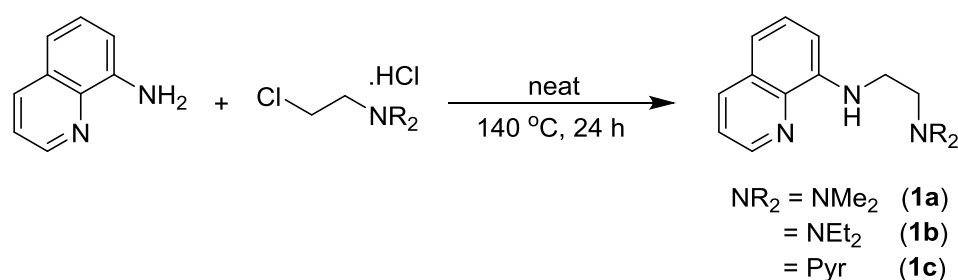
Synthesis of pincer ligands and their transition metal complexes has given significant attention because of their stability and diverse catalytic activity.¹⁻²⁷ Many nickel pincer complexes have been synthesized and demonstrated in various catalytic reactions such as traditional cross-coupling²⁸⁻³⁶ and C–H functionalization.³⁷⁻⁴² In general, the nickel pincer complex catalyzed reactions resulted in high turnover numbers and broad substrates scope than the similar reactions with a bidentate- or monodentate-ligated nickel catalyst. Recently, Hu developed [$\{\kappa^N, \kappa^N, \kappa^N\text{-}(\text{C}_6\text{H}_4\text{NMe}_2)_2(\mu\text{-N})\}\text{NiCl}$],⁴³ ($^{\text{Me}}\text{N}_2\text{N}$)NiCl and [$\{\kappa^N, \kappa^N, \kappa^N\text{-C}_6\text{H}_4\text{N}(\text{Me})_2(\mu\text{-N})(\text{CH}_2)_2\text{NMe}_2\}\text{NiCl}$]⁴⁴ (NNN^{Me_2})NiCl catalyst systems that were efficiently employed in the Sonogashira cross-coupling reaction. The ($^{\text{Me}}\text{N}_2\text{N}$)NiCl catalyst worked efficiently for the Sonogashira cross-coupling at 100 °C, whereas the hemilabile (NNN^{Me_2})NiCl catalyzed the same reaction at room temperature. The hemilabile coordination property of complex (NNN^{Me_2})NiCl facilitated the Sonogashira transformation very effectively under milder conditions. Recently our group developed the (quinolinyl)amido–nickel catalyst, [$\{\kappa^N, \kappa^N, \kappa^N\text{-Et}_2\text{NCH}_2\text{C}(\text{O})(\mu\text{-N})\text{C}_9\text{H}_6\text{N}\}\text{Ni}(\text{OAc})$],⁴⁵ that regioselectively catalyzes the alkylation and arylation of indoles with various alkyl and aryl halides, respectively through the monodentate-chelate assistance. Unfortunately, employing this catalyst system the methodology required a very high reaction temperature (150 °C), and needed KI in stoichiometric amount when Br- and Cl-alkyl electrophiles are used. Considering the advantage of hemilabile pincer system, in this chapter we have demonstrated the design and synthesis of hemilabile $\text{R}_2\text{N}(\text{CH}_2)_2(\text{NH})\text{C}_9\text{H}_6\text{N}$ ($^{\text{Q}}\text{NNN}^{\text{R}_2}$) ligand and complexes, and their application for the alkylation of indoles. The synthesized complexes were fully characterized by ^1H and ^{13}C NMR. The molecular structures of the complexes were established by X-ray structure determination. These complexes were screened for alkylation of indoles. In addition, the catalysts were also explored for the dehydrogenative alkylation of indolines to alkylated indoles.

5.2 RESULTS AND DISCUSSION

5.2.1 Synthesis and Characterization of ($^{\text{Q}}\text{NNN}^{\text{R}_2}$) Nickel Complexes

The tridentate (dialkylamino)-*N*-(quinolin-8-yl)ethane ligands ($\text{R}_2\text{NCH}_2\text{CH}_2(\text{NH})\text{C}_9\text{H}_6\text{N}$) ($\text{NR}_2 = \text{NMe}_2, \text{NEt}_2, \text{Pyr}$) were synthesized in excellent yield using reported procedure (Scheme 5.1). The reaction of 8-aminoquinoline with 2-chloro-*N,N*-dialkylethylamine hydrochloride

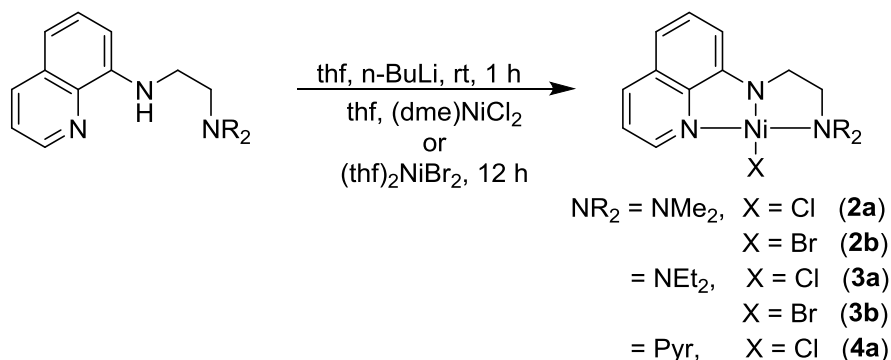
under neat reaction condition provided the desired ligand (dimethylamino)-*N*-(quinolin-8-yl)ethane (**1a**) and (diethylamino)-*N*-(quinolin-8-yl)ethane (**1b**) with 86% and 85% yield, respectively. Whereas the ligand (2-pyrrolidine)-*N*-(quinolin-8-yl)ethane (**1c**) was synthesized from the reaction of 8-aminoquinoline with 1-(2-chloroethyl)pyrrolidine hydrochloride with 86% yield. All the ligands synthesis was performed under neat reaction conditions at 140 °C for 24 h. These compounds were readily purified by column chromatography as a yellow liquid. The ^1H and ^{13}C NMR data of the ligands are consistent with the reported literature data for the same compounds.



Scheme 5.1 Synthesis of ($^{\text{Q}}\text{NNN}^{\text{R}2}$)-H pincer ligand.

The metalation reaction of the ligand ($^{\text{Q}}\text{NNN}^{\text{Me}2}$)-H (**1a**) with nickel precursor was performed by the first lithiation of ligand in THF at room temperature, and then by metalation using (dme)NiCl₂, which produced the pincer complex ($^{\text{Q}}\text{NNN}^{\text{Me}2}$)NiCl (**2a**) in good yield (Scheme 5.2). Similarly, the treatment of **1a** with (thf)₂NiBr₂ at room temperature afforded ($^{\text{Q}}\text{NNN}^{\text{Me}2}$)NiBr (**2b**). Both the nickel complexes were characterized by NMR spectroscopy as well as elemental analysis. In ^1H NMR spectra of complexes **2a** and **2b**, the disappearance of the N-H signal corresponds to the ligand suggests a covalent bonding between the central nitrogen atom and the nickel center. Further, the -NMe₂ protons in the complexes resonate in the range δ_{H} 2.76-2.45 ppm, which were significantly deshielded in comparison to those observed for the same protons in ligand **1a** (δ 2.31 ppm). One of the CH₂ protons of the side arm of the ligand (**1a**) is shifted and merged with the -N(CH₃)₂ proton in the complex, which indicates the coordination of 'N' to the nickel in **2a**. The C-H proton *ortho* to the quinolinyl nitrogen atom resonates differently than that in the free ligand **1a**. All these observations clearly suggest the

tridentate pincer coordination of the ligand to the Ni center in the complexes. The molecular structure of **2a** was further established by single-crystal diffraction studies.



Scheme 5.2 Synthesis of $(^{\text{Q}}\text{NNN}^{\text{R}2})\text{NiX}$ pincer complexes.

The pincer complexes $(^{\text{Q}}\text{NNN}^{\text{Et}2})\text{NiCl}$ (**3a**) and $(^{\text{Q}}\text{NNN}^{\text{Et}2})\text{NiBr}$ (**3b**) were synthesized in excellent yields by the reaction of $(^{\text{Q}}\text{NNN}^{\text{Et}2})\text{-H}$ (**1b**) with $(\text{dme})\text{NiCl}_2$ and $(\text{thf})_2\text{NiBr}_2$, respectively, following the similar procedure. These pincer nickel complexes were obtained as purple-violet solids. In the ^1H NMR spectra of complexes **3a** and **3b**, the $-\text{CH}_3$ protons of the $-\text{NEt}_2$ group desheilded to δ_{H} 1.97-1.78 ppm as compared to the one in the shielded region (δ_{H} 1.03-1.19 ppm) in the ligand **1b**. Very slight desheilding was observed in the $-\text{CH}_2$ protons of the complexes as compared to the ligand. All these complexes were characterized by ^{13}C NMR spectroscopy, HRMS, and elemental analysis techniques. The molecular structure of **3b** was determined by single-crystal diffraction studies. The pincer complex $(^{\text{Q}}\text{NNN}^{\text{Pyr}})\text{NiCl}$ (**4a**) was synthesized in good yield by the reaction of $(^{\text{Q}}\text{NNN}^{\text{Pyr}})\text{-H}$ (**1c**) with $(\text{dme})\text{NiCl}_2$ following the similar procedure. The molecular structure of the same was confirmed by single-crystal diffraction studies.

5.2.2 Molecular Structure of Nickel Complexes. The ORTEP diagrams of complexes **2a**, **3b** and **4a** are shown in Figures 5.1-5.3, respectively. Selected bond lengths and bond angles are given in Table 5.1. For these three complexes, the geometry around the nickel is slightly distorted from the expected square planar. The Ni–N1 bond lengths are in the range (1.960(3)-1.955(3) Å), which are comparable with the similar bond length in $(\text{NNN}^{\text{Me}2})\text{NiCl}$ (1.962(4) Å).⁴⁴ Similarly, the Ni–N2 bond lengths (1.831(2)-1.835(1) Å) in complexes **2a** and **3b** are

comparable to the Ni–N2 bond lengths (1.832(3) (Å)). The Ni–N3 bond lengths (1.916(2)-1.925(1) Å) are slightly shorter than the Ni–NMe₂ bond length (1.995 Å) in the complex (NNN^{Me2})NiCl. However, the Ni–Cl bond length (2.202 (1) Å) in complex **2a** is comparable to the bond length observed in the complex (NNN^{Me2})NiCl (Ni–Cl = 2.210 Å). The N1–Ni–N3 (167.6(1)°) bond angle in complex **2a** is significantly shorter than the similar bond angle in the complex (NNN^{Me2})NiCl (N1–Ni–N3 = 169.04(13)°, whereas N2–Ni–Cl bond angle in complex **2a** (178.5(1)°) is comparable to the similar bond angle in (NNN^{Me2})NiCl (N1–Ni–Cl = 178.3(1)°).

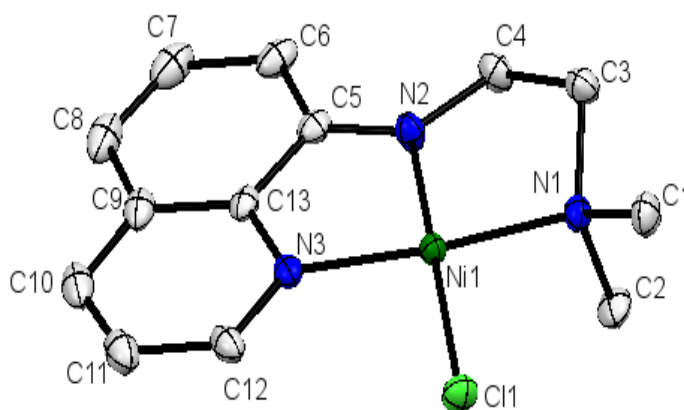


Figure 5.1 Thermal ellipsoid plot of (NNN^{Me2})NiCl (**2a**). All hydrogens atoms are omitted for clarity.

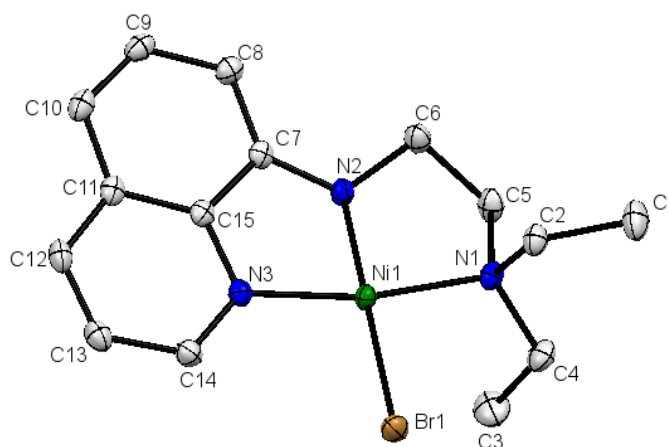


Figure 5.2 Thermal ellipsoid plot of (NNN^{NEt2})NiBr (**3b**). All hydrogens atoms are omitted for clarity.

The Ni–N1 bond length in complex **4a** is 1.955(3) Å, which is comparable with the similar bond length in (^{Me}₂NNN^{pyr})NiCl (1.968(4) Å). Similarly, the Ni–N2 bond length (1.829(3) Å) in complex **4a** is comparable to the Ni–N2 bond length (1.854(4) Å). The Ni–N3 bond length (1.924(4) Å) in **4a** is shorter than the Ni–NMe₂ bond length (1.963 Å) of the complex (^{Me}₂NNN^{pyr})NiCl. However, the Ni–Cl bond length (2.195(1) Å) in complex **4a** is also comparable to the bond length observed in the complex (^{Me}₂NNN^{pyr})NiCl (Ni–Cl = 2.213 Å). The N1–Ni–N3 (168.3(1)°) bond angles in complex **4a** is slightly smaller than the similar bond angles in the complex (NNN^{pyr})NiCl³⁴ (N1–Ni–N3 = 169.8(2)°), whereas N2–Ni–Cl bond angle in complex **4a** is (179.1(1)°) is comparable to the similar (NNN^{pyr})NiCl (N1–Ni–Cl = 179.3(1)°).

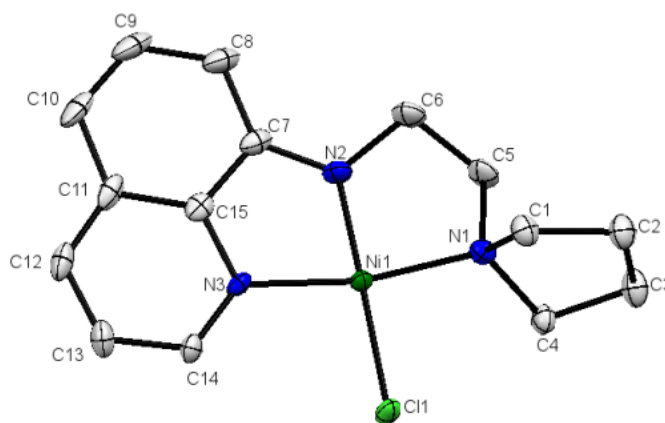


Figure 5.3 Thermal ellipsoid plot of (^QNNN^{pyr})NiCl (**4a**). All hydrogens atoms are omitted for clarity.

Table 5.1 Selected Bond Lengths (Å) and Angles (deg) for 2a, 3b, and 4a

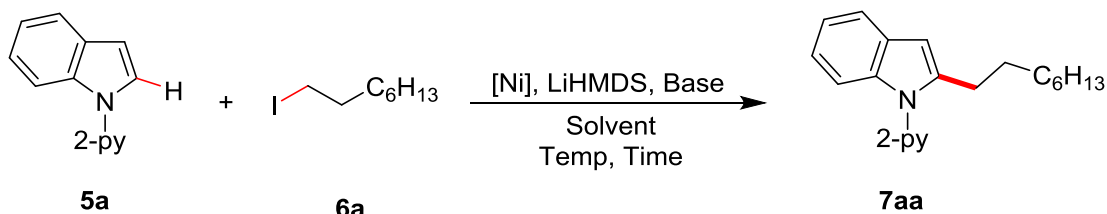
	2a	3b	4a
Ni(1)–N(1)	1.960(3)	1.978(2)	1.955(3)
Ni(1)–N(2)	1.831(3)	1.835(1)	1.829(3)
Ni(1)–N(3)	1.916(3)	1.925(1)	1.924(4)
Ni(1)–Cl(1)	2.202(1)		2.195(1)
Ni(1)–Br(1)		2.3505(3)	
N(1)–Ni(1)–N(2)	84.6(1)	85.25(6)	85.5(1)
N(1)–Ni(1)–N(3)	167.6(1)	168.51(6)	168.3(1)
N(2)–Ni(1)–N(3)	84.2(1)	83.93(6)	83.9(1)
Cl(1)–Ni(1)–N(1)	95.6(1)		95.4(1)
Cl(1)–Ni(1)–N(2)	178.5(1)		179.1(1)
Cl(1)–Ni(1)–N(3)	95.6(1)		95.3(1)
N(1)–Ni(1)–Br(1)		95.45(4)	
N(2)–Ni(1)–Br(1)		177.53(5)	
N(3)–Ni(1)–Br(1)		95.20(4)	

5.2.3 Pincer Nickel Complexes in Alkylation of Indoles.

We initiated optimization studies for the cross-coupling of indole **5a** with 1-iodooctane (**6a**) employing the Ni catalyst **2a** (Table 5.2). We started optimization using milder bases like Na₂CO₃, K₂CO₃, Cs₂CO₃, KOAc, CsOAc and K₃PO₄ in toluene. All bases were either ineffective or giving very less yield. The employment of a catalytic amount of LiHMDS (20 mol %) in addition to the milder bases were also ineffective and showed very less conversion and poor yield (entries 1-6). Reaction using LiO^tBu base and LiHMDS (20 mol %) provided good yield of indole alkylated product **7aa**. With the newly synthesized catalyst, use of 1.0 mL of toluene resulted in the partial formation of the benzylated product (2-benzyl-1-(pyridin-2-yl)-1*H*-indole) (12%) in addition to the desired compound **7aa** (73%), whereas the reaction with 0.15 mL of toluene gave 79% of the product **7aa** (entry 7). The most effective solvent was toluene and the alkylation in other solvents or in the absence of solvent was less efficient. The catalysis at 150 °C for less time (12 h) afforded the moderate yield (entry 8) where as catalysis at a lower temperature (100-130 °C) gave less yields (entries 9-10). Without the catalytic amount of

LiHMDS the reaction provided a very poor result with only 30% yield of product **7aa** (entry 11). The Ni-catalyst was essential for achieving the alkylation of indole; without that no coupling occurred (entry 12). All other nickel catalysts were also employed as catalysts that produced moderate to good yield of product **7aa**, however, slightly less efficient than catalyst **2a** (entries 13-16).

Table 5.2 Optimization of Reaction Conditions^a

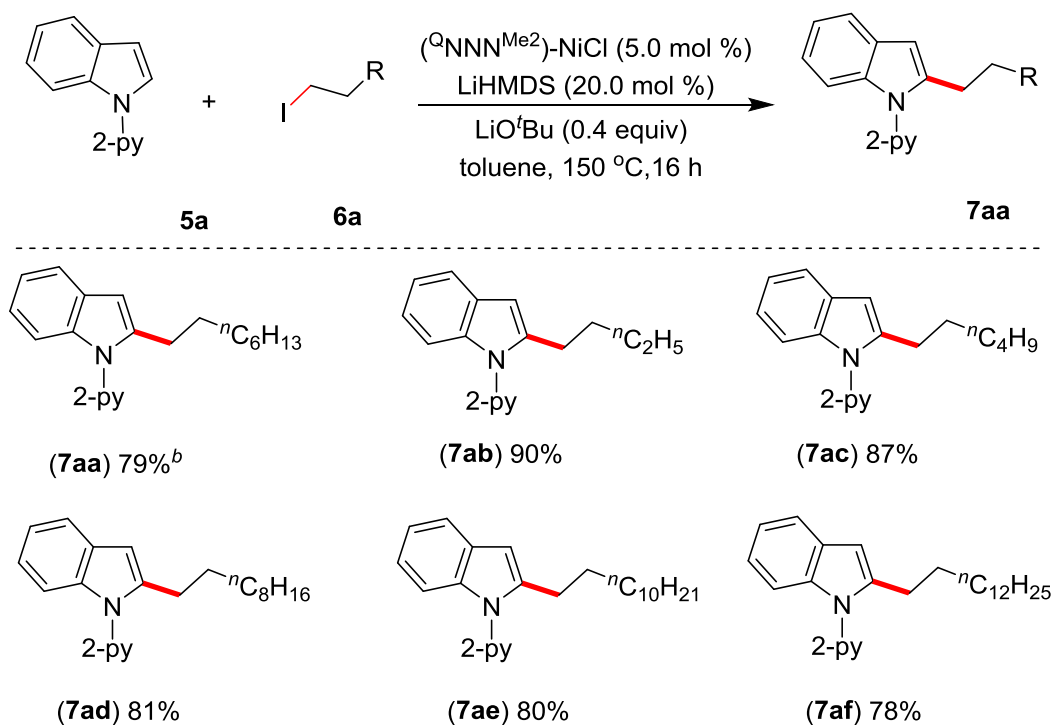


entry	[Ni] cat.	Base	Temp (°C)	Time (h)	GC Yield ^b (%)
1	2a	Na ₂ CO ₃	150	16	14
2	2a	K ₂ CO ₃	150	16	4
3	2a	Cs ₂ CO ₃	150	16	4
4	2a	KOAc	150	16	2
5	2a	CsOAc	150	16	3
6	2a	K ₃ PO ₄	150	16	17
7	2a	LiO^tBu	150	16	83 (79)^c
8	2a	LiO ^t Bu	150	12	65
9	2a	LiO ^t Bu	130	16	48
10	2a	LiO ^t Bu	100	24	17
11 ^d	2a	LiO ^t Bu	150	16	30
12 ^e	-	LiO ^t Bu	150	16	-
13	2b	LiO ^t Bu	150	16	55
14	3a	LiO ^t Bu	150	16	78
15	3b	LiO ^t Bu	150	16	50
16	4a	LiO ^t Bu	150	16	75

^aReaction conditions: **5a** (0.2 mmol), **6a** (0.4 mmol), and [Ni] cat. (5.0 mol %), LiOtBu (0.4 mmol), LiHMDS (20 mol %, 0.04 mmol). ^bGc yield using n-hexadecane as internal standard,

^cIsolated yield, ^dNo LiHMDS, ^eNo catalyst.

After rigorous optimization of indole alkylation using newly synthesized $(^Q\text{NNN}^{\text{Me}_2})\text{NiCl}$ complex, scope for the indole alkylation using different alkyl iodide was performed (Scheme 5.3). Alkyl halides having different chain length were subjected to optimized condition using indole pyridine. NMR yields were calculated for all the reaction and all the products were found to be in good to excellent yield. Since the catalytic performance of the newly synthesized $(^Q\text{NNN}^{\text{Me}_2})\text{NiCl}$ catalyst was found similar to the our previously described catalyst hence we have performed only few substrate scope for the indole alkylation.

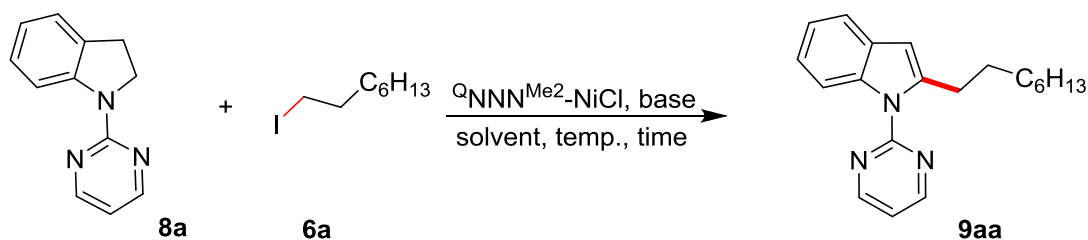


Scheme 5.3 Scope for alkylation of indole. indole **5a** (0.20 mmol), alkyl iodide **6** (0.40 mmol), cat. **2a** (0.003 g, 0.01 mmol, 5 mol %), LiHMDS (0.007 g, 0.04 mmol, 20 mol %), LiO^tBu (0.032 g, 0.40 mmol). ¹H NMR Yields of the products are calculated using CH₂Br₂ as internal standard. ^bIsolated Yield.

5.2.4 Dehydrogenative Alkylation of Indolines with Primary Halides.

Indolines and indoles are ubiquitous structural core found in organic dyes, numerous biologically active natural products, drugs and pharmaceutical compounds. Catalytic dehydrogenation of indoline reaction is a highly desired functionalization method for unreactive C(sp³)-H bonds since the corresponding alkenes are valuable synthetic intermediates for a variety of industrially important processes. Thus, there is a growing interest in the efficient and selective functionalization of indolines, particularly by developing the strategies based on transition-metal-catalyzed direct C-H bond activation. Herein, we have utilized the newly synthesized ^QNNN^{R2}-Ni complex for indoline C-H bond functionalization. Surprisingly, we observed the dehydrogenative alkylation of indoline at C-2 position. Most likely, in this catalytic transformation first indoline oxidizes to indole *via* 2-pyrimidinyl directed C-H bond activation and then β -hydride elimination in the presence of nickel catalyst. Once indoline has converted to indole, the C-H bond alkylation takes place at C-2 position of resulted indole by the nickel catalyst. Interestingly both the transformation took place in one pot.

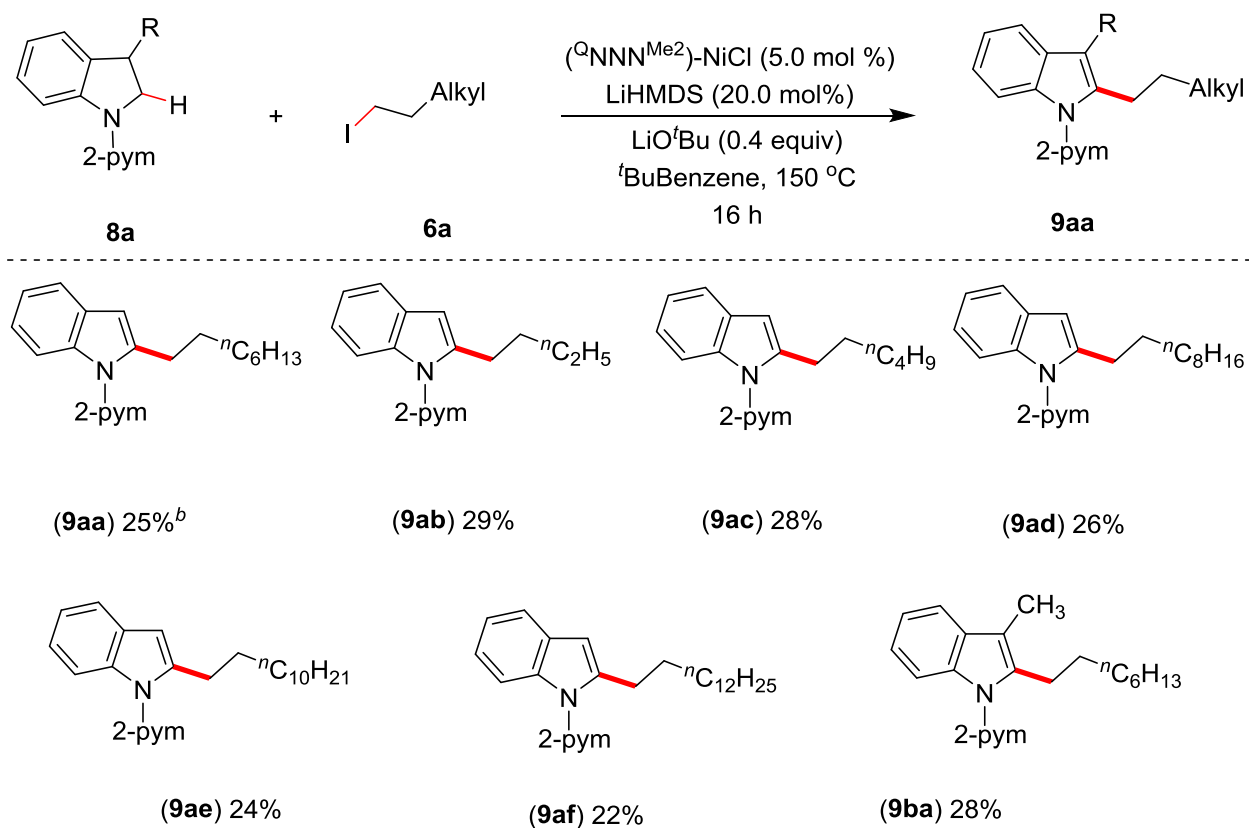
With some primitive observation we started optimization for the cross-coupling of 1-(pyrimidin-2-yl)indoline with 1-iodooctane employing the nickel catalyst **2a**, base LiO^tBu/LiHMDS and toluene (Table 5.3). Toluene was found to be partially coupled with indole (benzylated product 2-benzyl-1-(pyridin-2-yl)-1*H*-indole) along with the indoline dehydrogenative alkylated product **9aa**. Further, we have performed the reaction in other solvents like 1,4-dioxane, chlorobenzene, ^tButylbenzene, CF₃-Ph. etc (entries 2-6). Among all these solvents, ^tButylbenzene was more effective (entry 4). Apart from LiO^tBu some other bases were employed like NaO^tBu, Na₂CO₃, K₂CO₃, etc; but all other bases were found to be abortive (entries 7-9). The catalytic reaction provided similar result even in 16 h (entry 10). Reaction with an excess of catalyst (20 mol %) was ineffective and gave similar results (entry 11). Without catalyst no product was observed (entry 12). The employment of (^QNNN^{pyr})NiCl catalyst also gave similar result (44% of product) (entry 13). After rigorous optimization we could get the product in 29% (25%) yield.

Table 5.3 Optimization for Dehydrogenative Alkylation of Indoline^a

entry	solvent	base	temp (°C)	time (h)	9aa (%) ^b
1	toluene	LiO ^t Bu	150	24	48 ^c
2	1,4-dioxane	LiO ^t Bu	150	24	-
3	Cl-Ph	LiO ^t Bu	150	24	10
4	^t BuBenzene	LiO ^t Bu	150	24	45 (24) ^d
5	CF ₃ Ph	LiO ^t Bu	150	24	41
6	DMSO	LiO ^t Bu	150	24	-
7	^t BuBenzene	NaO ^t Bu	150	24	5
8	^t BuBenzene	Na ₂ CO ₃	150	24	-
9	^t BuBenzene	K ₂ CO ₃	150	24	-
10	^tBuBenzene	LiO^tBu	150	16	48 (25) ^d
11 ^e	^t BuBenzene	LiO ^t Bu	150	16	38
12 ^f	^t BuBenzene	LiO ^t Bu	150	16	-
13 ^g	^t BuBenzene	LiO ^t Bu	150	16	44

^aReaction conditions: **8a** (0.2 mmol), **6a** (0.4 mmol), and [Ni] cat. (5.0 mol %), ^bGc conv., ^c10% toluene coupled product, ^dIsolated Yield, ^ecat. (20 mol %), ^fNo catalyst, ^gQNN^{pyr}-NiCl as catalyst.

To demonstrate the versatility of the catalytic reaction we have employed various 1-iodo alkanes having different alkyl chain length in the catalytic transformation (Scheme 5.4). All the yields were obtained by ¹H NMR analysis of the crude reaction mixture using CH₂Br₂ as internal standard. The 3-methyl indoline was also used for the catalytic transformation and resulted with 28% NMR yield.



Scheme 5.4 Scope for dehydrogenative alkylation of indoline. indoline **8** (0.20 mmol), alkyl iodide **6** (0.40 mmol), cat. **2a** (0.003 g, 0.01 mmol, 5 mol %), LiHMDS (0.007 g, 0.04 mmol, 20 mol %), LiO^tBu (0.032 g, 0.40 mmol). ^1H NMR Yields of the product are calculated using CH_2Br_2 as internal standard. ^bIsolated Yield.

5.3 CONCLUSION

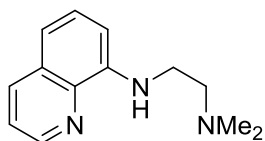
In summary, the inexpensive and novel pincer nickel complexes $(^Q\text{NNN}^{\text{R}_2})\text{NiX}$ were synthesized and fully characterized by various spectroscopic techniques. The molecular structures were confirmed by the X-ray crystallography technique. These complexes were screened and demonstrated for the C–H bond alkylation of important indoles with 1-iodoalkane containing β -hydrogen atoms. Further, the complexes were employed for the dehydrogenative C-2 alkylation of indoline using monodentate chelation assisted strategy. Newly synthesized complexes have shown double C–H activation in one pot, firstly dehydrogenation of indoline to indole and then C-2 alkylation. We have shown selected substrate scopes for the same.

5.4 EXPERIMENTAL

General Experiment

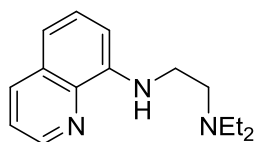
All manipulations were conducted under an argon atmosphere either in a glove box or using standard Schlenk techniques in pre-dried glass wares. The catalytic reactions were performed in flame-dried reaction vessels with Teflon screw cap. Solvents were dried over Na/benzophenone and distilled prior to use. Liquid reagents were flushed with argon prior to use. All other chemicals were obtained from commercial sources and were used without further purification. High resolution mass spectroscopy (HRMS) mass spectra were recorded on a Thermo Scientific Q-Exactive, Accela 1250 pump. NMR: (^1H and ^{13}C) spectra were recorded at 400 or 500 MHz (^1H), 100 or 125 MHz (^{13}C , DEPT (distortionless enhancement by polarization transfer)) respectively in CDCl_3 solutions, if not otherwise specified; chemical shifts (δ) are given in ppm. The ^1H and ^{13}C NMR spectra are referenced to residual solvent signals (CDCl_3 : $\delta \text{H} = 7.26$ ppm, $\delta \text{C} = 77.2$ ppm). NMR yields of the catalytic reactions were calculated by using CH_2Br_2 as an internal standard.

5.4.1 Procedure for Ligand Synthesis and Characterization Data

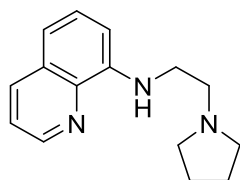


Synthesis of ($^{\text{O}}\text{NNN}^{\text{Me}_2}$)-H (1a): To a Schlenk tube, 8-aminoquinoline (2.0 g, 13.88 mmol) and 2-chloro-*N,N*-dimethylethan-1-amine hydrochloride (2.4 g, 16.66 mmol), was added under an argon atmosphere. The resulting solid mixture was heated at 140 °C for 24 h. After completion of the reaction, water (20 x 3 mL) was used to take out the entire compound in water (heated in water to get dissolved the compound). The water solution was cooled and the potassium carbonate was added into it, and then compound was extracted with ethyl acetate (30 mL x 3). The combined organic layer was washed with distilled water (30 mL x 3) and dried over Na_2SO_4 . The volatiles were evaporated under vacuum, and the crude mixture was purified by column chromatography on silica gel (petroleum ether/EtOAc: 5/1) to obtain a yellow liquid. Yield: 2.56 g, 86%. ^1H NMR (500 MHz, CDCl_3): $\delta = 8.73$ (dd, $J = 4.0, 1.7$ Hz, 1H, Ar-H), 8.01 (dd, $J = 8.4, 1.5$ Hz, 1H, Ar-H), 7.39 (t, $J = 8.0$ Hz, 1H, Ar-H), 7.31 (dd, $J = 8.0, 4.2$ Hz, 1H,

Ar-H), 7.04 (d, $J = 8.0$ Hz, 1H, Ar-H), 6.67 (d, $J = 7.2$ Hz, 1H, Ar-H), 6.49 (br. s., 1H, NH), 3.36 (q, $J = 6.1$ Hz, 2H, Ar-H), 2.68 (t, $J = 6.5$ Hz, 2H), 2.31 (s, 6H, CH₃). ¹³C NMR (125 MHz, CDCl₃): $\delta = 146.8$ (CH), 144.9 (C_q), 138.3 (C_q), 135.8 (CH), 128.6 (C_q), 127.7 (CH), 121.3 (CH), 113.7 (CH), 104.5 (CH), 58.1 (CH₂), 45.5 (2C, CH₃), 41.0 (CH₂). HRMS (ESI): m/z calcd for C₁₃H₁₇N₃+H⁺ [M + H]⁺ 216.1498, found 216.1495.



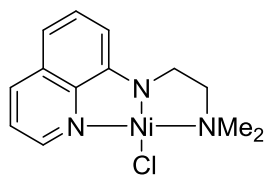
Synthesis of (QNNN^{Et2})-H (1b): This compound was synthesized following a procedure similar to the synthesis of **1a**, employing 8-aminoquinoline (2.0 g, 13.88 mmol) and 2-chloro-*N,N*-diethylethan-1-amine hydrochloride (2.8 g, 16.66 mmol), Yield: 2.85 g, 85%. ¹H NMR (500 MHz, CDCl₃): $\delta = 8.76$ (m, 1H, Ar-H), 8.12-8.01 (m, 1H, Ar-H), 7.43-7.38 (m, 1H, Ar-H), 7.32 (s, 1H, Ar-H), 7.06 (d, $J = 7.2$ Hz, 1H, Ar-H), 6.72 (d, $J = 5.7$, 1H, Ar-H), 6.58 (br s, 1H, NH), 3.39 (br s, 2H, CH₂), 2.85 (br s, 2H, CH₂), 2.68-2.54 (m, 4H, CH₂), 1.11 (br s, 6H, CH₃). ¹³C NMR (125 MHz, CDCl₃): $\delta = 146.6$ (CH), 145.0 (C_q), 138.3 (C_q), 135.6 (CH), 128.5 (C_q), 127.7 (CH), 121.1 (CH), 113.5 (CH), 104.4 (CH), 51.6 (CH₂), 46.9 (2C, CH₂), 41.2 (CH₂), 11.8 (2C, CH₃). HRMS (ESI): m/z calcd for C₁₅H₂₁N₃+H⁺ [M + H]⁺ 244.1814, found 244.1808.



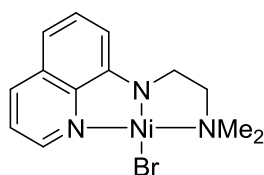
Synthesis of (QNNN^{pyr})-H (1c): This compound was synthesized following a procedure similar to the synthesis of **1a**, employing 8-aminoquinoline (2.0 g, 13.88 mmol) and 1-(2-chloroethyl)pyrrolidine hydrochloride (2.8 g, 16.66 mmol), Yield: 2.86 g, 86%. ¹H NMR (500 MHz, CDCl₃): $\delta = 8.69$ (dd, $J = 4.2, 1.5$ Hz, 1H, Ar-H), 7.96 (dd, $J = 8.0, 1.5$ Hz, 1H, Ar-H), 7.36 (t, $J = 7.8$ Hz, 1H, Ar-H), 7.31-7.22 (m, 1H, Ar-H), 7.00 (d, $J = 8.4$ Hz, 1H, Ar-H) 6.66 (d, $J = 7.6$ Hz, 1H, Ar-H), 6.44 (s, 1H, NH), 3.40 (q, $J = 6.5$ Hz, 2H, CH₂), 2.82 (t, $J = 6.7$ Hz, 2H, CH₂), 2.63-2.45 (m, 4H, CH₂), 1.83-1.69 (m, 4H, CH₂). ¹³C NMR (125 MHz, CDCl₃): $\delta = 146.6$ (CH), 144.8 (C_q), 138.2 (C_q), 135.7 (CH), 128.6 (C_q), 127.7 (CH), 121.2 (CH), 113.6 (CH),

104.4 (CH), 54.9 (CH₂), 54.1 (2C, CH₂), 42.3 (CH₂), 23.4 (2C, CH₃). HRMS (ESI): m/z calcd for C₁₅H₁₉N₃+H⁺ [M+H]⁺ 242.1656, found 242.1652.

5.4.2 Procedure for Synthesis of Complex and Characterization Data

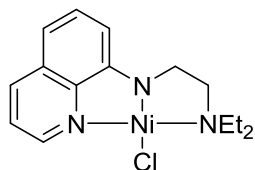


Synthesis of (QNNN^{Me2})NiCl (2a). The ⁿBuLi (1.5 mL, 2.55 mmol) was slowly added to a THF solution (10 mL) of ligand QNNN^{Me2}-H (1a; 0.500 g, 2.32 mmol) at 0 °C. The reaction mixture was stirred for 1 h at room temperature. This reaction mixture was added into a solution of (dme)NiCl₂ (0.510 g, 2.32 mmol) in THF (10 mL). The resulting solution was stirred overnight and then evaporated in vacuum. The residue was extracted with toluene (10 X 3 mL), and then was concentrated to 5 mL. Addition of pentane (20 mL) afforded a violet precipitate, which was filtered, washed with additional pentane, and vacuum dried.. Filtrate part was kept for slow evaporation which afforded violet crystals suitable for X-ray analysis. Yield: 0.490 g, 68%. Mp: 142–145 °C. ¹H NMR (500 MHz, CDCl₃): δ = 8.26 (d, J = 5.0, 1H, Ar-H), 7.97 (d, J = 8.2, 1H, Ar-H), 7.20-7.09 (m, 2H, Ar-H), 6.53 (d, J = 8.1, 1H, Ar-H), 6.19 (d, J = 7.8 Hz, 1H, Ar-H), 2.86 (t, J = 6.0, Hz, 2H, CH₂), 2.64-2.58 (m, 2H, CH₂; 6H, CH₃). ¹³C NMR (125 MHz, CDCl₃): δ 154.8 (C_q), 148.8 (CH), 145.6 (C_q), 137.7 (CH), 129.6 (C_q), 129.7 (CH), 121.0 (CH), 108.0 (CH), 104.4 (CH), 67.6 (CH₂), 49.4 (2C, CH₃), 44.5 (CH₂). HRMS (ESI): m/z calcd for C₁₃H₁₆ClN₃Ni+H⁺ [M+H]⁺ 308.0461, found 308.0459. Anal. Calcd for C₁₃H₁₆ClN₃Ni: C, 50.62; H, 5.23; N, 13.62. Found: C, 50.23; H, 5.07; N, 12.90.

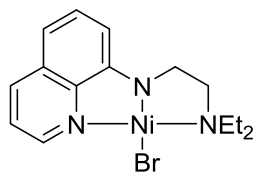


Synthesis of (QNNN^{Me2})NiBr (2b). This compound was synthesized following a procedure similar to the synthesis of **2a**, employing QNNN^{Me2}-H (1a; 0.50 g, 2.32 mmol), ⁿBuLi (1.5 mL, 2.55 mmol) and (thf)NiBr₂ (0.841 g, 2.32 mmol). Yield: 0.513 g, 63%. Mp: 170–174 °C. ¹H NMR (500 MHz, CDCl₃): δ = 8.56 (d, J = 4.6, 1H, Ar-H), 7.95 (d, J = 8.0, 1H, Ar-H), 7.16 (t, J

= 8.2, 1H, Ar-H), 7.09 (dd, $J = 8.0$, $J = 5.3$, 1H, Ar-H), 6.55 (d, $J = 8.0$ Hz, 1H, Ar-H), 6.22 (d, $J = 7.6$ Hz, 1H, Ar-H), 2.87 (t, $J = 6.1$, Hz, 2H, CH₂), 2.72 (s, 6H, CH₃), 2.62 (t, $J = 5.7$, Hz, 2H, CH₂). ¹³C NMR (125 MHz, CDCl₃): δ 154.8 (C_q), 151.1 (CH), 145.3 (C_q), 137.6 (CH), 129.6 (CH), 121.2 (CH), 108.2 (CH), 104.2 (CH), 67.6 (CH₂), 50.4 (2C, CH₃), 44.6 (CH₂). HRMS (ESI): m/z calcd for C₁₃H₁₆N₃BrNi+H⁺ [M+H]⁺ 351.9948, found 351.9954. Anal. Calcd for C₁₃H₁₆N₃BrNi: C, 44.25; H, 4.57; N, 11.91. Found: C, 43.78; H, 4.92; N, 10.38.

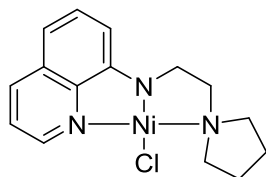


Synthesis of (QNNN^{Et2})NiCl (3a). This compound was synthesized following a procedure similar to the synthesis of **2a**, employing QNNN^{Et2}-H (1b; 0.50 g, 2.05 mmol), ⁿBuLi (1.4 mL, 2.25 mmol) and (dme)NiCl₂ (0.450 g, 2.05 mmol). Yield: 0.448 g, 65%. Mp: 168–170 °C. ¹H NMR (500 MHz, CDCl₃): δ = 8.28 (dd, $J = 5.3$, $J = 1.1$, 1H, Ar-H), 7.96 (dd, $J = 8.0$, $J = 1.1$, 1H, Ar-H), 7.16-7.10 (m, 2H, Ar-H), 6.52 (d, $J = 8.0$, 1H, Ar-H), 6.16 (d, $J = 7.6$ Hz, 1H, Ar-H), 3.25-3.18 (m, 2H, CH₂), 2.86 (t, $J = 6.1$ Hz, 2H, CH₂), 2.65 (t, $J = 6.1$ Hz, 2H, CH₂), 2.63-2.57 (m, 2H, CH₂), 1.84 (t, $J = 7.2$ Hz, 6H, CH₃). ¹³C NMR (125 MHz, CDCl₃): δ 154.8 (C_q), 148.6 (CH), 145.6 (C_q), 137.5 (CH), 129.4 (C_q), 129.6 (CH), 121.0 (CH), 107.8 (CH), 104.4 (CH), 57.2 (CH₂), 52.7 (2C, CH₂), 45.5 (CH₂), 11.6 (2C, CH₃). HRMS (ESI): m/z calcd for C₁₅H₂₀N₃ClNi+H⁺ [M+H]⁺ 336.0766, found 336.0772. Anal. Calcd for C₁₅H₂₀N₃ClNi: C, 53.54; H, 5.99; N, 12.49. Found: C, 53.83; H, 6.03; N, 12.04.



Synthesis of (QNNN^{Et2})NiBr (3b). This compound was synthesized following a procedure similar to the synthesis of **2a**, employing QNNN^{Et2}-H (1b; 0.50 g, 2.05 mmol), nBuLi (1.4 mL, 2.25 mmol) and (thf)NiCl₂ (0.743 g, 2.05 mmol). Yield: 0.484 g, 62%. Mp: 178–180 °C. ¹H NMR (500 MHz, CDCl₃): δ = 8.60 (d, $J = 4.6$, 1H, Ar-H), 7.96 (d, $J = 8.0$, 1H, Ar-H), 7.16 (t, $J = 7.6$, 1H, Ar-H), 7.11-7.09 (m, 1H, Ar-H), 6.55 (d, $J = 7.6$ Hz, 1H, Ar-H), 6.20 (d, $J = 7.2$ Hz,

^1H , Ar-H), 3.39-3.33 (m, 2H, CH_2), 2.88 (t, $J = 5.7$ Hz, 2H, CH_2), 2.69-2.65 (m, 4H, CH_2), 1.86 (t, $J = 6.9$ Hz, 6H, CH_3). ^{13}C NMR (125 MHz, CDCl_3): δ 155.0 (C_q), 151.1 (CH), 145.6 (C_q), 137.5 (CH), 129.5 (C_q), 129.6 (CH), 121.2 (CH), 108.1 (CH), 104.3 (CH), 56.9 (CH_2), 53.6 (2C, CH_2), 45.9 (CH_2), 11.9 (2C, CH_3). HRMS (ESI): m/z calcd for $\text{C}_{15}\text{H}_{20}\text{N}_3\text{BrNi}+\text{H}^+$ $[\text{M}+\text{H}]^+$ 380.0256, found 380.0267. Anal. Calcd for $\text{C}_{15}\text{H}_{20}\text{N}_3\text{BrNi}$: C, 47.29; H, 5.29; N, 11.03. Found: C, 47.10; H, 5.23; N, 10.86.



Synthesis of $(\text{QNNN}^{\text{pyr}})\text{NiCl}$ (4a). This compound was synthesized following a procedure similar to the synthesis of **2a**, employing $\text{QNN}^{\text{pyr}}\text{-H}$ (**1c**; 0.50 g, 2.07 mmol), $n\text{BuLi}$ (1.4 mL, 2.28 mmol) and $(\text{dme})\text{NiCl}_2$ (0.455 g, 2.05 mmol). Yield: 0.464, 67%. Mp: 160–164 °C. ^1H NMR (500 MHz, CDCl_3): δ = 8.29 (d, $J = 4.5$, 1H, Ar-H), 7.96 (d, $J = 8.1$, 1H, Ar-H), 7.22-7.03 (m, 2H, Ar-H), 6.51 (d, $J = 8.0$ Hz, 1H, Ar-H), 6.17 (d, $J = 7.3$ Hz, 1H, Ar-H), 3.88-3.63 (m, 2H, CH_2), 3.05-2.71 (m, 4H, CH_2), 2.70-2.46 (m, 2H, CH_2), 2.05-1.63 (m, 4H, CH_3). ^{13}C NMR (125 MHz, CDCl_3): δ 154.6 (C_q), 148.7 (CH), 145.7 (C_q), 137.6 (CH), 129.5 (C_q), 129.6 (CH), 121.0 (CH), 107.0 (CH), 104.3 (CH), 63.7 (CH_2), 57.4 (2C, CH_2), 46.3 (CH_2), 21.5 (2C, CH_2). HRMS (ESI): m/z calcd for $\text{C}_{15}\text{H}_{18}\text{ClN}_3\text{Ni}+\text{H}^+$ $[\text{M}+\text{H}]^+$ 334.0617, found 334.0615. Anal. Calcd for $\text{C}_{15}\text{H}_{18}\text{ClN}_3\text{Ni}$: C, 53.87; H, 5.42; N, 12.56. Found: C, 54.38; H, 4.95; N, 10.38.

5.4.3 Representative Procedure for Alkylation

Alkylation of Indoles: *Synthesis of 2-Octyl-1-(pyridin-2-yl)-1H-indole (7aa).* In a flame-dried screw-cap tube (5 mL) equipped with a magnetic stir bar were introduced 1-pyridin-2-yl-1H-indole (**5a**; 0.039 g, 0.20 mmol), 1-iodooctane (**6a**; 0.096 g, 0.40 mmol), catalyst **2a** (0.003 g, 0.01 mmol, 5.0 mol %), LiHMDS (0.010 g, 0.06 mmol, 20 mol %), and LiOtBu (0.038 g, 0.4 mmol) inside the glovebox. To the above mixture in the tube was added toluene (0.15 mL), and the resultant reaction mixture was stirred at 150 °C in a preheated oil bath for 16 h. At ambient temperature, the reaction mixture was quenched with distilled H_2O (10 mL) and then neutralized with 2 N HCl (0.5 mL). The crude product was then extracted with ethyl acetate (20 mL \times 3). The combined organic extract was dried over Na_2SO_4 , and the volatiles were evaporated in

vacuo. The remaining residue was purified by column chromatography on neutral alumina (petroleum ether/EtOAc: 50/1/) to yield **7aa** (0.048 g, 79%) as a light yellow liquid.

Alkylation of Indoline: *Synthesis of 2-Octyl-1-(pyrimidin-2-yl)-1H-indole (9aa):* The representative procedure of alkylation of indoles was followed, using substrate 1-(pyridin-2-yl)indoline (**8a**; 0.039 g, 0.20 mmol), 1-iodooctane (**6a**; 0.096 g, 0.40 mmol), catalyst **2a** (0.003 g, 0.01 mmol, 5.0 mol %), LiHMDS (0.010 g, 0.06 mmol, 20 mol %), and LiOtBu (0.038 g, 0.4 mmol). The resultant reaction mixture was stirred at 150 °C in a preheated oil bath for 16 h. At ambient temperature, the reaction mixture was quenched with distilled H₂O (10 mL). The crude product was then extracted with ethyl acetate (20 mL × 3). The combined organic extract was dried over Na₂SO₄, and the volatiles were evaporated in vacuo. The remaining residue was purified by column chromatography on neutral alumina (petroleum ether/EtOAc: 50/1/) to yielded **9aa** (0.016 g, 25%) as a light yellow liquid.

5.4.4 X-ray Structure Determination. X-ray intensity data measurements of compounds **2a**, **2b**, **3a**, **3b** and **5a** were carried out on a Bruker SMART APEX II CCD diffractometer with graphite-monochromatized (MoK_α= 0.71073 Å) radiation between 150(2) - 296 (2) K. The X-ray generator was operated at 50 kV and 30 mA. A preliminary set of cell constants and an orientation matrix were calculated from three sets of 12 frames (total 36 frames). Data were collected with ω scan width of 0.5° at eight different settings of φ and 2θ with a frame time of 10 sec keeping the sample-to-detector distance fixed at 5.00 cm for all the compounds. The X-ray data collection was monitored by APEX2 program (Bruker, 2006).⁴⁶ All the data were corrected for Lorentzian, polarization and absorption effects using SAINT and SADABS programs (Bruker, 2006). SHELX-97 was used for structure solution and full matrix least-squares refinement on F^2 .⁴⁷ Hydrogen atoms were placed in geometrically idealized position and constrained to ride on their parent atoms.

Crystal Data and Structure Refinement for Complexes 2a, 3b and 4a

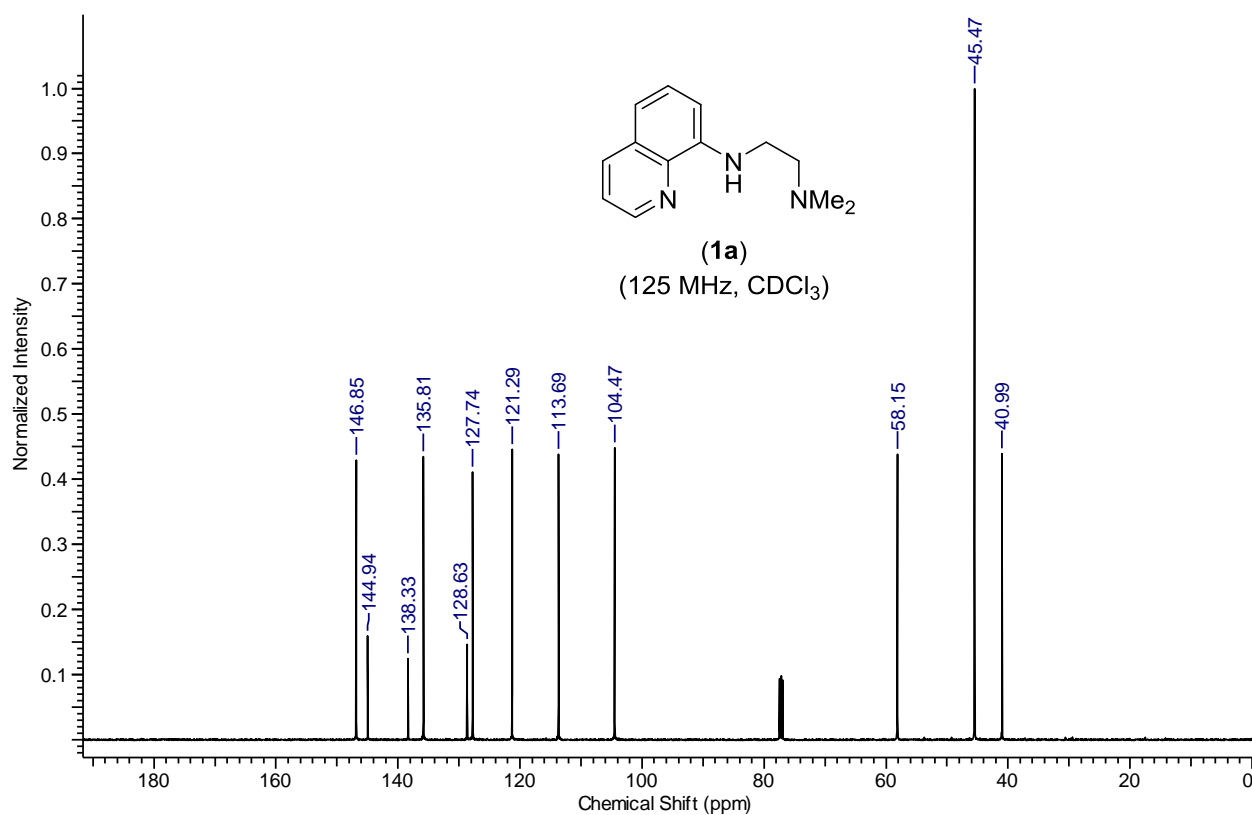
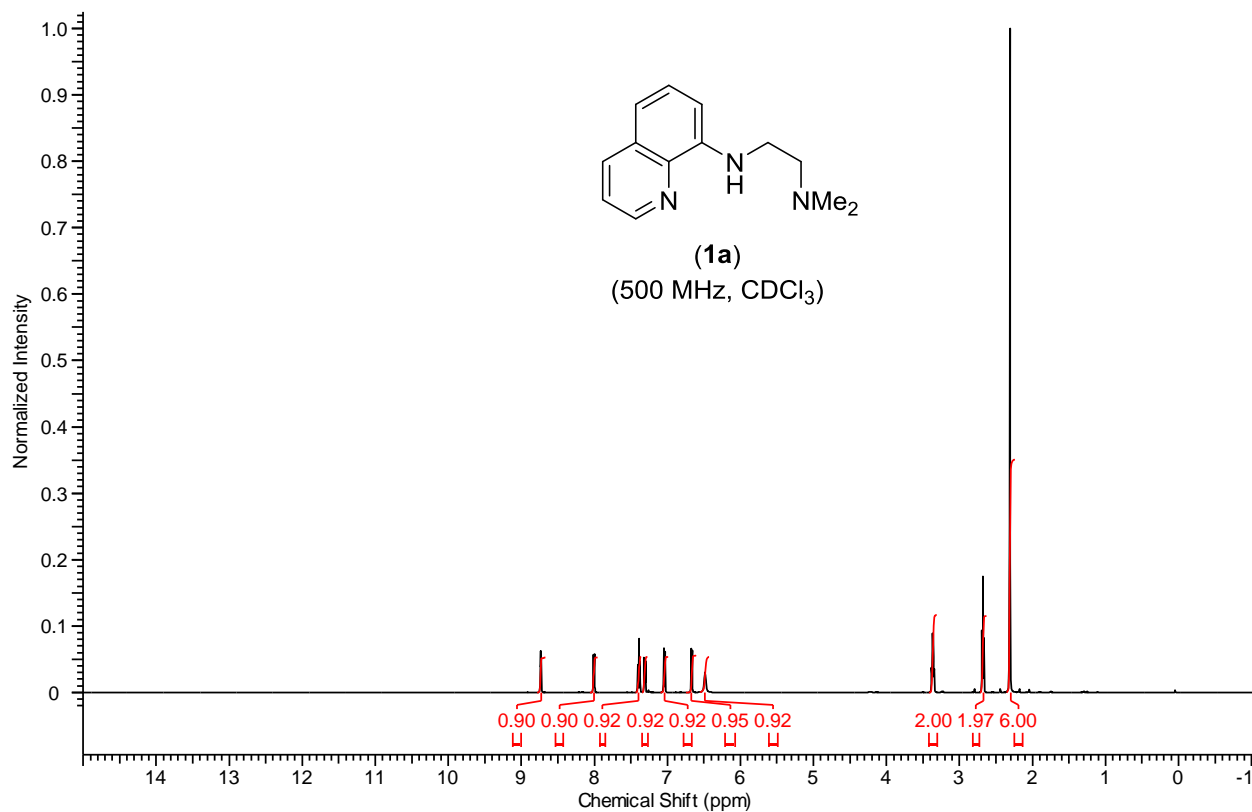
	2a	3b	4a
Empirical formula	C ₁₃ H ₁₆ ClN ₃ Ni	C ₁₅ H ₂₀ N ₃ BrNi	C ₁₅ H ₁₈ ClN ₃ Ni
Formula weight	308.43	380.94	333.47
Temperature, K	296(2) K	100(2) K	100(2) K
Cryst. Syst.	Orthorhombic	Orthorhombic	monoclinic
Space group	P b c a (61)	P 2 ₁ 2 ₁ 2 ₁ (19)	P 2 ₁ /n (14)
<i>a</i> (Å)	10.6351(2)	7.3020(2)	12.0842(3)
<i>b</i> (Å)	21.7017(5)	12.2147(3)	8.0478(2)
<i>c</i> (Å)	23.1374(5)	17.0510(5)	14.9369
α (°)	90	90	90
β (°)	90	90	100.108(10)
γ (°)	90	90	90
<i>V</i> (Å ³)	5340.1(2)	1520.81	1430.08(6)
<i>Z</i>	14	16	2
$\rho_{\text{calcd.}}$ g/cm ³	1.413	1.459	1.554
ε (mm ⁻¹)	1.437	1.4362	1.536
<i>F</i> (000)	2380	1232	696
Crystal size (mm)	0.23 x 0.17 x 0.15	0.31 x 0.21 x 0.17	0.29 x 0.30 x 0.25
θ (min, max) (°)	1.76, 24.998	2.914, 30.558	2.384, 24.996
R(int)	0.0341	0.0278	0.0432
Independent reflections	4711	4644	4983
Completeness to θ	100 %	99.9 %	99.7 %
Max. and min. transmission	0.6082, 0.7461	0.6401, 0.7461	0.4358, 0.7471
Data / restraints / parameters	4711 / 0 / 325	4644 / 0 / 184	4983 / 2 / 361
R ₁ , wR ₂ (<i>I</i> > 2 σ (<i>I</i>))	0.0455, 0.1362	0.0153, 0.0353	0.0297, 0.0787
R ₁ , wR ₂ (all data)	0.0483, 0.1389	0.0165, 0.0355	0.0301, 0.0795

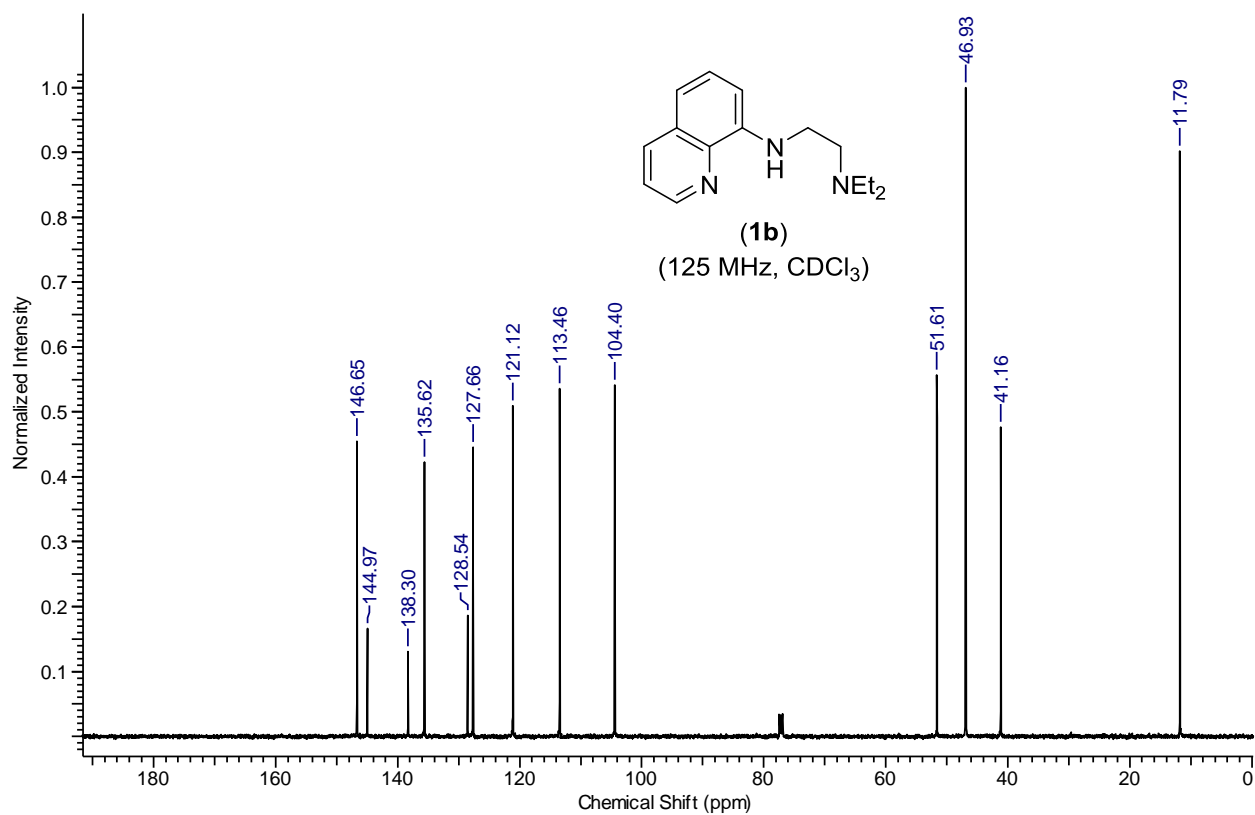
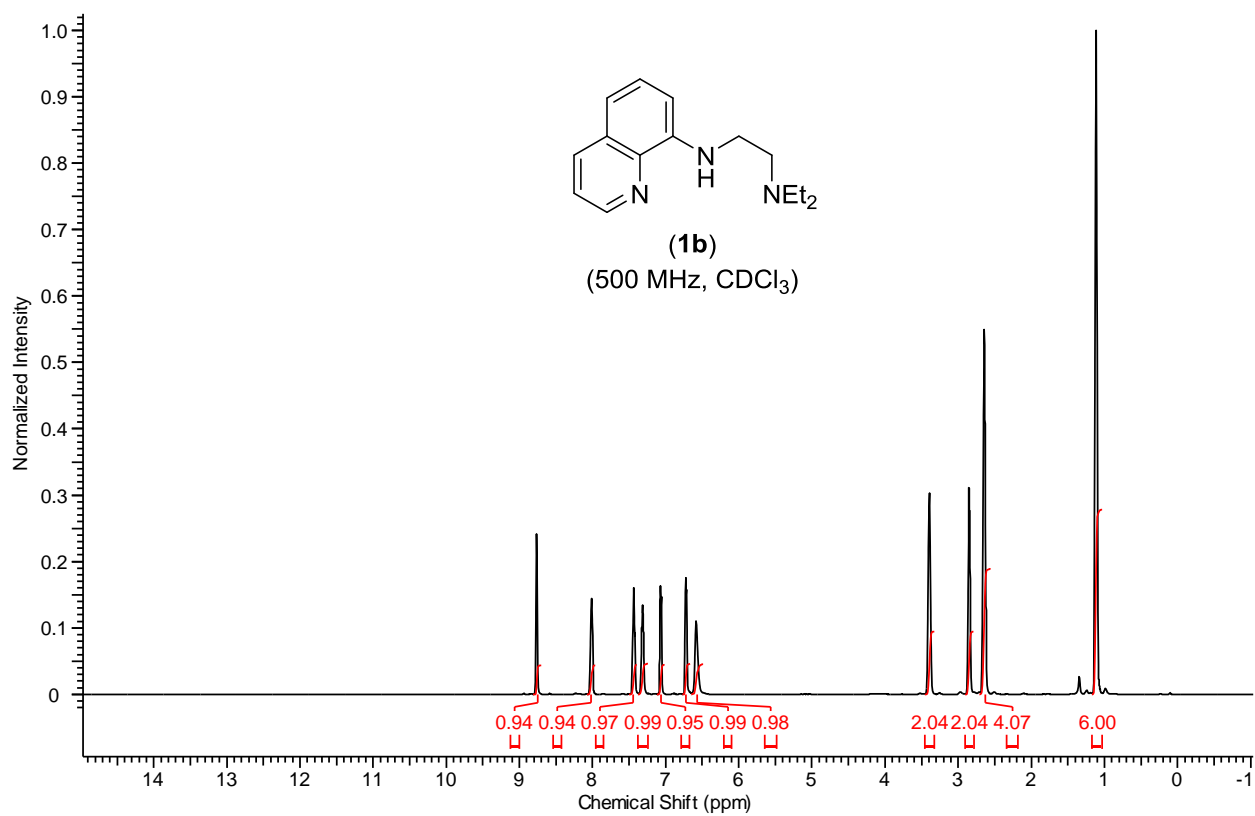
5.5 REFERENCES

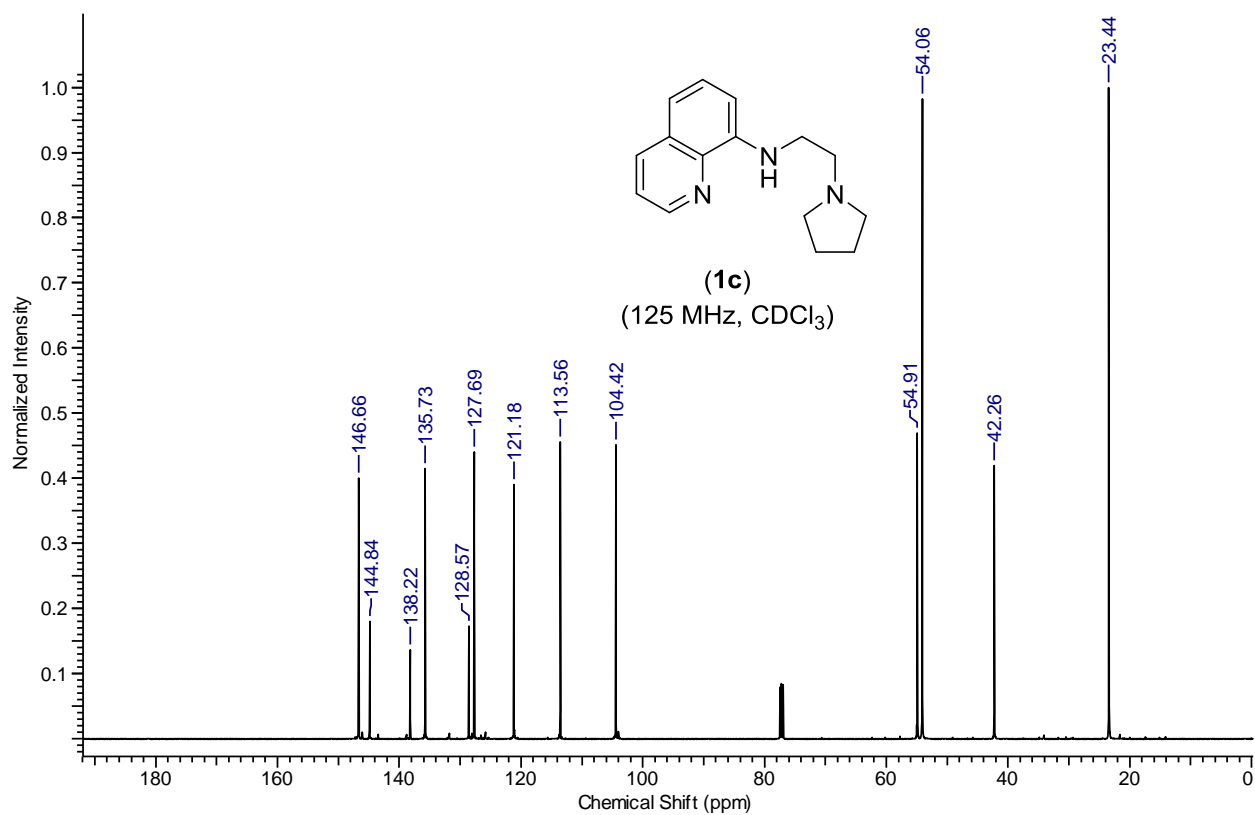
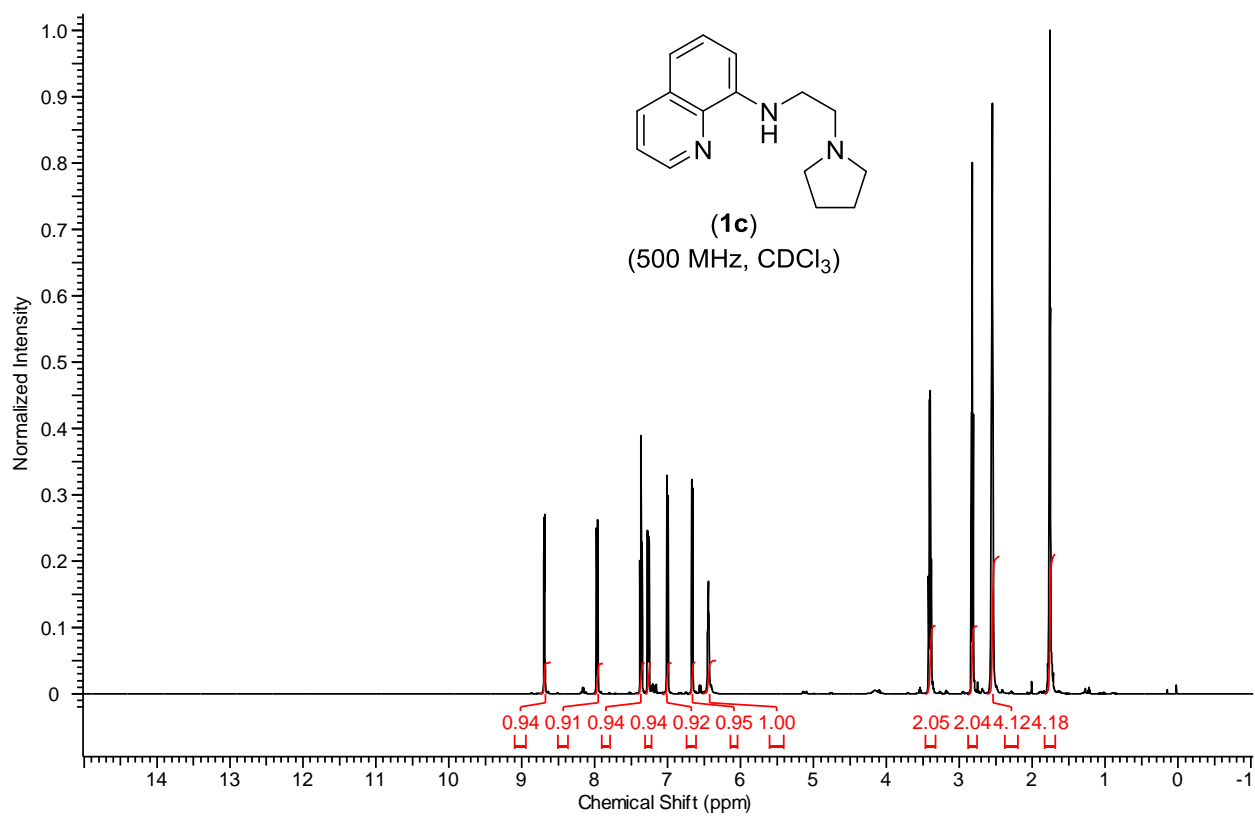
- (1) Tabrizi, L.; Chiniforoshan, H. *New J. Chem.* **2017**, *41*, 10972-10984.
- (2) Taghvaei, M.; Rodríguez-Álvarez, M. J.; García-Álvarez, J.; del Río, I.; Lough, A. J.; Gossage, R. A. *J. Organomet. Chem.* **2017**, *845*, 107-114.
- (3) Vasilenko, V.; Blasius, C. K.; Wadepohl, H.; Gade, L. H. *Angew. Chem. Int. Ed.* **2017**, *56*, 8393-8397.
- (4) Wenz, J.; Kochan, A.; Wadepohl, H.; Gade, L. H. *Inorg. Chem.* **2017**, *56*, 3631-3643.
- (5) Pocquet, L.; Vologdin, N.; Mangiatordi, G. F.; Ciofini, I.; Nicolotti, O.; Thorimbert, S.; Salmain, M. *Eur. J. Inorg. Chem.* **2017**, 3622-3634.
- (6) Pandiri, H.; Soni, V.; Gonnade, R. G.; Punji, B. *New J. Chem.* **2017**, *41*, 3543-3554.
- (7) Mastalir, M.; Pittenauer, E.; Stöger, B.; Allmaier, G.; Kirchner, K. *Org. Lett.* **2017**, *19*, 2178-2181.
- (8) Kumar, L. M.; Ansari, R. M.; Bhat, B. R. *Appl. Organomet. Chem.* **2018**, *32*, 4054.
- (9) Domyati, D.; Latifi, R.; Tahsini, L. *J. Organomet. Chem.* **2018**, *860*, 98-105.
- (10) Zohreh, N.; Jahani, M. *J. Mol. Catal. A: Chem.* **2017**, *426*, 117-129.
- (11) Garbe, M.; Junge, K.; Walker, S.; Wei, Z.; Jiao, H.; Spannenberg, A.; Bachmann, S.; Scalone, M.; Beller, M. *Angew. Chem. Int. Ed.* **2017**, *56*, 11237-11241.
- (12) Ehrlich, N.; Kreye, M.; Baabe, D.; Schweyen, P.; Freytag, M.; Jones, P. G.; Walter, M. D. *Inorg. Chem.* **2017**, *56*, 8415-8422.
- (13) Cope, J. D.; Denny, J. A.; Lamb, R. W.; McNamara, L. E.; Hammer, N. I.; Webster, C. E.; Hollis, T. K. *J. Organomet. Chem.* **2017**, *845*, 258-265.
- (14) Singh, M. P.; Saleem, F.; Rao, G. K.; Kumar, S.; Joshi, H.; Singh, A. K. *Dalton Trans.* **2016**, *45*, 6718-6725.
- (15) Reilly, S. W.; Webster, C. E.; Hollis, T. K.; Valle, H. U. *Dalton Trans.* **2016**, *45*, 2823-2828.
- (16) Murugesan, S.; Kirchner, K. *Dalton Trans.* **2016**, *45*, 416-439.
- (17) Ji, M.; Dong, C.; Yang, X. *J. Coord. Chem.* **2016**, *69*, 1380-1387.
- (18) Yang, L.; Zhang, X.; Mao, P.; Xiao, Y.; Bian, H.; Yuan, J.; Mai, W.; Qu, L. *RSC Adv.* **2015**, *5*, 25723-25729.
- (19) Salah, A.; Corpet, M.; Khan, N. U-H.; Zargarian, D.; Spasyuk, D. M. *New J. Chem.* **2015**, *39*, 6649-6658.

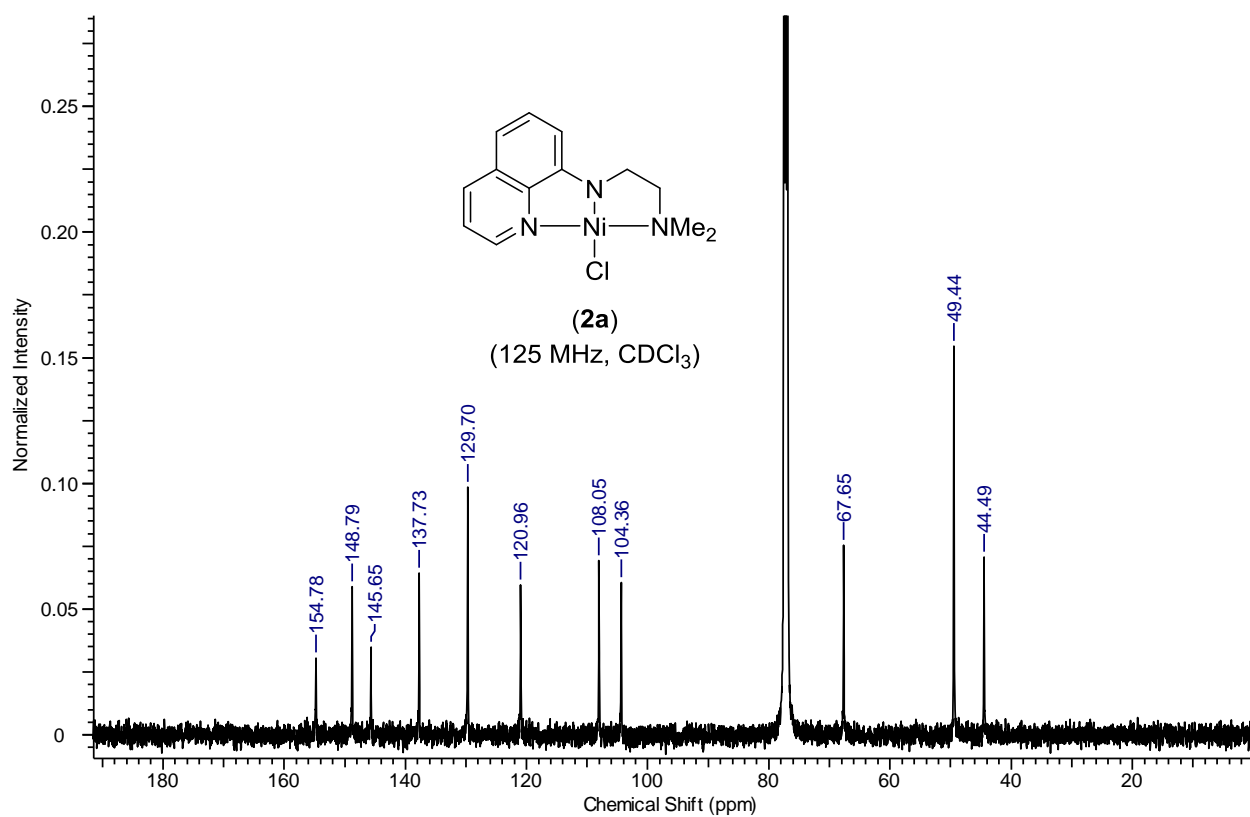
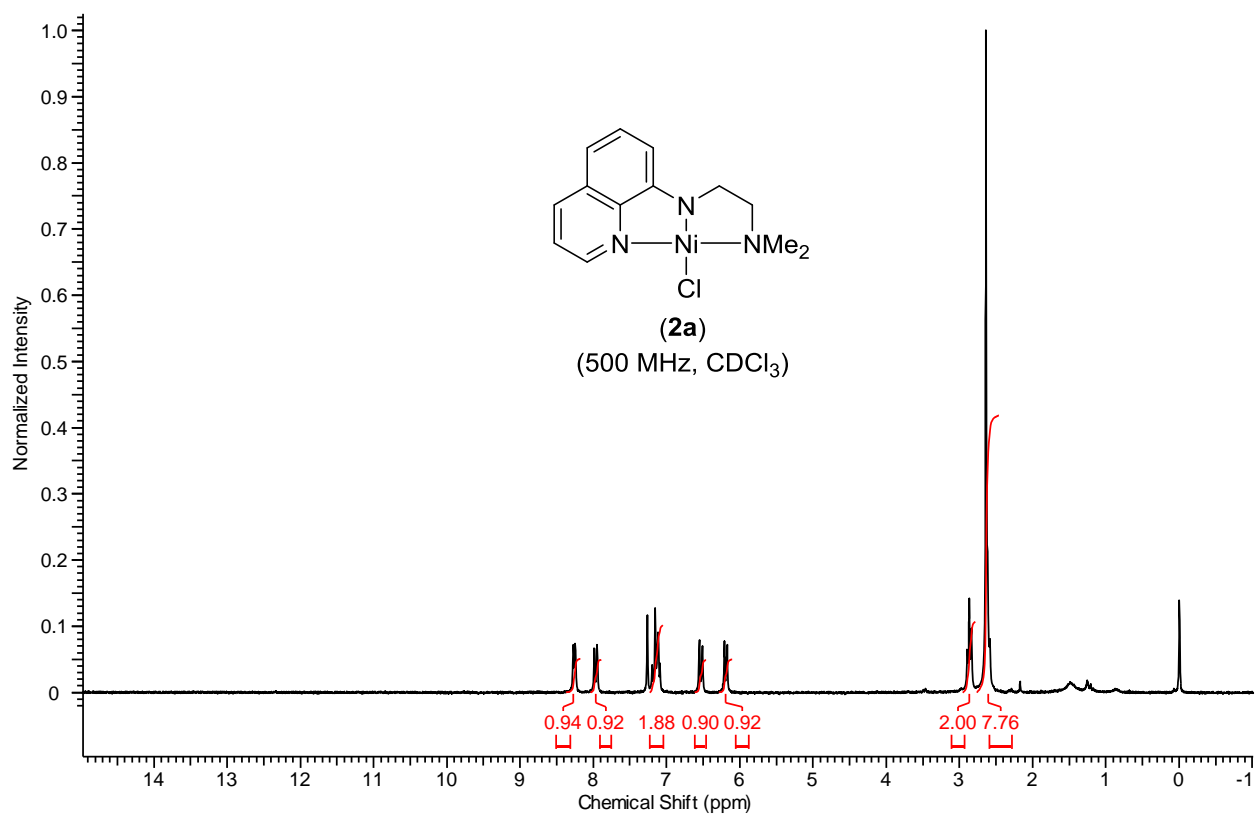
-
- (20) Lapointe, S.; Vabre, B.; Zargarian, D. *Organometallics* **2015**, *34*, 3520-3531.
- (21) Kumar, P.; Kashid, V. S.; Reddi, Y.; Mague, J. T.; Sunoj, R. B.; Balakrishna, M. S. *Dalton Trans.* **2015**, *44*, 4167-4179.
- (22) Fleckhaus, A.; Mousa, A. H.; Lawal, N. S.; Kazemifar, N. K.; Wendt, O. F. *Organometallics* **2015**, *34*, 1627-1634.
- (23) Madhira, V. N.; Ren, P.; Vechorkin, O.; Hu, X.; Vicic, D. A. *Dalton Trans.* **2012**, *41*, 7915-7919.
- (24) Shao, D.-D.; Niu, J.-L.; Hao, X.-Q.; Gong, J.-F.; Song, M.-P. *Dalton Trans.* **2011**, *40*, 9012-9019.
- (25) Kozhanov, K. A.; Bubnov, M. P.; Cherkasov, V. K.; Vavilina, N. N.; Efremova, L. Y.; Artyushin, O. I.; Odinets, I. L.; Abakumov, G. A. *Dalton Trans.* **2008**, 2849-2853.
- (26) Zargarian, D.; Castonguay, A.; Spasyuk, D. M. *Top Organomet. Chem.* **2013**, *40*, 131-174.
- (27) Hao, J.; Mougang-Soumé, B.; Vabre, B.; Zargarian, D. *Angew. Chem., Int. Ed.* **2014**, *53*, 3218-3222.
- (28) Wu, D.; Wang, Z.-X. *Org. Biomol. Chem.* **2014**, *12*, 6414-6424.
- (29) Vechorkin, O.; Godinat, A.; Scopelliti, R.; Hu, X. *Angew. Chem. Int. Ed.* **2011**, *50*, 11777-11781.
- (30) Buslov, I.; Becouse, J.; Mazza, S.; Montandon-Clerc, M.; Hu, X. *Angew. Chem. Int. Ed.* **2015**, *54*, 14523-14526.
- (31) Hu, X. *Chimia* **2012**, *66*, 154-158.
- (32) Rettenmeier, C. A.; Wenz, J.; Wadepohl, H.; Gade, L. H. *Inorg. Chem.* **2016**, *55*, 8214-8224.
- (33) Vechorkin, O.; Proust, V.; Hu, X. *J. Am. Chem. Soc.* **2009**, *131*, 9756-9766.
- (34) Pérez Garcia, P. M.; Di Franco, T.; Epenoy, A.; Scopelliti, R.; Hu, X. *ACS Catal.* **2016**, *6*, 258-261.
- (35) Gu, S.; Du, J.; Huang, J.; Guo, Y.; Yang, L.; Xu, W.; Chen, W. *Dalton Trans.* **2017**, *46*, 586-594.
- (36) Sun, Y.; Li, X.; Sun, H. *Dalton Trans.* **2014**, *43*, 9410-9413.
- (37) Johnson, S. A. *Dalton Trans.* **2015**, *44*, 10905-10913.
- (38) Vabre, B.; Petiot, P.; Declercq, R.; Zargarian, D. *Organometallics* **2014**, *33*, 5173-5184.

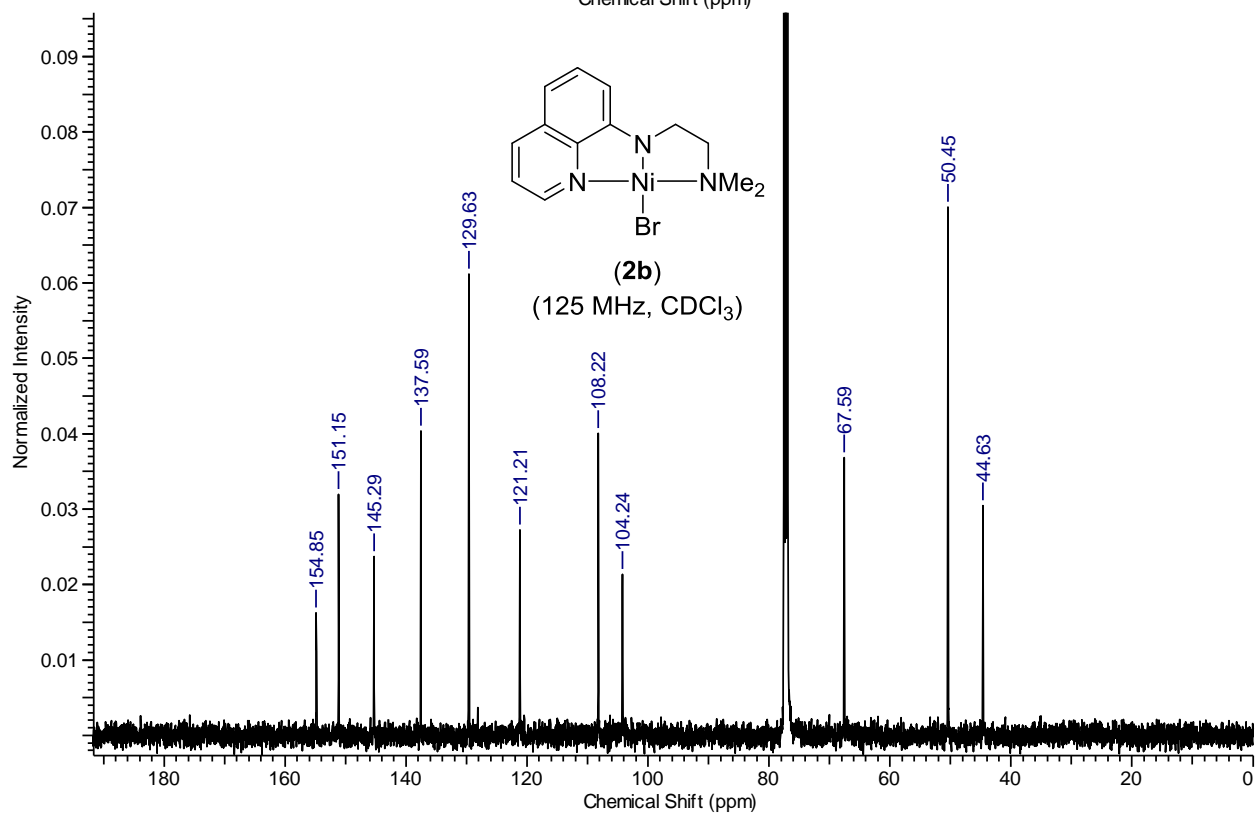
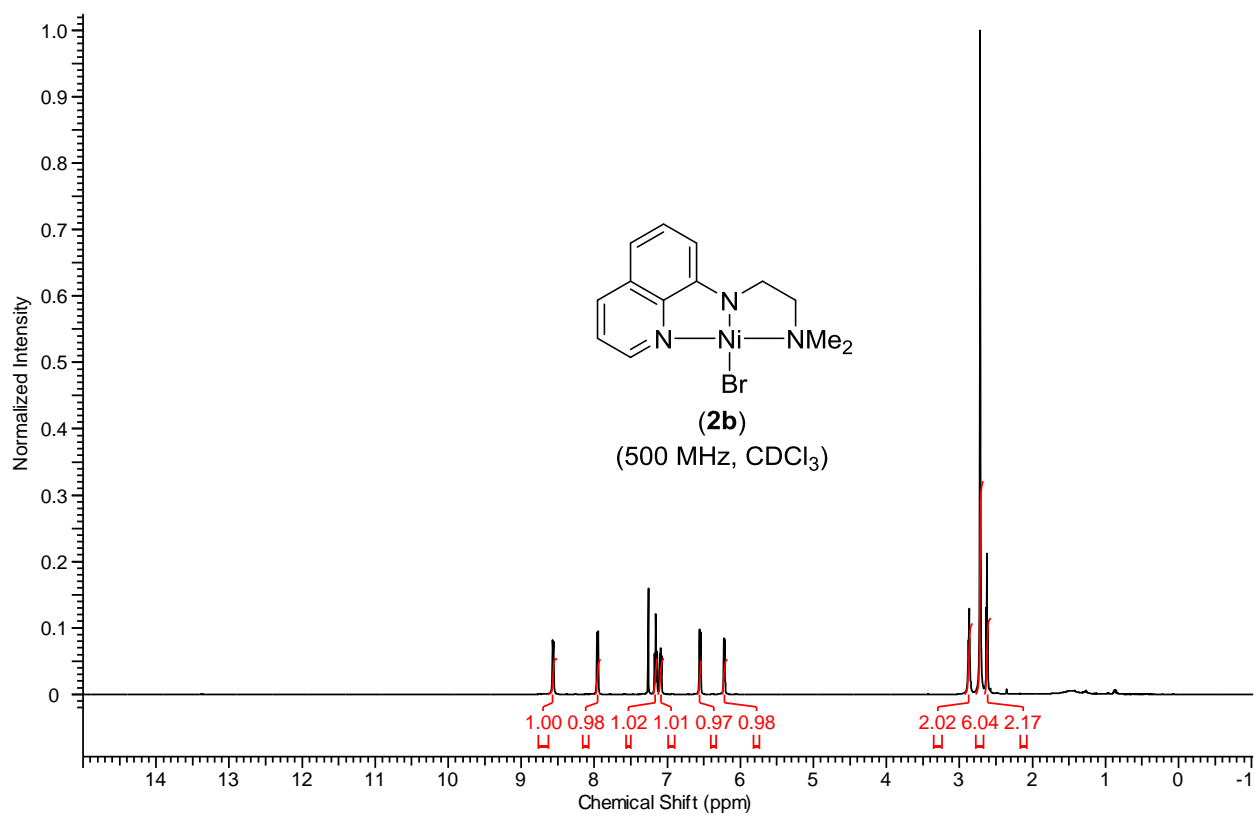
- (39) Patel, U. N.; Pandey, D. K.; Gonnade, R. G.; Punji, B. *Organometallics* **2016**, *35*, 1785-1793.
- (40) Pandiri, H.; Sharma, D. M.; Gonnade, R. G.; Punji, B. *J. Chem. Sci.* **2017**, *129*, 1161-1169.
- (41) Vechorkin, O.; Csok, Z.; Scopelliti, R.; Hu, X. *Chem. Eur. J.* **2009**, *15*, 3889-3899.
- (42) Liang, L.-C.; Chien, P.-S.; Huang, Y.-L. *J. Am. Chem. Soc.* **2006**, *128*, 15562-15563.
- (43) Csok, Z.; Vechorkin, O.; Harkins, S. B.; Scopelliti, R.; Hu, X. *J. Am. Chem. Soc.* **2008**, *130*, 8156-8157.
- (44) Pérez García, P. M.; Ren, P.; Scopelliti, R.; Hu, X. *ACS Catal.* **2015**, *5*, 1164-1171.
- (45) Soni, V.; Jagtap, R. A.; Gonnade, R. G.; Punji, B. *ACS Catal.* **2016**, *6*, 5666-5672.
- (46) APEX2, SAINT and SADABS. *Bruker AXS Inc.*, Madison, Wisconsin, USA **2006**.
- (47) Sheldrick, G. M. *Acta Crystallogr.* **2008**, *A64*, 112-122.

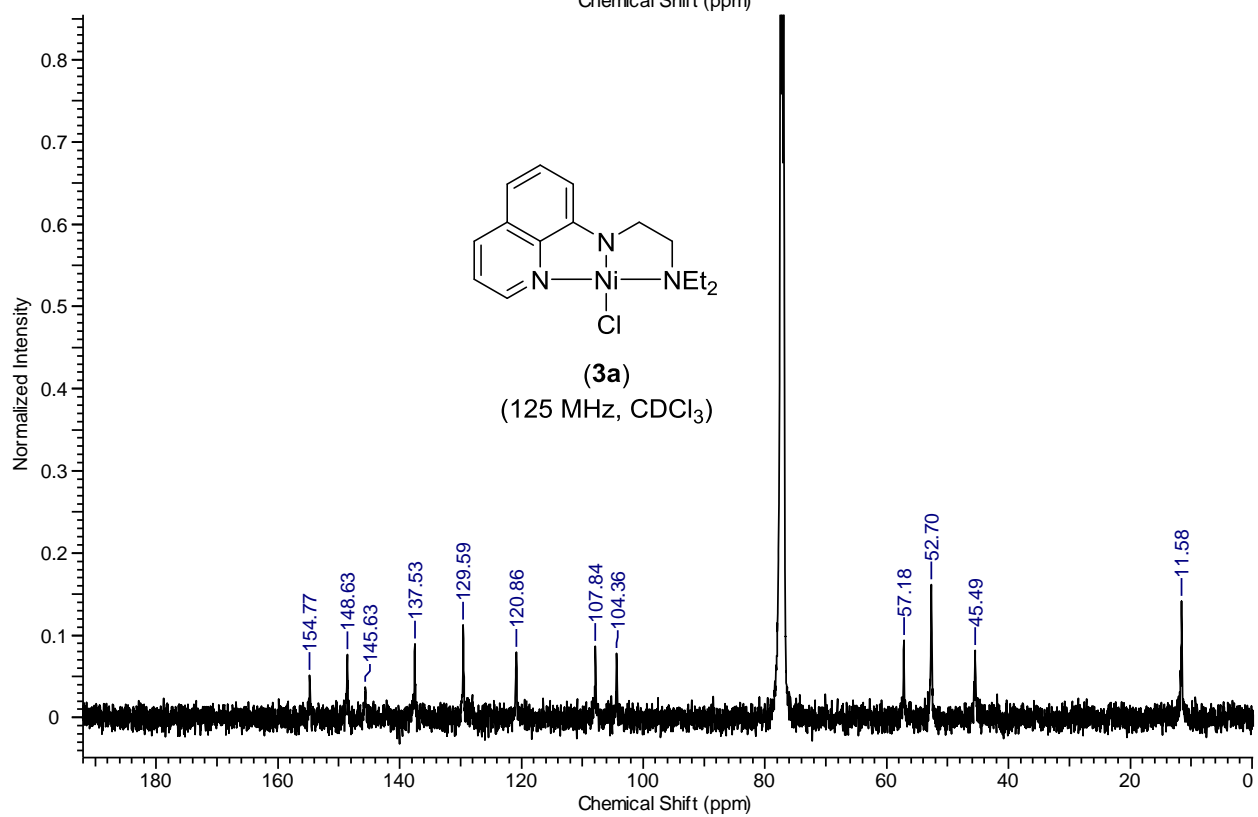
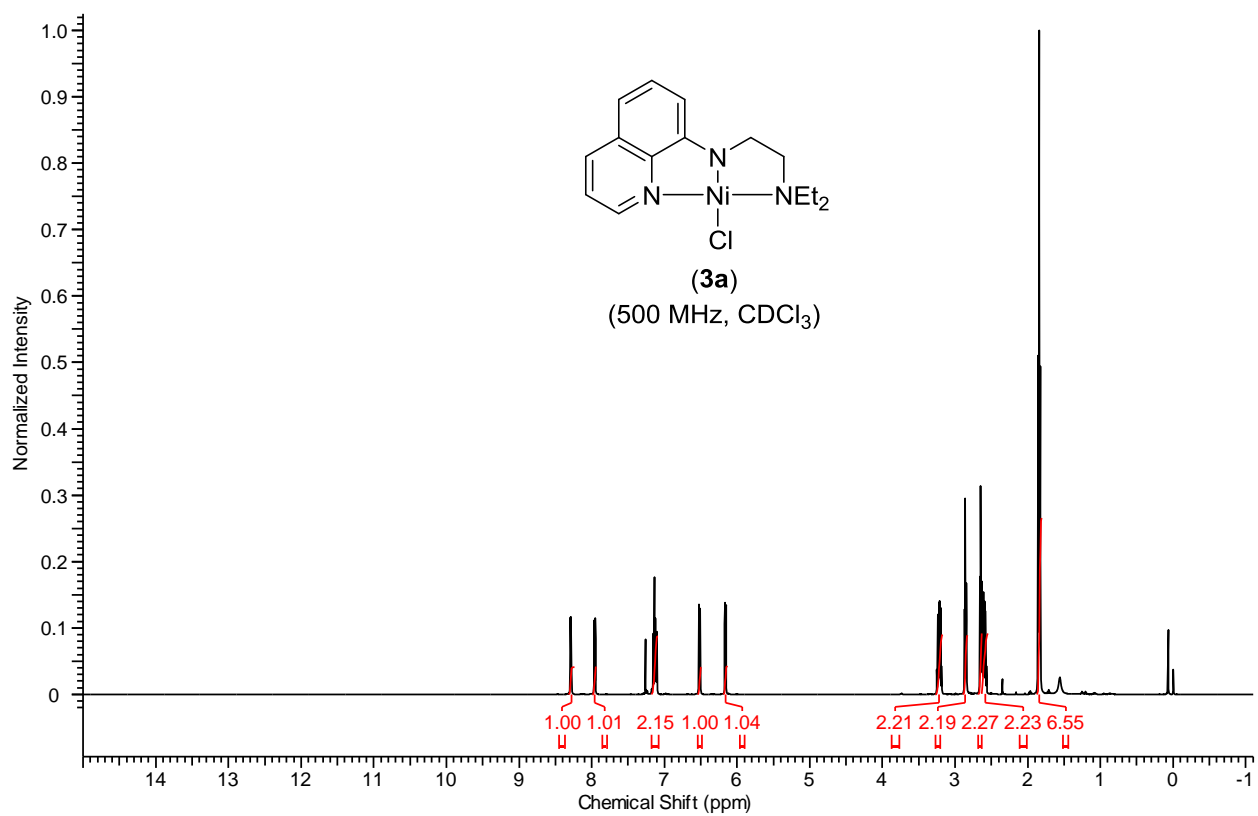
^1H and ^{13}C NMR Spectra of the Complexes

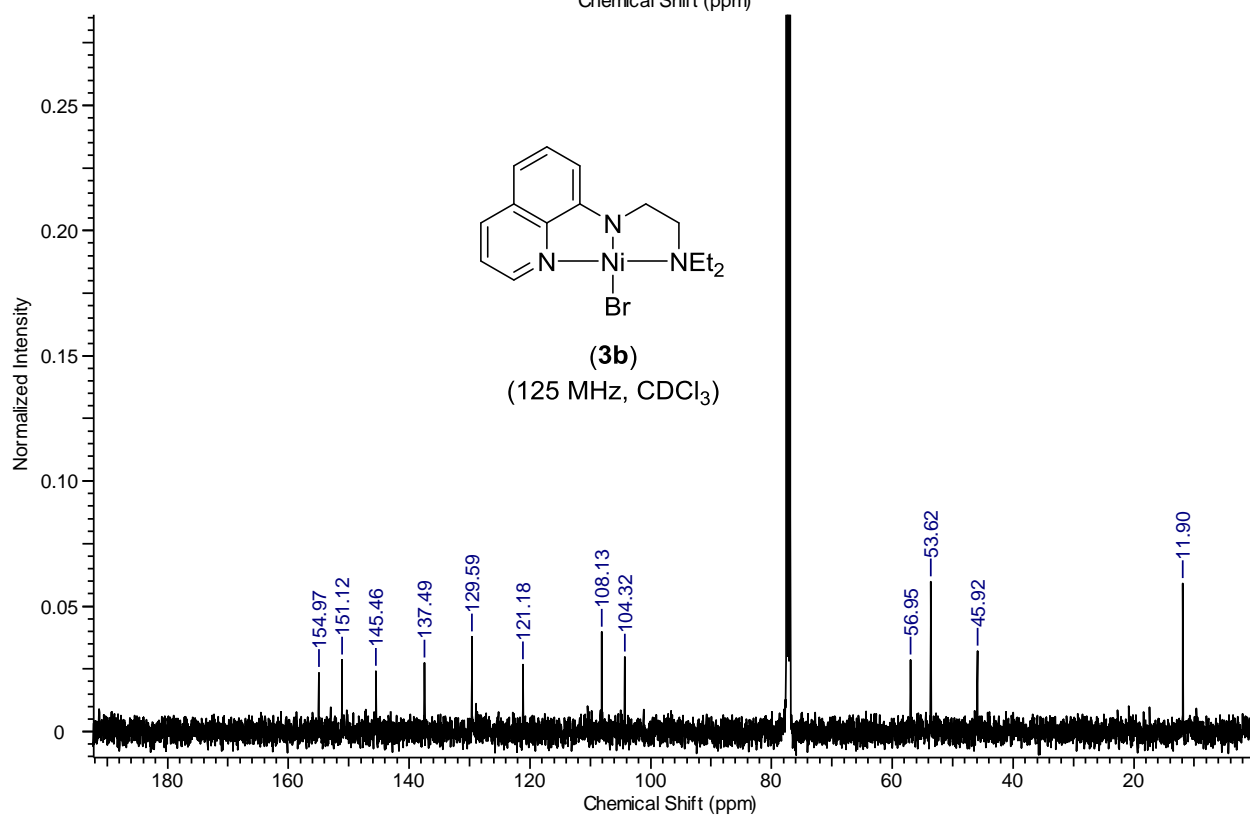
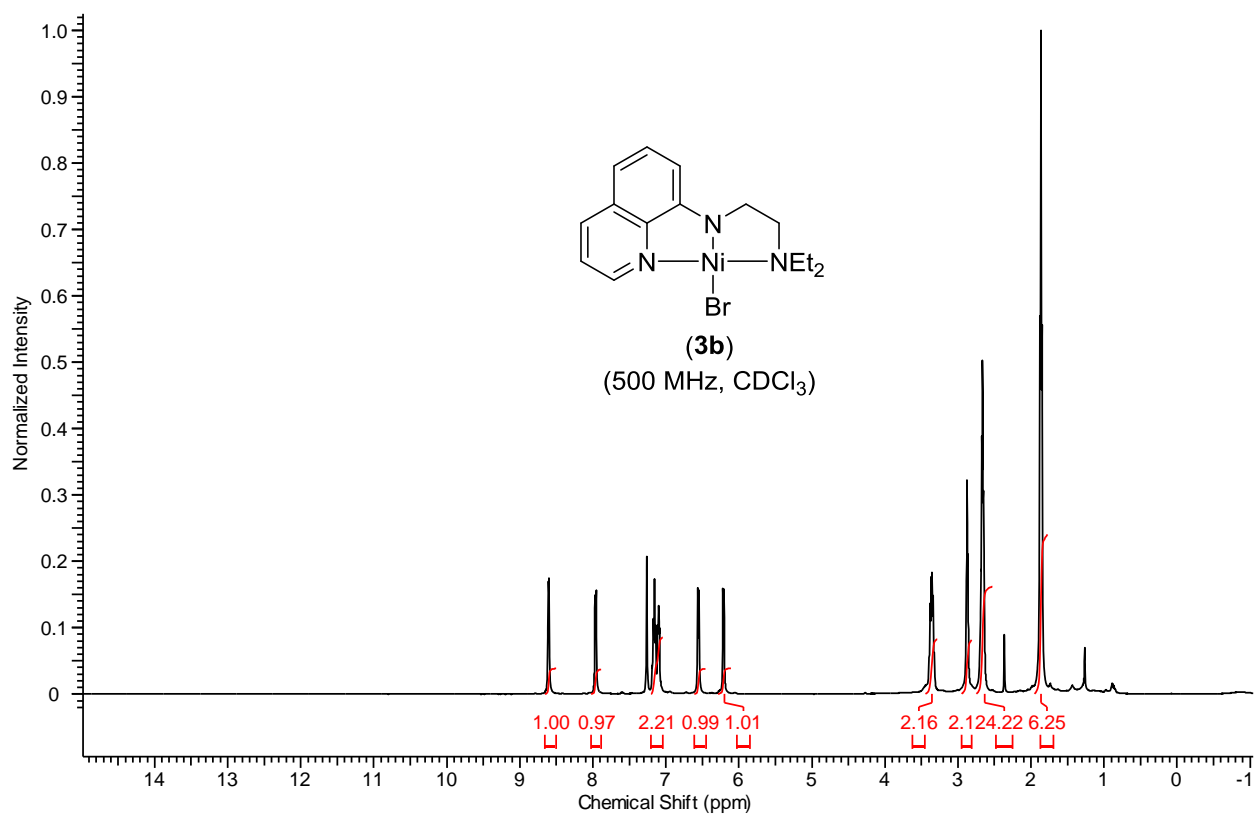


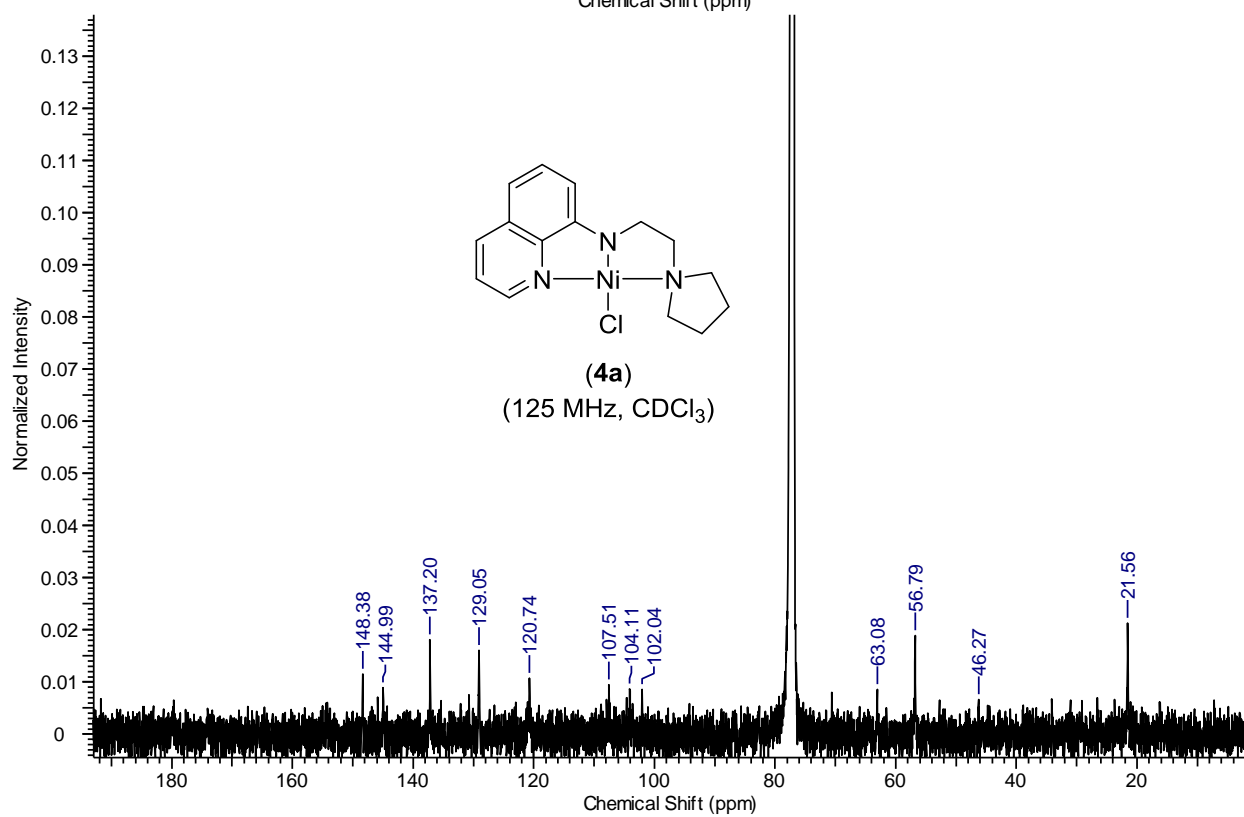
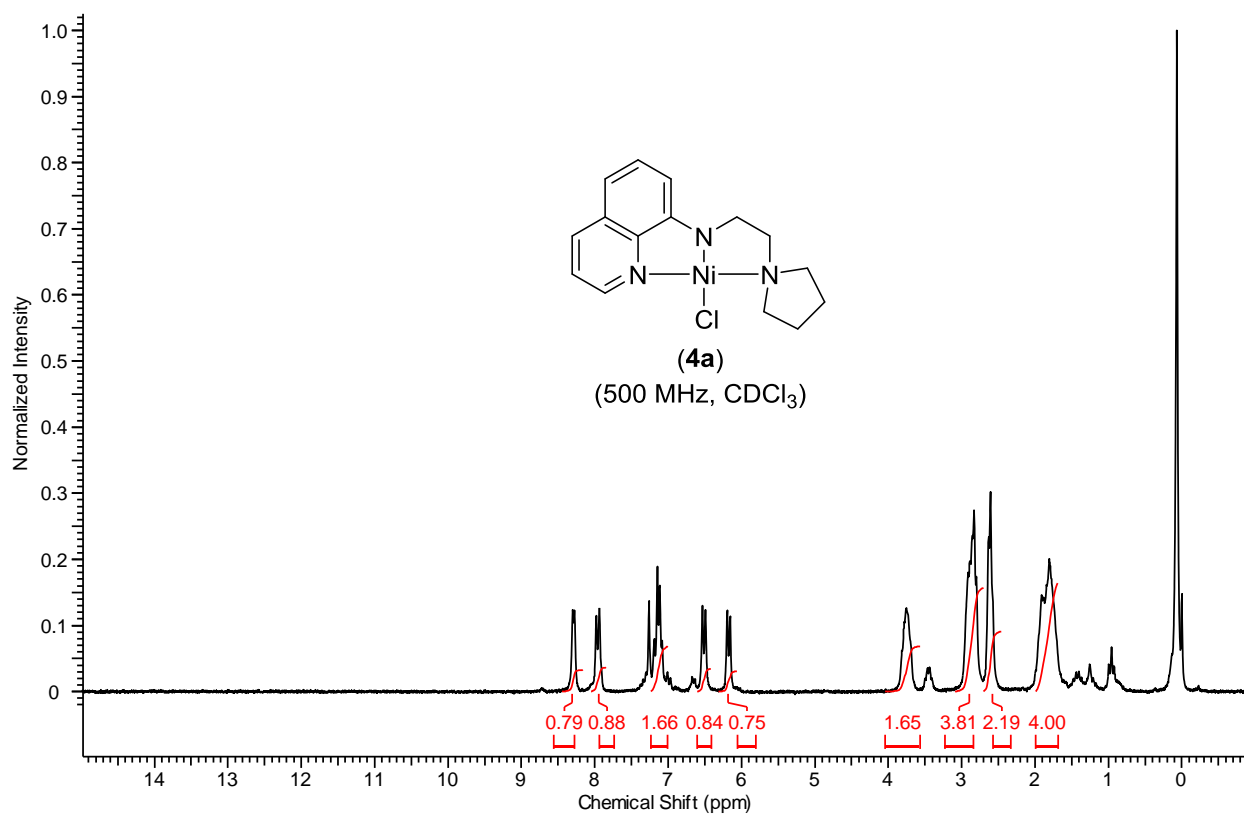












LIST OF PUBLICATIONS

1. **Pandey, D. K.**; Kumar V.; Punji, B.; Nickel-Catalyzed Regioselective Arylation of Indole with Aryl Chlorides, Manuscript under preparation.
2. **Pandey, D. K.**; Ankade S.; Ali A.; Vinod C. P.; Punji, B.; Unactivated Alkyl Chlorides in Nickel-Catalyzed C(2)-H Alkylation of Indoles: Evidence of a Ni(I) Active Species, Manuscript communicated.
3. Patel U. N.; Jain S.; **Pandey D. K.**; Gonnade R. G.; Vanka K.; Punji B.; “Mechanistic Aspects of Pincer Nickel(II)-Catalyzed C-H Bond Alkylation of Azoles with Alkyl Halides” *Organometallics*, **2018**, *37*, 1017–1025.
4. Patel U. N.; **Pandey D. K.**; Gonnade R. G.; Punji B.; Synthesis of Quinoline-Based NNN-Pincer Nickel(II) Complexes: A Robust and Improved Catalyst System for C-H Bond Alkylation of Azoles with Alkyl Halides, *Organometallics*, **2016**, *35*, 1785–1793.
5. **Pandey, D. K.**; Khake, S. M.; Gonnade, R. G.; Punji, B., “Mono- and Binuclear Palladacycles *via* Regioselective C-H Bond Activation: Syntheses, Mechanistic Insights and Catalytic Activity in Direct Arylation of Azoles”, *RSC Adv.*, **2015**, *5*, 81502 – 81514.